

# **The Synthesis of Oxime-and-Amide *bis*-Chelate Ligands**

by

**Thomas John Theron**

B.Sc. (Hons), (University of KwaZulu-Natal)

Submitted in fulfilment of the requirements  
for the degree of Master of Science in Chemistry  
School of Chemistry and Physics  
College of Agriculture, Engineering, and Science  
University of KwaZulu-Natal  
Pietermaritzburg

**2014**

## **A Note of Introduction**

This thesis reflects two essentially independent projects completed in fulfilment of the requirements for the degree of Masters of Science, and found under the same cover. Consequently, they are presented in Chapter A and Chapter B of the manuscript. The reason for such “doubling-up” is explained later in the thesis (at the end of Chapter A). As the contents of Chapter A and Chapter B are largely independent and are bound only by the common theme of oxime-and-amide ligands pursued in our research group, we decided to introduce independent numbering of figures, tables, schemes, references, and compounds in each of these chapters.

## Abstract for Chapter A

In this part of the thesis our intention was to pave the way for the synthesis of pentadentate ligands with the *bis*-chelate methyl-hydroxyacetamide binding centre augmented with a flexible pendant arm that may provide additional coordination from an axial direction (scorpionate action), Fig. 4.

Analysis of the possible synthetic approaches revealed that to realise a variety of ligands with the above features, a class of key intermediate compounds will have to be prepared, namely, 1,3-diaminopropanes with a flexible arm of variable length bearing terminal nucleophile and grafted on the C2-carbon, Figure 5. In principle, the synthesis of substituted 1,3-diaminopropanes can be achieved through a number of routes, Schemes 1A-6A, of which in present work we explored two.

In total, we have synthesised eleven compounds, five of them new: 2,2'-(2-hydroxypropane-1,3-diyl)bis(1*H*-isoindole-1,3(2*H*)-dione) (**2**), 2,2'-(2-bromopropane-1,3-diyl)bis(1*H*-isoindole-1,3(2*H*)-dione) (**3**), [2-(benzyloxy)ethyl]propanedinitrile (**22a**), [3-(benzyloxy)propyl]propanedinitrile (**22b**) and 2-(2-hydroxyethyl)propane-1,3-diaminium dichloride (**24a**). Previously known compounds were characterised by <sup>1</sup>H and <sup>13</sup>C NMR spectroscopy. New compounds were characterised by complete range of instrumental techniques described in Chapter A.

Pivotal 2-(2-hydroxyethyl)alkyl-1,3-diaminium dichloride precursor (**24a**) was synthesised via benzylic *mono*-protection of diols, followed by bromo-de-hydroxylation, alkylation of malononitrile at the C2 carbon with the intermediate prepared, deprotection, and catalysed hydrogenation. The reduction proved to be persistently difficult, and highly hydroscopic diamine hydrochloride salt formed in rather low yield.

An alternative route, emanating from bromo-de-hydroxylation of (**2**) into (**3**), was briefly explored but abandoned due to a regrettable oversight. As a matter of fact, the synthesis of (**3**) was accomplished successfully, and the routes that rely on this or similar Boc-protected intermediate (**13**), in retrospect, are probably the most promising ones.

## Abstract for Chapter B

In this part of the thesis we set out to synthesise new class of the *bis*-chelate *N,N'*-alkane-1,*x*-diylbis[2-cyano-2-(hydroxyimino)ethanamide] ligands, Fig. 6, with a variable length and nature of polymethylene bridge (ethyl, methyl, butyl and 1,3-diaminopropyl-2-ol) between the two cyanohydroxyiminoacetamide moieties. Prior to our work only one such ligand was reported in literature. These new compounds were synthesised for future studies of their thermodynamics of protonation and metallation with a range of transition metals.

In total, we have synthesised nine compounds in this chapter, of which three are new (**5a**, **5c**, and **5d**). Previously known compounds were characterised by <sup>1</sup>H and <sup>13</sup>C NMR spectroscopy. All new compounds were characterised by complete range of instrumental techniques described in Chapter B.

Two routes towards the synthesis of desired ligands were explored, and the path that relies on the intermediate *bis*-amides, Scheme 15 path A, turned out to be successful.

In particular,

- a) three of the four *bis*-cyanoamide precursors were synthesised in solvent medium, with the yield of 67% (**4a**), 76 % (**4b**) and 66 % (**4d**); the remaining *bis*-cyanoamide (**4c**) was synthesised in 87 % yield using a solvent-free procedure,
- b) all four desired *bis*-cyanoxime-and-amide ligands (**5a-d**) were prepared successfully in 3.6, 24, 6.6 and 6.2 % yield, respectively.

For two representative compounds, *N,N'*-ethane-1,2-diylbis(2-cyanoacetamide) (**4a**) and *N,N'*-ethane-1,2-diylbis[2-cyano-2-(hydroxyimino)ethanamide] (**5a**), we were able to obtain suitable single crystals and to determine their molecular and crystal structure by X-ray diffraction. Both crystals structures are the first of their kind.



# Acknowledgments

I would like to express sincere gratitude to:

my supervisor *Professor Igor Nikolayenko* for his assistance, patience, enthusiasm and attention to detail. The wealth of knowledge gained under his supervision has been invaluable, and will carry through to all future endeavours. His input while writing this thesis has been patient and constructive guiding me in the right direction.

*Mr Craig Grimmer* for all his assistance, not only in keeping NMR spectroscopy and the IT network running, but other matters regarding chemical reagents and lab safety, as well as his input on debates regarding NMR results.

*Dr Matthew Akerman* and *Professor Nikolay Gerasimchuck* for their assistance in the collection of single crystal X-ray data, and structural determinations.

*Mrs Cayrl Jansen van Rensburg* for her assistance with mass spectroscopy and elemental analysis.

*Mr Clarence Mortlock* for his assistance in making unusual synthetic glassware.

*my family* for the extended financial support over the years

the *National Research Foundation* for funding through the second year of this work

and the *University of KwaZulu-Natal* for providing research opportunities and the remission of fees at postgraduate level.

# Declaration

I, *Thomas J. Theron*, declare that:

1. The research presented in this thesis, except where otherwise stated, is solely my own work.
2. This research has not been submitted for any other degree or examination at another university.
3. This thesis does not contain other people's data, graphics or pictures unless acknowledged as being sourced from other relevant parties.
4. This thesis does not contain other researchers writing unless specifically stated as originating from them. In cases where other written sources have been used:
  - a) where their words were rewritten, the general information attributed to author/authors has been referenced,
  - b) where their words have been directly quoted, they were placed inside quotation marks, and referenced.

Signed: \_\_\_\_\_ (**Thomas J. Theron**) on this \_\_\_\_\_ day of \_\_\_\_\_ 2014

I hereby certify that this is correct, and as *Thomas J. Theron's* supervisor I **have/have not** approved this thesis for external examination and submission.

Signed: \_\_\_\_\_ **Professor I. Nikolayenko** on this \_\_\_\_ day of \_\_\_\_\_ 2014

# Table of Contents

## Chapter A

<b>1. Introduction</b>	1
<b>2. Literature Survey</b>	5
2.1 Oxime-and-amide chelates	5
2.1.1 Coordination chemistry of the oxime group	7
2.1.2 Coordination chemistry of the amide group	8
2.1.3 Coordination chemistry of the HIAA moiety	9
2.1.4 Coordination chemistry of the HIAA <i>bis</i> -chelates	10
2.2 Metal complexes in oxidation catalysis	13
<b>3. Towards the synthesis of functionalised propane-1,3-diamines</b>	17
3.1 Synthetic strategies considered	19
3.1.1 1,3-Diaminopropane-2-ol & 2-aminoethanol route	20
3.1.2 1,3-Diaminopropane-2-ol & t-butyl(2-aminoethyl)carbamate route	21
3.1.3 1,3-Diaminopropane-2-ol & 2-aminoethanol route	22
3.1.4 1,3-Dianimopropane-2-ol & 2-(2-aminoethyl)-1 <i>H</i> -isoindole-1,3(2 <i>H</i> ).... route	23
3.1.5 Malononitrile & ethane-1,2-diol route	24
3.1.6 Malononitrile & 2-bromoethanamine route	25
3.2 Literature review of the chemistry of synthetic steps	26
3.2.1 Protection of functional groups	26
3.2.2 Mono protection of terminal diols	38
3.2.3 Halide-de-hydroxylation	39
3.2.4 Condensation with malononitrile	40
3.2.5 Hydrogenation of substituted malononitriles	41
<b>4. Synthetic steps explored</b>	44
4.1 Synthesis of 2,2'-(2-Bromopropane-1,3-diyl)bis(1 <i>H</i> -iso-indole-1,3-(2 <i>H</i> )-dione)	44
4.2 Synthesis of mono-protected terminal diols	46
4.3 Synthesis of [(bromoalkoxy)methyl]benzenes	47
4.4 Synthesis of [n-(benzyloxy)alkyl]propanedinitriles	48
4.5 Synthesis of [n-(Benzyloxy)alkyl]-1,3-propanediamines	49
<b>5. Synthesis and characterisation</b>	54
5.1 Experimental	54

5.1.1 Solvents and reagents	54
5.1.2 Instrumental	56
5.1.3 Interpretation of NMR results	57
5.2 Intermediates with protected functional groups	59
5.2.1 Phthalimide di-protected-1,3-diaminopropan-2-ol	59
5.2.2 Mono-protected terminal diols	60
5.2.3 Boc protected 1,3-diaminopropan-2-ol	62
5.2.4 Boc mono-protected diamines	62
5.3 Products of bromo-de-hydroxylation	63
5.3.1 2,2'-(2-bromopropane-1,3-diyl)bis(1H-isoindole-1,3(2H)-dione)	63
5.3.2 [(n-bromoalkyloxy)methyl]benzenes	64
5.4 Condensation with malononitrile	66
5.5 Reduction of malononitrile intermediates	68
<b>6. Conclusions to chapter A</b>	<b>70</b>
<b>7. Future work emanating from chapter A</b>	<b>72</b>
<b>8. References from chapter A</b>	<b>74</b>

## Chapter B

<b>0. A Note on the notation</b>	<b>78</b>
<b>1. Introduction</b>	<b>78</b>
<b>2. Literature survey</b>	<b>82</b>
2.1 Introduction to cyanoximes	82
2.2 Coordination chemistry of isolated functional groups	83
2.3 Coordination by cyanoximes	83
2.4 Coordination chemistry of the CHIAA moiety	84
2.5 Bis-chelate ligands with CHIAA moieties	85
2.6 Possible applications of ligands with cyanoxime-and-amide chelates	87
2.7 Synthesis of the CHIAA moiety	88
2.7.1 General approach to the synthesis of cyanoxime-and-amides	88
2.7.2 Nitrosation followed by condensation	90
2.7.3 Condensation followed by nitrosation	90
2.8 Possible side reactions in the preparation of cyanoxime ligands	93

2.8.1 Nitrosation of ethyl cyanoacetate	93
2.8.2 Cross-protonation of diamines	93
2.8.3 Self-condensation of cyanoacetate esters	94
2.8.4 The Thorpe-Ziegler reaction	95
2.8.5 Side products determined by the reaction and workup temperature	97
2.9 Proposed synthetic routes	99
2.9.1 Nitrosation followed by condensation	100
2.9.2 Condensation followed by nitrosation	101
2.10 Comparative analysis of the characterisation data for cyanoxime-and-amide ligands	104
2.10.1 Characteristic IR data	104
2.10.2 Characteristic NMR data	106
<b>3. Synthesis and characterisation</b>	<b>108</b>
3.1 Experimental	108
3.1.1 Solvents and reagents	108
3.1.2 Instrumental	108
3.2 Synthesis of <i>bis</i> -cyanoacetamide precursors	109
3.3 Synthesis of bis-chelate cyanoxime-and-amide ligands	113
3.4 Solid state structures	121
3.4.1 <i>N,N</i> -Ethane-1,2-diylbis(2-cyanoacetamide)	121
3.4.2 <i>N,N</i> -Ethane-1,2-diylbis[2-cyano-2-(hydroxyimino)ethanamide]	128
<b>4. Discussion of synthetic results</b>	<b>136</b>
4.1 Two synthetic routes	136
4.2 Path B	137
4.2.1 Step one oximation	137
4.2.2 Step two condensation	137
4.3 Path A	139
4.3.1 Step one condensation	139
4.3.2 Step two oximation	141
4.3.3 Evidence of different molecular forms	152
<b>5. Conclusions for chapter B</b>	<b>156</b>
<b>6. Further work</b>	<b>157</b>
6.1 New ligand synthesis	157
6.2 Protonation studies	157

6.3 Conformational studies	.....	158
6.4 Metallation of the cyanoxime-and-amide ligands	.....	158
<b>7. References for chapter B</b>	.....	160
<b>Appendix</b>	.....	163

# List of Tables

## Chapter A

Table 1.	Conditions of stability and removal for the MOM ethers	.....	27
Table 2.	Conditions of stability and removal for the THP ethers	.....	28
Table 3.	Conditions of stability and removal for the <i>t</i> -buthyl ethers	.....	28
Table 4.	Conditions of stability and removal for the allylethers	.....	29
Table 5.	Conditions of stability and removal for the Bn ethers	.....	29
Table 6.	Conditions of stability and removal for the Ac ethers	.....	30
Table 7.	Conditions of stability and removal for the Pv esters	.....	30
Table 8.	Conditions of stability and removal for the Bz ester	.....	31
Table 9.	Conditions of stability and removal of Fmoc	.....	32
Table 10.	Conditions of stability and removal of Boc	.....	33
Table 11.	Conditions of stability and removal for Cbz	.....	33
Table 12.	Conditions of stability and removal for Ac	.....	34
Table 13.	Conditions of stability and removal for Trifluoroacetamides	.....	35
Table 14.	Conditions of stability and removal of Phth	.....	35
Table 15.	Conditions of stability and removal of Bn	.....	36
Table 16.	Conditions of stability and removal of Tr protection	.....	36
Table 17.	Conditions of stability and removal of benzylideneamine	.....	37
Table 18.	Conditions of stability and removal of Ts	.....	37
Table 19.	Common solvents used and internal purification procedures	.....	54
Table 20.	Commercially available reagents used for the synthesis in this chapter	.....	55

## Chapter B

Table 1.	Cyanoxime-and-amide ligands synthesised through acidic nitrosation	.....	89
Table 2.	Cyanoxime-and-amide ligands synthesised through basic nitrosation	.....	89
Table 3.	Yield of various <i>bis</i> -cyanoamides in Gazit <i>et al</i> procedure	.....	102
Table 4.	Wavenumbers (in cm <sup>-1</sup> ) of the characteristic valent vibrations in various cyanoxime-and-amide chelates according to literature	.....	104
Table 5.	Representative <sup>1</sup> H and <sup>13</sup> C NMR chemical shifts (in ppm) in various cyanoxime-and-amide chelates according to literature	.....	106
Table 6.	Common solvents used and internal purification procedures	.....	108
Table 7.	Commercially available reagents used for the synthesis in this chapter of the		
	Thesis	.....	108

Table 8.	Sample and crystal data for compound (4a)	..... 122
Table 9.	Selected geometric parameters for compound (4a)	..... 123
Table 10.	Hydrogen-bond geometry in crystal structure of (4a)	..... 125
Table 11.	Sample and crystal data for compound (5a)	..... 129
Table 12.	Selected geometric parameters for compound (5a)	..... 130
Table 13.	Hydrogen-bond geometry in crystal structure of (5a)	..... 132
Table 14.	Yield of <i>N,N'</i> -propane-1,3-diylbis(2-cyanoacetamide) (4b) per fraction in two different solvated systems	..... 139
Table 15.	Yield of <i>bis</i> -cyanoacetamides according to Gazit <i>et al</i> <sup>[37]</sup> (solvent-free) and our synthesis in MeOH/glass beads medium	..... 140
Table 16.	Yield of <i>bis</i> -chelate ligand (5c) for various ratios of starting materials	..... 147
Table 17.	Yield of <i>bis</i> -chelate ligand (5c) in comparable runs with different precursor to base ratios	..... 148
Table 18.	Yield of <i>bis</i> -chelate ligand (5c) in comparable runs with different amount of precursor present in solution	..... 149
Table 19.	Yield of <i>bis</i> -chelate ligand (5c) in two sequential bubblers using the same gas source	..... 150
Table 20.	Yield of <i>bis</i> -chelate ligand (5b), in comparable runs at different temperatures	..... 150
Table 21.	Yield of <i>bis</i> -chelate ligand (5d), in five identical runs	..... 151
Table 22.	Representative yield of the oximation step for different <i>bis</i> -chelate ligands synthesised in this project	..... 151



# List of Figures

## Chapter A

<b>Fig. 1.</b>	Generic structure of a ligand with hydroxyiminoacetamide (HIAA) chelating moiety	1
<b>Fig. 2.</b>	Typical structure of the Cu(II)- <i>N,N'</i> -propane-1,3-diylbis[2-(hydroxyimino)propanamide] (mhiaa <sub>2p</sub> ) complex	2
<b>Fig. 3.</b>	Kimura's catalytically active Ni(II)/Ni(III)-cyclic dioxopentamine complex	2
<b>Fig. 4.</b>	A concept of the metal complex with tetrapodal oxime-and-amide binding site augmented by a scorpion action.	3
<b>Fig. 5.</b>	Key synthetic intermediate required for the preparation of the ligands with scorpionic action	4
<b>Fig. 6.</b>	Adenosine Triphosphate, (ATP), and Adenosine Diphosphate, (ADP)	5
<b>Fig. 7.</b>	Reaction mechanism of the complex-catalysed hydrolysis of acetyl phosphate initially suggested by Lau and Gutsche	6
<b>Fig. 8.</b>	Alternative reaction mechanisms suggested in <sup>[5]</sup> for the hydrolysis of acetyl phosphate, catalysed by the Cu(II)-complex of an oxime-and-amide ligand with terminal nucleophile, that exhibited ten-fold increase in reaction rate in comparison to free ligand	6
<b>Fig. 9.</b>	1-Undecyl- <i>N,N'</i> -bis[(2-hydroxyimino)propanol]ethylenediamine ligand	6
<b>Fig. 10.</b>	Transition metal complex of 1-undecyl- <i>N,N'</i> -bis[(2-hydroxyimino)propanol]ethylenediamine, and proposed reaction mechanisms for the catalysed decomposition of acetyl phosphate	7
<b>Fig. 11.</b>	Generic view of an oxime, illustrating spatial location of the lone pairs that are available for metal coordination	8
<b>Fig. 12.</b>	Generic representation of the amide chemical group showing the existence of lone pairs on the oxygen and nitrogen	9
<b>Fig. 13.</b>	Generic structure of a ligand with 2-methyl hydroxyiminoacetamide (HIAA) chelating moiety	10
<b>Fig. 14.</b>	Various coordination modes of the metal ions by MHIAA moiety, including an illustration of the geometrical need for amide deprotonation to achieve N(ox)N(ad) chelation	10
<b>Fig. 15.</b>	<i>N,N'</i> -bis(2-hydroxyiminopropionyl)propane-1,3-diamine	11
<b>Fig. 16.</b>	The structure of Cu(II)- <i>N,N'</i> -propane-1,3-diylbis[2-(hydroxyimino)propanamide] (MLH <sub>3</sub> type)	11
<b>Fig. 17.</b>	Ni(II) macrocyclic pentadamine complex	13
<b>Fig. 18.</b>	Ni(II) cyclo dioxotertamine complex	13
<b>Fig. 19.</b>	Ni(II) macrocyclic dioxopentaamine complex	14
<b>Fig. 20.</b>	Ni(II) macrocyclic dioxopentaamine complex	14
<b>Fig. 21.</b>	Ni(III) macrocyclic dioxopentaamine complex	15
<b>Fig. 22.</b>	Generic view of the metal complex of C2-substituted hydroxyiminoacetamide (HIAA) <i>bis</i> -chelate ligand with a propane bridge, functionalised with a scorpionic arm terminated in a nucleophile	16
<b>Fig. 23.</b>	A ligand with methyl hydroxyiminoacetamide (HIAA) chelating moiety	17
<b>Fig. 24.</b>	Generic scheme of the condensation of ethyl-2-(hydroxyimino)propanoate with a suitable primary diamine	17
<b>Fig. 25.</b>	Generic structure of propane-1,3-diamines with a flexible alkyl chain grafted onto the C2-carbon of the propane backbone and terminated with a suitable nucleophile	18

Fig. 26.	Illustration of the labelling principle for homologue compounds adopted in this thesis. This example is for the aliphatic diols	19
Fig. 27.	Generic structure of a MOM ether	27
Fig. 28.	Generic structure of a THP ether	27
Fig. 29.	Generic structure of a <i>t</i> -butyl ether	28
Fig. 30.	Generic structure of an allyl ether	28
Fig. 31.	Generic structure of a Bn ether	29
Fig. 32.	Generic structure of an Ac ether	29
Fig. 33.	Generic structure of a Pv ester	30
Fig. 34.	Generic structure of a Bz ester	30
Fig. 35.	Williamson's ether synthesis	31
Fig. 36.	Generic structure of an Fmoc amide	32
Fig. 37.	Generic structure of a Boc amide	33
Fig. 38.	Generic structure of a Cbz amide	33
Fig. 39.	Generic structure of an Ac amide	34
Fig. 40.	Generic structure of a trifluoroacetamide	34
Fig. 41.	Generic structure of a Phth	35
Fig. 42.	Generic structure of a Bn	35
Fig. 43.	Generic structure of a Tr	36
Fig. 44.	Generic structure of a benzylideneamine	36
Fig. 45.	Generic structure of a Ts	37
Fig. 46.	Diagrammatic representation of a terminal diol oxygens coordinating to Ag <sub>2</sub> O catalyst in a bi-dentate fashion	39
Fig. 47.	Appel's chloro-de-hydroxylation mechanism	40
Fig. 48.	The structure of (2,2-dimethylpropyl)propanedinitrile	42
Fig. 49.	Bromo-de-hydroxylation step of Schemes 1 and 2	44
Fig. 50.	Chemical structure of <i>di</i> -butylpropanedinitrile	50

## Chapter B

Fig. 1.	Generic structure of a ligand with hydroxyiminoacetamide ( <b>hiao</b> ) chelating moiety	78
Fig. 2.	Solid state structure of the di-copper – di-ligand complex [Cu <sub>2</sub> (mhiao <sub>2</sub> eH-1) <sub>2</sub> ].	79
Fig. 3.	Solid state structure of the di-copper – di-ligand complex [Cu <sub>2</sub> (mhiao <sub>2</sub> bH-1) <sub>2</sub> ]	80
Fig. 4.	2-Cyano-2-(hydroxyimino)acetamide and 2-hydroxyiminopropanamide	81
Fig. 5.	Mhiao <sub>2</sub> ligands investigated in our group previously	81
Fig. 6.	<i>Bis</i> -chelate cyano-hydroxyiminoacetamide ( <b>chiaaz</b> ) ligands studied in Chapter B	81
Fig. 7.	The concept of synthetic approach to oximation after Victor Meyer	82
Fig. 8.	Generic view of the cyanoxime moiety in its most stable conformational form showing the location of lone pairs available for the metal coordination	83
Fig. 9.	2-Cyano-2-(hydroxyimino)ethanamide ( <b>chiaad</b> ), the first cyanoxime-and-amide chelating ligand ...	84
Fig. 10.	(2 <i>E</i> )- <i>N</i> -(2-aminoethyl)-2-cyano-2-(hydroxyimino)ethanamide ligand	84

Fig. 11.	(2 <i>E</i> ,2 <i>E'</i> )- <i>N,N'</i> -propane-1,3-diylbis[2-cyano-2-(hydroxyimino)ethan amide] ( <b>chiaa<sub>2</sub>p</b> ) ligand	85
Fig. 12.	Molecular structure of 3,3'-Piperazine-1,4-diylbis[2-(hydroxyimino)-3-oxopropane-nitrile] or ( <b>chiaa<sub>2</sub>ppz</b> ) ligand	85
Fig. 13.	Molecular structure of 2-(hydroxyimino)-3-(morpholin-4-yl)-3-oxopropanenitrile	87
Fig. 14.	<i>N,N</i> -(2-aminoethyl)-2-cyano-2-(hydroxyimino)ethanamide	90
Fig. 15.	2-Cyano-2-(hydroxyimino)- <i>N,N</i> -dimethylethanamide	90
Fig. 16.	2-Cyano-2-(hydroxyimino)- <i>N,N</i> -dimethylethanethioamide	91
Fig. 17.	(2 <i>E</i> ,2' <i>E'</i> )- <i>N,N'</i> -propane-1,3-diylbis[2-cyano-2-(hydroxyimino)ethan amide] ligand	92
Fig. 18.	Three structurally similar to the desired ligands compounds, which syntheses have been reported in literature: (2 <i>E</i> )- <i>N</i> -(2-aminoethyl)-2-cyano-2-(hydroxyimino)ethanamide ( <b>chiaaea</b> ), (2 <i>E</i> ,2' <i>E'</i> )- <i>N,N'</i> -propane-1,3-diylbis[2-cyano-2-(hydroxyimino)ethanamide] ( <b>chiaa<sub>2</sub>p</b> ), and (2 <i>E</i> ,2' <i>E'</i> )-3,3'-piperazine-1,4-diylbis[2-(hydroxyimino)-3-oxopropanenitrile] ( <b>chiaa<sub>2</sub>ppz</b> )	99
Fig. 19.	(2 <i>E</i> ,2' <i>E'</i> )- <i>N,N'</i> -propane-1,3-diylbis[2-cyano-2-(hydroxyimino)ethan amide] ( <b>chiaa<sub>2</sub>p</b> ) ligand synthesised by Kolotilov <i>et al</i>	101
Fig. 20.	The range of <i>N,N'</i> -alkyl-diylbis[2-(hydroxyimino)propanamides] synthesised in the research group previously	102
Fig. 21.	Diagrammatic representation of the apparatus for the oximation of <i>bis</i> -cyanacetamides	113
Fig. 22.	Image of the actual methyl nitrite generating vessel employed in the above process.	115
Fig. 23.	Overview of the actual apparatus employed in the above process.	115
Fig. 24.	A view of the molecular structure of ( <b>4a</b> ) with the numbering scheme.	123
Fig. 25.	A view of the molecular structure of ( <b>4a</b> ) illustrating the planarity of the cyanoacetamide moieties	124
Fig. 26.	A packing diagram viewed down <i>a</i> -axis for the crystal structure of ( <b>4a</b> )	124
Fig. 27.	H-Bonding interactions in the crystal structure of ( <b>4a</b> )	125
Fig. 28.	Representative H-bonding interactions in the crystal structure of ( <b>4a</b> ) that involve amine and carbonyl groups	125
Fig. 29.	$\pi$ -Stacking interaction of the first kind in the crystal structure of ( <b>4a</b> )	126
Fig. 30.	$\pi$ -Stacking interaction of the second kind in the crystal structure of ( <b>4a</b> )	126
Fig. 31.	Two intersecting molecular strands arising from $\pi$ -stacking interactions in the crystal structure of ( <b>4a</b> )	126
Fig. 32.	A view of the crystal structure of ( <b>5a</b> ) down <i>a</i> -axis	126
Fig. 33.	A view of the crystal structure of ( <b>4a</b> ) down the axis of strands	127
Fig. 34.	A view of the crystal structure of ( <b>4a</b> ) perpendicular to the axis of strands	127
Fig. 35.	A view of the molecular structure of ( <b>5a</b> ) with the numbering scheme	131
Fig. 36.	A view of the molecular structure of ( <b>5a</b> ) illustrating the planarity of chelating moieties	131
Fig. 37.	A packing diagram viewed down <i>b</i> -axis for the crystal structure of ( <b>5a</b> )	132
Fig. 38.	Major types of H-bonding interactions in the crystal structure of ( <b>5a</b> )	132
Fig. 39.	Representative H-bonding interactions in the crystal structure of ( <b>5a</b> ) that involve oxime and carbonyl groups	133
Fig. 40.	Representative H-bonding interactions in the crystal structure of ( <b>5a</b> ) that involve amine and nitrile groups	133
Fig. 41.	$\pi$ -Stacking interaction of the first kind in the crystal structure of ( <b>5a</b> )	134

<b>Fig. 42.</b> $\pi$ -Stacking interaction of the second kind in the crystal structure of (5a)	.....	134
<b>Fig. 43.</b> Two types of molecular strands arising from $\pi$ -stacking interactions in the crystal structure of (5a)	.....	134
<b>Fig. 44.</b> Two intersecting molecular strands in the crystal structure of (5a)	.....	135
<b>Fig. 45.</b> A view of the crystal structure of (5a) down $a$ -axis	.....	135
<b>Fig. 46.</b> Suggested Zwitter-ion type stabilisation of cyanoxime-amide-amine <i>mono</i> -condensates	.....	138
<b>Fig. 47.</b> An apparatus for oximation with a single common laboratory bubbler	.....	142
<b>Fig. 48.</b> An apparatus for oximation with a large volume bubbler adorned with a coarse ceramic frit	.....	143
<b>Fig. 49.</b> An apparatus for oximation with two sequential common laboratory bubblers	.....	144
<b>Fig. 50.</b> $^1\text{H}$ NMR spectrum of the molecular form of <i>bis</i> -cyanacetamide (4c)	.....	153
<b>Fig. 51.</b> $^1\text{H}$ NMR spectrum of the suspected tetra sodium salt of <i>bis</i> -cyanacetamide (4c)	.....	153
<b>Fig. 52.</b> $^1\text{H}$ NMR spectrum of ligand (5c), showing the mixture of suspected conformers	.....	154
<b>Fig. 53.</b> COSY NMR spectrum of ligand (5c), indicating the mixture of two conformers	.....	154
<b>Fig. 54.</b> 2-Hydroxyiminopropanamide or mhiaa, left, and 2-cyano-2-(hydroxyimino)acetamide or chiaa, right	.....	157
<b>Fig. 55.</b> Mhiaazz and mhiaaza ligands investigated in our group previously	.....	159
<b>Fig. 56.</b> Two new classes of 2-cyano-(2-hydroxyimino)acetamide ligands, chiaazz and chiaaza, designated for the future metallation studies	.....	159

# CHAPTER A.

## Towards the Synthesis of Oxime-and-Amide Ligands with Scorpionic Action

### 1. Introduction

In recent years the interest in the research group to which I belong, the group Prof I Nikolayenko, is focused on the synthesis, characterisation, and both solid state and solution studies of the *mono*- and *bis*-chelate ligands with the hydroxyiminoacetamide (HIAA) moiety, Figure 1, as well as their metal complexes with late *3d*-transition metals.

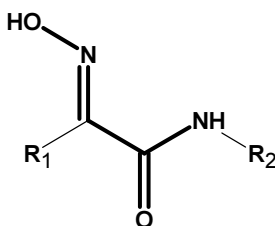


**Fig. 1.** Generic structure of a ligand with hydroxyiminoacetamide (HIAA) chelating moiety (highlighted).

There are four donor centres in the HIAA moiety, two oxygen atoms and two nitrogen atoms, which leads to a large variety of metal complexes, depending on the *pH* and metal to ligand ratio. When two such moieties are joined by a flexible polymethylene bridge, one is faced with *bis*-chelate ligands.

One stable isolatable and persistent *mono*-nuclear complex of a ligand with propane bridge is that of  $MLH_3$  stoichiometry. It corresponds to triply deprotonated pseudo-macrocyclic structure, and forms at equimolar metal to ligand ratio in the *pH* range from weakly acidic to strongly basic (exact range is metal dependent). A representative structure of such complex is shown below, Figure 2.

A few examples of the TM-mhiaa<sub>2</sub>p complexes, with Ni(II) and Cu(II), were reported in literature prior to the work of our group.<sup>[1]</sup> Both are of the above  $MLH_3$  type, and are characterised by the following attractive features. First, the ligand in the complex is folded to provide square-planar  $2N_{ox}2N_{am}$  coordination environment around the metal, and the steric strain on the bridge is relieved by adopting an envelope conformation (the middle methylene group of the spacer is out of plane in an otherwise

nearly perfectly planar complex). The square-planar complex structure is assisted by the fact that both chelating units are already planar in free ligand, due to the  $\pi$ -conjugation of oxime and amide groups. The complex is further stabilised by the formation of a pseudo-macrocyclic structure as a result of hydrogen bonding between one protonated and one deprotonated oxime group.

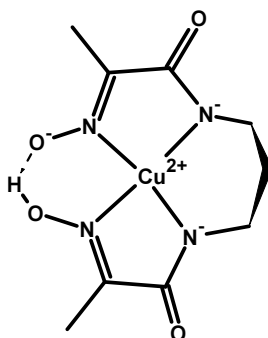


**Fig. 2.** The structure of a stable Cu(II)-*N,N'*-propane-1,3-diylbis[2-(hydroxyimino)propanamide] (**mhiaa<sub>2</sub>p**) complex (MLH<sub>3</sub> type).

High thermodynamic stability and attractive geometric features of such complexes prompted conceptual idea of this project.

In the early 1990's Kimura<sup>[2]</sup> discovered that Ni(II)/Ni(III) complex of a pentadentate tetrapodal ligand dioxopentamine, Figure 3, was capable of oxidising benzene to phenol under very mild conditions. Essential feature of such square-pyramid binding is squeezing of the metal ion into a higher oxidation state (as its reduced ionic radius allows better orbital overlap and hence stabilizes the complex), while still allowing a substrate access to the metal centre from an unoccupied axial direction. Both of these features are essential for the catalysis.

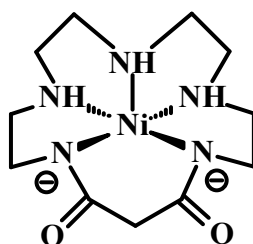


**Fig. 3.** Kimura's catalytically active Ni(II)/Ni(III)-cyclic dioxopentamine complex.

In view of what has been said above, the conceptual idea for this project was to augment attractive square-planar 4N binding centre of the *bis*-chelate oxime-and-amide ligands with additional monodentate binding to the transition metal centre from one axial direction. As we have discussed, M-(hiaa<sub>2</sub>pH<sub>3</sub>) complexes adopt envelope conformation on the bridge when the ligand is coordinated

to Ni(II) or Cu(II) in pseudo-macrocyclic triply deprotonated MLH<sub>3</sub> fashion; grafting a pendant flexible arm equipped with a terminal nucleophile group in the centre of polymethylene bridge should lead to square pyramidal\* coordination, Figure 4.

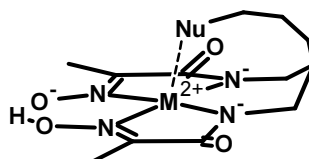


**Fig. 4.** A concept of the metal complex with tetrapodal oxime-and-amide binding site augmented with a scorpion action.

Once synthesised, such ligands are expected to form stable metal complexes where pressure is exerted on the metal centre to reduce its ionic radius, improve orbital overlap, and thus stabilize higher oxidation state. At the same time, free access of a substrate to the metal ion is still possible from the side opposite to the one where terminal nucleophile bites. As we have mentioned earlier, both of these features are desirable for an oxidation catalysis.

Consequently, the ultimate aim of the project was to develop ligands of this kind, prepare their metal complexes, and test for catalytic activity in the oxidation reactions.

In view of the preferred donor atoms for late transition metals, we thought that terminal hydroxyl or amino group might work well. As far as geometrical considerations for a pendant arm are concerned, a chain of two to four methylene groups<sup>†</sup> terminated in a suitable nucleophile and grafted on the C2 carbon of the ligand bridge should give the most favourable coordination geometry.

It soon became obvious that to realise a variety of ligands with the above features, a class of key intermediate compounds will have to be prepared, namely, 1,3-diaminopropanes with a flexible arm of variable length bearing terminal nucleophile and grafted on the C2-carbon, Figure 5.

\* In some literature it is called pentadentate *tetrapodal* coordination, though almost always it is associated with heterocyclic species. We prefer to call such coordination geometry *square-pyramidal* (when it is well defined) or *scorpionic* in general. The term arises from the scorpion's ability to hold its prey with its pincers and to sting and inject venom from above with its tail; in our case, the pincers are equivalent to planar *bis*-chelate part of the ligand, and the tail represents the pendant flexible arm responsible for the axial coordination.

<sup>†</sup> One of them could be an amino group as it is more accessible synthetically.

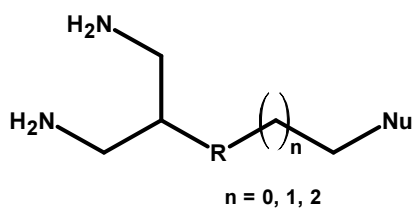


**Fig. 5.** Key synthetic intermediate required for the preparation of ligands with scorpionic action.

$\text{R} = \text{CH}_2$  or  $\text{NH}$ .



## 2. Literature survey

### 2.1 Oxime-and-Amide Chelates

An early interest in the metal complexes of multidentate oxime-and-amide donor ligands, similar to the kind discussed in this thesis, is traceable to their ability to catalyse hydrolysis of acetyl phosphate.<sup>[3]</sup> Acetyl phosphate decomposition is an important model reaction from a biological perspective as it mimics a step of the key energy transfer cycle, namely, conversion of adenosine triphosphate, **ATP**, to adenosine diphosphate, **ADP**.<sup>[4]</sup>

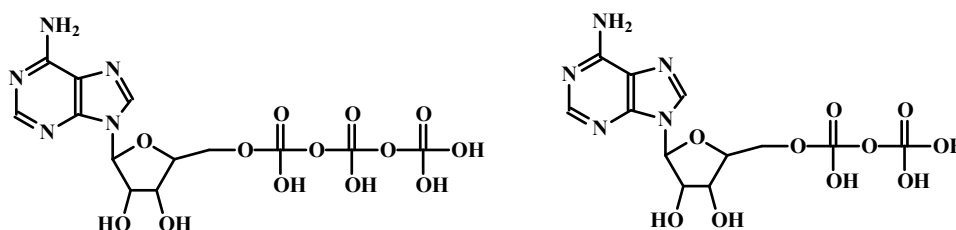


**Fig. 6.** Adenosine Triphosphate, (ATP), and Adenosine Diphosphate, (ADP).

Melhado and Gutsche<sup>[3]</sup> discovered that late transition metal complexes of 5-dodecyltriethylenetetramine catalysed acetyl phosphate decomposition. It was established that free ligand had no effect on the reaction rate. In the presence of Zn(II) ions the rate of acetyl phosphate decomposition decreased compared to that of the free ligand, for Ni(II) ions it remained unchanged, while in the presence of Cu(II) ions a two-fold increase in the rate was observed. Consequently, it was concluded that catalytic action is associated with the presence of a metal complex. Further work, published by Lau and Gutsche,<sup>[5]</sup> explored these findings further. The focus of that extended study was to look at the effect the addition of a nucleophile, attached to the N-terminus of triethylenetetramine, would have on the reaction rate.<sup>[5]</sup>

The concept of possible catalytic action according to Lau and Gutsche<sup>[5]</sup> is illustrated by Figure 7.

Of particular interest to the work carried out in our group was a Cu(II)-oxime-and-amide complex that showed ten-fold increase in catalytic activity in comparison to free ligand,<sup>[5]</sup> Figure 8. Two possible mechanisms, postulated by the authors, are shown in this Figure; both of them are conceivable as nucleophilic groups are present at both ends of the ligand. Some years later Gutsche and Mei<sup>[6]</sup> synthesised a symmetric *bis*-chelate ligand with a long aliphatic chain attached to the spacer to make it soluble in lipid layers and micelles, 1-undecyl-*N,N'*-bis[(2-hydroxyimino)propanol]ethylenediamine, Figure 9.

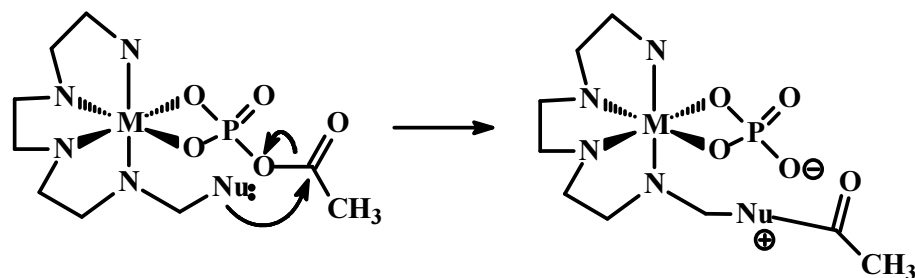


**Fig. 7.** Reaction mechanism of the complex-catalysed hydrolysis of acetyl phosphate initially suggested by Lau and Gutsche.<sup>[5]</sup>

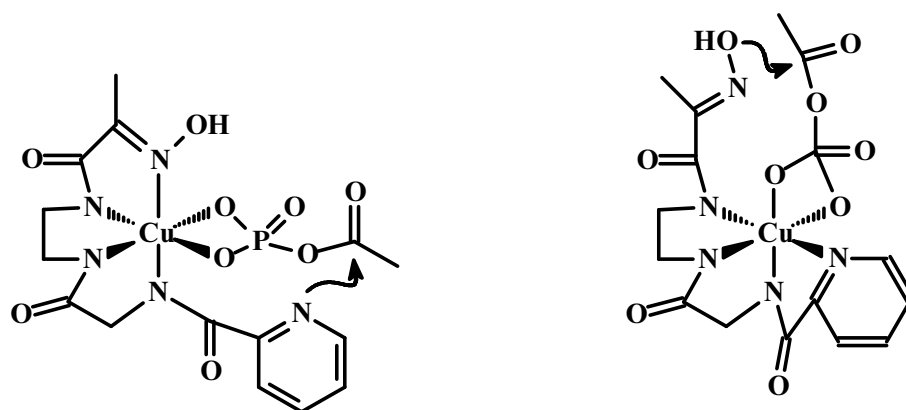


**Fig. 8.** Alternative reaction mechanisms suggested in<sup>[5]</sup> for the hydrolysis of acetyl phosphate, when catalysed by the Cu(II)-complex of oxime-and-amide ligand with a terminal nucleophile. Ten-fold increase in reaction rate in comparison to free ligand was observed in this case.

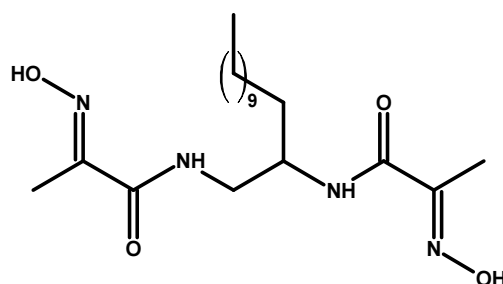


**Fig. 9.** 1-Undecyl-*N,N'*-bis[(2-hydroxyimino)propanol]ethylenediamine ligand.

Similar approach to the testing of effects of the presence or absence of transition metal complexes on the rate of acetyl phosphate decomposition was undertaken. Substantial positive catalytic activity was confirmed for the free ligand and its complexes with Ni(II), Cu(II), and Zn(II),<sup>[6]</sup> though, the last one has never been isolated or characterised. These results pointed to a possibility of advancement in the ligand design. Again, two mechanisms were proposed for the catalytic action, with the first being very similar to previous suggestions, Figure 10.

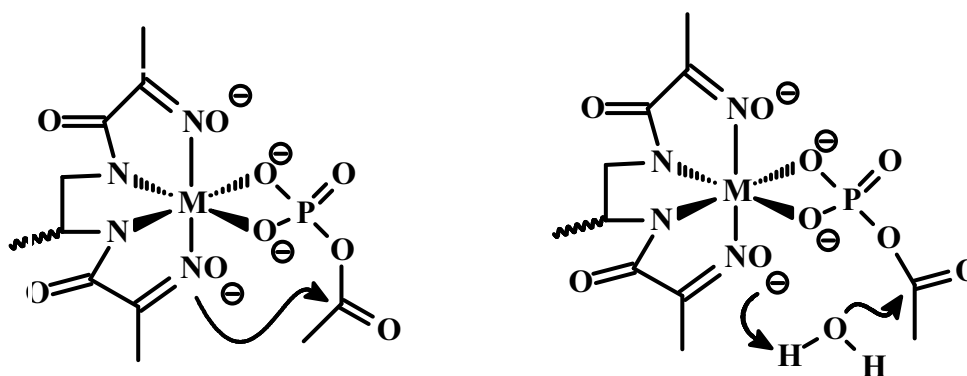


**Fig. 10.** Transition metal complex of 1-undecyl-*N,N'*-bis[(2-hydroxyimino)propanol]ethylenediamine, and proposed reaction mechanisms for the catalysed decomposition of acetyl phosphate.

According to the first mechanism, the 1-undecyl-*N,N'*-bis[(2-hydroxyimino)propanol]ethylenediamine metal complex acts as a catalyst under basic conditions; in the presence of the chelated oxime an acyl transfer to the oxime oxygen occurs, followed by rapid hydrolysis of oxime acetate.

According to the second mechanism, the complex in question can be considered as a *phosphatase* mimic, as it catalyses the transfer of the acetyl group from acetyl phosphate to water. In the latter case, the oxime abstracts a proton from an appropriately positioned water molecule. This, in turn, generates a hydroxide in the vicinity of acetyl phosphate, and liberates acetic acid directly without the formation of an acyl intermediate.<sup>[6]</sup>

The field remained relatively quiet for the next decade. In 1995 Onindo *et al*<sup>[7]</sup> published a study of *N*-pyruvoylaminoacid oximes, ( $\text{CH}_3\text{C}(\text{=NOH})\text{CONHRCO}_2\text{H}$ ), in an attempt to gain better understanding of the metal-protein interactions. These ligands were structurally similar to dipeptides but for the oxime moieties in place of the amino groups. Solution equilibrium studies indicated the formation of a range of stable Cu(II)-complexes of *N*-pyruvoylaminoacid oximes. The analysis of solid state structures of these complexes revealed that such ligands are ambidentate and that their coordination properties are highly influenced by the  $\text{CH}_3\text{C}(\text{=NOH})\text{CONH}$  planar framework, which leads to the formation of nearly planar complexes. Two principal chelation modes were established for Cu(II) cation: a) N(oxime),N(amide) chelation and b) conformationally altered N(oxime),O(carbonyl) chelation.<sup>[7-8]</sup> With the knowledge that the  $\text{CH}_3\text{C}(\text{=NOH})\text{CONH}$  moiety strongly chelates Cu(II)-ions, let us now have a closer look at the individual functional groups involved.

### 2.1.1 Coordination Chemistry of the Oxime Group

*Oxime* or *hydroxyimino* functional group consists of a nitrogen atom on one side double-bonded to a carbon and on the other side bearing a hydroxyl. The general formula for oximes is  $\text{R}_1\text{R}_2\text{CN}=\text{OH}$ , and they can act both as weak acids and weak bases. Hydroxyimino group is a very weak acid, with typical

$pK_a$  values in the range from 8 to 12, and is fully deprotonated only in alkaline solutions. Oxime nitrogen is a very weak base; it can be protonated but only in highly acidic medium at  $pH$  less than 1. From a geometrical point of view, the most stable conformation for an oxime is the one shown below, with three lone electron pairs located on the oxygen and nitrogen atoms, Figure 11.

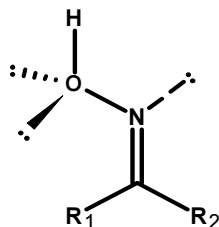


**Fig. 11.** Generic view of an oxime, illustrating spatial location of the lone pairs that are available for metal coordination.

The structure is commonly planar unless distorted by bulky substituent groups  $R_1$  and  $R_2$ . Two lone pairs carried by the oxygen atom are out of plane of the molecule, while the nitrogen lone pair is in plane. Presence of these lone pairs and the ability of the oxime groups to deprotonate account for the metal coordination in a number of modes. Coordination can occur in monodentate manner to oxime nitrogen<sup>[8]</sup> or oxime oxygen,<sup>[9]</sup> in chelate manner to N-O unit by the same metal,<sup>[10]</sup> or in a bridging manner when two different metal centres are simultaneously coordinated to the N-O pair.<sup>[11]</sup> Metal coordination tends to be stronger for deprotonated oximes.<sup>[12]</sup> The ability to form hydrogen bonds adds to the appeal of oxime group as a building block in ligand structures, and helps with the formation of crystal lattices. Conventionally, oximes are synthesised via acid or base catalysed hydroxylamination of active methylenic carbons.<sup>[13-16]</sup>

### 2.1.2 Coordination Chemistry of the Amide Group

Amides are exceptionally well studied compounds in view of their significance for the polypeptide and protein chemistry. Conventionally, they are formed in the reaction between an acyl halide and an amine, or via condensation of an ester with primary amine.<sup>[17-18]</sup> Geometrically their structure is also planar, with the lone electron pair on nitrogen atom occupying  $p_z$ -orbital perpendicular to the plane of the amide group, Figure 12. Two more lone pairs are resident on the carbonyl oxygen and both are in plane of the amide moiety.

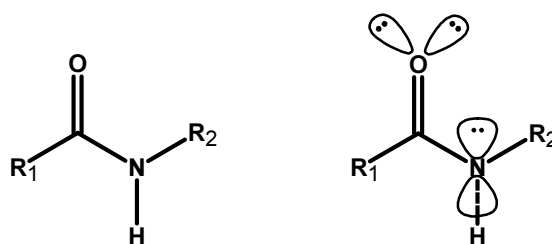


**Fig. 12.** Generic representation of the amide group illustrating special location of the lone pairs on oxygen and nitrogen atoms.\*

The amide group is an exceptionally weak acid, with  $pK_a \geq 15$ . Consequently, ionisation of the amide hydrogen is not observed in aqueous solutions of free amides but does happen in the presence of metal ions, when the formation of a metal complex compensates for the thermodynamically unfavourable cleavage of the N-H bond.<sup>[15]</sup>

The amide group has two donor centres, O and N, and can coordinate to metals through both of them. When the amide hydrogen is ionised, N-donor centre becomes significantly more nucleophilic. In addition, the lone pair on N-centre bodes well for the formation of hydrogen bonds.<sup>1</sup>

### 2.1.3 Coordination Chemistry of the HIAA Moiety

Combining oxime and amide functionalities in one unit, in an oxime-and-amide or as we prefer to call it **HydroxyIminoAcetAmide** (HIAA) moiety, Figure 13, does not simply add up their individual properties but also confers new structural and functional features onto it in a synergetic manner.

The first of these new features is almost perfect planarity of the moiety, caused by  $\pi$ -conjugation across the whole -N=C-C(=O)-N- framework, as each of the mentioned atoms has an electron in the  $p_z$ -orbital perpendicular to the plane of the molecule. Any rotation around indicated bonds will disrupt such planarity, reduce the  $\pi$ -orbital overlap and destabilise the structure. The second feature is the intramolecular hydrogen bonding of the amide proton to the oxime nitrogen as shown in Figure 13. These two features combined lead to the conformational shape shown above, namely, *E*-type arrangement of the double bonds. This has been confirmed by us both in direct structural studies (single crystal XRD) and quantum mechanical calculations at high level of the DFT (see later in the Experimental section).

\* Formally, an amide may contain yet another substituent group on the nitrogen atom. Only  $R_1$  and  $R_2$  substituents are shown in Figure 12 because in the scope of current thesis the third group is always hydrogen.

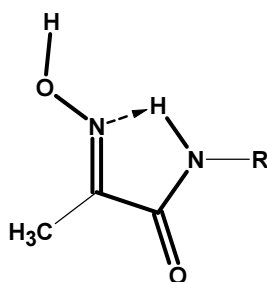


**Fig. 13.** Generic structure of a ligand with 2-methyl hydroxyiminoacetamide (HIAA) chelating moiety.

There are four donor centres in the HIAA moiety, two oxygen atoms and two nitrogen atoms, which lead to a large variety of metal complex structures depending on the  $pH$  and metal to ligand ratio, Figure 14.

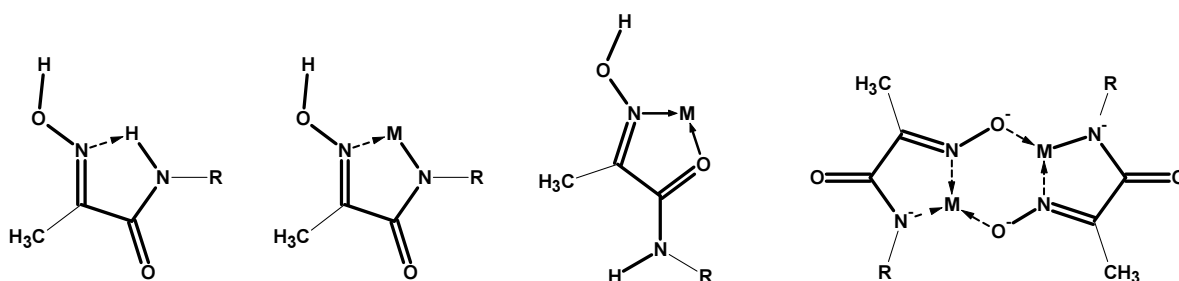


**Fig. 14.** Various coordination modes of the metal ions by MHIAA moiety, including an illustration of the geometrical need for amide deprotonation to achieve N(ox)N(ad) chelation.

In summary, the following attributes can be assigned to the HIAA chelating unit. It is ambidentate and can bind through N(ox) and O(ad) in regions of low  $pH$ , where both the oxime and amide groups are still protonated (note that amide proton blocks the N(ox)N(ad) metal chelation). At higher  $pH$  deprotonation of the oxime group occurs, enabling the coordination through O(ox). In the presence of a suitable metal in this  $pH$  region the amide proton can also be ionised, leading to the N(ox)N(ad) chelation. In addition, coordination through oxime oxygen allows the bridging of two metal centres, as shown in Figure 14, right-hand side structure.

#### 2.1.4 Coordination Chemistry of the HIAA *bis*-Chelates

Naturally, with the knowledge of HIAA moiety being favourable binding site for the transition metal coordination, further work led to the preparation of *bis*-chelate ligands of this nature.

The first ligand of this kind, *N,N'*-bis(2-hydroxyiminopropionyl)ethylenediamine, was synthesised in 1978 by Lau and Gutsche.<sup>[5]</sup> In 1997 Duda *et al*.<sup>[1]</sup> reported the preparation of *N,N'*-bis(2-hydroxyimino-propionyl)propane-1,3-diamine ligand. The interest in these types of ligands at the time was due to the fact that dioximes had been used extensively in analytical chemistry and

metallurgy as very efficient complexing agents. It was thought that ligands including HIAA functionality would also prove to be effective chelates. Duda *et al.*<sup>[1]</sup> performed potentiometric and spectroscopic investigation of the new ligand, *N,N'*-bis(2-hydroxyiminopropionyl)propane-1,3-diamine, Figure 15, as well as its Ni(II) and Cu(II) complexes.

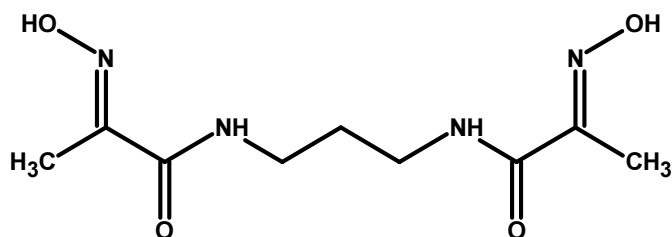


**Fig. 15.** *N,N'*-Bis(2-hydroxyiminopropionyl)propane-1,3-diamine.

Their study indicated tetradentate 2N(ox)N(ad) coordination in square-planar pseudo-macrocyclic structure for both Ni(II)- and Cu(II)-complexes,<sup>[1]</sup> Figure 16, assisted by the deprotonation of oxime and amide groups.

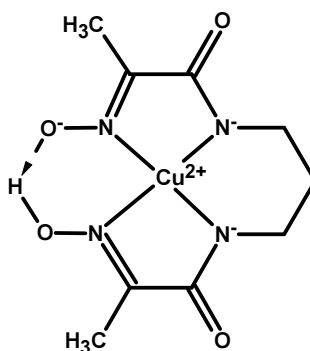


**Fig. 16.** The structure of Cu(II)-*N,N'*-propane-1,3-diylbis[2-(hydroxyimino)propanamide] (*mhiaa*<sub>2p</sub>) complex (MLH<sub>3</sub> type).

N(ox)O(ad) chelation mode was reported a year later<sup>[8]</sup> for Cu(II)-*N,N'*-bis(2-hydroxyiminopropionyl)butane-1,4-diamine complex, which was isolated in the solid state. XRD structure of this complex was entirely different, representing di-copper di-ligand arrangement.<sup>[8]</sup> In this new complex two Cu(II)-ions are sandwiched between two relatively linear ligands, forming a stepwise structure. Each copper ion is chelated by two N(ox)O(ad) moieties that belong to two different ligands. Such coordination arrangement highlighted the importance of dimers in these types of systems.<sup>[8,20]</sup>

To reiterate, the solid state studies of the Ni(II)- and Cu(II)-complexes with *N,N'*-bis(2-hydroxyiminopropionyl)propane-1,3-diamine revealed square-planar coordination; the ligand being triply deprotonated with the remaining oxime proton stabilising the pseudo-macrocyclic structure by hydrogen-bonding to the deprotonated oxime terminal. Conformation of the propane bridge in the complex was “flap of the envelope” type, with the middle methylene group significantly out of plane

of the complex.<sup>[1]</sup> *N,N'*-Bis[(3*E*)-3-(hydroxyimino)-2-methylbutan-2-yl]propane-1,3-diamine and two analogues with variable length of the methylene bridge were also synthesised.<sup>[19]</sup> Thermodynamic stability of their Cu(II)-complexes was studied by potentiometry, and the results confirmed the peak of stability for the ligand with the propane bridge.<sup>[19]</sup> The reason for this is the relief of the steric strain on the bridge and the optimum bite angle for the metal centre.



## 2.2 Metal Complexes in Oxidation Catalysis

The concept of catalysis was first introduced by Jons Jacob Berzelius in 1835. He rationalised a number of isolated scientific observations made by members of the scientific community and postulated the existence of substances that “awaken affinities, which are asleep at particular temperatures by their mere presence and not by their own affinity”. He called this phenomenon “catalytic power”. The concept of catalysts and their behaviour was debated for almost a century without much of clear understanding.<sup>[21-22]</sup> Modern interpretation of the catalytic action is, probably, traceable to the close inspection of the Deacon “Chlorine process” by Falkenstine, who in 1906 outlined the following features of catalytic behaviour: “... the catalysis was perceived as operation to produce equilibrium in a system more rapidly than could be achieved in the absence of a catalyst. However, the catalyst could not shift the equilibrium position; it was independent of the catalyst’s nature”.<sup>[21]</sup>

The concept that metal complexes may act as catalytic centres in, say, oxidation reactions (which is essentially behind this chapter of the thesis), stems from the study of electrochemical and structural behaviour of Ni(II) macrocyclic dioxopentamines.<sup>[2]</sup> It was determined that in the Ni(II) macrocyclic pentamine complex, Figure 17, Ni(II) is high spin with the square-pyramidal coordination geometry around it, and the complex has half-wave redox potential for the Ni (III)/Ni (II) couple,  $E_{1/2}^{\ominus}$ , of 0.66 V. In comparison, in the Ni(II) cyclo dioxotertamine complex, Figure 18, Ni(II) is low spin, coordination geometry is square-planar, and  $E_{1/2}^{\ominus}$  value is 0.81 V.

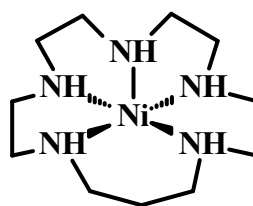


Fig. 17. Ni(II) macrocyclic pentamine complex.

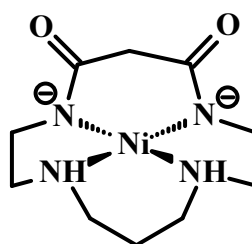
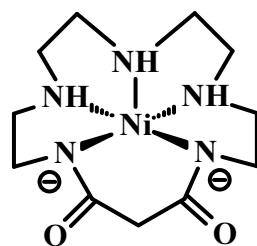


Fig. 18. Ni(II) cyclo dioxotertamine complex.

In light of these redox potential values, a complex was synthesised in the Kimura group where the ligand combined structural features of the above two ligands, Figure 19.



**Fig. 19.** Ni(II) macrocyclic dioxopentaamine complex.

Ni(II)-complex of this new ligand displayed Ni(III)/Ni(II) redox half-wave potential of only 0.24 V under the same conditions. This was one of the lowest  $E_{1/2}^{\ominus}$  values ever reported for the Ni(III)/Ni(II) redox couple in the macrocyclic polyamine coordination environment in aqueous medium. Such low potential represents an easy oxidation of Ni(II) to Ni(III). Solid state XRD studies of both Ni(II)- and Ni(III)-complexes were obtained,<sup>[2]</sup> Figures 20-21, and the following observations made.

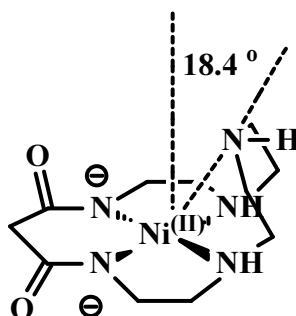


**Fig. 20.** Ni (II) macrocyclic dioxopentaamine complex viewed from the side.

In the square-pyramidal Ni(II) macrocyclic dioxopentaamine complex the steric strain is evident, with axial N-donor being at an angle of  $18.4^{\circ}$  to the optimal axial direction. Oxidation of the metal centre in this complex leads to reduction of the metal ion size, better fit into the ligand binding site, and significant relief of the steric strain. The solid state structure of Ni(III) macrocyclic dioxopentaamine complex, Figure 21, shows this relief as the axial N-donor now deviates only by  $7.7^{\circ}$  from the axis perpendicular to the complex plane.<sup>[2]</sup> Consequently, the lower oxidation state of the metal centre, in this case, Ni(II), is destabilised by the steric strain, while the higher, Ni(III), oxidation state is stabilised by its relief in the complex. Both phenomena contribute to the extremely low value of the redox potential.

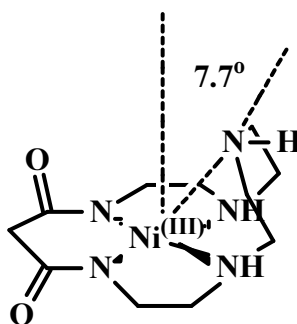


**Fig. 21.** Ni (III) macrocyclic dioxopentaamine complex viewed from the side.

Interestingly, the above Ni (II) complex is able to bind dioxygen,  $O_2$  (g), and to catalyse oxidation of toluene to phenol at room temperature and atmospheric pressure,<sup>[2]</sup> very mild reaction conditions in comparison to the ones employed at present in the industrial manufacture of phenol.<sup>[23]</sup>

The concept of imposing steric strain on a transition metal centre in a complex with square-pyramidal environment seems enhanced and even more attractive with the ligands of interest to our research group, Figure 22, for the following reasons:

1. *Bis*-chelate HIAA ligands easily form complexes of square-planar geometry of variable thermodynamic stability with a range of different transition metals. 4N equatorial coordination environment anchors the metal centre, while its planarity is conducive to the approach from both axial directions; that is by the fifth nucleophilic group and catalysed reaction substrate.
2. The length and conformation of the spacer that separates two chelating units determines the size of the metal receptor site, resulting in the thermodynamic stability based selectively; metal ions of the matching size, will bind the strongest.
3. Formation of the strong and short hydrogen bond between a deprotonated and a protonated oxime terminal adds to the complex stability through the pseudo-macrocyclic effect.
4. The complex stability is strongly pH dependent:
  - a) the very nature of the 2N(ox),2N(ad) coordination requires deprotonation of the amide nitrogens; the pH at which this happens is strongly metal dependent
  - b) for the effect 3 above, partial deprotonation of the oxime terminals is also required.
5. The fifth donor centre and its scorpionic action account for the stabilisation of a higher oxidation state and the destabilisation of a lower oxidation state of the metal in the complex as discussed above. This enhances catalytic activity of the complex in oxidation reactions.

6. As already mentioned, an unrestricted access by substrate to the catalytic centre from the “South Pole” axial direction is essential feature of a functioning catalytic system.

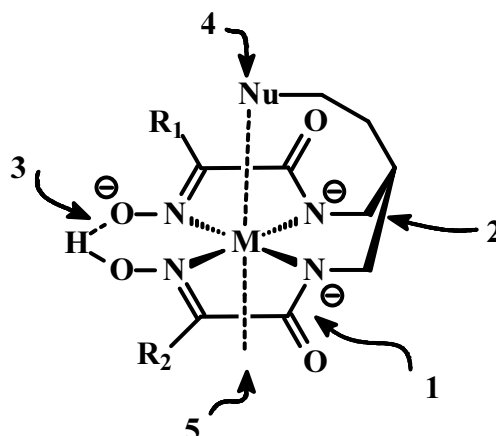


**Fig. 22.** Generic view of the metal complex of hydroxyiminoacetamide (HIAA) *bis*-chelate ligand with a propane bridge, functionalised with a scorpionic arm terminated in a nucleophile. The key to the numbers on the figure is as follows:

1. Oxime-and-amide moieties are planar due to the double-bond conjugation.
2. The length and conformation of the bridge between two chelate moieties determines the metal receptor size.
3. Intramolecular H-bond between two oxime groups completes pseudo-macrocyclic structure and adds to the complex stability.
4. Pendant arm with a terminal Nu-group, grafted on the spacer like a scorpion's tail, is essential for the steric stress on metal a centre in the complex.
5. The “South Pole” axial direction is free for the access of reaction substrate and the removal of reaction intermediate or product.<sup>†</sup>

With the above in mind, we set out to synthesise new ligands with an expectation that their metal complexes might exhibit catalytic activity.

We shall conclude this brief literature survey by mentioning that in recent years work has started on a class of tetrapodial pentadentate, MAE<sub>4</sub>, (M = Metal, A = Axial nucleophile, E = Equatorial nucleophile), complexes. The authors' interest in ligands of this nature is linked to mimicking biological systems, such as hemes, in the oxidation of alkanes.<sup>[24]</sup> In addition, Wiedemann *et al*<sup>[25]</sup> have recently published a paper, where they are applying the above principles to the preparation of photo-electrochemical sensors.

<sup>†</sup> Although only substrate access has been discussed here, this site also lends itself to entry and exit of the catalyst reactivation agent.

## 3. Towards the Synthesis of Functionalised Propane-1,3-diamines

### 3.0 Propane-1,3-diamine as a Key Intermediate

As discussed previously, recent interest of our research group is focused on the synthesis, characterisation, and both solid state and solution studies of the *mono*- and *bis*-chelate ligands with the (HIAA) moiety; the methyl derivative being of interest to this project.

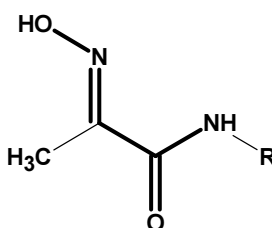


**Fig. 23.** A ligand with 2-methyl hydroxyiminoacetamide (HIAA) chelating moiety (highlighted).

The synthesis of *bis*-chelate ligands involves condensation of two equivalents of ethyl-2-(hydroxyimino)propanoate (HIPA) with a suitable primary diamine, Figure 24.

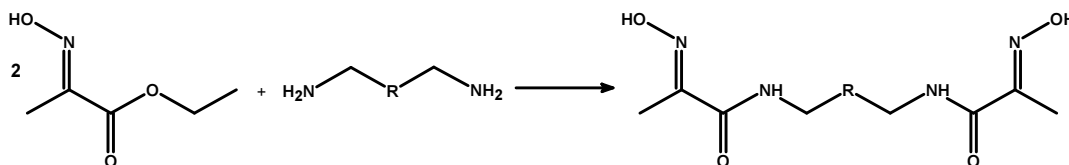


**Fig. 24.** Generic scheme of the condensation of ethyl-2-(hydroxyimino)propanoate with a suitable primary diamine.<sup>[1,15]</sup>

Variation of the length of the bridge between the two chelating moieties allows fine-tuning of the ligand binding cavity size to a specific metal ion. Potentiometric studies by Jackson *et al*<sup>[19]</sup> on *N,N'*-bis[(3)-3-(hydroxyimino)-2-methylbutan-2-yl]propane-1,3-diamine and its two analogues with variable length of the polymethylene linker indicated the propane bridge affording the most stable Cu(II)-complex.

Taking into account that in this project we are interested in the stable Ni(II)- or Cu(II)-complexes of a modified ligand, the propane bridge between the two chelating units is a necessary choice. It will give the ligand optimum size of the binding site for these metal ions. Consequently, the synthesis of derivatised propane-1,3-diamines with a flexible alkyl chain grafted onto the C2 carbon of the propane

backbone and terminated with a suitable nucleophile, Figure 25, becomes strategically essential synthetic step.

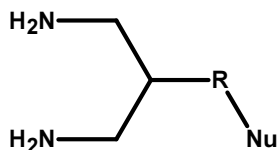


**Fig. 25.** Generic structure of propane-1,3-diamine with a flexible alkyl chain grafted onto the C2-carbon of the propane backbone and terminated with a suitable nucleophile.

As will become clear in the following section, once the preparation of derivatised propane-1,3-diamines is accomplished, the path to the desired ligands is cleared as the rest of the synthetic steps is being well practiced by us. However, preparation of the compounds shown in Figure 25 is far from trivial.

### 3.1 Synthetic Strategies Considered

In principle, a number of synthetic strategies can be employed to prepare *bis*-chelate ligands of interest with HIAA-units. Before we outline these strategies, it would be useful to mention a few points of general nature that merit consideration:

- a) one has to form the HIAA chelating moiety
- b) then, one has to assemble two of such moieties into a *bis*-chelate ligand
- c) as has been discussed in 3.0, derivatised propane-1,3-diamine is the key intermediate for point b) above.

From practical perspective,

- d) one has to review available starting materials and
- e) consider the need and sequence of protection/deprotection of the sensitive functional groups.

Six synthetic routes, potentially leading to the desired ligands, have been considered in this project. They are classified on the basis of two factors:

1. The starting material at the route inception.
2. The nature of compound to be grafted as a pendant arm on the ligand in a condensation step.

To simplify the presentation of the proposed synthetic routes, only derivatives with two methylene carbons in the pendant arm will be shown. Longer polymethylene chains are also of interest in this work and are likely to be synthesised through the same steps, unless stated otherwise.

Each compound in the following reaction schemes is assigned unique number under which it will be referred to everywhere in this thesis. Homologue compounds of similar nature are labelled in alpha-numerical manner as shown below for aliphatic diols, Figure 26.

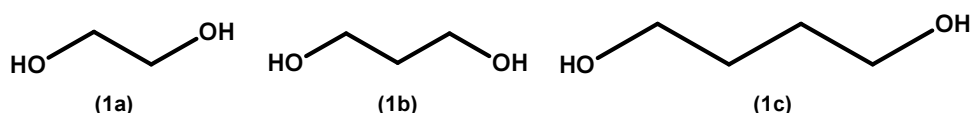
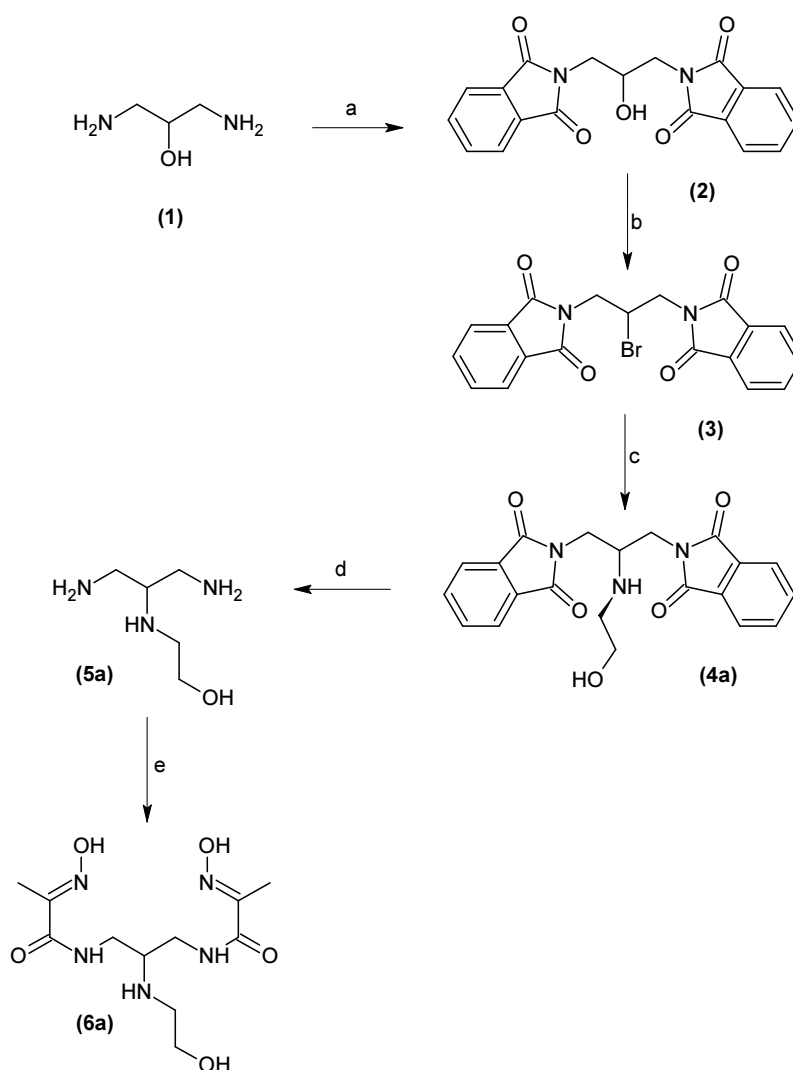


**Fig. 26.** Illustration of the labelling principle for homologue compounds adopted in this thesis. This example is for the aliphatic diols.

### 3.1.1 1,3-Diaminopropane-2-ol & 2-Aminoethanol Route

The only commercially available propane-1,3-diamine derivatised at C2-carbon is 1,3-diaminopropane-2-ol (DAPOL). In the reaction scheme presented below, Scheme 1, two terminal amino groups of the starting compound are first protected with phthalimide, step a; the product is then converted into a bromide derivative, step b; then, the desired pendant arm is grafted in a condensation reaction, step c; followed by the deprotection, step d; and finally, attachment of two HIAA moieties in yet another condensation step, step e.

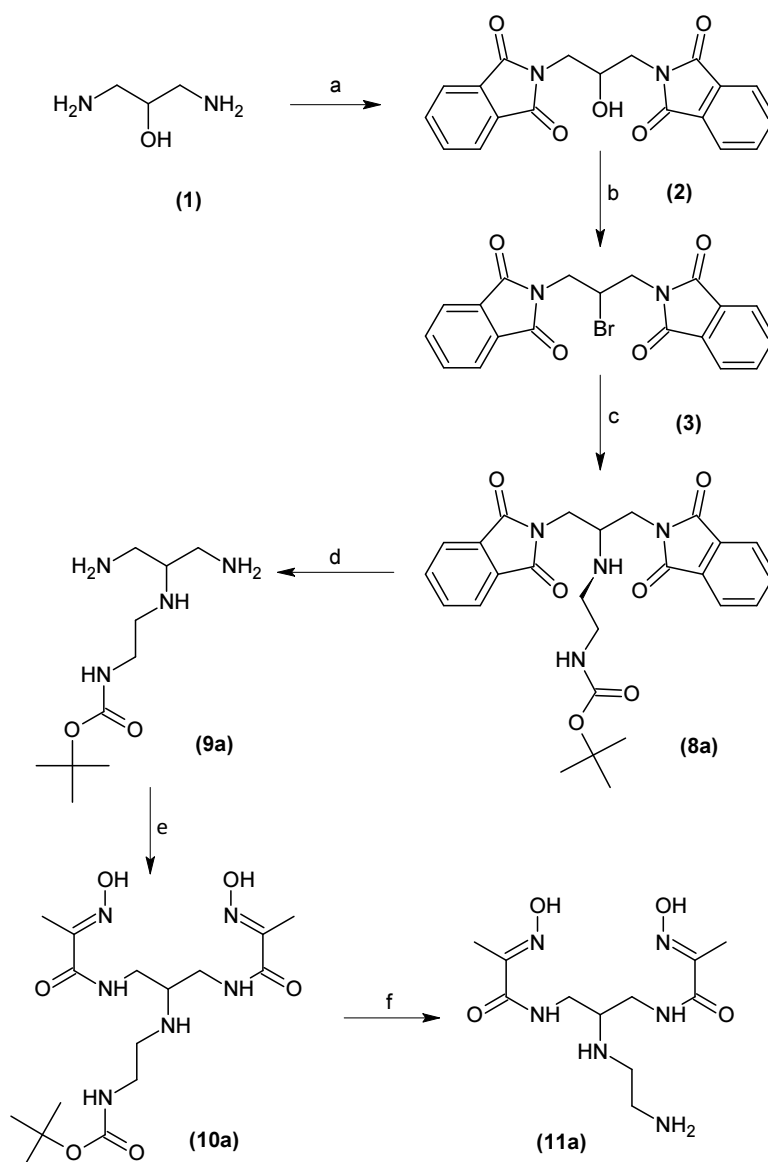


**Scheme 1.** Sequence of the reaction steps for the 1,3-diaminopropane-2-ol and 2-aminoethanol route. Reagents required at different stages as well as essential external conditions are as follows: a) Phthalic anhydride, b) HBr/CBr<sub>4</sub>PPh<sub>3</sub>, c) HOCH<sub>2</sub>CH<sub>2</sub>NH<sub>2</sub>, d) pH 12, RT, e) CH<sub>3</sub>C(=NOH)COOC<sub>2</sub>H<sub>5</sub>.



### 3.1.2 1,3-Diaminopropane-2-ol & *t*-Butyl(2-aminoethyl)carbamate Route

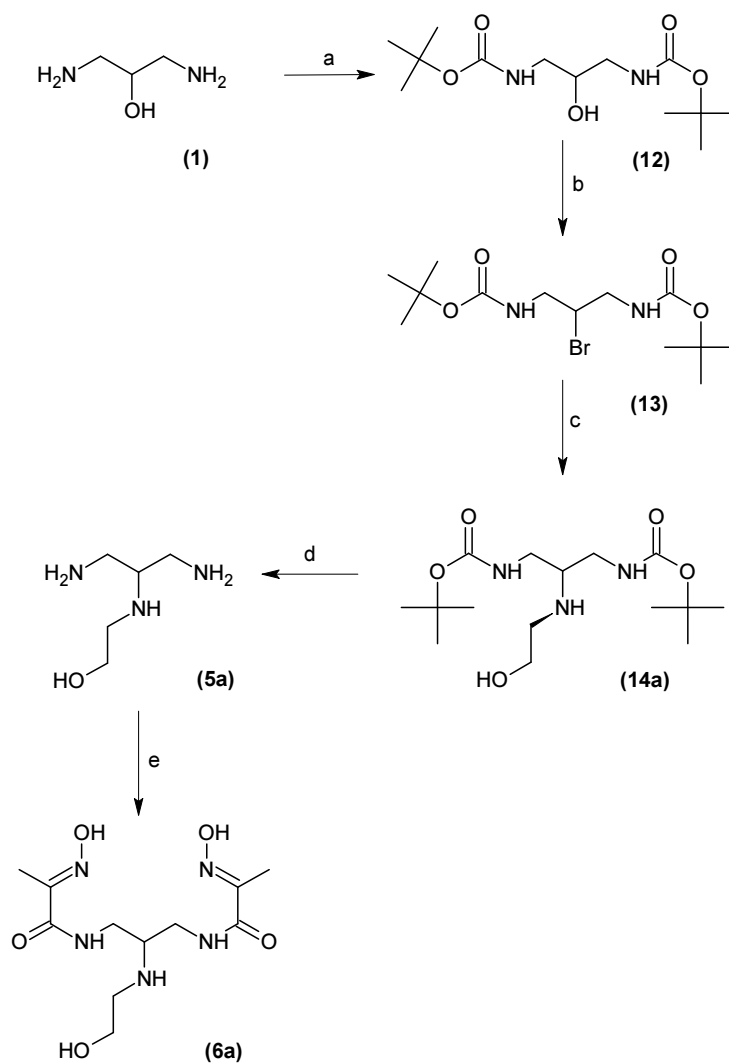
This route is similar to the previous one but for the diamine to be grafted as a pendant arm instead of aminoalcohol, Scheme 2. The major difference is that the terminal amino-group of the pendant arm has to be protected to prevent formation of the undesirable side-products in steps c and d; final step f represents removal of the Boc-protection.



**Scheme 2.** Sequence of the reaction steps for the 1,3-diaminopropan-2-ol & *t*-butyl(2-aminoethyl) carbamate route. Reagents required at different stages as well as essential external conditions are as follows: a) Phthalic anhydride, b) HBr/CBr<sub>4</sub> PPh<sub>3</sub>, c) HN<sub>2</sub>CH<sub>2</sub>CH<sub>2</sub>NH-Boc, d) LiAlH<sub>4</sub>, e) CH<sub>3</sub>C(=NOH)COOC<sub>2</sub>H<sub>5</sub>, f) HCl.

### 3.1.3 1,3-Diaminopropane-2-ol & 2-Aminoethanol Route

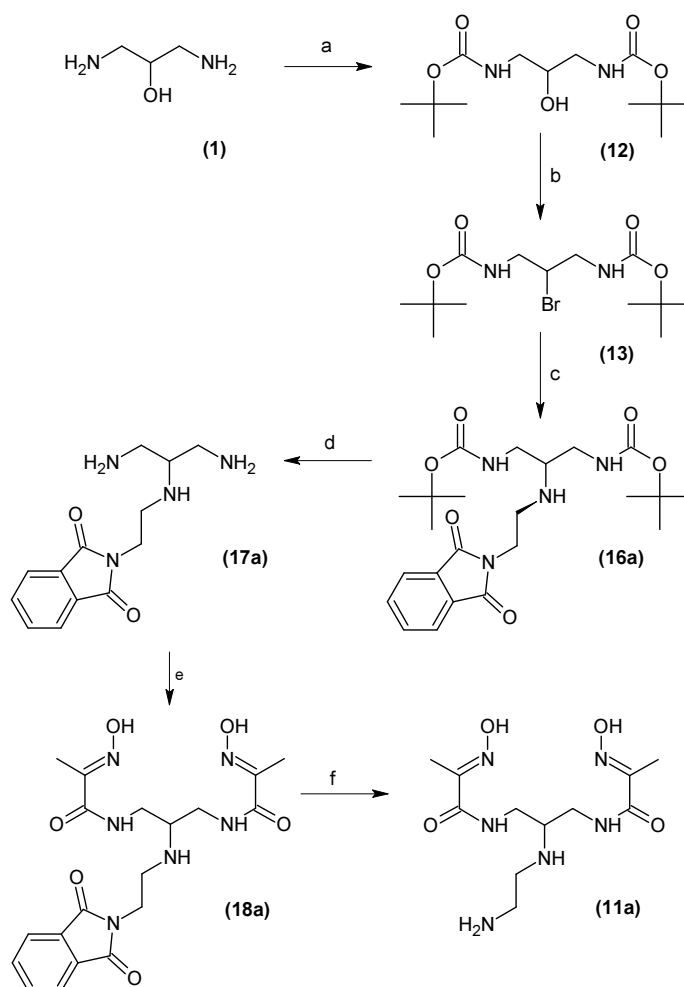
This route is nearly identical to route one but for the Boc-protection of the starting diamine instead of the phthalamide protection, Scheme 3. It has its potential advantages, in particular, in steps b and c, which will be discussed later.



**Scheme 3.** Sequence of the reaction steps for the 1,3-diaminopropane-2-ol & 2-aminoethanol route. Reagents required at different stages as well as essential external conditions are as follows: a) Boc, b)  $\text{CBr}_4/\text{PPh}_3$ , c)  $\text{HN}_2\text{CH}_2\text{CH}_2\text{OH}$ , d)  $\text{LiAlH}_4$ , e)  $\text{CH}_3\text{C}(=\text{NOH})\text{COOC}_2\text{H}_5$ .

### 3.1.4 1,3-Diaminopropane-2-ol & 2-(2-Aminoethyl)-1*H*-isoindole-1,3(2*H*)-dione Route

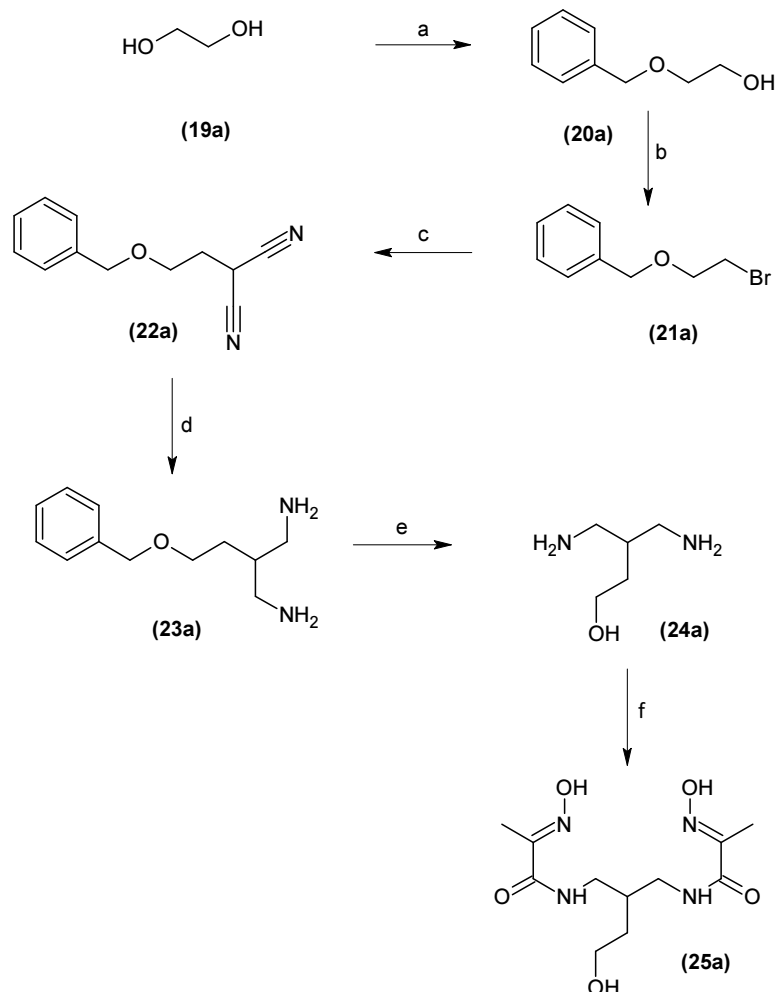
This route is similar to route three but for the diamine to be grafted as a pendant arm instead of aminoalcohol, Scheme 4. It was also considered an advantage to protect the terminal amino-group of the pendant arm with phthalamide, as it will remain in place in step d; that should reduce the formation of undesirable side-products in step e. Final step f represents removal of the phthalamide protection.



**Scheme 4.** Sequence of the reaction steps for the 1,3-diaminopropan-2-ol & 2-(2-aminoethyl)-1*H*-isoindole-1,3(2*H*)-dione route. Reagents required at different stages as well as essential external conditions are as follows: a) Boc, b) CBr<sub>4</sub>/PPh<sub>3</sub>, c) HN<sub>2</sub>CH<sub>2</sub>CH<sub>2</sub>OH d) pH 1, RT, e) CH<sub>3</sub>C(=NOH)COOC<sub>2</sub>H<sub>5</sub>, f) pH 1, 100 °C.

### 3.1.5 Malononitrile & Ethane-1,2-diol Route

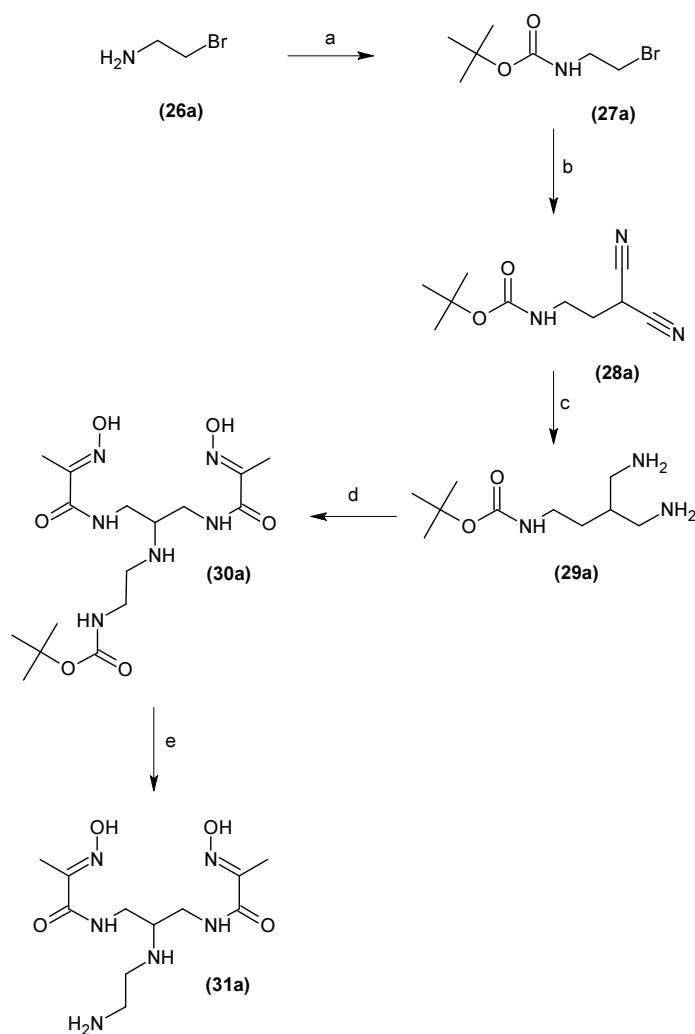
This route entails the use of malononitrile as the starting compound, Scheme 5. In the first step a diol is mono-protected with benzyl bromide; the product is then converted to a bromide derivative, step b; followed by the condensation with malononitrile, step c. Then, the product is reduced to a derivatised 1,3-propanediamine; followed by the deprotection of alcohol group, step e; and finally, two HIAA moieties are attached in yet another condensation step, step f.



**Scheme 5.** Sequence of the reaction steps for the malononitrile & ethane-1,2-diol route. Reagents required at different stages as well as essential external conditions are as follows: a) benzyl bromide, b) HBr/CBr<sub>4</sub> PPh<sub>3</sub>, c) NCCH<sub>2</sub>CN *t*-BuOK, d) LiAlH<sub>4</sub>, e) Pd/C H<sub>2</sub>, f) CH<sub>3</sub>C(=NOH)COOC<sub>2</sub>H<sub>5</sub>.

### 3.1.6 Malononitrile & 2-Bromoethanamine Route

This route is similar to that of Scheme 5 but for a bromoamine being used in place of the diol, Scheme 6. In the first step amino-group is protected with Boc, step a; followed by the condensation with malononitrile, step b. Then, the product is reduced to a derivatised 1,3-propanediamine; followed by the attachment of two HIAA moieties in yet another condensation step, step d; and finally, the removal of Boc protection, step e.



**Scheme 6.** Sequence of the reaction steps for the malononitrile & ethane-1,2-diol route. Reagents required at different stages as well as essential external conditions are as follows: a) Boc protection, b)  $\text{CNCH}_2\text{CN}$  *t*-BuOK, c)  $\text{NaBH}_4$ , d)  $\text{CH}_3\text{C}(=\text{NOH})\text{COOC}_2\text{H}_5$ , e) HCl.

## 3.2 Literature Review of the Chemistry of Synthetic Steps

### 3.2.1 Protection of Functional Groups

In the process of a multistep organic synthesis steps are often undertaken to derivatise certain functional groups in a molecule sequentially, one at a time, for which suitable reagents are chosen. It is not uncommon, upon completion of a particular step and analysis of results, to discover that in addition to the desired change other functionalities in the molecule have been modified. The solution to this problem is the protection of sensitive functional groups by suitable agents (during those steps when they may be altered) and removal of such modifications at the end of the multistep synthesis (deprotection). The choice of a suitable protection group is not a trivial one; it has to be inert or relatively inert towards all reagents and products in the reaction scheme between the stages of protection and deprotection. Additional problem arises when a molecule has two identical or similar functional groups but only one is to be modified in a particular reaction step. By a choice of suitable conditions the protection of a single group may be achieved, though one has to make sure the right group is protected. Alternatively, the protection of both groups can be done using two different reagents for certain functionalities, and only one of them removed at a later stage. In any case, both protecting groups have to remain in place for the steps between protection and deprotection. The conditions of deprotection of one group need to be sufficiently different from the ones for another to enable only *mono*-deprotection of the same functional group within the molecule to occur and to make the route viable.

For the purposes of this project we will look at the protection and deprotection of alcohols and amines. With the above in mind, one has to look at the proposed synthetic path and make one's choice of protecting group(s) based on chemical compatibility with further steps. Other factors that also have to be considered are the ease of deprotection and the ability of modified molecules to survive the deprotection intact. The addition of a protection group normally adds up to the mass of a molecule. Consequently, the removal of such a group will have an effect of decreasing the mass of the molecule. At every step in a synthesis it is desirable to isolate the product; the reason for this being less interfering species at later stages. A general trend in chemistry is the heavier a molecule gets, the more likely it is to be a solid at room temperature.<sup>[26]</sup> Separation of solid products from a reaction mixture is generally easier than the separation of oils. Hence, employment of heavier protection groups might be beneficial to the separation in later steps.

With all this in mind, it would be logical to review protecting groups, first, by their chemical inertness, and second, by the ease of protection and deprotection.

### 3.2.1.1 Protection of the Alcohol Group

The synthetic path shown in Scheme 5 required *mono*-protection of linear diols. To the best of our knowledge, three major classes of protection groups employed for this purpose are listed below:

1. Ethers.
2. Esters.
3. Silyls.

The target molecules contain large number of polar functional groups, and steps in aqueous medium (during the separation or purification) are likely to be needed. We have left silyl-type protection out of consideration, as these groups cleave under aqueous conditions.<sup>[27]</sup> Another factor against using silyl-type protection is that it is not very amenable to chromatographic separation.<sup>[27]</sup>

#### 3.2.1.1.1 Ether-Type Protection

##### Methoxymethyl ethers (MOM)

Generic structure of a MOM ether is shown below.

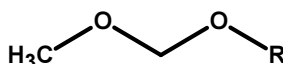


**Fig. 27.** Generic structure of a MOM ether.

Conditions of stability and conditions under which such protection group can be removed are summarised in Table 1.

**Table 1.** Conditions of stability and removal for the MOM ethers.<sup>[28-29]</sup>

Labile	pH ≤ 1 Reduction: Zn/HCl Oxidation: Br <sub>2</sub> and Cl <sub>2</sub>
Moderately stable	pH ≥ 12 Oxidation: Acetic acid

##### Tetrahydropyranyl ethers (THP)

Generic structure of a THP ether is shown below.

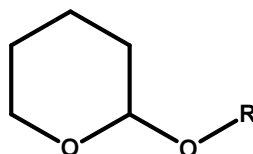


**Fig. 28.** Generic structure of a THP ether.

Conditions of stability and removal for this protection group are summarised in Table 2.

**Table 2.** Conditions of stability and removal for the THP ethers.<sup>[28-29]</sup>

Labile	pH ≤ 1 Reduction: Zn/HCl Oxidation: Br <sub>2</sub> and Cl <sub>2</sub>
Moderately stable	pH ≤ 4 Oxidation: Acetic acid

### ***t*-Butyl ethers**

Generic structure of a THP ether is shown below.

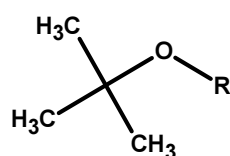


**Fig. 29.** Generic structure of a *t*-butyl ether.

Conditions of stability and removal for this protection group are summarised in Table 3.

**Table 3.** Conditions of stability and removal for the *t*-butyl ethers.<sup>[28-29]</sup>

Labile	pH ≤ 1 above 100 °C
Conditions of moderate stability	None

### **Allyl ethers**

Generic structure of an allyl ether is shown below.

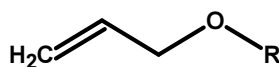


**Fig. 30.** Generic structure of an allyl ether.

Conditions of stability and removal for this protection group are summarised in Table 4.

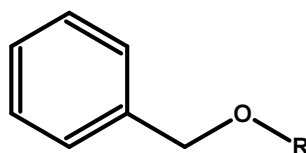


**Table 4.** Conditions of stability and removal for the allylethers.<sup>[28-29]</sup>

Labile	pH $\leq$ 1 above 100 °C, pH $\geq$ 12 above 100 °C Bases: <i>t</i> -BuOK Nucleophiles: NaOCH <sub>3</sub> Electrophiles: Bu <sub>3</sub> SnH Reduction: H <sub>2</sub> /Ni Oxidation: KMnO <sub>4</sub> , Acetic acid, Br <sub>2</sub> and Cl <sub>2</sub> .
Conditions of moderate stability	pH $\geq$ 12 Oxidation: I <sub>2</sub>

**Benzyl ethers (Bn)**

Generic structure of a Bn ether is shown below.

**Fig. 31.** Generic structure of a Bn ether.

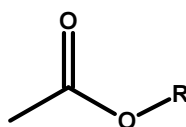
Conditions of stability and conditions under which such protection group can be removed are summarised in Table 5.

**Table 5.** Conditions of stability and removal for the Bn ethers.<sup>[28-29]</sup>

Labile	pH $\leq$ 1 above 100 °C Reduction: Ni/H <sub>2</sub> and Na/NH <sub>3</sub>
Conditions of moderate stability	Oxidation: Br <sub>2</sub> and Cl <sub>2</sub>

**3.2.1.1.2 Ester-Type Protection****Acetate ester (Ac)**

Generic structure of an Ac ester is shown below

**Fig. 32.** Generic structure of an Ac ester.

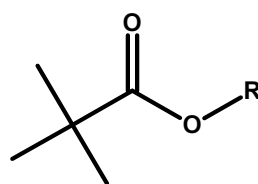
Conditions of stability and conditions under which such protection group can be removed are summarised in Table 6.

**Table 6.** Conditions of stability and removal for the Ac esters.<sup>[28-29]</sup>

Labile	pH ≤ 1 above 100 °C, pH ≥ 12 Bases: LDA and <i>t</i> -BuOK Nucleophiles: Grignard reagents Reduction: LiAlH <sub>4</sub> and Na/NH <sub>3</sub>
Conditions of moderate stability	pH ≥ 9 Nucleophiles: NH <sub>3</sub> and RNH <sub>2</sub> .

**Pivalate ester (Pv)**

Generic structure of a Pv ester is shown below.

**Fig. 33.** Generic structure of a Pv ester.

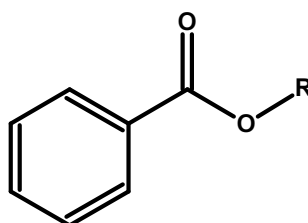
Conditions of stability and conditions under which such protection group can be removed are summarised in Table 7.

**Table 7.** Conditions of stability and removal for the Pv esters.<sup>[28-29]</sup>

Labile	pH ≤ 1 above 100 °C, pH ≥ 12 above 100 °C Bases: <i>t</i> -BuOK Nucleophiles: NH <sub>3</sub> and RNH <sub>2</sub> Reduction: Na/NH <sub>3</sub> and LiAlH <sub>4</sub>
Conditions of moderate stability	pH ≥ 12 Nucleophiles: Grignard reagents and NaOCH <sub>3</sub> Reduction: Na/NH <sub>3</sub> and LiAlH <sub>4</sub>

**Benzoate ester (Bz)**

Generic structure of a Bz ester is shown below

**Fig. 34.** Generic structure of a Bz ester.

Conditions of stability and conditions under which such protection group can be removed are summarised in Table 8.

**Table 8.** Conditions of stability and removal for the Bz ester.<sup>[28-29]</sup>

Labile	pH $\leq$ 1 above 100 °C, pH $\geq$ 12 above 100 °C Nucleophiles: Grignard reagents Reduction: Na/NH <sub>3</sub> and LiAlH <sub>4</sub>
Conditions of moderate stability	pH $\geq$ 12 Nucleophiles: NH <sub>3</sub> /RNH <sub>2</sub> and NaOCH <sub>3</sub>

### Choosing the Protection Group

Grafting a pendant arm with the terminal hydroxyl functionality onto C2-carbon of 1,3-diaminopropane, Scheme 5, requires *mono*-protection of a relevant diol. Suitable protection group must meet the following criteria:

1. Be suitable for the diol *mono*-protection.
2. Remain inert to *t*-BuOK used in the activation of malononitrile.
3. Remain relatively inert to LiAlH<sub>4</sub> used for the reduction of dinitriles.

The choice that comes to mind is benzyl bromide as it fits all the above criteria, and is of high molecular mass, which is beneficial for separation.

The applicability of a particular step is always benefited by mechanistic thinking (the consideration of the reaction mechanism, when known). The protection of alcohol functionalities by benzyl bromide is achieved in *the Williamson ether synthesis*, first accomplished in 1850.<sup>[30]</sup> The mechanistic details are as follows:

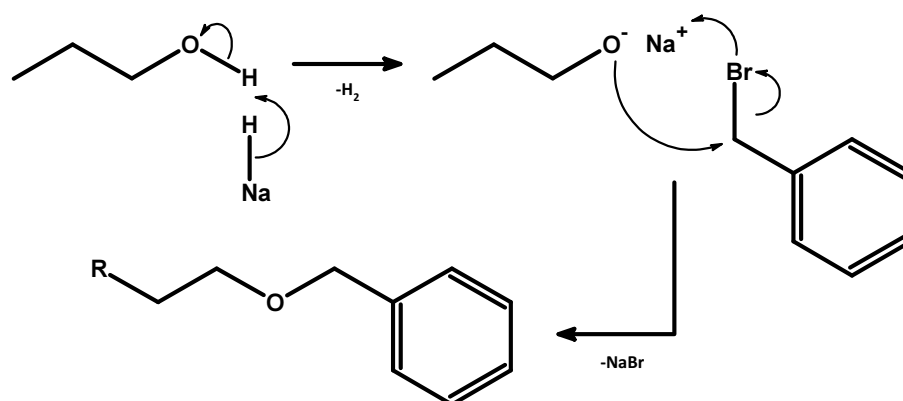


**Fig. 35.** Williamson's ether synthesis.<sup>[17]</sup>

The deprotonation can be achieved using strong base, such as NaH. However, in cases where selective substitution is needed, for example, discussed above case of *mono*-protection of diols, a weaker base, such as Ag<sub>2</sub>O, is preferred.<sup>[29]</sup>

The removal of benzyl protection can be done through Pd/C hydrogenation under mild conditions if the desired product has no unsaturated double bonds.<sup>[31]</sup>

### 3.2.1.2 Protection of the Amino Group

The synthetic paths shown in Schemes 1-4, 6 require protection of terminal amino groups. Large variety of protecting agents for primary and secondary amines are reported in literature. We will present most common of them briefly before focusing on the ones chosen in this project.

#### 9-Fluorenylmethyl carbamate (Fmoc)

Generic structure of an Fmoc product is shown below.

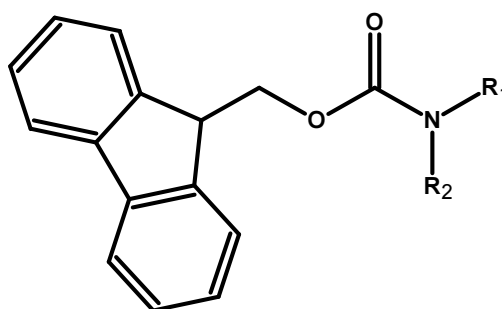


**Fig. 36.** Generic structure of an Fmoc amide.

Conditions of stability and conditions under which such protection group can be removed are summarised in Table 9.

**Table 9.** Conditions of stability and removal of Fmoc.<sup>[28, 32]</sup>

Conditions of lability	H <sub>2</sub> O: pH ≤ 1 above 100 °C, pH ≥ 12 above 100 °C Nucleophiles: Grignard reagents, NH <sub>3</sub> and RNH <sub>2</sub> Reduction: Na/ NH <sub>3</sub> Oxidation: CrO <sub>3</sub> / Py
Conditions of moderate stability	H <sub>2</sub> O: pH ≥ 12, pH ≤ 1 Bases: NEt <sub>3</sub> and Py Nucleophiles: NaOCH <sub>3</sub> Reduction: LiAlH <sub>4</sub>

**t-Butyl carbamate (Boc)**

Generic structure of a Boc product is shown below.

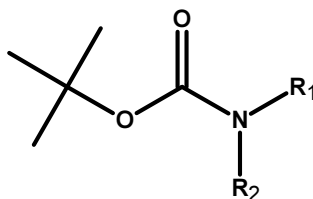


**Fig. 37.** Generic structure of a Boc amide.

Conditions of stability and conditions under which such protection group can be removed are summarised in Table 10.

**Table 10.** Conditions of stability and removal of Boc.<sup>[28, 32]</sup>

Conditions of lability	H <sub>2</sub> O: pH ≤ 1 Nucleophiles: Grignard reagents Reduction: Zn/ HCl
Conditions of moderate stability	H <sub>2</sub> O: pH ≥ 12 Reduction: LiAlH <sub>4</sub>

**Benzyl carbamate (Cbz)**

Generic structure of a Cbz product is shown below.

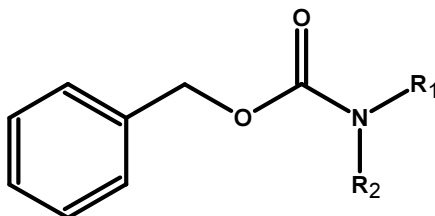


**Fig. 38.** Generic structure of a Cbz amide.

Conditions of stability and conditions under which such protection group can be removed are summarised in Table 11.

**Table 11.** Conditions of stability and removal for Cbz.<sup>[28, 32]</sup>

Conditions of lability	H <sub>2</sub> O: pH ≤ 1 above 100 °C, pH ≥ 12 above 100 °C Nucleophiles: Grignard reagents, NH <sub>3</sub> , RNH <sub>2</sub> , Reduction: H <sub>2</sub> /Ni, Na/NH <sub>3</sub> and LiAlH <sub>4</sub>
Conditions of moderate stability	H <sub>2</sub> O: pH ≤ 1 Reduction: Zn/HCl

**Acetamide (Ac)**

Generic structure of an Ac product is shown below.

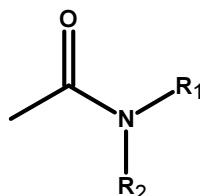


**Fig. 39.** Generic structure of an Ac amide.

Conditions of stability and conditions under which such protection group can be removed are summarised in Table 12.

**Table 12.** Conditions of stability and removal for Ac.<sup>[28, 32]</sup>

Conditions of lability	H <sub>2</sub> O: pH ≤ 1 above 100 °C, pH ≥ 12 above 100 °C Bases: LDA Nucleophiles: NH <sub>3</sub> and RNH <sub>2</sub> Reduction: Na/NH <sub>3</sub> and LiAlH <sub>4</sub>
Conditions of moderate stability	H <sub>2</sub> O: pH ≥ 12 Nucleophiles: Grignard reagents Reduction: Zn/HCl

**Trifluoroacetamide**

Generic structure of a trifluoroacetamide is shown below.

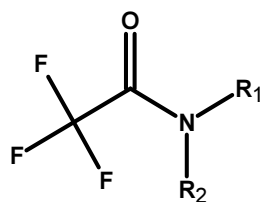


**Fig. 40.** Generic structure of a trifluoroacetamide.

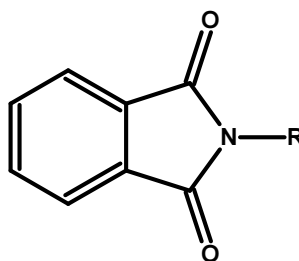
Conditions of stability and conditions under which such protection group can be removed are summarised in Table 13.

**Table 13.** Conditions of stability and removal for Trifluoroacetamides.<sup>[28, 32]</sup>

Conditions of lability	H <sub>2</sub> O: pH ≤ 1 above 100 °C, pH ≥ 12 Nucleophiles: Grignard reagents, NH <sub>3</sub> and RNH <sub>2</sub> Reduction: Na/ NH <sub>3</sub> Oxidation: CrO <sub>3</sub> /Py
Conditions of moderate stability	H <sub>2</sub> O: pH ≥ 12, pH ≤ 1 Bases: NEt <sub>3</sub> and Py Nucleophiles: NaOCH <sub>3</sub> Reduction: LiAlH <sub>4</sub>

**Phthalimide (Phth)**

Generic structure of a Phth product is shown below.

**Fig. 41.** Generic structure of a Phth.

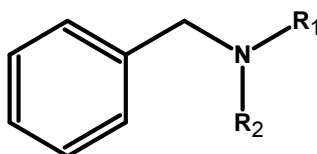
Conditions of stability and conditions under which such protection group can be removed are summarised in Table 14.

**Table 14.** Conditions of stability and removal of Phth.<sup>[28, 32]</sup>

Conditions of lability	H <sub>2</sub> O: pH ≤ 1 above 100 °C, pH ≥ 12 above 100 °C Nucleophiles: NH <sub>3</sub> and RNH <sub>2</sub> , Reduction: H <sub>2</sub> /Rh, Na/NH <sub>3</sub> and LiAlH <sub>4</sub>
Conditions of moderate stability	H <sub>2</sub> O: pH ≥ 12 Nucleophiles: Grignard reagents

**Benzylamine (Bn)**

Generic structure of a benzylamine product is shown below.

**Fig. 42.** Generic structure of a Bn.

Conditions of stability and conditions under which such protection group can be removed are summarised in Table 15.

**Table 15.** Conditions of stability and removal of Bn.<sup>[28, 32]</sup>

Conditions of lability	H <sub>2</sub> O: pH ≤ 1 above 100 °C Electrophiles: CH <sub>3</sub> I Reduction: H <sub>2</sub> /Ni, Na/NH <sub>3</sub> Oxidation: KMnO <sub>4</sub> , CrO <sub>3</sub> /Py, RCOOH, Br <sub>2</sub> and Cl <sub>2</sub>
Conditions of moderate stability	None

### Triphenylmethyamine (Tr)

Generic structure of a Tr product is shown below.

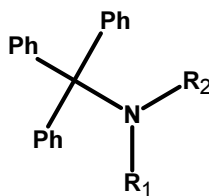


**Fig. 43.** Generic structure of a Tr.

Conditions of stability and conditions under which such protection group can be removed are summarised in Table 16.

**Table 16.** Conditions of stability and removal of Tr protection.<sup>[28, 32]</sup>

Conditions of lability	H <sub>2</sub> O: pH ≤ 1 Electrophiles: CH <sub>3</sub> I Reduction: H <sub>2</sub> /Ni, Zn/HCl and Na/NH <sub>3</sub> Oxidation: KMnO <sub>4</sub> , CrO <sub>3</sub> /Py, RCOOH, Cl <sub>2</sub> and Br <sub>2</sub>
Conditions of moderate stability	H <sub>2</sub> O: pH ≤ 4

### Benzylideneamine

Generic structure of a benzylideneamine is shown below.

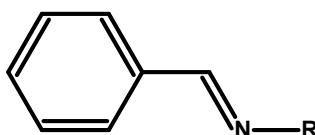


**Fig. 44.** Generic structure of a benzylideneamine.

Conditions of stability and conditions under which such protection group can be removed are summarised in Table 17.

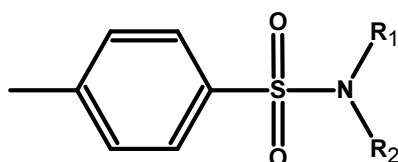


**Table 17.** Conditions of stability and removal of benzylideneamine protection.<sup>[28, 32]</sup>

Conditions of lability	H <sub>2</sub> O: pH ≤ 1, pH ≥ 12 above 100 °C Nucleophiles: Grignard reagents, NH <sub>3</sub> and RNH <sub>2</sub> Reduction: H <sub>2</sub> /Ni, Zn/HCl, Na/NH <sub>3</sub> and LiAlH <sub>4</sub> Oxidation: KMnO <sub>4</sub> , CrO <sub>3</sub> /Py, RCOOH, Cl <sub>2</sub> , I <sub>2</sub> and Br <sub>2</sub>
Conditions of moderate stability	H <sub>2</sub> O: pH ≥ 12, pH ≤ 4 Nucleophiles: RCuLi Electrophiles: CH <sub>3</sub> I Reduction: NaBH <sub>4</sub>

***p*-Toluenesulfonamide (Ts)**

Generic structure of a Ts product is shown below.

**Fig. 45.** Generic structure of a Ts protection.

Conditions of stability and conditions under which such protection group can be removed are summarised in Table 18.

**Table 18.** Conditions of stability and removal of Ts.<sup>[28, 32]</sup>

Conditions of lability	H <sub>2</sub> O: pH ≤ 1 above 100 °C Electrophiles: Grignard reagents Reduction: Zn/HCl and Na/NH <sub>3</sub>
Conditions of moderate stability	No moderately stable chemical condition

**Choosing the Protection Group**

Upon extensive consideration, we have settled on the use of *t*-butyl carbamate (Boc) and phthalimide (Phth) protection of amino groups in this project. Both offer a wide range of stability, with Boc amides being stable against NaBH<sub>4</sub> and acetic acid. The latter allows selective Phth-deprotection of amino groups, as discussed earlier.<sup>[33]</sup>

*Mono*-Boc protection of terminal diamines has been successfully achieved by Ms E. Diu, a postgraduate student in our research group, while the removal of Boc-protection in acidic conditions should not be a problem. According to observations from our potentiometric work, the ligands of this nature are fairly resilient on exposure to acidic conditions.

Phthalimide protection of 1,3-diamino-2-propanol has also been achieved previously in our research group by a postgraduate student, Mr A. Naseen. The deprotection can be enacted by a combination of  $\text{NaBH}_4$  and acetic acid.<sup>[33]</sup>

In the following sections 3.2.2-3.2.5 we will consider in some detail reaction particulars reported in literature for the protection steps **actually attempted** in this project.

### 3.2.2 *Mono-Protection of Terminal Diols*

It has been reported that the treatment of diols with hydroxyl protecting agents in a 1 : 1 molar ratio results in a mixture of *mono*- and *di*-protected species as well as unreacted diol, usually, in the ratio of 1 : 2 : 1.<sup>[34]</sup> This can be overcome by adding large excess of diol but the efficiency drops and separation becomes more difficult. To address the latter, Bouzide *et al*<sup>[34]</sup> suggested the use of  $\text{Ag}_2\text{O}$  as a co-catalyst. They observed, in the preparation of HIV-1 protease inhibitors, that protection of diols with benzyl bromide,  $\text{NaH/THF}$ ,  $\text{Na/DMF}$  (which are challenging reagents), and phase transfer catalysts gave *di*-protected products, while, the use of  $\text{Ag}_2\text{O}$  resulted in predominately *mono*-protected species (in 97 : 3 ratio). The optimum stoichiometric ratios were determined to be diol : benzyl bromide :  $\text{Ag}_2\text{O}$  = 1 : 1.2 : 1.5. We tested the applicability of such ratios in a range of solvents, and  $\text{CH}_2\text{Cl}_2$ ,  $\text{CH}_3\text{Cl}$ ,  $\text{EtOEt}$  and  $\text{EtOAc}$  proved to be suitable. Acetonitrile gave reduced yields, while THF should be avoided due to its ring opening behaviour.<sup>[34]</sup> Yields of 70 % for 2-(benzyloxy)ethanol and 87 % for 3-(benzyloxy)propan-1-ol, which are target intermediates in this project, were reported with minimal quantities of the *di*-protected species formed ( $\leq 3$  %).

$\text{Ag}_2\text{O}$ -catalysed *mono*-protection of secondary alcohols proceeds less favourably, though catalytic amounts of KI can be added to aid the reaction.<sup>[34]</sup>

To the best of our knowledge, the exact mechanism of this reaction is not yet known. It has been suggested  $\text{Ag}_2\text{O}$  coordinates to the diol oxygens in a *bi*-dentate fashion,<sup>[34]</sup> which increases the lability of a hydroxyl proton, particularly, if it is not involved in the intra-molecular hydrogen bonding. This is illustrated by the figure below.

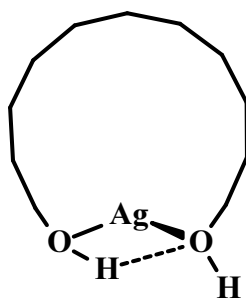


**Fig. 46.** Diagrammatic representation of a terminal diol oxygens coordinating to  $\text{Ag}_2\text{O}$  catalyst in a *bi*-dentate fashion.

### 3.2.3 Halide-de-Hydroxylation

Conversion of alcohols to alkyl halides can be done with a number of halogenating reagents. Among them are halogen acids, such as HCl, HBr and HI,<sup>[35]</sup> and inorganic halides, such as  $\text{SOCl}_2$ ,  $\text{PCl}_3$  and  $\text{POCl}_3$ .<sup>[35]</sup> The formation of iodinated substituents employing HI can be troublesome, as it is known to reduce double bonds. Chloro- and bromo-de-hydroxylation of terminal alkyl alcohols with halogen acids works well but appears a slow reaction for secondary and tertiary alcohols. The lack of reactivity can be altered by the addition of catalytic amounts of zinc chloride,<sup>[35]</sup> or by using glacial acetic acid as the solvent that aids activation.<sup>[35]</sup>

Other halogenation options also exist. Popular among them is the conversion of terminal alkyl alcohols to terminal alkyl halides by using the  $\text{CCl}_4/\text{PPh}_3$  or  $\text{CBr}_4/\text{PPh}_3$  combination. Chemical conditions in this conversion are mild and the yields are good.<sup>[36]</sup> The drawbacks to this route are: a) the formation of *tri*-phenylphosphine oxide (*t*-PPO), which has to be removed from the reaction medium, and b) the steric bulk of the three phenyl groups hindering the active site. In consequence, the reaction works well with terminal alkyl alcohols as they can readily access the active site.

The issue of separating *t*-PPO by-product have been partially solved by us by “crashing it out” of solution with hexane or cold diethyl ether; this only works when the reaction products are soluble in either of the above mentioned solvents. In industry this problem was tackled by converting *t*-PPO to something else. Natural attempts to regenerate it back to *tri*-phenylphosphine (*t*-PP) proved to be difficult in view of the stability of phosphorus-oxygen double bond.<sup>[37]</sup> The approach by Denton *et al*.<sup>[37]</sup> was to convert the *t*-PPO into a chlorophosphonium salt, which then was tested successfully on decanol as a chlorinating agent. Alternative approach to the problem is to re-think the phosphorylating agent. Work was done by Kalkeren *et al*.<sup>[38]</sup> that included regeneration of the phosphorus intermediate in the primary reaction cycle. The authors tested a number of heterocyclic type phosphorous reagents with some success.

Reaction mechanism of chloro-de-hydroxylation, proposed by Appel,<sup>[36]</sup> is shown below.

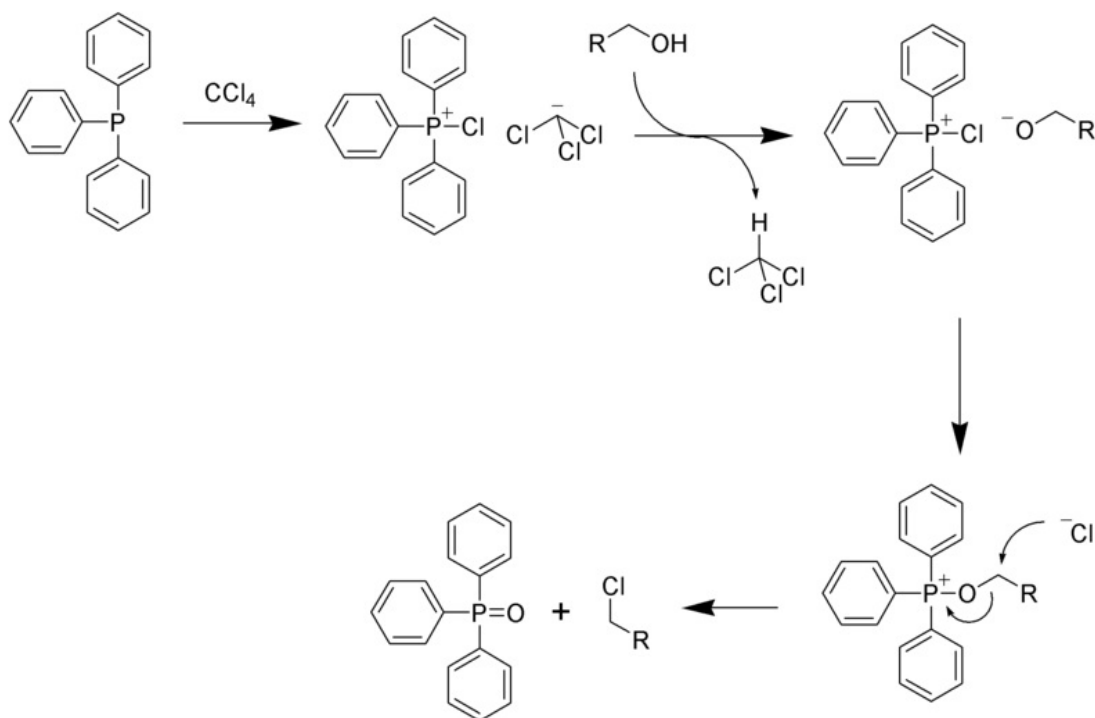


Fig. 47. Appel's chloro-de-hydroxylation mechanism.<sup>[39]</sup>

### 3.2.4 Condensation with Malononitrile

Preparation of alkylmalononitriles can be achieved by one of the two methods:

- in a direct synthesis, where malononitrile is alkylated with terminal alkyl halides, or
- in an indirect synthesis, where compounds with the alkylmalononitrile skeleton undergo certain transformation.

Numerous direct methods of preparation *di*-substituted alkylmalononitriles were reported,<sup>[40]</sup> while *mono*-substituted derivatives were synthesised by indirect methods, such as alkylidene malononitrile reduction, diamide or cyanoacetamide dehydration, to name a few. No generic method of synthesising *mono*-substituted malononitriles existed<sup>[41]</sup> until the work of Diez-Barra *et al*,<sup>[40]</sup> who discovered the phase transfer catalyst route. They observed alkylation of malononitrile with terminal alkyl halides under solvent free conditions in the presence of a base and a phase transfer catalyst. Three bases were found to be effective for the deprotonation of malononitrile (essential activation step): potassium carbonate, potassium *tert*-butoxide, and sodium hydrogen carbonate. The base is chosen on the grounds of alkyl halide reactivity towards malononitrile.<sup>[40]</sup> Thus, potassium carbonate is used with more reactive alkyl halides. With less reactive alkyl halides, potassium *t*-butoxide is a preferred choice.

In a study with *tert*-butyl ammonium bromide, phase transfer catalyst at 4 mol percent of alkyl halide was employed.<sup>[40]</sup> With malononitrile being highly reactive, questions arose what molar ratios would be appropriate for *mono*-alkylation? With more reactive alkyl halides the following two ratios were found to work well (malononitrile : alkyl halide : base = 2 : 1 : 1 and 2 : 1 : 2) with the first set of ratios delivering higher yields. The less reactive alkyl halides were found to give the highest yields when the ratio was 2 : 1 : 1.5.<sup>[40]</sup> Optimum temperature and reaction time<sup>[40]</sup> were found to be specific to the alkyl halide used.

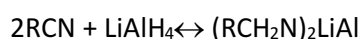
Closer to our work, malononitrile *mono*-alkylation with 1-bromobutane and 1-bromooctane was reported,<sup>[40]</sup> which gave a set of starting conditions to work out in our malononitrile *mono*-substitution step.

### 3.2.5 Hydrogenation of Substituted Malononitriles

Nitrile groups can be hydrogenated with a multitude of reagents. Among them are: LiAlH<sub>4</sub>,<sup>[42]</sup> Pd/C, BF<sub>3</sub>/Ether, BH<sub>3</sub>·S(CH<sub>3</sub>)<sub>2</sub>, NaBH<sub>4</sub>/BF·Ether, BF<sub>3</sub>·THF,<sup>[43]</sup> and PtO<sub>2</sub>/H<sub>2</sub>.<sup>[44]</sup>

#### Lithium aluminium hydride

Historically the first reagent tried was LiAlH<sub>4</sub>, which was extensively studied by Amundsen and co-workers in 1951.<sup>[42]</sup> At that time, LiAlH<sub>4</sub> had been shown to be a useful reagent for the reduction of nitriles to amines. The aim of their work was to develop a procedure that worked across a wide range of nitriles, and to resolve remaining ambiguity about optimal molar ratio.<sup>[42]</sup> Earlier work suggested that half a mole of LiAlH<sub>4</sub> was needed per mole on nitrile as the reaction was perceived as follows:



Results of Amundsen and Nelson<sup>[42]</sup> suggested otherwise. A set of studies on octanenitrile was performed with the aim to optimise reaction conditions, in particular, the molar loading, amount of solvent, and temperature. These studies yielded the following results: a) molar ratios of LiAlH<sub>4</sub> to RCN = 0.63 : 1, 1:1 and large excess : 1 were tried, with the equimolar and excess ratios giving the highest yields. Difference in yield between the equimolar and LiAlH<sub>4</sub> excess ratios was insignificant.<sup>[42]</sup> Reduction of octanenitrile was carried out at three different temperatures: 0, 25 and 35 °C, with the yield varying about 3 % across the temperature range. The effect of solvent volume on the reaction outcome was also studied but revealed no appreciable change in yield. The hydrolysis of LiAlH<sub>4</sub> was carried out with aqueous sodium hydroxide solution.<sup>[42]</sup>

## Boranes

Another option for the reduction of *di*-nitriles is the use of borane reagents.

In the synthesis, one of the two forms of borane is used: either a solution of  $\text{BH}_3$ , normally stabilised by coordination to a solvent, e.g.,  $\text{BH}_3 \cdot \text{S}(\text{CH}_3)_2$  or  $\text{BH}_3 \cdot \text{THF}$ , or a borane generated *in situ* in the reaction vessel.

Due to the issue with stability, commercially available sources of boranes are 1.0 M  $(\text{BH}_3 \cdot \text{THF})^{[45]}$  or 2.0 M  $(\text{BH}_3 \cdot \text{S}(\text{CH}_3)_2)^{[46]}$  solutions in THF. One disadvantage of these solutions is that an appreciable quantity is needed to make up molar equivalents in the reaction mixture. What is more, they age rather quickly after opening, even if refrigerated. The *in situ* generation of  $\text{BH}_3$  can be achieved in the reaction between  $\text{NaBH}_4$  and  $\text{BF}_3 \cdot \text{Ether}$ . However, complications arise from the fact that the  $\text{BF}_3 \cdot \text{Ether}$  complex is unstable at atmospheric conditions. To avoid  $\text{BF}_3 \cdot \text{Ether}$  inactivity, it is distilled daily before use under inert atmosphere, and transferred to the reaction vessel under the same anaerobic conditions.

The reduction of *di*-nitriles of the kind relevant to this project has been reported previously by Hutching and Maryanoff,<sup>[43]</sup> who undertook the reduction of (2,2-dimethylpropyl) propanedinitrile, Figure 48.

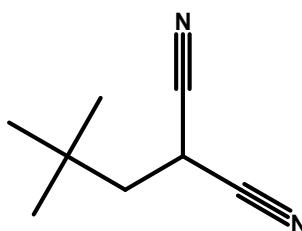


**Fig. 48.** The structure of (2,2-dimethylpropyl)propanedinitrile.

## Direct hydrogenation

Yet another option for the reduction of *di*-nitriles is the catalysed hydrogenation with dihydrogen gas.

Among the catalysts of choice, we will consider  $\text{PtO}_2$ . Reading about this catalyst revealed that, unlike the palladium immobilised on carbon system, it is capable of reducing carbonyls, indicating that it is a stronger hydrogenation catalyst. A literature search on the applicability of  $\text{PtO}_2$  to reduce 1,3-dinitriles of the *mono*-substituted malononitrile framework returned two publications.<sup>[44, 47]</sup> In both of them the hydrogenation was performed at 30 to 50 % catalyst loading by weight in the presence of aqueous hydrochloric acid to afford the formation of ammonium salt. In one case<sup>[44]</sup> dihydrogen gas at an elevated pressure of 460 kPa was used, in contrast to the hydrogenation at atmospheric pressure (of about 100 kPa), commonly used with Pd/C catalyst. Additional advantage of this procedure is that two nitrile groups can be reduced and the benzylic hydroxyl protection removed at the same time.

However, significant drawback of this route is high cost of the catalyst (in excess of R2,000 per gram) and the requirement of high catalyst loading.

Another hydrogenation catalyst, the Raney nickel,<sup>[48]</sup> also reported to reduce nitriles well but experimental conditions usually call for the hydrogen gas pressures upwards of 42 atm at temperatures above 70 °C.<sup>[49]</sup> The cost of Raney nickel is significantly lower than that of PtO<sub>2</sub>, however, it requires high-pressure hydrogenator.

## 4. Synthetic Steps Explored

In this section we will present reaction particulars, observations, and outcomes of the synthetic steps undertaken in this part of the project.

### 4.1 Synthesis of 2,2'-(2-Bromopropane-1,3-diyl)bis(1*H*-isoindole-1,3-(2*H*)-dione) (3)

As phthalimide protection of 1,3-propane-2-ol has been accomplished in our research group by my predecessor, Mr A. Naseem, I could proceed directly to the bromo-de-hydroxylation step, Figure 49.

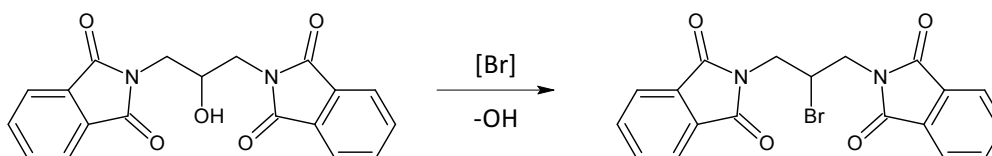


**Fig. 49.** Bromo-de-hydroxylation step of Schemes 1 and 2.

The synthesis of 2,2'-(2-bromopropane-1,3-diyl)bis(1*H*-isoindole-1,3(2*H*)-dione) (3) from 2,2'-(2-hydroxypropane-1,3-diyl)bis(1*H*-isoindole-1,3(2*H*)-dione) (2) was attempted with two sets of halogenating reagents; HBr/CH<sub>3</sub>COOH and CBr<sub>4</sub>/PPh<sub>3</sub>. In both cases molar loading and solvent volumes were kept the same, though, variations in the reaction time and temperature were explored.

The generic procedure for the CBr<sub>4</sub>/PPh<sub>3</sub> route was as follows.

Tri-phenylphosphine (0.393 g, 1.50 mmol) was weighed into a 100 mL two-neck RBF flushed with argon, followed by (2) (0.525 g, 1.5 mmol) in dry CH<sub>2</sub>Cl<sub>2</sub> (20 mL). Then a solution of carbon tetrabromide (0.497 g, 1.50 mmol) in dry CH<sub>2</sub>Cl<sub>2</sub> (10 mL) was added drop-wise to the reaction mixture.

- a) **Conditions:** The reaction mixture was stirred for 12 hours under N<sub>2</sub>(g) at room temperature. Hexane was added, precipitated solid filtered off, and the mother liquor concentrated under reduced pressure. Remaining oil was separated by column chromatography (CH<sub>2</sub>Cl<sub>2</sub> : EtOAc = 9 : 1).

**Outcome:** <sup>1</sup>H and <sup>13</sup>C NMR spectra of column fractions indicated un-reacted starting material and brominating agents.



- b) **Conditions:** The reaction mixture was stirred for 12 hours under nitrogen at 35 °C. Hexane was added, precipitated solid filtered off, and the mother liquor concentrated under reduced pressure.

**Outcome:** <sup>1</sup>H and <sup>13</sup>C NMR analysis of the concentrated mother liquor indicated presence of the starting material (**2**) and brominating reagents.

The failure of the CBr<sub>4</sub>/PPh<sub>3</sub> bromo-de-hydroxy conversion, possibly, can be attributed to a steric hindrance of the reaction site. According to the reaction mechanism,<sup>[36]</sup> an activated complex with a bond between the phosphorus atom of *tri*-phenylphosphine and the electrophilic carbon (C2-carbon) of the substrate molecule has to form, prior to the nucleophilic attack by bromine and the cleavage of hydroxyl. This might be difficult for (**2**), as it involves close interaction of five aromatic rings (two from the phthalimide reagent and three from the *tri*-phenylphosphine). Suggestions to overcoming this difficulty included using molar excess of carbon tetrabromide and *tri*-phenylphosphine.<sup>[50]</sup> We struggled to see the merit of this suggestion, as the formation of alcohol-TPP intermediate is required *prior* to the bromide attack, while carbon tetrabromide is already in excess. Excess of a brominating agent might be beneficiary from the perspective of Le Chatelier's principle, although, such reactions give excellent yields already at equimolar ratio. Mentioned above excess of brominating species arises from the carbon tetrabromide ability of exchanging all four bromine atoms in the reaction cycle sequentially.<sup>[36]</sup> Other suggestions included raising the reaction temperature and duration to aid bonds formation and cleavage.<sup>[51]</sup> Unfortunately, this proved unsuccessful in our case.

The generic procedure for the HBr/CH<sub>3</sub>COOH route was as follows.

Compound (**2**) (0.250 g, 0.71 mmol) was weighed into a 100 mL RBF, glacial acetic acid (10 mL) added, followed by HBr(48 wt. %), (75 μL, 0.66 mmol).

- a) **Conditions:** The mixture was refluxed under low light conditions, to reduce decomposition rate of HBr, for 24 hours. Once cooled to RT, the contents of the RBF were neutralised with Na<sub>2</sub>CO<sub>3</sub> (80 mL, 10 %), and the brine added (10 mL). The aqueous layer was extracted with CH<sub>2</sub>Cl<sub>2</sub> (2×100 mL), organic fractions combined and concentrated under the reduced pressure. The remaining residue was separated by column chromatography (Hexane : EtOAc = 1 : 4).

**Outcome:** <sup>1</sup>H NMR spectra showed un-reacted starting material.

- b) **Conditions:** Similar to a) but refluxed for 48 hours.

**Outcome:** <sup>1</sup>H and <sup>13</sup>C NMR analysis indicated a mixture closely resembling starting materials.

Upon later review (during the preparation of this manuscript) of the NMR and IR data for the samples from the HBr/CH<sub>3</sub>COOH attempts it was realised that the starting material (**2**) and desired product (**3**)

have very similar “fingerprints”. When multiple samples were compared side by side, it became evident two distinctly different species, the starting material and the desired product, were present. It is regrettable this oversight has occurred, and the parameters of the procedure were not finalised, as the outcome of this synthetic step at the time was considered a failure. Consequently, synthetic routes represented by Schemes 1 and 2, which depended on this intermediate, were never explored.

## 4.2 Synthesis of *mono*-Protected Terminal Diols (20a-c)

As at this point preparation of (**3**) was thought to be a failure, alternative routes were considered, and attention switched to a malononitrile one, Schemes 5-6.

As mentioned earlier, treatment of diols with the hydroxyl protecting agents in a 1 : 1 molar ratio results in a mixture of *mono*- and *di*-protected species, as well as unreacted diol (usually, in the ratio of 1 : 2 : 1). To improve on this, Bouzide and Sauvé<sup>[34]</sup> proposed the use of Ag<sub>2</sub>O as a co-catalyst, and the optimum stoichiometric ratio was determined to be (diol : benzyl bromide : Ag<sub>2</sub>O) = (1 : 1.2 : 1.5). We have performed the synthesis in CH<sub>2</sub>Cl<sub>2</sub> as it was the solvent quoted in literature to work for this type of reaction. All starting reagents but Ag<sub>2</sub>O were soluble in it and the low boiling point of CH<sub>2</sub>Cl<sub>2</sub> made the concentration of the mother liquor easier.

The authors<sup>[34]</sup> claimed yield of 70 % for 2-(benzyloxy)ethanol and 87 % for 3-(benzyloxy)propan-1-ol, but initially we have observed the yields of only 10 to 15 %. To improve on these, we followed their suggestion of using freshly prepared co-catalyst.

Ag<sub>2</sub>O was prepared in a manner similar to that of Tanabe and Peters,<sup>[52]</sup> although, we did not dry it under high vacuum, as suggested in the paper. Instead, we transferred it into a 500 mL RBF and dried it by rotary evaporation under reduced pressure. The bath temperature was kept at 80 °C, which significantly shortened drying time.

Use of fresh dry Ag<sub>2</sub>O in the *mono*-protection reaction improved yields by a few percent. Another observation made was the existence of “dead areas” in the RBF (the areas where stirring was absent) due to the high content of solid Ag<sub>2</sub>O. To counteract this phenomenon, RBF was replaced with a wide beaker and large stirrer bars just fitting into it. Such arrangement improved interaction of Ag<sub>2</sub>O with the solvent mixture. This left one more problem with the experimental setup to solve. It turned out, the solvent, (CH<sub>2</sub>Cl<sub>2</sub>), kept evaporating during the reaction. The latter is undesirable as it leads to inefficient stirring of the reaction mixture and formation of a viscous paste that sticks to the reactor walls. An attempt to cover the beaker with a watch glass did not work because the reaction, being exothermic, heated and evaporated the solvent through the beaker pouring lip. Finally, we used filter

paper to cap the beaker, and then sealed the top with a Parafilm "M". This afforded reasonable protection of the parafilm, which otherwise is decomposed on exposure to the  $\text{CH}_2\text{Cl}_2$  vapour. The yield has improved to 31 % for 2-(benzyloxy)ethanol (**20a**) and 47 % for 3-(benzyloxy)propan-1-ol (**20b**) but still remained far below claimed in literature.<sup>[34]</sup>

### 4.3 Synthesis of [(Bromoalkoxy)methyl]benzenes (**21a-c**)

Both [(2-Bromoethoxy)methyl]benzene (**21a**) and [(3-bromopropoxy)methyl]benzene (**21b**) were successfully synthesised from their precursors (**20a-b**) via the  $\text{CBr}_4/\text{PPh}_3$  route. Careful drying of the reagents and glassware substantially aids the yield of this reaction,<sup>[53]</sup> so *tri*-phenylphosphine and carbon tetrabromide were kept under argon in a desiccator with phosphorus pentoxide drying agent. Glassware was dried in an oven at  $110^\circ\text{C}$  for 12 hours, and the solvent transferred through a dry cannula from a solvent purifying station. All solvent bottles as well as collecting flasks were kept under  $\text{N}_2$  atmosphere. The reaction was performed in  $\text{CH}_2\text{Cl}_2$  with the molar ratio of  $\text{CBr}_4 : \text{PPh}_3 : \text{R-OH} = 1 : 1 : 1$ , as suggested by Appel's mechanism.<sup>[36]</sup> At room temperature the reaction proceeded to relative completion in 3 hours with only mild heating of the mixture due to exothermic nature of the reaction. However, the heat dissipation became a concern when the procedure was scaled up four-fold. To address this problem the reactor was placed in an ice bath prior to the addition of  $\text{CBr}_4$  solution. Upon completion of the reaction the mixture was reduced on rotary evaporator. At this stage two separation options were explored. The first of them was to separate the entire mixture by chromatography, while the second was to add cold hexane to precipitate out *tri*-phenylphosphine-oxide (TPPO), leaving predominantly the brominated product in solution. The latter is effective only if the desired product is soluble in hexane; which is the case with (**21a-b**). Neither of the separation methods turned trouble free. With the first, equimolar quantity of TPP contributes approximately a third of the load mass on a chromatographic column; as it is fairly polar compound, it moves through the column slowly and requires a lot of solvent to elute. This would not be a huge problem, were the intention to discard the residual TPPO together with the silica waste. However, recyclable columns for an automated system were used in this work, and the cost of their replacement was not insignificant. With the second, adding hexane to the concentrated reaction mixture caused the formation of TPPO clumps, trapping product (**21a**) or (**21b**) inside, and lowering the yield. The problem of TPPO clumping was solved by drop-wise addition of hexane and vigorous stirring of the reaction mixture. Leaving the mixture flask stoppered with a septum and stirring it overnight took care of any remaining clumps (they were broken into smaller particles). Analysis of the reaction mixture after the removal of TPPO revealed that it contained about 20 mol percent of starting material. These residual components were

separated from the product by column chromatography. The first fraction, fairly non-polar, was the product; the second, was a mixture of unconverted reagents and starting materials. The volume of solvent required to elute the latter was greatly reduced in comparison to solely chromatographic separation, affording more economical procedure. Achieved yield of **(21a)** and **(21b)** was 76 % and 84 %, respectively.

#### 4.4 Synthesis of [*n*-(Benzyloxy)alkyl]propanedinitriles (22a-c)

We have found no mention of compounds **(22a-c)** in literature. Referring to the procedure of Diez-Barra *et al.*,<sup>[40]</sup> who discovered the phase-transfer catalyst route and synthesised among other products 1-bromobutane, we started with the conditions described in their synthesis as a template for our work. Initially, potassium carbonate was employed as a base but the outcome was unsuccessful. We replaced it with potassium *t*-butoxide, which happened to work well for both products **(22a-b)**.

As these compounds are new and were synthesised by us for the first time, a range of reaction conditions were explored. The best yield was achieved at the molar ratio (malononitrile : alkyl halide : base) = (3 to 4 : 1 : 1). Reaction times from 24 to 132 hours were tried but the yield of product stopped increasing after 48 hours. Limiting the amount of potassium *t*-butoxide and employing an excess of malononitrile ensured that only *mono*-deprotonation of the latter occurred.

At first, the reaction mixture was extracted with CH<sub>2</sub>Cl<sub>2</sub>, which left the salts behind, the organic fractions were combined and the solvent removed by rotary evaporation. Separation of the product was attempted on a chromatographic column but met with some difficulties. After trying a number of solvent systems we settled on CHCl<sub>3</sub>, the only solvent that worked reasonably well. Although we could get the mixture moving on the column with CHCl<sub>3</sub>, malononitrile co-eluted with the product fraction. Attempts to vary the flow rate or column loading failed to overcome this difficulty. At this point, a column pre-wash procedure was considered, and it turned out that pre-washing concentrated organic fractions with water and hexane helped. Hexane helped removing unreacted alkyl halide, while water took care of unreacted malononitrile. Two additional problems were associated with this procedure. The first was that the reaction mixture could not be washed with hexane and water simultaneously. Our attempts of washing with a mixture of immiscible solvents give widely variable results. This problem was solved by washing the mixture sequentially, first with hexane and then with water. In addition, target compounds **(22a-b)** were partially soluble both in water and hexane. Consequently, the volume of hexane and water used became critical, as too much water would wash away not only

malononitrile but also (**22a-b**); too little would leave unreacted malononitrile in the product fraction. Hexane behaved in a similar manner but for leaving unreacted [(bromoalkoxy)methyl]benzene in the product fraction instead of malononitrile. Optimal volume of each of these solvents in the separation procedure had to be determined independently for both homologues (**22a-b**) as somewhat higher loading of malononitrile was used in the [3-(benzyloxy)propyl]propanedinitrile synthesis. Attempts to separate the hexane and water layers from the concentrated reaction mixture by using a filter paper cone turned upside down worked as it did not let higher viscosity product through. We also tried centrifugal separation as an alternative, and it worked well. Chromatographic separation of the pre-washed mixture proved successful as residual traces of malononitrile did not co-elute with the target compounds. The yield of 34 % was achieved for (**22a**) and of 38 % for (**22b**).

Isolated products were characterised by  $^1\text{H}$  and  $^{13}\text{C}$  NMR spectroscopy. In addition, as they were new compounds, a range of 2D and correlation NMR spectra were recorded. This information helped to assign chemical shifts in all three structures unambiguously (see experimental section 5.4). In particular, we paid close attention to the chemical shifts at the sites that were derivatised. Thus,  $\delta$  values for  $^{13}\text{C}$  in NCCHCH are 19.7 for (**22a**) and 22.6 ppm for (**22b**). They compare favourably with chemical shifts of 22.7 ppm for prop-2-en-1-ylpropanedinitrile, 24.7 ppm for benzylpropanedinitrile, and 22.8 ppm for prop-2-yn-1-ylpropanedinitrile reported Diez-Barra *et al.*<sup>[40]</sup> This confirmed the fact reported previously<sup>[40]</sup> that  $^{13}\text{C}$  resonance of the CH group, sandwiched between two nitriles, is relatively unaffected by the nature of the  $\beta$ -carbon on the grafted pendant arm.  $^1\text{H}$  resonances of the same group, CH, in two of our compounds vary slightly more. Thus, previously reported values were in the range 3.54 to 3.78 ppm, while we observed the shifts at 3.92 and 4.07 ppm.  $^{13}\text{C}$  resonances of the nitrile group carbons, 112 and 113 ppm for (**22a**) and (**22b**), respectively, compare well with the range characteristic of this group, 105 to 117 ppm.<sup>[40, 54]</sup>

In addition, (**22b**) was characterised by high-resolution mass spectroscopy, which confirmed its molecular composition and verified the synthetic procedure.

Our experience showed that compounds (**22a-b**) are best kept refrigerated, and they should not be exposed to temperatures exceeding 40 °C.

## 4.5 Synthesis of [*n*-(Benzyloxy)alkyl]-1,3-propanediamines (**23a-c**)

The reduction of derivatised malononitriles (Scheme 5, step **d**) was first attempted by us with  $\text{LiAlH}_4$  following reaction conditions suggested in 1951 by Amundsen *et al.*<sup>[42]</sup> They concluded that an optimal

molar ratio was (LiAlH<sub>4</sub> : RCN) = (1 : 1), with both reagents dissolved in dry THF. With this in mind, the following procedure was attempted on intermediate (**22b**).

- a) LiAlH<sub>4</sub> (0.151 g, 3.63mmol) was weighed into a round bottom flask blanketed with argon. Dry THF or diethyl ether (25 mL) was added to the flask through a cannula, followed by the solution of (**22b**) (0.323 g, 1.51 mmol) in THF or ether (10 mL). The mixture was refluxed for 1 hour, allowed to cool to room temperature, and left stirring for 24 hours under N<sub>2</sub> atmosphere. After that, it was placed in an ice bath and quenched slowly with water (0.137 mL), NaOH (10 %, 0.274 mL), and more water (0.411 mL). The mixture was filtered and the mother liquor concentrated under reduced pressure.

<sup>1</sup>H NMR spectra of the concentrated mother liquor indicated the reaction did not occur with either of the solvents, so a test reaction on malononitrile was set up under the same conditions but for stirring the reaction mixture for 72 hours at room temperature. <sup>1</sup>H NMR spectrum of the mother liquor from this attempt still revealed absence of 1,3-diaminopropane. Next, the condition of LiAlH<sub>4</sub> was checked by a reaction with water, which proved to be very vigorous. Consequently, an alternative approach was considered at this point. As the target molecules have no double bonds, their precursors could be hydrogenated under more strenuous conditions. The hydrogenation of [n-(benzyloxy)alkyl]propanedinitrile homologues was tried with H<sub>2</sub>(g) on Pd/C catalyst in ethanol and on Pd/C catalyst in acetic acid, which is an activating solvent. Unfortunately, in both cases the reaction failed. Any concerns about the age and activity of the of Pd/C catalyst were dispelled by successful test reaction. We think, the above failure might have been caused by the intramolecular interaction between freshly reduced amine group and still in place nitrile group. Such possibility was first mentioned by Briggs *et al*<sup>[55]</sup> in their synthesis of non-ionic surfactants with malononitrile backbone. According to the study of *di*-butylpropanedinitrile, by Briggs *et al*, Figure 50, the reduction of 1,3-dinitriles does not proceed with a wide range of hydrogenation catalysts and under a variety of conditions. Unfortunately, exact nature of the catalysts tried by Briggs *et al*<sup>[55]</sup> was not specified. Paradoxically, the reaction was reported to proceed successfully when LiAlH<sub>4</sub> was used.<sup>[55]</sup>

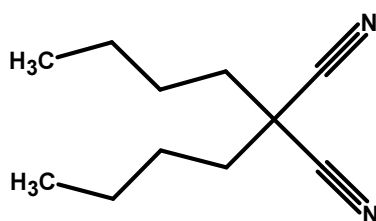


**Fig. 50.** Chemical structure of *di*-butylpropanedinitrile, which reduction was investigated by Briggs *et al*.<sup>[55]</sup>

To summarise our laboratory experience up to this point, attempts at reduction of 1,3-dinitrile with either  $\text{LiAlH}_4$  or  $\text{H}_2(\text{g})$  on Pd/C catalyst in ethanol failed. The only notable difference between the structure of *di*-butylpropanedinitrile and those of [n-(benzyloxy)alkyl]propanedinitriles, synthesised in this work, is the presence of a proton on C2 carbon atom of the malononitrile fragment.

At this point direct hydrogenation was abandoned and alternative reducing agents looked at.

Reduction of *di*-nitriles of similar nature, in particular, of (2,2-dimethylpropyl)propanedinitrile, has been reported previously in Organic Synthesis by Hutching and Maryanoff.<sup>[43]</sup> We have decided to follow their procedure in an attempt to reduce [n-(benzyloxy)alkyl]propanedinitrile via in situ borane generation. NMR spectra indicated a mixture of products, repeatability in producing the same mixture proved to be tricky, while the separation of fractions was difficult. In the case of (2,2-dimethylpropyl)propanedinitrile, last two fractions were separated by distillation. For the compounds of interest in this work, the latter was not feasible due to their higher molecular mass and higher boiling points. With (2,2-dimethylpropyl)propanedinitrile already distilling at 100 °C (at 27 mbar), this separation approach for target compounds had to be abandoned; as mentioned earlier, they are not sufficiently heat resistant. To save the effort and cost of purification, while still looking for the conditions of successful reduction, we decided to use crude [n-(benzyloxy)alkyl]propanedinitriles (generated via borane reduction). Various conditions were tried for the deprotection of the benzylic moiety in the crude material; in particular,  $\text{H}_2$  on Pd/C in EtOH,  $\text{H}_2$  on Pd/C in  $\text{CH}_3\text{COOH}$ , and reflux in aqueous HCl (pH 0.5) for 12 hours; all without success. Next, we tried  $\text{BF}_3$ -Ether as a hydrogenation catalyst. The results were complicated and inconclusive (difficult multicomponent mixture ensued). Before we finished working with the  $\text{BH}_3$  generated in situ, the ability to make it was lost as the commercial manufacture of its precursor,  $\text{BF}_3$ -ether, was discontinued.

One last catalyst for hydrogenation that we could think of was platinum dioxide,  $\text{PtO}_2$ . Platinum dioxide catalysed hydrogenation was approached with caution, keeping in mind the statement by Briggs *et al*.<sup>[55]</sup> that such reduction of 1,3-dinitriles to diamines failed. First, test reactions were performed on the hydrogenation of malononitrile and deprotection of 3-(benzyloxy)propan-1-ol. In both cases  $\text{PtO}_2$  performed successfully at times of 7 and 9 hours, respectively. Next, as we desired to prepare free amine, the hydrogenation in dry ethanol without a hydrogen chloride source was tried but failed to reduce the dinitriles. Finally, with the above in mind, the following procedure was settled on.

**Procedure:** [2-(Benzyloxy)ethyl]propanedinitrile (287 mg, 1.31 mmol) was weighed into a 100 mL RBF, followed by  $\text{PtO}_2$  (143 mg, 50 wt. %), dry EtOH (90 mL) and concentrated aqueous HCl (32 %, 895  $\mu\text{L}$ ). The mixture was stirred under  $\text{H}_2$  (460 kPa) for 48 hours. Resulting solution was filtered through two filter papers, and mother liquor concentrated under reduced pressure. The residue was re-dissolved

in EtOH (5 mL) and C<sub>2</sub>H<sub>5</sub>OC<sub>2</sub>H<sub>5</sub> (45 mL) was added to it in a centrifuge tube. The precipitate was dried over P<sub>2</sub>O<sub>5</sub> for two weeks resulting in a fine yellow highly hygroscopic powder.

The amount of acid was chosen in line with the Sundarmoorthie and Keenan's recommendation of three molar equivalents of acid per nitrile unit,<sup>[44]</sup> and the volume of solvent was chosen to keep pH at about 1. The reaction mixture was filtered through two filter papers to allow recovery and reuse of the PtO<sub>2</sub> (the literature cited using celite). Once the mother liquor was catalyst-free and reduced to a small volume of ethanolic solution, addition of larger volumes of C<sub>2</sub>H<sub>5</sub>OC<sub>2</sub>H<sub>5</sub> became possible. The ether changes polarity of the solvent system and the amine hydrochloride salt precipitates out. The yield of this reaction with product (24b) was approximately 3%, which is, of course, unsatisfactory from practical perspective. Nevertheless, this desired new compound has been undoubtedly synthesised. <sup>1</sup>H and <sup>13</sup>C NMR spectroscopy confirmed the nature of 2-(2-hydroxyethyl) propane-1,3-diaminium dichloride beyond any doubt (see section 5.5). As it turned out, this ammonium salt is extremely hygroscopic. Drying off a sample for the NMR studies took two weeks in a vacuum desiccator over phosphorus pentoxide.

Below is the summary of our attempts at the reduction of dinitriles.

(2,2-Dimethylpropyl)propanedinitrile can be reduced with LiAlH<sub>4</sub> but not with dihydrogen gas, no matter which catalyst is used. In contrast, reduction of [2-(benzyloxy)ethyl]propanedinitrile with LiAlH<sub>4</sub> failed. The only structural difference between two substrates that might affect their ability to undergo reduction is that one is *mono*-alkylated on the C2-carbon of malononitrile, while the other *bi*-alkylated.

The reduction of nitrile groups in compounds (**23a-b**) possibly occurs with BH<sub>3</sub>, though it failed to occur with LiAlH<sub>4</sub>; unfortunately, we were unable to complete this part of the work conclusively. Such outcome is fascinating, as the reaction mechanism is expected to be similar for both reagents.

The results of direct catalysed hydrogenation, with H<sub>2</sub>(g), are puzzling. With PtO<sub>2</sub> catalyst, separate deprotection of benzyl bromide and reduction malononitrile is achieved in good yield. However, when both derivatisations were attempted in one pot, deprotection of the alcohol group occurred, and the reduction of dinitriles was achieved but in very poor yields. And this was with reaction times being at least four times longer than for the separate reactions. Such behaviour is odd and, probably, should be investigated in a separate project where comparative reduction of the nitrile groups of *mono*- and *bi*-alkylated malononitrile derivatives is investigated.

At this stage the project described in this chapter, chapter A, was shelved for two reasons. First, we ran out of time. It took nearly two years of work to reach this point. Trying anything else along similar lines might have put at risk successful completion of this MSc project. The time frame for the preparation of intermediate compounds (**22a-b**) was about six weeks and the synthesis had been done



twice already. Second, the cost of the work escalated to the level where it was considered unsustainable. Prohibitively high cost of the platinum dioxide catalyst, at over R2,000 per gram, and the need of its 50 percent loading by weight, with about 3 percent intermediate product yield and two more sequential synthetic steps still to go, made continuation of this pursuit untenable.

## 5. Synthesis and Characterisation

In this section we will present particulars of synthetic procedures followed and instrumental techniques used for the compound characterisation. For each compound synthesised by us in this part of the project we will report instrumental data collected and the structure assigned.

### 5.1 Experimental

#### 5.1.1 Solvents and Reagents

The solvents and starting materials used are listed in Tables 19 and 20, respectively.

**Table 19.** Common solvents used and internal purification procedures

Solvent	Claimed Purity	Purification procedure
Water	Level II, 15 M $\Omega$ cm	ELGA <sup>a</sup>
Methanol	≥98 %	Distillation
Ethanol	≥98 %	None
Ethyl acetate	≥98 %	None
Dichloromethane	≥98 %	Molecular sieves <sup>b</sup>
Chloroform	≥98 %	None
Tetrahydrofuran	≥98 %	Molecular sieves <sup>b</sup>
Diethyl ether	≥98 %	Molecular sieves <sup>b</sup>
Hexane	≥95 %	Distillation

a) Water purification system: ELGA Veolia, Option R/7.

b) Multi-solvent purification system: Innovative Technology Inc., Model PS-ND-7.

**Table 20.** Commercially available reagents used for the synthesis in this chapter of the thesis.\*

Name	Structure	Assay/ %	MW/ g mol <sup>-1</sup>	Phase state at 25 °C	Density/ g cm <sup>-3</sup>
1,2- Ethanediamine		99	60.10	l	0.900
1,3-Propanediamine		99	74.13	l	0.888
1,3-Diaminopropan-2-ol		95	90.13	s	
Ethylene glycol		99	62.07	l	1.113
1,3-Propanediol		98	76.10	l	1.053
1, 6-Hexanediol		99	118.18		
Malononitrile		98	66.06	s	
(Bromomethyl)benzene		98	171.04	l	1.438
2-Bromoethanamine hydrobromide		95	204.89	s	
2-Aminoethanol		98	61.08	l	1.012
3-Aminopropanol		99	71.11	l	0.982
Silver oxide	Ag <sub>2</sub> O <sub>2</sub>	97	231.735	s	
Triphenylphosphine		99	262.29	s	
Tetrabromomethane		99	331.63	s	
Tetrabutylammonium bromide		99	322.37	s	
Potassium t-butoxide		98	112.21	s	

\*) All reagents were purchased from Sigma-Aldrich and used without further purification.

## 5.1.2 Instrumental

**IR:** FTIR spectra were recorded on Perkin Elmer Spectrum 100 in the range of 450 to 4000  $\text{cm}^{-1}$  with a resolution of 1  $\text{cm}^{-1}$ . All samples were recorded in KBr disks unless otherwise stated.

**CHN:** Elemental analysis was performed on Thermo-Scientific Flash 2000 Organic Elemental CHNS-O Analyser.

**NMR:**  $^1\text{H}$  and  $^{13}\text{C}$  NMR spectra were recorded on Bruker Avance III 400 MHz or Bruker Avance III 500 MHz spectrometer at frequencies of 400/500 MHz (for  $^1\text{H}$  nucleus) and 100/125 MHz (for  $^{13}\text{C}$  nucleus). One of the following probes was used in each case: 5 mm BBOZ probe  $^{19}\text{F}$ - $^{31}\text{P}$ - $^{109}\text{Ag}$ - $\{^1\text{H}\}$ , 5 mm BBIZ probe  $^1\text{H}$ - $\{^{31}\text{P}$ - $^{109}\text{Ag}\}$ , or 5 mm TBIZ probe  $^1\text{H}$ - $\{^{31}\text{P}$ - $^{31}\text{P}$ - $^{103}\text{Rh}\}$ . All proton and carbon chemical shifts are quoted relative to the relevant solvent signal (e.g., for DMSO- $\text{d}_6$ ,  $^1\text{H}$ : 2.500 ppm,  $^{13}\text{C}$ : 39.500 ppm). Proton-proton coupling constants are reported in Hertz (Hz). All experiments, unless stated otherwise, were conducted at 30  $^\circ\text{C}$ .

**MS/ToF:** High-resolution mass spectra were recorded on Waters Acquity UPLC+LCT Premier ToF-MS spectrometer. Samples were dissolved in DMSO to a concentration of approximately 2  $\text{ng } \mu\text{L}^{-1}$ . For low resolution measurements, the instrument was internally calibrated with either reserpine (positive ionisation mode) or raffinose (negative ionisation mode). High resolution measurements were performed using DMSO as the lock mass standard. Cone voltage was kept at 20 kV in all cases unless stated otherwise. All samples were directly injected into the MS port, i.e. bypassing the LC system.

**Flash Chromatography:** Gradient chromatography was used in majority of cases. The notation explained below was adopted for the description of solvent ramping:

“EtOH : Hex = (0:1) to (1:0) solvent system. Product fraction (2)”

This notation first introduces the solvent system, in the above case “EtOH : Hex”; then, the volume ratio of solvents at the start and at the end of elution period is given “(0:1) to (1:0)”; and finally, the number of a product fraction is specified (fractions are counted in order, in which they leave the column) “(2)”.

### 5.1.3 Interpretation of the NMR Results

No single approach to the elucidation of chemical structure from the NMR data exists. The procedure adopted by us, which is explained below, worked well for the type of molecules encountered in this thesis. Routinely, we have recorded  $^1\text{H}$  and  $^{13}\text{C}$  spectra. For all new substances, as well as for the substances not extensively studied previously, in addition, we have recorded a range of 2D- and correlation spectra, e.g., *g*-COSY, DEPT-135, DEPT-90, NOESY, HSQC, HMBC, etc.

The first spectrum interpreted is “dept-135” for the  $^{13}\text{C}$  nucleus. It allows one to associate carbon resonances with the  $\text{CH}_3$ ,  $\text{CH}_2$ , or  $\text{CH}$  groups, with the methylene signals appearing as lines of opposite sign in the spectrum. Remaining ambiguity in the assignment of  $\text{CH}_3$  and  $\text{CH}$  carbon signals (both resonances appear as positive lines in the spectrum) is then resolved in the  $^{13}\text{C}$  “dept-90” spectrum, where positive lines appear only for the  $\text{CH}$  nuclei. Once this is done, the whole of  $^{13}\text{C}$  spectrum is interpreted by assigning all remaining lines to the quaternary carbons.

Next, assignment of the protons to carbon centres, to which they are covalently bound, is carried out by analysing the HSQC spectrum; the latter indicates short distance carbon-proton correlations. With this information in hand, one can check whether the number of protons, derived from the integrated signals for each proton resonance in the  $^1\text{H}$  spectrum, matches the number expected from the DEPT spectra. If the two agree, one has established the number of hydrogen atoms connected to each non-quaternary carbon.

At this stage, an issue of carbon connectivity can be considered. It is based on a) the analysis of multiplet structure of  $^1\text{H}$  resonances (unfortunately, the usefulness of this approach is limited by first-order spectra) and b) interpretation of the HMBC spectra.

Separation of the lines in a proton spectrum that are suspected to belong to a multiplet can be checked and, if it turns out to be same, confirms the multiplet nature, affords the coupling constant, and gives the number of equivalent protons ( $N+1$  rule) in the groups directly connected to parent carbon atom.

HMBC spectra allow to detect the correlation between protons and carbon atoms separated by two, three and, on occasion, four bonds. In part, it provides information similar to the one derived from the ( $N + 1$ ) rule; this allows cross-checking of the HMBC assignment. However, cases exist where the HMBC interpretation fails; say, when a chain of quaternary carbons occurs in a molecule. On occasion, the HMBC spectrum gives one the same correlation as the HSQC spectrum. The latter accounts for which protons are connected to which carbon, and the former accounts for which protons are connected to carbons adjacent to the carbon of interest. Similarity of the HSQC and HMBC correlations happens for the molecules of symmetrical nature, which makes sense as one carbon correlates to the proton on

the carbon equivalent to it. Yet again, this takes place only if the separation between equivalent carbons is less than approximately four bonds. The presence of equivalent hydrogens is also reflected in higher values of signal integrals in the  $^1\text{H}$  spectrum.

In addition, the values of chemical shifts can be taken into account to aid structural assignment. When present in certain functional groups, both proton and carbon atoms display characteristic chemical shifts, which are altered relatively little by the rest of molecular structure.

Correlation of the protons through space is another useful NMR technique, which helps to choose the most likely conformational structure.

Finally, incremental and quantum mechanical modelling of both  $^1\text{H}$  and  $^{13}\text{C}$  NMR spectra became useful additional tool in testing the correctness of assignment of molecular structures.

## Compounds Synthesised

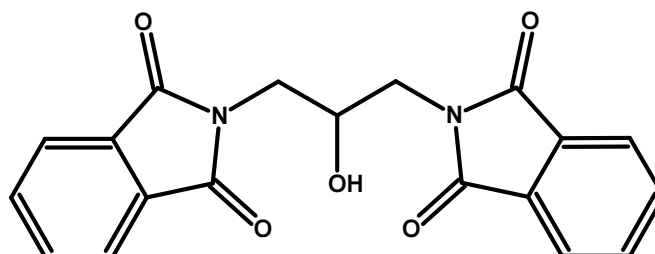
In total, we have synthesised eleven compounds in this part of the project, of which five were new. Whether the compound is new or is known in literature is stated in the relevant section that describes its preparation and characterisation.

In addition to their systematic names, compounds synthesised and isolated by us are labelled with integer numbers that already appeared in Schemes 1-6, Section 3. For homologous compounds with variable length of the alkane chain, a letter is added to the number; in particular, letter "a" designates ethane chain, letter "b" propane one, and letter "c" hexane one. For example, **(20c)** would mean compound of class 20, which is a *mono*-protected diol with hexane chain, i.e. 6-(benzyloxy)hexan-1-ol.

### 5.2 Intermediates with protected functional groups

First, we will present compounds prepared by protecting alcohol or amine functional groups.

#### 5.2.1 Phthalimide *di*-protected 1,3-diaminopropan-2-ol (**2**)



**Procedure:** 1,3-Diaminopropan-2-ol (2.76g, 30.6 mmol) was added to a RBF, followed by phthalic anhydride (9.01g, 60.8 mmol). The mixture was dissolved in toluene (155 mL) and triethylamine (0.42 mL, 3.01 mmol) pipetted in. Reaction mixture was refluxed for 10 hours under Dean-Stark conditions. Once cooled to RT, the mixture was filtered and solids recrystallised from glacial acetic acid. Product has appearance of colourless needles.

#### **(2)** 2,2'-(2-Hydroxypropane-1,3-diyl)bis(1*H*-isoindole-1,3(2*H*)-dione)

This compound is known in literature.<sup>[56]</sup>

**Yield:** 10.1 g, 29.1 mmol (95 %).

**IR** (KBr,  $\bar{\nu}$  /  $\text{cm}^{-1}$ ): 3489(br, O-H), 2948, 2893, 1770, 1710 (s, C=O), 1612, 1466, 1420, 1394 (s, C-N), 1361, 1342, 1191, 1156, 1128, 1089, 1066 (s, C-OH), 1038 (s, C-OH), 1012, 996, 910, 875, 846, 797, 744, 722 (s), 717 (s), 695, 679, 531(s).

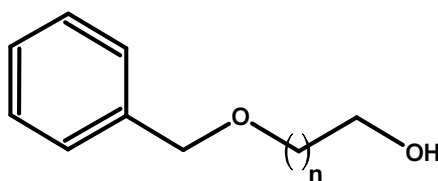
**$^1\text{H}$  NMR** (400 MHz,  $\text{CDCl}_3$ ,  $\delta$ / ppm): 3.55-3.69 (m, 4H,  $-\text{CH}_2-$ ), 4.15-4.20 (m, 1H,  $-\text{CH}(\text{OH})-$ ), 5.29 (d,  $J = 5.3$  Hz, 1H,  $-\text{OH}$ ), 7.82-7.85 (m, 8H, Ar).

**$^{13}\text{C}$  NMR** (400 MHz,  $\text{CDCl}_3$ ,  $\delta$ / ppm): 42.0 (t,  $-\text{CH}_2-$ ), 65.0 (d,  $-\text{CH}(\text{OH})-$ ), 122.9 (d,  $-\text{CHC}(\text{C}=\text{O})-$ ), 131.6 (s,  $-\text{C}(\text{C}=\text{O})-$ ), 134.3 (d,  $-\text{CHCHC}(\text{C}=\text{O})-$ ), 167.8 (s, C=O).

Original spectra for this compound are presented in appendix A, Figures A1-A7.

Characterisation was achieved by means of  $^1\text{H}$ ,  $^{13}\text{C}$ , and correlation NMR spectra. Analysis of the data indicated that the desired species has been synthesised. No comparable data was reported in the Appleton and Hall paper.<sup>[56]</sup>

## 5.2.2 Mono-protected terminal diols (20a-c)



$n = 1, 2, 5$

**Generic procedure:**  $\text{CH}_2\text{Cl}_2$  (30 mL) and fresh  $\text{Ag}_2\text{O}$  (12.1 g, 52.0 mmol) were charged to a beaker, and a diol of interest (34.6 mmol) was added to it with stirring, followed by benzyl bromide (4.62 mL, 38.1 mmol). The beaker was covered, first, with paper and, then, with parafilm. The mixture was stirred at room temperature for 3 hours.  $\text{Ag}_2\text{O}$  was filtered off and washed with  $\text{CH}_2\text{Cl}_2$  (3x10 mL). Then, it was suspended in more dichloromethane and filtered off; yet again, it was washed with  $\text{CH}_2\text{Cl}_2$  (3x10 mL). The  $\text{CH}_2\text{Cl}_2$  extracts were combined and shaken, first, with  $\text{Na}_2\text{CO}_3$  (5%, 5 mL) and then, with brine (5 mL). The aqueous layers were combined and extracted with  $\text{CH}_2\text{Cl}_2$ . All organic layers were combined, and the solvent removed by rotary evaporation. The residual brown liquid was purified by column chromatography using (EtOH : Hex) = (0:1) to (1:0) solvent system. Product fraction (fraction 2) was reduced in volume by rotary evaporation at 80 °C. Residual liquid was purified by distillation at atmospheric pressure. The products were golden-brown viscous liquids.

### (20a) 2-(Benzyloxy)ethanol

This compound is known in literature.<sup>[57-58]</sup>



**Yield:** 1.64 g, 10.6 mmol (31 %).

**<sup>1</sup>H NMR** (400 MHz, CDCl<sub>3</sub>, δ/ ppm): 3.44-3.47 (m, 2H, -OCH<sub>2</sub>CH<sub>2</sub>-), 3.74-3.77 (m, 2H, -CH<sub>2</sub>OH), 4.56 (s, 2H, PhCH<sub>2</sub>-), 7.24-7.35 (m, 5H, Ph).

**<sup>13</sup>C NMR** (100 MHz, CDCl<sub>3</sub>, δ/ ppm): 62.0 (t, -CH<sub>2</sub>OH), 71.6 (t, -OCH<sub>2</sub>CH<sub>2</sub>-), 73.4 (t, PhCH<sub>2</sub>-), 127.1 (d, Ph), 128.8 (d, Ph), 138.1 (s, Ph).

Original spectra for this compound are presented in appendix A, Figures A8-A10.

### **(20b) 3-(Benzyloxy)propan-1-ol**

This compound is known in literature.<sup>[59-60]</sup>

**Yield:** 2.89 g, 16.3 mmol (47 %).

**<sup>1</sup>H NMR** (400 MHz, CDCl<sub>3</sub>, δ/ ppm): 1.87 (p, *J* = 5.7 Hz, 2H, -CH<sub>2</sub>CH<sub>2</sub>OH), 3.67 (t, *J* = 5.8 Hz, 2H, -OCH<sub>2</sub>CH<sub>2</sub>-), 3.79 (t, *J* = 5.7 Hz, 2H, -CH<sub>2</sub>OH), 4.53 (s, 2H, PhCH<sub>2</sub>-), 7.26-7.34 (m, 5H, Ph).

**<sup>13</sup>C NMR** (100 MHz, CDCl<sub>3</sub>, δ/ ppm): 32.3 (t, -CH<sub>2</sub>CH<sub>2</sub>OH), 62.1 (t, -CH<sub>2</sub>OH), 69.6 (t, -OCH<sub>2</sub>CH<sub>2</sub>-), 73.5 (t, PhCH<sub>2</sub>-), 127.8 (d, Ph), 127.9 (d, Ph), 128.6 (d, Ph), 138.3 (s, Ph).

**HRMS** (ES-, *m/z*): [M + Na]<sup>+</sup> calcd. for C<sub>10</sub>H<sub>14</sub>O<sub>2</sub>Na, 189.0891; found, 189.0893.

Original spectra for this compound are presented in appendix A, Figures A11-A18.

### **(20c) 6-(Benzyloxy)hexan-1-ol**

This compound is known in literature.<sup>[61-62]</sup>

**Yield:** 2.85 g, 13.68 mmol (40%).

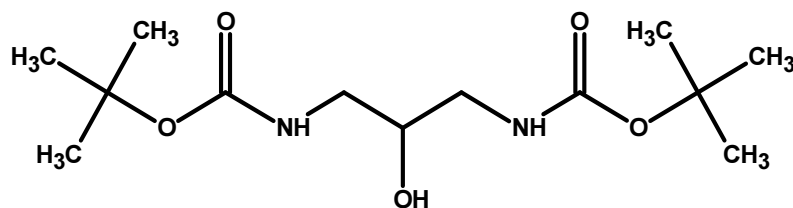
**<sup>1</sup>H NMR** (400 MHz, CDCl<sub>3</sub>, δ/ ppm): 1.30-1.34 (m, 4H, -OCH<sub>2</sub>CH<sub>2</sub>CH<sub>2</sub>CH<sub>2</sub>-), 1.50 (p, *J* = 6.9 Hz, 2H, -CH<sub>2</sub>CH<sub>2</sub>CH<sub>2</sub>OH), 1.56 (p, *J* = 6.9 Hz, 2H, -OCH<sub>2</sub>CH<sub>2</sub>CH<sub>2</sub>-), 3.40 (t, *J* = 6.5 Hz, 2H, PhCH<sub>2</sub>OCH<sub>2</sub>-), 3.56 (t, *J* = 6.6 Hz, 2H, -CH<sub>2</sub>OH), 4.43 (s, 2H, PhCH<sub>2</sub>-) 7.19-7.27 (m, 5H, Ph).

**<sup>13</sup>C NMR** (100 MHz, CDCl<sub>3</sub>, δ/ ppm): 25.8 (t, -OCH<sub>2</sub>CH<sub>2</sub>CH<sub>2</sub>-), 26.2 (t, -CH<sub>2</sub>CH<sub>2</sub>OH), 29.9 (t, -OCH<sub>2</sub>CH<sub>2</sub>CH<sub>2</sub>-), 32.9 (t, -CH<sub>2</sub>CH<sub>2</sub>CH<sub>2</sub>OH), 63.1 (t, -CH<sub>2</sub>OH), 70.5 (t, PhCH<sub>2</sub>OCH<sub>2</sub>-), 73.1 (t, PhCH<sub>2</sub>-), 127.7 (d, Ph), 127.8 (d, Ph), 128.5 (d, Ph), 138.9 (s, Ph).

Original spectra for this compound are presented in appendix A, Figures A19-A24.

Characterisation was achieved by means of IR, <sup>1</sup>H, <sup>13</sup>C, and correlation NMR; as well as IR. Analysis of the data indicated that the desired species has been synthesised. For all three *mono*-protected diols, <sup>1</sup>H and <sup>13</sup>C NMR data are in satisfactory agreement with the values reported in literature.<sup>[57-62]</sup>

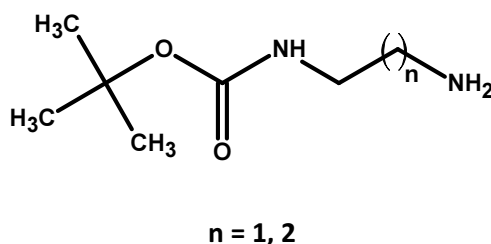
### 5.2.3 Boc protected 1,3-diaminopropan-2-ol (12)



#### (12) *Di-t-butyl(2-hydroxypropane-1,3-diyl)bis-carbamate*

The above Boc *di*-protected 1,3-diaminopropan-2-ol is of relevance to the synthetic path presented in Scheme 4. Unfortunately, it was not explored by us due to time constraints. The synthesis of this compound in our research group has been accomplished by Elizabeth Diu. However, taking into account deviation from the original direction of her PhD work, the particulars of such synthesis are not included in Elizabeth's dissertation. For the completeness of record on the work done on scorpionate ligands, the specifics of this preparation are included in appendix A of this report, Figure A25.

### 5.2.4 Boc mono-protected diamines (7)

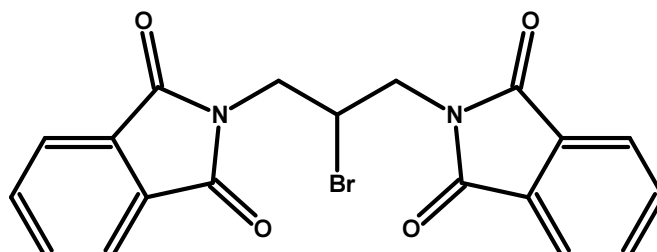


#### (7a-b) *t*-Butyl(*n*-aminoalkyl)carbamates

The above Boc *mono*-protected aliphatic diamines are of relevance to the synthetic route presented in Scheme 2. Due to time constraints we have not explored this path. The synthesis of these compounds in our research group has been accomplished by Elizabeth Diu, but taking into account deviation from the original direction of her PhD work, the particulars of their preparation are not included in Elizabeth's dissertation. For the completeness of record on the work done on scorpionate ligands, the specifics of this synthetic step are included in appendix A of our report, Figure A26.

## 5.3 Products of bromo-de-hydroxylation

### 5.3.1 2,2'-(2-Bromopropane-1,3-diyl)bis(1H-isoindole-1,3(2H)-dione) (3)



**Procedure:** 2,2'-(2-Hydroxypropane-1,3-diyl)bis(1H-isoindole-1,3(2H)-dione), (**2**), (0.250 g, 0.71 mmol) was weighed into a RBF, and acetic acid (10 mL) and HBr (48 wt. %) (75  $\mu$ L, 0.66 mmol) added sequentially. The mixture was refluxed under low light conditions for 24 hours. Once cooled to RT, the contents of the flask were neutralised with Na<sub>2</sub>CO<sub>3</sub> (10 %) (80 mL) and washed with brine (10 mL). The aqueous layer was extracted with CH<sub>2</sub>Cl<sub>2</sub> (2 $\times$ 100 mL). Organic fractions were combined and concentrated by rotary evaporation. The residue was separated by column chromatography using (EtOAc : Hexane) = (4 : 1) solvent system. Resulting product is a white powder.

#### (**3**) 2,2'-(2-Bromopropane-1,3-diyl)bis(1H-isoindole-1,3(2H)-dione)

This compound is **new**.

It was first synthesised in our research group by Ahmed Naseem in 2008.<sup>[63]</sup>

**Yield:** Not measured.

**IR** (KBr,  $\bar{\nu}$  / cm<sup>-1</sup>): 3435(br, O-H), 2938, 1774, 1772, 1726(s), 1713 (s, C=O), 1612, 1466, 1433, 1423, 1397 (s, C-N), 1372, 1291, 1276, 1189, 1120, 999 (s, C-Br), 906, 882, 845, 798, 744, 724, 715, 695, 532(s).

**<sup>1</sup>H NMR** (400 MHz, CDCl<sub>3</sub>,  $\delta$ / ppm): 3.82-3.91 (m, 4H, -CH<sub>2</sub>-), 5.29-5.35 (m, 1H, -CHBr-), 7.84-7.92 (m, 8H, Ar).

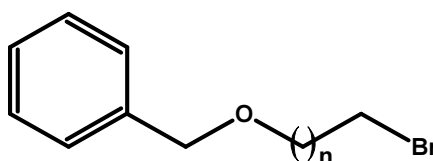
**<sup>13</sup>C NMR** (100 MHz, CDCl<sub>3</sub>,  $\delta$ / ppm): 38.9 (t, -CH<sub>2</sub>-), 68.9 (d, -CHBr-), 123.1 (d, -CHC(C=O)-), 131.3 (-C(C=O)), 131.5 (d, -CHCH(C=O)-), 167.6 (C=O).

Original spectra for this compound are presented in appendix A, Figures A27-A32.

The comparison of NMR and IR data for compounds (**2**) and (**3**) revealed a high level of similarity; one major band shift in the IR spectra was from 1038 (s, C-OH) to 999 (s, C-Br) cm<sup>-1</sup>, and a small shift in <sup>13</sup>C

NMR spectra for the derivatised was carbon from 65.00 (d, -CH(OH)-) to 68.93 (d, -CHBr-) ppm. Initially we thought that compound (3) was not obtained, as its IR and NMR spectra were very close to those of (2), and we could not get positive MS results indicating it was indeed the bromine homologue. Only at the stage of compiling this thesis when we compared our results with those of Ahmed and analysed large numbers of reaction samples derived from the use of different bromo-de-hydroxylation agents, did we realise that they closely resembling each other but are nevertheless distinctly different compounds (2) and (3) were present. A regrettable oversight.

### 5.3.2 [(n-Bromoalkoxy)methyl]benzenes, (21)



$n = 1, 2, 5$

**Generic procedure:** Triphenylphosphine (2.86g, 10.8 mmol) was dissolved in  $\text{CH}_2\text{Cl}_2$  (30 mL) in a RBF and relevant (benzyloxy)alcohol (10.6 mmol) added to it. A solution of carbon tetrabromide (3.62 g, 10.8 mmol) in  $\text{CH}_2\text{Cl}_2$  (10 mL) was added drop-wise to the flask, which was kept in an ice bath. The mixture was allowed to warm up and was stirred for 3 hours at RT under  $\text{N}_2$ . The organic layer was washed with  $\text{Na}_2\text{CO}_3$  (aq, 5 wt. %) (5 mL), and brine (5 mL). Aqueous layers were extracted with  $\text{CH}_2\text{Cl}_2$ , organic fractions combined, and concentrated by rotary evaporation. The residue was re-dissolved in hexane (30 mL), which was added slowly with stirring, and left stirring overnight. Resulting white solid was filtered off and mother liquor concentrated by rotary evaporation. The residue was purified by column chromatography, ( $\text{CH}_2\text{Cl}_2$  : EtOAc) = (1:0) to (0:1). The product fraction (fraction 1) was collected and distilled at atmospheric pressure (90 °C). The product is a golden-brown liquid.

#### (21a) [(2-Bromoethoxy)methyl]benzene

This compound is known in literature.<sup>[64-65]</sup>

**Yield:** 1.83 g, 8.20 mmol (76%).

**$^1\text{H}$  NMR** (400 MHz,  $\text{CDCl}_3$ ,  $\delta$ / ppm): 3.49 (t,  $J = 6.2$  Hz, 2H,  $-\text{CH}_2\text{Br}$ ), 3.79 (t,  $J = 6.2$  Hz, 2H,  $-\text{CH}_2\text{CH}_2\text{Br}$ ), 4.59 (s, 2H,  $\text{PhCH}_2-$ ), 7.29-7.36 (m, 5H, Ph).

**$^{13}\text{C}$  NMR** (100 MHz,  $\text{CDCl}_3$ ,  $\delta$ / ppm): 30.6 (t,  $-\text{CH}_2\text{Br}$ ), 70.2 (t,  $-\text{CH}_2\text{CH}_2\text{Br}$ ), 73.4 (t,  $\text{PhCH}_2-$ ), 127.9 (d, Ph), 128.1 (d, Ph), 128.68 (d, Ph), 138.0 (s, Ph).

Original spectra for this compound are presented in appendix A, Figures A33-A38.

Characterisation was achieved by means of  $^1\text{H}$ ,  $^{13}\text{C}$ , and correlation NMR spectra. Analysis of the data indicated that the desired species has been synthesised.

### **(21b) [(3-Bromopropoxy)methyl]benzene**

This compound is known in literature.<sup>[59]</sup>

**Yield:** 2.04 g, 8.71 mmol (84%).

**$^1\text{H}$  NMR** (400 MHz,  $\text{CDCl}_3$ ,  $\delta$ / ppm): 2.14 (p,  $J = 6.2$  Hz, 2H,  $-\text{CH}_2\text{CH}_2\text{Br}$ ), 3.54 (t,  $J = 6.6$  Hz, 2H,  $-\text{CH}_2\text{Br}$ ), 3.61 (t,  $J = 5.8$  Hz, 2H,  $-\text{OCH}_2-$ ), 4.52 (s, 2H,  $\text{PhCH}_2-$ ), 7.26-7.36 (m, 5H, Ph).

**$^{13}\text{C}$  NMR** (100 MHz,  $\text{CDCl}_3$ ,  $\delta$ / ppm): 30.8 (t,  $-\text{CH}_2\text{Br}$ ), 33.1 (t,  $-\text{CH}_2\text{CH}_2\text{Br}$ ), 67.9 (t,  $-\text{OCH}_2-$ ), 73.3 (t,  $\text{PhCH}_2-$ ), 127.8 (d, Ph), 127.9 (d, Ph), 128.6 (d, Ph), 138.5 (s, Ph).

Original spectra for this compound are presented in appendix A, Figures A39-A43.

Characterisation was achieved by means of  $^1\text{H}$ ,  $^{13}\text{C}$ , and correlation NMR spectra. Analysis of the data indicated that the desired species has been synthesised.

### **(21c) {[6-Bromoethyl]oxy}methyl}benzene**

This compound is known in literature.<sup>[66-67]</sup>

**Yield:** 2.32 g, 8.56 mmol (81 %).

**$^1\text{H}$  NMR** (400 MHz,  $\text{CDCl}_3$ ,  $\delta$ / ppm): 1.38-1.50 (m, 4H,  $-\text{CH}_2\text{CH}_2\text{CH}_2\text{CH}_2\text{Br}$ ), 1.64 (p,  $J = 7.0$  Hz, 2H,  $-\text{OCH}_2\text{CH}_2-$ ), 1.87 (p,  $J = 6.9$  Hz, 2H,  $-\text{CH}_2\text{CH}_2\text{Br}$ ), 3.41 (t,  $J = 6.8$  Hz, 2H,  $-\text{CH}_2\text{Br}$ ), 3.48 (t,  $J = 6.5$  Hz, 2H,  $-\text{OCH}_2-$ ), 4.51 (s, 2H,  $\text{PhCH}_2-$ ), 7.29-7.35 (m, 5H, Ph).

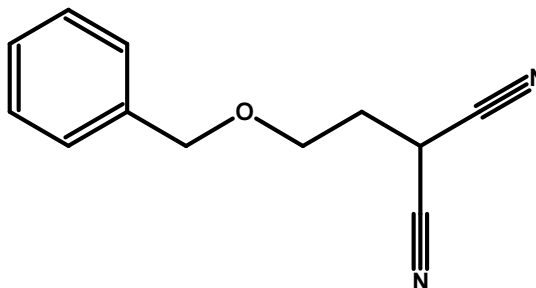
**$^{13}\text{C}$  NMR** (100 MHz,  $\text{CDCl}_3$ ,  $\delta$ / ppm): 25.6 (t,  $-\text{CH}_2\text{CH}_2\text{CH}_2\text{Br}$ ), 28.2 (t,  $-\text{OCH}_2\text{CH}_2\text{CH}_2-$ ), 29.8 (t,  $-\text{OCH}_2\text{CH}_2-$ ), 32.9 (t,  $-\text{CH}_2\text{CH}_2\text{Br}$ ), 34.0 (t,  $-\text{CH}_2\text{Br}$ ), 70.4 (t,  $-\text{OCH}_2-$ ), 73.1 (t,  $\text{PhCH}_2-$ ), 127.7 (d, Ph), 127.8 (d, Ph), 128.5 (d, Ph), 138.8 (s, Ph).

Original spectra for this compound are presented in appendix A, Figures A44-A49.

Characterisation was achieved by means of  $^1\text{H}$ ,  $^{13}\text{C}$ , and correlation NMR spectra. Analysis of the data indicated that the desired species has been synthesised. For all compounds in this category,  $^1\text{H}$  and  $^{13}\text{C}$  NMR data are in satisfactory agreement with the values reported in literature.<sup>[59, 64-67]</sup>

## 5.4 Condensation with malononitrile

### (22a) [2-(Benzyloxy)ethyl]propanedinitrile



This compound is **new**.

**Procedure:** Malononitrile (3.30 g, 49.5 mmol) was weighed into a dry 100 mL RBF flushed with Ar. [(2-Bromoethoxy)methyl]benzene (3.70g, 16.5 mmol), *t*-butylammonium bromide (0.215 g, 0.66 mmol) and dry THF (10 mL) were added sequentially. After stirring for 1 hour, potassium *t*-butoxide (2.11 g, 18.5 mmol) was added. The reaction mixture was stirred for further 12 hours under N<sub>2</sub> at 60 °C. The mixture was extracted with CH<sub>2</sub>Cl<sub>2</sub> (3×100 mL) and the residual solid filtered off. It was washed with CH<sub>2</sub>Cl<sub>2</sub> (60 mL). The dichloromethane fractions were combined and the solvent removed under reduced pressure at RT to a CH<sub>2</sub>Cl<sub>2</sub> free residue, which was washed, first, with hexane (74 mL), and then, with water (30 mL). Each time two-phase liquid system was filtered through a double paper filter that removed the solvent layer but left the viscous liquid phase on top. This phase was transferred to a RBF and the residual solvent removed under vacuum. Thereafter, a small amount of EtOH was added to the residue and it was separated by column chromatography using (CHCl<sub>3</sub> : EtOH) = (1 : 0)- (0 : 1) solvent system. Resulting product is a pale-brown viscous liquid.

**Note:** The product is heat sensitive and should not be subjected to temperatures above 40 °C in the separation procedure! On average, we had a success with this separation procedure four times out of five. In the case of failure, one should re-combine all fractions, remove the solvents by evaporation, and try the separation again.

**Yield:** 1.18 g, 5.55 mmol (34%).

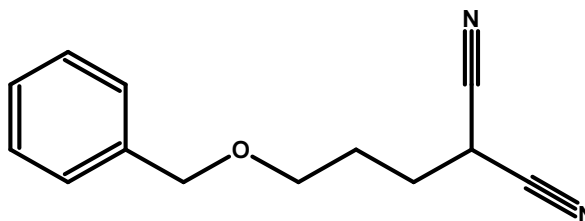
**<sup>1</sup>H NMR** (400 MHz, CDCl<sub>3</sub>, δ/ ppm): 2.28-2.31 (m, 1H, -CH<sub>2</sub>CH(CN)<sub>2</sub>), 2.30-2.33 (m, 1H, -CH<sub>2</sub>CH(CN)<sub>2</sub>), 3.69 (t, *J* = 11.0 Hz, 2H, -OCH<sub>2</sub>CH<sub>2</sub>-), 4.07 (t, *J* = 7.6 Hz, 1H, -CH(CN)<sub>2</sub>), 4.55 (s, 2H, PhCH<sub>2</sub>-), 7.31-7.39 (m, 5H, Ph).

**<sup>13</sup>C NMR** (100 MHz, CDCl<sub>3</sub>, δ/ ppm): 19.7 (d, -CH(CN)<sub>2</sub>), 31.7 (t, -CH<sub>2</sub>CH(CN)<sub>2</sub>), 64.7 (t, -OCH<sub>2</sub>-), 73.8 (t, PhCH<sub>2</sub>-), 112.6 (s, -C≡N), 128.1 (d, Ph), 128.4 (d, Ph), 128.8 (d, Ph), 137.3 (s, Ph).

Original spectra for this compound are presented in the appendix A, Figures A50-A54.

Characterisation was achieved by means of  $^1\text{H}$ ,  $^{13}\text{C}$ , and correlation NMR spectra. Analysis of the data indicated that the desired species has been synthesised.

### (22b) [3-(Benzyloxy)propyl]propanedinitrile



This compound is **new**.

**Procedure:** Malononitrile (0.87 g, 13.1 mmol) was weighed in a dry 100 mL RBF flushed with Ar. [(3-Bromopropoxy)methyl]benzene (1.00g, 4.36 mmol), *t*-butylammonium bromide (0.039 g, 0.12 mmol), and dry THF (10 mL) were added sequentially. After stirring for 1 hour potassium *t*-butoxide (0.376 g, 3.29 mmol) was added. The reaction mixture was stirred for further 12 hours under  $\text{N}_2$  at 60 °C. Then it was extracted with  $\text{CH}_2\text{Cl}_2$  (3×32 mL) and the residual solid filtered off. It was washed with  $\text{CH}_2\text{Cl}_2$  (20 mL) and all dichloromethane fractions combined. The solvent was removed under reduced pressure at RT to a  $\text{CH}_2\text{Cl}_2$  free residue, which was washed, first, with hexane (16 mL), and then, with water (8 mL). Each time two-phase liquid system was filtered through a double paper filter that removed the solvent layer but left the viscous liquid phase on top. This phase was transferred to a RBF and the residual solvent removed under vacuum. Thereafter, a small amount of EtOH was added to the residue, and it was separated by column chromatography using  $(\text{CHCl}_3 : \text{EtOH}) = (1 : 0)$  to  $(0 : 1)$  solvent system. Resulting product is a pale-brown viscous liquid.

**Note:** The product is heat sensitive and should not be subjected to temperatures above 40 °C in the separation procedure!

**Yield:** 0.373 g, 1.65 mmol (38%).

$^1\text{H}$  NMR (400 MHz,  $\text{CDCl}_3$ ,  $\delta$ / ppm): 1.89-1.94 (m, 2H,  $-\text{OCH}_2\text{CH}_2-$ ), 2.16-2.21 (m, 2H,  $-\text{CH}_2\text{CH}(\text{CN})_2$ ), 3.57 (t,  $J = 5.6$  Hz, 2H,  $-\text{OCH}_2-$ ), 3.91 (t,  $J = 7.3$  Hz, 1H,  $-\text{CH}(\text{CN})_2$ ), 4.51 (s, 2H,  $\text{PhCH}_2-$ ), 7.30-7.37 (m, 5H, Ph).

$^{13}\text{C}$  NMR (100 MHz,  $\text{CDCl}_3$ ,  $\delta$ / ppm): 22.6 (d,  $-\text{CH}(\text{CN})_2$ ), 26.5 (t,  $-\text{OCH}_2\text{CH}_2-$ ), 29.1 (t,  $-\text{CH}_2\text{CH}(\text{CN})_2$ ), 68.7 (t,  $-\text{OCH}_2-$ ), 73.4 (t,  $\text{PhCH}_2-$ ), 112.9 (s,  $-\text{C}\equiv\text{N}$ ), 127.9 (d, Ph), 128.1 (d, Ph), 128.8 (d, Ph), 137.9 (s, Ph).

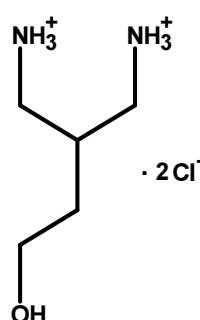
**HRMS** (ES $^-$ ,  $m/z$ ):  $[\text{M} + \text{Na}]^+$  calcd. for  $\text{C}_{13}\text{H}_{14}\text{N}_2\text{ONa}$ , 237.1004; found, 237.1009.

Original spectra for this compound are presented in the appendix A, Figures A55-A61.

As both of the above two species are new, full NMR characterisation was carried out. The assignment of the structure was achieved by analysing 1D, 2D, and correlation spectra, ( $^1\text{H}$ ,  $^{13}\text{C}$ , dept-135, dept-90, hsqc, hmbc, cosy). Molecular formula of (22b) was confirmed by high-resolution mass spectroscopy.

## 5.5 Reduction of malononitrile intermediates

### (24a) 2-(2-Hydroxyethyl)propane-1,3-diaminium dichloride



This compound is **new**.

**Procedure:** [n-(Benzyloxy)ethyl]propanedinitrile (287 mg, 1.31 mmol) was weighed into a 100 mL RBF, to which  $\text{PtO}_2$  (143 mg, 50 wt. %), dry EtOH (90 mL), and concentrated aqueous HCl (32 wt. %, 895  $\mu\text{L}$ ) were added sequentially. The mixture was stirred under  $\text{H}_2$  (at 460 kPa) for 48 hours. Resulting mixture was filtered through two filter papers, and mother liquor concentrated under reduced pressure. The residue was re-dissolved in EtOH (5 mL) and transferred to a centrifuge tube, where  $\text{C}_2\text{H}_5\text{OC}_2\text{H}_5$  (45 mL) was added in. The precipitate formed was centrifuged, and dried over  $\text{P}_2\text{O}_5$  for two weeks, resulting in a fine yellow highly hygroscopic powder.

**Note:** pH of the solvent mixture should not exceed 1! The choice of  $\text{D}_2\text{O}$  for NMR studies was caused by the fact that the product failed to dissolve in either  $\text{CDCl}_3$  or  $\text{DMSO-d}_6$ .

**Yield:** Approximately 3 wt. %.

$^1\text{H}$  NMR (400 MHz,  $\text{D}_2\text{O}$ ,  $\delta$ / ppm): 1.84-1.89 (m, 2H,  $\text{HOCH}_2\text{CH}_2-$ ), 2.35-2.40 (m, 1H,  $-\text{CH}_2\text{CH}(\text{CH}_2)_2$ ), 3.20-3.24 (m, 4H,  $-\text{CH}_2\text{NH}_3^+$ ), 3.82-3.85 (t,  $J = 11.8$  Hz, 2H,  $\text{HOCH}_2-$ )<sup>†</sup>.

<sup>†</sup>) Sample had some impurities, which caused the loss of resolution in the  $^1\text{H}$  spectrum; the value of the splitting constant is provisional.



$^{13}\text{C}$  NMR (100 MHz,  $\text{D}_2\text{O}$ ,  $\delta$ / ppm): 31.1 (t,  $\text{HOCH}_2\text{CH}_2^-$ ) 33.4 (d,  $-\text{CH}(\text{CH}_2)_2^-$ ), 40.8 (t,  $-\text{CH}_2\text{NH}_3^+$ ), 58.5 (t,  $\text{HOCH}_2^-$ ).

Original spectra for this compound are presented in the appendix A, Figures A62-A66.

As this compound is new, assignment of the NMR data was achieved with the aid of 1D, 2D, and correlation spectra.

## 6. Conclusions for Chapter A

1. In total, we have synthesised eleven compounds, of which five were new (**2**, **3**, **22a**, **22b**, and **23b**). Previously known compounds were characterised by  $^1\text{H}$  and  $^{13}\text{C}$  NMR spectroscopy; in all cases the comparison with literature data was satisfactory. New compounds were characterised by complete range of instrumental techniques described in this Chapter.
2. The *mono*-protection of diols was achieved with benzyl bromide and silver oxide as a co-catalyst. Yields for *mono*-protected species were 31 % for 2-(benzyloxy)ethanol (**20a**), 47 % for 3-(benzyloxy)propan-1-ol (**20b**), and 40 % for 6-(benzyloxy)hexan-1-ol (**20c**). This is lower than the values in excess of 70 percent, claimed in literature, despite extensive optimisation of the synthetic procedure undertaken by us. The reaction was performed on more than six occasions and the procedure proved repeatable.
3. Two different brominating agents were employed in the conversion of protected alcohols (**2** and **20**) to the respective bromides (**3** and **21**):
  - a) Bromo-de-hydroxylation of (**2**), 2,2'-(2-hydroxypropane-1,3-diyl)bis(1*H*-isoindole-1,3(2*H*)-dione), was attempted with  $\text{CBr}_4/\text{PPh}_3$  and  $\text{HBr}/\text{CH}_3\text{COOH}$ , and initially thought to have failed in both cases. On review of the data from a number of attempts, we realised the  $\text{HBr}/\text{CH}_3\text{COOH}$  route was successful.
  - b) Bromo-de-hydroxylation of alcohols (**20a-c**) to bromides (**21a-c**) proceeded well via the  $\text{CBr}_4/\text{PPh}_3$  route. Yields of 75 percent or higher were in accord with reported in literature.
4. Two of the six synthetic routes considered in Chapter A required intermediate (**3**), 2,2'-(2-bromopropane-1,3-diyl)bis(1*H*-isoindole-1,3(2*H*)-dione), the synthesis of which was attempted by the bromo-de-hydroxylation of compound (**2**). We have abandoned this direction as at the time it was believed that preparation of (**3**) has failed. Later review of experimental evidence changed that conclusion and, in fact, the synthesis of (**3**) was successfully achieved. In particular, IR and NMR data for both compounds were very close but for a couple of small differences in certain parts of the spectra. When spectra for a range of samples were compared side by side, it became clear they represent two distinctly different species. Regrettably, this oversight was corrected only recently. Hence, the parameters of the procedure were not finalised, and two synthetic paths that depended on intermediate (**3**) were not followed.
5. According to the experience gained in our research group, *mono*-substitution of malononitriles at C2-carbon has always been difficult due to the lability of hydrogen atom remaining on this

carbon. In all previous attempted syntheses with various halogenating agents, *bi*-substitution occurred. We have succeeded to achieve *mono*-substitution with intermediates (**21a-b**) by employing potassium *t*-butoxide and a three-fold excess of malononitrile. Yields of derivatised malononitriles (**22a-b**) were in the range of 30 to 40 percent.

6. Conversion of intermediates (**22a-b**) to 1,3-diamino-2-alkyl derivatives (**24a-b**) involves two separate reactions. The first is de-protection of the *mono*-protected benzyl ether alcohol, and the second is reduction of the di-nitrile. Initially we thought both steps could be achieved with the palladium-on-carbon hydrogenation catalyst, but it proved unsuccessful even in activating solvents. Various other reducing agents were tried, among them LiAlH<sub>4</sub> and BH<sub>3</sub>, without success. The first proved unable to reduce *mono*-substituted dinitriles, while the second resulted in the formation of inseparable mixtures.
7. Hydrogenation of [3-(benzyloxy)propyl]propanedinitrile (**22b**) to 2-(2-hydroxyethyl)propane-1,3-diamonium dichloride salt (**24b**) was achieved for the first time with PtO<sub>2</sub> catalyst under acidic conditions. Highly hygroscopic product was isolated in approximately 3 % yield. Low yield for this one-pot reaction is puzzling, as the test reactions on stepwise hydrogenation – de-protection afforded moderate to high yields.

It took us two years of work to arrive at the results just summarised above. Although, much was learned and many useful synthetic steps accomplished, our primary objective – to synthesise derivatised 1,3-propanediamines – was not met in satisfactory fashion. At this stage, upon consultation with my supervisor, it was decided to shelve present project for two reasons. First, we ran out of time. Trying anything else along similar lines would require another year, year and a half, without certainty that it will work, and might have put at risk successful completion of this MSc project. Second, the cost of the work escalated to the level where it was considered unsustainable. Prohibitively high cost of the platinum dioxide catalyst, at over R2,000 per gram, and the need of its 50 percent loading by weight, with about 3 percent intermediate product yield and two more sequential synthetic steps still to go, made continuation of this pursuit untenable.

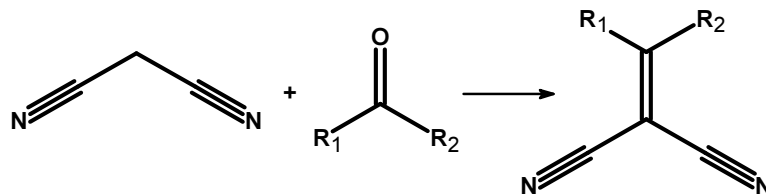
Overall feeling that the project was not a success, after so much work and effort, led to another suggestion of my supervisor, which I accepted. It was to change synthetic direction to the synthesis of novel *bis*-chelate cyanoxime-and-amide ligands, which at the time was just tested and shown promise. Consequently, Chapter B that follows is a reflection of the essence and outcome of this second effort in my Master's work.

## 7. Future Work Emanating from Chapter A

Preparation of the *bis*-chelate ligands with oxime-and-amide moieties, derivatised at some point of an aliphatic bridge, remains important synthetic target in our research group. Below are some suggestion for the future work, formulated on the basis of experience gained in the course of performing this project.

1. Considering the failure of most common hydrogenation catalysts employed by us to reduce substituted malononitriles, hydrogenation under harsh conditions, such as H<sub>2</sub>(g) at 200 atm in liquid ammonia in the presence of a suitable composite metal catalyst, should be tried. We could not try this in the current project, as it requires highly specialised apparatus. Capital investment in such equipment will be difficult to justify within our department, and its cost is very substantial (a few million Rand). The best solution would be to find collaborators overseas, who already possess such apparatus, and to arrange trial runs at their facility.
2. If mechanistic questions about the reduction of substituted malononitriles are to be answered, one may consider more systematic study, where a range of derivatives is prepared with and without a hydrogen atom on the C2-carbon of malononitrile, followed by an investigation of their reactivity. In particular, a range of mono-alkylated products may be synthesised according to Diez-Barra *et al*<sup>[40]</sup>, and another range of derivatives, with the olefin-type grafting (see Scheme 7), may be prepared according to Zhang *et al*<sup>[68]</sup> or Moussaoui and Salem.<sup>[69]</sup> By subjecting these analogues to hydrogenation with a number of reducing agents (among them: LiAlH<sub>4</sub>, BH<sub>3</sub>, refluxing with concentrated acids, and direct hydrogenation with a range of catalysts), one might gain an understanding of factors essential to the reduction of substituted malononitriles to derivatised 1,3-diaminopropanes.
3. In view of the difficulties encountered with the reduction of substituted malononitriles, one should revisit the preparation of brominated compound (**3**), and explore synthetic routes presented in Schemes 1-2. Alternatively, if the above proves difficult, Boc-protection of 1,3-diaminopropane-2-ol should be considered, and Schemes 3-4 followed.
4. Otherwise, an entirely new approach might be considered. The fact that malononitrile has two fairly acidic protons allows it to undergo a Knoevenagel condensation, which is yet another way of grafting an arm onto C2-carbon of malononitrile, Scheme 7. Knoevenagel condensation products are synthesised on alumina under solvent free conditions, or by grinding neat reagents with K<sub>2</sub>CO<sub>3</sub>. The reaction gives slightly better yields if R<sub>1</sub> is hydrogen and R<sub>2</sub> is carbon β to an

aromatic moiety, though, yields in the region of 50 % were achieved for non-aromatic substituents. This approach may allow a wide range of arms to be grafted on C2-carbon of malononitrile.<sup>[68]</sup> Reduction of the nitrile groups that follows might at the same time convert the double bond into a saturated hydrocarbon chain, as desired in this project.



**Scheme 7.** Generic Knoevenagel condensation of malononitrile with ketones.

## 8. References for Chapter A

1. Duda, A.M.; Karaczyn, A.; Kozlowski, H.; Fritsky, I.O.; Glowiak, T.; Prisyazhnaya, E.V.; Sliva, S.Y.; Swiatek-Kozlowska, J. Co-ordination of copper(II) and nickel(II) ions by a novel open-chain oxime ligand. *J. Chem. Soc. Dalton Trans.* 1997, **20**, 3853-3859.
2. Kimura, E. Macrocyclic Polyamines with Intelligent Functions. *Tetrahedron.* 1992, **48**, 30, 6175-6217.
3. Melhado, L.L.; Gutsche, C.D. Association phenomena 2. Catalysis of the decomposition of acetyl phosphate by chelate micelles and by amine-ammonium micelles. *J. Am. Chem. Soc.* 1978, **100**, 6, 1850-1856.
4. Puri, D. *Medicinal Book of Biochemistry*, 2<sup>nd</sup> ed., Elsevier: India, 2005.
5. Lau, H.-P.; Gutsche, C.D. Association phenomena 3. Polyfunctional catalysis of acetyl phosphate decomposition. *J. Am. Chem. Soc.* 1978, **100**, 23, 1857-1865.
6. Gutsche, C.D.; Mei, M. Association phenomena 7. Mixed chelate and co-micellar catalysis of acetyl phosphate "olysis" reactions. *J. Am. Chem. Soc.* 1985, **107**, 26, 7964-7967.
7. Onindo, C.O.; Sliva, T.Y.; Kowalik-Jankowska, T.; Fritsky, I.O.; Buglyo, P.; Pettit, L.D.; Kozlowski, H.; Kiss, T. Copper(II) co-ordination by oxime analogues of amino acids and peptides. *J. Chem. Soc. Dalton Trans.* 1995, 23, 3911-3915.
8. Fritsky, I.O.; Kozlowski, H.; Prisyazhnaya, E.V.; Rzaczyńska, Z.; Karaczyn, A.; Sliva, T.Y.; Glowiak, T. Co-ordination ability of novel tetradentate amide-and-oxime ligands: differential binding to Cu<sup>II</sup> and Ni<sup>II</sup>. *J. Chem. Soc. Dalton Trans.* 1998, 21, 3629-3634.
9. Domasevitch, K.V.; Gerasinchuk, N.N.; Mokhir, A. Organoantimony(V) cyanoximates: Synthesis, spectra and crystal structures. *Inorg. Chem.* 2000, **39**, 6, 1227-1237.
10. Pathak, M.; Bohra, R.; Mehrotra, R. C.; Lorenz, I.; Pitrowski, H. Heteroleptic complexes of zirconium acetylacetonates: structural characterisation of [(acac)<sub>2</sub>Zr(ONC(Me)py-2)]<sub>2</sub>. *Z. Anorg. Allg. Chem.* 2003, **629**, 14, 2493-2498.
11. Burdinski, D.; Bill, E.; Brielbach, F.; Wieghardt, K.; Chaudhuri, P. Long range exchange interactions and integer-spin S<sub>T</sub> = 2 EPR spectra of a Cr(III)Zn(II)Cr(III) species with multiplet mixing. *Inorg. Chem.* 2001, **40**, 1160-1166.
12. Aakeroy, C.B.; Sinha, A.S.; Epa, K.N.; Chopade, P.D.; Smith, M.M.; Desper, J. Structural chemistry of oximes. *Cryst. Growth Des.* 2013, **13**, 6, 2687-2695.
13. Fischer, H. 2,4-Dimethyl-3,5-dicarbethoxypyrrole. *Org Synth.* 1935, **15**, 17-19.
14. Fischer, H. Cryptopyrrole (2,4-dimethyl-3-ethylpyrrole). *Org Synth.* 1941, **21**, 67-70.
15. *Private communication.* Nikolayenko, I.V. 2008.
16. Cheadle, C.; Gerasimchuk, N.N.; Barnes, C.L.; Tyukhtenko, S.I.; Silchenko, S. The first bis-cyanoxime: synthesis and properties of a new versatile and accessible polydentate bi-functional building block for coordination and supramolecular chemistry. *Dalton Trans.* 2013, **42**, 14, 4931-4946.
17. Bruice, P.Y. *Organic Chemistry*, 5<sup>th</sup> ed., Pearson International: Saddle River, 2007.
18. Clayden, J.; Greeves, N.; Warren, S.; Wothers, P. *Organic Chemistry*. Oxford: USA, 2000.
19. Jackson, G.E.; Nakani, B.S. A potentiometric and spectroscopic study of copper(II) diaminodioxime complexes. *J. Chem. Soc. Dalton Trans.* 1996, 7, 1373-1377.
20. Fritsky, I.O.; Karaczyn, A.; Kozlowski, H.; Glowiak, T.; Prisyazhnaya, E.V. Crystal and molecular structure of two tetradentate "oxime-and-amide" ligands. *Z. Naturforsch.*, 1999, **54**, 4, 456-460.
21. Roberts, M.W. Birth of the catalytic concept. *Catal. Lett.* 2000, **67**, 1, 1-4.
22. Rutger, S. *Catalysis: from principles to applications*, 1<sup>st</sup> ed., Wiley, 2012.

23. Flickinger, E.D.; Isom, J.T. Process of treating a reaction mixture from the production of phenol to cumene. G.B. Patent 1207133. November 23, 1966.
24. Morin, T. J.; Bennet, B.; Lindeman, S. V.; Gardinier, J. R. First-Row Transition-Metal Complexes of a new Pentadentate Ligand,  $\alpha, \alpha', \alpha''$ -Tetra(pyrazolyl)lutidine. *Inorg. Chem.* **2008**, 47(17), 7468-7470.
25. Wiedemann, D.; Swietek, E.; Macyk, W.; Grohmann, A. Copper(I) and Iron(II) complexes of a novel tris(pyridyl)ethane-derived N<sub>4</sub> Ligand: Aspects of redox behaviour and bioinorganic physiochemistry. *Z. Anorg. Allg. Chem.* 2013, **639**, 8-9, 1483-1490.
26. Stephen Stoker, H. *General Organic and Biological Chemistry*. 6<sup>th</sup> ed., Brooks/Cole: Belmont, 2011.
27. University of Windsor. Protecting Groups. <http://mutuslab.cs.uwindsor.ca/green/4531/Protecting%20Groups.pdf> (accessed Dec 18, 2013)
28. Green, T.W.; Wuts P.G. M. *Protective Groups in Organic Synthesis*; Wiley-Interscience: New York, 1999.
29. Organic Chemistry Portal. Protecting Group Stability. <http://www.organic-chemistry.org/protectivegroups/hydroxyl.shtm> (accessed Feb 02, 2011)
30. Williamson, A. Theory of aetherification. *Philosophical Magazine*, 37, 1850, pp 350-356.
31. Cristau, H.J.; Herve, A.; Loiseau, F.; Virieux, D. Synthesis of a new arylhydroymethylphosphinic acid and derivatives. *Synthesis*, 2003, **14**, 2216-2220.
32. Organic Chemistry Portal. Protecting Group Stability <http://www.organic-chemistry.org/protectivegroups/amino.shtm>. (accessed Feb 02, 2011)
33. Osby, J.O.; Martin, M.G.; Ganem, B. An exceptionally mild deprotection of phthalimides. *Tetrahedron Lett.* 1984, **25**, 20, 2093-2096.
34. Bouzide, A.; Sauvé, G. Highly selective silver(I) oxide mediated monoprotection of symmetrical diols. *Tetrahedron Lett.* 1997, **38**, 34, 5945-5948.
35. Smith, M.B.; March, J. *March's Advanced Organic Chemistry*, 6<sup>th</sup> Ed.; Wiley-Interscience: New Jersey, 2007.
36. Appel, R. Tertiary phosphene/tetrachloromethane, a versatile reagent for chlorination, dehydration, and P-N Linkage. *Angew. Chem. Int. Ed.* 1975, **14**, 12, 801-811.
37. Denton, R.M.; An, J.; Blake, A. J.; Lewis, W.; Poulton, A.M. Catalytic phosphorous(V)-mediated nucleophilic substitution reactions: development of a catalytic Appel reaction. *J. Org. Chem.* 2011, **76**, 16, 6749-6767.
38. Kalkeren, A.H.; Leenders, S.H.A.M.; Hommersom, C.R.A.; Rutjes, F.P. J.T.; Delft, F.L. In situ phosphine oxide reduction: a catalytic Appel reaction. *Chem. Eur. J.* 2011, **17**, 40, 11290-11295.
39. Appel Reaction Mechanism. [http://en.wikipedia.org/wiki/File:Appel\\_Reaction\\_Mechanism.png](http://en.wikipedia.org/wiki/File:Appel_Reaction_Mechanism.png) (accessed Jan 14. 2014).
40. Díez-Barra, E.; de la Hoz, A.; Moreno, A.; Sánchez-Verdú, P. Phase transfer catalysis without solvent: selective mono- or di-alkylation of malononitrile. *J. Chem. Soc., Perkin Trans. 1* , 1991, **10** , 2589-2592.
41. Curran, D.P.; Min Seong, C. Radical annulation reactions of allyl iodomalnonitriles. *Tetrahedron* , 1992, **48**, 11, 2175-2190.
42. Amundsen, L.H.; Nelson, L.S. Reduction of nitriles to primary amines with lithium aluminum hydride. *J. Am. Chem. Soc.* , 1951, **73**, 242-244.
43. Hutchings, R.O.; Maryanoff, B.E. 2-tert-Butyl-1,3-diaminopropane. *Org Synth.* 1973, **53**, 22.
44. Sundaramoorthi, R.; Keenan, T.P. Hydrogenation of imino-bisnitriles-synthesis of novel triamines. *Synth Comm.* 2007, **37**, 3, 417-423.
45. Sigma Aldrich Catalogue. <http://www.sigmaaldrich.com/chemistry/chemical-synthesis/technology-spotlights/bh3-thf-solutions.html>. (accessed Feb 11, 2014)
46. Sigma Aldrich Catalogue. <http://www.sigmaaldrich.com/catalog/product/aldrich/192120?lang=en&region=ZA>. (accessed Feb 11, 2014)

47. Inaba, Y.; Fujimoto, T.; Ono, H.; Obata, M.; Yano, S.; Mikata, Y. A general route to pendant C-glycosyl 1,2- and 1,3-diamines. *Carbohydrate Research*. 2008, **343**, 5, 941-950.
48. Whitmore, Raney, M. Method of preparing catalytic material. U.S. Patent 1,563,587, December 1, 1925.
49. Albertson, N.F.; Archer, S. A synthesis of di-ornithine hydrochloride. *J. Am. Chem. Soc.* 1945, **67**, 2043-2044.
50. Akerman, M.P., Structural, physical and biological studies of gold(III)-bis(pyrrrolide-imine) Schiff base complexes: potential chemotherapeutic agents. Ph.D. Dissertation, University of Kwa-Zulu Natal, Pietermaritzburg, South Africa, 2010.
51. Olmsted, J.; Williams, G. M. *Chemistry.*; 3<sup>rd</sup> ed.; Wiley: New York, 2002.
52. Tanabe, M.; Peters, H. (*R,S*)-Mevalonolactone-2-<sup>13</sup>C. *Org. Synth.* 1981, **60**, 92.
53. Calzada, J.G.; Hooz, J. Geranyl Chloride. *Org. Synth.* 1974, **54**, 63.
54. Wang, K.; Nguyen, K.; Huang, Y.; Dömling, A. Cyanoacetamide multicomponent reaction (I): parallel synthesis of cyanoacetamides. *J. Comb. Chem.* 2009, **11**, 5, 920-927.
55. Briggs, C.B.A.; Newington, I.M.; Pitt, A.R. Synthesis and properties of some novel non-ionic polyol surfactants. *J. Chem. Soc. Chem. Commun.* 1995, **3**, 379-380.
56. Appleton, T.G.; Hall, R.J. Complexes with six-membered chelate rings. IV. Preparation of some complexes of 1,3-diaminopropan-2-ol and chloropropane-1,3-diamine with Platinum and Palladium. *Inorg. Chem.* 1972, **11**, 112-117.
57. Gaunt, M.J.; Yu, J.; Spencer, J.B. Rational design of benzyl-type protecting groups allowed sequential deprotection of hydroxyl groups by catalytic hydrogenolysis, *J. Org. Chem.* 1998, **63**, 4172-4173.
58. Kutiyaama, W.; Matsumoto, T.; Ogata, O.; Ino, Y.; Aoki, K.; Tanaka, S.; Ishida, K.; Kobayashi, T.; Sayo, N.; Saito, T. *Organic Process Research and Development*. Catalytic hydrogenation of esters. Development of an efficient catalyst and processes for synthesising (*R*)-1,2-propanediol and 2-(*l*-menthoxy) ethanol. 2012, **16**, 1, 166-171.
59. Frankowski, K.J.; Golden, J.E.; Zeng, Y.; Lei, Y.; Aubé, J. Syntheses of the stemona alkaloids (+/-)-stenine, (+/-)-neostenine, and (+/-)-13-epineostenine using a sterodivergent Diels-Alder/Azido-Schmidt reaction. *J. Am. Chem. Soc.* 2008, **130**, 18, 6018-6024.
60. Dickschat, J.S.; Citron, C.A.; Nelson, L. Brock, N.L.; Riclea, R.; Kuhz, H. Synthesis of deuterated mevalonoacetone isotopomers. *Eup. Org. Chem.* 2011, **18**, 3339-3346.
61. Halcomb, R.L.; Huang, H.; Wong, C-H. Solution- and solid-phase synthesis of inhibitors of *H. pylori* attachment and e-selectin-mediated leukocyte adhesion. *J. Am. Chem. Soc.* 1994, **116**, 25, 11315-11322.
62. Tucker, J.W.; Narayanam, T.M.R.; Shah, P.S.; Stephenson, C.R.J. Oxidative photoredox catalysis: mild and selective deprotection of PMB ethers mediated by visible light. *Chem. Commun.* 2011, **47**, 11, 5040-5042.
63. *Private communication*, Naseem, A. 2008.
64. Hammerschmidt, F.; Kählig, H. Biosynthesis of natural products with a P-C Bond. 7. Synthesis of [1,1-<sup>2</sup>H<sub>2</sub>]-, [2,2-<sup>2</sup>H<sub>2</sub>]-, (*R*)- and (*S*)-[1-<sup>2</sup>H<sub>1</sub>](2-hydroxyethyl)phosphonic acid and (*R,S*)-[1-<sup>2</sup>H<sub>1</sub>](1,2-dihydroxyethyl)phosphonic acid and incorporation studies into fosfomycin in streptomyces fardiae. *J. Org. Chem.* 1991, **56**, 7, 2364-2370.
65. Machida, S.; Kato, N.; Harada, K.; Ohkanda, J. Bivalent inhibitors for disrupting protein surface-substrate interactions and dual inhibition of protein prenyltransferases. *J. Am. Chem. Soc.* 2011, **133**, 4, 958-963.
66. Jew, S.; Kim, H.; Jeong, B.; Park, H. Asymmetric synthesis of (*R*)-(+)-etomoxir. *Tetrahedron: Asymmetry*. 1997, **8**, 8, 1187-1192.
67. Dai, C.; Jagan, M.R.; Stephenson, C.R.J. Visible light mediated conversion of alcohols to halides. *Nature Chemistry*. 2011, **3**, 2, 140-145.
68. Zhang, M.; Zhang, A-Q.; Chen, H-H.; Chen, J.; Chen, H-Y. Fast methods for synthesis of ylidenemalononitriles. *Synthetic Communications*. 2006, **36**, 22, 3441-3445.



69. Moussaoui, Y.; Salem, R.B. Catalysed Knoevenagel reactions on inorganic solid supports: application to the synthesis of coumarine compounds. *C. R. Chimie.* 2007, **10**, 1162-1169.

# CHAPTER B

## New Cyanoxime-and-Amide *bis*-Chelate Ligands

### 0. A Note On the Notation

As the contents of Chapter A and Chapter B are essentially independent and are bound only by the common theme of oxime-and-amide ligands pursued in our research group, we have decided to introduce independent numbering of Figures, Tables, Schemes, References, compounds, etc. in each of these Chapters. If a reference, say, to a Figure 5 from Chapter A is made in Chapter B, it would be expanded to Figure 5A. Within the same Chapter it would be referred to simply as Figure 5.

### 1. Introduction

As has already been mentioned in the introduction to Chapter A, the interest in the research group to which I belong is focused on the synthesis, characterisation, and both solid state and solution studies of the *mono*- and *bis*-chelate ligands with the hydroxyiminoacetamide (**hiao**) moiety, Figure 1, as well as their metal complexes with late *3d*-transition metals.

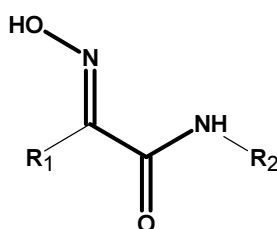


**Fig. 1.** Generic structure of a ligand with hydroxyiminoacetamide (**hiao**) chelating moiety (highlighted).

Prior to present work, most of the research published in literature, as well as research performed in our group, was centred on ligands with  $R_1 = \text{CH}_3$ . *Bis*-chelates of such nature (we shall abbreviate them

as **mhiaa<sub>2</sub>z**<sup>\*</sup>) and their metal complexes possess a range of attractive structural and physical properties. Please refer to the introduction in Chapter A for more detail. In addition to the Ni(II) and Cu(II) pseudo-macrocyclic *mono*-nuclear **mhiaa<sub>2</sub>z** complexes of the MLH<sub>3</sub> composition,<sup>[1-3]</sup> which we have discussed previously, **mhiaa<sub>2</sub>z** ligands with even number of methylene groups in the bridge, namely, **mhiaa<sub>2</sub>e** and **mhiaa<sub>2</sub>b**, were shown to form dinuclear-diligand complexes with Cu(II).<sup>[4]</sup> Spectroscopic (UV-Vis and ESR) and structural studies of these complexes indicated different coordination environment around the metal. In particular, for [M] : [L] = 1 : 1, in the pH range from fairly acidic to slightly basic (where the deprotonation of only oxime groups occurs), conformation of the oxime-and-amide moiety changes from *E* to *Z*, and the square-planar coordination environment around copper(II) becomes 2N(ox)2O(ad), the mode entirely different from the 2N(ox)2N(ad) coordination environment discussed previously for the mono-dentate complexes.

Reported initially by Fritsky *et al.*,<sup>[4]</sup> as well as confirmed in our group,<sup>[5]</sup> crystal structures of such complexes revealed chelation not previously observed for these ligands, Figures 2-3. Inability of the *bis*-chelate to bind the same Cu(II) centre in its protonated amide conformation led to interesting two-platforms di-metal di-ligand complexes (see below). As already mentioned, such structures arise both in solution and in solid state only if the flexible bridge between two chelate units consists of an even number of methylene groups (2 or 4). For **mhiaa<sub>2</sub>p** ligand, where the bridge consists of 3 methylene groups, no formation of such complex is observed at all.

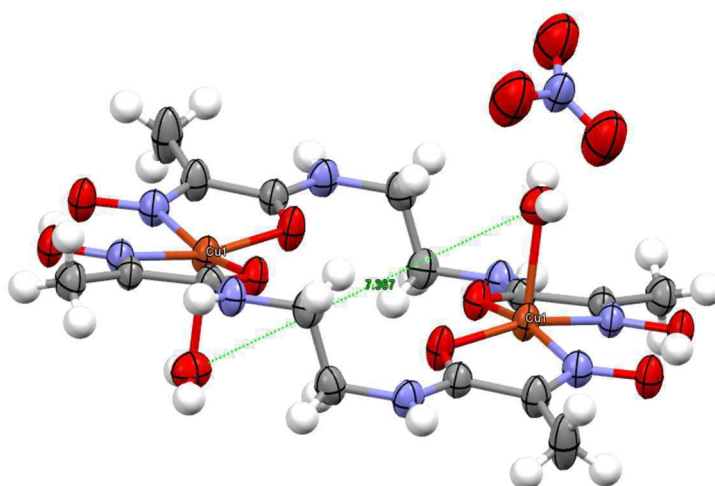


**Fig. 2.** Solid state structure of the di-copper – di-ligand complex [Cu<sub>2</sub>(mhiaa<sub>2</sub>eH.1)<sub>2</sub>].<sup>[5]</sup>

\* This abbreviation is derived from two **methylhydroxyiminoacetamide** units and **z** representing the nature of a flexible bridge, e.g., z = e for ethane, z = p for propane, etc.

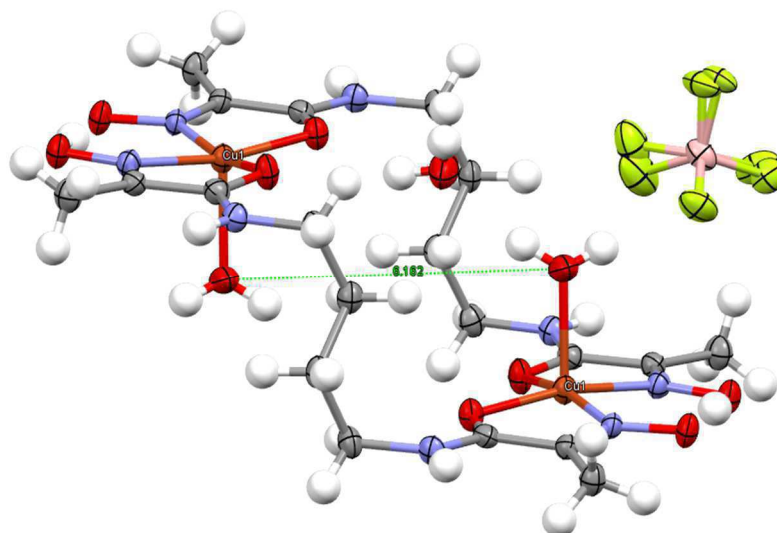


**Fig. 3.** Solid state structure of the di-copper – di-ligand complex  $[\text{Cu}_2(\text{mhiala}_2\text{bH.1})_2]$ .<sup>[5]</sup>

Among distinctive geometrical features of these complexes are: a) square-planar 2N(ox)2O(ad) coordination environment around copper, b) “two-platform” stepwise shape, c) relief of a steric strain on the polymethylene bridge via adopting a “zig-zag” conformation. Nevertheless, as for 2N(ox)2N(ad) complexes, the planarity of the metal bound sites is aided by the fact that both chelating units are in prearranged planar conformation due to the  $\pi$ -conjugation of oxime and amide groups. Another essential stabilising feature is partial deprotonation of the terminal oxime groups and the formation of short intra-molecular hydrogen bond between one ligand deprotonated and another ligand still protonated oxime group. The latter adds pseudo-macrocyclic character to the complex structure and increases its thermodynamic stability.

Taking into account the formation of stable Ni(II)- and Cu(II)-complexes with **mhiala<sub>2</sub>** ligands, where the planarity of **mhiala** moiety, the nucleophilicity of its donor centres, and the conformational shape of the chelate all play essential role, we deemed it extremely interesting to explore the influence of an electron withdrawing group in place of the methyl group on the above factors, as well as on the complex stability. Supported in part by quantum-mechanical modelling in our group, the expectation was that strongly electron withdrawing functional group (such as nitrile) will render oxime (and possibly amide) protons of **hiala** more acidic, resulting in their early (at lower pH) deprotonation and affecting the stability of metal complexes. Also, we were curious to explore how this newly increased acidity of the oxime groups will affect intra-molecular hydrogen bonding of the pseudo-macrocyclic complexes, and thus reveal its relative significance in stabilising such structures.

The first test of the concept of electron redistribution within the **hiala** moiety, came from the comparison of the protonation behaviour of two similar acetamides,  $\text{NCC(=NOH)C(=O)NH}_2$  (**chiala**) and  $\text{H}_3\text{CC(=NOH)C(=O)NH}_2$ , (**mhiala**), Figure 4.

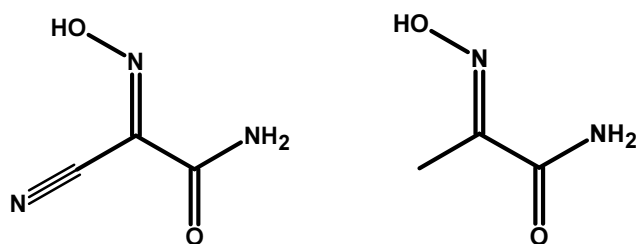


**Fig. 4.** 2-Cyano-2-(hydroxyimino)acetamide or **chiaa** (left) and 2-hydroxyiminopropanamide or **mhiaa** (right).

According to Sliva *et al*,<sup>[6]</sup> oxime protonation constants for **mhiaa** and **chiaa** were found to be 9.87 and 5.12 (for  $\log_{10}K$ ), respectively. As anticipated, there is huge increase (by more than 4 orders of magnitude!) in the acidity of the oxime proton, in response to placement of the electron withdrawing nitrile group in immediate vicinity of the oxime group.

The thermodynamics of protonation and metallation of a range of *bis*-chelate **mhiaa<sub>2z</sub>** ligands, Figure 5, with Co(II), Ni(II), and Cu(II) in aqueous solutions have been investigated in our group in recent years.<sup>[5]</sup>

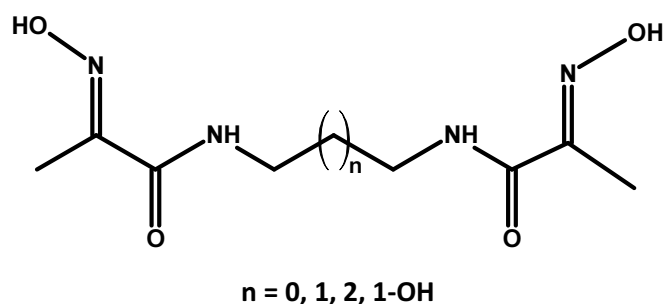


**Fig. 5.** **Mhiaa<sub>2z</sub>** ligands investigated in our group previously.<sup>[5]</sup>

In line with the considerations expressed above, in this Chapter of the thesis we will describe the synthesis and characterisation of a range of similar **chiaa<sub>2z</sub>** ligands, Figure 6, intended for the future protonation and metallation thermodynamic studies.

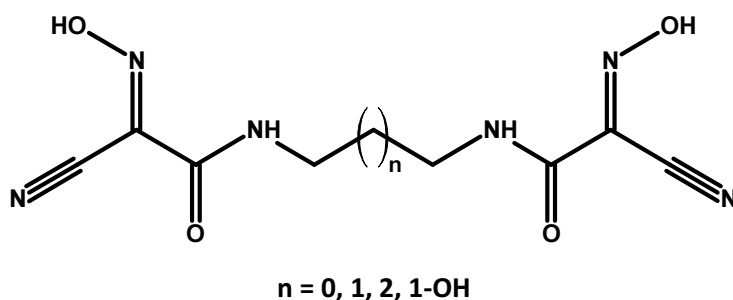


**Fig. 6.** *Bis*-chelate cyano-hydroxyiminoacetamide (**chiaa<sub>2z</sub>**) ligands to be studied in the second part of the project.

## 2 Literature Survey

### 2.1 Introduction to Cyanoximes

Early addition of the hydroxyimino (oxime) group to an organic molecule is traceable to the work of Victor Meyer and Alios Janny, who explored the synthesis of aldoximes and ketoximes, Figure 7.<sup>[7-8]</sup>

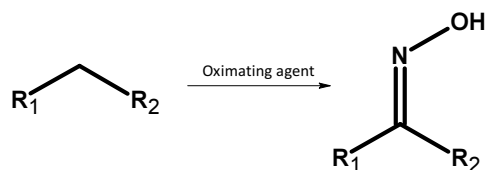


**Fig. 7.** The concept of synthetic approach to oximation after Victor Meyer.<sup>[8]</sup>

By constraining one of the above substituent groups to a nitrile, first cyanoximes were prepared. They have found application as intermediates in the synthesis of heterocyclic systems.<sup>[9-11]</sup> Oximes also proved useful in the area of coordination chemistry, as they form fairly stable complexes or salts with a variety of metal ions; among them, Ni(II), Cu(II), Pb(II), Ag(I), Tl(I) and Sb(V), to mention a few.<sup>[6, 12, 13]</sup> In recent years oximes have attracted attention as building blocks in supramolecular assemblies,<sup>[14, 15]</sup> possible gas sensors,<sup>[16]</sup> and medical indwelling devices.<sup>[17]</sup>

Our interest in this area is associated with the oxime-and-amide ligands, traceable to the study of 2-(hydroxyimino)propanamides, H<sub>3</sub>C-C(=NOH)CONH-, by Lau and Gutsche,<sup>[18]</sup> and later by Onindo *et al.*<sup>[19]</sup> Structurally such ligands are similar to dipeptides but for the oxime functionality in place of the terminal amino group. XRD data for a number of Cu(II)-complexes of *N*-pyruvoylaminoacid oximes confirmed the fact that the ligand chelate moiety was ambidentate, and the square-planar complexes formed were characterised by high degree of planarity. Two major chelation modes were established: a) N(oxime) N(amide) and b) a conformationally altered N(oxime) O(carbonyl).<sup>[1, 2, 19]</sup>

As already mention in the Introduction to this Chapter, conceptual idea for this part of the project was to look at the consequences the replacement of the methyl group riding oxime carbon with strongly electron withdrawing group (such as nitrile) would have on the properties of *bis*-chelate ligands, as well as on their binding of transition metals. First potentiometric and spectroscopic data by Sliva *et al.*<sup>[6]</sup> for the ligand with 2-cyan(hydroxyimino)acetamide moiety confirmed very substantial change in the protonation and metallation behaviour in comparison to the methylated ligand.

At this point we would like to review coordination properties of individual functional groups and their combinations in the ligands under discussion.

## 2.2 Coordination Chemistry of Isolated Functional Groups

Coordination behaviour of the isolated oxime and amide groups has been already reviewed in chapter A, and the reader is advised to consult it, (pages 7-9). We will also skip the discussion of coordination behaviour of an isolated nitrile group as it not relevant to the focus of present work.\*

## 2.3 Coordination by Cyanoximes

As already mentioned in the Introduction, the *cyanoxime moiety* consists of a hydroxyimino group with one of the substituents being a nitrile. In general the formula is:  $\text{N}\equiv\text{C}-\text{C}(\text{=N-OH})\text{R}_1$ , Figure 8.

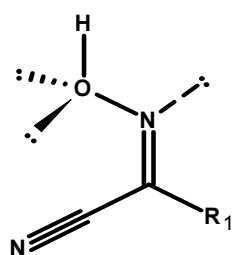


**Fig. 8.** Generic view of the cyanoxime moiety in its most stable conformational form with the lone pairs available for the metal coordination displayed.

Cyanoxime moiety is effectively planar for most of the substituent groups R<sub>1</sub>. Two lone pairs carried by the oxygen atom are out of plane of this moiety, while the oxime nitrogen lone pair is in plane. The very existence of these lone pairs and the ability of oxime group to deprotonate allow for the metal to be coordinated in a number of modes. Among them are monodentate coordination to oxime nitrogen<sup>[2]</sup> or oxime oxygen,<sup>[20]</sup> chelating coordination to the N-O unit by the same metal,<sup>[21]</sup> or monodentate coordination of two metal centres to the same N-O pair;<sup>[13]</sup> with the involvement of two or more ligands the latter commonly results in the formation of polynuclear complexes, where the metal ions are linked in a bridging manner. Cyanoximes have the ability to form salts or stable complexes with a variety of metals; the examples include benzoylcyanoxime complexes of Ni(II), Cu(II) and Ag(I) and hydroxyiminopropanamide complexes of Sb(V) and Sn(IV), to mention a few.<sup>[12, 20, 22]</sup>

\* It will be briefly considered later in the section on crystallography (Section 3.4).

## 2.4 Coordination Chemistry of the CHIAA Moiety.

Placing the cyanoxime and amide functionality in immediate vicinity of each other in the same molecule leads to the ligands with strong chelation preference towards transition metals. Coordination chemistry of the HIAA moiety has been already discussed in chapter A. A reader is advised to consult the relevant section of the thesis (pages 9-10).

The first ligand of this kind, 2-cyano-2-(hydroxyimino)ethanamide, Figure 9, was synthesised in 1909 by Conrad and Schulze,<sup>[23]</sup> though its coordination behaviour remained unexplored until the 1997 work of Sliva *et al.*<sup>[6]</sup>

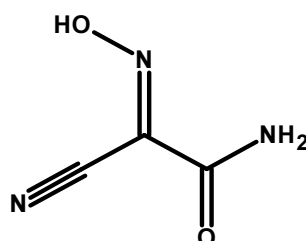


**Fig. 9.** 2-Cyano-2-(hydroxyimino)ethanamide (**chiaad**), the first cyanoxime-and-amide chelating ligand.

From the spectroscopic and solid state studies of the Ni(II) complexes of this ligand the authors concluded that the metal centre in them was in a distorted square planar N4 coordination environment. Two ligand molecules coordinated the same metal in a chelate manner and were *trans* to each other.<sup>[6]</sup> A year later Sliva *et al.*<sup>[13]</sup> synthesised the first ligand derived from a diamine, (2*E*)-*N*-(2-aminoethyl)-2-cyano-2-(hydroxyimino)ethanamide (**chiaaea**), Figure 10. On the grounds of spectroscopic evidence it was also shown to bind Cu(II).

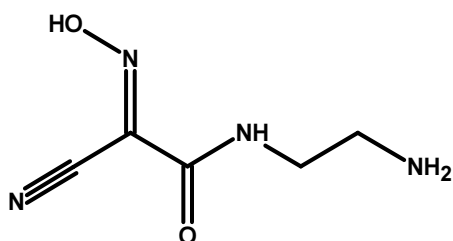


**Fig. 10.** (2*E*)-*N*-(2-aminoethyl)-2-cyano-2-(hydroxyimino)ethanamide ligand.

Since then, more than a dozen of other cyanoxime-and-amide ligands and their metal complexes were reported in literature. We will provide the list of synthesised to date **chiaa** ligands in section 2.7.



## 2.5 Bis-Chelate Ligands with CHIAA Moieties

Combining two cyanoxime-and-amide moieties in one molecule leads to *bis*-chelate ligands, which are the subject of our project.

To the best of our knowledge only two cyanoxime-and-amide *bis*-chelate ligands were reported previously. The first of them, **chiaa<sub>2</sub>p** ligand, Figure 11, was synthesised by Kolotilov *et al.*,<sup>[24]</sup> who also studied magnetic properties of the materials derived from its dinuclear and trinuclear Cu(II) amido oximate complexes.

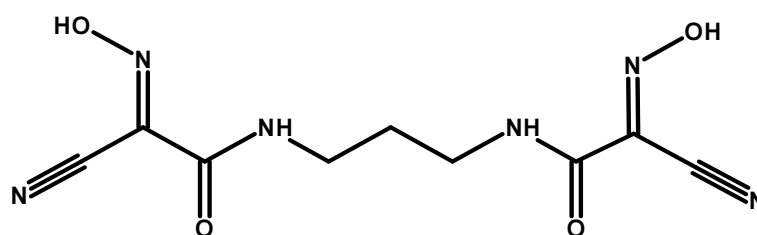


**Fig. 11.** (2*E*,2*E'*)-*N,N'*-propane-1,3-diylbis[2-cyano-2-(hydroxyimino)ethanamide] (**chiaa<sub>2</sub>p**) ligand.

Clearly, the ligand was able to bind copper centres, though no meaningful characterisation of such complexes was reported. Individual complexes were spontaneously assembled into multinuclear metal clusters, and the authors were primarily interested in the magnetic properties of the latter.

The second ligand, (2*E*,2*E'*)-3,3'-piperazine-1,4-diylbis[2-(hydroxyimino)-3-oxopropanenitrile] or (**chiaa<sub>2</sub>ppz**), was prepared by Cheadle *et al.*<sup>[15]</sup> as a bifunctional building block for supramolecular and coordination chemistry, Figure 12.

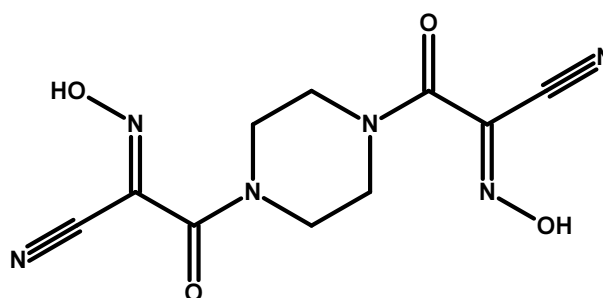


**Fig. 12.** Molecular structure of (2*E*,2*E'*)-3,3'-Piperazine-1,4-diylbis[2-(hydroxyimino)-3-oxopropane-nitrile] or (**chiaa<sub>2</sub>ppz**) ligand.<sup>[15]</sup>

As shown by the XRD structure of **chiaa<sub>2</sub>ppz** Tl(I)-complex, the metal centre in it is coordinated to five deprotonated oxime groups. A number of other metal ions also formed complexes with this ligand; among them were monovalent sodium, silver and thallium, and divalent nickel, palladium and platinum.

The mention of **chiaa<sub>2</sub>p** ligands in literature inspired optimism, as it was one of the series of ligands desired in this project. We hoped that its preparation<sup>[24]</sup> will provide a template for the synthesis of other new ligands of this series.

In conclusion, we can reiterate that two examples of the *bis*-chelate ligands with cyanoxime-and-amide moieties have been reported in literature, and that such ligands have been shown to bind Ni(II) and Cu(II) strongly, both in solution and in the solid state.

## 2.6 Possible Applications of Ligands with Cyanoxime-and-Amide Chelates

In this section we will take a brief look at the real world applications of cyanoximes.

A number of cyanoximes have found industrial applications as plant growth regulators, e.g., 2-cyano-2-(hydroxyimino)ethanamide or  $\text{NCC(=N-OH)C(=O)NH}_2$ , and antidotes for pesticides, e.g., 2-cyano-2-(hydroxyimino)-*N,N*-dimethylethanamide or  $\text{NCC(=N-OH)C(=O)N(CH}_3)_2$ .<sup>[12, 20]</sup>

A range of promising sophisticated uses of this type of ligands and their metal complexes is expanding. Among some of them reported recently are tin(IV) cyanoximates as anti-cancer agents,<sup>[22]</sup> and precursors to peptide coupling agents.<sup>[25,26]</sup> Pd(II) and Pt(II) complexes of 2-(hydroxyimino)-3-(morpholin-4-yl)-3-oxopropanenitrile (**hmco**), Figure 13, were also shown to have anticancer activity,<sup>[27]</sup>

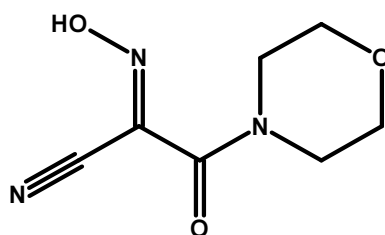


**Fig. 13.** Molecular structure of (2*E*)-2-(hydroxyimino)-3-(morpholin-4-yl)-3-oxopropanenitrile (**hmco**).

Ag(I)-2-cyano-2-(hydroxyimino)ethanamide or  $\text{NCC(=NOAg)C(=O)NH}_2$  and silver (I) salts of other cyanoximes studied by Gerasimchuck *et al*.<sup>[16]</sup> exhibited long term light insensitivity, which is unusual for the silver(I) compounds of this nature. However, in the presence of NO(g), HCCH(g), H<sub>2</sub>(g), CO(g) or C<sub>2</sub>H<sub>4</sub> (g) with light exposure certain amount of visible degradation occurred. Such behaviour allows these types of silver oxime salts to be used as non-electric gas sensors.<sup>[16]</sup>

Silver(I) complexes of cyanoxime-and-amide ligands show high thermal stability, low solubility in aqueous environments and antibiotic activity, which are desired qualities for medical indwelling<sup>†</sup> antimicrobial agents.<sup>[17]</sup>

Also, a range of Mn(II) 2-pyridylcyanoximes have been investigated recently as promising magnetic materials.<sup>[28]</sup>

<sup>†</sup> The term **indwelling antimicrobial agent** in this context refers to a device that is fixed to a bone near an implant with a purpose of suppressing microbial matter that threatens to infect the site and cause the implant rejection.

## 2.7 Synthesis of the CHIAA moiety

With the synthesis of *bis*-chelate **chiaa** ligands being primary aim of the project, in this section we will take a look at how a number of structurally similar cyanoxime-and-amide species have been prepared, in a search for general synthetic path.

### 2.7.1 General approach to the synthesis of cyanoxime-and-amide molecular fragment

To the best of our knowledge, the first case of preparation cyanoxime-and-amide fragment is the nitrosation of 2-cyanoacetamide or  $\text{NCCH}_2\text{CONH}_2$  according to Conrad and Schulze,<sup>[23]</sup> which can be classified as a Meyer-type reaction.<sup>[8]</sup> In this process, 2-cyanoacetamide is treated with aqueous solution of sodium nitrate and glacial acetic acid, resulting in the conversion of methylene group into a deprotonated oxime group. Following treatment of the crude product (oxime sodium salt) with acid affords free cyanoxime-and-amide chelate.<sup>[23]</sup>

The preceding paragraph gave an example of oximation under acidic conditions; later it was found that similar conversion will proceed also under basic conditions. Indeed, a number of examples relevant to this work exist where such conditions were employed. Consequently, two major routes need to be considered for the 2-cyanamide oximation: acidic and basic oximation. A number of different acids were used in the low *pH* synthesis; also, a wide range of different bases and various alkyl nitrite agents were used under the basic conditions. In addition, a variation in the sequence of oximation and condensation synthetic steps was reported.

In the following two tables, Table 1 and 2, we have summarised the bulk of published information on the preparation of cyanoxime-and-amide species; in particular, we reflected on the order of synthetic steps and reaction conditions.

The data presented in the tables allow to classify preparation of **chiaa** ligands on the basis of nitrosation conditions (acidic or basic) and the sequence of synthetic steps (nitrosation before condensation<sup>†</sup> or vice versa). From this viewpoint, their preparation can be subdivided into four classes. In the next two sections we will discuss a few examples chosen from each class.

---

<sup>†</sup> In this thesis the reaction between an amine and an ester, resulting in the formation of an amide, will be referred to as a condensation as it gives off an alcohol.

**Table 1.** Cyanoxime-and-amide ligands synthesised via acidic nitrosation.

No	Oxime	Precursor	Step one	Step two	Solvent	Nitrite source	Acid	Reference
1	$\text{NCC(=N-OH)C(=O)NH}_2$	$\text{NCCH}_2\text{C(=O)NH}_2$	Cond.	Nitr.	H <sub>2</sub> O	NaNO <sub>2</sub>	Acetic	[23, 6]
2	$\text{NCC(=N-OH)C(=O)NHCH}_2\text{CH}_2\text{NH}_2$	$\text{NCC(=N-OH)C(=O)OCH}_2\text{CH}_3$	Nitr.	Cond.	H <sub>2</sub> O	NaNO <sub>2</sub>	Acetic	[13 <sup>§</sup> ]
3	$\text{NCC(=N-OH)C(=O)N(CH}_3)_2$	$\text{NCCH}_2\text{C(=O)N(CH}_3)_2$	Cond.	Nitr.	H <sub>2</sub> O	KNO <sub>2</sub>	Acetic	[20]
4	$\text{NCC(=N-OH)C(=S)N(CH}_3)_2$	$\text{NCCH}_2\text{C(=S)N(CH}_3)_2$	Cond.	Nitr.	H <sub>2</sub> O	NaNO <sub>2</sub>	HCl	[20]

**Table 2.** Cyanoxime-and-amide ligands synthesised via basic nitrosation.\*\*

Nö	Oxime	Precursor	Step one	Step two	Solvent	Nitrite source	Base	Reference
1	$\text{NCC(=N-OH)C(=O)NH}_2$	$\text{NCCH}_2\text{C(=O)NH}_2$	Cond.	Nitr.	EtOH / MeOH	EtONO / MeONO	EtONa / MeONa	[29, 30]
2	$\text{NCC(=N-OH)C(=O)NHCH}_3$	$\text{NCCH}_2\text{C(=O)NHCH}_3$	Cond.	Nitr.	EtOH	EtONO	EtONa	[29, 31]
3	$\text{NCC(=N-OH)C(=O)NHPh}$	$\text{NCCH}_2\text{C(=O)NHPh}$	Cond.	Nitr.	EtOH	EtONO	EtONa	[29, 31]
4	$\text{NCC(=N-OH)C(=O)NHC}_6\text{H}_{11}\text{-Cyclic}$	$\text{NCCH}_2\text{C(=O)NHC}_6\text{H}_{11}\text{-Cyclic}$	Cond.	Nitr.	EtOH	EtONO	EtONa	[29]
5	$\text{NCC(=N-OH)C(=O)NHC}_6\text{H}_4\text{Br}$	$\text{NCCH}_2\text{C(=O)NHC}_6\text{H}_4\text{Br}$	Cond.	Nitr.	EtOH	EtONO	EtONa	[29]
6	$\text{NCC(=N-OH)C(=O)NHCH}_2\text{Ph}$	$\text{NCCH}_2\text{C(=O)NHCH}_2\text{Ph}$	Cond.	Nitr.	EtOH	EtONO	EtONa	[31]
7	$\text{NCC(=N-OH)C(=O)N(CH}_2)_5\text{-Cyclic}$	$\text{NCCH}_2\text{C(=O)N(CH}_2)_5\text{-Cyclic}$	Cond.	Nitr.	<i>i</i> -PrOH / MeOH	<i>t</i> -BuONO / MeONO	<i>i</i> -PrONa / MeONa	[32], [30]
8	$\text{NCC(=N-OH)C(=O)N(CH}_2)_4\text{O-Cyclic}$	$\text{NCCH}_2\text{C(=O)N(CH}_2)_4\text{O-Cyclic}$	Cond.	Nitr.	<i>i</i> -PrOH / MeOH	<i>t</i> -BuONO / MeONO	<i>i</i> -PrONa / MeONa	[32], [30]
9	$\text{NCC(=N-OH)C(=O)NH(CH}_2)_3\text{NHC(=O)C(=N-OH)CN}$	$\text{NCCH}_2\text{C(=O)NH(CH}_2)_3\text{NHC(=O)CH}_2\text{CN}$	Cond.	Nitr.	EtOH	EtONO	EtONa	[24]
10	$\text{NCC(=N-OH)C(=O)NHC}_2\text{H}_5$	$\text{NCCH}_2\text{C(=O)NHC}_2\text{H}_5$	Cond.	Nitr.	MeOH	MeONO	MeONa	[30]
11	$\text{NCC(=N-OH)C(=O)N(CH}_2)_4\text{NC(=O)C(=N-OH)CN}$	$\text{NCCH}_2\text{C(=O)N(CH}_2)_4\text{NC(=O)CH}_2\text{CN}$	Cond.	Nitr.	<i>i</i> -PrOH	MeONO	<i>i</i> -PrONa	[15]

<sup>§</sup> Precursor is synthesised according to.<sup>[6]</sup>

\*\* The summary of nitrosation under acidic and basic conditions, presented in the above two tables, is not an exhaustive account of all published cases of preparation cyanoxime-and-amide chelates; rather it serves to provide representative examples. A number of cyanoxime-and-amide ligands with aryl functionalities were also reported. These were excluded

## 2.7.2 Nitrosation followed by condensation

One species of interest to this project, *N,N*-(2-aminoethyl)-2-cyano-2-(hydroxyimino)ethanamide, Figure 14, was synthesised by condensing ethyl 2-cyano(hydroxyimino)acetate, an already oximated intermediate, with 1,2-diaminopropane.<sup>[13]</sup>

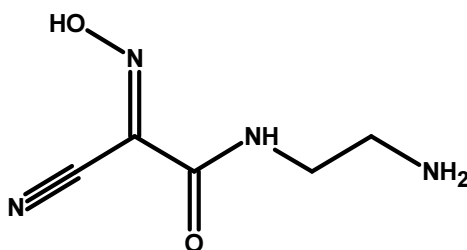


Fig. 14. *N,N*-(2-aminoethyl)-2-cyano-2-(hydroxyimino)ethanamide.

## 2.7.3 Condensation followed by nitrosation

The number of cyanoxime-and-amide ligands synthesised in this manor far exceeds the number of compounds from the previous section. We will consider representative examples in chronological order. The first two examples, 2-cyano-2-(hydroxyimino)-*N,N*-dimethylethanamide **H(DCO)**, Figure 15, and 2-cyano-2-(hydroxyimino)-*N,N*-dimethylethanethioamide, **H(TDCO)**, Figure 16, were synthesised by oximating 2-cyano-*N,N*-dimethylacetamide or  $\text{NCCH}_2\text{C}(=\text{O})\text{N}(\text{CH}_3)_2$  and 2-cyano-*N,N*-dimethylethanethioamide or  $\text{NCCH}_2\text{C}(=\text{S})\text{N}(\text{CH}_3)_2$ , respectively, with the aim to explore their antimony complexes.<sup>[20]</sup>

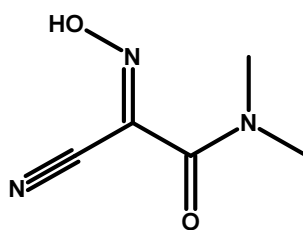
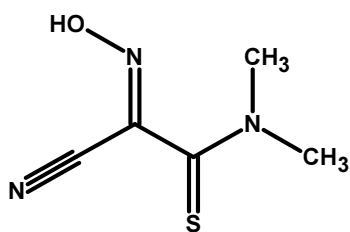


Fig. 15. 2-Cyano-2-(hydroxyimino)-*N,N*-dimethylethanamide or **H(DCO)**.

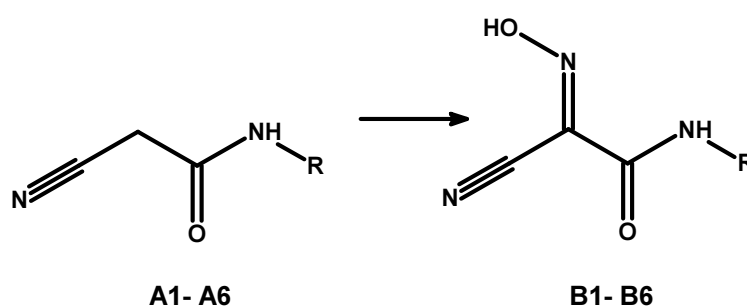
---

from the tables. Fairly extensive list of the cyanoximes studied to date can also be found in the supplementary information to the paper by Cheadle *et al.*<sup>[15]</sup>



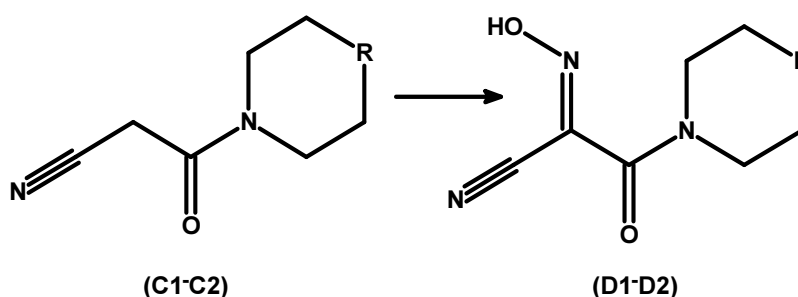
**Fig. 16.** 2-Cyano-2-(hydroxyimino)-*N,N*-dimethylethanethioamide or **H(TDCO)**.

The applicability of nitrosation after condensation route was further illustrated by the work of Kislyi *et al.*<sup>[31]</sup> and Bakulev *et al.*<sup>[29]</sup> on the cyclization reactions, for which they synthesised precursors shown below, Scheme 1.



**Scheme 1.** Cyanoxime-and-amide precursors for the cyclisation reactions, R = CH<sub>3</sub>, CH<sub>2</sub>Ph, C<sub>6</sub>H<sub>11</sub>, Ph, C<sub>6</sub>H<sub>4</sub>OCH<sub>3</sub> and C<sub>6</sub>H<sub>4</sub>Br.

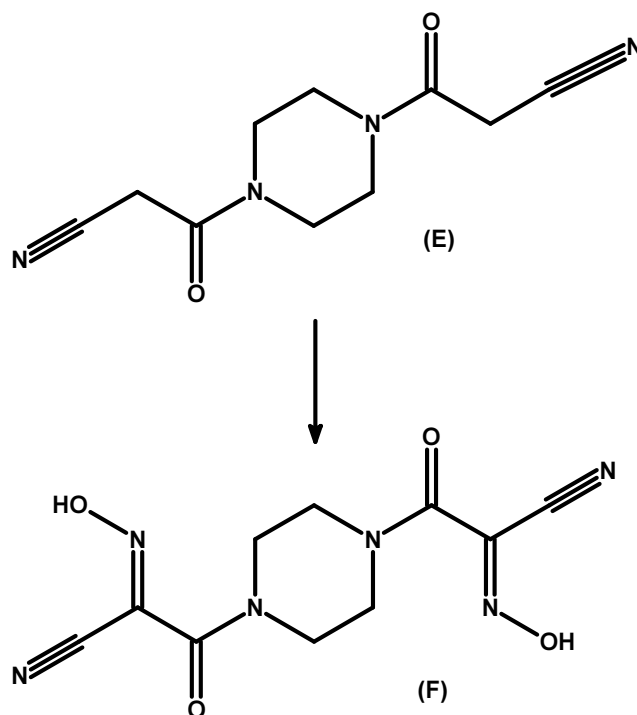
Wide range of substituents connected to the amide nitrogen (from methyl to cycloalkanes to aromatic derivatives) indicates that the process of nitrosation is fairly insensitive to the nature of the substituent group.<sup>[29, 31]</sup> The latter is encouraging if one desires to prepare a range of modified molecules. Even more complex analogues were derived from the condensation products of secondary amines, e.g., 2-(hydroxyimino)-3-oxo-3-(piperidin-1-yl)propanenitrile or **(HPiPCO)**, Scheme 2.<sup>[32]</sup>



**Scheme 2.** Reaction path for the preparation of **HPiPCO** (R = CH<sub>2</sub>) and **HMCO** (R = O).

Cyanoxime-and-amide *bis*-chelates can also be prepared in a similar manner, e.g., the condensation of ethyl cyano(hydroxyimino)ethanoate with piperazine leads to

3,3'-piperazine-1,4-diylbis(3-oxo-propanenitrile), which is then converted to 3,3'-piperazine-1,4-diylbis[2-(hydroxyimino)-3-oxo-propanenitrile], Scheme 3.<sup>[15]</sup>



**Scheme 3.** Preparation of the 3,3'-piperazine bridged *bis*-cyano(hydroxyimino)acetamide ligand (F) from intermediate *bis*-cyanoacetamide (E).

To the best of our knowledge, the publication by Cheadle *et al*<sup>[15]</sup> is the only reported case of a *bis*-cyanoxime-and-amide ligand with the tertiary amine linker between the two chelating units. It was synthesised by the condensation of piperazine, which as a secondary diamine is in general less reactive than similar primary diamines, with cyano acetamide, followed by the nitrosation step. One may infer from these results that the condensation step should proceed well when more active primary diamines are involved.

Such inference is confirmed by the work of Kolotilov *et al*,<sup>[24]</sup> who synthesised *N,N'*-propane-1,3-diylbis[2-cyano-2-(hydroxyimino)ethanamide], Figure 17, the first and only one of the *bis*-chelate **chiaa** ligands targeted in this project that was reported in literature.

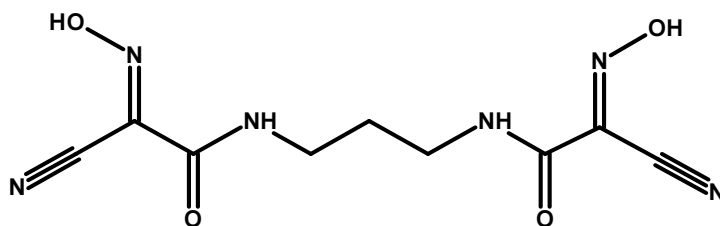


**Fig. 17.** (2*E*,2'*E*)-*N,N'*-propane-1,3-diylbis[2-cyano-2-(hydroxyimino)ethanamide] ligand.<sup>[24]</sup>

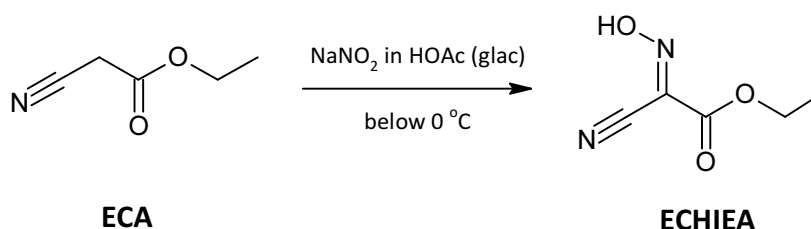


## 2.8 Possible Side Reactions in the Preparation of Cyanoxime Ligands

A number of side reactions may occur at various stages in the preparation of cyanoxime ligands. As they will affect the yield and even outcome of the relevant synthetic steps, it is important to understand the mechanisms and conditions under which they proceed prolifically, so that one may suppress or at least minimise such undesirable complications.

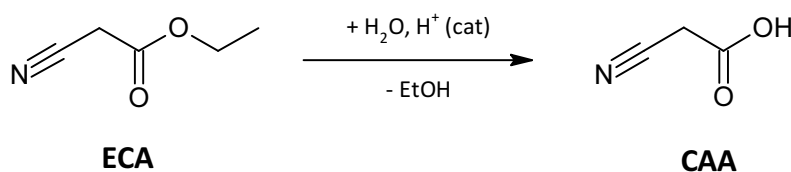
### 2.8.1 Nitrosation of ethyl cyanoacetate

Classical nitrosation of ethyl cyanoacetate according to Conrad and Schulze<sup>[23]</sup> is carried out on the mixture chilled below 0 °C, Scheme 4.



**Scheme 4.** Nitrosation of ethyl cyanoacetate (ECA) to ethyl (2E)-cyano(hydroxyimino)ethanoate (ECHIEA) after Conrad and Schulze.<sup>[23]</sup>

Low temperature is required to avoid the saponification of the ester in acidic medium, Scheme 5.



**Scheme 5.** Possible saponification of ethyl cyanoacetate (ECA) to ethyl cyanoacetic acid (CAA).

### 2.8.2 Cross-protonation of diamines

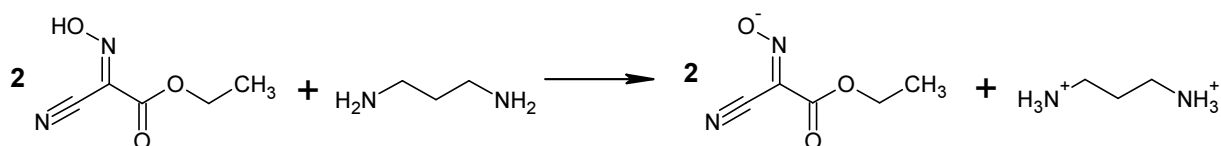
Our attempts at direct condensation of ECHIEA with various diamines revealed the following facts:

- Instantaneous formation of ammonium salts upon mixing.<sup>††</sup>
- Total absence of condensation products at the ECHIEA : diamine = 2 : 1 molar ratio.

<sup>††</sup> Also confirmed in private communication by Professor N.N. Gerasimchuk.

c) Formation of only mono-condensate products at molar ratios 1 : 1 and 1 : 2.

Our interpretation of these results is that much increased acidity of the oxime group of ECHIEA (Sliva *et al*<sup>[13]</sup> reported the value of  $\log K = 6.61$  for this group in 2-cyano-2-(hydroxyimino)acetic acid), is sufficient to protonate amino groups of the diamines, and thus render them unreactive,<sup>††</sup> Scheme 6.



**Scheme 6.** Cross-protonation of diamines caused by increased acidity of the oxime group in ECHIEA.

A few suggestions to consider in order to overcome this undesirable effect are:

- to use sterically hindered strong base to deprotonate ECHIEA prior to the addition of a diamine
- employ dry aprotic solvents
- use an excess of diamine in relation to ECHIEA<sup>§§</sup>.

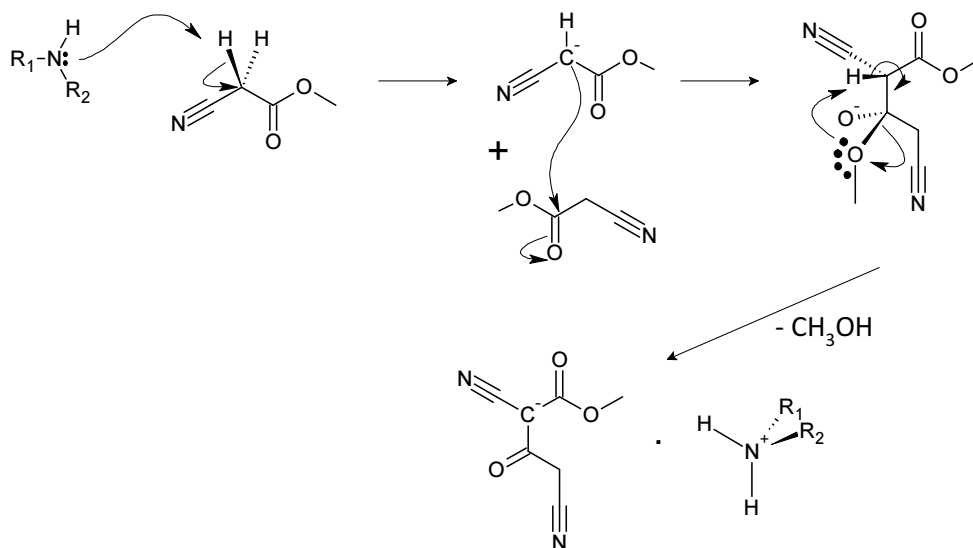
### 2.8.3 Self-condensation of cyanoacetate esters

In the presence of sterically hindered amines, e.g., di-*iso*-propyl amine, ethyl cyanoacetate undergoes self-condensation resulting in the formation of ammonium salt.<sup>[33]</sup> Initially, fairly acidic methylene group of the cyanoacetate ester is deprotonated, affording a carboanion. Nucleophilic attack by this anion on the carbonyl carbon of another ester molecule follows and, upon rearrangement, an organic ammonium salt is formed, Scheme 7.

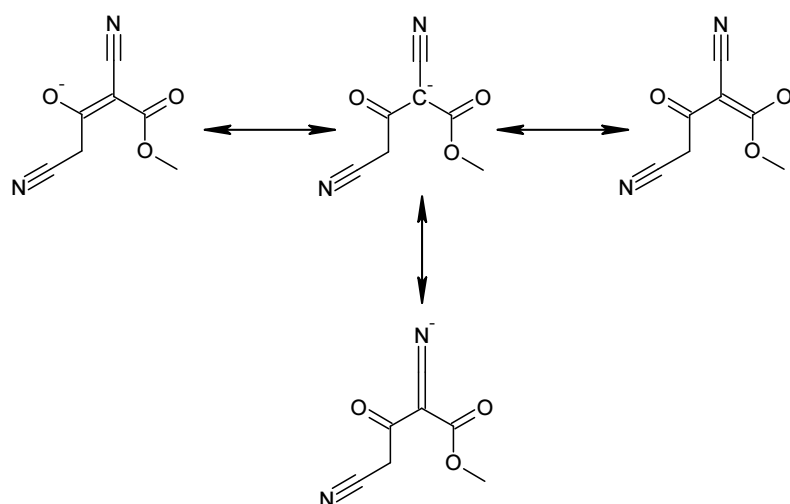
The carboanion in question is stabilised by the delocalisation of negative charge. The latter is distributed between three strongly electron withdrawing groups, Scheme 8, and consequently, is highly delocalised. A number of possible mesomeric forms confer high thermodynamic stability on the product in addition to the stabilising cation-anion Coulomb interaction. Of course, such increased stability of the side-product is undesired, and measures may need to be taken to suppress its formation, in particular, if this product is isolated from the reaction mixture.

<sup>††</sup> Ammonium groups are non-nucleophilic.

<sup>§§</sup> However, the latter makes preparation of *bis*-chelates difficult.



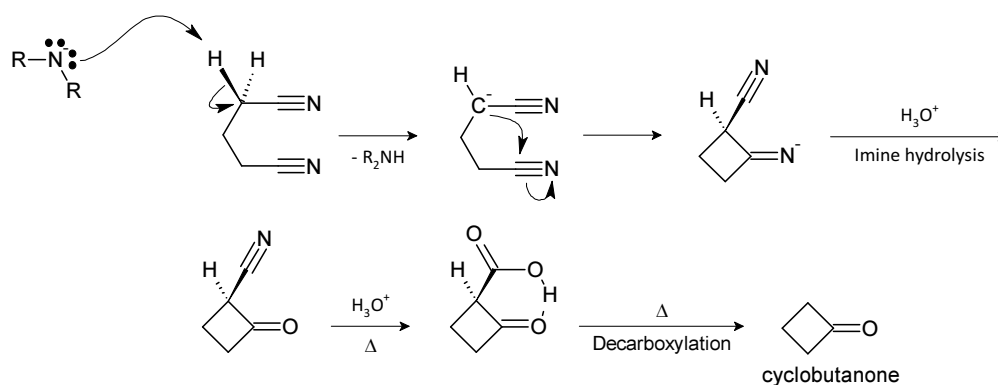
**Scheme 7.** Self-condensation of ethyl cyanoacetate in the presence of a sterically hindered amine.



**Scheme 8.** Possible resonance forms of the 1,3-dicyano-1-(methoxycarbonyl)-2-oxopropane-1-ide.

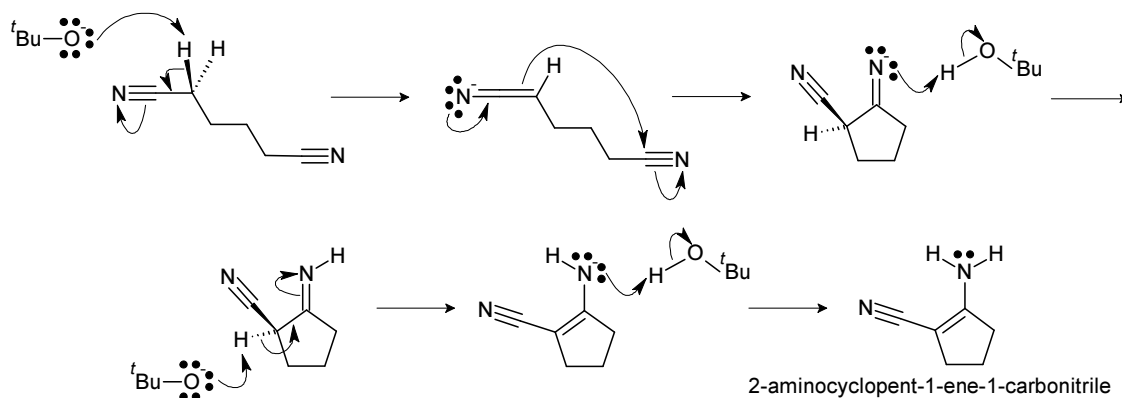
### 2.8.4 The Thorpe-Ziegler reaction

Yet another possible side reaction is a Thorpe-Ziegler cyclisation.<sup>[34]</sup> In the presence of strong non-coordinating bases  $\alpha$ -alkyl nitrites undergo self-condensation, with enamines being common products. Similar to the previous case, deprotonation of the acidic methylene group by a non-coordinating base leads to the di-nitrile carboanion, which upon a series of rearrangements, hydrolysis, and decarboxylation affords the cyclic ketone product of Thorpe-Ziegler reaction, Scheme 9.



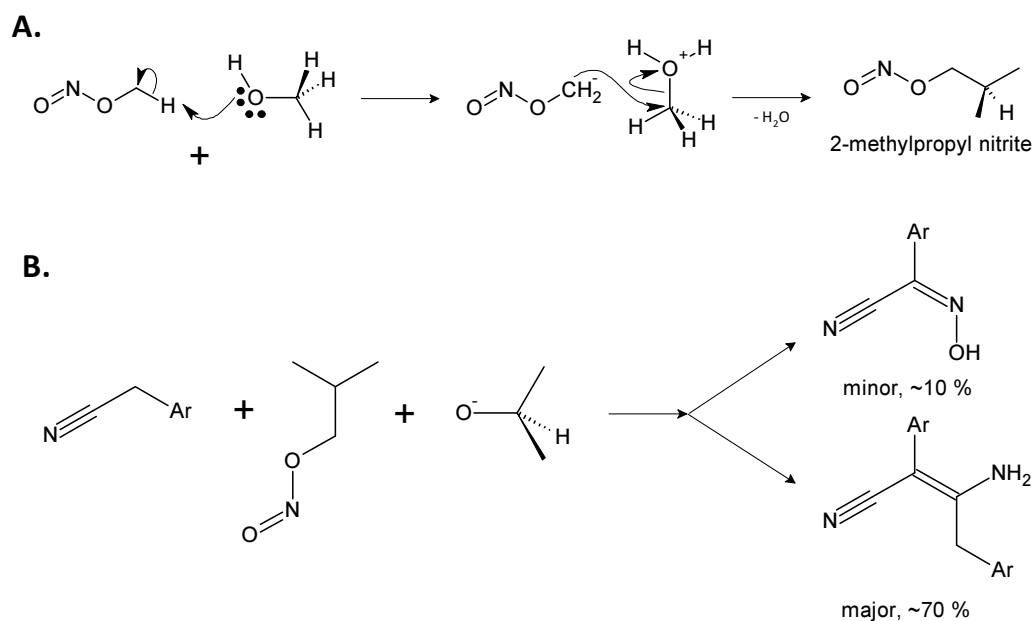
**Scheme 9.** An example of the Thorpe-Ziegler self-condensation of pentanedinitrile with an amine base.

Even more important to our case is the Thorpe-Ziegler reaction in the presence of an alkoxide base, Scheme 10.



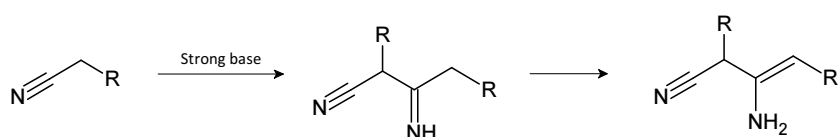
**Scheme 10.** An example of the Thorpe-Ziegler self-condensation of hexanedinitrile with <sup>t</sup>butoxide base.

According to Gerasimchuk *et al.*,<sup>[35]</sup> when a substituted acetonitrile (the substrate) remains for a few hours in the alcoholic solution in the presence of a strong base and alkylnitrite, the following variant of the Thorpe self-condensation is observed, Scheme 11.



**Scheme 11.** A variant of the Thorpe-Ziegler self-condensation of substituted acetonitriles in the presence of methyl nitrite according to Gerasimchuk *et al.*<sup>[35]</sup>

In the context of our synthesis (section 2.9), the Thorpe side reaction is a self-condensation of aliphatic nitriles catalysed by a strong base to form enamines, Scheme 12.

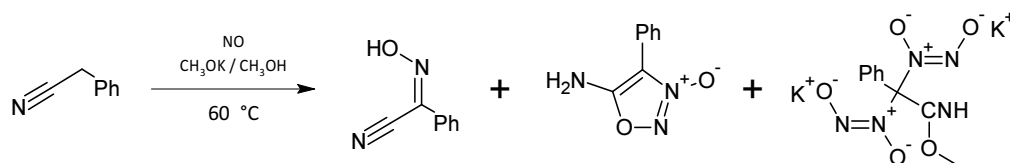


**Scheme 12.** Generic representation of the Thorpe self-condensation of substituted aliphatic acetonitriles in the presence of a strong base, resulting in the formation of enamines.

An important consequence to our work from the above is the need to acidify the reaction mixture, as soon as the formation of cyanoxime ligand is believed to be complete. We shall elaborate on this point later in the thesis.

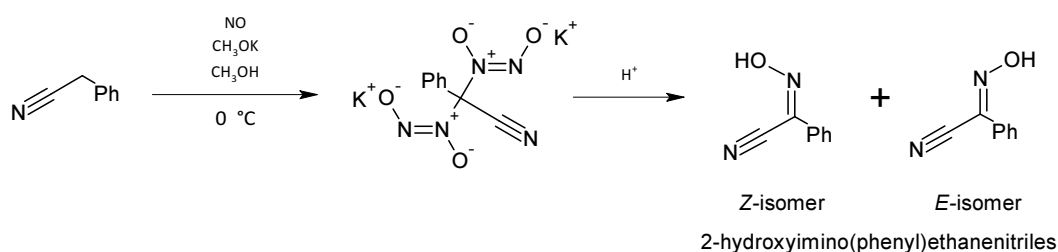
## 2.8.5 Side products affected by the reaction and work-up temperature

Finally, we will mention side products that arose at different temperatures in the reaction of nitrosation and work-up in the course of preparation 2-hydroxyimino(phenyl)ethanenitrile. Two interesting observations have been made during an extensive recent study by Bohle *et al.*<sup>[36]</sup> The authors have synthesised the title compound via the nitrosylation of phenylacetonitrile, Scheme 13. They isolated three products when the reaction was conducted at 60 °C, the major of them being Z-isomer of hydroxyimino(phenyl)ethanenitrile, Scheme 13.



**Scheme 13.** Reaction products for the nitrosylation of phenylacetonitrile at 60 °C.<sup>[36]</sup>

However, when the mixture was cooled to 0 °C and the reaction allowed to proceed for 48 hours, the major product isolated was dipotassium salt of *bis*-diazoniumdiolate, which formed in excellent yield, Scheme 14. Careful control of the temperature during the acidification of this salt allows selective formation of *E/Z* isomers of the oximes: thus, acidification at 0 °C in water or methanol gives predominantly *E*-isomer (less than 5 % of *Z*-isomer).



**Scheme 14.** Diazoniumdiolation products of benzyl cyanide.

Bohle *et al*<sup>[36]</sup> also found that the composition of the conformer mixture was dependent on the reaction temperature even in cases when the dipotassium salt failed to appear, as well as on the temperature of work-up. These observations led them to a natural conclusion that conformational rearrangement is possible at elevated temperatures.

Clearly, monitoring reaction conditions in the synthesis of desired cyanoxime-and-amide ligands is important. Careful characterisation of all products isolated is also desirable, as it might shed light on the conformational equilibria.

## 2.9 Proposed Synthetic Routes

In this section we propose two synthetic routes to the desired cyanoxime-and-amide *bis*-chelate ligands. As no universally applicable oximation procedure was found in literature, we decided to design our synthetic strategy around three published cases, where products with similar structural features were isolated, Figure 18.

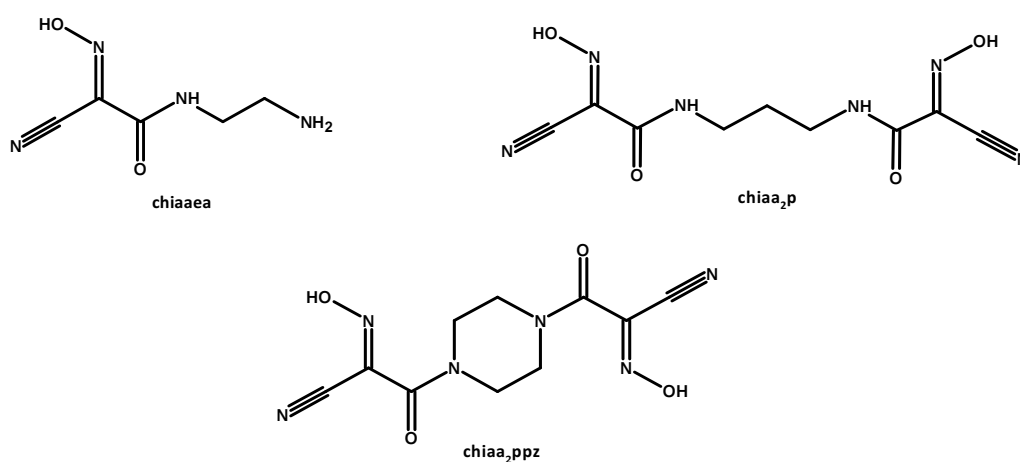
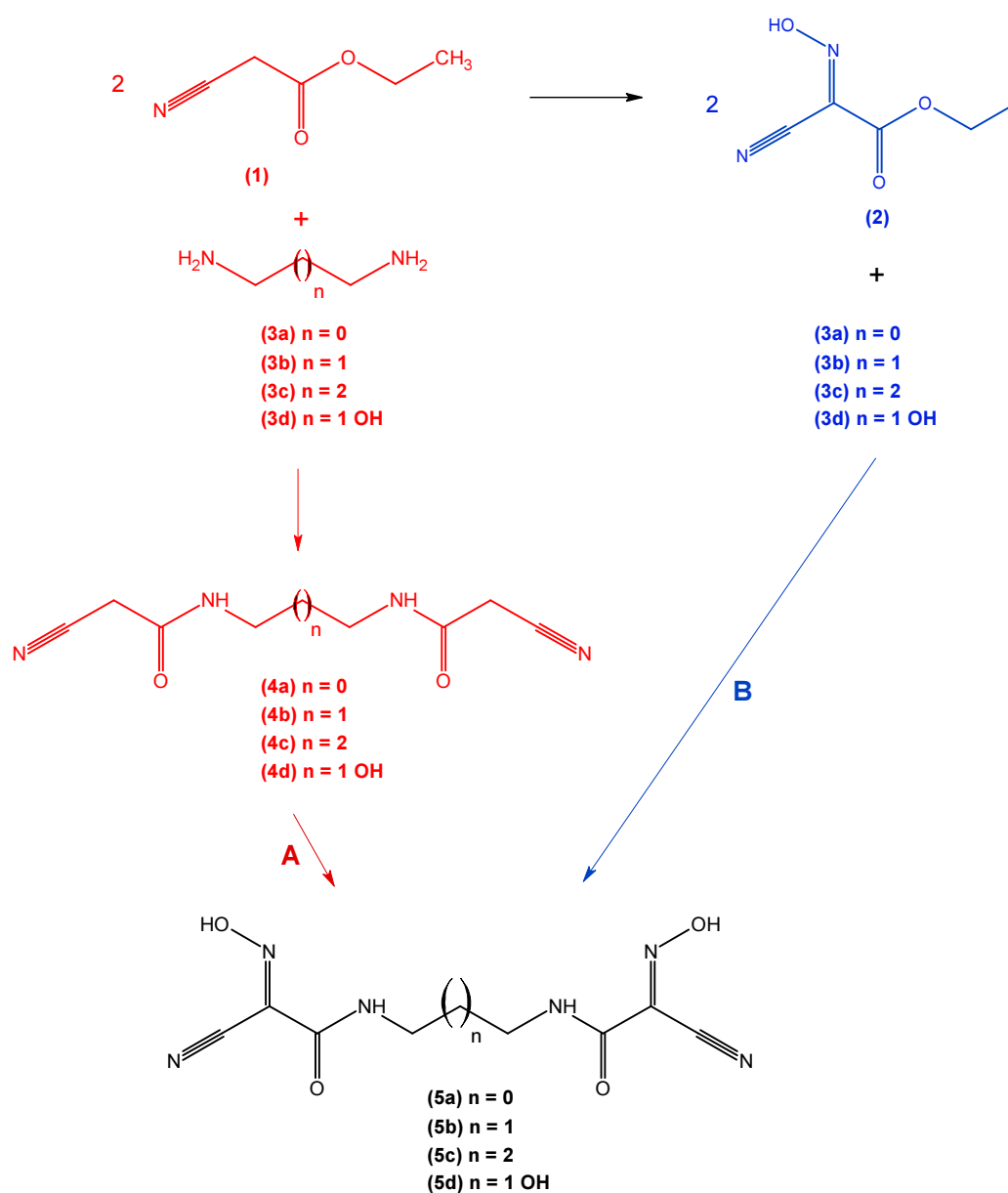


**Fig. 18.** Three structurally similar to the desired ligands compounds, which syntheses have been reported in literature: (2E)-N-(2-aminoethyl)-2-cyano-2-(hydroxyimino)ethanamide (**chiaaea**),<sup>[13]</sup> (2E,2E')-N,N'-propane-1,3-diylbis[2-cyano-2-(hydroxyimino)ethanamide] (**chiaa2p**),<sup>[24]</sup> and (2E,2E')-3,3'-piperazine-1,4-diylbis[2-(hydroxyimino)-3-oxopropanenitrile] (**chiaa2ppz**).<sup>[15]</sup>

The first product, **chiaaea**, was synthesised by Sliva *et al*<sup>[13]</sup> in a condensation reaction of ethyl-cyano(hydroxyimino)ethanoate (**chiaee**) with ethane-1,2-diamine (**en**). Equimolar quantities of the reactants were employed in original publication, and a *mono*-chelate product was obtained. An option to use stoichiometric ratio of cyanoxime ester to diamine (**chiaee** : **en** = 2 : 1) may be considered in order to prepare the desired *bis*-chelate ligands.

Both *bis*-chelate products, **chiaa2p** and **chiaa2ppz**, were synthesised in a two-stage process. First, ethyl cyanoacetate (**eca**) was condensed with a primary (1,3-diaminopropane) or a secondary (piperazine) terminal diamine. Next, intermediate *bis*-amides were oximated under strongly basic conditions to the products shown in Figure 18. Consequently, such approach was considered a viable option in the preparation of ligands desired in this project.

As is evident from the above analysis, two sequences of synthetic steps may be followed to prepare *bis*-chelate ligands of the kind desired in this project, Scheme 15.



**Scheme 15.** Two synthetic routes towards the desired cyanoxime-and-amide *bis*-chelate ligands proposed in the current project.

Both of them employ similar synthetic steps but in different order. Of the steps mentioned, one involves grafting a hydroxyimino group and another involves the formation of amide bonds. Each sequence has its merits and shortcomings. Which one to follow in particular circumstances, as well as reaction specifics, are discussed in the next section.

### 2.9.1 Nitrosation followed by condensation

Route **B**, Scheme 15, starts with ethyl cyanoacetate (**1**), which is available commercially. Oxime (**2**) can be easily synthesised from it in high yield following the Conrad and Schulze procedure.<sup>[23]</sup>



All four diamines (**3a-d**) required for the condensation with (**2**) are also available commercially. The second step can be carried out after Sliva *et al.*<sup>[13]</sup> with the adjusted reactant ratio as discussed above.

## 2.9.2 Condensation followed by nitrosation

Route **A**, Scheme 15, is the one followed by Kolotilov *et al.*<sup>[24]</sup> in the preparation of ligand (**5b**), Figure 19, the only cyanoxime-and-amide *bis*-chelate ligand of this type synthesised prior to our work.

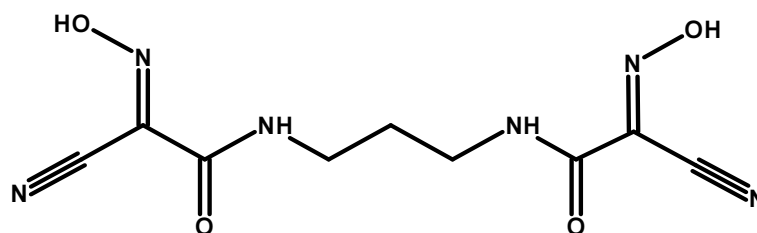


**Fig. 19.** (2*E*,2*E'*)-*N,N'*-propane-1,3-diylbis[2-cyano-2-(hydroxyimino)ethanamide] (**chiaa<sub>2p</sub>**) ligand synthesised by Kolotilov *et al.*<sup>[24]</sup>

Extending this synthetic approach to the preparation of new ligands (**5a**, **5c**, and **5d**), Scheme 15, would require the condensation of two equivalents of ethyl cyanoacetate (**1**) with one equivalent of a primary diamine (**3a-d**). Such task has been accomplished successfully on numerous occasions, and extensive literature on the matter exists. We will refrain from presenting complete and exhaustive literature review of this matter here but rather account for a few most important and relevant publications.

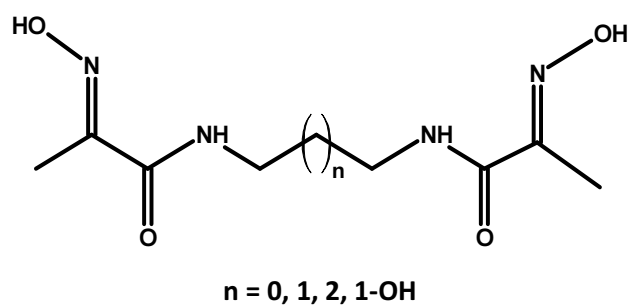
Gazit *et al.*<sup>[37]</sup> synthesised three of the four *bis*-amide precursors of interest to this work (**3a-c**) in their study of benzylidene-malononitriles. Taking into consideration that both reactants were liquid, they chose to run the reaction under solvent-free conditions. The authors observed exothermic heat effect upon addition of the diamine to a stirred ethyl cyanoacetate, followed by the formation of a white precipitate; the latter was filtered off and re-crystallised from ethanol. NMR data confirmed the solids to be the desired *bis*-cyanoamides.<sup>[37]</sup> Product yields claimed by Gazit *et al.* for three *bis*-amides are given in Table 3:

**Table 3.** Yield of various *bis*-cyanoamides in Gazit *et al* procedure.<sup>[37]</sup>

n	<i>bis</i> -Cyanoamide	Yield (%)
0	<i>N,N'</i> -ethane-1,2-diylbis(2-cyanoacetamide)	86
1	<i>N,N'</i> -propane-1,3-diylbis(2-cyanoacetamide)	74
2	<i>N,N'</i> -butane-1,4-diylbis(2-cyanoacetamide)	69

Such high yields (upwards of 69 %) are synthetically attractive as they show high atom efficiency, and usually result in a fairly pure product. Within a year of the original publication, similar procedure was successfully applied to eight linear diamines (from ethane to octane), though no yield values were reported.<sup>[38]</sup> Remaining fourth precursor *bis*-amide (derived from the 1,3-diaminopropan-2-ol), required in this project, was synthesised in 2005 by Hill and Odell<sup>[39]</sup> in 90 % yield following the same procedure. We are aware of a number of more recent publications, where the preparation of the same *bis*-cyanoamides was reported.<sup>[40-43]</sup> However, in essence they all follow original procedure of Gazit *et al*.

Solvent-free condensation of ethyl cyanoacetate with diamines affords the highest possible concentration of the reagents and eliminates the chance of solvent molecules becoming trapped in the crystal lattice of the product; it has been the norm in most publication to date. In contrast, condensation of ethyl pyruvate oxime with linear diamines proceeds better under solvated conditions, as was established in our research group previously, e.g., in the synthesis of various *N,N'*-alkyl-diylbis[2-(hydroxyimino)propanamides], Figure 20.<sup>[44]</sup>

**Fig. 20.** The range of *N,N'*-alkyl-diylbis[2-(hydroxyimino)propanamides] synthesised in the research group previously.

Two solvents were found to perform well in the above condensation,<sup>\*\*\*</sup> namely, CH<sub>2</sub>Cl<sub>2</sub> and MeOH. The latter one accounts for slightly better yields due to its better activating properties. One also must keep in mind that the rate constant for the condensation of this nature exhibits “bell-shaped” profile, peaking in the pH range between 4 and 6;<sup>[44]</sup> consequently, a mild acid catalyst should be used. One that performs this task well and can be easily removed afterwards, is the acid washed glass beads. We intend to try both of the above approaches in the synthesis of *bis*-cyanoamides intermediates, Scheme 15 Route **A**, and follow it with the nitrosation of four precursors in a procedure similar to that of Kolotilov *et al.*<sup>[24]</sup> In particular, we intend to employ CH<sub>3</sub>ONO(g) as a nitrosation agent, in an aprotic *iso*-propanol medium in the presence of strong base such as sodium *iso*-propoxide.

With the above in mind we set out to synthesise the four desired *bis*-chelate cyanoxime-and-amide ligands.

---

<sup>\*\*\*</sup> Please note that in this synthesis the oximation step precedes the condensation one.

## 2.10 Comparative Analysis of the Characterisation Data for Ligands with Cyanoxime-and-Amide Chelates

This section contains a summary of the characterisation data for a range of cyanoxime-and-amide chelates found in literature. Such comparative analysis is informative, helps with the identification of compounds, and is presented here for future reference.

### 2.10.1 Characteristic IR Data

**Table 4.** Wavenumbers (in  $\text{cm}^{-1}$ ) of the characteristic valent vibrations in various cyanoxime-and-amide chelates according to literature.<sup>†††</sup>

No	Compound	$\nu$ (O-H)	$\nu$ (N-H)	$\nu$ (C≡N)	$\nu$ (Amide I)	$\nu$ (Amide II)	$\nu$ (N-O)	Reference
1	NCC(=N-OH)CONH <sub>2</sub>			2239				[45]
2	NCC(=N-OH)CONHCH <sub>2</sub> CH <sub>2</sub> NH <sub>2</sub>		3340, 3300, 3060 <sup>†††</sup>		1648	1552	1130	[13]
3	NCC(=N-OH)CON(CH <sub>3</sub> ) <sub>2</sub>							[20]
4	NCC(=N-OH)CSN(CH <sub>3</sub> ) <sub>2</sub>							[20]
5	NCC(=N-OH)CONHCH <sub>3</sub>			2244	1664	1552		[31]
6	NCC(=N-OH)CONHPh			2250, 2240	1680, 1660	-, 1548		[29, 31]
7	NCC(=N-OH)CONHC <sub>6</sub> H <sub>11</sub> Cyclic			2225	1665			[29]
8	NCC(=N-OH)CONHC <sub>6</sub> H <sub>4</sub> Br			2235	1650			[29]
9	NCC(=N-OH)CONHCH <sub>2</sub> Ph			2242	1660	1550		[31]
10	NCC(=N-OH)CON(CH <sub>2</sub> ) <sub>5</sub> -Cyclic	2945		2236	1630		1036	[32]
11	NCC(=N-OH)CON(CH <sub>2</sub> ) <sub>4</sub> O Cyclic	2977		2236	1627		1006	[32]
12	NCC(=N-OH)CONHC <sub>2</sub> H <sub>5</sub>							[30]
13	NCC(=N-OH)CON(CH <sub>2</sub> ) <sub>4</sub> NOCC(=N-OH)CN			2232	1625		1047	[15]
14	NCC(=N-OH)CONH(CH <sub>2</sub> ) <sub>3</sub> NHOCC(=N-OH)CN		3370	2110	1680	1560		[24]

The data presented above reveal a number of regularities that may be summarised as follows:

- a) sharp peak in the range 3300 - 3370  $\text{cm}^{-1}$  is attributable to the N-H stretch

<sup>†††</sup> Empty cells in the table mean that IR data were not reported. For some compounds the reference quoted is not the first ever account of the synthesis but the first traceable reference with IR data.

<sup>†††</sup> Three absorptions bands were attributed to the N-H vibration in this case; elsewhere in the table double entries arise from different papers.

- b) valent vibration of the nitrile group ( $C\equiv N$ ) is observed in the region  $2110 - 2250\text{ cm}^{-1}$  and in many cases is surprisingly weak<sup>§§§</sup>; low signal to noise ratio is normally a concern but in this case it is easily identifiable as very few functional groups have transitions in this region of the spectrum
- c) amide functional group is characterised by two strong bands in the region  $1540 - 1620\text{ cm}^{-1}$ ; the first of them, at about  $1650\text{ cm}^{-1}$  and labelled as **amide I**, corresponds to the carbonyl bond stretch, while the second, at about  $1550\text{ cm}^{-1}$  and labelled as **amide II**, represents essentially C-N stretch of this group
- d) N-O valent stretch of the oxime group is normally observed in the region of  $1030 - 1130\text{ cm}^{-1}$  and is fairly intense.

---

<sup>§§§</sup> The intensity of the band is low due to “increased polarizability of the cyano moiety in the conjugated anion”<sup>[16]</sup>

## 2.10.2 Characteristic NMR data

**Table 5.** Representative  $^1\text{H}$  and  $^{13}\text{C}$  NMR chemical shifts (ppm) in various cyanoxime-and-amide chelates according to literature. \*\*\*\*

No	Oxime	Solvent	$^1\text{H}$ (=N-OH)	$^1\text{H}$ (-C(=O)NHR)	$^{13}\text{C}$ (NCC(=N-OH)-)	$^{13}\text{C}$ (NCC(=N-OH)-)	$^{13}\text{C}$ (-C(=O)NR-)	Reference
1	NCC(=N-OH)CONH <sub>2</sub>	DMSO-d <sub>6</sub> CDCl <sub>3</sub>	- , 13.38	7.85, 7.07	109.3, 109.45	128.1, 128.58	160.2, 160.32	[45, 30]
2	NCC(=N-OH)CONHCH <sub>2</sub> CH <sub>2</sub> NH <sub>2</sub>	DMSO-d <sub>6</sub>		8.15				[13]
3	NCC(=N-OH)CON(CH <sub>3</sub> ) <sub>2</sub>	n/a						[20]
4	NCC(=N-OH)CSN(CH <sub>3</sub> ) <sub>2</sub>	n/a						[20]
5	NCC(=N-OH)CONHCH <sub>3</sub>	n/a	14.4	8.3				[31]
6	NCC(=N-OH)CONHPh	n/a	- , 14.5	9.98, 10.3				[29, 31]
7	NCC(=N-OH)CONHC <sub>6</sub> H <sub>11</sub> Cyclic	n/a		8.21				[29]
8	NCC(=N-OH)CONHC <sub>6</sub> H <sub>4</sub> Br	n/a		10.51				[29]
9	NCC(=N-OH)CONHCH <sub>2</sub> Ph	n/a	14.5	9.0				[31]
10	NCC(=N-OH)CON(CH <sub>2</sub> ) <sub>5</sub> -Cyclic	DMSO-d <sub>6</sub>		N/A	109.79	127.44	157.73	[30]
11	NCC(HO-N=)CON(CH <sub>2</sub> ) <sub>4</sub> O-Cyclic	DMSO-d <sub>6</sub>	13.12	N/A	109.79	127.31	158.32	[30]
12	NCC(=N-OH)CONHC <sub>2</sub> H <sub>5</sub>	DMSO-d <sub>6</sub>	13.59	7.83	108.39	157.96	158.01	[30]
13	NCC(=N-OH)CON(CH <sub>2</sub> ) <sub>4</sub> NOCC(=N-OH)CN	DMSO-d <sub>6</sub>	14.27	N/A	109.2	130.1	158	[15]
14	NCC(=N-OH)CONH(CH <sub>2</sub> ) <sub>3</sub> NHOCC(=N-OH)CN	DMSO-d <sub>6</sub>						[24]

The data presented above reveal a number of trends that may be summarised as follows:

- chemical shift for the hydroxyimino proton is found in the range 13.1 to 14.5 ppm, a characteristically far downfield signal; the latter can be attributed to its highly de-shielded state, being  $\beta$  to a strongly electron withdrawing nitrile group
- chemical shift of the amide proton shows considerable variation (from 7 to 10.5 ppm), which can be attributed to the induction effects of functional groups  $\alpha$  to the amide nitrogen
- chemical shift of the nitrile carbon is found in a narrow range between 127 – 130 ppm, which is characteristic of the cyanoxime-and-amide chelates studied so far
- chemical shift of the quaternary carbon that is  $\alpha$  to both oxime and nitrile group is highly characteristic and confined to a narrow region at about 109 ppm.

\*\*\*\* Empty cells in the table mean that NMR data were not reported; in some cases NMR shifts were reported to one decimal place only. Synthesis of some of the compounds was reported earlier than the references in the table but no NMR data was given; consequently, we quote the first (and following) NMR containing references.

- e) chemical shift of the carbonyl carbon in amide moiety is pegged at about 158 ppm, in line with the well-known behaviour of this functional group.

## 3. Synthesis and Characterisation

In this section we will present particulars of synthetic procedures followed in the preparation of compounds and instrumental techniques used for their characterisation. For each substance synthesised we will report instrumental data collected and the structure assigned on their basis.

### 3.1 Experimental

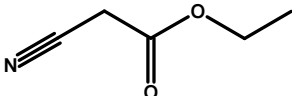
#### 3.1.1 Solvents and Reagents

Most of the common solvents and reagents used have already been described in section 5.1.1, Chapter A. Consequently, only items new to this part of the project are reported below, Tables 6 and 7.

**Table 6.** Common solvents used and internal purification procedures.

Solvent	Supplied Purity	Purification procedure
<i>iso</i> -Propanol	≥98%	Distillation

**Table 7.** Commercially available reagents used for the synthesis in this chapter of the thesis.\*

Name	Structure	Assay/ %	MW/ g mol <sup>-1</sup>	Phase state at 25 °C	Density/ g cm <sup>-3</sup>
Ethyl cyanoacetate		98	113.12	l	1.06

#### 3.1.2 Instrumental

Most of the instrumental procedures employed for characterisation have also been described in section 5.1.2, Chapter A. Please, refer to this section for particulars. The only new technique used in this part of the project was single crystal X-ray diffraction, and the specific information for it is given in section 3.4 of this chapter.

\*<sup>1</sup>) Purchased from Sigma-Aldrich and used without further purification.



## Compounds Synthesised

In total, we have synthesised nine compounds in this part of the project, of which **three** were new. Whether the compound is new or is known in literature is stated in the relevant section that describes its preparation and characterisation.

In addition to their systematic names, compounds synthesised and isolated by us are labelled with integer numbers that already appeared in Scheme 8, section 2 of this Chapter. For homologous compounds with variable length of the alkane chain, a letter is added to the number; in particular, letter “a” designates ethane chain, letter “b” propane one, letter “c” butane one, and letter “d” 2-hydroxypropane one. For example, **(4c)** would mean compound of class 4, which is *bis*-hydroxyimino-acetamide, with a butane bridge, i.e. *N,N'*-butane-1,4-diylbis(2-cyanoacetamide).

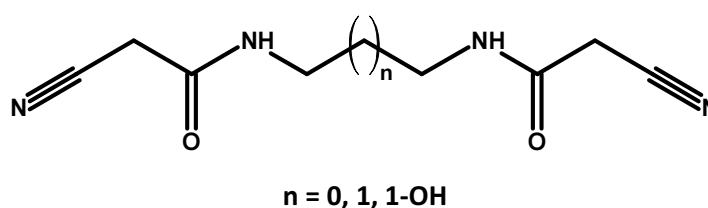
As has been discussed in the preceding section, we explored two different paths that might lead from the starting compound **(1)**, ethyl cyanoacetate, to the desired *bis*-hydroxyiminoacetamides **(5)**, Scheme 15.

### Path A:

Along this route **(1)** is condensed with a suitable diamine **(3)** to form *bis*-cyanoacetamide **(4)**, which is then oximated according to Kolotilov *et al.*<sup>[24]</sup> This proved to be a successful approach and all desired compounds (four *bis*-cyanoacetamides **(4)** and four *bis*-cyano(hydroxyimino)acetamides **(5)**) were synthesised, isolated, and characterised by following it.

## 3.2 Synthesis of the *bis*-Cyanoacetamide Precursors

Two variations of the synthetic procedure were employed for the preparation *bis*-cyanoamides. The first was a catalysed condensation in solvent medium, and the second was a solvent-free condensation. Three of the four compounds of interest were synthesised via the former procedure, and the remaining one via the latter. The procedure below refers to compounds (4a, 4b, and 4d).



**Procedure:** Ethyl cyanoacetate (5.43 mL, 50.0 mmol) was pipetted into a 100 mL RBF flushed with Ar, followed by dry methanol (25 mL) and a catalytic amount of the acid washed glass beads (106  $\mu\text{m}$ ).

Thereafter, relevant alkyl-diamine (25.5 mmol) was slowly injected through a septum, and the mixture stirred at room temperature for 24 hours. White precipitate that formed was filtered off, washed first with methanol (100 mL), then with aqueous HCl (0.1 M, 100 mL), and dried on a watch glass, affording white powder.

#### **(4a) *N,N'*-Ethane-1,2-diylbis(2-cyanoacetamide)**

This compound is known in literature.<sup>[37, 39, 41]</sup>

**Yield:** 3.56 g, 18.1 mmol (67 %).

**CHN:** Calcd. for C<sub>8</sub>H<sub>10</sub>N<sub>4</sub>O<sub>2</sub>: C, 49.48; H, 5.19; N, 28.85. Found: C, 49.70; H, 5.20; N, 28.57.

**<sup>1</sup>H NMR** (400 MHz, DMSO-d<sub>6</sub>, δ/ ppm): 3.13-3.15 (m, 4H, -CH<sub>2</sub>NH-), 3.59 (s, 4H, -CH<sub>2</sub>C≡N), 8.26 (t-br, 2H, -NH-).

**<sup>13</sup>C NMR** (100 MHz, DMSO-d<sub>6</sub>, δ/ ppm): 25.3 (t, -CH<sub>2</sub>NH-), 38.4 (t, -CH<sub>2</sub>C≡N), 116.0 (s, -C≡N), 162.3 (s, -C(=O)-).

Original spectra for this compound are presented in Appendix B, Figures B1-B4.

#### **(4b) *N,N'*-Propane-1,3-diylbis(2-cyanoacetamide)**

This compound is known in literature.<sup>[37, 39, 41]</sup>

**Yield:** 4.11 g, 19.6 mmol (76 %).

**<sup>1</sup>H NMR** (400 MHz, DMSO-d<sub>6</sub>, δ/ ppm): 1.56 (p, *J* = 7.0 Hz, 2H, -CH<sub>2</sub>CH<sub>2</sub>CH<sub>2</sub>-), 3.06-3.11 (m, 4H, -CH<sub>2</sub>NH-), 3.60 (s, 4H, -CH<sub>2</sub>C(=O)-), 8.19 (t-br, *J* = 4.8 Hz, 2H, -NH-).

**<sup>13</sup>C NMR** (100 MHz, DMSO-d<sub>6</sub>, δ/ ppm): 25.2 (t, -CH<sub>2</sub>CH<sub>2</sub>CH<sub>2</sub>-), 28.5 (t, -CH<sub>2</sub>NH-), 36.9 (t, -CH<sub>2</sub>C), 116.1 (s, -C≡N), 162.0 (s, -C(=O)-).

Original spectra for this compound are presented in Appendix B, Figures B5-B7.

#### **(4d) *N,N'*-(2-Hydroxypropane-1,3-diyl)bis(2-cyanoacetamide)**

This compound is known in literature.<sup>[39]</sup>

**Yield:** 4.09 g, 18.0 mmol (66 %).

**CHN:** Calcd. for C<sub>9</sub>H<sub>12</sub>N<sub>4</sub>O<sub>3</sub>: C, 48.21; H, 5.39; N, 24.99. Found: C, 48.14; H, 5.01; N, 25.21.

**<sup>1</sup>H NMR** (400 MHz, DMSO-d<sub>6</sub>, δ/ ppm): 2.99-3.05 (m, 2H, -CH(a)H(b)NH-), 3.11-3.17 (m, 2H, -CH(a)H(b)NH-), 3.55-3.60 (m, 1H, -CH(OH)-), 3.63 (s, 4H, -CH<sub>2</sub>C≡N), 5.08 (d, *J* = 5.0 Hz, 1H, -OH), 8.19 (t, *J* = 5.1 Hz, 2H, -NH-).

$^{13}\text{C}$  NMR (100 MHz, DMSO- $d_6$ ,  $\delta$ / ppm): 25.2 (t, -CH<sub>2</sub>NH-), 43.3 (t, -CH<sub>2</sub>C $\equiv$ N), 67.6 (d, -CH(OH)-), 116.2 (s, -C $\equiv$ N), 162.3 (-C(=O)-).

HRMS (ES-, m/z): [M + Na]<sup>+</sup> calcd. for C<sub>9</sub>H<sub>12</sub>N<sub>4</sub>O<sub>3</sub>Na, 247.0807; found, 247.0813.

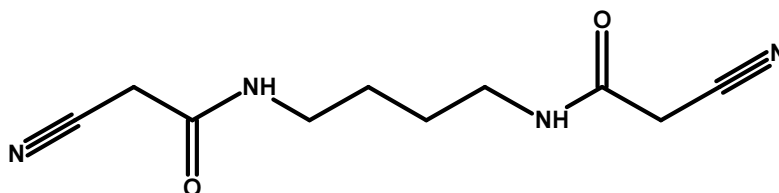
Original spectra for this compound are presented in Appendix B, Figures B11-B15.

Characterisation of the above three compounds was done by means of  $^1\text{H}$  and  $^{13}\text{C}$  NMR spectroscopy. In all three cases data are in satisfactory agreement with the values reported in literature,<sup>†, [39, 41-43]</sup> which indicates that the desired substances have been prepared. For compounds (**4a** and **4d**) we have obtained additional characterisation data, which up to now were not reported in literature. In particular, we have performed microanalysis on compounds (**4a** and **4d**), and obtained high-resolution mass-spectrum for compound (**4d**).

### (4c) *N,N'*-butane-1,4-diylbis(2-cyanoacetamide)

This compound is known in literature.<sup>[37, 39, 41]</sup>

We have synthesised this compound via a solvent-free variation of the condensation procedure described below.



**Procedure:** Ethyl cyanoacetate (8.69 mL, 80.0 mmol) was pipetted into a 100 mL RBF flushed with Ar. Butane-1,4-diamine (4.14 mL, 40.8 mmol) was slowly injected through a septum, and the mixture stirred at room temperature for 24 hours. White precipitate that formed was filtered off, washed with ethanol (40 mL), and dried on a watch glass, affording white powder.

**Yield:** 7.20 g, 35.3 mmol (87 %).

$^1\text{H}$  NMR (400 MHz, DMSO- $d_6$ ,  $\delta$ / ppm): 1.38-1.41 (m, 4H, -CH<sub>2</sub>CH<sub>2</sub>NH-), 3.04-3.09 (m, 4H, -CH<sub>2</sub>NH-), 3.58 (s, 4H, -CH<sub>2</sub>C(=O)-), 8.19 (t-br,  $J$  = 4.9 Hz, 2H, -NH-).

$^{13}\text{C}$  NMR (100 MHz, DMSO- $d_6$ ,  $\delta$ / ppm): 25.2 (t, -CH<sub>2</sub>CH<sub>2</sub>NH-), 26.1 (t, -CH<sub>2</sub>NH-), 38.7 (t, -CH<sub>2</sub>C $\equiv$ N), 116.2 (s, -C $\equiv$ N), 161.9 (s, -C(=O)-).

Original spectra for this compound are presented in Appendix B, Figures B8-B10.

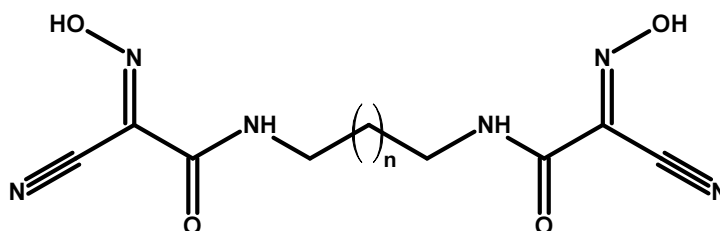
<sup>†</sup> References that follow are not the first where the synthesis of these compounds was reported, but the first where reliable NMR spectra in DMSO- $d_6$  were obtained.

Compound (**4c**) was characterised by NMR spectroscopy, and the data are in satisfactory agreement with values reported in literature.<sup>‡, [39, 41, 43]</sup> Other characterisation data for this compound are also reported.

---

<sup>‡</sup>) References that follow are not the first where the synthesis of these compounds was reported, but the first where reliable NMR spectra in DMSO-d<sub>6</sub> were obtained.

### 3.3 Synthesis of the *bis*-Chelate Cyanoxime-and-Amide Ligands



Preparation of the desired cyanoxime-and-amide *bis*-chelate ligands required generation of the methyl nitrite gas and its use in the oximation process. As the conditions of the former and latter are dramatically different, the reaction could not be carried out in one pot. Consequently, we have employed an apparatus shown below, Figures 21-23. As its nature falls outside of the day-to-day used synthetic setup in organic chemistry, we shall explain the procedure in some detail.

The apparatus with two bubbles was employed to better utilise the methyl nitrite gas by increasing both the contact area and the contact time between the gas bubbles with the basic solution of *bis*-cyanoacetamide. We also thought that the second bubbler might act in part as a scrubber, thus, reducing the amount of highly toxic gas discharged into the extraction cabinet.

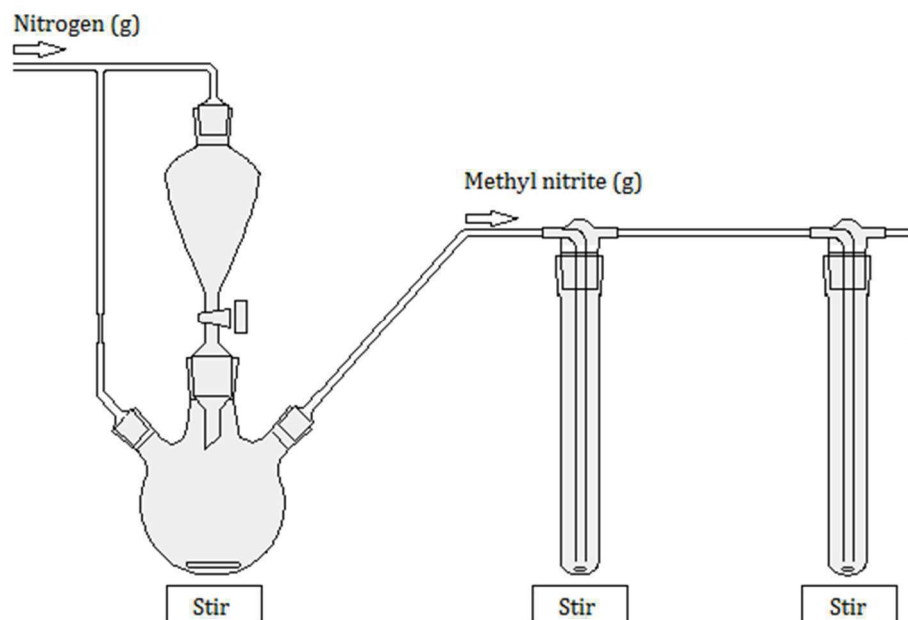


**Fig. 21.** Diagrammatic representation of the apparatus for the oximation of *bis*-cyanoacetamides.

In the generic procedure that follows we will refer to three solutions labelled as A, B, and C. Their composition and preparation is briefly described below.

**Solution A:** Aqueous H<sub>2</sub>SO<sub>4</sub> (6.25 M).

Chilled (ice bath) deionised water (200 mL) was placed in a 500 mL beaker, and concentrated sulphuric acid (98 wt. %, 100 mL) added in small portions of about 5-10 mL.<sup>§</sup>

**Solution B:** NaNO<sub>2</sub> solution (1.00 M) in H<sub>2</sub>O : MeOH = 1 : 1 mixed solvent.

NaNO<sub>2</sub> (13.94 g, 200 mmol) was weighed out and dissolved in deionised water (100 mL) in a 500 mL RBF. Thereafter, methanol (100 mL, 2.46 mol) was added and the mixture left stirring until needed.

**Solution C:** *Bis*-cyanoacetamide (3.00 mmol) and sodium *iso*-propoxide (0.038 M) in *iso*-propanol.

Sodium metal was washed with *n*-hexane from the storage oil, oxidised surface layer scrapped with a sharp knife, and the shiny bar of it (*ca.* 0.152 g, 6.00 mmol) weighed in a beaker filled with Ar gas. The ingot was cut into thin slivers and placed into a 250 mL RBF flushed with argon. Freshly distilled *iso*-propanol (160 mL) was added to the flask and the contents stirred under nitrogen until all of the sodium has dissolved. On average, the process of dissolution took between 2 and 3 hours. Before use clear solution was decanted from the trace quantities of the products of oxidation (undissolved) of the sodium metal. Respective *bis*-cyanoacetamide (3.00 mmol)\*\* was weighed into a 500 mL Erlenmeyer flask, and the above sodium *iso*-propoxide solution added to it. The mixture was stirred for about 30 min, during which time some of the *bis*-amide has dissolved but most remained in a suspended state.

Respective solutions were charged to the following parts of the apparatus:

*Solution A* was placed in the dropping funnel attached to the three-neck round bottom reactor.

*Solution B* was placed in the three-neck reactor.

*Solution C* was divided into two equal parts by volume and placed in two bubblers.

---

<sup>§</sup>) CAUTION! The process is highly exothermic and can lead to splashes, which may cause severe burns.

\*\*\*) In view of the two bubblers employed in the apparatus, the solution of *bis*-cyanoacetamide (3.00 mmol) in solution B (160 mL) was split equally between them.

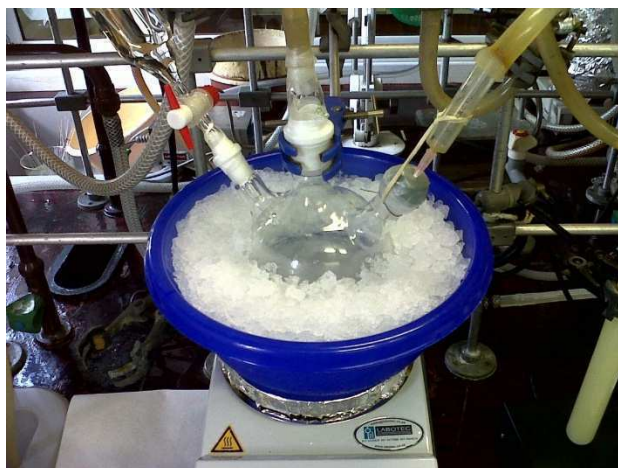


**Fig. 22.** An image of the actual methyl nitrite generating vessel employed in the above process.



**Fig. 23.** Overview of the actual apparatus employed in the above process.

**Procedure:** Solution A (60 mL) was placed in a 100 mL dropping funnel, solution B (200 mL) was charged to the three-neck reactor, and suspension C (160 mL), subdivided into two equal halves, was placed into two bubblers; each of the three vessels had a magnetic stirrer bar in it. The apparatus was assembled and flushed with a flow of  $N_2$  gas for a few minutes. RBF with solution B was kept in an ice-bath throughout the synthesis. Dropping funnel containing solution A was back-pressured with  $N_2$  gas and aqueous sulphuric acid added drop-wise (at the rate of about 1 drop per minute). Generated MeONO gas, with a co-flow of  $N_2$  gas, was discharged through the bubblers. Solution B and suspension C in both bubblers were continuously stirred through the duration of the synthesis. Within seconds of bubbling methyl nitrite gas through suspension C, it turned visibly yellow, and the colour intensified as oximation progressed. After approximately 3 hours, the contents of two bubblers were combined, undissolved *bis*-cyanoamide filtered off, and the mother liquor reduced by rotary evaporation to yellow crystals. The latter were re-dissolved in hot deionised water (20 mL), allowed to cool to a room temperature, and acidified with aqueous HCl (2.0 M) to pH of 2.8 (controlled by pH meter with a glass-sensor). Slow evaporation of the resulting solution on a watch glass afforded the desired product.

**(5a) *N,N'*-Ethane-1,2-diylbis[2-cyano-2-(hydroxyimino)ethanamide]**

This compound is **new**.

**Yield:** 0.027 g, 0.10 mmol (3.6%), yellow crystals.

**CHN:** Calcd. for C<sub>8</sub>H<sub>8</sub>N<sub>6</sub>O<sub>4</sub>: C, 38.10; H, 3.20; N, 33.32. Found: C, 37.78; H, 3.02; N, 33.17.

**IR** (KBr,  $\bar{\nu}$  / cm<sup>-1</sup>): 3391 (s, N-H), 3147, 2968, 2241, 1676 (s, C=O), 1542 (s, C-N), 1451, 1243 (s), 1172, 1073 (s, N-O), 872, 755, 633.

**<sup>1</sup>H NMR** (400 MHz, DMSO-d<sub>6</sub>,  $\delta$ / ppm): 3.31-3.33 (m, 2H, -CH<sub>2</sub>-), 8.56 (t, *J* = 5.51 Hz, 2H, -NH-), 14.44 (s, 2H, -OH).

**<sup>13</sup>C NMR** (100 MHz, DMSO-d<sub>6</sub>,  $\delta$ / ppm): 38.5 (t, -CH<sub>2</sub>-), 108.9 (s, -C(=NOH)-), 128.1 (s, -C≡N), 158.3 (s, -C(=O)-).

**HRMS** (ES-, *m/z*): [MH<sub>-1</sub>]<sup>-</sup>, calcd. for C<sub>8</sub>H<sub>7</sub>N<sub>6</sub>O<sub>4</sub>, 251.0529; found, 251.0526 (-1.2 ppm).

Original spectra for this compound are presented in Appendix B, Figures B16-B25.

**(5b) *N,N'*-Propane-1,3-diylbis[2-cyano-2-(hydroxyimino)ethanamide]**

A single reference to this compound was found in literature.<sup>[24]</sup>

**Yield:** 0.194 g, 0.725 mmol (24 %), light to dark yellow crystals.

**IR** (KBr,  $\bar{\nu}$  / cm<sup>-1</sup>): 3369 (s, N-H), 3131 (br, O-H), 2182, 2235, 1679 (s, C=O), 1553 (s, C-N), 1457, 1449, 1414 (s), 1373, 1306, 1224 (s), 1182, 1082 (s, N-O), 1066 (s), 923, 829, 798, 750 (s), 655, 519, 479.

**<sup>1</sup>H NMR** (400 MHz, DMSO-d<sub>6</sub>,  $\delta$ / ppm): 1.66 (p, *J* = 6.74 Hz, 2H, -CH<sub>2</sub>CH<sub>2</sub>CH<sub>2</sub>-), 3.17-3.22 (m, 4H, -CH<sub>2</sub>NH-), 8.51 (t, *J* = 5.93 Hz, 2H, -NH-), 14.45 (s, 2H, -OH).

**<sup>13</sup>C NMR** (100 MHz, DMSO-d<sub>6</sub>,  $\delta$ / ppm): 28.6 (t, -CH<sub>2</sub>CH<sub>2</sub>CH<sub>2</sub>-), 36.4 (t, -CH<sub>2</sub>NH-), 108.9 (s, -C(=NOH)-), 128.1 (s, -C≡N), 158.0 (s, -C(=O)-).

**HRMS** (ES-, *m/z*): [MH<sub>-1</sub>]<sup>-</sup>, calcd. for C<sub>9</sub>H<sub>9</sub>N<sub>6</sub>O<sub>4</sub>, 265.0685; found, 265.0689 (+1.5 ppm).

Original spectra for this compound are presented in Appendix B, Figures B26-B34.

**(5c) *N,N'*-Butane-1,4-diylbis[2-cyano-2-(hydroxyimino)ethanamide]**

This compound is **new**.

**Yield:** 0.056 g, 0.20 mmol (6.6 %), dark yellow crystals.

**CHN:** Calcd. for C<sub>10</sub>H<sub>12</sub>N<sub>6</sub>O<sub>4</sub>: C, 42.86; H, 4.32; N, 29.99. Found: C, 43.24; H, 4.26; N, 29.61.



**IR** (KBr,  $\bar{\nu}$  /  $\text{cm}^{-1}$ ): 3346 (s, N-H), 3139 (br, O-H), 2975, 2364, 1662 (s, C=O), 1543 (s, C-N), 1445, 1396 (s), 1366, 1249, 1200, 1175, 1059 (s, N-O), 1039, 969, 935, 812, 758 (s), 686.

**$^1\text{H}$  NMR** (400 MHz, DMSO- $d_6$ ,  $\delta$ / ppm): 1.45-1.46 (m, 2H, - $\text{CH}_2\text{CH}_2\text{NH}$ -), 3.17-3.18 (m, 4H, - $\text{CH}_2\text{NH}$ -), 8.51 (t,  $J$  = 5.84 Hz, 2H, - $\text{NH}$ -), 14.39 (s-br, 2H, -OH).

**$^{13}\text{C}$  NMR** (100 MHz, DMSO- $d_6$ ,  $\delta$ / ppm): 26.2 (t, - $\text{CH}_2\text{CH}_2\text{NH}$ -), 38.7 (t, - $\text{CH}_2\text{NH}$ -), 108.9 (s, - $\text{C}(\text{=NOH})$ -), 128.1 (s, - $\text{C}\equiv\text{N}$ ), 157.9 (s, - $\text{C}(\text{=O})$ -).

**HRMS** (ES-,  $m/z$ ):  $[\text{MH}_-1]^-$ , calcd. for  $\text{C}_{10}\text{H}_{11}\text{N}_6\text{O}_4$ , 279.0842; found, 279.0840 (-0.7 ppm).

Original spectra for this compound are presented in Appendix B, Figures B35-B45.

### **(5d)** *N,N'*-(2-Hydroxypropane-1,3-diyl)bis[2-cyano-2-(hydroxyimino)ethanamide]

This compound is **new**.

**Yield:** 0.053 g, 0.19 mmol (6.2 %), white powder.

**CHN:** Calcd. for  $\text{C}_9\text{H}_{10}\text{N}_6\text{O}_5$ : C, 38.30; H, 3.57; N, 29.78. Found: C, 38.15; H, 3.43; N, 29.63.

**IR** (KBr,  $\bar{\nu}$  /  $\text{cm}^{-1}$ ): 3381, 3324, 2960, 2363, 1684 (s, C=O), 1618, 1546 (s, N-H), 1421, 1242, 1180, 1110 (s, C-OH), 1067 (s, N-O), 712.

**$^1\text{H}$  NMR** (400 MHz, DMSO- $d_6$ ,  $\delta$ / ppm): 3.13-3.26 (m, 4H, - $\text{CH}_2$ -), 3.73 (p,  $J$  = 5.32 Hz, 1H, - $\text{CH}(\text{OH})$ -), 5.11 (s-br, 1H, - $\text{CH}(\text{OH})$ -), 8.34 (t,  $J$  = 6.03 Hz, 2H, - $\text{NH}$ -), 14.49 (s-br, 2H, = $\text{N-OH}$ ).

**$^{13}\text{C}$  NMR** (100 MHz, DMSO- $d_6$ ,  $\delta$ / ppm): 42.7 (t, - $\text{CH}_2$ -), 67.3 (d, - $\text{CH}(\text{OH})$ -), 108.9 (s, - $\text{C}(\text{=NOH})$ -), 128.0 (s, - $\text{C}\equiv\text{N}$ ), 158.2 (s, - $\text{C}(\text{=O})$ -).

**HRMS** (ES-,  $m/z$ ):  $[\text{MH}_-1]^-$ , calcd. for  $\text{C}_9\text{H}_9\text{N}_6\text{O}_5$ , 281.0634; found 281.0636 (+0.7 ppm).

Original spectra for this compound are presented in Appendix B, Figures B46-B55.

All but one (**5b**) of these compounds are new. All of them have been characterised by microanalysis, IR, NMR ( $^1\text{H}$ ,  $^{13}\text{C}$ , 2D, correlation) and high-resolution MS spectrometry. Experimental data were consistent with the expected compounds, and we were able to assign molecular structures with confidence.

Our  $^1\text{H}$  NMR data for compound (**5b**), the only one reported previously, compare well with the literature values.<sup>[24]</sup> In addition, we have recorded  $^{13}\text{C}$  and correlation NMR spectra for this compounds, as well as its high-resolution mass-spectrum. We have also performed elemental analysis of this compound.

The nitrile IR band appearing at 2241 to 2364  $\text{cm}^{-1}$  in these compound is weak but discernable. Oxime proton shifts  $^1\text{H}$  proved very characteristic across the range of compounds (**5a-d**): all of them confined

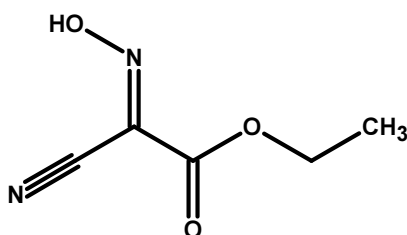
to a narrow range of 14.39-14.49 ppm.  $^{13}\text{C}$  MNR data showed a pattern similar to the published results for cyanoxime-and-amide moieties as shown in Table 5.

## Path B:

Along this route, compound (1) is first oximated to ethyl (2*E*)-cyano(hydroxyimino)ethanoate (2), which is subsequently condensed with a suitable diamine (3). Compound (2) was successfully synthesised, isolated, and characterised by us. However, not even trace quantities of *bis*-cyano(hydroxyimino)acetamides (5) were detected among products of condensation with diamines. In general, this synthetic step led to mixtures that were difficult to separate. Under certain conditions, which will be described elsewhere, this step led to the formation of (2*E*)-*N*-(*X*-aminoalkyl)-2-cyano-2-(hydroxyimino)ethanamides, of which all but one were new. It was decided to exclude these compounds from the present thesis as they will constitute the basis of future work. Hence, only data pertinent to compound (2) are presented below.

### (2) Ethyl (2*E*)-cyano(hydroxyimino)ethanoate

This compound is known in literature.<sup>[23]</sup>



**Procedure:** Sodium nitrate (20.91 g, 300.0 mmol) was weighed into a RBF, water (110 mL) added, and the mixture stirred until all of the solid had dissolved. The flask was placed in an ice bath and ethyl cyanoacetate (27.1 mL, 250 mmol) pipetted into it, followed by glacial acetic acid (19.8 mL, 345 mmol), which was added slowly. Thereafter, the mixture was stirred for 24 hours. This afforded primary precipitate, which was filtered off, and the mother liquor. The former was washed in a beaker with aqueous HCl (2M, 100 mL), then filtered off and dried on a watch glass ( $\alpha$  fraction). Within thirty minutes secondary precipitate has formed in the filtrate; it was also filtered off and left to dry on a watch glass ( $\beta$  fraction), while the filtrate was set aside (acidic filtrate fraction). Mother liquor was extracted with ether (3 $\times$ 50 mL) and aqueous HCl (2M, 80 mL) added to it. Both acidic fractions were combined and extracted again, this time with CH<sub>3</sub>Cl (3 $\times$ 65 mL). All organic fractions were combined and reduced to a solid by rotary evaporation ( $\gamma$  fraction).

Once  $\alpha$ ,  $\beta$  and  $\gamma$  were confirmed to be the same desired product by <sup>1</sup>H NMR, all three were combined and recrystallized from hot water.

**Yield:** 26.8 g, 0.188 mol (75 %).

**$^1\text{H}$  NMR** (400 MHz, DMSO,  $\delta$ / ppm): 1.28 (t,  $J = 7.1$  Hz, 3H,  $-\text{CH}_3$ ), 4.31 (q,  $J = 7.1$  Hz, 2H,  $-\text{CH}_2-$ ), 15.07 (s-br, 1H,  $=\text{N}-\text{OH}$ ).

**$^{13}\text{C}$  NMR** (100 MHz, DMSO,  $\delta$ / ppm): 13.8 (t,  $-\text{CH}_3$ ), 62.5 (d,  $-\text{CH}_2-$ ), 108.8 (s,  $-\text{C}(=\text{N}-)$ ), 125.7 (s,  $\text{N}\equiv\text{C}-$ ), 158.4 (s,  $-\text{C}(=\text{O})-$ ).

In addition to  $^1\text{H}$  and  $^{13}\text{C}$  NMR spectra we have also recorded dept-135,  $g$ -hsqc,  $g$ -hmbsc, and  $g$ -cosy spectra for this compound. They all were consistent with the structure expected.

Original spectra for this compound are presented in Appendix B, Figures B56-B57.

As this compound is known, its characterisation by NMR spectroscopy was deemed sufficient. Spectroscopic data conclusively indicated that the desired product has been synthesised.

## 3.4 Solid State Structures

We have succeeded in crystallising out two compounds, one *bis*-cyanoacetamide and one *bis*-chelate ligand, and determined their structure by single crystal X-ray diffraction. Each primary data set was collected in a different laboratory, the first by Dr M. Ackerman at UKZN and the second by Professor N.N. Gerasimchuck at MSU, to whom we express our sincere appreciation. We also gratefully acknowledge their assistance with the solution of crystal structures. The results of these determinations are presented in this section.

### 3.4.1 *N,N'*-Ethane-1,2-diylbis(2-cyanoacetamide) (**4a**)

This compound is known. Its synthesis and properties are describe in a number of publications,<sup>[37, 39, 41]</sup> but no known crystal structure has been reported so far.

## Experimental

**General:** The X-ray data were recorded on a Bruker Apex Duo diffractometer equipped with an Oxford Instruments Cryojet operating at 100(2) K and an Incoatec microsource operating at 30 W power. The data were collected with Mo K $\alpha$  ( $\lambda = 0.71073 \text{ \AA}$ ) radiation at a crystal-to-detector distance of 50 mm. The data collections were performed using  $\omega$  and  $\psi$  scans with exposures taken at 30 W X-ray power and  $0.50^\circ$  frame widths using APEX2.<sup>[46]</sup> The data were reduced with the programme SAINT<sup>[46]</sup> using outlier rejection, scan speed scaling, as well as standard Lorentz and polarisation correction factors. A SADABS semi-empirical multi-scan absorption correction<sup>[46]</sup> was applied to the data. Direct methods, SHELXS-97<sup>[47]</sup> and WinGX<sup>[48]</sup> were used to solve the structure. All non-hydrogen atoms were located in the difference density map and refined anisotropically with SHELXL-97.<sup>[47]</sup> All hydrogen atoms were included as idealized contributors in the least squares process. Their positions were calculated using a standard riding model with C–H<sub>methylene</sub> distances of  $0.99 \text{ \AA}$  and  $U_{\text{iso}} = 1.2 U_{\text{eq}}$ . Amide hydrogen atoms, N–H, were located in the difference density map, and refined isotropically.

The checkCIF report is included in Appendix B, Figure B58.

**Specific:** A clear yellow needle-like single crystal was selected after inspection under microscope. It was mounted with the help of a mitegen loop.

Crystal and structure refinement data are given in Table 8.

**Table 8.** Sample and crystal data for compound (**4a**).

Name	<i>N,N'</i> -ethane-1,2-diylbis(2-cyanoacetamide)	
Chemical Formula	C <sub>8</sub> H <sub>10</sub> N <sub>4</sub> O <sub>2</sub>	
Formula weight	97.10	
Temperature	100 K	
Wavelength	0.71073 Å	
Crystal size	0.25 × 0.10 × 0.10 mm	
Crystal appearance	clear yellow needle	
Crystal system	monoclinic	
Space Group	P 2 <sub>1</sub> /c	
Unit cell dimensions	<i>a</i> = 4.4555(5) Å	α = 90°
	<i>b</i> = 8.7443(7) Å	β = 99.125(7) °
	<i>c</i> = 11.6123(10) Å	γ = 90°
Volume	446.69(7) Å <sup>3</sup>	
Z	4	
Density (calculated)	1.444 g cm <sup>-3</sup>	
Absorption coefficient	0.108 mm <sup>-1</sup>	
F(000)	204	
Theta range for data collection	2.93 to 26.27°	
Index ranges	-5 ≤ h ≤ 4, -10 ≤ k ≤ 10, -14 ≤ l ≤ 14	
Reflections collected	3802	
Independent reflections	862 [R <sub>int</sub> = 0.0402]	
Max. and min. transmission	0.9893 and 0.9735	
Refinement method	Full-matrix least-squares on F <sup>2</sup>	
Function minimized	Σ w(F <sub>o</sub> <sup>2</sup> - F <sub>c</sub> <sup>2</sup> ) <sup>2</sup>	
Data / restraints / parameters	862 / 0 / 64	
Goodness-of-fit on F <sup>2</sup>	1.09	
Final R indices	782 data; I > 2σ(I)	R1 = 0.0408, wR2 = 0.1151
	all data	R1 = 0.0446, wR2 = 0.1190
Weighing scheme	w = 1/[σ <sup>2</sup> (F <sub>o</sub> <sup>2</sup> ) + (0.0666P) <sup>2</sup> + 0.2084P], where P = (F <sub>o</sub> <sup>2</sup> + 2F <sub>c</sub> <sup>2</sup> )/3	
Largest diff. peak and hole	0.308 and -0.213 eÅ <sup>-3</sup>	
RMS deviation from mean	0.056 eÅ <sup>-3</sup>	

Selected bond lengths and angles are given in Table 9.

**Table 9.** Selected geometric parameters for compound (4a).

Bond lengths (Å)			
N1—C1	1.144 (2)	C2—O1	1.234 (2)
C1—C2	1.462 (2)	C3—N2	1.330 (2)
C2—C3	1.533 (2)	C2—C4	1.460 (2)
Bond angles (°)			
N1-C1-C2	179.20 (19)	O1-C3-N2	124.32 (14)
C1-C2-C3	110.43 (12)	C3-N2-C4	122.72 (12)
C2-C3-N2	114.06 (12)	C3-N2-H1	118.6
Torsion angles (°)			
N1-C1-C2-C3	103 (11)	O1-C3-N2-C4	-3.9 (3)
C1-C2-C3-O1	5.7 (2)	O1-C3-N2-H1	176.03
C1-C2-C3-N2	-174.76 (13)		

## Molecular Structure

The title compound is centrosymmetric, Figure 24. Selected bond distances are given in Table 9, and are fairly representative of such compounds.<sup>[49]</sup> 2-Cyano-ethanamide moiety is essentially planar. The most distant atom from the average plane drawn through all non-hydrogen atoms of this fragment is methylene group carbon (at 0.061 Å), Figure 25. Within the moiety nitrile and carbonyl groups are *cis* to each other.

Essential feature of the molecular structure of (4a) is that the molecule is not in linear but in the step-wise “two parallel platform” conformation, with the distance between average platform planes of 1.841 Å, Figure 25. Terminal cyanoacetamide moieties are *trans* to each other. Two methylene groups of the ethane bridge are in a staggered conformation.

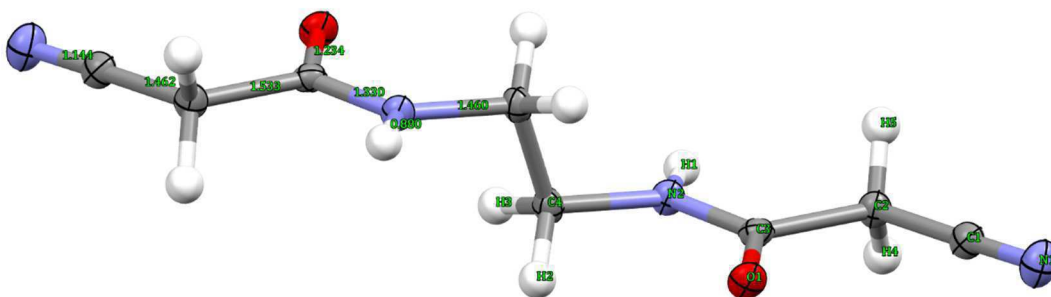


**Fig. 24.** A view of the molecular structure of (4a) with the numbering scheme. Displacement ellipsoids (Mercury 3.3) are drawn at the 50 % probability level; representative bond distances are given in Angstroms (Å).

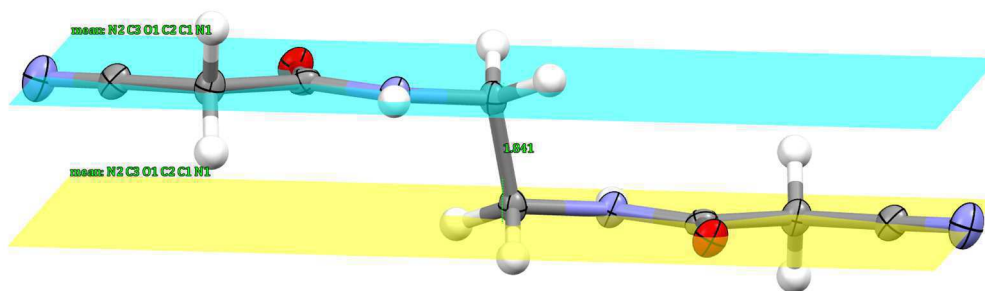


**Fig. 25.** A view of the molecular structure of **(4a)** illustrating the planarity of the cyanoacetamide moieties.

## Crystal Structure

As can be seen from Figure 24, solid phase of **(4a)** is solvent-free. A packing diagram for the crystal structure of this compound is shown in Figure 26. It crystallises in  $P 2_1/c$  space group of the monoclinic system. At 100 K the unit cell has a volume of  $446.69 \text{ \AA}^3$ , and contains 4 asymmetric units.

The spatial arrangement of molecules is influenced by two major factors: a) multiple intermolecular hydrogen bonds, and b)  $\pi$ -stacking interactions between double and triple bonds on neighbouring **(4a)** molecules.

There are four hydrogen-bonding interaction between amine and carbonyl groups per molecule, Figure 27. Geometric parameters of such interactions are given in Table 10. Amine-carbonyl interactions are also shown in Figure 28. They represent hydrogen bonding of moderate strength, and are characterised by the bond length of  $2.11 \text{ \AA}$ , and bond angle of  $156.4^\circ$ .

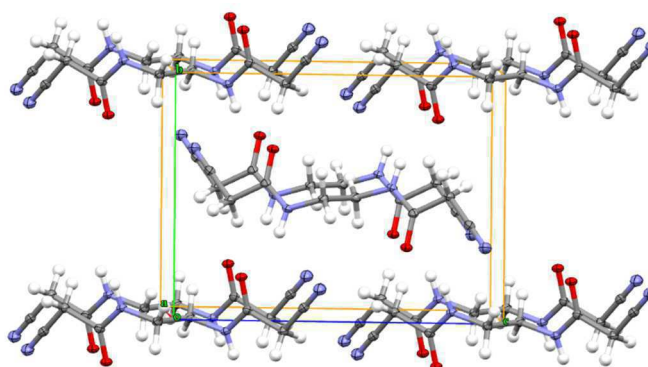


**Fig. 26.** A packing diagram viewed down  $a$ -axis for the crystal structure of **(4a)**.



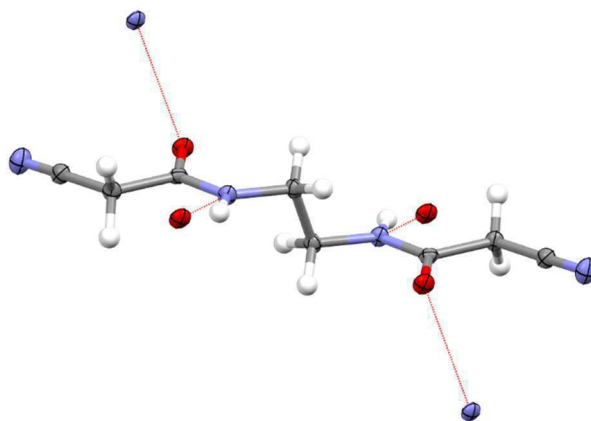


**Fig. 27.** H-Bonding interactions in the crystal structure of (**4a**).

**Table 10.** Hydrogen-bond geometry in crystal structure of (**4a**).

D—H...A	Distance (Å)			Angle (°)
	D—H	H...A	D...A	
N2—H1...O1 <sup>i</sup>	0.88	2.11	2.94(2)	156.4

Symmetry codes: (i)  $-x, -1/2+y, 1/2-z$ .

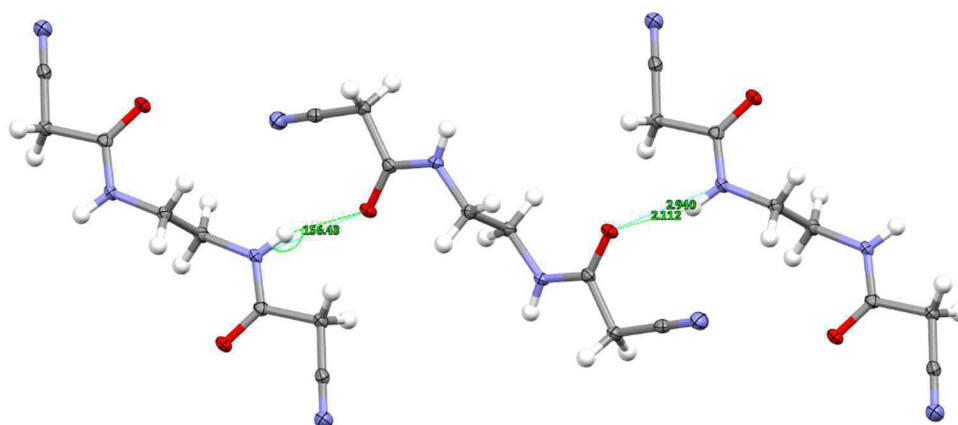


**Fig. 28.** Representative H-bonding interactions in the crystal structure of (**4a**) that involve amine and carbonyl groups.

$\pi$ -Stacking plays important role in the formation of this crystal structure. There are two types of such interaction. The first of them are shown in Figures 29 and 30. The first of them represents back-to-back  $\pi$ -stacking of terminal nitrile groups, while the second represents stacking of the nitrile and carbonyl functional groups. Molecules linked by these interactions form infinite linear strands, which intersect as shown in Figure 31. The combination of hydrogen bonding,  $\pi$ -stacking interactions and weak van der Waals forces affords three-dimensional crystal structure. A view of the fragment of this structural down  $a$ -axis is shown in Figure 32. It also can be described as a stack of parallel molecular strands, shown in Figures 33 and 34.

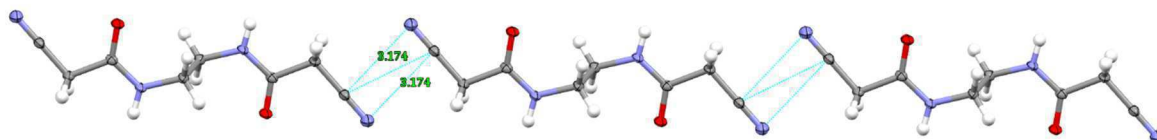


**Fig. 29.**  $\pi$ -Stacking interaction of the first kind in the crystal structure of (4a).

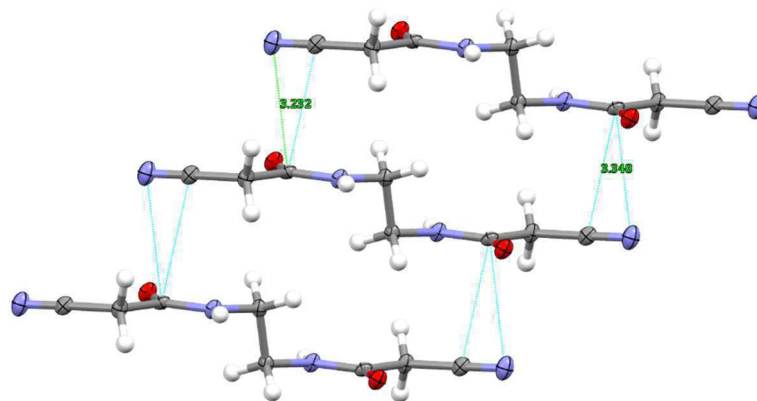


**Fig. 30.**  $\pi$ -Stacking interaction of the second kind in the crystal structure of (4a).

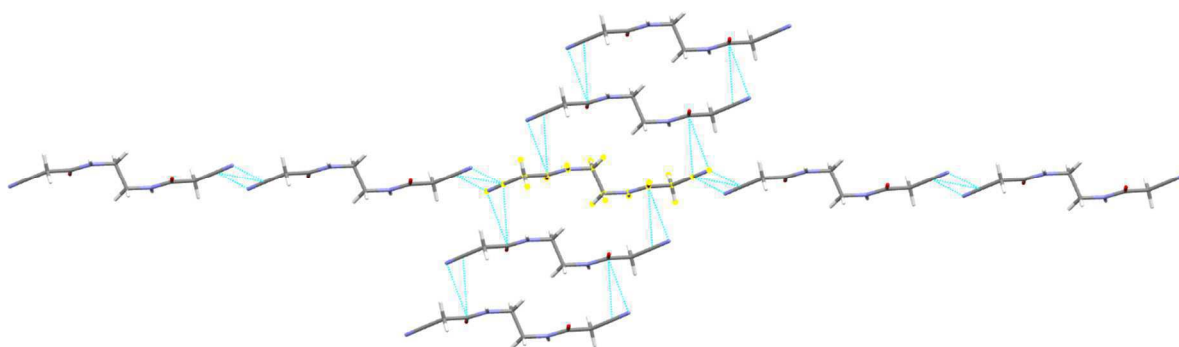


**Fig. 31.** Two intersecting molecular strands arising from  $\pi$ -stacking interactions in the crystal structure of (4a).

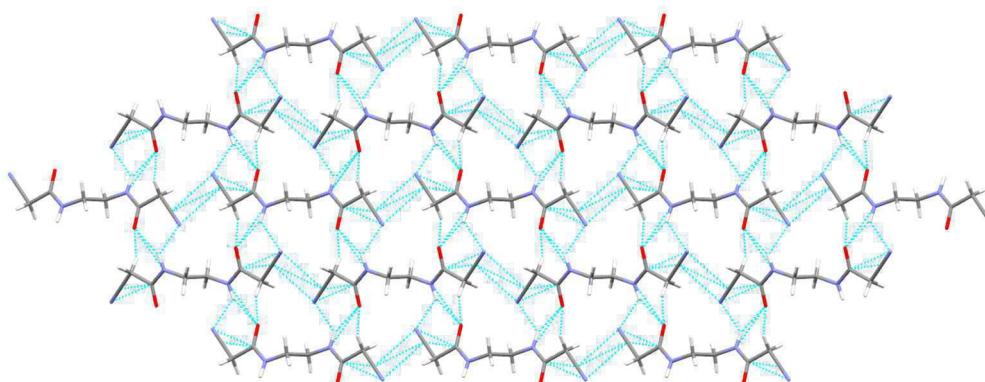


**Fig. 32.** A view of the crystal structure of (5a) down  $a$ -axis.

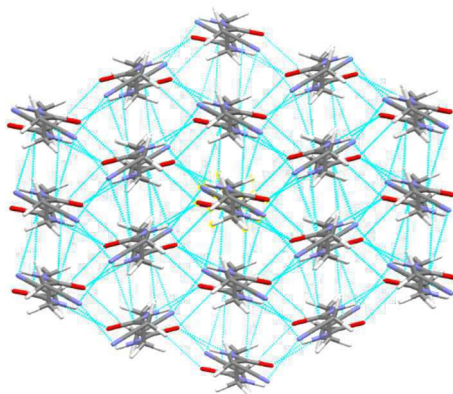


**Fig. 33.** A view of the crystal structure of (4a) down the axis of strands.

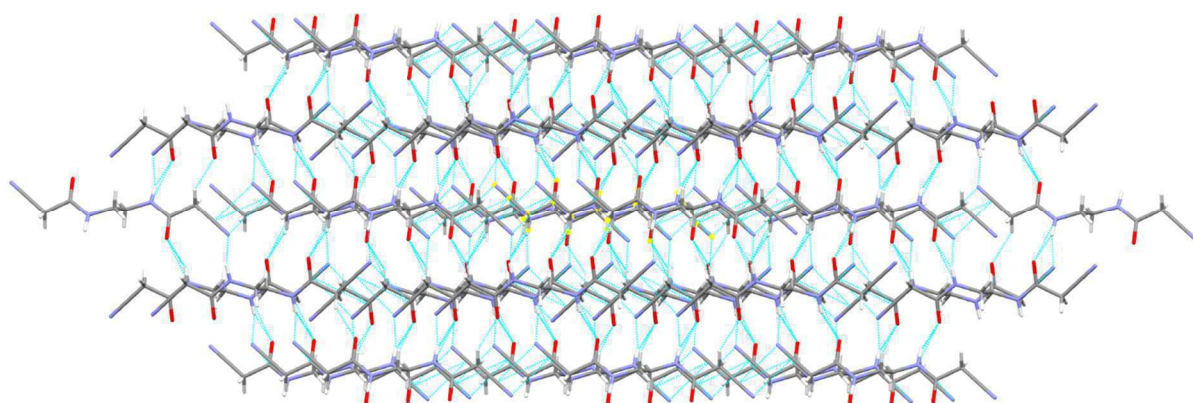


**Fig. 34.** A view of the crystal structure of (4a) perpendicular to the axis of strands.

### 3.4.2 *N,N'*-Ethane-1,2-diylbis[2-cyano-2-(hydroxyimino)ethanamide] (5a)

This compound is new. Consequently, the crystal structure determined is the first for the new class of *bis*-chelate cyanoxime-and-amide ligands.

#### Experimental

**General:** Crystal data were collected on the Bruker APEX 2 diffractometer, equipped with a SMART CCD area detector. The intensity data were collected in  $\omega$  scan mode using the Mo tube ( $K_{\alpha}$  radiation;  $\lambda = 0.71073 \text{ \AA}$ ) with a highly oriented graphite monochromator. Intensities were integrated from 4 series of 364 exposures, each covering  $0.5^{\circ}$  in  $\omega$  at 20 seconds of acquisition time, with the total data set being a sphere.<sup>[50]</sup> Determination of the space group was done with the aid of XPREP software.<sup>[50]</sup> The absorption correction was performed by the numerical method using the set of images obtained from the video-microscope and using the SADABS program from Bruker AXS software package.<sup>[51]</sup> The structure was solved by direct methods and refined by least squares on weighted  $F^2$  values for all reflections using the SHELXTL program. Drawing of crystal structures and packing diagrams was done using the ORTEP<sup>[52]</sup> and Mercury software packages.<sup>[53]</sup> The crystal structure has been deposited into the CCDC, deposition numbers: 992014-992015. The PLATON<sup>[54]</sup> checkCIF report is included in Appendix B, Figure B59.

**Specific:** A clear platelet-like single crystal was selected after inspection under polarized light. With the help of vacuum grease it was mounted on a thin galls fibre attached to the copper-pin positioned on the goniometer head of the Bruker APEX 2 diffractometer. A total of 1456 frames were collected. Overall exposure time was 8.09 hours. Integration of the data for a monoclinic unit cell yielded a total of 6787 reflections to the maximum  $\theta$  angle of  $27.48^{\circ}$  ( $0.77 \text{ \AA}$  resolution), of which 1273 were independent (average redundancy 5.332, completeness 99.8%,  $R_{\text{int}} = 5.08\%$ ) and 897 (70.46%) were greater than  $2\sigma(F^2)$ . The final cell constants,  $a = 8.170(2) \text{ \AA}$ ,  $b = 6.6782(18) \text{ \AA}$ ,  $c = 10.309(3) \text{ \AA}$ ,  $\beta = 99.320(4)^{\circ}$ , volume =  $555.0(3) \text{ \AA}^3$ , are based on the refinement of XYZ-centroids for the reflections above  $20 \sigma(I)$ . The calculated minimum and maximum transmission coefficients (based on the crystal size) are 0.7268 and 0.7456.

The structure was solved and refined using Bruker SHELXTL Software Package, for the space group  $P 2_1/n$ , with  $Z = 4$  for the asymmetric formula unit,  $C_4H_4N_3O_2$ . The final anisotropic full-matrix least-squares refinement on  $F^2$  with 97 variables converged at  $R1 = 4.59 \%$ , for the observed data, and  $WR2 = 12.60 \%$  for all data. The goodness-of-fit was 1.039. The largest peak in the final difference

electron density map was  $0.453 \text{ e}/\text{\AA}^3$  and the largest hole was  $-0.268 \text{ e}/\text{\AA}^3$  with the RMS deviation of  $0.065 \text{ e}/\text{\AA}^3$ . On the basis of the final model, the calculated density was  $1.509 \text{ g cm}^{-3}$  and  $F(000)$  was 260 e-.

Remarkable feature of this data set was that all hydrogen atoms in the structure were located in the difference density map and, consequently, refined anisotropically.

The summary of crystal data and refinement parameters is presented in Table 11, while selected geometric parameters are given in Table 12.

**Table 11.** Sample and crystal data for compound (5a).

Name	<i>N,N</i> -ethane-1,2-diylbis[2-cyano-2-(hydroxyimino)ethanamide]	
Chemical Formula	$\text{C}_8\text{H}_8\text{N}_6\text{O}_4$	
Formula weight	126.10	
Temperature	120(2) K	
Wavelength	0.71073 Å	
Crystal size	0.090 × 0.230 × 0.340 mm	
Crystal appearance	clear light colourless plate	
Crystal system	monoclinic	
Space Group	P 2 <sub>1</sub> /n	
Unit cell dimensions	$a = 8.170(2) \text{ \AA}$	$\alpha = 90^\circ$
	$b = 6.6782(18) \text{ \AA}$	$\beta = 99.320(4)^\circ$
	$c = 10.309(3) \text{ \AA}$	$\gamma = 90^\circ$
Volume	$555.0(3) \text{ \AA}^3$	
Z	4	
Density (calculated)	$1.509 \text{ g cm}^{-3}$	
Absorption coefficient	$0.124 \text{ mm}^{-1}$	
$F(000)$	260	
Theta range for data collection	2.96 to 27.48°	
Index ranges	$-10 \leq h \leq 10, -8 \leq k \leq 8, -13 \leq l \leq 13$	
Reflections collected	6787	
Independent reflections	1273 [ $R_{\text{int}} = 0.0508$ ]	
Max. and min. transmission	0.7456 and 0.7268	
Structure solution technique	direct methods	
Structure solution program	SHELXS-1013 (Sheldrick, 2013)	
Refinement method	Full-matrix least-squares on $F^2$	
Refinement program	SHELXL-2013 (Sheldrick, 2013)	
Function minimized	$\sum w(F_o^2 - F_c^2)^2$	
Data / constraints / parameters	1273 / 0 / 97	
Goodness-of-fit on $F^2$	1.039	
Final R indices	897 data; $l > 2\sigma(l)$	$R1 = 0.0459, wR2 = 0.1056$
	all data	$R1 = 0.0730, wR2 = 0.1260$
Weighing scheme	$w = 1/[\sigma^2(F_o^2) + (0.0479P)^2 + 0.5247P]$ , where $P = (F_o^2 + 2F_c^2)/3$	
Largest diff. peak and hole	$0.453$ and $-0.268 \text{ e}\text{\AA}^{-3}$	
RMS deviation from mean	$0.065 \text{ e}\text{\AA}^{-3}$	

## Molecular Structure

The title compound is centrosymmetric, Figure 35. Selected bond distances are given in Table 12, and are fairly representative of such compounds.<sup>[49]</sup> 2-Cyano-2-(hydroxyimino)ethanamide moiety is essentially planar, as expected on the grounds of  $\pi$ -conjugation of double bonds. The most distant atom from the average plane drawn through all non-hydrogen atoms of this fragment is carbonyl oxygen (at 0.084 Å), Figure 36. Oxime and carbonyl groups within the moiety are *trans* to each other, as is the case in almost all known to us oxime-and-amide compounds. Intramolecular hydrogen bond between the amide hydrogen and oxime nitrogen is weak, and at  $N_{ox} \cdots H_{ad}$  distance of 2.323 Å, probably, can be discounted.

**Table 12.** Selected geometric parameters for compound (5a).

Bond lengths (Å)			
C1-N1	1.287(3)	C1-C2	1.446(3)
C1-C3	1.499(3)	C2-N2	1.140(3)
C3-O2	1.242(2)	C3-N3	1.322(3)
N1-O1	1.360(2)	N3-H1N3	0.85(3)
O1-H1O1	0.97(3)		
Bond angles (°)			
N1-C1-C2	123.45(19)	N1-C1-C3	118.88(18)
C2-C1-C3	117.61(18)	N2-C2-C1	178.5(2)
O2-C3-N3	124.7(2)	O2-C3-C1	119.10(18)
N3-C3-C1	116.18(18)	N3-C4-C4	110.6(2)
C1-N1-O1	113.41(17)	N1-O1-H1O1	100.2(15)
Torsion angles (°)			
N1-C1-C3-O2	172.8(2)	C2-C1-C3-N3	176.6(2)
N1-C1-C3-N3	-5.8(3)	C2-C1-N1-O1	1.3(3)
O2-C3-N3-C4	-1.9(3)	O2-C3-N3-H1N1	-178.6(2)
C1-N1-O1-H1O1	177.4(2)	C1-C3-N3-H1N3	0.1(3)

Essential feature of the molecular structure of (5a) is that the molecule is not in a linear but in the step-wise “two parallel platform” conformation, with the distance between average platform planes of 1.420 Å, Figure 36. This feature was also present in the structure of anhydrous 2-methyl-2-(hydroxyimino)ethanamide analogue obtained in our research group previously,<sup>[5]</sup> as well as in the structure published by Fritsky *et al.*<sup>[49]</sup> Terminal 2-cyano-2-(hydroxyimino)ethanamide chelating moieties are also *trans* to each other. The methylene groups of the ethane bridge are in a staggered conformation.

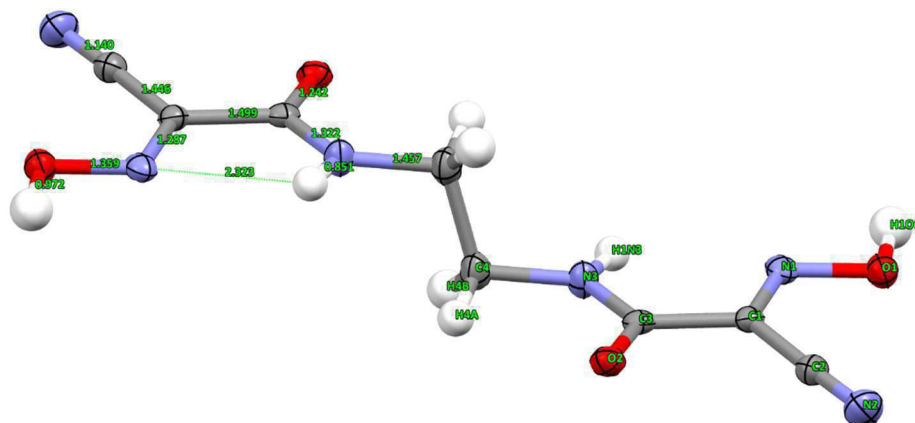


**Fig. 35.** A view of the molecular structure of **(5a)** with the numbering scheme. Displacement ellipsoids (Mercury 3.3) are drawn at the 50 % probability level; representative bond distances are given in Angstroms (Å).

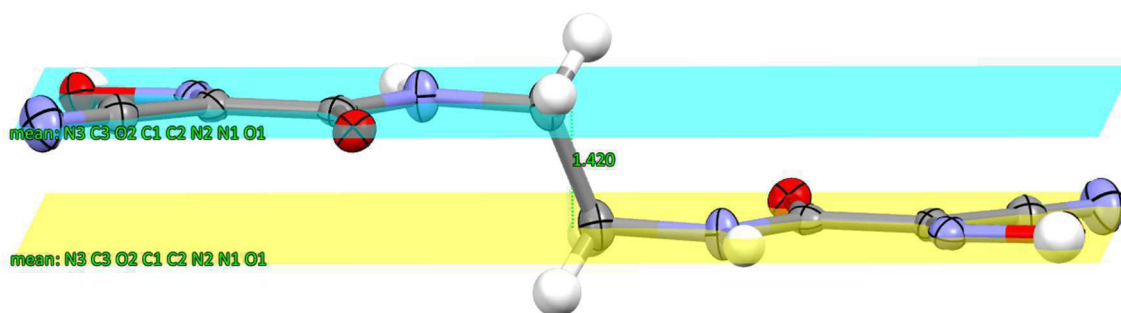


**Fig. 36.** A view of the molecular structure of **(5a)** illustrating the planarity of chelating moieties.

## Crystal Structure

As can be seen from Figure 35, solid phase of **(5a)** is solvent-free. A packing diagram for the crystal structure of this compound is shown in Figure 37. It crystallises in  $P2_1/n$  space group of the monoclinic system. At 120 K the unit cell has a volume of  $555.0(3) \text{ \AA}^3$ , and contains 4 asymmetric units.

The spatial arrangement of molecules is influenced by two major factors: a) intricate system of multiple intermolecular hydrogen bonds, and b) multiple  $\pi$ -stacking interactions between conjugate systems of the double bonds on neighbouring **(5a)** molecules.

There are four hydrogen-bonding interaction between oxime and carbonyl groups per molecule, and four more such interactions between amine and nitrile groups, Figure 38. Geometric parameters of such interactions are given in Table 13. Oxime-carbonyl interactions are also shown in Figure 39. They represent strong hydrogen bonding, and are characterised by rather short bond length,  $1.66(3) \text{ \AA}$ , and nearly optimal bond angle,  $172.8^\circ$ . In comparison, amine-nitrile interactions are significantly weaker.

As can be seen from Figure 40, the bond length at 2.37(3) Å is longer, and the bond angle at 133.2° is far from optimal.

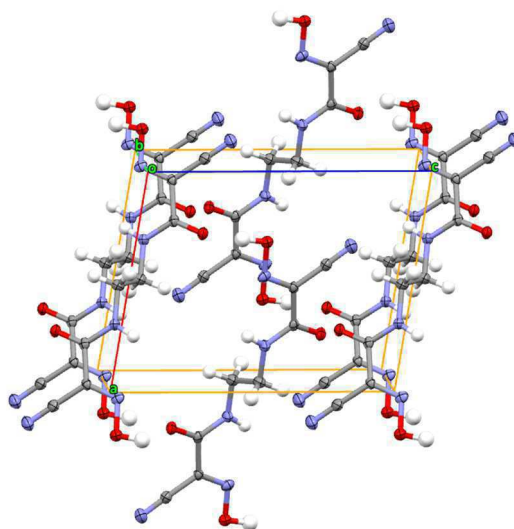


**Fig. 37.** A packing diagram viewed down *b*-axis for the crystal structure of (5a).

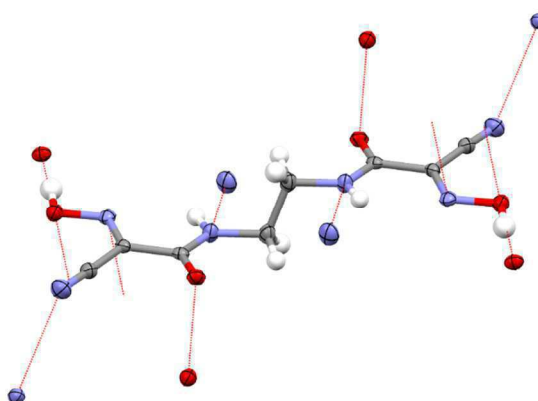


**Fig. 38.** Major types of H-bonding interactions in the crystal structure of (5a).

**Table 13.** Hydrogen-bond geometry in crystal structure of (5a).

D—H···A	Distance (Å)			Angle (°)
	D—H	H···A	D···A	
O1-H1O1···O2 <sup>i1</sup>	0.97(3)	1.66(3)	2.627(2)	172.8
N3-H1N3···N2 <sup>i2</sup>	0.85(3)	2.37(3)	3.018(3)	133.2

Symmetry codes: (i1)  $\frac{1}{2}+x, 1.5-y, \frac{1}{2}+z$ ; (i2)  $-\frac{1}{2}+x, 1.5-y, \frac{1}{2}+z$ .



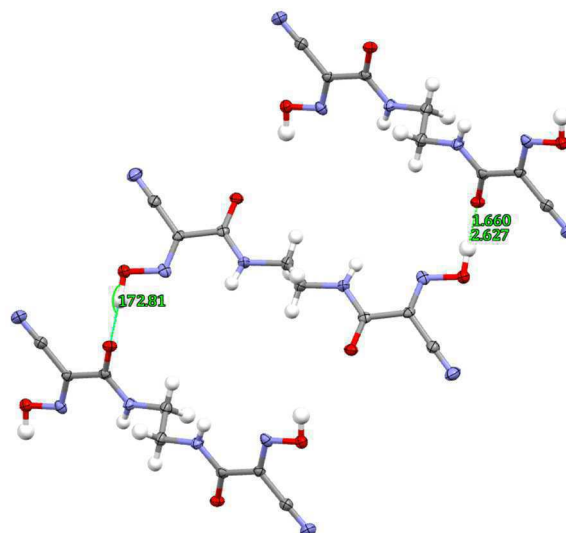


**Fig. 39.** Representative H-bonding interactions in the crystal structure of (5a) that involve oxime and carbonyl groups.

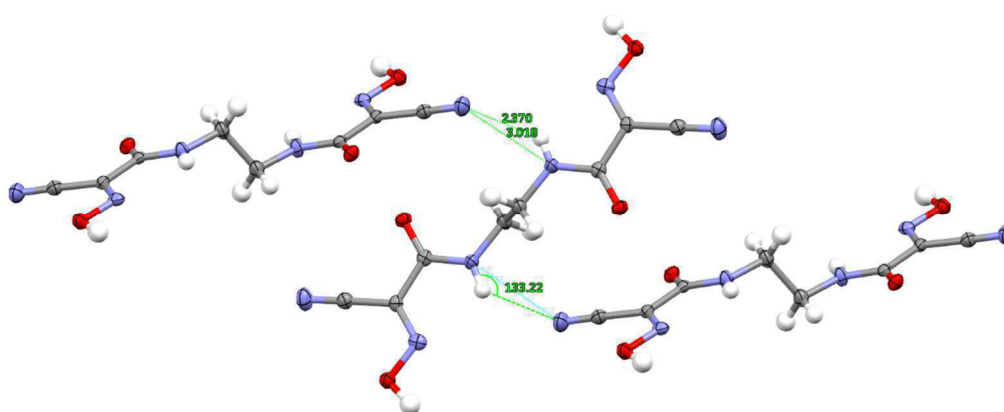


**Fig. 40.** Representative H-bonding interactions in the crystal structure of (5a) that involve amine and nitrile groups.

As has already been mentioned, high degree of planarity of cyanoxime-and-amide chelates is the reflection of extended  $\pi$ -conjugation of their double bonds.  $\pi$ -Stacking of these extended systems plays important role in the formation of crystal structure. Two types of such interactions are shown in Figures 41 and 42. The first of them represents back-to-back  $\pi$ -stacking of terminal oxime groups, while the second represents four-centre stacking of the oxime-and-amide moieties. Molecules linked by each kind of these interactions form infinite linear strands, Figure 43, which intersect as shown in Figure 44. Sheets of such stands are stitched by hydrogen bonds into three-dimensional networks. Weak van der Waals intermolecular forces complement the above two kinds of interactions, and in combination are responsible for intricate three-dimensional crystal structure. A view of the fragment of this structural down  $a$ -axis is shown in Figure 45; as can be seen from this angle, the molecules form beautiful undulating array.

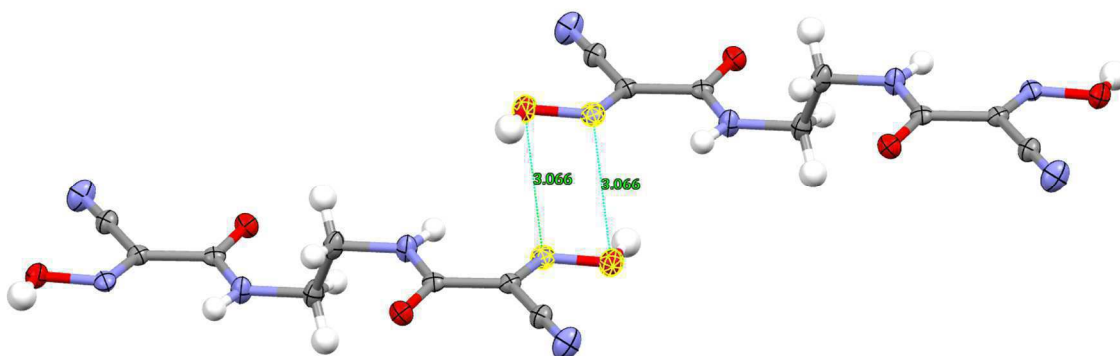


Fig. 41.  $\pi$ -Stacking interaction of the first kind in the crystal structure of (5a).

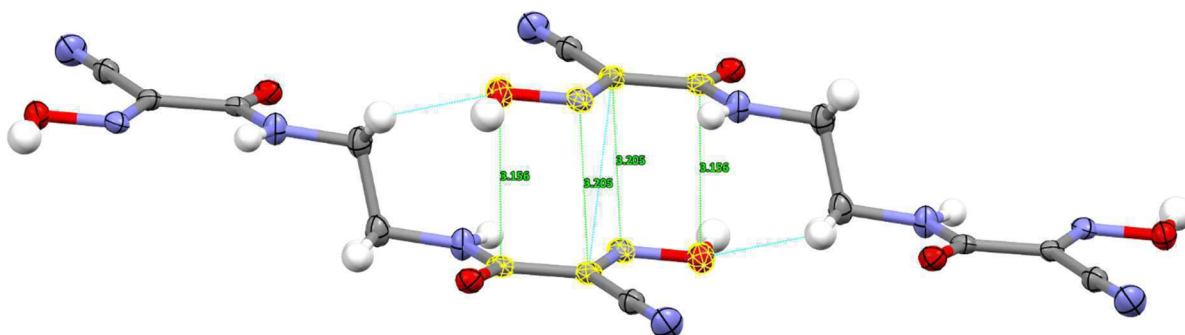


Fig. 42.  $\pi$ -Stacking interaction of the second kind in the crystal structure of (5a).

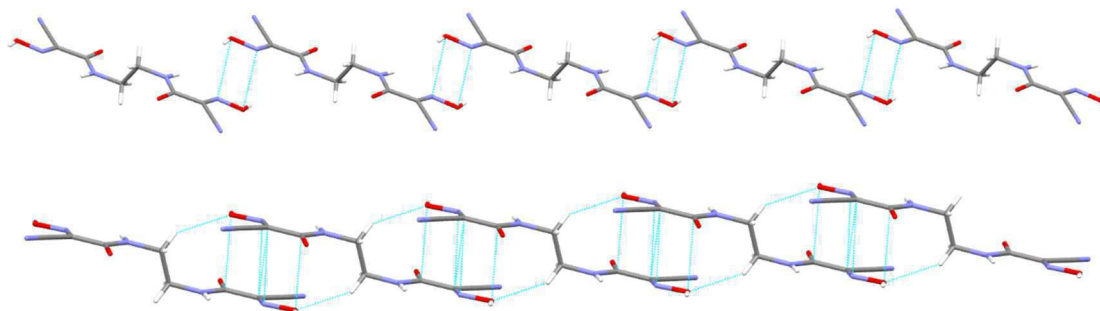
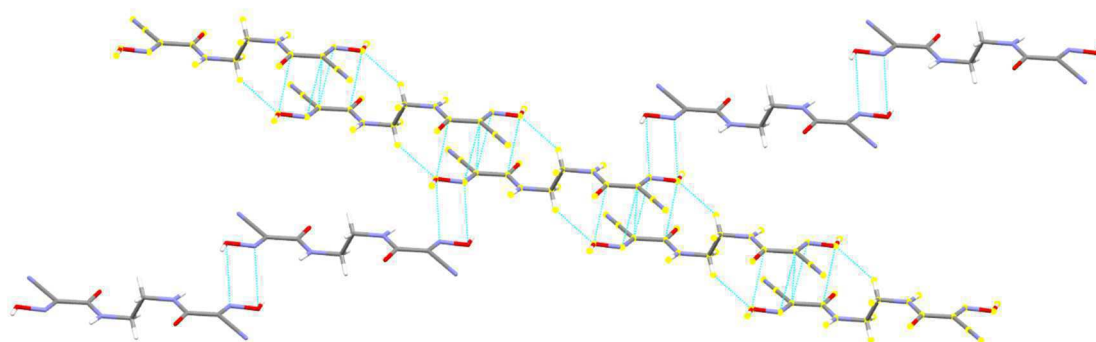
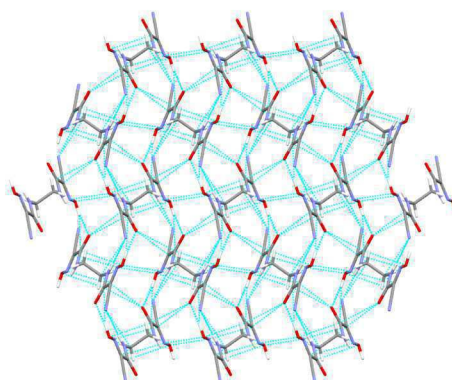


Fig. 43. Two types of molecular strands arising from  $\pi$ -stacking interactions in the crystal structure of (5a).



**Fig. 44.** Two intersecting molecular strands in the crystal structure of **(5a)**.



**Fig. 45.** A view of the crystal structure of **(5a)** down *a*-axis.

## 4. Discussion of the Synthetic Results

In this section we will discuss our findings and observations accumulated in the course of ligand synthesis. Among other matters we will consider the sequence of steps, apparatus design, and evidence for the conformers formation.

### 4.1 Two Synthetic Routes

In view of two possible synthetic routes towards the desired cyanoxime-and-amide *bis*-chelates, which have been considered earlier, Scheme 15, we will take a close look at the reagents and starting materials used in each of them. The first step of each path, path A and path B, was accomplished by us with relative ease, and does not merit much of further discussion here. Ethyl cyanoacetate (**1**) and four diamines (**3a-d**) required for the precursor synthesis are all commercially available.

The second step of **path A**, Scheme 15, implies bubbling  $\text{CH}_3\text{ONO}$  gas\* through a solution/suspension of *bis*-cyanoamide precursor in *iso*-propanol that also contains sodium *iso*-propoxide. Advantages of this approach include gaseous nitrosation agent, which is easy to remove from the reaction mixture, and the synthesis of intermediate *bis*-cyanoamides (**4a-d**) that is well documented in literature.<sup>[37, 39]</sup> The latter are synthesised in one-pot reactions, in high yield, and with very little separation required. Drawbacks of this approach are the need of daily preparation of the *iso*-propoxide base<sup>†</sup> and the complication of working with a highly toxic methyl nitrite gas.

The second step of **path B**, Scheme 15, involves condensation of ethyl-cyano(hydroxyimino) ethanoate (**2**) with four diamines (**3a-d**). Similar reactions have been carried out successfully in our group previously in dry methanol in the presence of acid washed glass beads as a catalyst.

From a pragmatic point of view path **B** appears advantageous to path **A** as it does not require preparation of strong unstable base or use of a toxic nitrosation agent. In addition, one might argue the merit of each path in terms of time and effort spent on step one. In truth, both sets of precursors are made with relative ease and in high yield. However, path **B** is more appealing from this perspective as only one rather than four precursors need to be made.

---

\* Which is generated in a separate container by the drop wise addition of sulfuric acid to a solution of sodium nitrite in a mixed water-MeOH medium.

† This involves dissolving sodium metal in freshly distilled *iso*-propanol.

## 4.2. Path B

We will start with this path for two reasons: a) it was the first path we tried, and b) it failed completely to deliver *bis*-chelates.

### 4.2.1 Step One: Oximation

This synthetic step is described in section 3. It was completed successfully, and we have no additional comments about it.

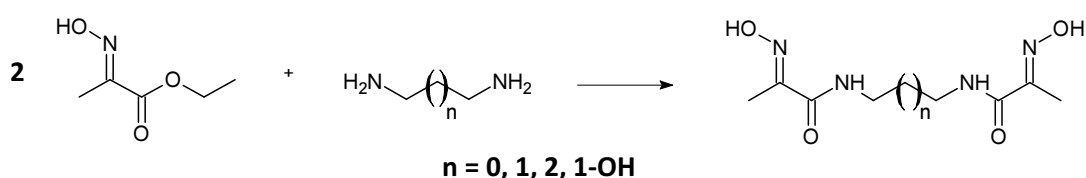
### 4.2.2 Step Two: Condensation

Four attempts to synthesise the desired ligands following Scheme 15 path **B** were made with diamines (**3a-d**). The generic procedure employed is given below.

**Generic Procedure:** Ethyl-cyano(hydroxyimino)ethanoate (**2**) (1.03 g, 7.00 mmol) was weighed into a RBF (100 mL), flushed with Ar, and dry MeOH added. The flask was sealed with a septum and the diamine (**3a-d**) (3.50 mmol) added dropwise.<sup>‡</sup> The mixture was stirred for 12 hours, the solvent removed by rotary evaporation, and the crude material analysed by means of <sup>1</sup>H and <sup>13</sup>C NMR spectroscopy.

Despite using stoichiometric ratio of the ester to diamine (2 : 1), in all four cases characterisation data indicated exclusive formation of *mono*-condensates, without even trace quantities of *bis*-chelates. In addition, separation of the products proved rather difficult, as is known to be the case from the work on a line of similar *mono*-chelate ligands (**mhiaa**) by Ms E. Diu, a postgraduate student in our research group.

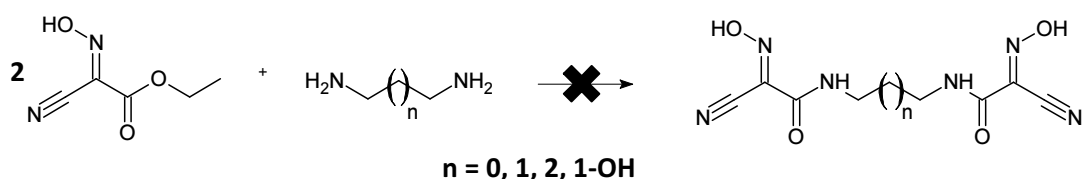
Initially, these results puzzled us, because similar approach worked well for the preparation of methyl substituted analogues, *N,N'*-alkyl-diylbis[2-(hydroxyimino)propanamide]s, (**mhiaaz**), Scheme 16.<sup>[44]</sup>



**Scheme 16.** Synthesis of *N,N'*-alkyl-diylbis[2-(hydroxyimino)propanamide]s.

<sup>‡</sup> In the case of 1,3-diaminopropan-2-ol, which is solid at room temperature, its solution in MeOH was used.

However, it completely failed when the methyl group  $\alpha$  to oxime was replaced with nitrile, Scheme 17.



**Scheme 17.** Attempted condensation step (step two) of path **B**.

We have already discussed possible reasons for such failure in section 2.8.2. In addition to what was said there, we offer the following explanation to exclusive formation of *mono*-condensates. Strictly stoichiometric ratio of ethyl-cyano(hydroxyimino)ethanoate (**2**) to diamine (**3a-d**) (2 : 1) results in complete protonation of both amino groups and, consequently, lack of any condensation products. In practice, slight excess of a diamine is employed (about 5 to 10 %) to compensate for its partial oxidation and loss due to evaporation. This excessive quantity of diamine remains in its molecular form and is able to attack electrophilic carbonyl carbon of the ester, affording *mono*-condensed product. However, once such product is formed, Figure 46, involvement of the second amino group into condensation process becomes impossible, no matter how large excess of the diamine is present. We think, the reason for it is additional Coulomb, and possibly hydrogen-bonding intramolecular stabilisation due to the formation of Zwitter-ions, as shown below.

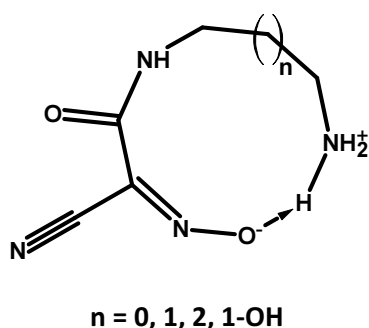


**Fig. 46.** Suggested Zwitter-ion type stabilisation of cyanoxime-amide-amine *mono*-condensates.

This stabilisation is responsible for the fact that the terminal amino group of the *mono*-condensate is always going to be in protonated state, rather than other sacrificial amine or diamine. Consequently, further condensation with another unit of ester (**2**) becomes impossible as the terminal amino group of *mono*-condensate is “switched off”.

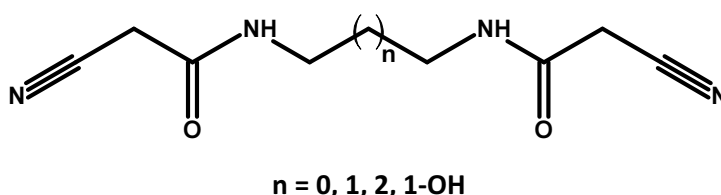
Having realised that this presents an unsurmountable obstacle on the way to *bis*-chelate ligands, we focused our synthetic efforts on path **A**, Scheme 15.

### 4.3. Path A:

The sequence of synthetic steps similar to the ones represented in path A, Scheme 15, led to the preparation of the first, and prior to our work the only, desired *bis*-chelate cyanoxime-and-amide ligand (**5b** or **chiaa<sub>2p</sub>**).<sup>[24]</sup> This was encouraging, and we proceeded to repeat the preparation of this and synthesise three new ligands of the series (**5a**, **5c** and **5d**).

#### 4.3.1 Step One: Condensation

Four homologue *bis*-cyanoacetamides shown below, required as intermediates, were synthesised following two procedures. On three occasions, the reaction was carried out in solvent medium. In another instance neat reagents were used in a solvent-free synthesis. Some of the relevant issues have already been discussed in section 2.9.2, and an interested reader is advised to consult it.



Initially, the synthesis of *N,N'*-propane-1,3-diylbis(2-cyanoacetamide) (**4b**) was attempted in  $\text{CH}_2\text{Cl}_2$  medium without a catalyst and in MeOH medium with acid washed glass beads catalyst. In both cases the synthesis proceeded well, precipitating out the product within a few hours.

Correspondingly, the merit of each solvent system was judged by the yield achieved in two synthetic attempts. In addition, we recorded the yield at every stage of the working up of the product mixture. Our data show that the product was recovered as a primary precipitate and from the mother liquor on both occasions, with the yields given below.

**Table 14.** Yield of *N,N'*-propane-1,3-diylbis(2-cyanoacetamide) (**4b**) per fraction in two different solvated systems.

Solvent system	Yield (%) from primary precipitate yield	Yield (%) from mother liquor precipitates
$\text{CH}_2\text{Cl}_2$	59	38
MeOH/Glass Beads	76	10

As can be seen from the table, more (**4b**) product was isolated as primary precipitate when the reaction was run in methanol in the presence of the catalyst, 76 % as opposed to 59 %. However, more product

was recovered from the dichloromethane mother liquor, 38 % versus 10 %. Overall yield, excellent on both occasions, nevertheless give slight advantage to the CH<sub>2</sub>Cl<sub>2</sub> medium (yield 97 %) against MeOH/beads system (yield 86 %). On the downside of the CH<sub>2</sub>Cl<sub>2</sub> system, was the need to work-up more synthetic fractions, which takes both time and effort. Such approach is justified if the starting materials are expensive. This was not the case, with ethyl cyanoacetate (**1**) and four diamines (**3a-d**) being affordable. Consequently, with time being of essence, we opted for the MeOH/catalyst system in the preparation of *bis*-cyanoacetamides (**3a**, **3b**, and **3d**), and decided to sacrifice residual amount of product still present in the mother liquor.

Now that we have considered the case of condensation reaction in two solvent media, we will turn our attention to the procedure of Gazit *et al.*,<sup>[37]</sup> who synthesised the same compounds without any solvent at all, Table 15.

**Table 15.** Yield of *bis*-cyanoacetamides according to Gazit *et al.*<sup>[37]</sup> (solvent-free) and in our synthesis in MeOH/glass beads medium.

No	<i>Bis</i> -cyanoacetamide	Yield (%) Gazit <i>et al.</i>	Yield (%) MeOH/glass beads
4a	<i>N,N'</i> -ethane-1,2-diylbis(2-cyanoacetamide)	86	67
4b	<i>N,N'</i> -propane-1,3-diylbis(2-cyanoacetamide)	74	76

As the data from the table indicate, both procedures are viable, with one giving better yield for compound (**4a**) and another giving slightly better yield for compound (**4b**).

Major shortcomings of the Gazit *et al.*<sup>[37]</sup> approach are the danger of heat induced side-reactions, and the need for more rigorous separation work-up. Being run without the solvent, the reaction mixture becomes very viscous and could experience local overheating. The latter is thermodynamically undesirable, as it may lead to decomposition and side reactions. Dissolving such mixtures, sometimes fused and in addition containing poorly soluble side products, is also problematic. For these reasons, we opted mostly for the MeOH/catalyst syntheses, as mentioned above.

However, the Gazit *et al.* procedure<sup>[37]</sup> has an advantage of the glass beads being absent from primary precipitate. General way of removing them, is to re-dissolve the precipitate and filter the beads off. This works well for reasonably soluble condensation products but presents a problem for our *bis*-cyanoacetamides. They are poorly soluble in the common organic solvents. Even in the most suitable solvents found by us, alcohols, their solubility does not exceed 0.5 g L<sup>-1</sup>, with the consequence of large volumes of solvent needed to purify just a few grams.



At this point we considered what consequences leaving the glass beads in the crude would have on the overall success of the synthetic route. Taking into account that typical catalyst load was about 11 mg per 5 g of substrate (or 0.22 wt. %), we elected to leave the glass beads in the mixture as they would be neutralised by an excess of strong base in the succeeding oximation step, rendered indifferent, and finally, separated from the product solution by filtration.

When the characterisation data on *bis*-cyanoacetamides were required, small portions of the crude were dissolved, the glass beads filtered off, and the product re-crystallised.

Another positive fact related to this synthesis was the ease of removal of unreacted reagents. The wash solvents employed in this synthesis were 0.1 M HCl and MeOH. The aqueous hydrochloric acid protonates any remaining diamine into ammonium hydrochloride salt, which is perfectly soluble in water and washes away easily. On the other hand, ethyl cyanoacetate is very soluble in methanol. Sequential rinsing with these two solvents efficiently removes starting materials from the product, which is, as mentioned earlier, practically insoluble in water and relatively insoluble in methanol.

### 4.3.2 Step Two: Oximation

Here we will consider chemical factors and the impact of external conditions on the outcome of oximation step.

#### 4.3.2.1 Initial attempts at oximation

The first successful oximation of a *bis*-cyanoacetamide to the desired *bis*-chelate ligand was reported by Kolotilov *et al.*,<sup>[24]</sup> and refers to the preparation of *N,N'*-propane-1,3-diylbis[2-cyano-2-(hydroxyimino)ethanamide] (**5b**). An excerpt from their procedure reads as follows:

"*N,N'*-propane-1,3-diylbis(2-cyanoacetamide) (10 mmol) was partially dissolved/suspended in a solution of NaOEt (20 mmol) (prepared from 0.46 g, 20 mmol of Na) in 60 mL of absolute EtOH, and treated with gaseous EtONO (20.5 mmol) prepared separately by reaction of NaNO<sub>2</sub> (1.42 g, 20.5 mmol) with an excess H<sub>2</sub>SO<sub>4</sub> in EtOH-water solution. After 5 hours 2 equivalents of aqueous HCl were added to the mixture, which was then filtered and concentrated by rotary evaporation until yellow orange crystals appeared", ..., "yield 0.93 g, 35 %".<sup>[24]</sup>

Our first attempt at the oximation reaction under the conditions suggested above was the synthesis of *N,N'*-butane-1,4-diylbis(2-cyanoacetamide) (**4c**). It immediately became clear that the starting *bis*-cyanoacetamide was poorly soluble in basic alkoxide-alcohol medium and the bubbler mixture was fairly viscous; both factors causing hydrodynamic resistance to the gas flow. Upon processing the

product mixture, we also established that the yield of new ligand was much less than 35 % claimed by Kolotilov *et al.*<sup>[24]</sup> The fact that this was the only set of synthetic conditions proposed literature, and they did not work very well for new ligands, lead to the realisation that we would have to optimise chemical and external parameters for such reactions.

#### 4.3.2.2 The bubbler design

As the glassware used in this synthesis was outside of the routine set employed by organic chemists, we have included short description of the laboratory setup and a few diagrams to aid the discussion.

Synthetic procedure and the composition of three solutions charged to the apparatus are described in section 3.3; we advise the reader interested in details to consult this section.

Initially, we attempted to pass methyl nitrite gas through a single common laboratory bubbler, as shown in Figure 47.

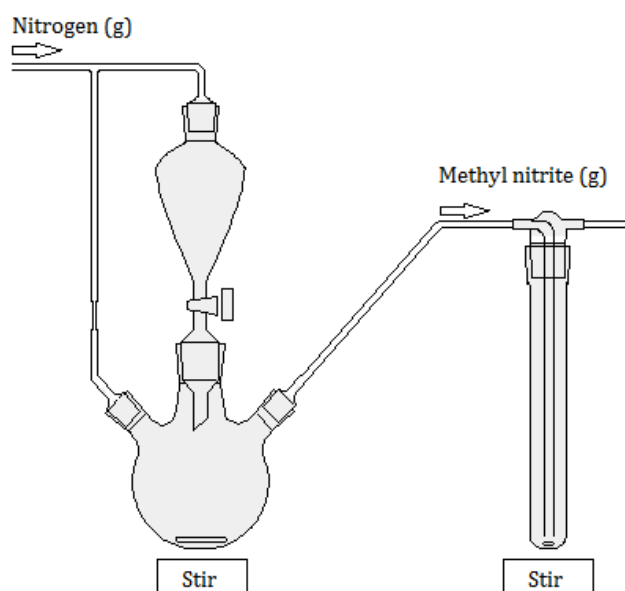


**Fig. 47.** An apparatus for oximation with a single common laboratory bubbler.

During the pilot run with this apparatus two observations were made, which gave cause to concern. First, it was noticed that the *bis*-cyanoacetamide failed to dissolve fully in the sodium propoxide/ *iso*-propanol solution.<sup>§</sup> Second, the gas bubbles emerging from the end of a spout were quite large, between 5 and 7 mm in diameter. Both these facts were unfortunate from the perspective of maximising the product yield. From our understanding of the reaction mechanism, at the activation stage the methylene group  $\alpha$  to the nitrile group of *bis*-cyanoacetamide has to be deprotonated, which

<sup>§</sup> Solution in the bubbler.

should make the latter reasonably soluble in the basic *iso*-propanol medium. The fact that it remained largely in suspended solid state was somewhat puzzling. Of course, solid suspension offers much diminished contact area with gas bubbles in comparison to the matter fully dissolved in liquid medium. Second, large size methyl nitrite bubbles also reduce contact area and contact time with liquid solution of reactant, with obvious kinetic and thermodynamic implications.

We tried to combat these problems by adding a coarse ceramic frit at the end of a spout, which was expected to break the gas flow into large number of small bubbles (of 1 mm diameter or less), and increasing the bubbler volume (to accommodate more solvent) to dissolve more of the precursor *bis*-cyanoacetamide. Diagrammatic view of the modified apparatus is shown in Figure 48.

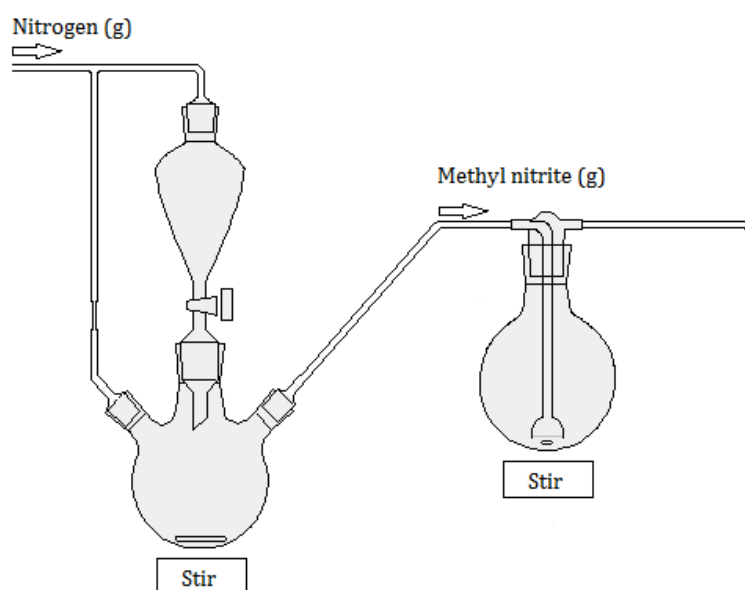


**Fig. 48.** An apparatus for oximation with a large volume bubbler adorned with a coarse ceramic frit.

Pilot run with the new apparatus afforded two observations. First, the pressure required for the gas to bubble through the frit was much higher than through the open tube. Second, the level of undissolved *bis*-cyanoacetamide has dropped, which was a positive sign. However, when we analysed the product mixture, the results were discouraging. The yield of desired product fell to about half of the value achieved previously in the standard bubbler type apparatus.

Careful analysis brought forward the theory that much higher gas pressure, required to overcome resistance caused by the frit, caused more methyl nitrite gas escaping through the glass ground joints of the apparatus. Even when we took additional precautions, by adding PTFE tape and employing Keck clips on every joint to stop gas leaks, certain amount of leakage remained. A consideration to cut down on the number of glass joints in the apparatus was rejected on practical grounds; it would complicate cleaning and hinder access to the inner part of the apparatus.

Hence, we reverted back to a design with an open tube bubbler. However, to increase the contact time of larger bubbles with the solution, we decided to go for a thinner internal tube and a longer bubbler. As practical considerations (such as the height of extraction cabinet, etc.) impose constraints on the usable height of a bubbler, we opted for a design with two relatively tall narrow sequential bubblers. It would allow, on one hand, to use larger quantity of solvent and, consequently, to dissolve more of the *bis*-cyanoacetamide precursor, and on the other hand, to increase the contact time between the gas and the solution. The new apparatus we settled on is shown in Figure 49.

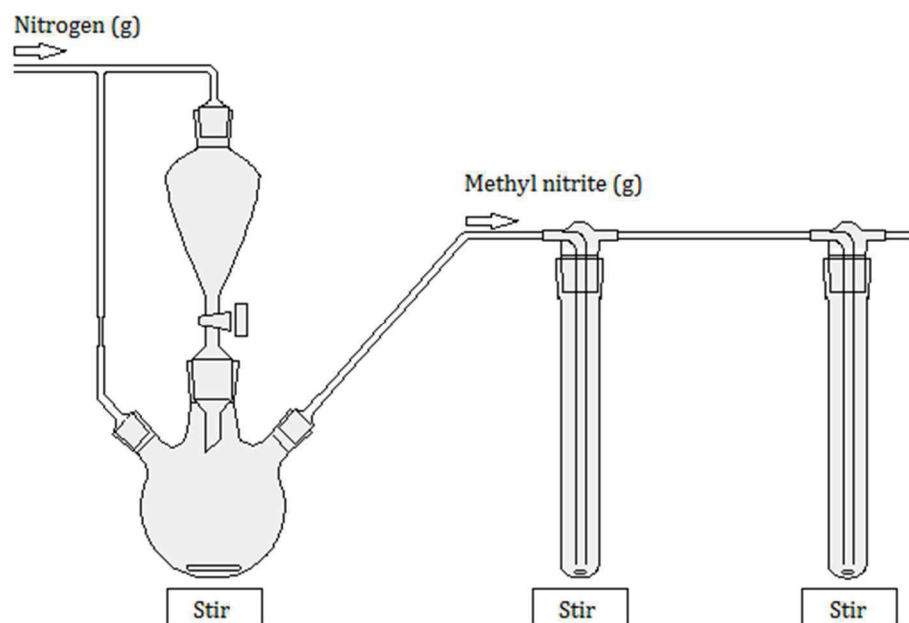


**Fig. 49.** An apparatus for oximation with two sequential common laboratory bubblers.

This design proved to be superior to the two discussed previously. In general, the apparatus works well, though on a few occasions the contents of one bubbler were partially blown over into the next one by a flow of  $N_2$  gas during the purge of the system. To prevent this from happening again, we introduced a gas flow restriction device, which came in the form of thin tube about 1 mm diameter and 45 mm long, and was installed on the incoming nitrogen supply line just before the flask where methyl nitrite gas was generated. Its role was to filter large shock waves in the gas supply line by constricting the flow.

Also, as can be seen from the diagram, the dropping funnel is backed by the nitrogen gas from the same line, equilibrating pressure on both sides of the dropping funnel solution; the latter aids controlled continuous drop-wise addition of this solution to the reaction flask and prevents emerging methyl nitrite from bubbling through the funnel. An advantage of such fine control of the methyl nitrite production is the ability to create stable, continuous, slow gas stream, which allows longer contact time of the bubbles of an acceptable size with the solution.

Subsequently, this apparatus was employed for the synthesis of remaining ligands.

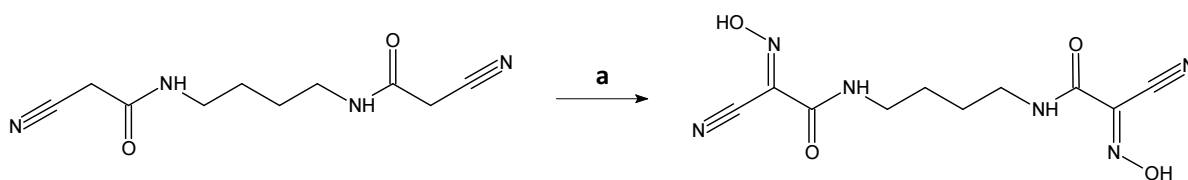
### 4.3.2.3 Optimising the conditions for oximation

As already mentioned, our early attempts at the oximation step under the conditions proposed by Kolotilov *et al*<sup>[24]</sup> were not entirely satisfactory as the yield was significantly lower than reported by authors 35 %. Consequently, we decided to optimise reaction conditions with the aim of improving the yield. The plan was to carry out the reaction under a range of conditions, changing one at a time, and to file the outcome, in terms of yield and product purity, in a matrix type map. The following conditions were considered important, and were altered as primary variables.

1. The nature of base and solvent and the source of a nitrosation agent.
2. Base to *bis*-cyanoacetamide ratio (base loading).
3. Base and *bis*-cyanoacetamide concentration.
4. Temperature.

#### Chemical parameters of oximation

First, we review the kind of reagents used in three selective oximation reactions reported in literature. Our test substance in this case was *N,N'*-butane-1,4-diylbis(2-cyanoacetamide) (**4c**), and the attempted reaction is shown in Scheme 18.



a : Base, RONO

**Scheme 18.** Oximation of *N,N'*-butane-1,4-diylbis(2-cyanoacetamide) (**4c**) to bis-chelate (**5c**) used as a test reaction for the optimisation of external conditions.

Two strong bases used previously were NaOCH<sub>3</sub> and NaOC<sub>2</sub>H<sub>5</sub> in the solution of a parent alcohol.<sup>[24, 15]</sup> Considering the structure of our *bis*-cyanoacetamide, it was decided that somewhat stronger and more

hindered base would be a better choice.\*\* Consequently, we settled on sodium *iso*-propoxide in *iso*-propanol.

According to Bohle *et al.*,<sup>[36]</sup> different oximation products and in different ratio were formed when the same base but with different counter ion ( $\text{Na}^+$  or  $\text{K}^+$ ) was used. As our work is closely related to the synthesis of 3,3'-piperazine-1,4-diylbis[2-(hydroxyimino)-3-oxopropanenitrile]<sup>[15]</sup> and *N,N'*-propane-1,3-diylbis[2-cyano-2-(hydroxyimino)ethanamide],<sup>[24]</sup> it was decided to employ the same cation, namely  $\text{Na}^+$ , in both cases.

Next, we considered practical aspects of the preparation of such sodium alkoxide solution. The choice was between dissolving sodium hydroxide or sodium metal in dry alcohol. By-product of the latter reaction is dihydrogen gas, while by-product of the former is water. For obvious reasons we have chosen dissolving metallic sodium in freshly distilled *iso*-propanol as a preferred procedure.

The third factor is the choice of nitrosation agent. Two such agents,  $\text{CH}_3\text{ONO}$  and  $\text{C}_2\text{H}_5\text{ONO}$ , were employed in a similar reaction previously.<sup>[24, 15]</sup> We settled on  $\text{CH}_3\text{ONO}$ , which is a gas at RT and can be easily synthesised in a secondary reaction vessel. It can be easily removed from the oximation reactor and, probably, has higher chemical reactivity.<sup>††</sup>

With the base and nitrosation agent settled, next we looked at the stoichiometric ratio of the base to starting material. Experimental results are presented in Table 16, which specifically refers to the oximation of *N,N'*-butane-1,4-diylbis(2-cyanoacetamide) (**4c**).

---

\*\* The base is required to deprotonate the methylene group but should not participate in any condensation reactions of its own.

†† The latter assumption is based on lesser steric hindrance this agent might experience during the electrophilic attack on rather crowded bis-amide precursor.

**Table 16.** Yield of *bis*-chelate ligand (**5c**) for various ratios of starting materials.

Run	<i>Bis</i> -amide ( <b>4c</b> ) (mmol)	<i>i</i> PrONa (mmol)	<i>i</i> PrOH (mL)	Yield (%)	Product Purity
4 <sup>††</sup>	1.5	3.0	85	24	High
5	1.0	1.0	65	13	Contained about 10 % of starting material
6a <sup>§§</sup>	1.0	2.2	65	10	High
6b	1.0	2.2	65	7.9	High
7a	1.0	3.1	65	4.2	High
7 <sup>***</sup>	1.0	3.1	65	0	No <i>bis</i> -chelate detected as no CH <sub>3</sub> ONO was bubbled
8a	1.5	3.0	80	13	High
8	1.5	9.0	80	5.4	High

A few conclusions can be drawn from the data presented in this table; they are discussed below.

### Base loading

Two subsets of comparable data, different only by the *bis*-cyanacetamide to base ratio, are shown in Table 17.

<sup>††</sup> Runs listed in the table do not start from 1 due to the fact that a few experiments were conducted earlier to optimise the apparatus setup.

<sup>§§</sup> Entries that are labelled as **a** or **b** refer to the experiments where the contents of two sequentially connected bubblers were worked up separately.

<sup>\*\*\*</sup> This sample was run with methyl nitrite source disconnected from the bubbler. The purpose was to check whether nitrosation agent plays any role in the deprotonation of *bis*-cyanacetamides.

**Table 17.** Yield of *bis*-chelate ligand (**5c**) in comparable runs with different precursor to base ratios.

Run	<i>Bis</i> -amide ( <b>4c</b> ) (mmol)	<i>i</i> PrONa (mmol)	Yield (%)
5	1	1	13 <sup>+++</sup>
6a	1	2.2	10
7a	1	3.1	4.2
8a	1.5	3	13
8	1.5	9	5.4

Analysis of these data allows to draw a few conclusions. Runs 5, 6a and 7a were performed under identical conditions but for the increasing base loading. Same applies to runs 8a and 8, though, they were carried out with increased overall amount of *bis*-cyanacetamide.

Starting with run 5, which was carried out at *bis*-cyanoacetamide to base ratio of 1 : 1, rather than at stoichiometric 1 : 2 ratio, somewhat to our surprise, fairly high yield of the product (about 11.5 %) was achieved. However, recovered from the mother liquor product contained not only *bis*-chelate cyanoxime-and-amide ligand but also about 10 % of the unreacted starting material. Further increase of the base loading in runs 6a and 7a to 1 : 2.2 and 1 : 3.1, respectively, caused the yield to fall from 10 % to 4.2 %.<sup>+++</sup> Similar outcome was recorded for runs 8a and 8, where increasing the base loading from 1 : 2 to 1 : 6, dropped the yield from 13 to 5.4 %.

Overall conclusion from these two sets of runs and similar data for other ligands is that optimal yield is achieved at stoichiometric precursor to base ratio (1 : 2). Crude product obtained under such conditions is characterised by low level of impurities and can be upgraded to an analytical sample through the separation procedure. Similar yield may be achieved with lower base loading of about 1 : 1.1 ratio. However, in the latter case the sample is contaminated with noticeable amount of the *bis*-cyanacetamide salt, which is more difficult to separate from the target product.

### ***Bis*-cyanoacetamide concentration**

The next factor to consider is *bis*-cyanacetamide concentration in the bubbler. Given that *bis*-cyanacetamide precursors (**4a-c**) are poorly soluble in most solvents, including sodium

---

<sup>+++</sup> 13 % yield value is overestimated. It was derived from the weight of a sample, which upon analysis turned out to be a mixture of product and approximately 10 % of starting *bis*-cyanacetamide. The real yield was under 11.5 %. In contrast, the yield for all other runs in the table represents analytically pure product.

<sup>+++</sup> In truth, the yield at 1 : 2 ratio might have been the highest. Unfortunately, we did not prepare exact stoichiometric ratio in run 6a. Small excess (about 10 %) of the base over the above ratio, probably, had detrimental effect on the yield.



*iso*-propoxide/*iso*-propanol system charged to the bubbler, it was difficult to estimate actual precursor concentration in different runs. In fact, as was evident from experimental observations, most of the *bis*-cyanacetamide in the bubbler remained undissolved through the process of oximation. The best comparison we can offer in this regard is between runs 6a and 8a, Table 18, where the last column is not the true concentration in solution, which is much lower, but formal ratio of the precursor amount to the volume of liquid phase used.

**Table 18.** Yield of *bis*-chelate ligand (5c) in comparable runs with different amount of precursor present in solution.

Run	<i>Bis</i> -amide (4c) (mmol)	<sup>i</sup> PrONa (mmol)	<sup>i</sup> PrOH (mL)	Yield (%)	Formal (4c) to <sup>i</sup> PrOH ratio (M)
6a	1.0	2.2	65	10	0.0154
8a	1.5	3.0	80	13	0.0188

The difference in yield is not significant enough to draw far reaching conclusions. It may well be caused by slightly higher base loading in run 6a. On the other hand, if we assume the solubility of the precursor in *iso*-propanol medium being the same, higher yield in run 8a may signify an advantage of having larger overall amount of the reactant in solution. Probably, larger overall volume of solution in the bubbler also helps as it increases the contact time.

### Efficiency of sequential bubblers

Next we will consider the efficiency of sequential bubblers.

As we have been compelled to introduce the second bubbler in our apparatus design, it became of interest how much of the generated methyl nitrite gas goes through it after a portion was consumed in the first bubbler. At the first glance, one might expect some decrease in yield in the second bubbler due to lower partial pressure of the nitrosation agent in the gas mixture (CH<sub>3</sub>ONO flow is complemented by the stream of N<sub>2</sub>). However, as the reaction was run with large excess of methyl nitrite over the *bis*-cyanacetamide (at about 200 : 1 molar ratio), that seemed unlikely. Nevertheless, noticeable drop in the conversion ratio between the two bubblers was observed in all such experiments. The data in Table 19 illustrate this point.

**Table 19.** Yield of *bis*-chelate ligand (**5c**) in two sequential bubblers using the same gas source.

Run	Yield (%)
6a	10
6b	7.9

We do not have convincing explanation to this effect. However, from a practical point a view, it is well worth the trouble of setting up additional bubbler and getting 7.9 % extra material from the same oximation process.

### Temperature

As is well known from chemical thermodynamics, the temperature may have profound effect on reaction yield. Logically, in view of its importance, the issue of reaction temperature in the bubblers should have been considered earlier. We have deferred it until now because the temperature effect on yield was studied by us only for ligand (**5b**), *N,N*-propane-1,3-diylbis[2-cyano-2-(hydroxyimino)ethanamide] and not for ligand (**5c**), as was the case with the rest of external factors.

Two comparable runs were made in the preparation of (**5b**); the first with the bubblers at RT and the second with the bubblers submerged in an oil bath maintained at 65 °C. The results of this experiment are presented in Table 20.

**Table 20.** Yield of *bis*-chelate ligand (**5b**), *N,N*'-propane-1,3-diylbis[2-cyano-2-(hydroxyimino)ethan-amide] in comparable runs at different temperatures.

Run	Temperature (°C)	Yield (%)
3	27	24
4	65	17

As can be seen from the above table, heating the oximation vessel is counterproductive to the product yield. The latter also implies exothermic enthalpy of reaction.

### Synthetic Repeatability

To justify trust in the above results, we also tested synthetic repeatability by carrying multiple repetitive runs for one chosen ligand.

The oximation reaction aimed at the preparation of ligand (**5d**), *N,N'*-(2-hydroxypropane-1,3-diyl)*bis*[2-cyano-2-(hydroxyimino)ethanamide], was performed last. By this time final synthetic procedure

was well established. The following five synthetic runs were carried out following the same generic procedure, which allowed us to test the repeatability of our approach, Table 21.

**Table 21.** Yield of *bis*-chelate ligand (**5d**), *N,N'*-(2-hydroxypropane-1,3-diyl)bis[2-cyano-2-(hydroxyimino)ethanamide], in five identical runs.

Run	Yield (%)
1	5.1
2	5.4
3	4.7
4	4.7
5	6.6

Average yield was  $(5.3 \pm 2.35)$  % at the 95 % probability level.

### Yield figures for different ligands

Finally, we will present average yields of the desired compounds in the oximation step across the series of *bis*-chelate cyanoxime-and-amide ligands, Table 22. All such runs were performed under comparable conditions following the optimised generic procedure.

**Table 22.** Representative yield of the oximation step for different *bis*-chelate ligands synthesised in this project.

Ligand	Yield (%)
<i>N,N'</i> -ethane-1,2-diylbis[2-cyano-2-(hydroxyimino)ethanamide], (n=0) ( <b>5a</b> )	3.6
<i>N,N'</i> -propane-1,3-diylbis[2-cyano-2-(hydroxyimino)ethanamide], (n=1) ( <b>5b</b> )	24
<i>N,N'</i> -butane-1,4-diylbis[2-cyano-2-(hydroxyimino)ethanamide], (n=2) ( <b>5c</b> )	13
<i>N,N'</i> -(2-hydroxypropane-1,3-diyl)bis[2-cyano-2-(hydroxyimino)ethanamide], (n=1-OH) ( <b>5d</b> )	5.1

As can be seen from the table, oximation with methyl nitrite agent works best for the ligand with propane spacer between two chelate moieties. The ligand with butane spacer is next in line. However, the ligands with shorter (ethane) or more complex (2-hydroxyethane) linkers form in lower yield. This is likely to be attributed to steric difficulties in the formation of reaction intermediate.

### 4.3.3 Evidence of different molecular forms

In the course of synthetic work on this project we have made two interesting observations, which lead us to believe that on two occasions we isolated different molecular forms of the same compound.

#### ***Bis-cyanoacetamide salt***

The first observation pertains to the recovered unreacted *bis*-cyanoacetamide material. As has been mentioned earlier, during the oximation procedure some of the *bis*-cyanoacetamide precursor remains in suspension, and is filtered off at the end of the reaction. The solid suspension is predominantly starting material (white) mixed with another solid phase (yellow). <sup>1</sup>H NMR spectrum of this second phase is similar to the spectrum of precursor *bis*-cyanoacetamide with only slightly altered values of chemical shifts. However, most striking feature of the spectrum is complete absence of all methylene protons signals on the carbons  $\alpha$  to nitrile groups. This secondary species is fairly stable, but reverts to the original precursor when dissolved in hot water, acidified to pH 2.8, and left to precipitate. <sup>1</sup>H NMR analysis of this recovered solid is identical to the original *bis*-cyanoacetamide.

These facts, complemented by the knowledge that cyanamide salts are yellow, lead us to conclude that the secondary species is a tetra sodium salt of original *bis*-cyanoacetamide. Two additional observations fit well with such suggestion: a) the solubility of yellow compound is much higher than that of molecular *bis*-cyanoacetamides, which is characteristic of salts, and b) when we acidify the solid mixture only molecular *bis*-cyanoacetamides precursor precipitates out.

<sup>1</sup>H NMR spectra of the molecular form and its suspected tetra sodium salt are presented below in Figures 50-51.

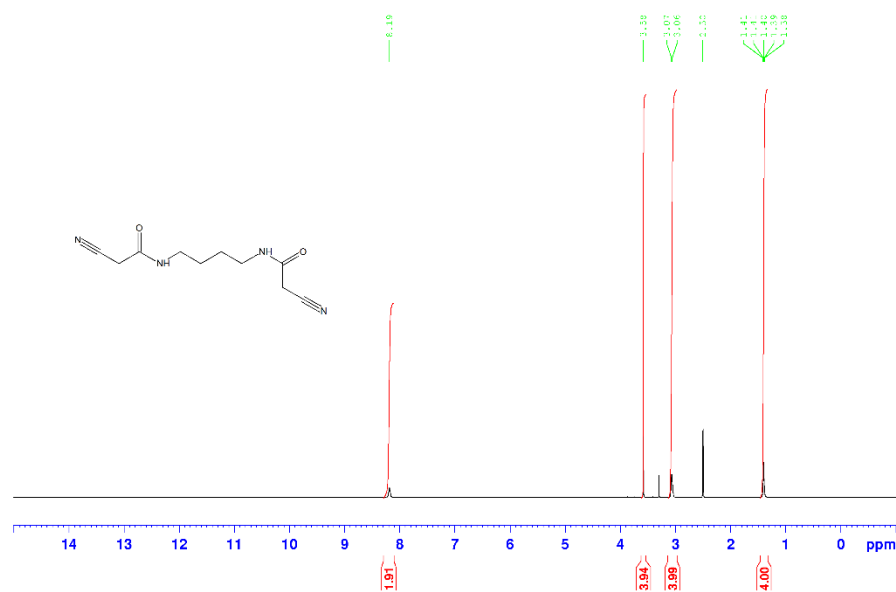


Fig. 50.  $^1\text{H}$  NMR spectrum of the molecular form of *bis*-cyanacetamide (**4c**).

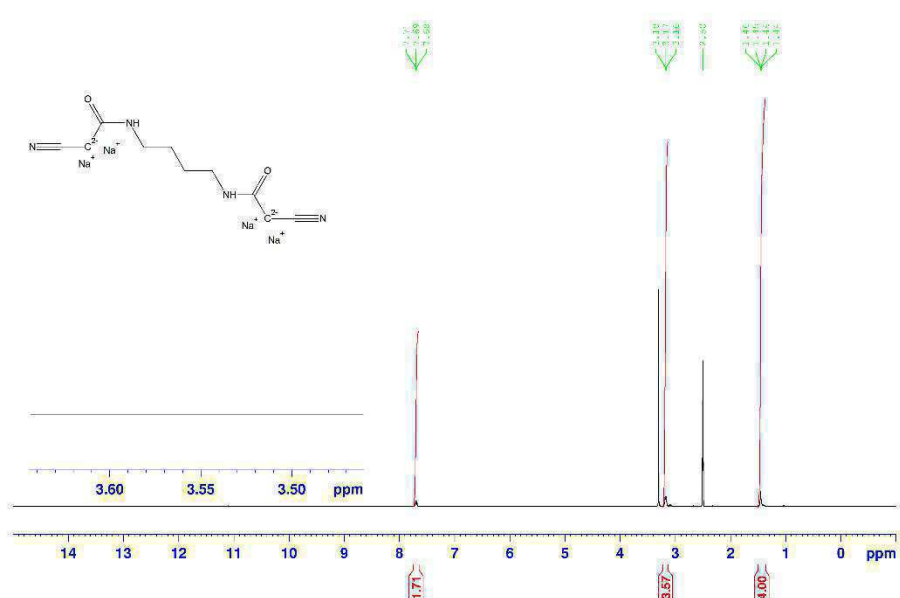
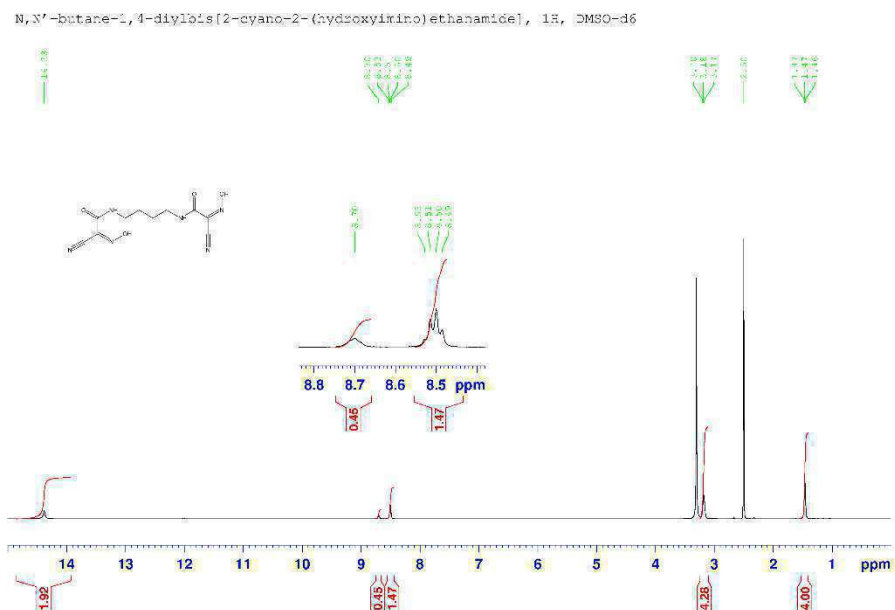


Fig. 51.  $^1\text{H}$  NMR spectrum of the suspected tetrasodium salt of *bis*-cyanacetamide (**4c**).

### Conformers

During the synthesis of ligand (**5c**), *N,N'*-butane-1,4-diyldis[2-cyano-2-(hydroxyimino)ethanamide], which we repeated numerous times, on occasion, secondary amide peak (at about 8.7 ppm) was detected in the  $^1\text{H}$  NMR spectrum of the product, Figure 52.



**Fig. 52.**  $^1\text{H}$  NMR spectrum of ligand (**5c**), hinting at the mixture of two conformers.

Analysis of the NMR data indicated that it was unrelated to any starting material but, in fact, was associated with the product. Additional COSY spectrum of this sample, Figure 53, confirmed that both peaks of interest correlate with the methylenic protons  $\alpha$  to amide nitrogen (3.17-3.20 ppm).

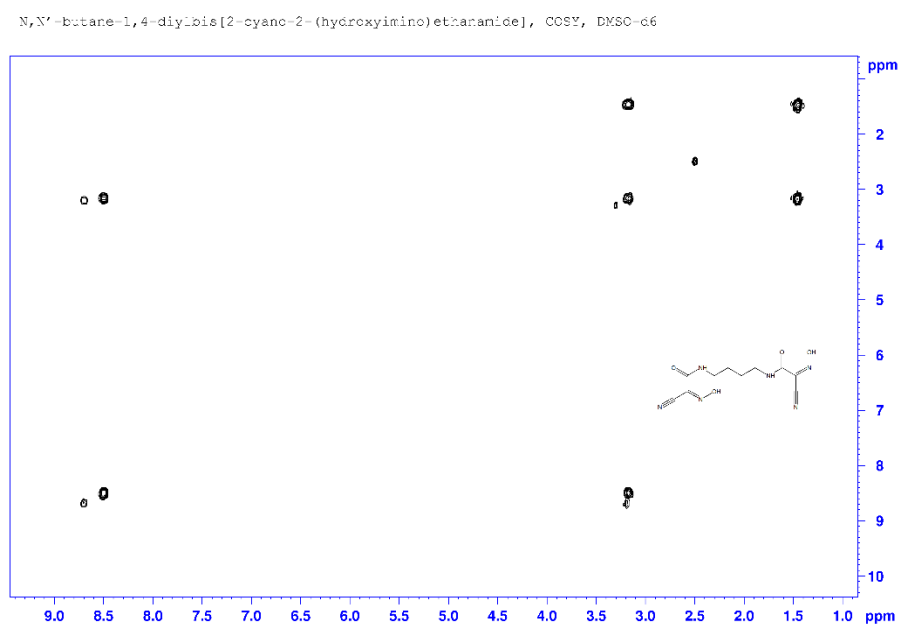


**Fig. 53.** COSY NMR spectrum of ligand (**5c**), indicating the mixture of two conformers.

Such behaviour is characteristic of a mixture of conformers, where two amide protons are in slightly different environments. Based on the integrated proton signals, the ratio of two conformers in the mixture appears to be 3 : 1. It is also interesting to note that the amide proton signal of the major

conformer is a well resolved multiplet, implying strong coupling to the protons of neighbouring methylene group. In contrast, similar signal for the minor conformer is unresolved broad singlet.

As for the exact nature of these conformers, it is yet unknown to us and will be the subject of future computational work emanating from this chapter. At this stage, we are only prepared to say that the major conformer is likely to be structurally constrained, probably due to the intramolecular hydrogen bonding of the amide proton, while its minor counterpart lacks such interaction and has an amide group with a more exchangeable proton.

## 5. Conclusions for Chapter B

1. In total, we have synthesised nine compounds in this chapter, of which three are new (**5a**, **5c**, and **5d**). Previously known compounds were characterised by  $^1\text{H}$  and  $^{13}\text{C}$  NMR spectroscopy, and in all cases the comparison with literature data was satisfactory. For a few compounds certain characterisation data were not reported in literature (e.g.,  $^{13}\text{C}$  NMR spectra, high-resolution MS spectra, etc.). For these compounds such measurements were performed and the blanks filled. All new compounds were characterised by complete range of instrumental techniques described in this Chapter.
2. Three of the four *bis*-cyanoamide precursors, Scheme 15 path A (p. 101), were synthesised in solvent medium, with the yield of 67% (**4a**), 76 % (**4b**) and 66 % (**4d**). The fourth *bis*-cyanoamide (**4c**) was synthesised in 87 % yield using a solvent-free procedure.
3. All four desired *bis*-cyanoxime-and-amide ligands (**5a-d**), three of which are new (**5a**, **5c**, **5d**), were successfully prepared following path A, Scheme 15 (p. 101). The yield was 3.6, 24, 6.6 and 6.2 % for compounds (**5a-d**), respectively.
4. All our attempts at the preparation of ligands (**5a-d**) following path B, Scheme 15 (p. 101), failed. The likely reason for this is high acidity of the oxime group in cyanoxime compounds, leading to the cross-protonation of diamine substrates. Resulting ammonium salts are non-nucleophilic and are unable to engage the cyanoxime ester in the condensation reaction.



## 6. Further Work

We fully intend to continue the investigation of this new class of cyanoxime-and-amide *bis*-chelate ligands at the PhD level. In particular, we would like to expand the work in three directions. First, we will synthesise four cyanoxime-and-amide molecules, this time of a *mono*-chelate nature, which will constitute yet another new class of ligands. Second, we will undertake thermodynamic investigation of the ligand protonation in aqueous medium. Finally, we would like to explore interaction of the above ligands with a few divalent late *3d*-transition metals, both in solution and in solid state.

These plans are explained in more detail below.

### 6.1 New ligand synthesis

We have already developed an approach toward the synthesis of cyanoxime-and-amide *mono*-chelate ligands, and synthesised a few of them. In future, we will complete the synthesis of a representative range of such ligands, isolate and characterise them.

### 6.2 Protonation studies

As has been already established by Sliva et al,<sup>[6]</sup> substitution of the methyl group in **mhiaa** ligand for the strongly electron withdrawing nitrile group in **chiaa** ligand, Figure 54, lead to significant increase in acidity of the oxime group.

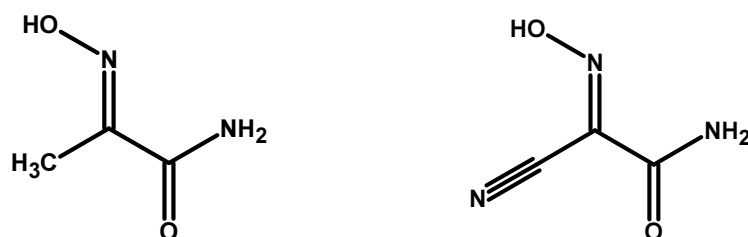


**Fig. 54.** 2-Hydroxyiminopropanamide or **mhiaa**, left, and 2-cyano-2-(hydroxyimino)acetamide or **chiaa**, right.

In particular, the value of  $\log_{10}K$ , where  $K$  is the protonation constant, has dropped from 9.87 for **mhiaa** to 5.12 for **chiaa**.<sup>[6]</sup> This four orders of magnitude increase in acidity makes the oxime proton ionisable in the biological pH region. Consequently, the ligands of this nature are expected to coordinate metal

ions in much more acidic solutions, and possibly in a different manner, than the ligands with conventional oxime functionalities.

Our future intention is to investigate the protonation behaviour of these two new classes of cyanoxime ligands by means of potentiometric, spectroscopic and calorimetric titrations. Expected outcomes here would be protonation constants, enthalpies of protonation and entropies of protonation.

### 6.3 Conformational studies

Due to intra-molecular hydrogen bonding and  $\pi$ -conjugation, the ligands under consideration may exist in a variety of conformational states. In future work we intend to probe this variety by quantum-mechanical calculations at the DFT level with two objectives in mind: a) to relate experimental thermodynamic quantities of protonation to particular conformational structures, and b) to relate such structures to the experimental conditions, under which ligands were synthesised or isolated.

For example, during the synthesis of *N,N'*-butane-1,4-diylbis[2-cyano-2-(hydroxyimino)ethanamide] (**5c**), on occasion secondary amide peak appeared in the  $^1\text{H}$  NMR spectrum at about 8.7 ppm that was unrelated to any starting material. The COSY correlation spectrum indicated it to originate from the same species. Such behaviour is characteristic of two amide protons being in non-equivalent magnetic environment. We interpret it as a mixture of conformers, in this case conformers of ligand (**5c**). The exact nature of the second suspected conformer is not yet known, and we will try to elucidate it computationally. Also, taking into account the work of Bohle *et al.*,<sup>[36]</sup> who have shown that the temperature of acidification has a profound effect on the ratio of conformers isolated in a similar oximation reaction, future synthetic attempts of this nature should cover the range of temperatures of acidification (and, in general, other synthetic conditions) and their comparison to the ratio of isolated conformers.

### 6.4 Metallation of the Cyanoxime-and-Amide Ligands

Stability constants for Co(II), Ni(II) and Cu(II) complexes in aqueous solutions with a range of *mono*- and *bis*-chelate **mhiaa<sub>2</sub>z** and **mhiaaza** ligands, Figure 55, have been investigated in our group in recent years.<sup>[5]</sup>

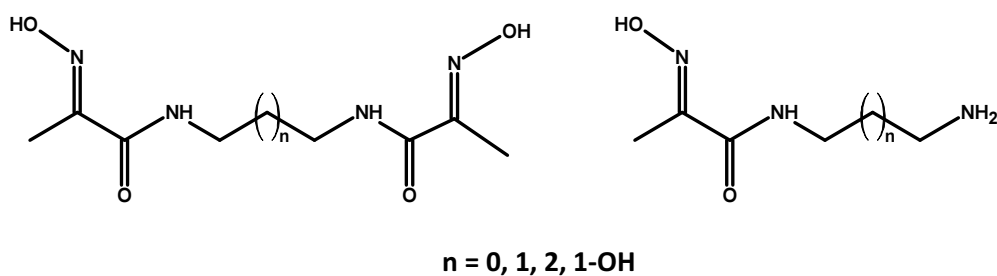


**Fig. 55.** Mhiaa<sub>2z</sub> and mhiaaza ligands investigated in our group previously.<sup>[5]</sup>

Numerous complex compositions and structures were determined in this study, and interesting trends and regularities correlating complex stability to its structure were established.

Of equal interest would be a comparative study of cyanoxime ligands, Figure 56, in particular, with respect to the effect an electron withdrawing functionality has on the complex stability and structure.

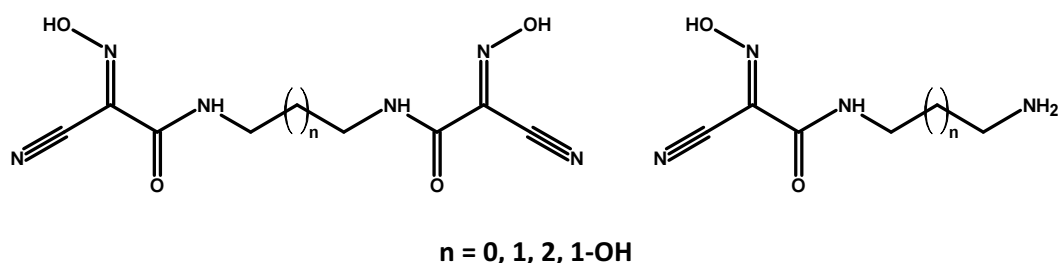


**Fig. 56.** Two new classes of 2-cyano-(2-hydroxyimino)acetamide ligands, chiaa<sub>2z</sub> and chiaaza, designated for the future metallation studies.

In addition, novel multinuclear Cu(II) and Pt(II) metal clusters are expected to form with the new class of tridentate, N(ox)N(ad)N(am), ligands, as has been established recently in our group for their methyl-analogues.<sup>[55]</sup>

We plan to measure thermodynamic stability of these two new classes of cyanoxime ligand complexes in aqueous solutions by means of potentiometric, spectroscopic and calorimetric titrations. We also intend to isolate a range of such complexes in solid state, grow their monocrystals, and to determine their molecular and crystal structure by X-ray diffraction.

Expected outcomes here would include stability constants, enthalpies and entropies of complex formation, and complex molecular structures.

## 7. References for Chapter B

1. Duda, A.M.; Karaczyn, A.; Kozlowski, H.; Fritsky, I.O.; Glowiak, T.; Prisyazhnaya, E.V.; Sliva, T.Y.; Swiatek-Kozlowska, J. Co-ordination of copper(II) and nickel(II) ions by a novel open chain oxime ligand. *J. Chem. Soc. Dalton Trans.* 1997, **20**, 3853-3859.
2. Fritsky, I.O.; Kozlowski, H.; Prisyazhnaya, E.V.; Rzaczyńska, Z.; Karaczyn, A.; Sliva, T.Y.; Glowiak, T. Co-ordination ability on novel tetradentate amide-and-oxime ligands: differential binding to Cu(II) and Ni(II). *J. Chem. Soc. Dalton Trans.* 1998, **21**, 3629-3633.
3. Fritsky, I.O. New ring-closure reaction involving co-ordinated amide groups. *J. Chem. Soc. Dalton Trans.* 1999, **6**, 825-826.
4. Fritsky, I.O.; Kozlowski, H.; Prisyazhnaya, E.V.; Karaczyn, A.; Kalibabchuk, V.A.; Glowiak, T. A short intramolecular hydrogen bond is a key factor in the self-assembly of a dimeric complex with a 22-membered metallamacrocyclic cavity. *J. Chem. Soc. Dalton Trans.* 1998, **10**, 1535-1536.
5. *Private communication.* Nikolayenko, I. 2013
6. Sliva, T.Y.; Duda, A.M.; Glowiak, T.; Fritsky, I.O.; Amirkhanov, V.M.; Mokhir, A.A.; Kozlowski, H. Co-ordination ability of amino acid oximes. Potentiometric, spectroscopic and structural studies of complexes of 2-cyano-2-(hydroxyimino)acetamide. *J. Chem. Soc. Dalton Trans.* 1997, **2**, 273-276.
7. Wikipedia. [http://en.wikipedia.org/wiki/Victor\\_Meyer](http://en.wikipedia.org/wiki/Victor_Meyer) (accessed Mar 18 2014).
8. Meyer, V. Ueber die Nitroverbindungen der Fettreihe. *Berichte.* 1873, **6**, 1492.
9. Plate, R.; Nivard, R.J.F.; Ottenheijm, H.C.J. Conversion of N-hydroxytryptophans into  $\alpha,\beta$ -dehydrotryptophan. An approach to the neoechinulin series. *J. Chem. Soc. Perkin Trans.* 1987, **11**, 2473-2480.
10. Sauerberg, P.; Olesen, P.H.; Nielsen, S.; Treppendahl, S.; Sheardown, M.J.; Honore, T.; Mitch, C.H.; Ward, J.S.; Pike, A.J.; Bymaster, F.P.; Sawyer, B.D.; Shannon, H.E. Novel functional M<sub>1</sub> selective muscarinic agonists and structure-activity relationships of 3-(1,2,5-thiadiazolyl)-1,2,5,6-tetrahydro-1-methylpyridines. *J. Med. Chem.* 1992, **35**, 12, 2274-2283.
11. Wamhoff, H.; Berresse, R.; Nieger, M. Efficient synthesis of fused isothiazole C-nucleosides. 1. Synthesis of a 3- $\beta$ -D-ribofuranosylisothiazolo[4,5-*d*]pyrimidin-7(6*H*)-one isostere of inosine. *J. Org. Chem.* 1993, **58**, 19, 5181-5185.
12. Ponomareve, V.V.; Dalley, N.K.; Kou, X.; Gerasimchuk, N.N.; Domasevitch, K.V. Synthesis, spectra and crystal structures of complexes of ambidentate C<sub>6</sub>H<sub>5</sub>C(O)C(NO)CN. *J. Chem. Soc. Dalton Trans.* 1996, **11**, 2351-2359.
13. Sliva, T.Y.; Dobosz, A.; Jerzykiewicz, L.; Karaczyn, A.; Moreeuw, A.M.; Swiatek-Kozlowska, J.; Glowiak, T.; Kozlowski, H. Copper(II) and Nickel (II) complexes with oxime analogues of amino acids. Potentiometric, spectroscopic and X-ray studies of complexes with 2-cyano-2-(hydroxyimino)acetic acid and its ethane-1,2-diamine derivative. *J. Chem. Soc. Dalton Trans.* 1998, **11**, 1863-1867.
14. Aakeroy, C.B.; Smith, M.M.; Desper, J.  $\alpha,\alpha,\alpha$ -Tris(hydroxyimino)-1,3,5-benzenetriacetonitrile: A three-fold symmetric, versatile and practical supramolecular building block. *Cryst. Eng. Comm.* 2012, **14**, 71-74.
15. Cheadle, C.; Gerasimchuk, N.; Barnes, C.L.; Tyukhtenko, S.I.; Silchenko, S. The first bis-cyanoxime: synthesis and properties of a new versatile and accessible polydentate bifunctional building block for coordination and supramolecular chemistry. *J. Chem. Soc. Dalton Trans.* 2013, **42**, 14, 4931-4946.
16. Gerasimchuk, N.; Esaulenko, A.N.; Dalley, K.N.; Moore, C. 2-Cyano-2-isonitrosoacetamide and its Ag(I) complexes. Silver(I) cyanoximate as non-electric gas sensors. *J. Chem. Soc. Dalton Trans.* 2010, **39**, 3, 749-764.
17. Gerasimchuk, N.; Gamian, A.; Glover, G.; Szponar, B. Light insensitive silver(I) cyanoximates as antimicrobial agents for indwelling medical devices. *Inorg. Chem.* 2010, **49**, 21, 9863-9874.

18. Lau, H.-P.; Gutsche, C.D. Association phenomena. 3. Polyfunctional catalysis of acetyl phosphate decomposition. *J. Am. Chem. Soc.* 1978, **100**, 6, 1857-1863.
19. Onindo, C.O.; Sliva, T.Y.; Kowalik-Jankowska, T.; Fritsky, I.O.; Buglyo, P.; Pettit, L.D.; Kozlowski, H.; Kiss, T. Copper(II) co-ordination by oxime analogues of amino acids and peptides. *J. Chem. Soc. Dalton Trans.* 1995, **23**, 3911-3915.
20. Domasevitch, K.V.; Gerasimchuck, N.N.; Mokhir, A. Organoantimony(V) cyanoximates: synthesis, spectra and crystal structures. *Inorg. Chem.* 2000, **39**, 6, 1227-1237.
21. Pathak, M.; Bohra, R.; Mehrotra, R.C.; Lorenz, I.-P.; Pirtowski, H. Heteroleptic complexes of zirconium acetylacetonates: better precursors for the preparation of zirconia. Structural characterisation of [(acac)<sub>2</sub>Zr{ONC(Me)py-2}<sub>2</sub>]. *Z. Anorg. Allg. Chem.* 2003, **629**, 14, 2493-2498.
22. Gerasimchuck, N.; Maher, T.; Durham, P.; Domasevitch, K.V.; Wilking, J.; Mokhir, A. Tin(IV) cyanoximates: synthesis, characterisation, and cytotoxicity. *Inorg. Chem.* 2007, **46**, 18, 7268-7284.
23. Conrad, M.; Schulze, A. Uebernitro-cyanessigsäure. *Berichte.* 1909, **42**, 735.
24. Kolotilov, S.V.; Schollmeyer, D.; Thompson, L.K.; Golub, V.; Addison, A.W.; Pavlishchuk, V.V. Synthesis, structure and magnetic properties of oligometallic systems derived from di- and trinuclear copper(II) amido-oximate complexes. *J. Chem. Soc. Dalton Trans.* 2008, **22**, 3007-3014.
25. El-Faham, A.; Fanosas, R.S.; Prohens, R.; Albericio, F. Comu: a safer and more effective replacement for benzotriazole-based uronium coupling reagents. *Chem. Eur. J.* 2009, **15**, 37, 9404-9416.
26. Khattab, S.N.; Subiros-Funosas, R.; El-Faham, A.; Albericio, F. Screening of *N*-alkyl-cyanoacetamide oximes as substitutes for *N*-hydroxysuccinimide. *ChemistryOpen.* 2012, **1**, 3, 147-152.
27. Ratcliff, J.; Durham, P.; Keck, M.; Mokhir, A.; Gerasimchuck, N. Part 2: in vitro cytotoxicity studies of two ML<sub>2</sub> complexes (M= Pd, Pt; L = 2-cyano-2-isonitroso-*N*-morpholyacetamide, HMCO). *Inorganica Chimica Acta.* 2012, **385**, 11-20.
28. Alcazar, L.; Cordero, B.; Esteban, J.; Tangoulis, V.; Font-Bardia, M.; Calvet, T.; Escuer, A. Manganese clusters derived from 2-pyridylcyanoxime: new topologies and large spin ground state in pyridyloximate chemistry. *J. Chem. Soc. Dalton Trans.* 2013, **42**, 34, 12334-12345.
29. Bakulev, V.A.; Morzerin, Y.Y.; Shafran, Y.Y.; Mokrushin, V.S. Tandem pseudo-pericyclic processes in the cyclization of  $\alpha$ -diazonitriles to 5-halo-1,2,3-triazoles. Scope and limitations. *Arkivoc.* 2002, **8**, 5, 166-179.
30. Khattab, S.N.; Subiros-Funosas, R.; El-Faham, A.; Albericio, F. Cyanoacetamide-based oxime carbonates: an efficient, simple alternative for the introduction of fmoc with minimal dipeptide formation. *Tetrahedron.* 2012, **68**, 14, 3056-3062.
31. Kislyi, V.P.; Danilova, E.B.; Zakharov, E.P.; Semenov, V.V. Synthesis of 4-aminoisoxazole-3-carboxamides using base-promoted nitrosation of *N*-substituted cyanoacetamides. *Russian Chemical Bulletin Int. Ed.* 2004, **53**, 3, 622-628.
32. Eddings, D.; Barnes, C.; Gerasimchuck, N.; Durham, P.; Domasevich, K. First bivalent palladium and platinum cyanoximates: synthesis, characterisation, and biological activity. *Inorg. Chem.* 2004, **43**, 13, 3894-3909.
33. Cheadle, C.E. Synthesis and studies of N<sup>1</sup>,N<sup>2</sup>-piperazine bis-(2-oximino-2-cyano)acetamide and its several metal complexes. Missouri State University, Missouri, 2008.
34. Fleming, F.F.; Shook, B.C. Nitrile anion cyclizations. *Tetrahedron.* 2002, **58**, 1, 1-23.
35. Gerasimchuk, N.; Goeden, L.; Durham, P.; Barnes, C.; Cannon, J.F.; Silchenko, S.; Hidalgo, I. Synthesis and characterisation of disubstituted arylcyanoximes and their several metal complexes. *Inorganica Chimica Acta.* 2008, **361**, 7, 1983-2001.
36. Bohle, D.S.; Chua, Z.; Perepichka, I.; Rosaduik, K. E/Z oxime isomerism in PhC(NO<sub>2</sub>)CN. *Chem. Eur. J.* 2013, **19**, 13, 4223-4229.
37. Gazit, A.; Osherov, N.; Gilon, C.; Levitzki, A. Tyrphostins. 6. Dimeric benzylidenemalononitrile tyrphostins: potent inhibitors of EGF receptor tyrosine kinase in vitro. *J. Med. Chem.* 1996, **39**, 25, 4905-4911.

38. Alexandre, C.; Melikian, G.; Rouessac, F. Synthesis and reactivity of *bis*-lactamic compounds. *Synth. Commun.* 1997, **27**, 11, 1919-1925.
39. Hill, T.; Odell, L.R.; Edwards, J.K.; Graham, M.E.; McGeachie, A.B.; Rusak, J.; Quan, A. Abagyan, R.; Scott, J.L.; Robinson, P.J.; McCluskey, A. Small molecule inhibitors of dynamin 1 GTPase activity: development of dimeric tyrophostins. *J. Med. Chem.* 2005, **48**, 24, 7781-7788.
40. Proenca, F.; Costa, M. A simple and eco-friendly approach for the synthesis of 2-imino and 2-oxo-2H-chromene-3-carboxamides. *J. Chem. Soc. Green Chem.* 2008, **10**, 9, 995-998.
41. Wang, K.; Nguyen, K.; Huang, Y.; Dumling, A. Cyanoacetamide multicomponent reaction (1): parallel synthesis of cyanoacetamides. *J. Comb. Chem.* 2009, **11**, 5, 920-927.
42. Cheikh, N.; Bar, N.; Choukhou-Braham, N.; Mostefa-Kara, B.; Lohier, J.-F.; Sopkova, J.; Villemin, D. Efficient synthesis of new butenolides by subsequent reactions: application for the synthesis of original iminolactones, *bis*-iminolactones and *bis*-lactones. *Tetrahedron.* 2011, **67**, 8, 1540-1551.
43. Elenairy, M.A.A.; Mekky, A.E.M.; Ahmed, A.A.M. Bis-(cyanoacetamide)alkanes in hetrocyclic synthesis: synthesis of *bis*-heteryl(carboxymido)alkanes and *bis*-(heteryl)alkanes of thiophene, pyrrole, thiazole and pyrimidione series. *J. Sulfur. Chem.* 2012, **33**, 3, 373-383.
44. a) *Private Communication*. Barry J. 2008, b) Jencks, W.P. Studies on the mechanism of oxime and semicarbazone formation. *J. Am. Chem. Soc.* 1959, **81**, 2, 475-481, c) Talvik, A-T.; Tuulmets, A.; Vanio, E. Kinetics and mechanism of aminolysis of aliphatic esters in aprotic solvents. *J. Physical Org. Chem.* 1999, **12**, 10, 747-750.
45. Arulsamy, N.; Bohle, D.S. Nucleophilic addition of hydroxylamine, methoxylamine, and hydrazine to malononitrileoxime. *J. Org. Chem.* 2000, **65**, 4, 1139-1143.
46. *Bruker APEX2, SAINT and SADABS*, Bruker AXS Inc.: Madison, Wisconsin, 2012
47. Sheldrick, G.M. A short history of SHELX. *Acta Cryst.* 2008, **A64**, 112-122
48. Farrugia, L.J. WinGX and ORTEP for windows update. *J. Appl. Cryst.* 2012, **45**, 849 -854.
49. Fritsky, I.O.; Karaczyn, A.; Kozlowski, H.; Glowiac, T.; Prisyazhnaya, E.V. Crystal and molecular structure of two tetradentate "oxime-and-amide" ligands. *Z. Naturforsch.*, 1999, **54**, 4, 456-460.
50. *Software Package for Crystal Structure Solution, APEX 2 suit*. Bruker AXS Inc.: Madison, Wisconsin, 2013
51. (a) Blessing, R.H. An empirical correction for absorption anisotropy. *Acta Cryst.* 1995, **A51**, 33-38; (b) Sheldrick, G. M. SADABS Area-detector Absorption Correction, 2.03; University of Göttingen, Göttingen, Germany, 1999.
52. (a) Farrugia, L.J. ORTEP-3 for Windows. *J. Appl. Cryst.* 1997, **30**, 565; (b) Burnett, M. N.; Johnson, C. K. ORTEP III: Report ORNL-6895; Oak Ridge National Laboratory: Oak Ridge, Tennessee, 1996.
53. *Mercury 2.4.. crystallographic viewing and graphing software package*. CCD.: Cambridge, 2013.
54. Platon: crystallographic software package at <http://www.cryst.chem.uu.nl/spek/platon/>.
55. *Private communication*. Diu, E. 2014

# Appendices

## **Use of this section.**

The following section shows raw characterisation data for the compounds discussed in the thesis.

Subsequently, all spectra have been presented as figures, which are listed with either an “A” or “B” prefix. Using an alpha numeral reference allows us to easily distinguish between species discussed in chapters A and B of the text. The exact position of **information pertaining to a particular synthetic product is shown** by a list of numbers summarised **under the characterisation specifics of that species in the relevant** sections. (Chapter A, 4.1-4.5 and Chapter B, 3.2-3.3)

Reynstallised, Prismatic  
**1,3-diphthalimido-2-bromopropane-MeCN- Attempt2/CBr4**

3 Sep 2008

<b>File Name</b>	F:\NASEEM PROJECTS\IR DATA\BR-DIAPHTHALIMIDE ATTEMPT2-CBR4 MECN.SP		<b>Date Stamp</b>	tue sep 02 10:49:37 2008
<b>Date</b>	Tue Sep 02 10:50:28 2008		<b>Technique</b>	Infrared
<b>Spectral Region</b>	IR	<b>X Axis</b> Wavenumber (cm-1)	<b>Y Axis</b> %Transmittance	<b>Instrument</b> Spectrum One
<b>Points Count</b>	3551	<b>Data Spacing</b> 1.0000	<b>Spectrum Range</b> 450.0000 - 4000.0000	

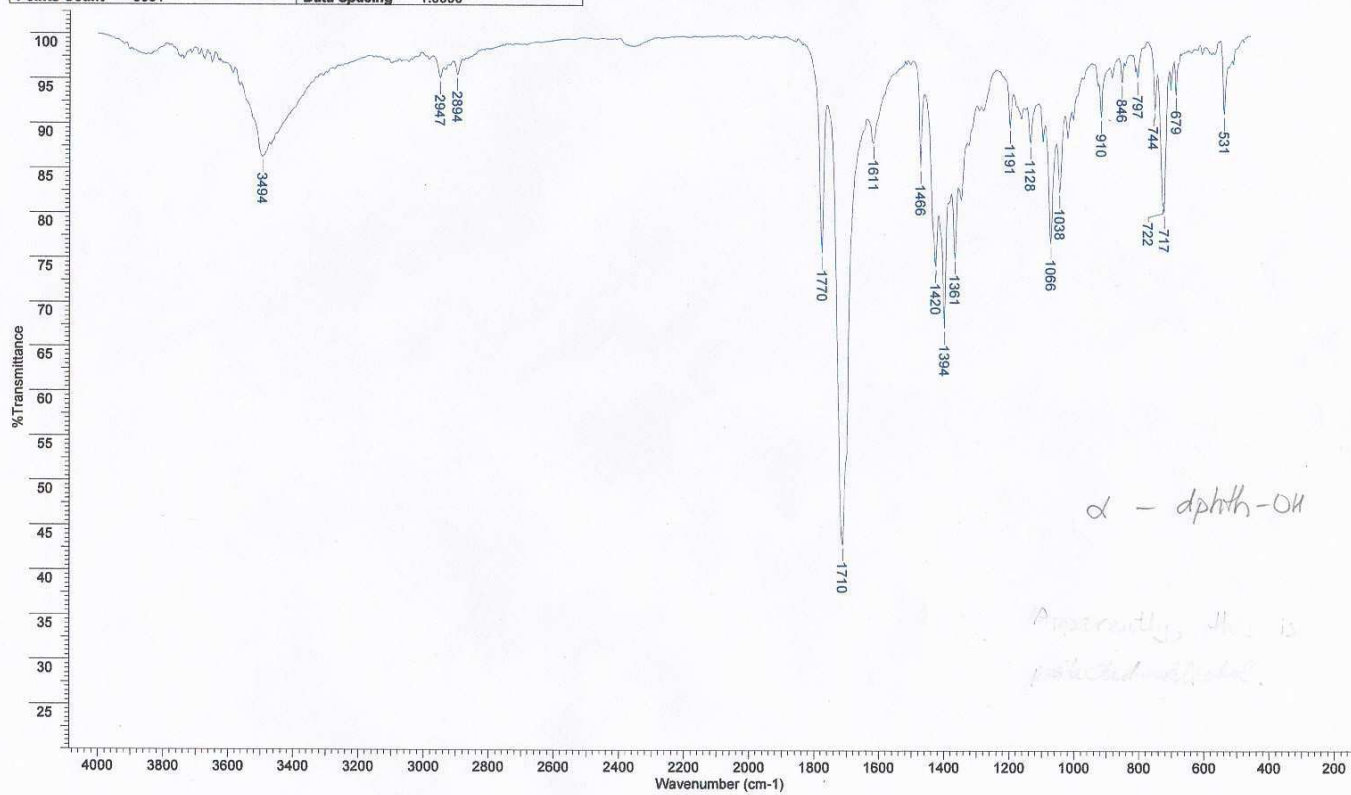


**Fig. A1.** Representative IR spectrum of 2,2'-(2-hydroxypropane-1,3-diyl)bis(1*H*-isoindole-1,3(2*H*)-dione).



2,2'-(2-hydroxypropane-1,3-diyl)bis(1H-isoindeole-1,3(2H)-dione), 1H, DMSO-d6

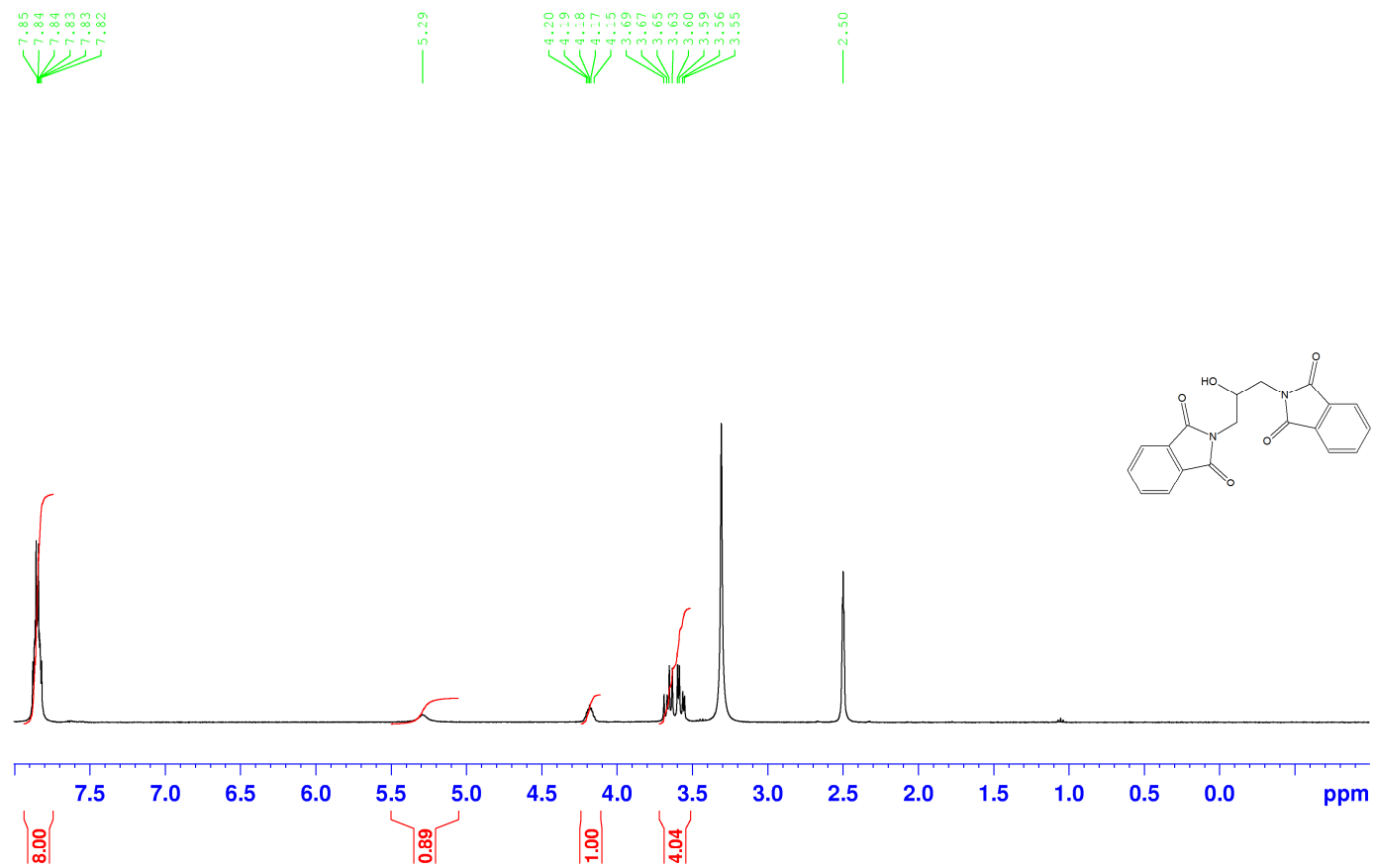
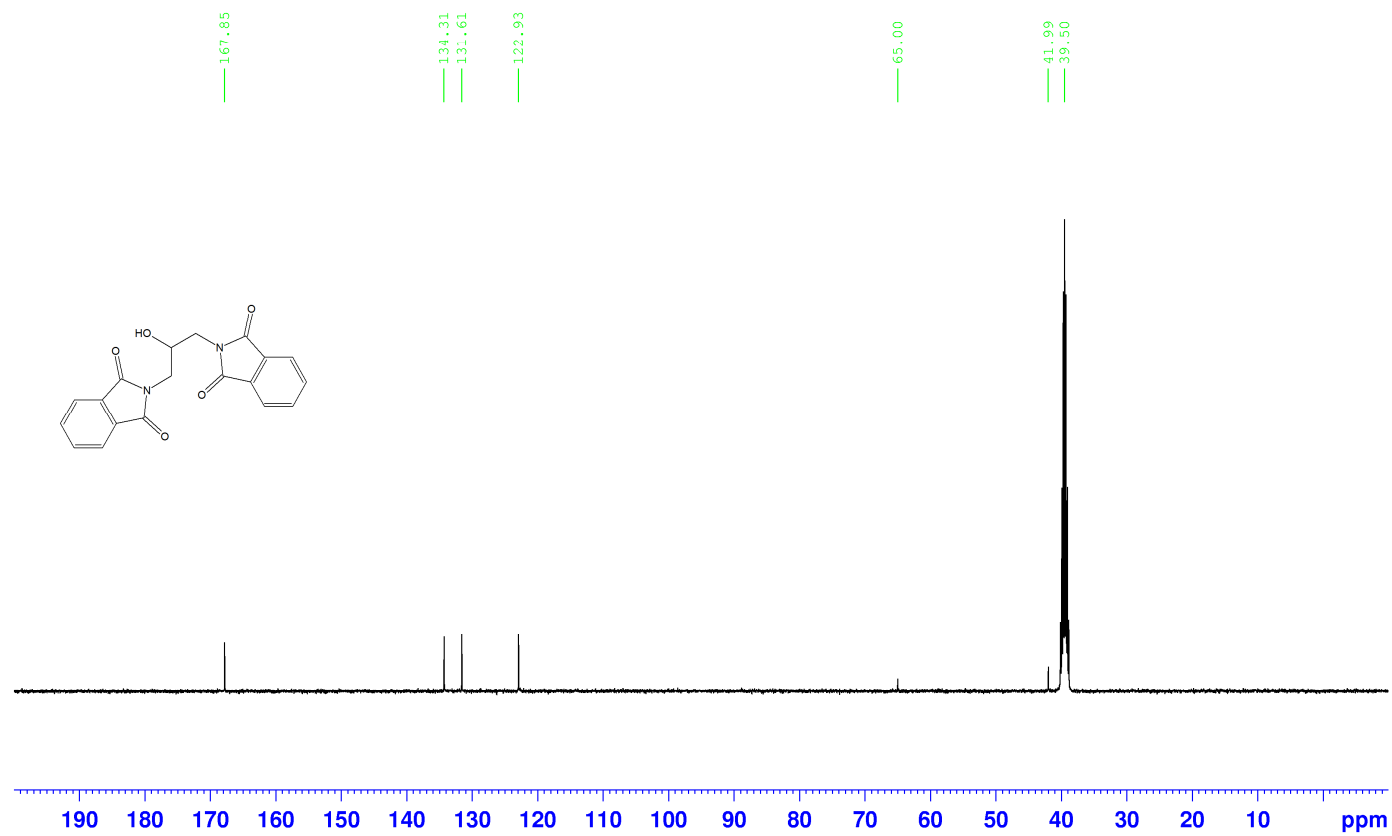


Fig. A2. <sup>1</sup>H NMR spectrum of 2,2'-(2-hydroxypropane-1,3-diyl)bis(1H-isoindeole-1,3(2H)-dione).

2,2'-(2-hydroxypropane-1,3-diyl)bis(1H-isoinidole-1,3(2H)-dione), <sup>13</sup>C, DMSO-d<sub>6</sub>



**Fig. A3.** <sup>13</sup>C NMR spectrum of 2,2'-(2-hydroxypropane-1,3-diyl)bis(1H-isoinidole-1,3(2H)-dione).

2,2'-(2-hydroxypropane-1,3-diyl)bis(1*H*-isoindole-1,3(2*H*)-dione), DEPT 135, DMSO-d<sub>6</sub>

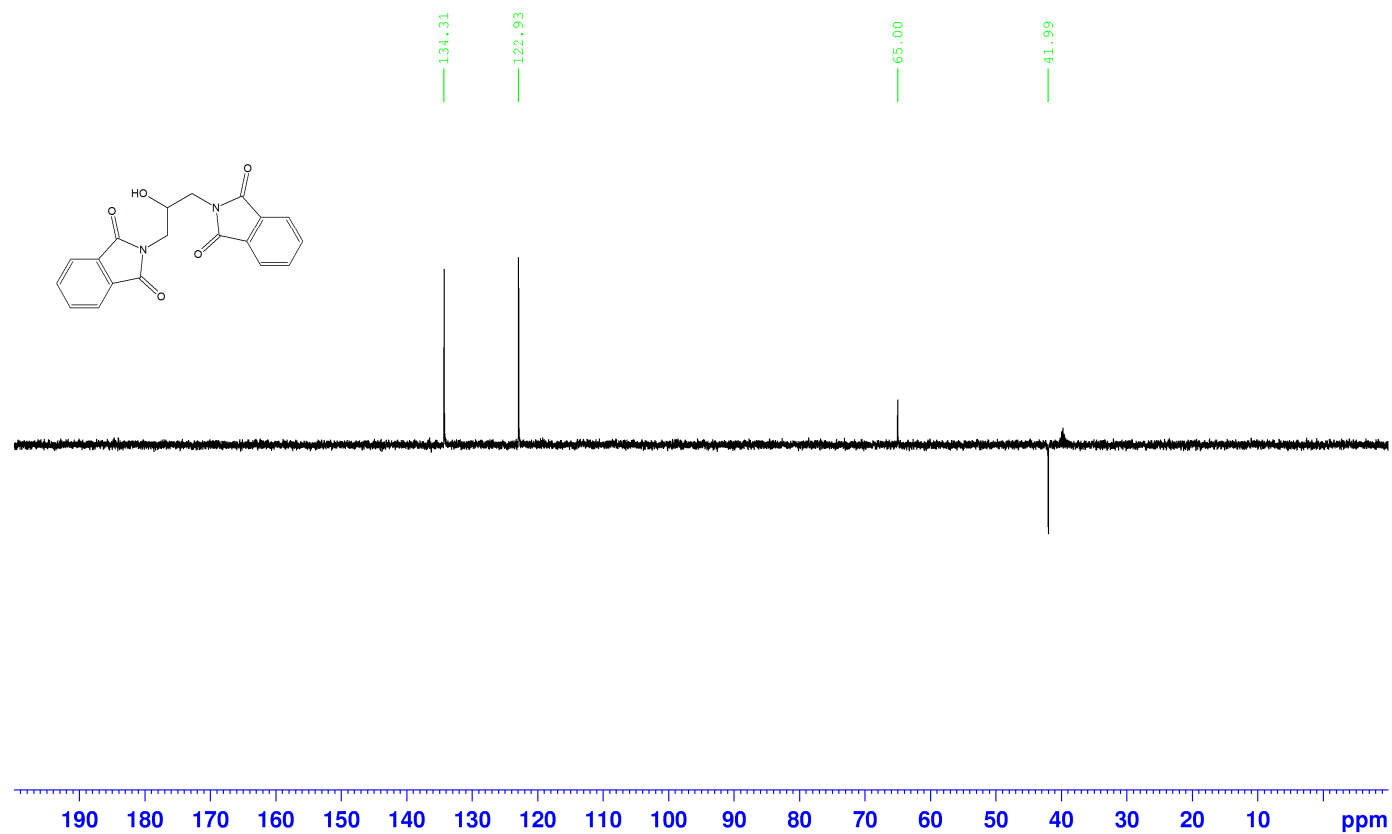


**Fig. A4.** DEPT 135 NMR spectrum of 2,2'-(2-hydroxypropane-1,3-diyl)bis(1*H*-isoindole-1,3(2*H*)-dione).

2,2'-(2-hydroxypropane-1,3-diyl)bis(1H-isoindole-1,3(2H)-dione), HSQC, DMSO-d6

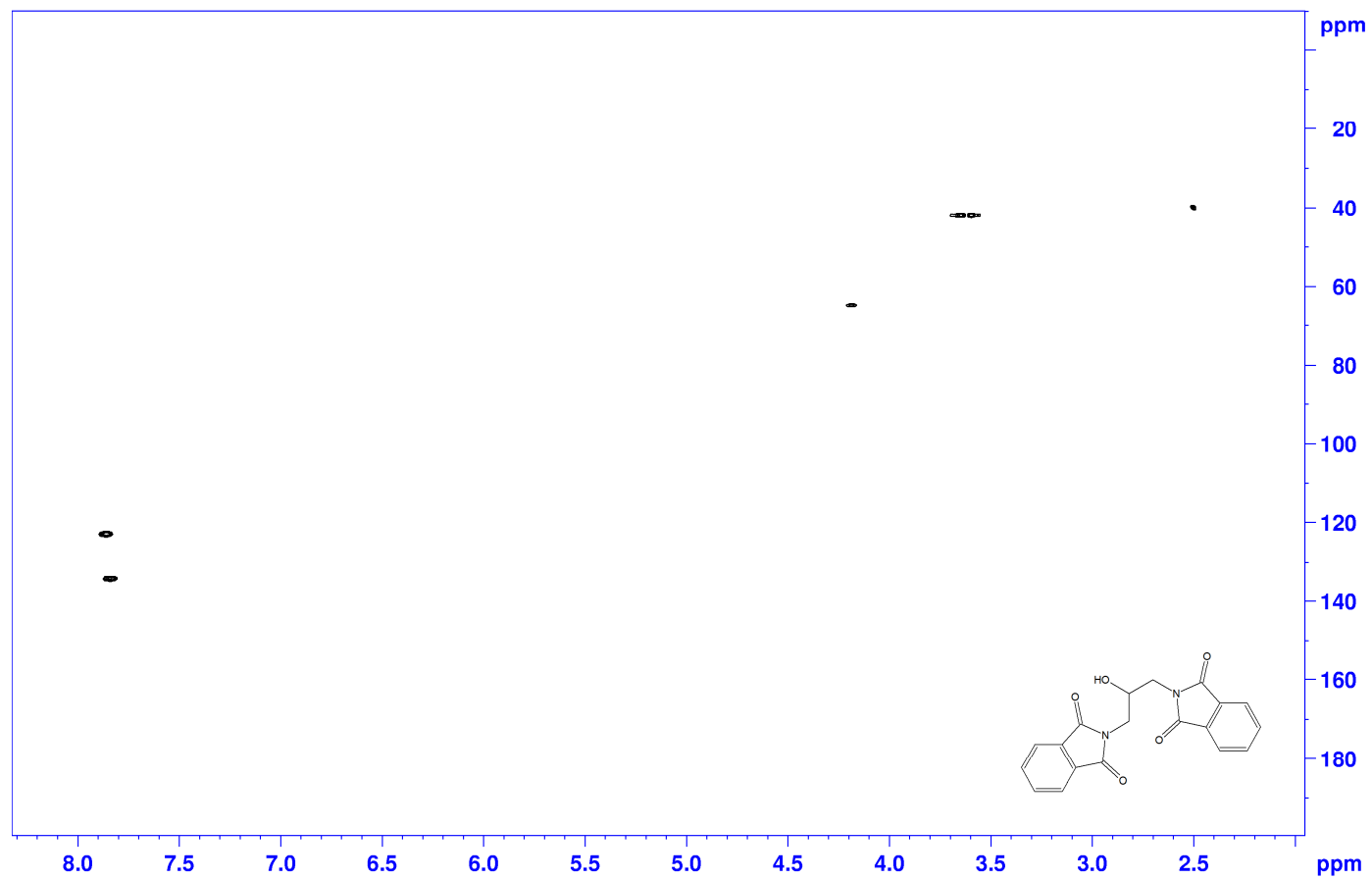


**Fig. A5.** HSQC NMR spectrum of 2,2'-(2-hydroxypropane-1,3-diyl)bis(1H-isoindole-1,3(2H)-dione).

2,2'-(2-hydroxypropane-1,3-diyl)bis(1*H*-isoindole-1,3(2*H*)-dione), HMBC, DMSO-d<sub>6</sub>

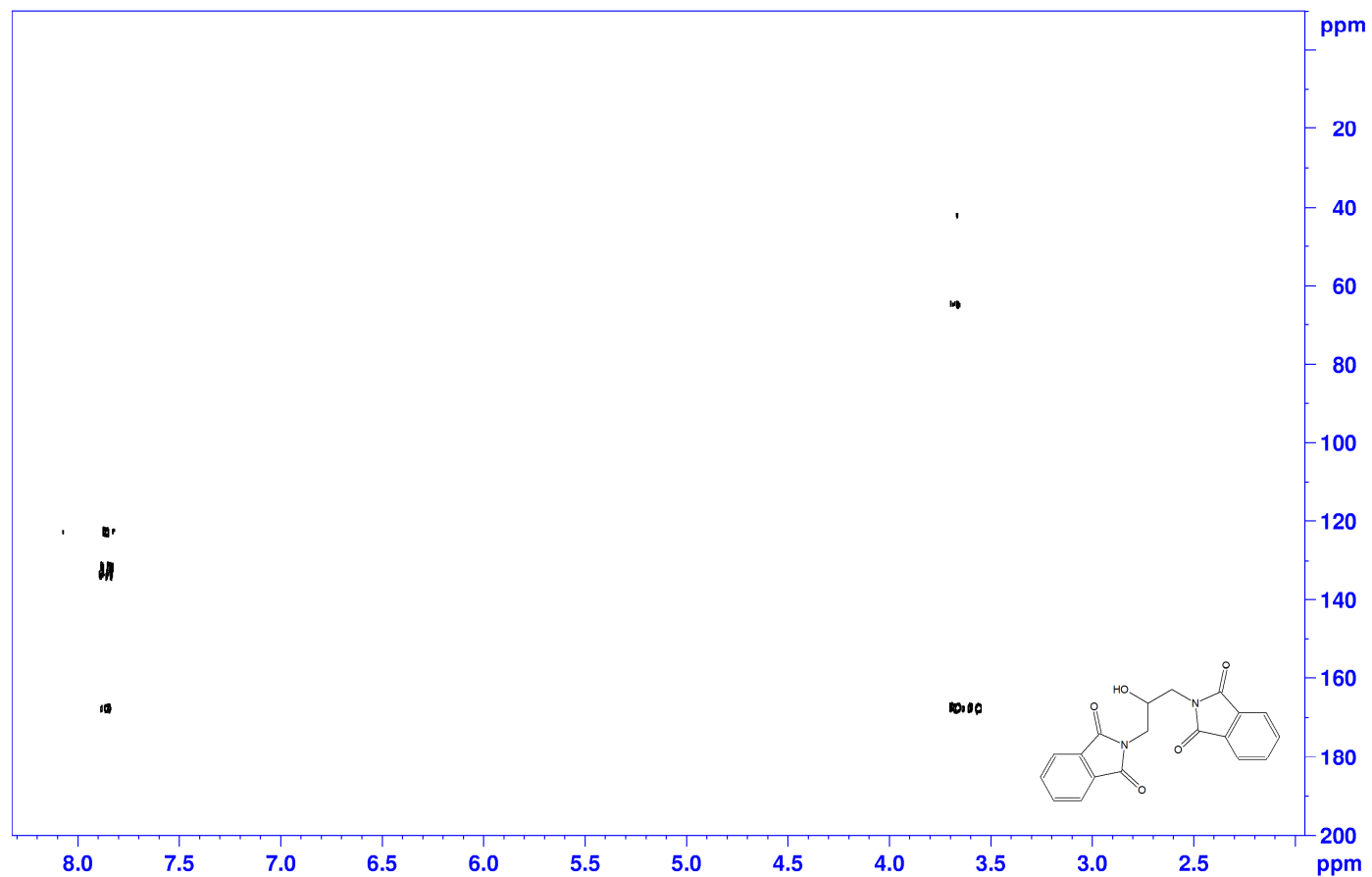
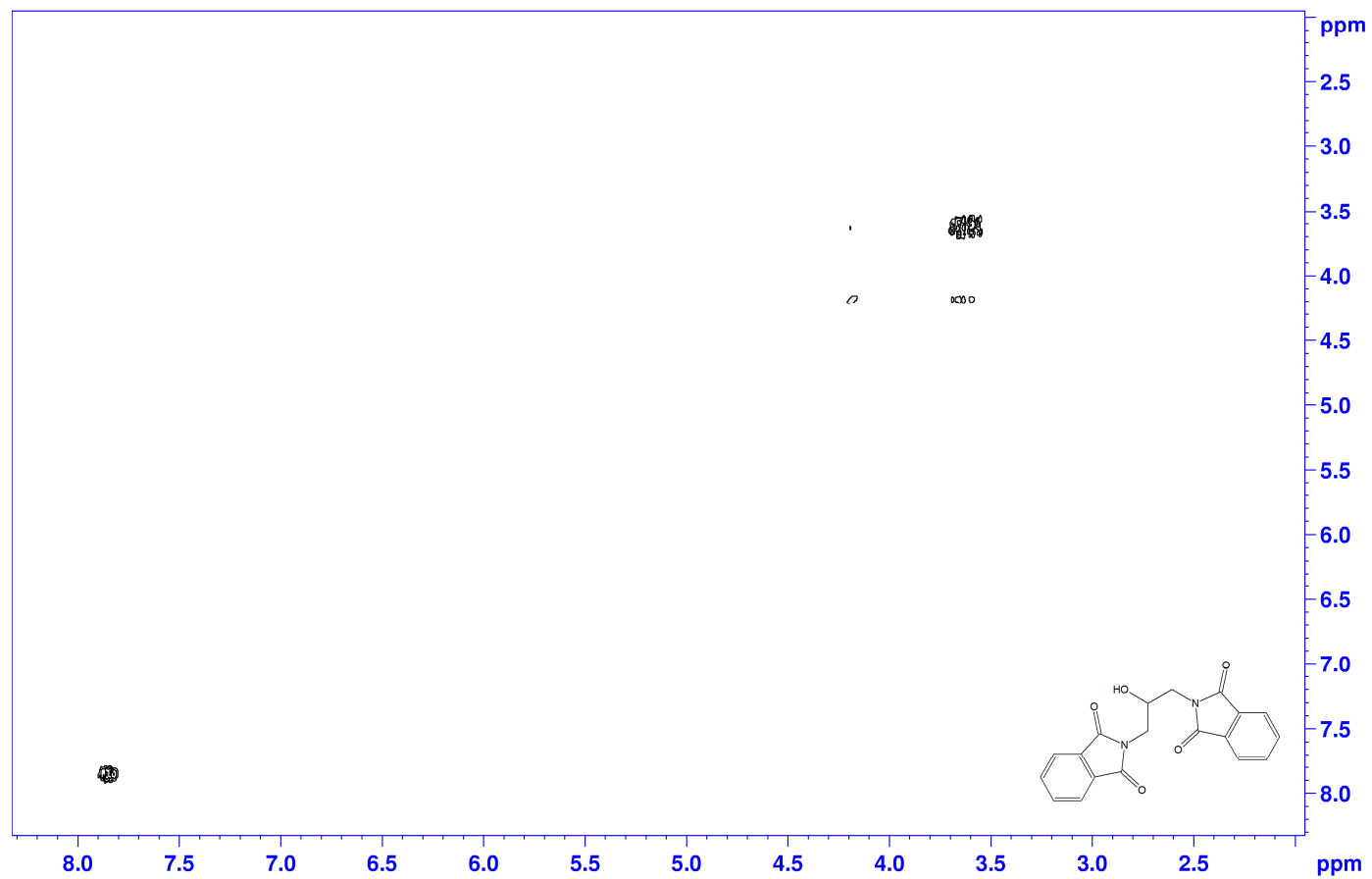


Fig. A6. HMBC NMR spectrum of 2,2'-(2-hydroxypropane-1,3-diyl)bis(1*H*-isoindole-1,3(2*H*)-dione).

2,2'-(2-hydroxypropane-1,3-diyl)bis(1H-isoinidole-1,3(2H)-dione), COSY, DMSO-d6



**Fig. A7.** COSY NMR spectrum of 2,2'-(2-hydroxypropane-1,3-diyl)bis(1H-isoinidole-1,3(2H)-dione).

2-(benzyloxy)ethanol, 1H, CDCl3

7.35  
7.34  
7.33  
7.31  
7.30  
7.29  
7.28  
7.27  
7.26  
7.25  
7.24

4.56

3.77  
3.76  
3.74  
3.47  
3.46  
3.44

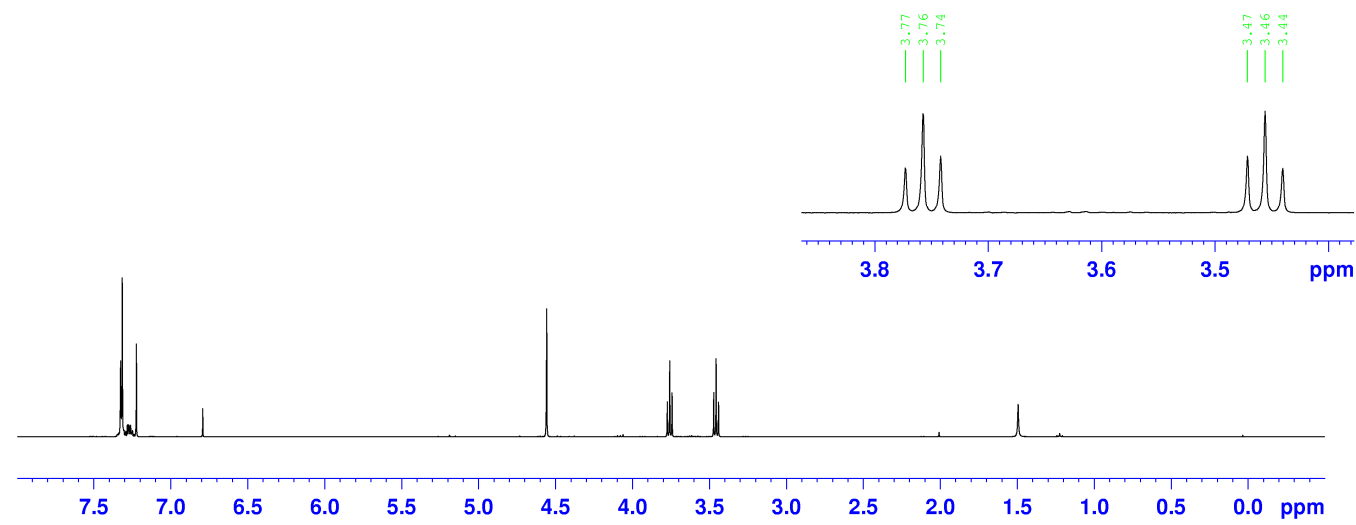
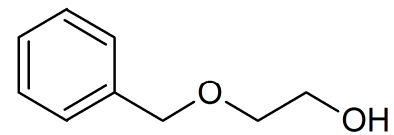
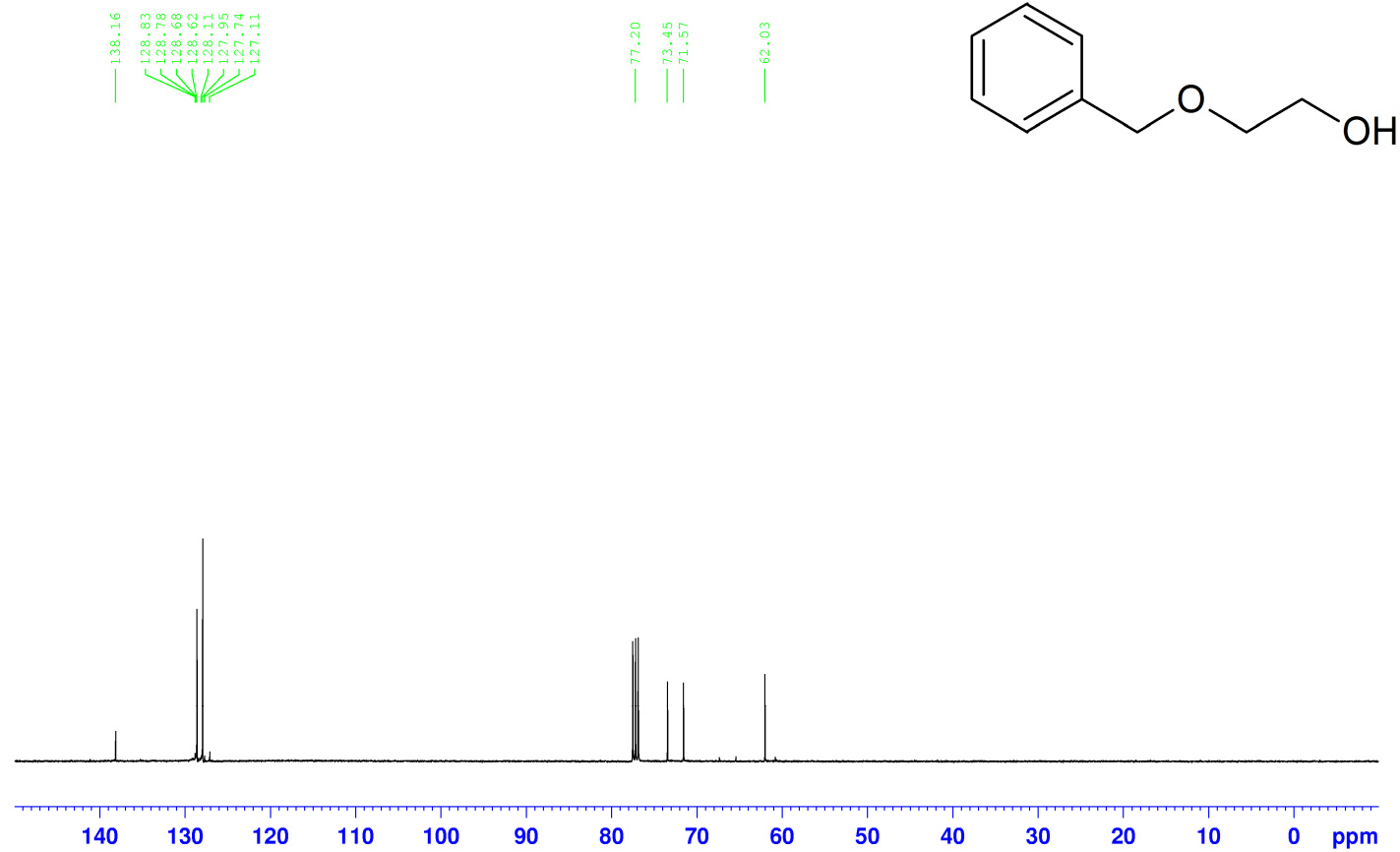


Fig. A8. <sup>1</sup>H NMR spectrum of 2-(benzyloxy)ethanol.

2-(benzyloxy)ethanol,  $^{13}\text{C}$ ,  $\text{CDCl}_3$



**Fig. A9.**  $^{13}\text{C}$  NMR spectrum of 2-(benzyloxy)ethanol.



2-(benzyloxy)ethanol, DEPT 135, CDCl<sub>3</sub>

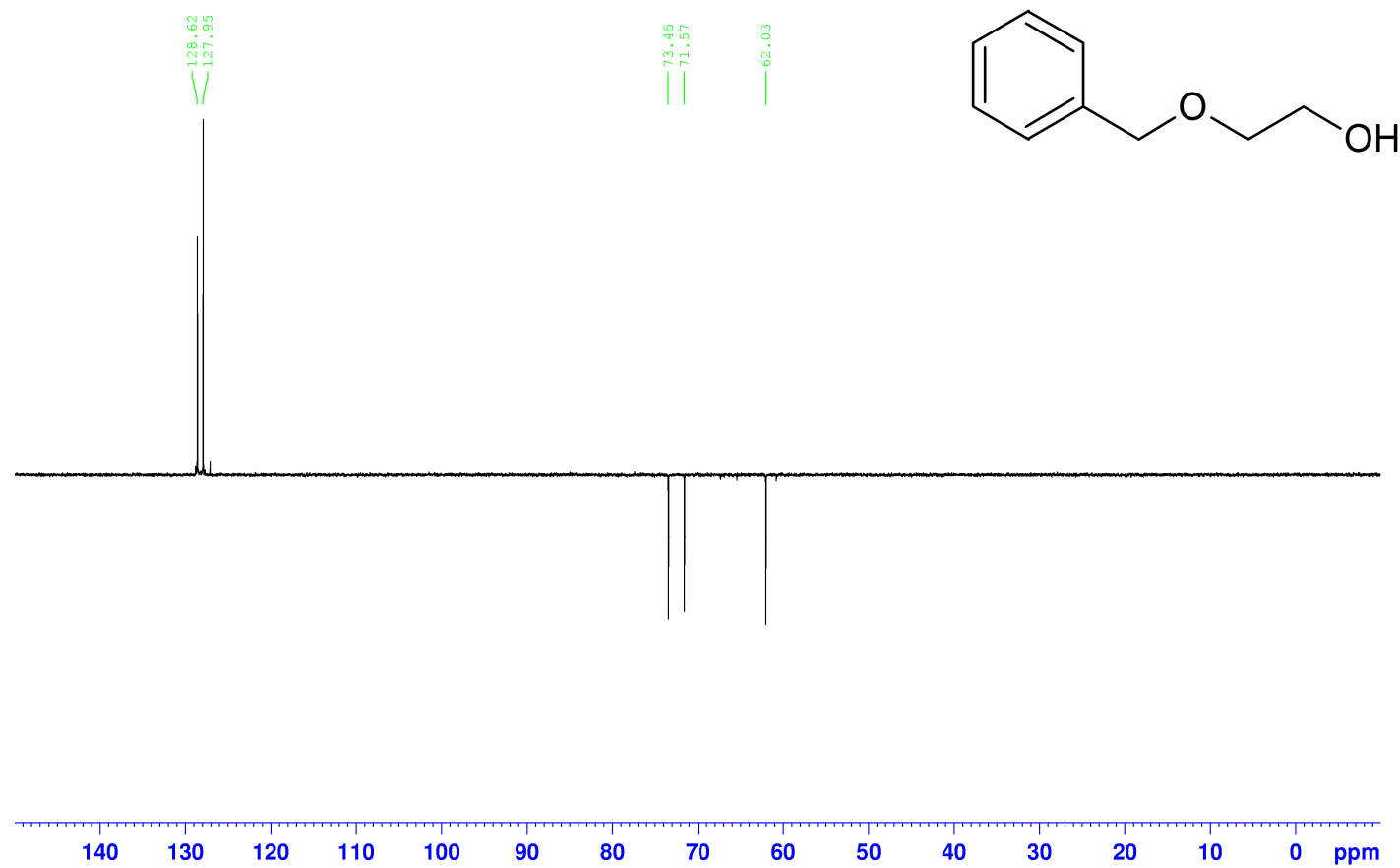


**Fig. A10.** DEPT 135 NMR spectrum of 2-(benzyloxy)ethanol.

3-(benzyloxy)propan-1-ol, 1H, CDCl3

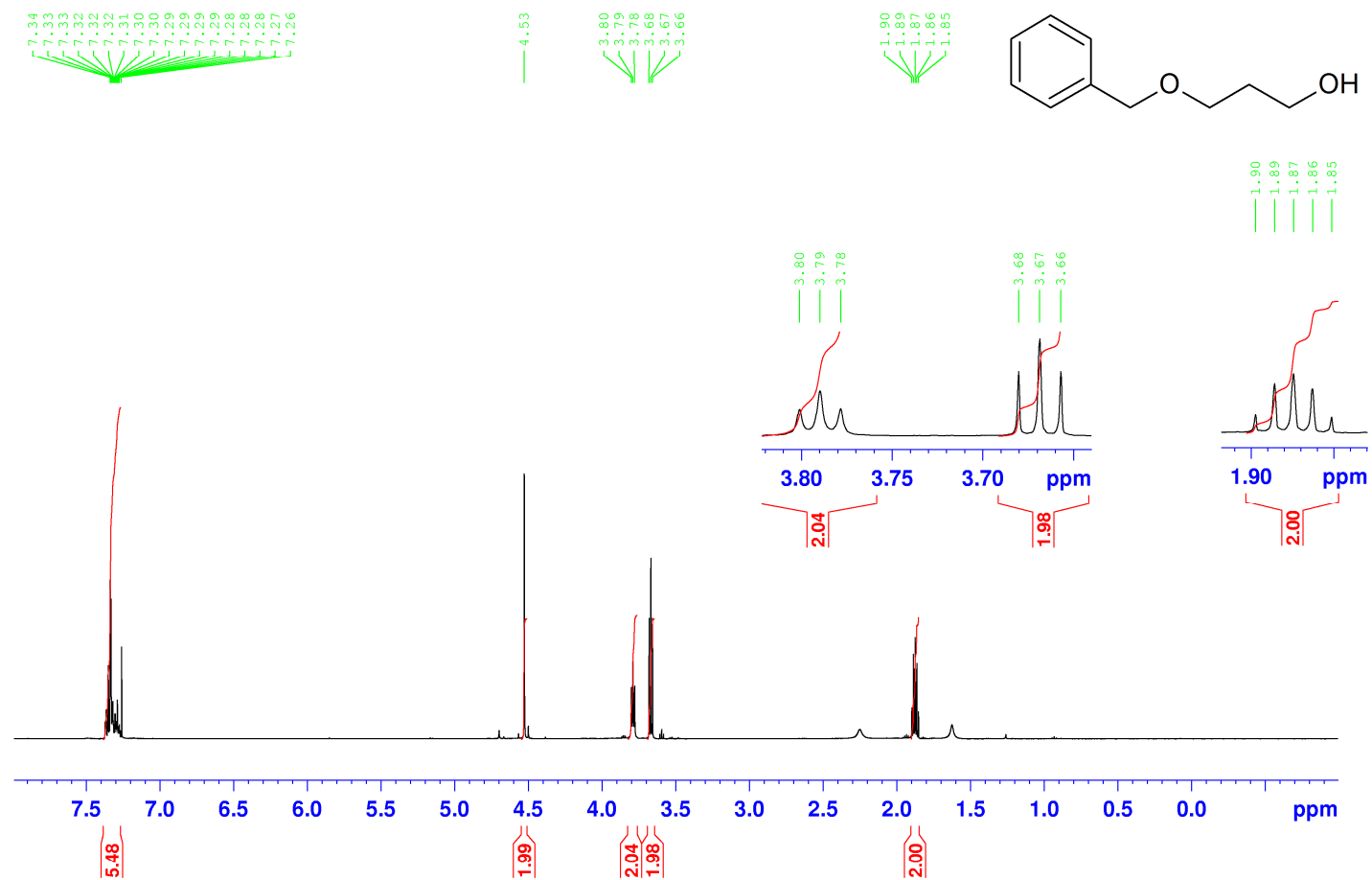
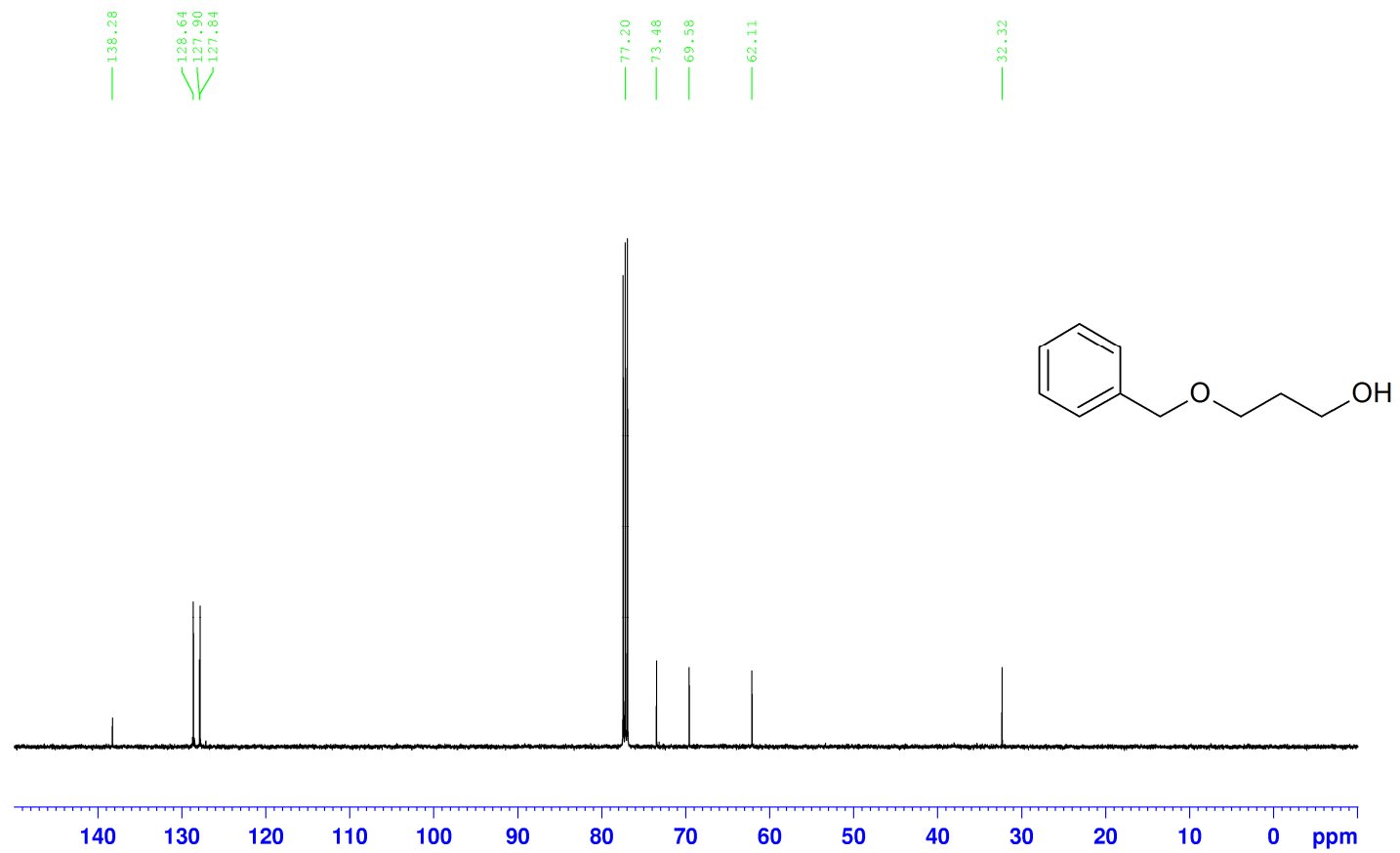


Fig. A11. <sup>1</sup>H NMR spectrum of 3-(benzyloxy)propan-1-ol.

3-(benzyloxy)propan-1-ol,  $^{13}\text{C}$ ,  $\text{CDCl}_3$



**Fig. A12.**  $^{13}\text{C}$  NMR spectrum of 3-(benzyloxy)propan-1-ol.

3-(benzyloxy)propan-1-ol, DEPT 135, CDC13

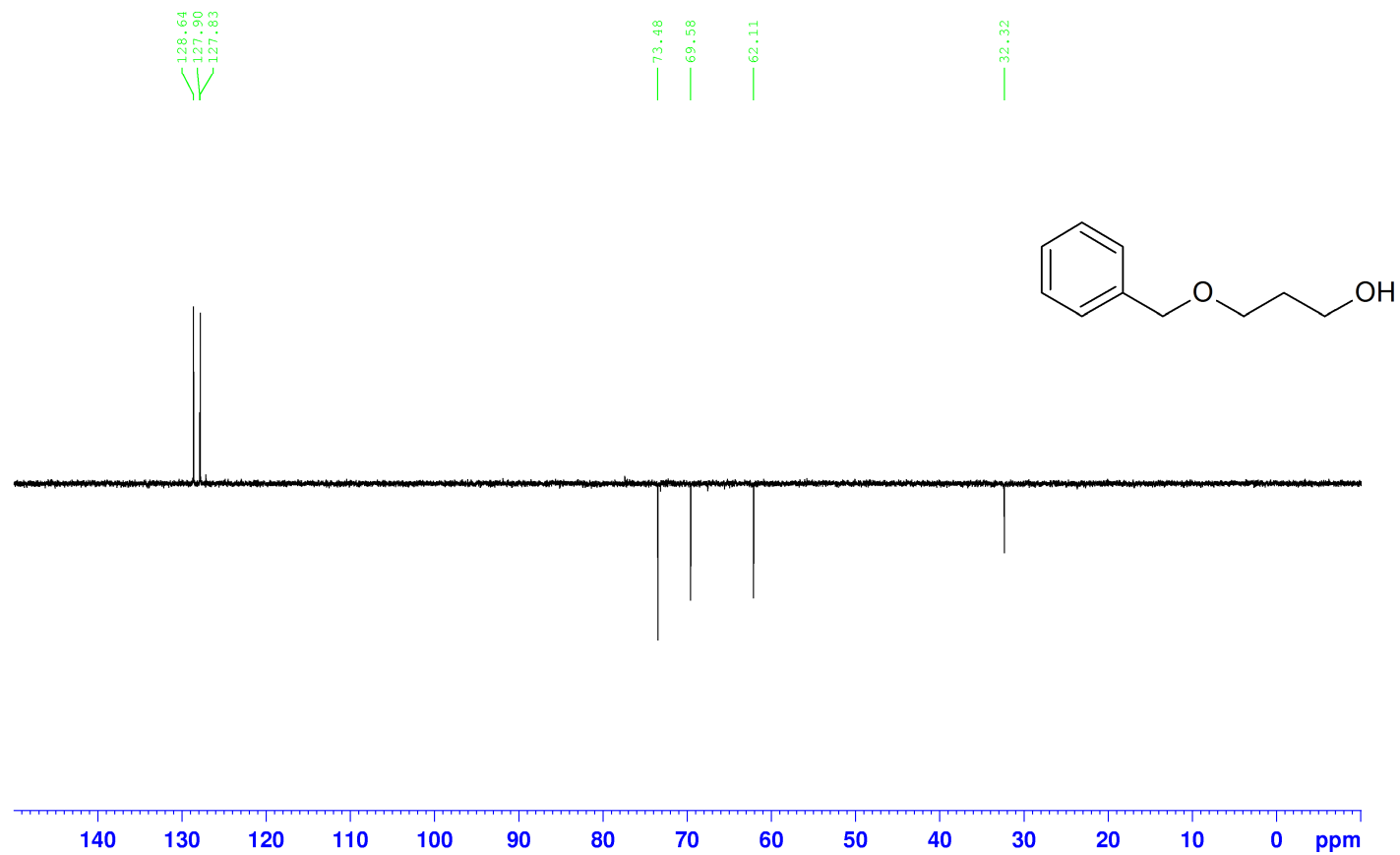
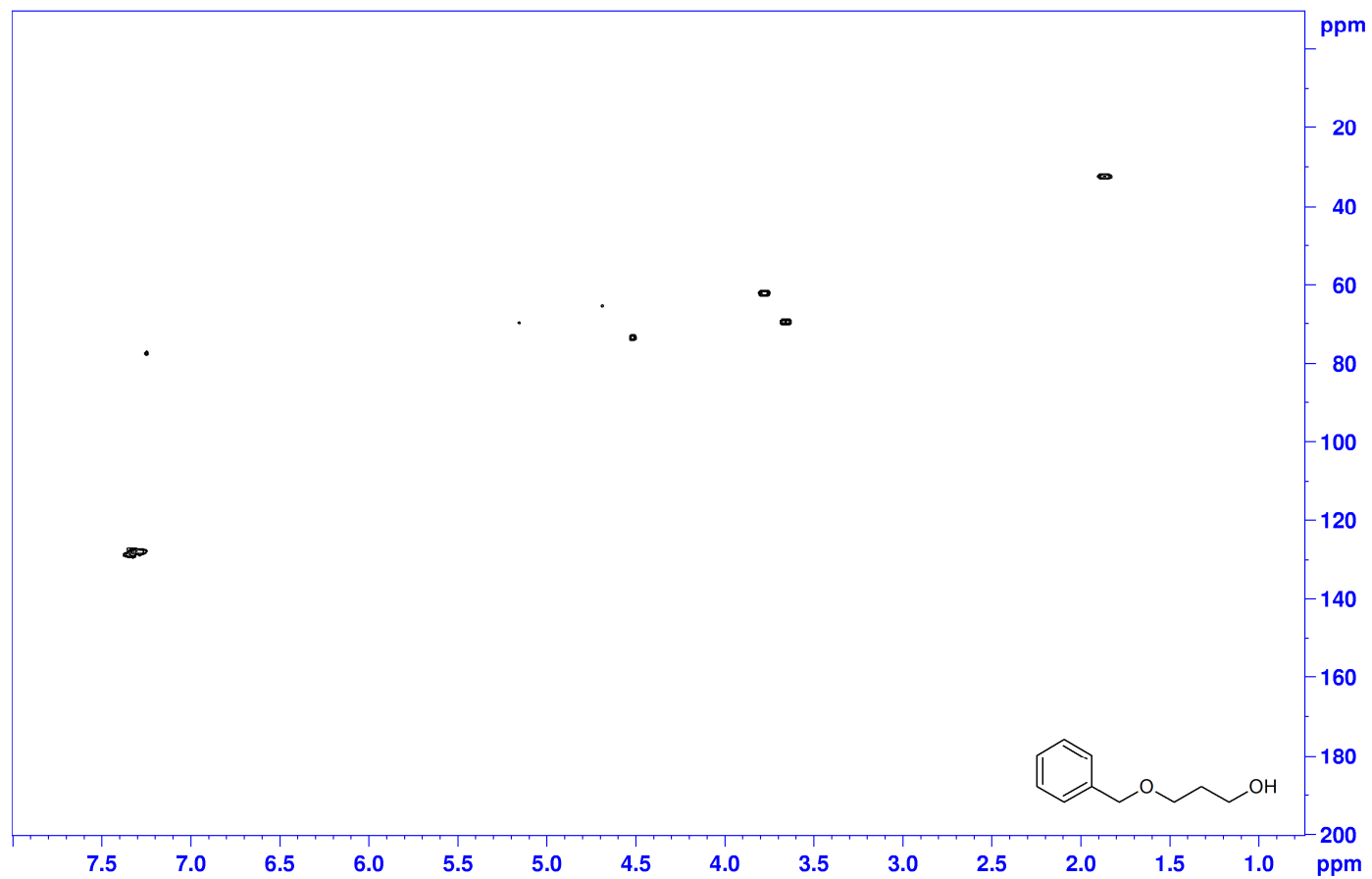


Fig. A13. DEPT 135 NMR spectrum of 3-(benzyloxy)propan-1-ol.

3-(benzyloxy)propan-1-ol, HSQC, CDC13



**Fig. A14.** HSQC NMR spectrum of 3-(benzyloxy)propan-1-ol.

3-(benzyloxy)propan-1-ol, HMBC, CDCl<sub>3</sub>

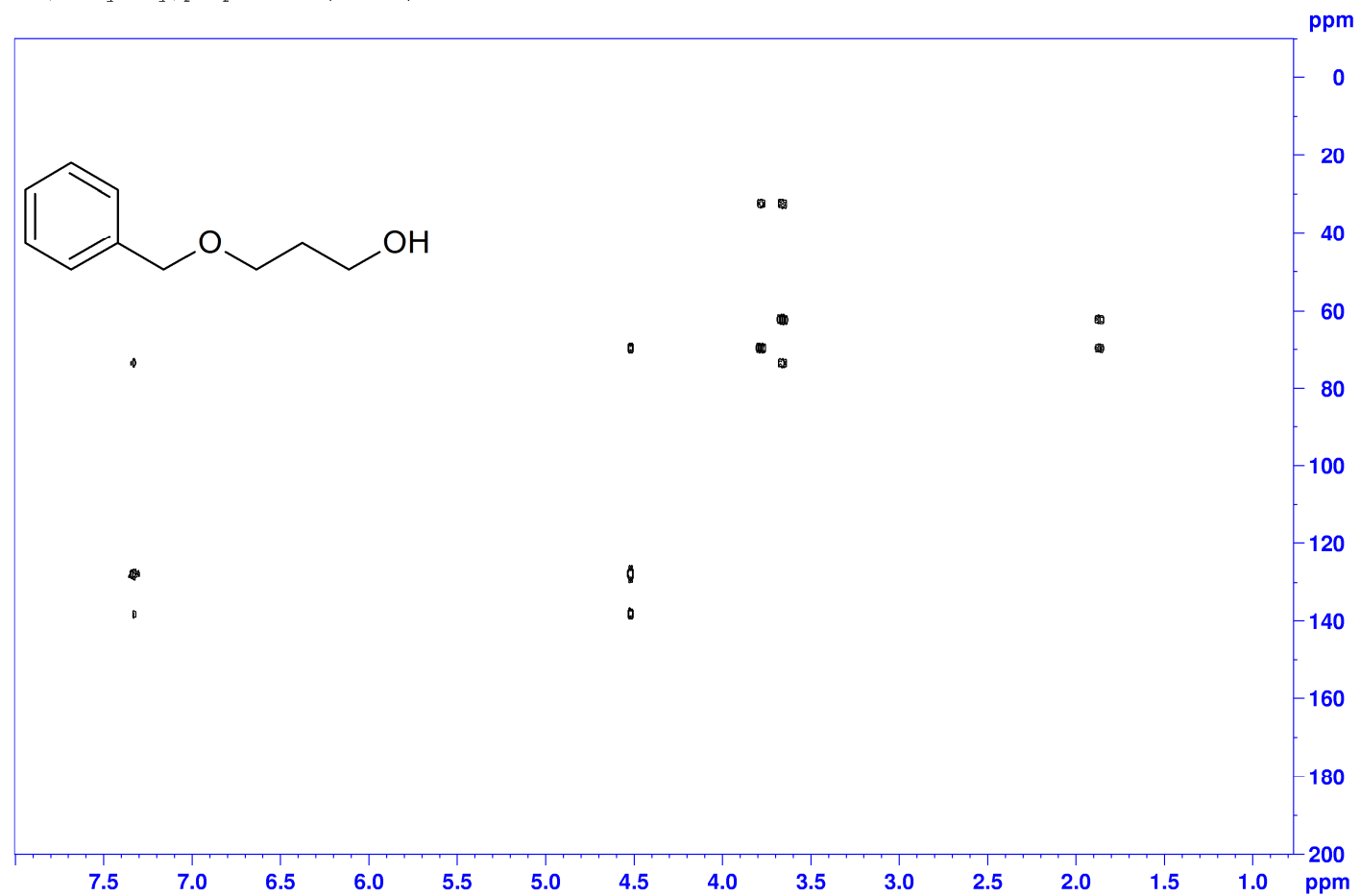


**Fig. A15.** HMBC NMR spectrum of 3-(benzyloxy)propan-1-ol.

3-(benzyloxy)propan-1-ol, COSY, CDCl<sub>3</sub>

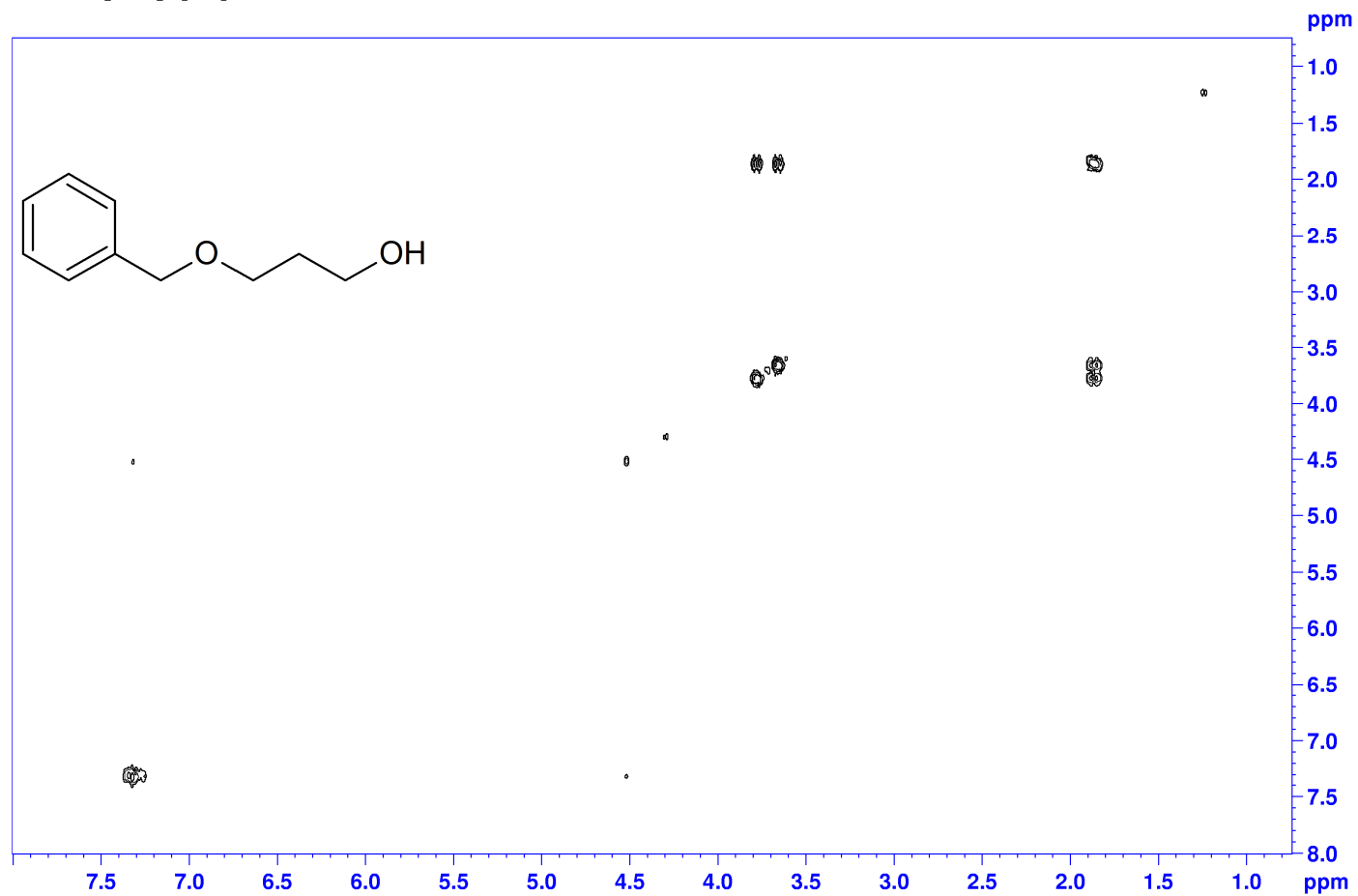


**Fig. A16.** COSY NMR spectrum of 3-(benzyloxy)propan-1-ol.

3-(benzyloxy)propan-1-ol, LRMS

13bnbr LRMS 2 (0.017) Cm (1:31)

TOF MS ES+  
7.51e4

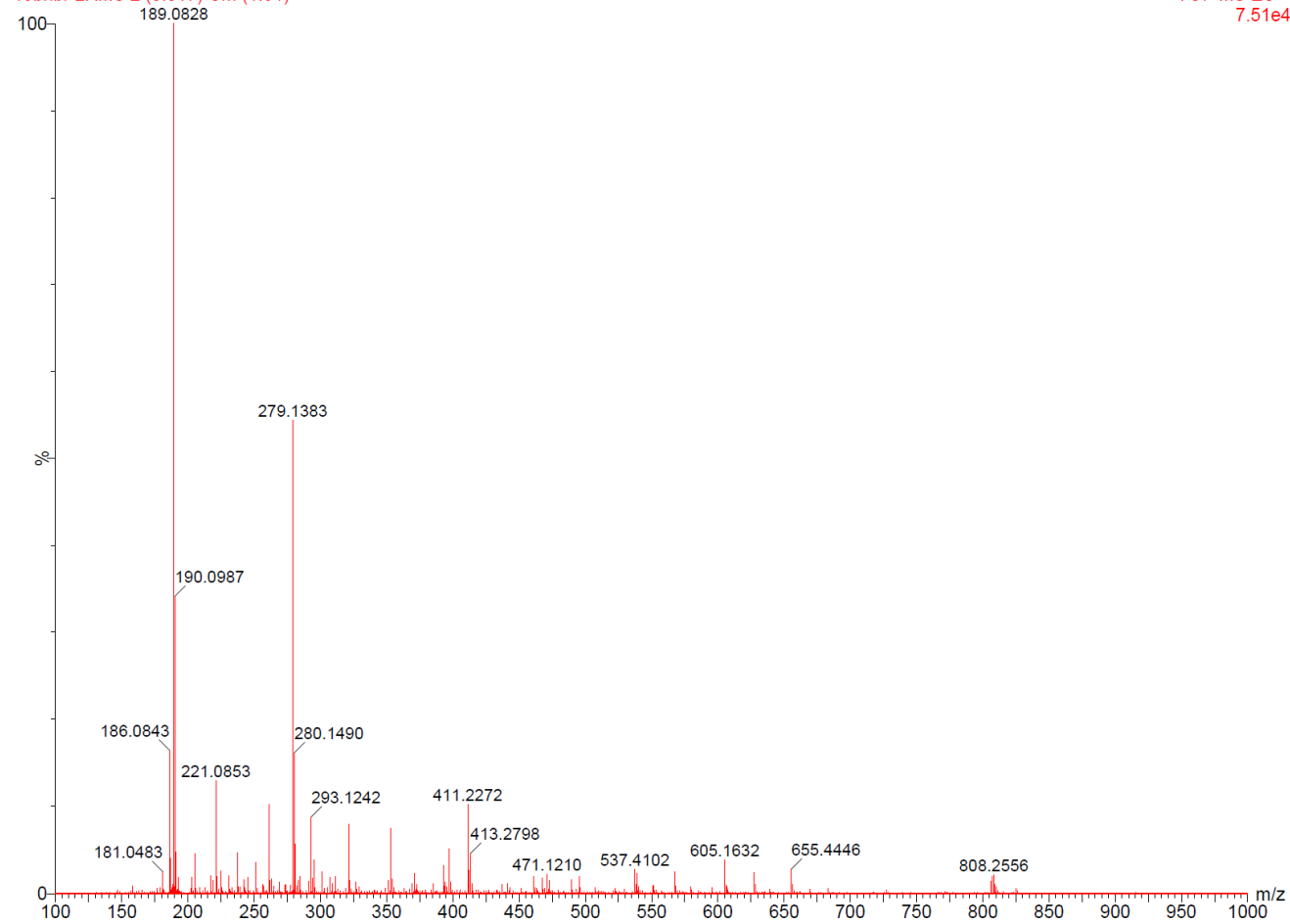


Fig. A17. Mass spectrum of 3-(benzyloxy)propan-1-ol without mass lock..



**Single Mass Analysis**

Tolerance = 50.0 PPM / DBE: min = -1.5, max = 50.0

Element prediction: Off

Number of isotope peaks used for i-FIT = 3

Monoisotopic Mass, Even Electron Ions

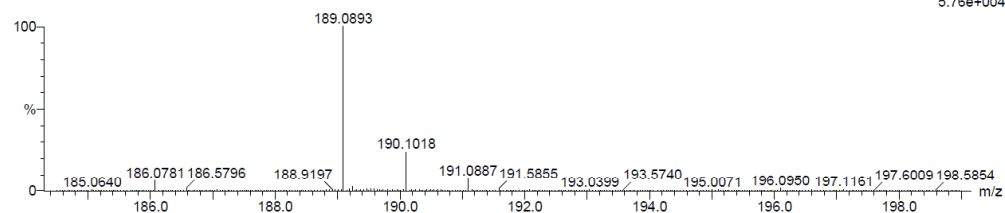
7 formula(e) evaluated with 1 results within limits (up to 50 best isotopic matches for each mass)

Elements Used:

C: 5-10 H: 10-15 O: 0-5 Na: 0-1

13bnbr 9 (0.137) Cm (1:30)

TOF MS ES+



Minimum: -1.5  
 Maximum: 50.0

Mass	Calc. Mass	mDa	PPM	DBE	i-FIT	i-FIT (Norm)	Formula
189.0893	189.0891	0.2	1.1	3.5	638.1	0.0	C10 H14 O2 Na

**Fig. A18.** Mass spectrum of 3-(benzyloxy)propan-1-ol with mass lock..

6-(benzyloxy)hexan-1-ol, 1H, CDCl<sub>3</sub>

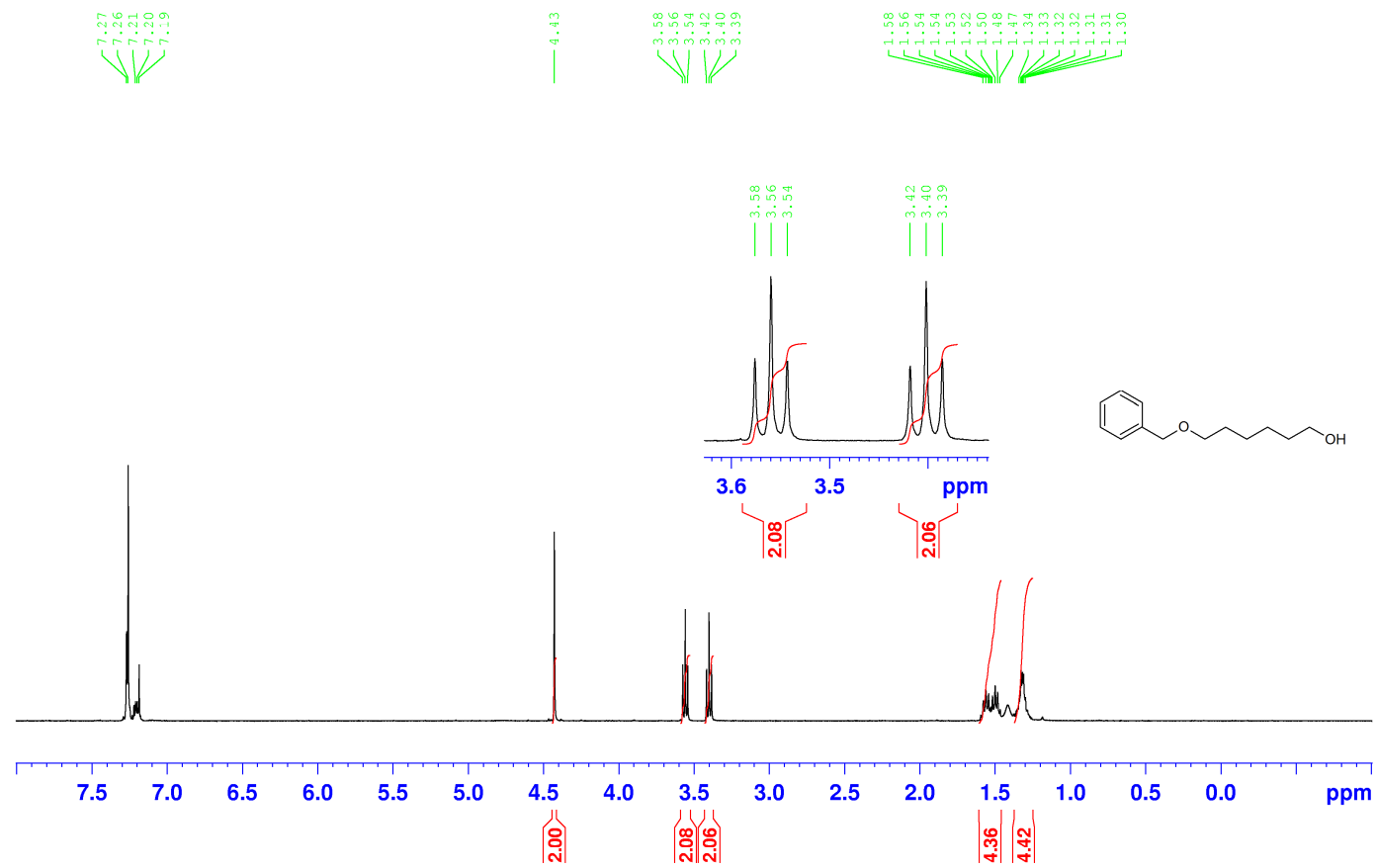
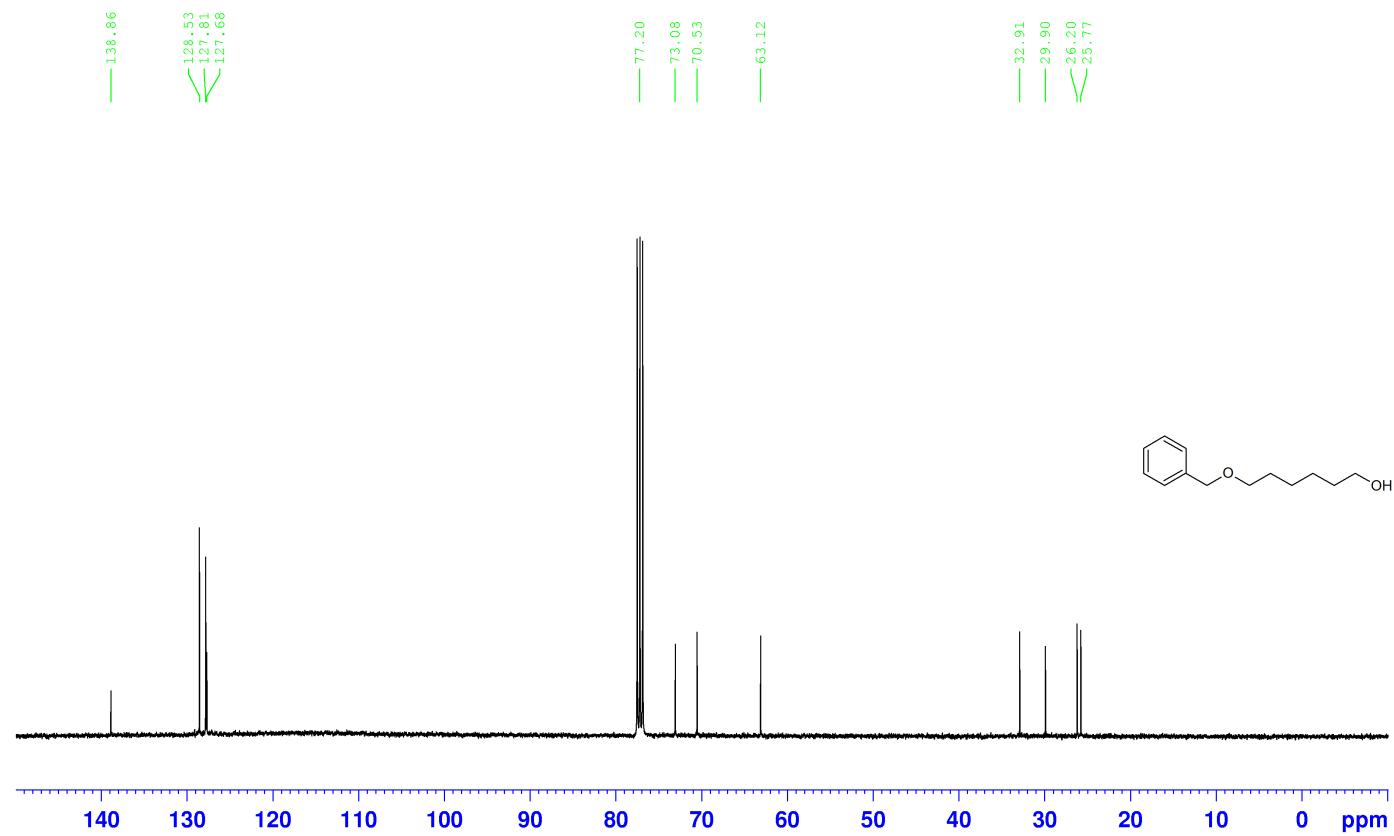


Fig. A19. <sup>1</sup>H NMR spectrum of 6-(benzyloxy)hexan-1-ol.

6-(benzyloxy)hexan-1-ol,  $^{13}\text{C}$ ,  $\text{CDCl}_3$



**Fig. A20.**  $^{13}\text{C}$  NMR spectrum of 6-(benzyloxy)hexan-1-ol.

6-(benzyloxy)hexan-1-ol, DEPT135, CDC13

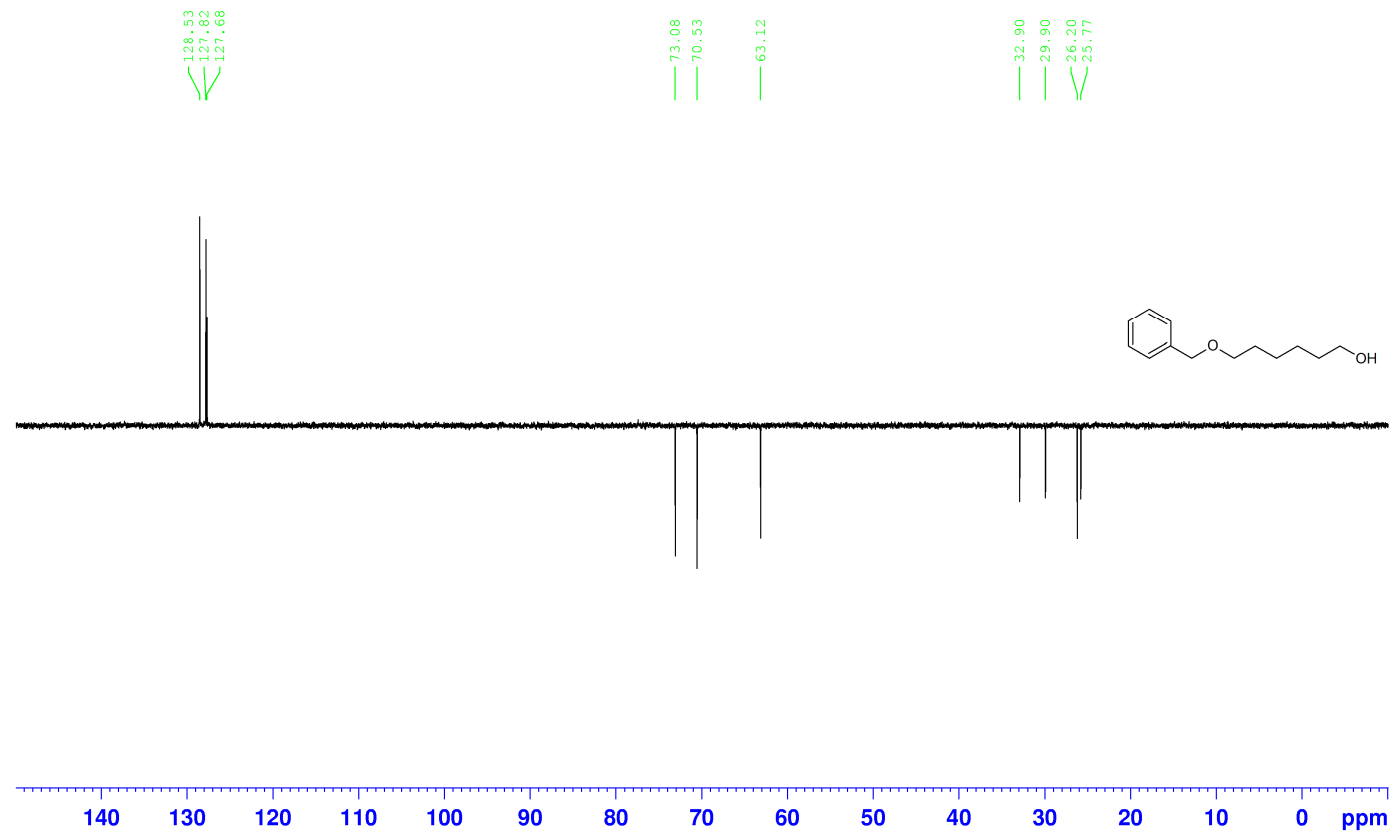


**Fig. A21.** DEPT 135 NMR spectrum of 6-(benzyloxy)hexan-1-ol.

6-(benzyloxy)hexan-1-ol, HSQC, CDCl<sub>3</sub>

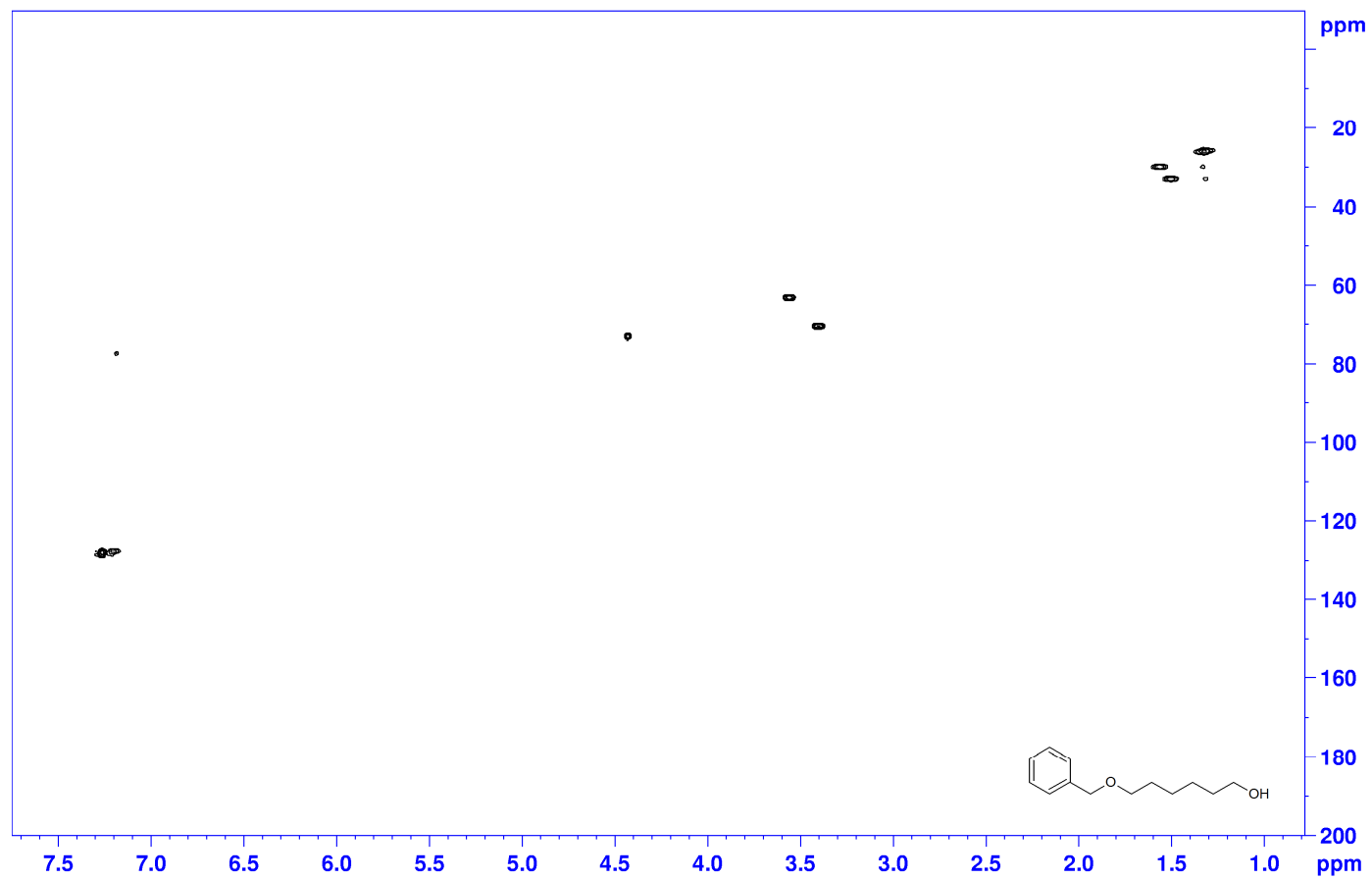


**Fig. A22.** HSQC NMR spectrum of 6-(benzyloxy)hexan-1-ol.

6-(benzyloxy)hexan-1-ol, HMBC, CDCl<sub>3</sub>

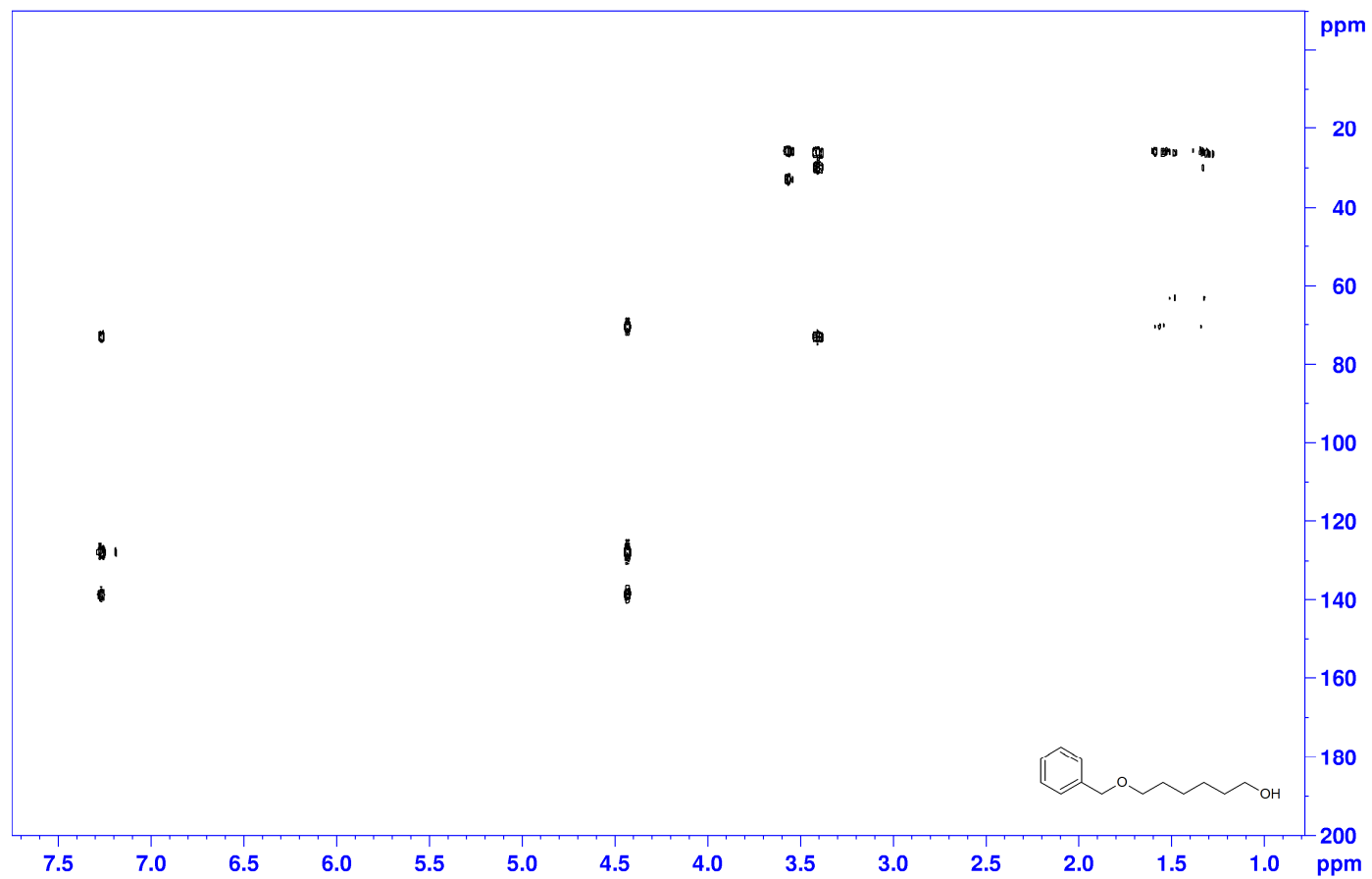


**Fig. A23.** HMBC NMR spectrum of 6-(benzyloxy)hexan-1-ol.

6-(benzyloxy)hexan-1-ol, COSY, CDCl<sub>3</sub>

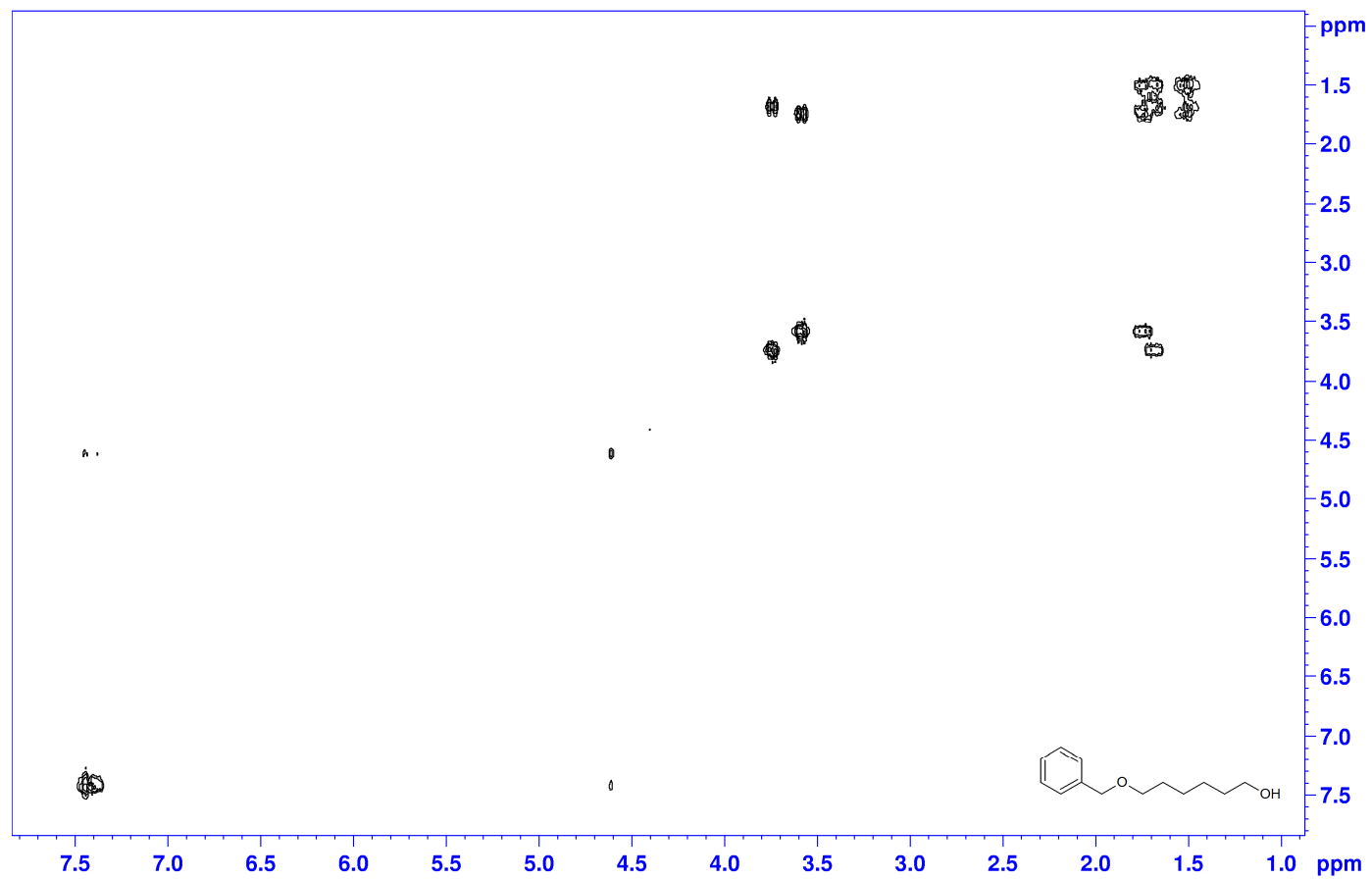
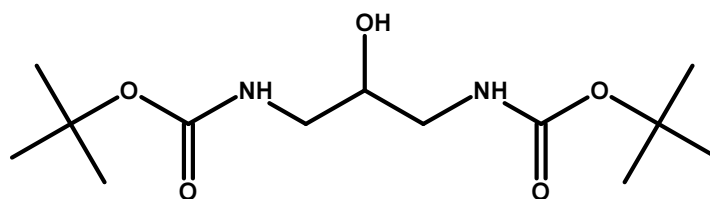


**Fig. A24.** COSY NMR spectrum of 6-(benzyloxy)hexan-1-ol.



**Procedure:** An equal mixture of acetonitrile : water (35 mL) in 250 mL RBF was chilled to 4 °C in an ice bath; NaHCO<sub>3</sub> (5.04 g, 60.0 mmol) added. In a separate vessel 1,3-diamino-2-propanol ( 1.26 g: 14.0 mmol) and di-tert-butyl-carbonate (26.9 mmol, 5.86 g) dissolved in an equal mixture of acetonitrile : water (35 mL). This mixture was added drop wise to the contents of the RBF and stirred on ice for 2 hours and overnight at RT. The acetonitrile was removed under reduced pressure and the remaining aqueous layer extracted with CH<sub>2</sub>Cl<sub>2</sub> (3x40 mL). The organic fraction were combined, dried over magnesium sulphate and concentrated under reduced pressure; resulting oil re-crystallised from diethyl ether : hexane.

**Di-tert-butyl (2-hydroxypropane-1,3-diyl)biscarbamate**

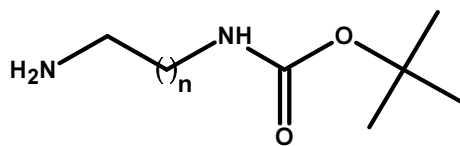
**Yield:** 3.19g, 10.9 mmol (78 %)

<sup>1</sup>H NMR (400 MHz, CDCl<sub>3</sub>, δ/ ppm): 1.44 (s, 18H, -C(CH<sub>3</sub>)<sub>3</sub>), 2.58 (s, 1H, OH), 3.13-3.27 (m, 4H, -CH<sub>2</sub>CH(OH)-) 3.76-3.71 (m, 1H, -CH(OH)-), 5.07(s, 2H, -HN-)

<sup>13</sup>C NMR (100 MHz, CDCl<sub>3</sub>, δ/ ppm): 28.3, 43.8, 71.3, 79.9, 157.3.

**Fig. A25. Synthetic procedure for di-tert-butyl (2-hydroxypropane-1,3-diyl)biscarbamate.**





$n = 1, 2$

**Generic procedure:** An alkanediamine (54 mmol) was added to a RBF and dissolved in  $\text{CH}_2\text{Cl}_2$  (17 mL). Di-tert-butyl-carbonate (9.0 mmol, 2.06 mL) dissolved in 120 mL  $\text{CHCl}_3$  and added drop wise with stirring to the contents of the RBF on ice. The mixture was stirred for 24 hours at RT and then concentrated under reduced pressure. Residual oil/solid dissolved in aqueous  $\text{CaCO}_3$  (2 M), (100 mL) and extracted with  $\text{CH}_2\text{Cl}_2$  (2x100 mL). The organic fractions combined, dried over  $\text{MgSO}_4$  and concentrated under reduce pressure. The product appears as pale yellow liquid.

**tert-Butyl (2-aminoethyl)carbamate, (n = 1)**

**Yeild:** 1.40g, 8.8 mmol (97 %), Pale yellow liquid.

$^1\text{H NMR}$  (400MHz,  $\text{CDCl}_3$ ,  $\delta$ / ppm): 1.40 (s, 9H, -  $\text{C}(\text{CH}_3)_3$ ), 2.25 (s, 2H,  $\text{H}_2\text{N}$ -), 2.78 (t, 2H,  $\text{H}_2\text{NCH}_2$ -), 3.12-3.17 (m, 2H,  $-\text{CH}_2\text{NH}$ -), 5.11 (s, 1H,  $-\text{NH}$ -).

$^{13}\text{C NMR}$  (100 MHz,  $\text{CDCl}_3$ ,  $\delta$ / ppm): 28.32, 41.61, 42.99, 79.15, 156.22.

**tert-Butyl (3-aminopropyl)carbamate, (n =2)**

**Yield:** 1.44 g, 8.3 mmol (92 %)

$^1\text{H NMR}$  (400MHz,  $\text{CDCl}_3$ ,  $\delta$ / ppm): 1.41 (s, 9H,  $-\text{C}(\text{CH}_3)_3$ ), 1.70 (s, 2H,  $\text{H}_2\text{N}$ -), 1.59-1.65 (q, 2H,  $-\text{CH}_2\text{CH}_2\text{CH}_2-$ ), 2.75-2.79 (t, 2H,  $\text{H}_2\text{NCH}_2-$ ) 3.17-3.23 (q, 2H,  $-\text{CH}_2\text{NH}$ -), 4.88 (s,  $-\text{NH}$ -).

$^{13}\text{C NMR}$  ( $\text{CDCl}_3, \delta$ ): 28.41, 33.23, 39.60, 79.12, 156.18, Unknown.

**Fig. A26.** Synthetic procedure for two tert-Butyl (n-aminoalkyl)carbamates.

### 1,3-diaphthalimido-2-bromopropane (Attempt-3) CBr4/PPh3

20 Aug 2008

<b>File Name</b>	F:\NASEEM PROJECTS\IR DATA\BR-DIAPHTHALIMIDE CBR4 ATTEMPT3 FROM ET-OH.SP		<b>Date Stamp</b>	tue aug 19 12:59:23 2008	
<b>Date</b>	Tue Aug 19 13:00:51 2008		<b>Technique</b>	Infrared	
<b>Spectral Region</b>	IR	<b>X Axis</b>	Wavenumber (cm-1)	<b>Instrument</b>	Spectrum One
<b>Points Count</b>	3551	<b>Data Spacing</b>	1.0000	<b>Spectrum Range</b>	450.0000 - 4000.0000

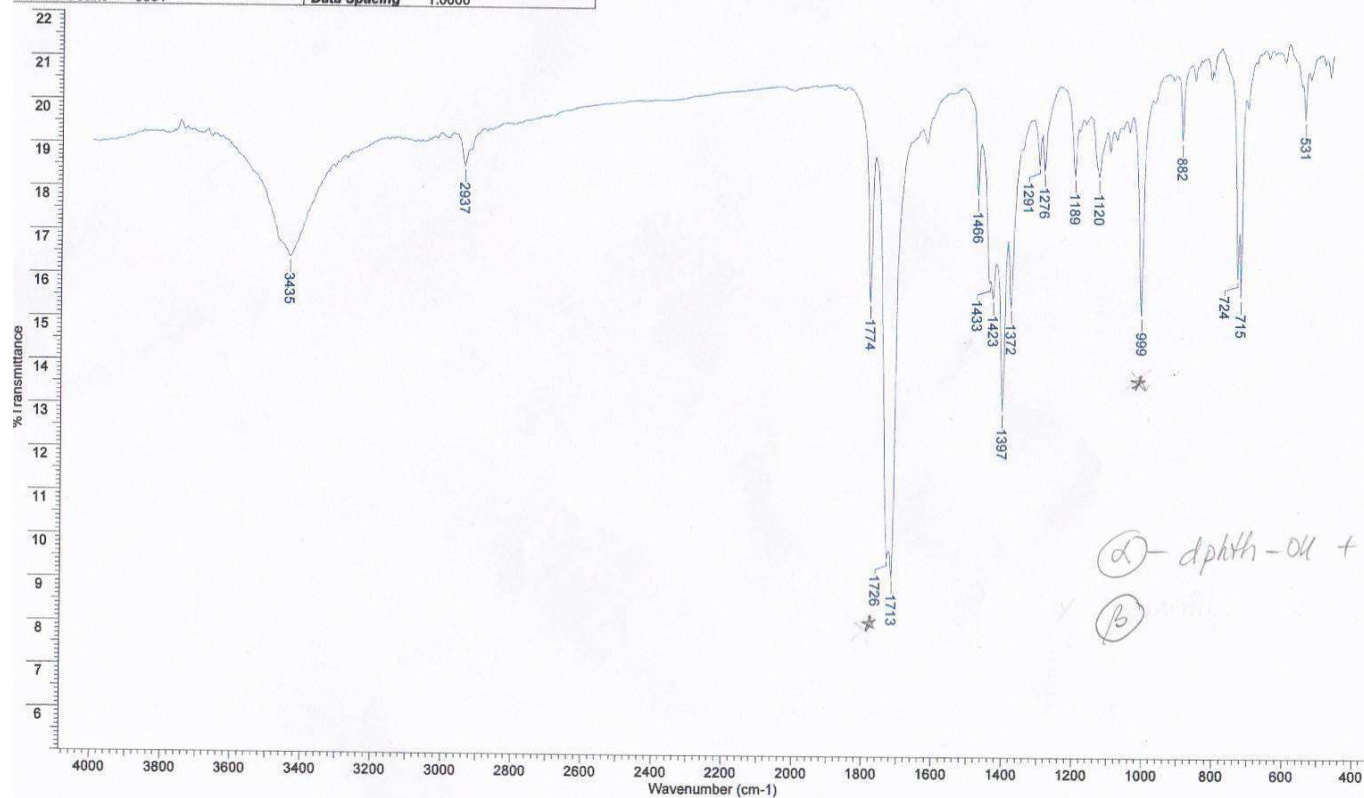


**Fig. A27.** Representative IR spectrum of 2,2'-(2-bromopropane-1,3-diyl)bis(1*H*-isoindole-1,3(2*H*)-dione).

2,2'-(2-bromopropane-1,3-diyl)bis(1*H*-isoindole-1,3(2*H*)-dione), 1*H*, DMSO-*d*<sub>6</sub>

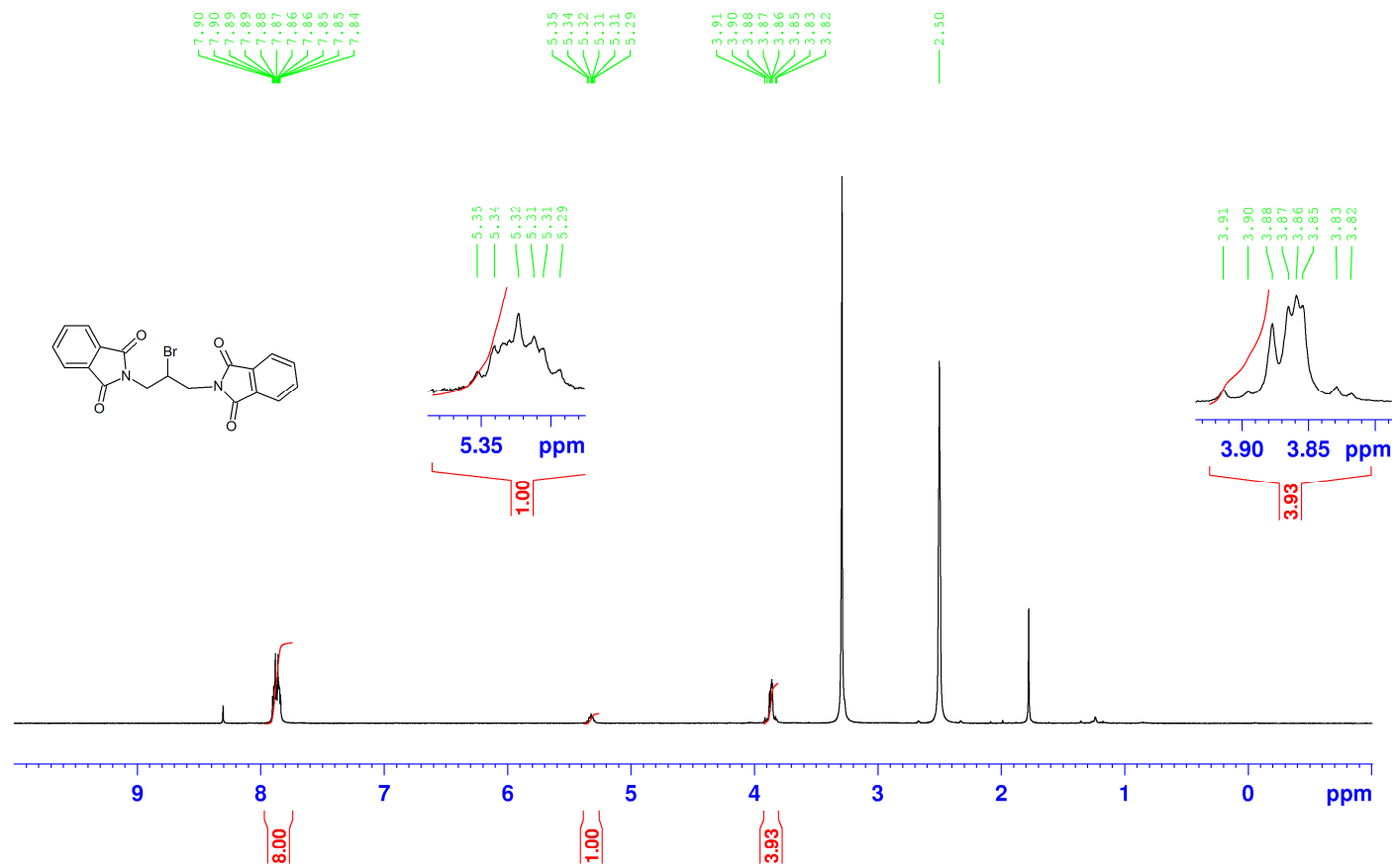


**Fig. A28.** <sup>1</sup>H NMR spectrum of 2,2'-(2-bromopropane-1,3-diyl)bis(1*H*-isoindole-1,3(2*H*)-dione).

2,2'-(2-bromopropane-1,3-diyl)bis(1H-isocindole-1,3(2H)-dione), <sup>13</sup>C, DMSO-d<sub>6</sub>

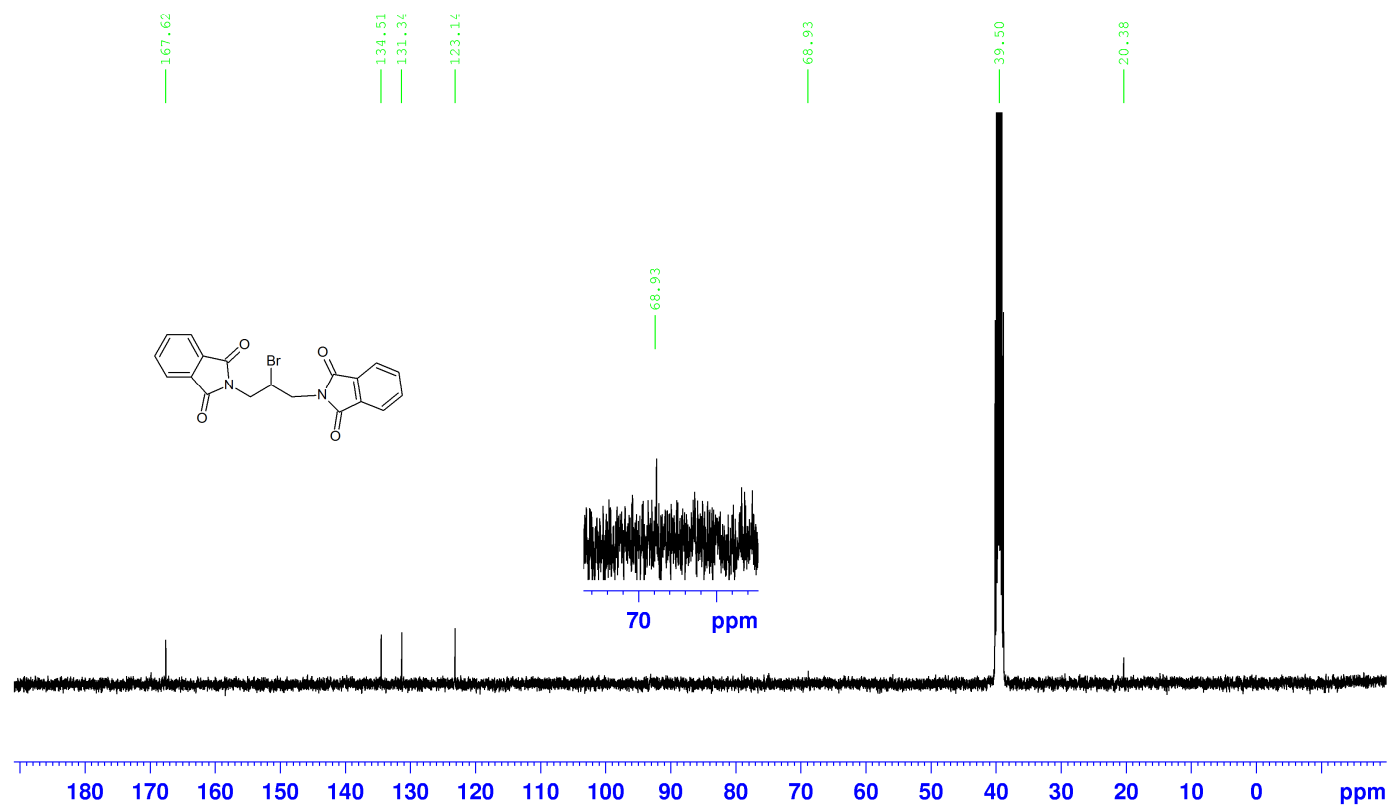


**Fig. A29.** <sup>13</sup>C NMR spectrum of 2,2'-(2-bromopropane-1,3-diyl)bis(1H-isocindole-1,3(2H)-dione).

2,2'-(2-bromopropane-1,3-diyl)bis(1*H*-isoindole-1,3(2*H*)-dione), DEPT 135, DMSO-d<sub>6</sub>

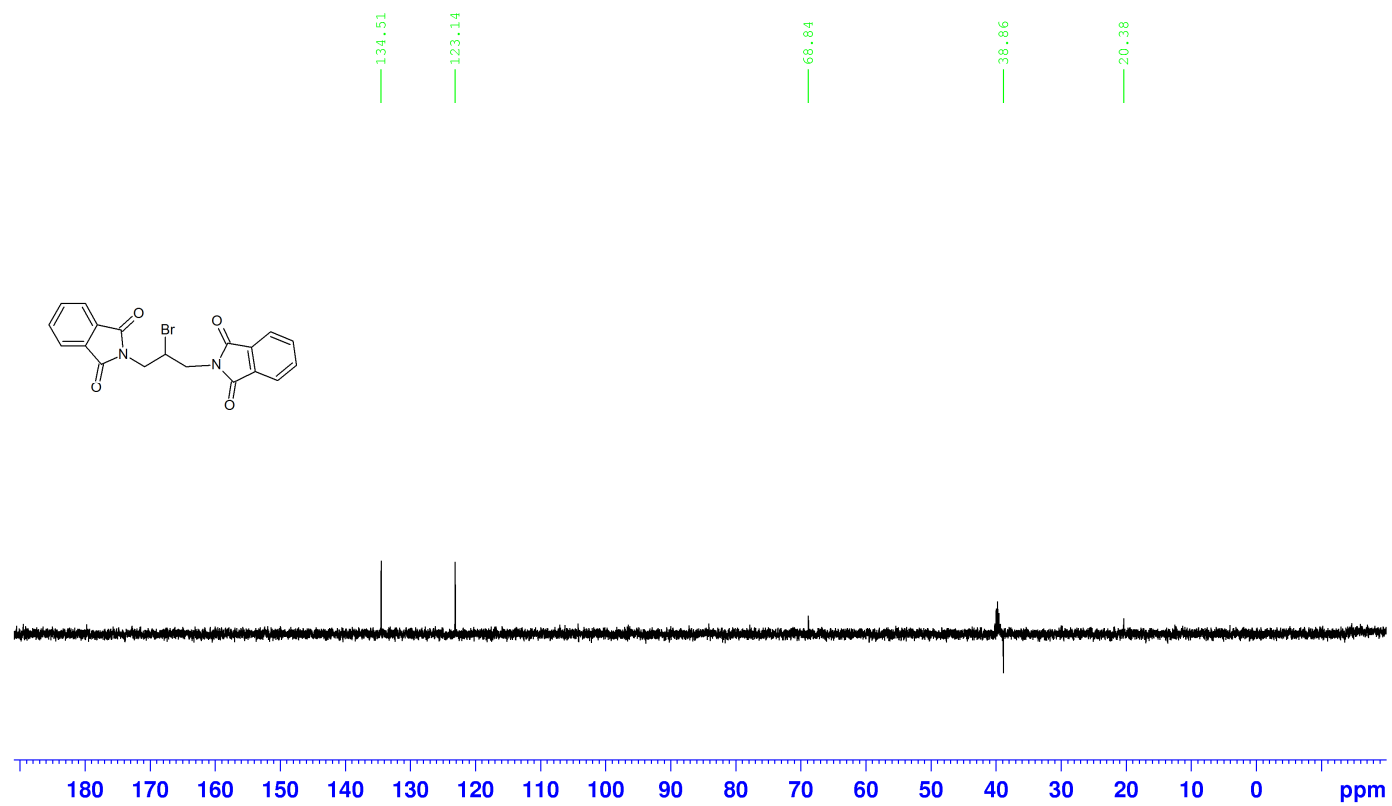


**Fig. A30.** DEPT 135 NMR spectrum of 2,2'-(2-bromopropane-1,3-diyl)bis(1*H*-isoindole-1,3(2*H*)-dione).

2,2'-(2-bromopropane-1,3-diyl)bis(1H-isindole-1,3(2H)-dione), HSQC, DMSO-d6

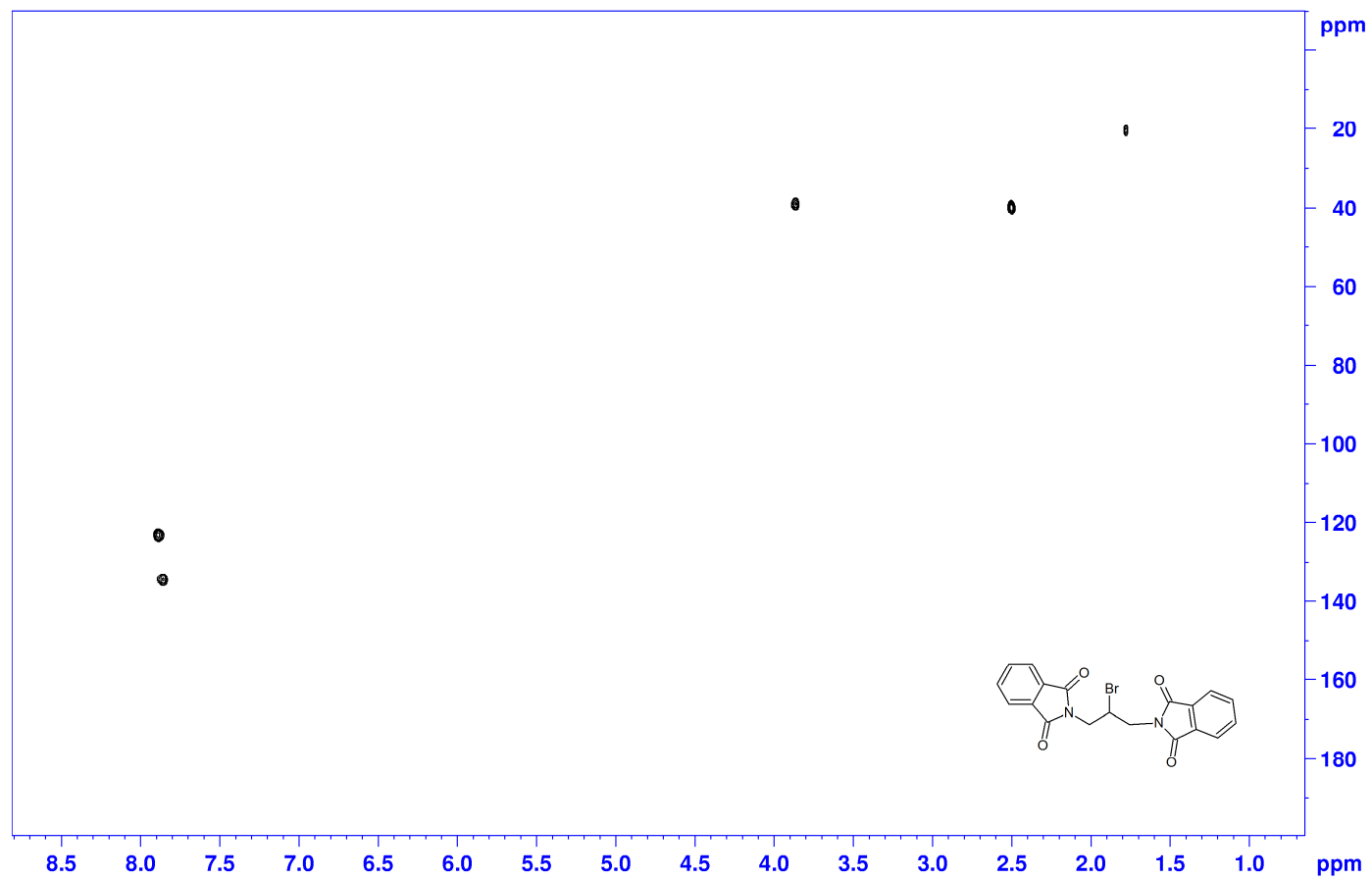


**Fig. A31.** HSQC NMR spectrum of 2,2'-(2-bromopropane-1,3-diyl)bis(1H-isindole-1,3(2H)-dione).

2,2'-(2-bromopropane-1,3-diyl)bis(1H-isindole-1,3(2H)-dione), COSY, DMSO-d6

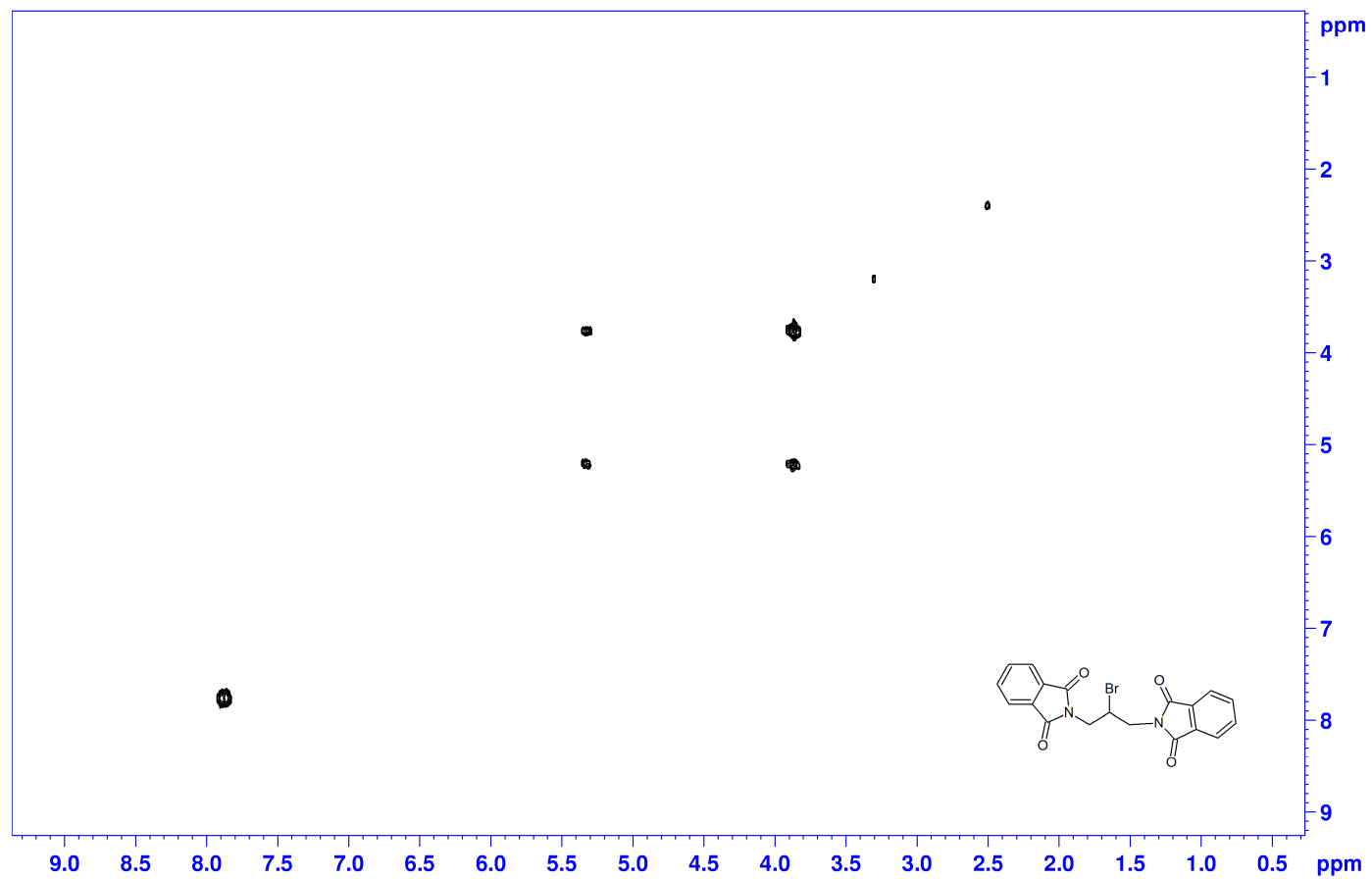


**Fig. 32.** COSY NMR spectrum of 2,2'-(2-bromopropane-1,3-diyl)bis(1H-isindole-1,3(2H)-dione).

[(2-bromoethoxy)methyl]benzene, 1H, CDCl3

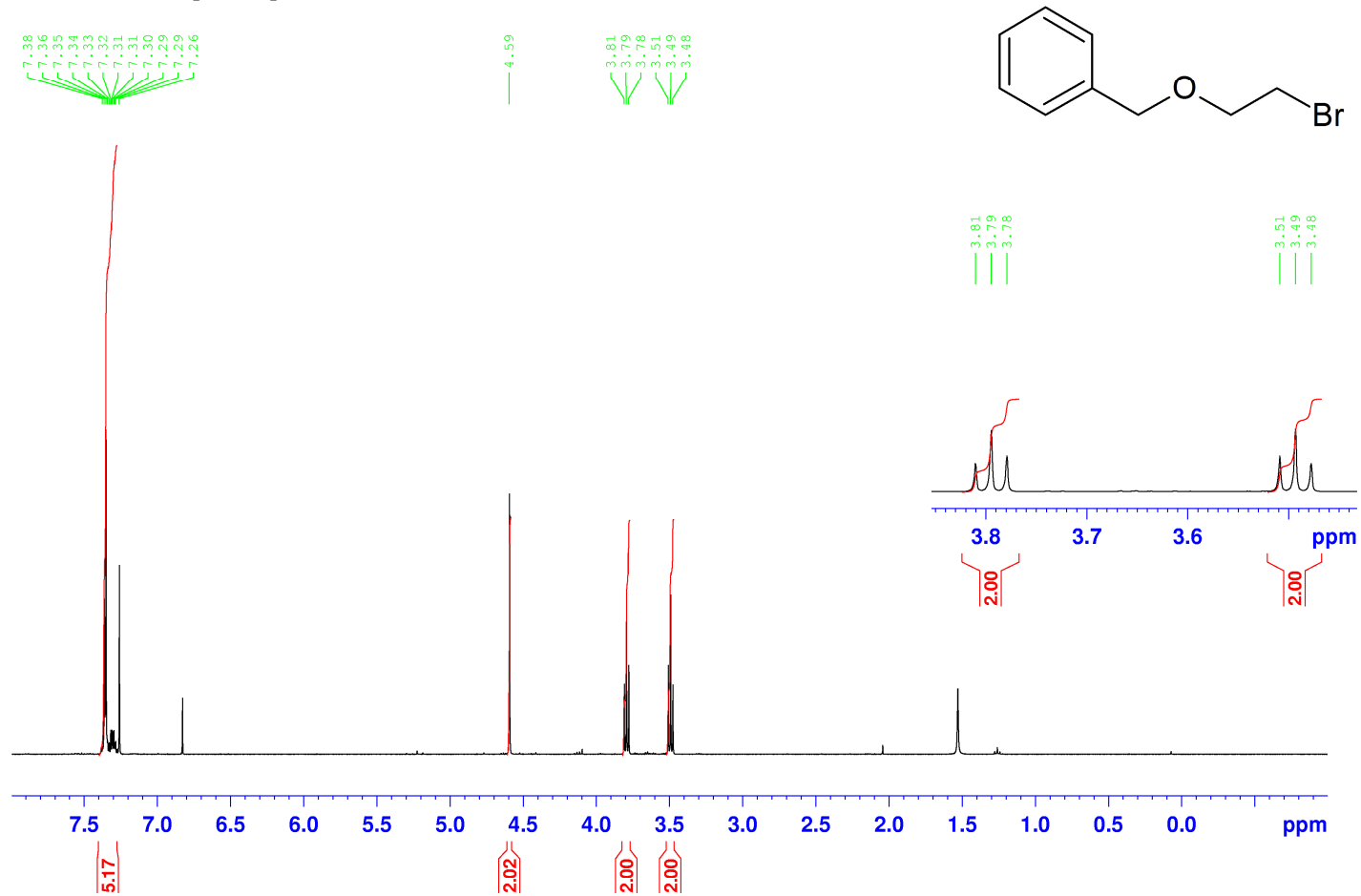
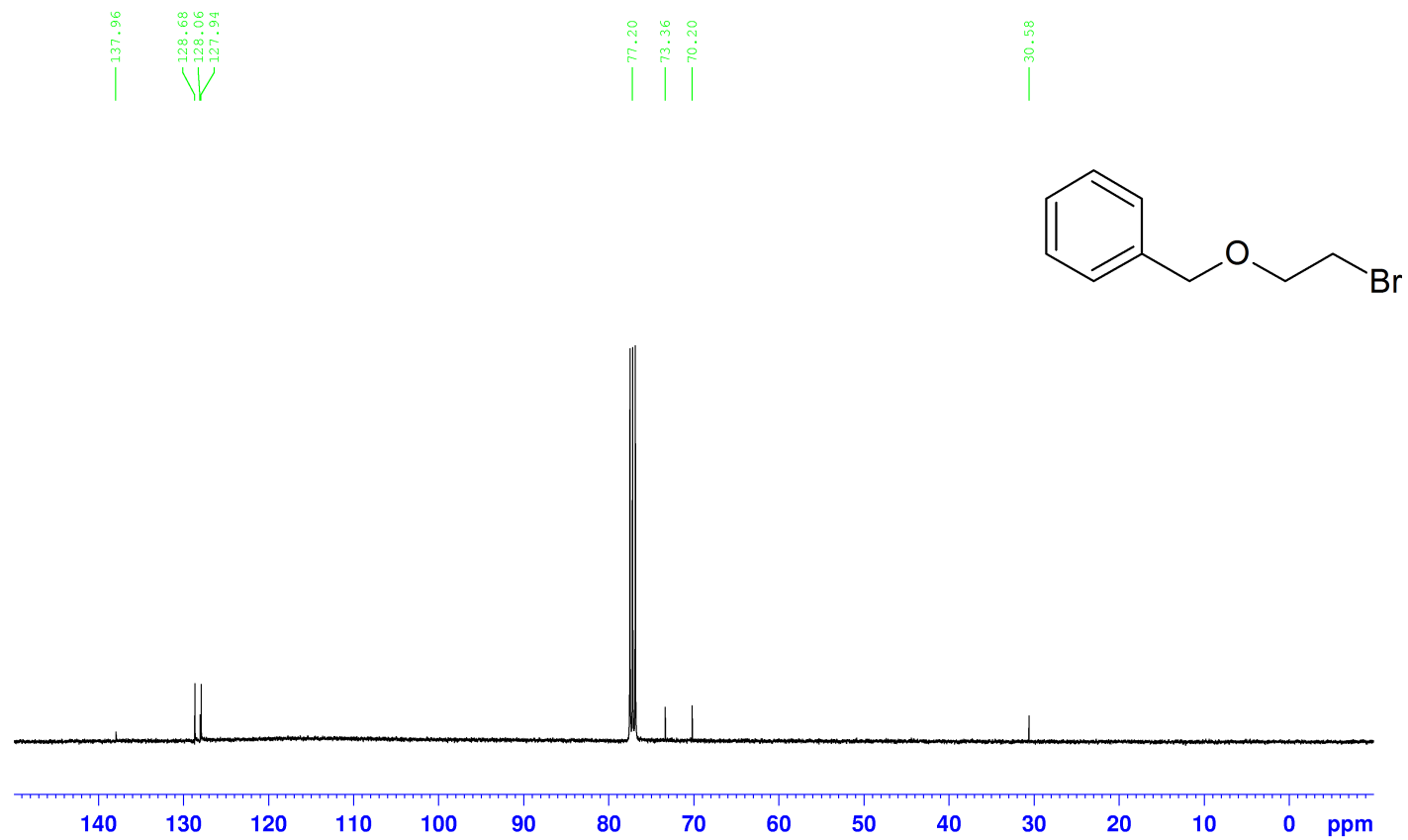


Fig. A33.  $^1\text{H}$  NMR spectrum of [(2-bromoethoxy)methyl]benzene.



[(2-bromoethoxy)methyl]benzene,  $^{13}\text{C}$ ,  $\text{CDCl}_3$



**Fig. A34.**  $^{13}\text{C}$  NMR spectrum of [(2-bromoethoxy)methyl]benzene.

[(2-bromoethoxy)methyl]benzene, DEPT 135, CDCl<sub>3</sub>

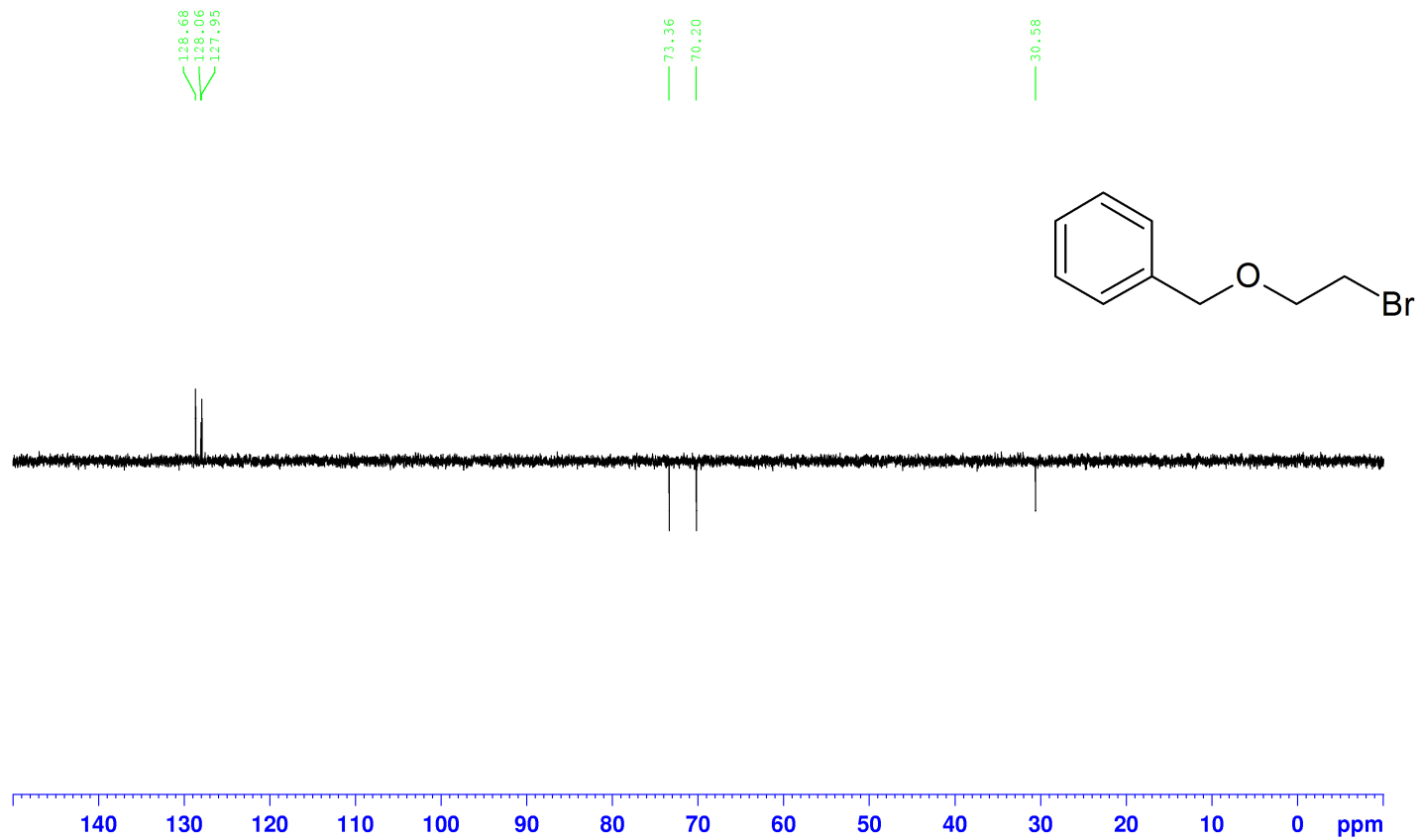
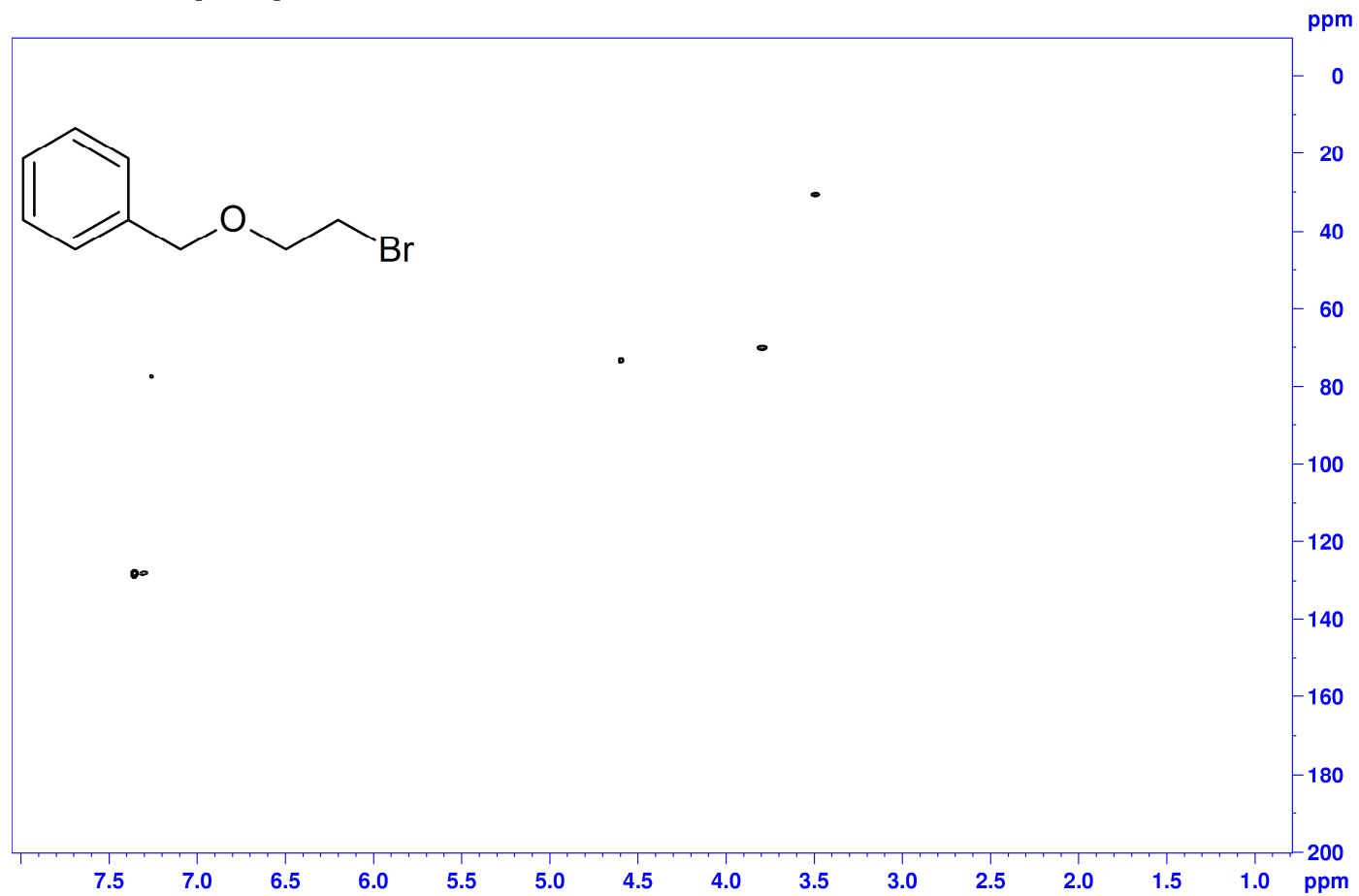


Fig. A35. DEPT 135 NMR spectrum of [(2-bromoethoxy)methyl]benzene.

[(2-bromoethoxy)methyl]benzene, HSQC, CDCl<sub>3</sub>



**Fig. A36** . HSQC NMR spectrum of [(2-bromoethoxy)methyl]benzene.

[(2-bromoethoxy)methyl]benzene, HMBC, CDCl<sub>3</sub>

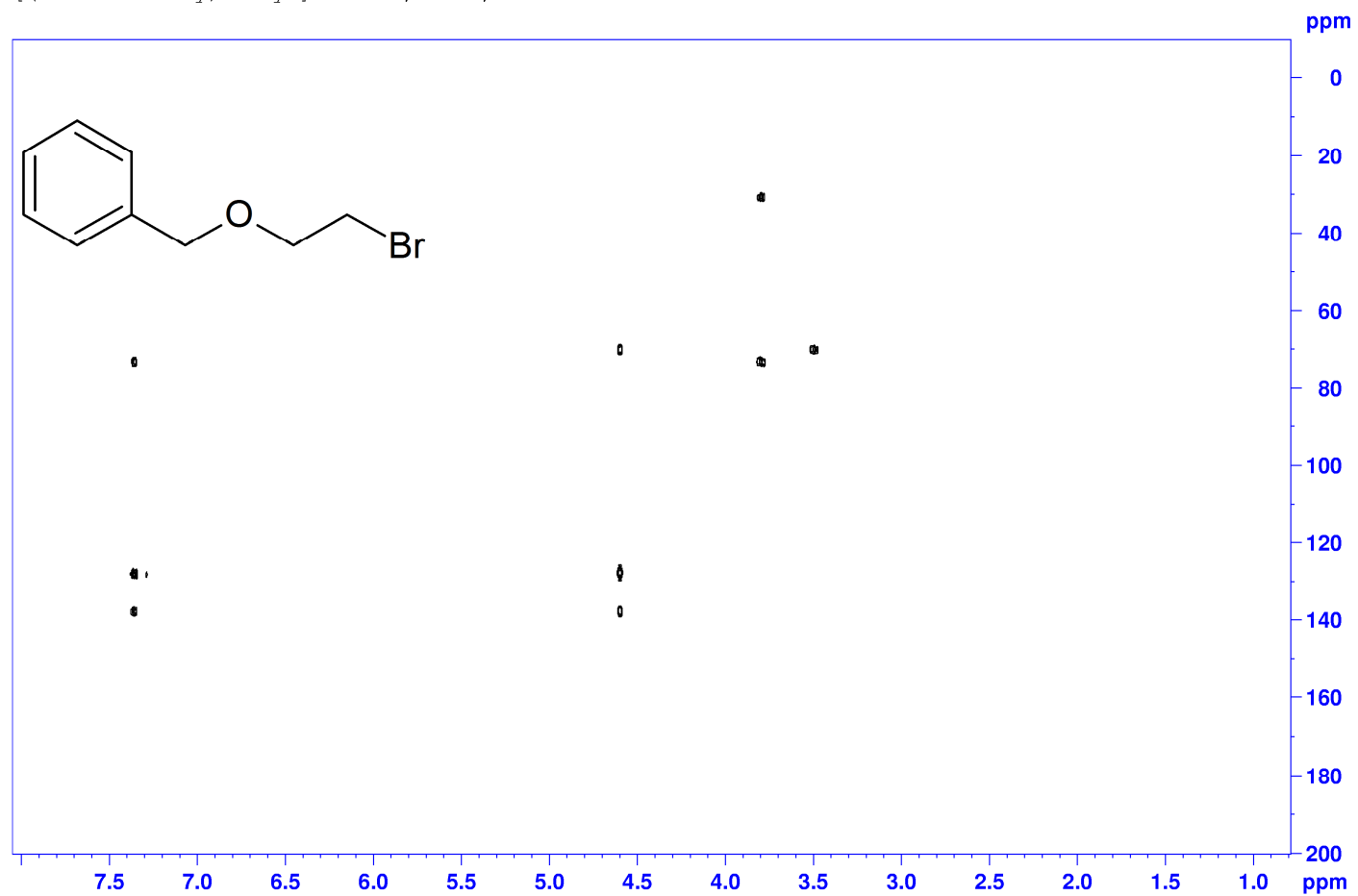


**Fig. A37.** HMBC NMR spectrum of [(2-bromoethoxy)methyl]benzene.

[(2-bromoethoxy)methyl]benzene, COSY, CDCl<sub>3</sub>

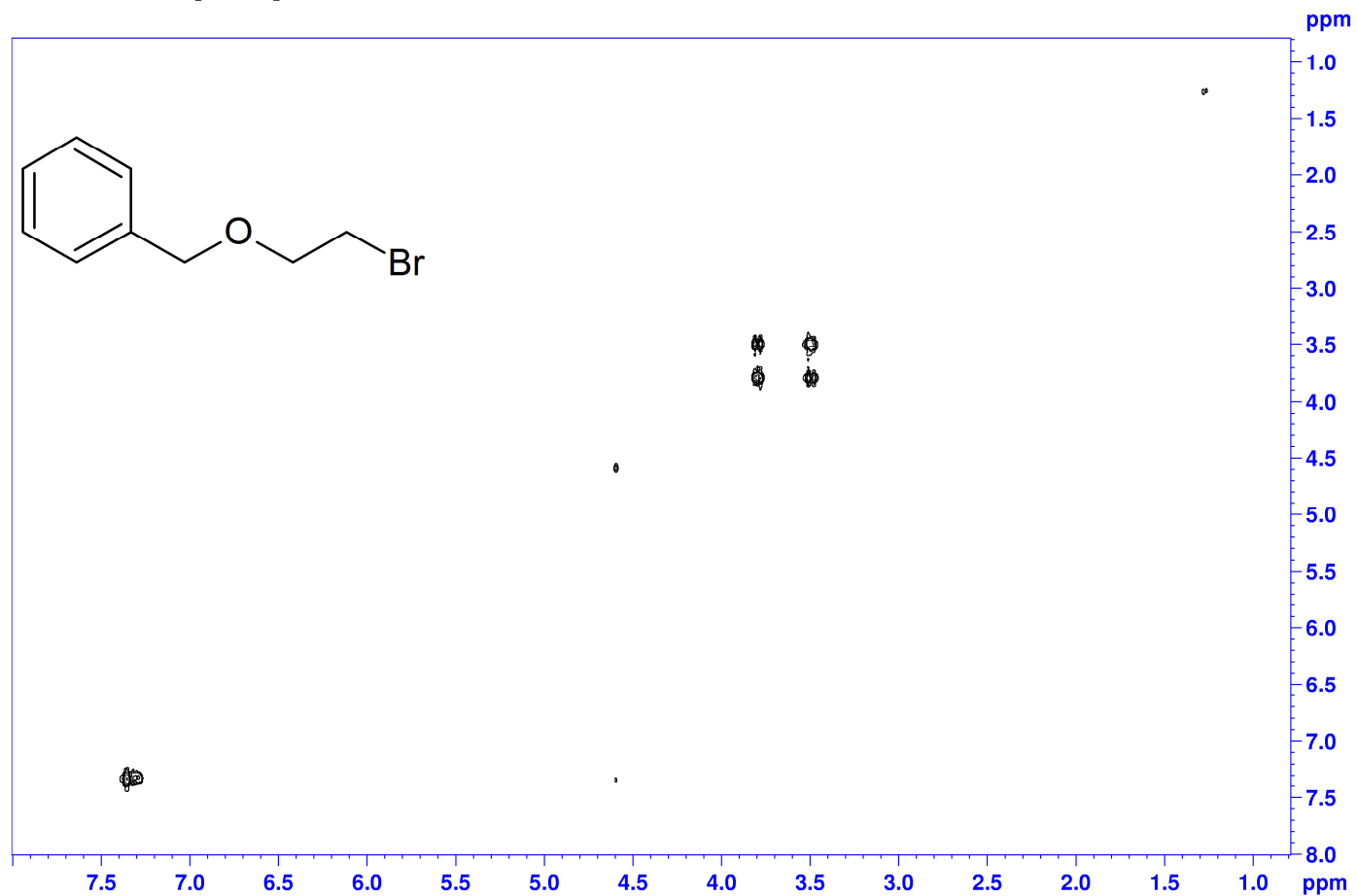


**Fig. A38.** COSY NMR spectrum of [(2-bromoethoxy)methyl]benzene.

[(3-bromopropoxy)methyl]benzene,  $^1\text{H}$ ,  $\text{CDCl}_3$

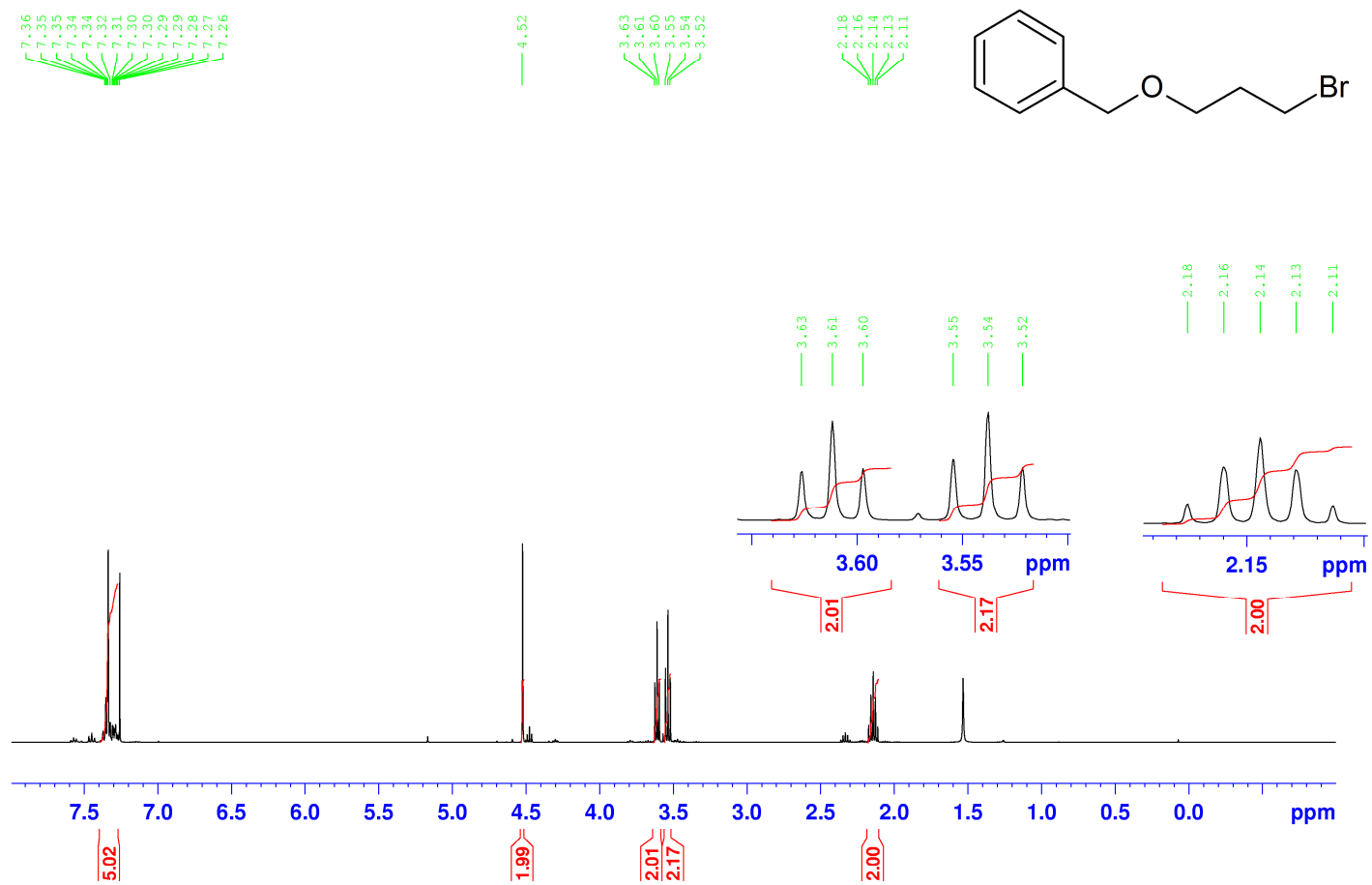
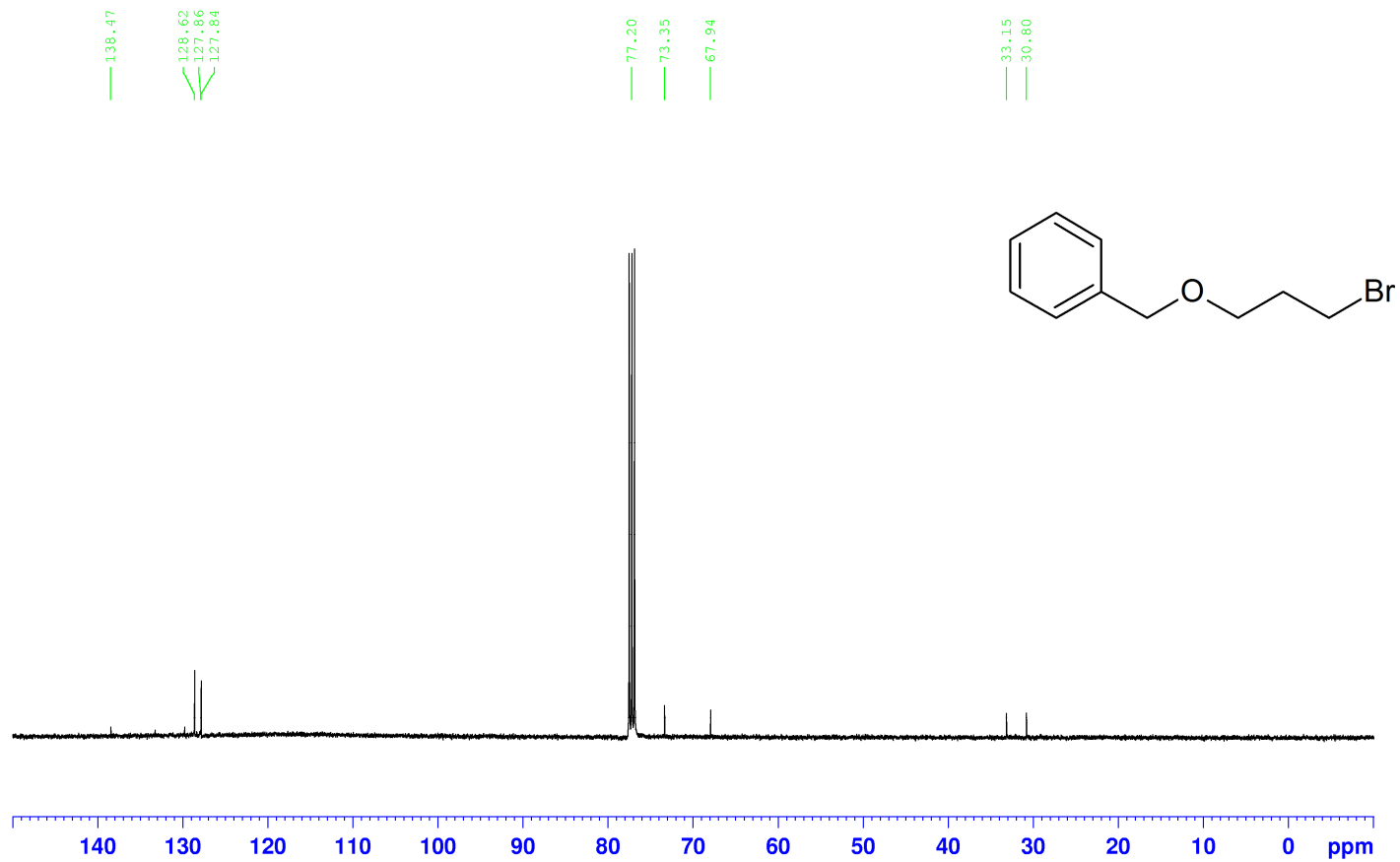


Fig. A39.  $^1\text{H}$  NMR spectrum of [(3-bromopropoxy)methyl]benzene.

[(3-bromopropoxy)methyl]benzene,  $^{13}\text{C}$ , CDC13



**Fig. A40.**  $^{13}\text{C}$  NMR spectrum of [(3-bromopropoxy)methyl]benzene.

[(3-bromopropoxy)methyl]benzene,  $^{13}\text{C}$ , DEPT 135

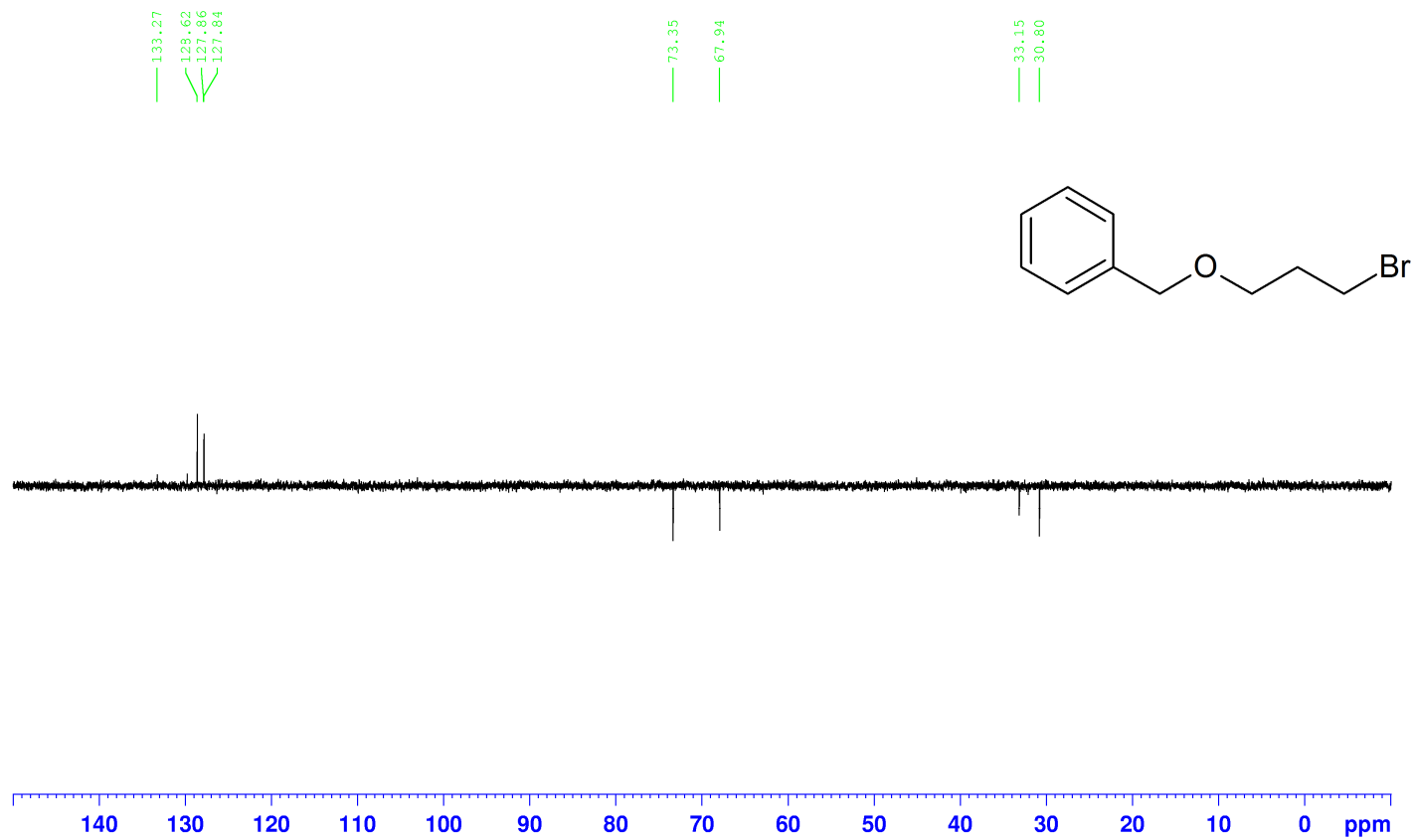


**Fig. A41.** DEPT 135 NMR spectrum of [(3-bromopropoxy)methyl]benzene.



[(3-bromopropoxy)methyl]benzene, HSQC, CDCl<sub>3</sub>

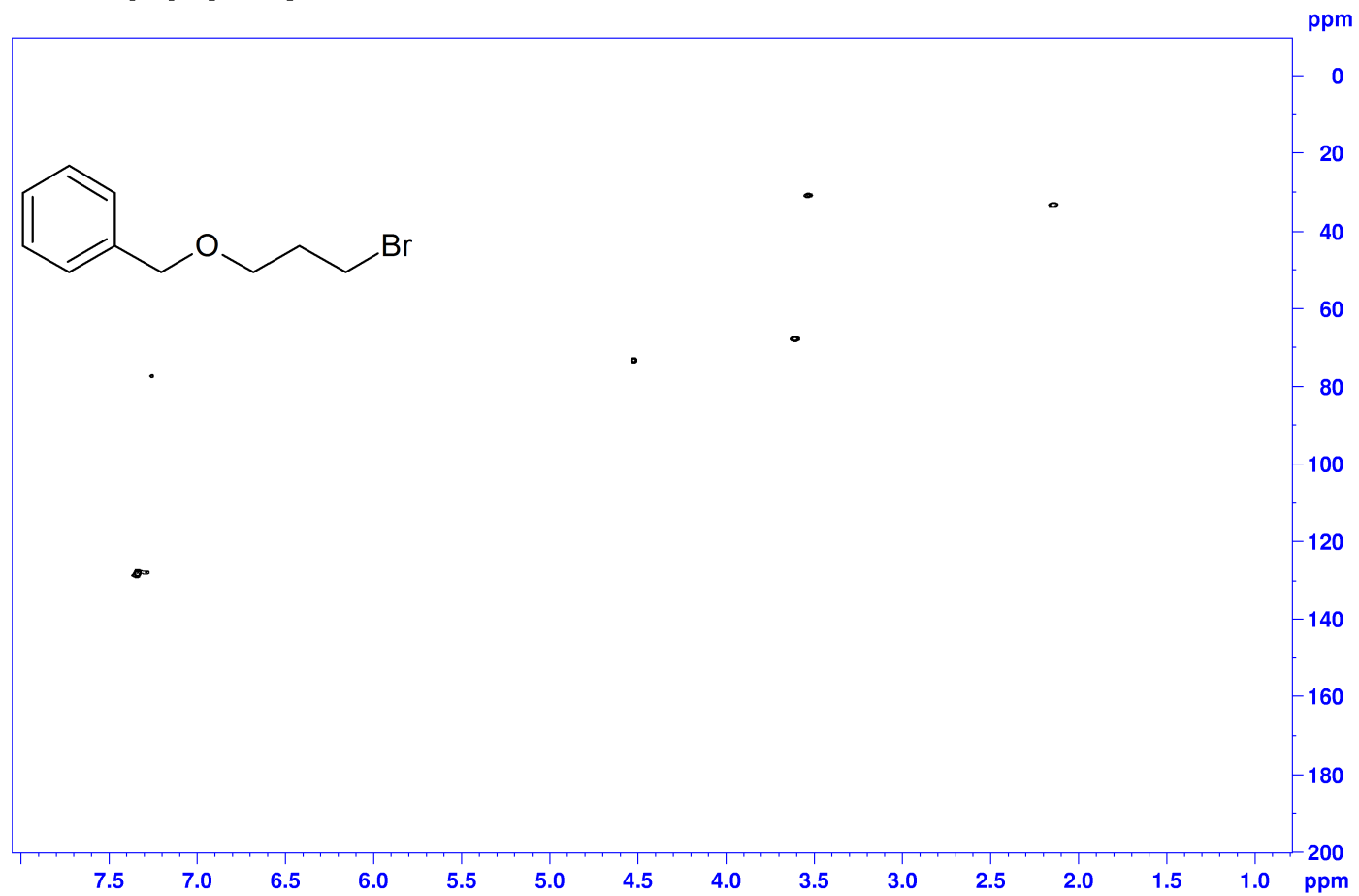


**Fig. A42.** HSQC NMR spectrum of [(3-bromopropoxy)methyl]benzene.

[(3-bromopropoxy)methyl]benzene, HMBC, CDCl<sub>3</sub>

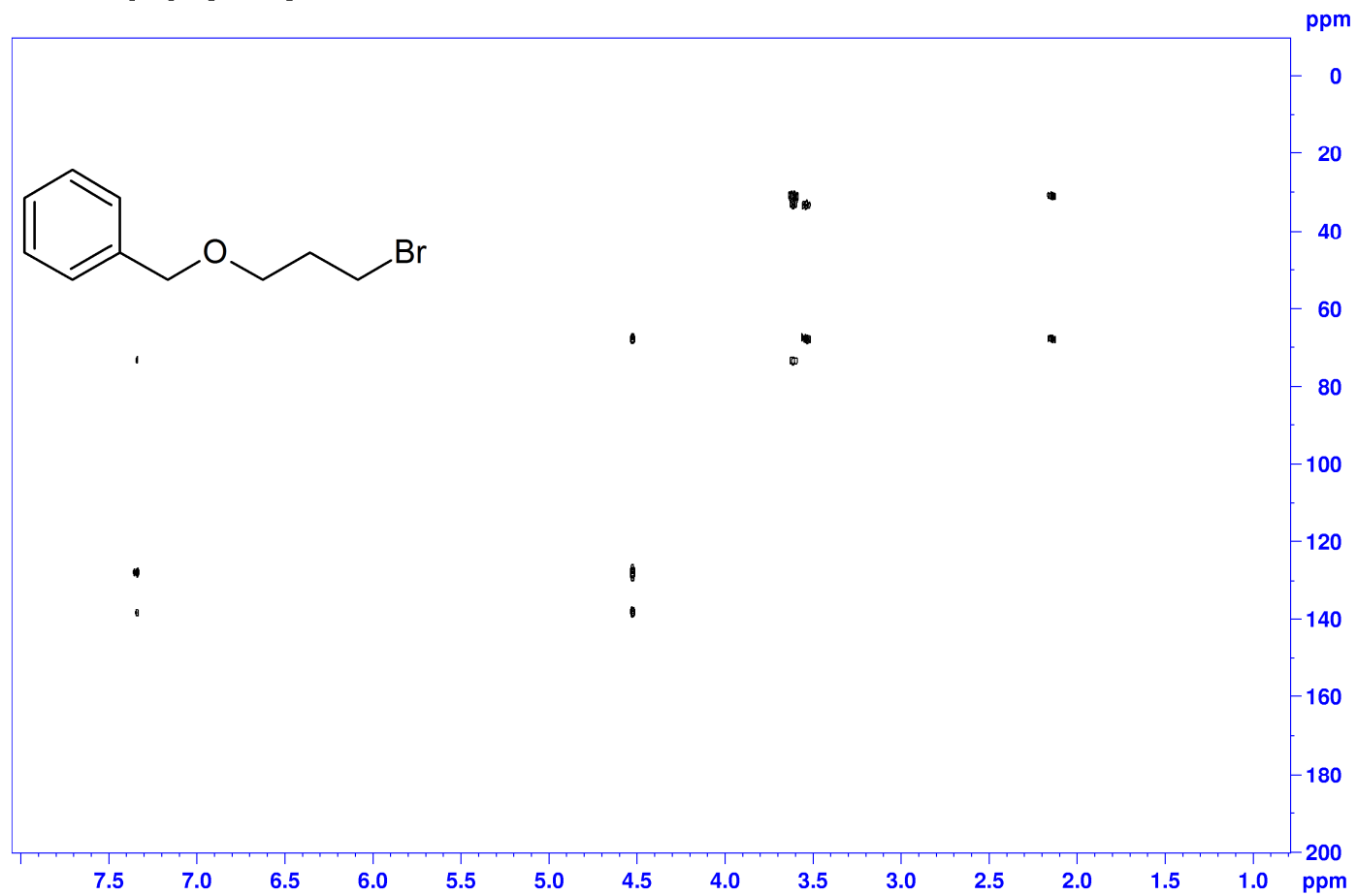


**Fig. A43.** COSY NMR spectrum of [(3-bromopropoxy)methyl]benzene.

{[(6-bromohexyl)oxy]methyl}benzene, 1H, CDCl3

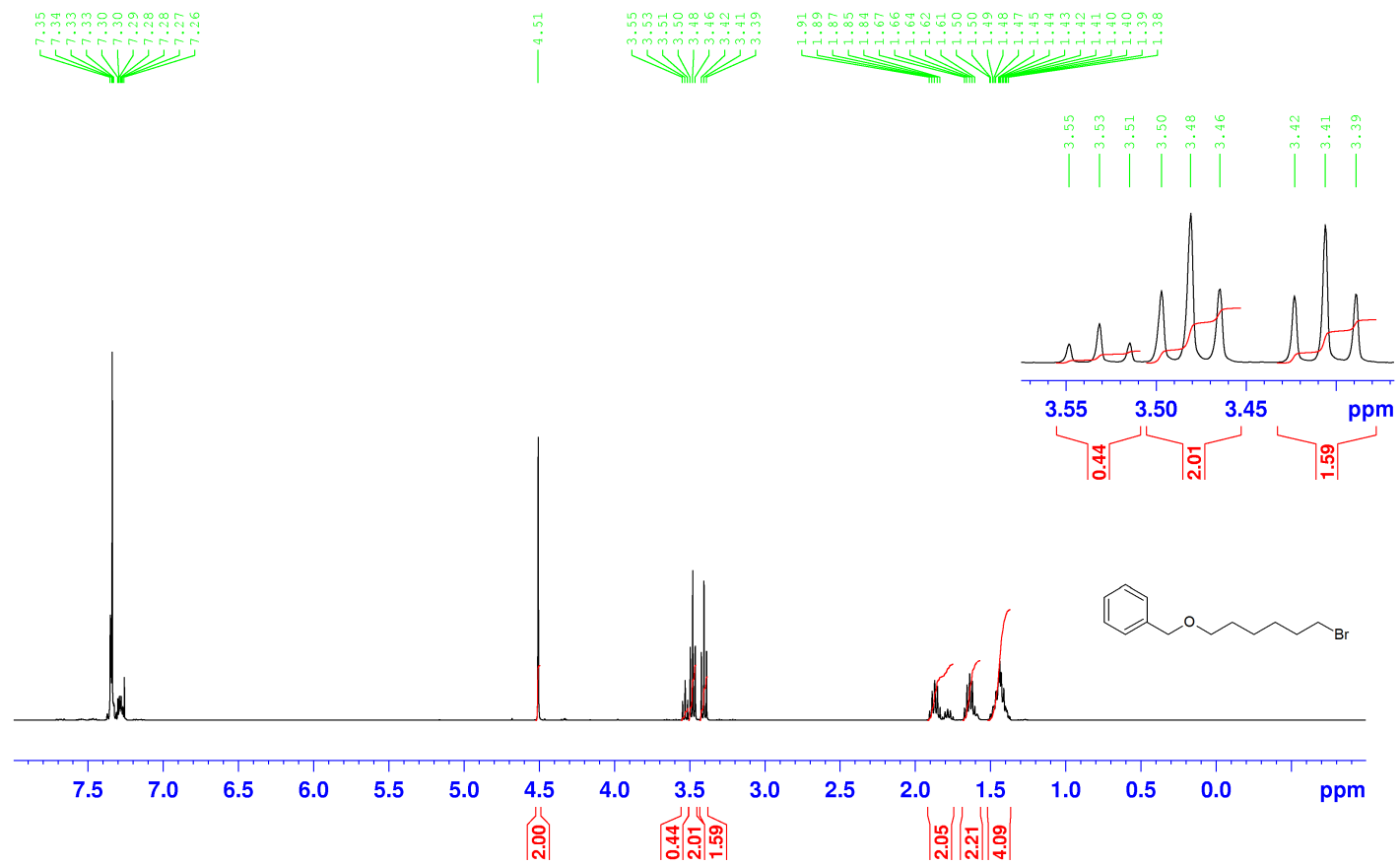
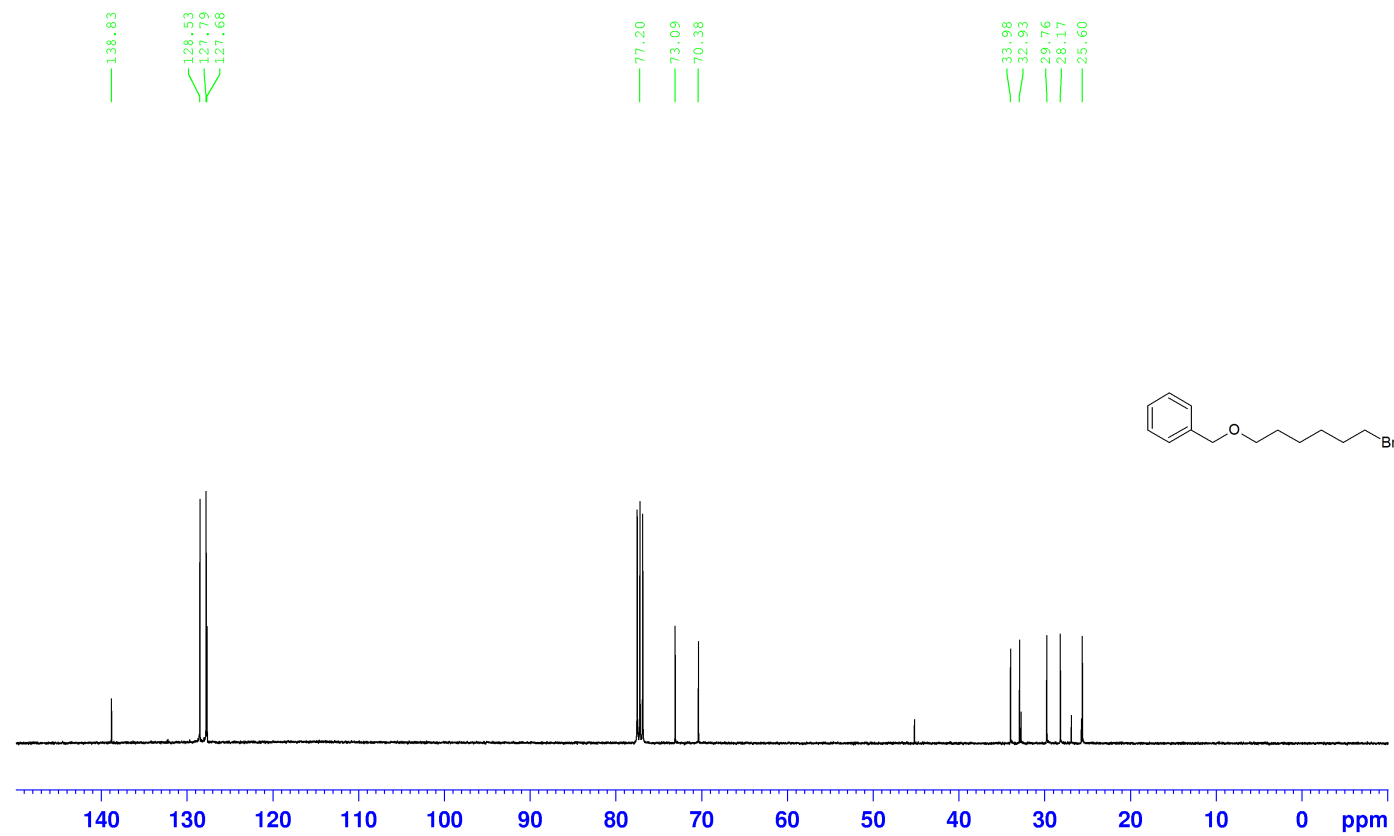


Fig. A44. <sup>1</sup>H NMR spectrum of. {[(6-bromohexyl)oxy]methyl}benzene.

{[(6-bromohexyl)oxy]methyl}benzene,  $^{13}\text{C}$ ,  $\text{CDCl}_3$



**Fig. A45.**  $^{13}\text{C}$  NMR spectrum of. {[(6-bromohexyl)oxy]methyl}benzene.

{[(6-bromohexyl)oxy]methyl}benzene, DEPT 135, CDCl<sub>3</sub>

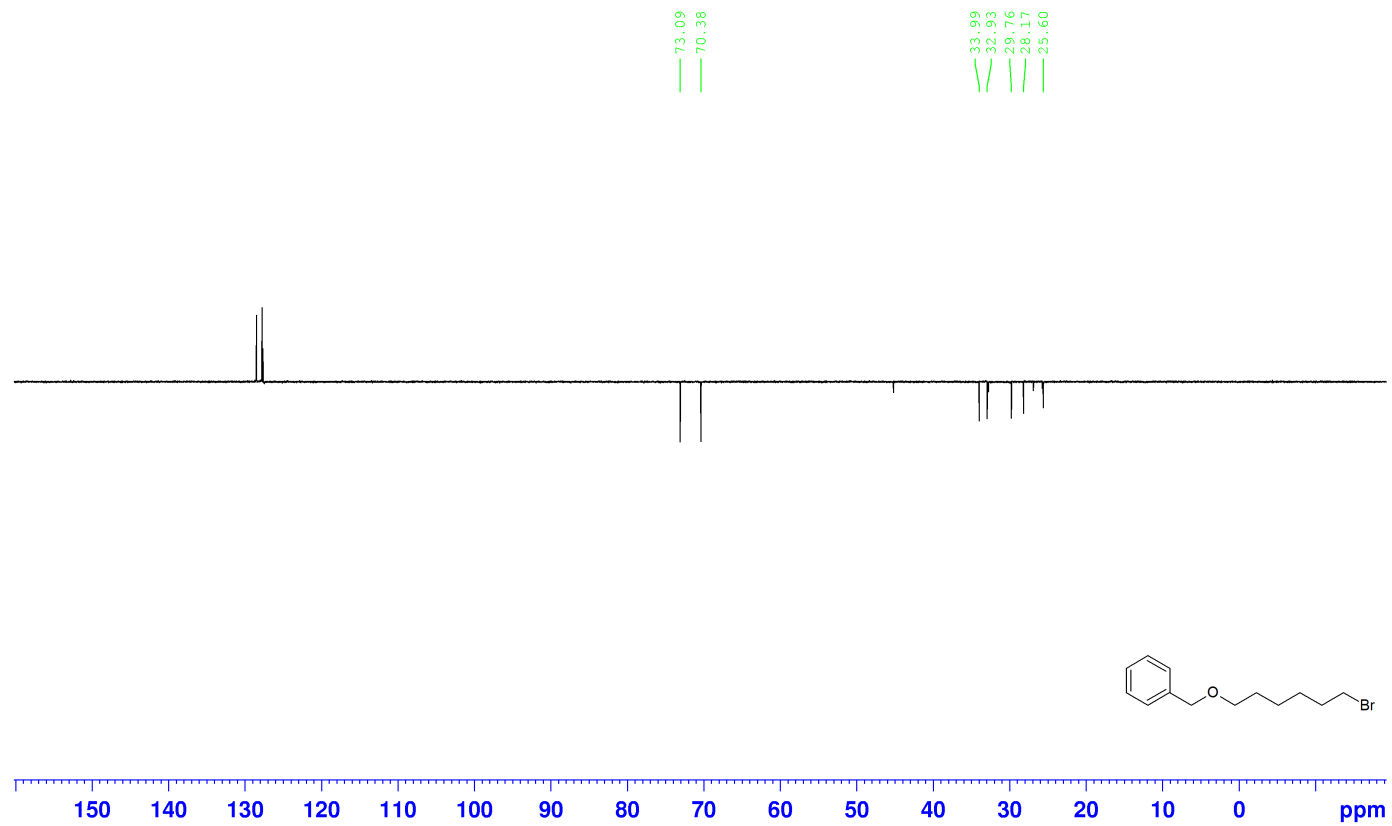


**Fig. A46.** DEPT 135 NMR spectrum of {[(6-bromohexyl)oxy]methyl}benzene.

{[(6-bromohexyl)oxy]methyl}benzene, HSQC, CDCl<sub>3</sub>

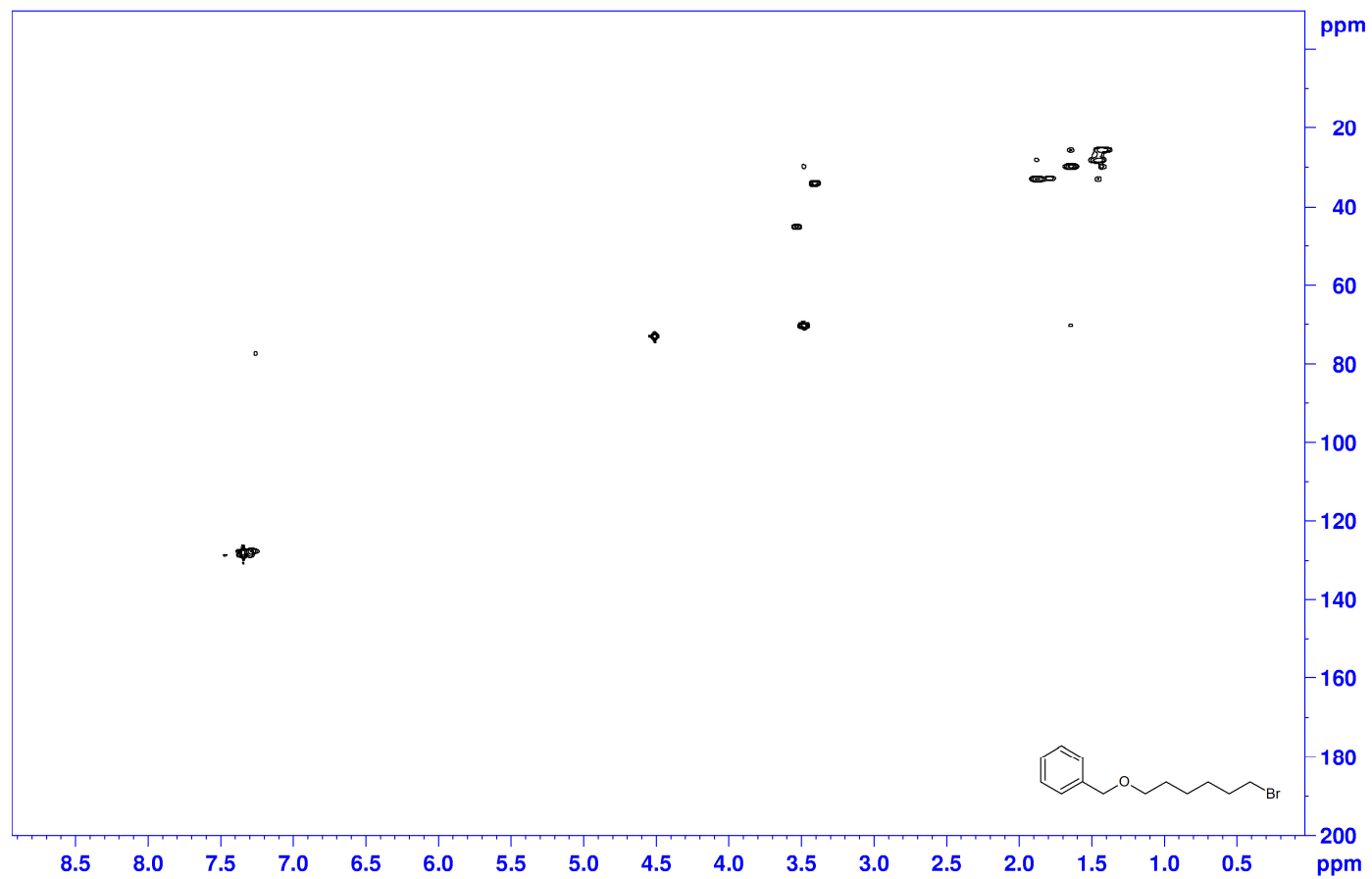


**Fig. A47.** HSQC NMR spectrum of. {[(6-bromohexyl)oxy]methyl}benzene.

{[(6-bromohexyl)oxy]methyl}benzene, HMBC, CDCl<sub>3</sub>

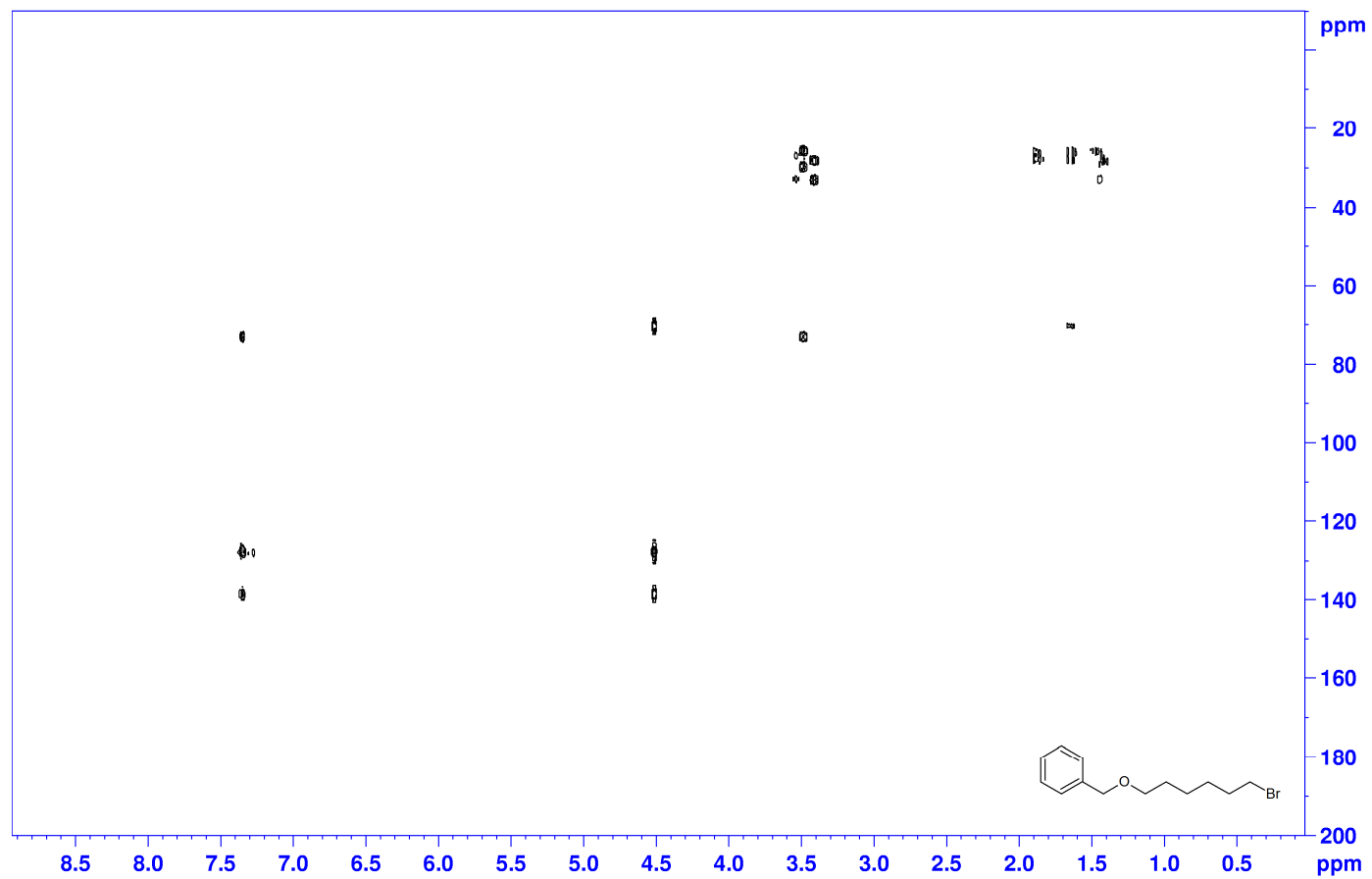


**Fig. A48.** HMBC NMR spectrum of. {[(6-bromohexyl)oxy]methyl}benzene.

{[(6-bromohexyl)oxy]methyl}benzene, COSY, CDC13

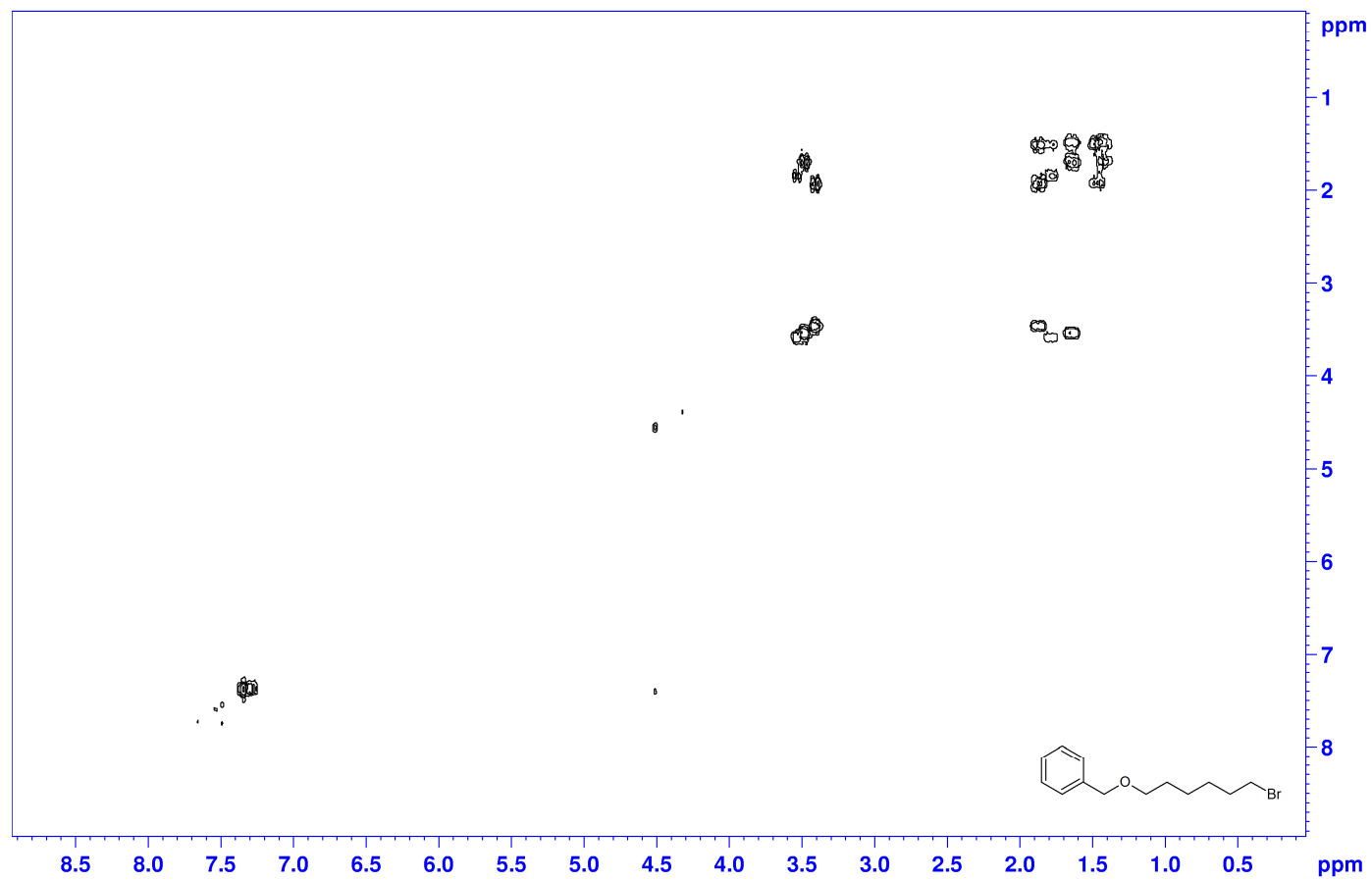


**Fig. A49.** NMR spectrum of. {[(6-bromohexyl)oxy]methyl}benzene.



[2-(benzyloxy)ethyl]propanedinitrile, <sup>1</sup>H, CDCl<sub>3</sub>

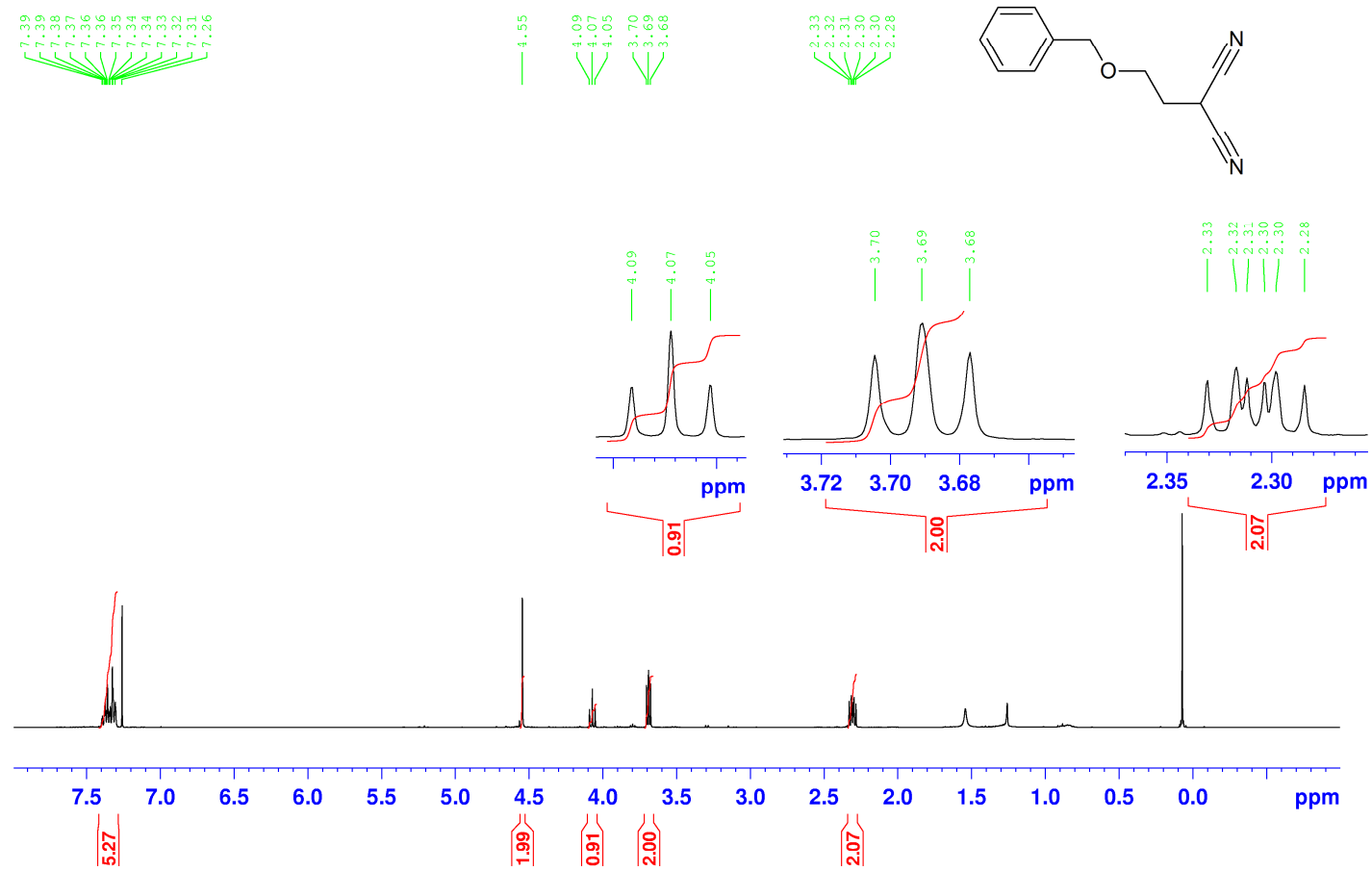
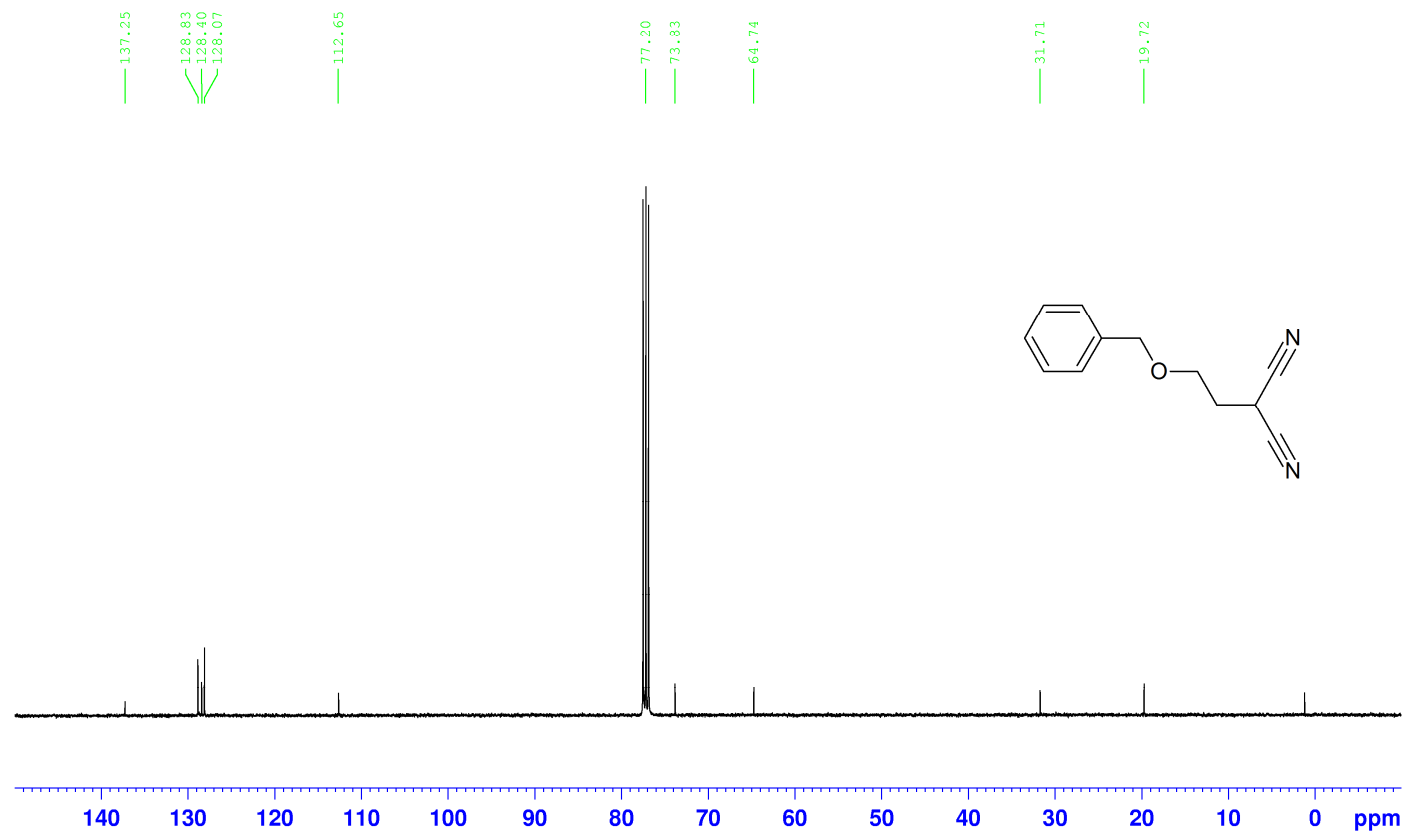


Fig. A50. <sup>1</sup>H NMR spectrum of [2-(benzyloxy)ethyl]propanedinitrile.

[2-(benzyloxy)ethyl]propanedinitrile,  $^{13}\text{C}$ ,  $\text{CDCl}_3$



**Fig. A51.**  $^{13}\text{C}$  NMR spectrum of [2-(benzyloxy)ethyl]propanedinitrile.

[2-(benzyloxy)ethyl]propanedinitrile, DEPT 135, CDCl<sub>3</sub>

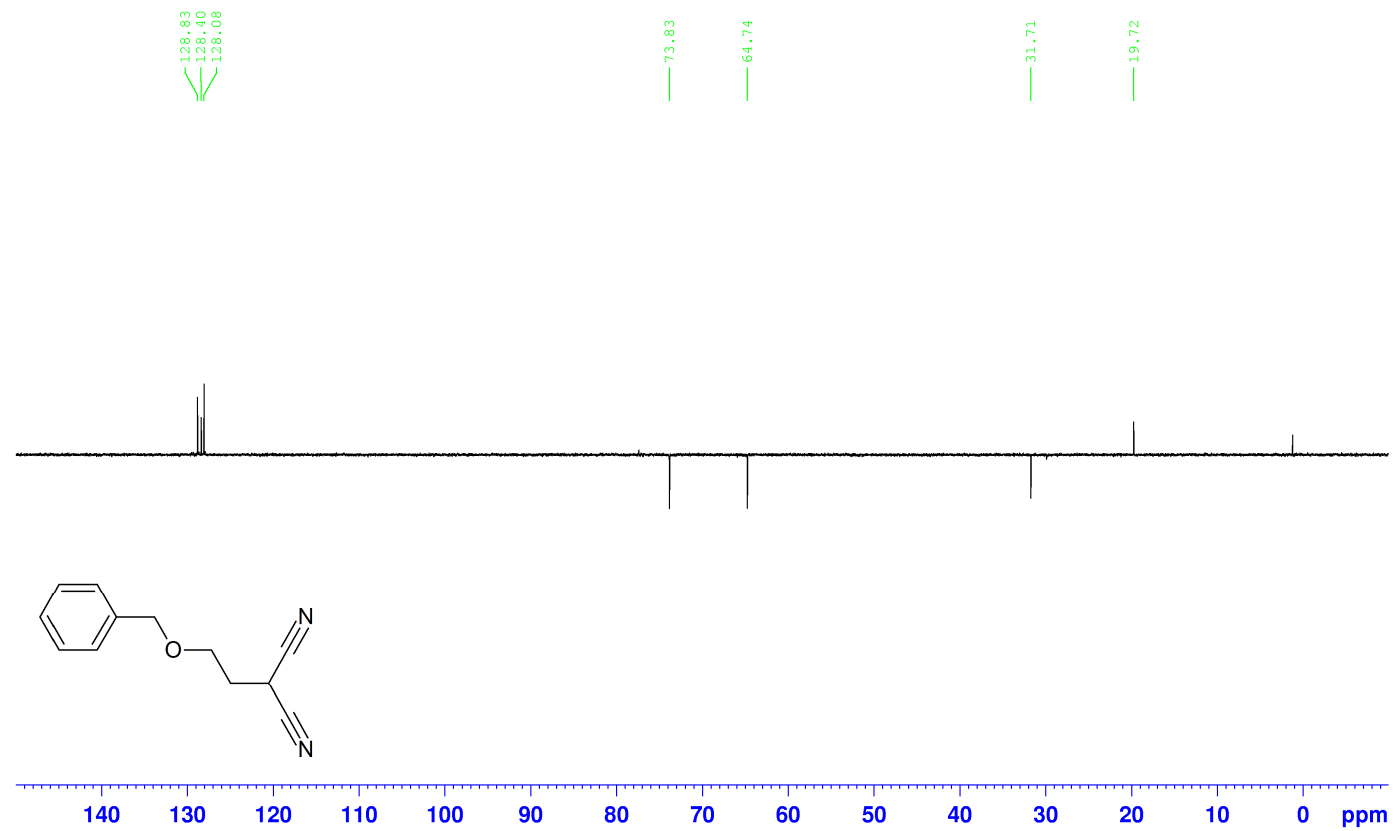


**Fig. A52.** DEPT 135 NMR spectrum of [2-(benzyloxy)ethyl]propanedinitrile.

[2-(benzyloxy)ethyl]propanedinitrile, HSQC, CDCl<sub>3</sub>

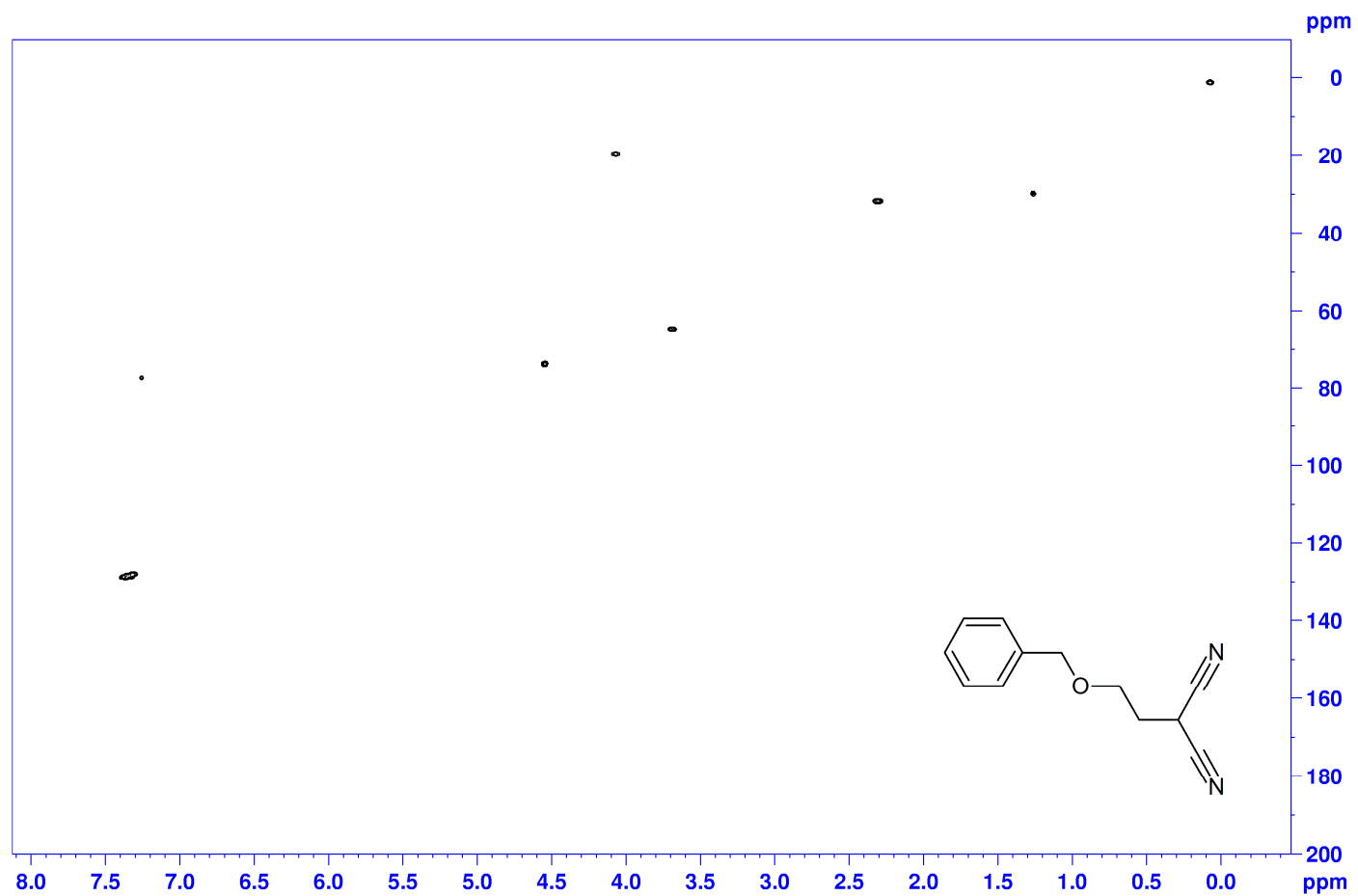


Fig. A53. HSQC NMR spectrum of [2-(benzyloxy)ethyl]propanedinitrile.

[2-(benzyloxy)ethyl]propanedinitrile, HMBC, CDC13

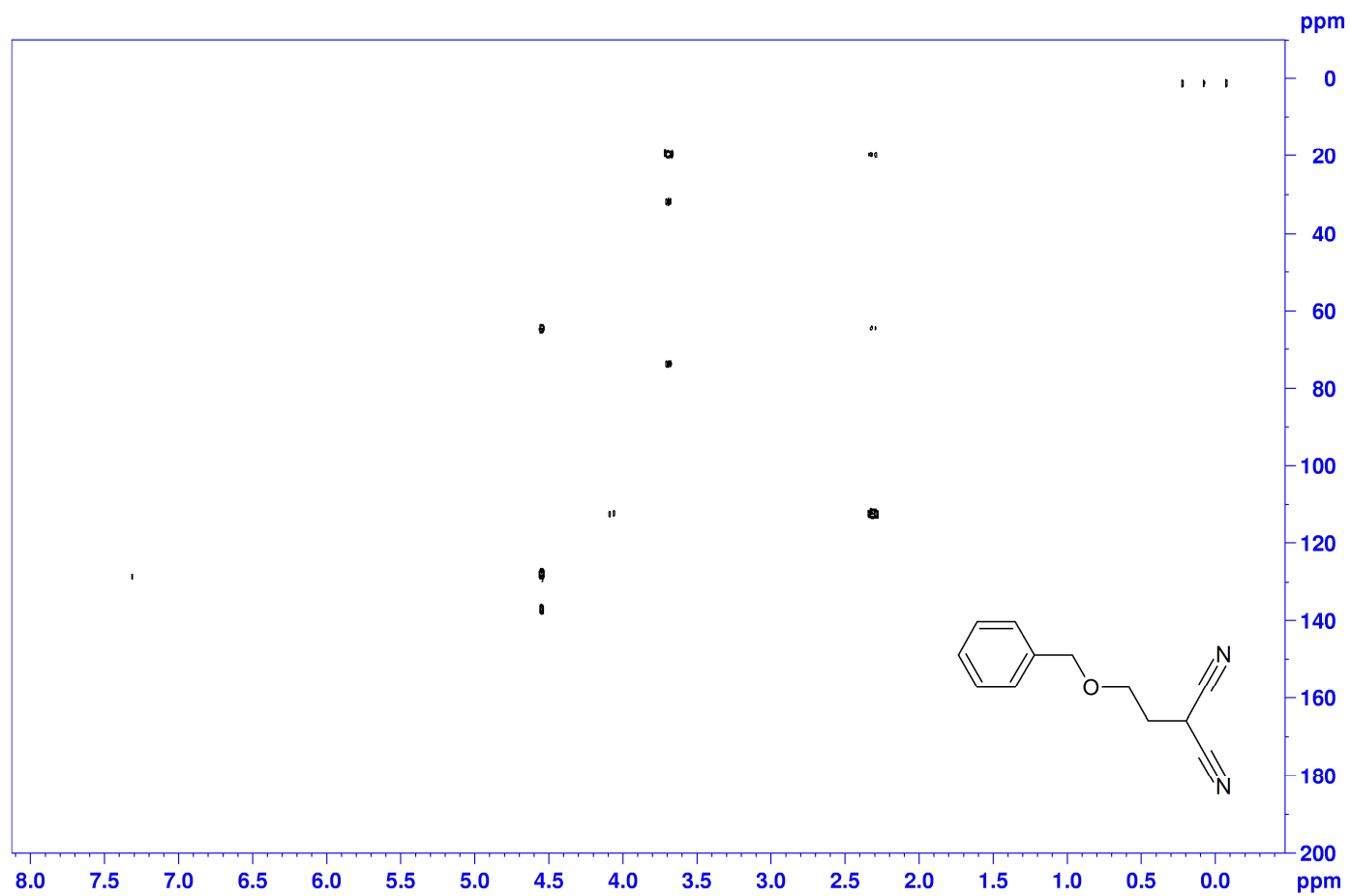


Fig. A54. HMBC NMR spectrum of [2-(benzyloxy)ethyl]propanedinitrile.

[3-(benzyloxy)propyl]propanedinitrile, 1H, CDC13

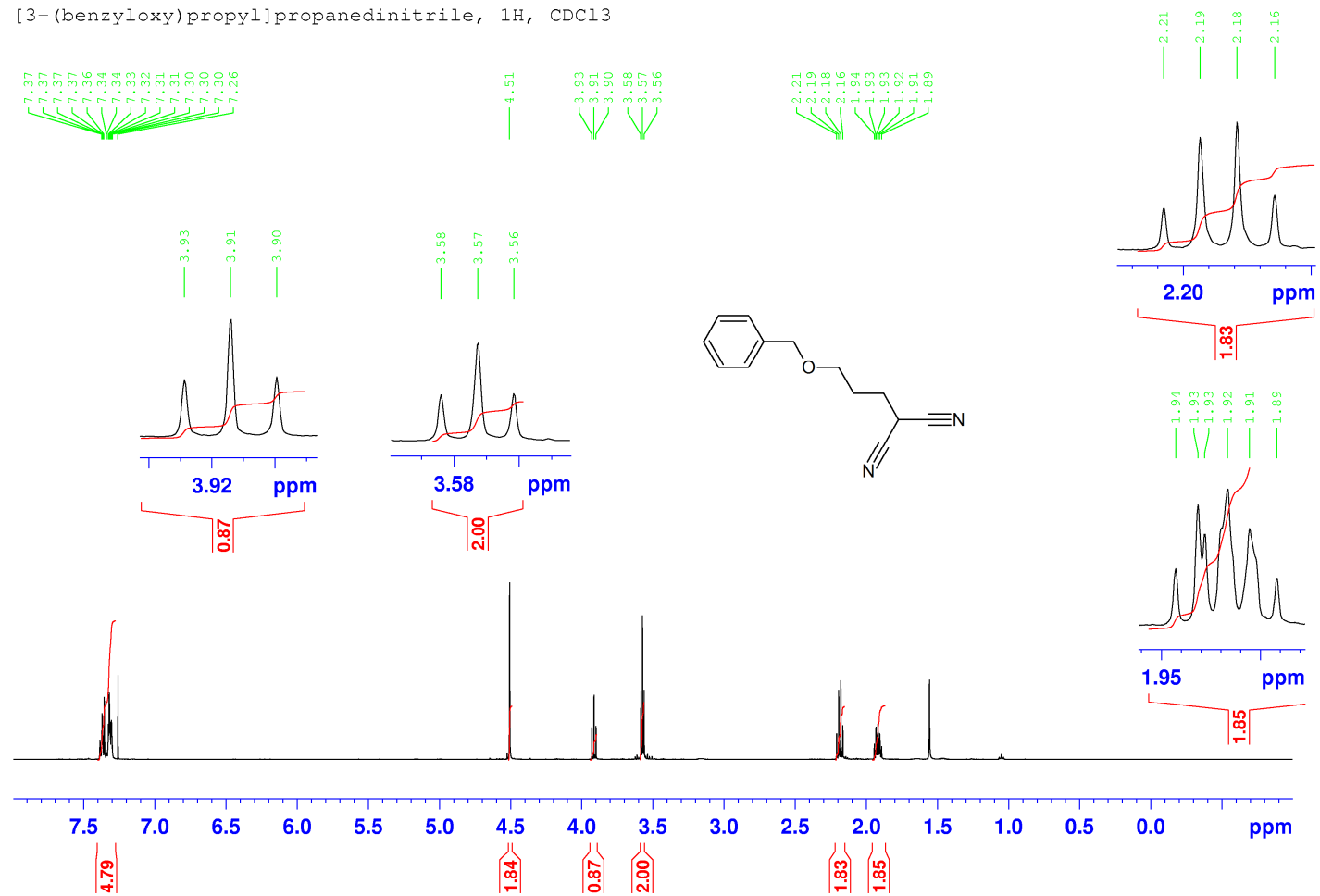
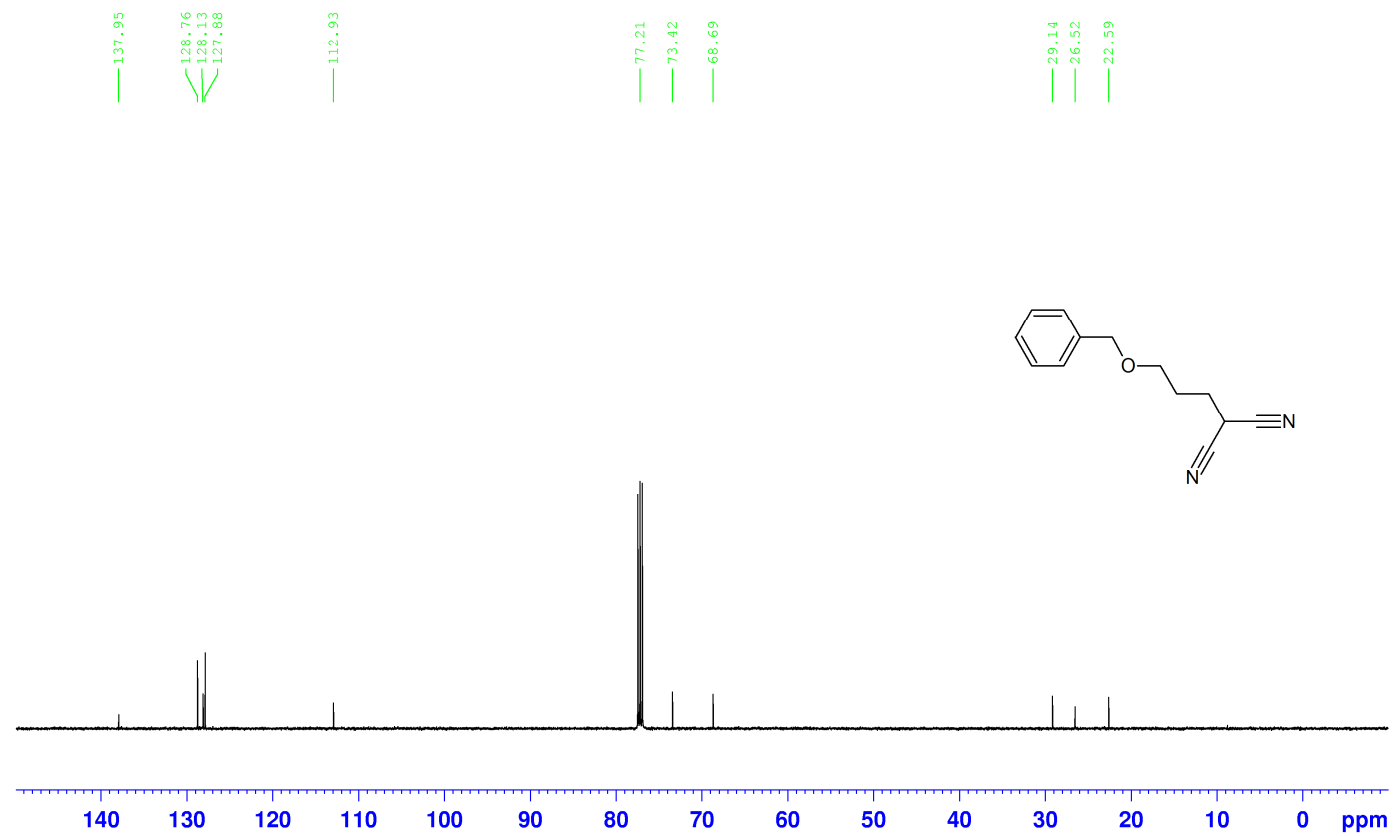


Fig. A55. <sup>1</sup>H NMR spectrum of [3-(benzyloxy)propyl]propanedinitrile.

[3-(benzyloxy)propyl]propanedinitrile,  $^{13}\text{C}$ ,  $\text{CDCl}_3$



**Fig. A56.**  $^{13}\text{C}$  NMR spectrum of [3-(benzyloxy)propyl]propanedinitrile.

[3-(benzyloxy)propyl]propanedinitrile, DEPT 135, CDC13

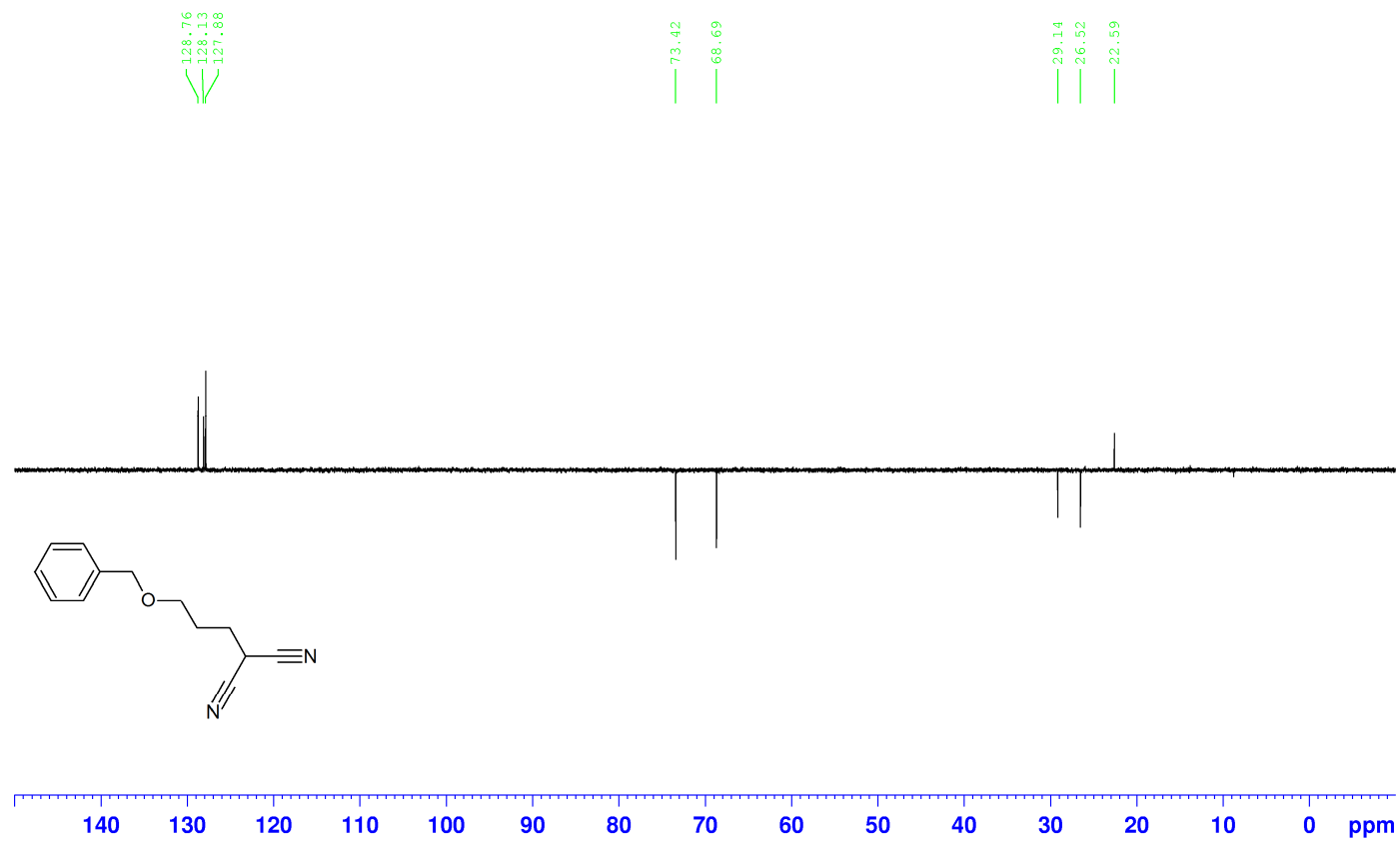


Fig. A57. DEPT 135 NMR spectrum of [3-(benzyloxy)propyl]propanedinitrile.



[3-(benzyloxy)propyl]propanedinitrile, DEPT 90, CDC13

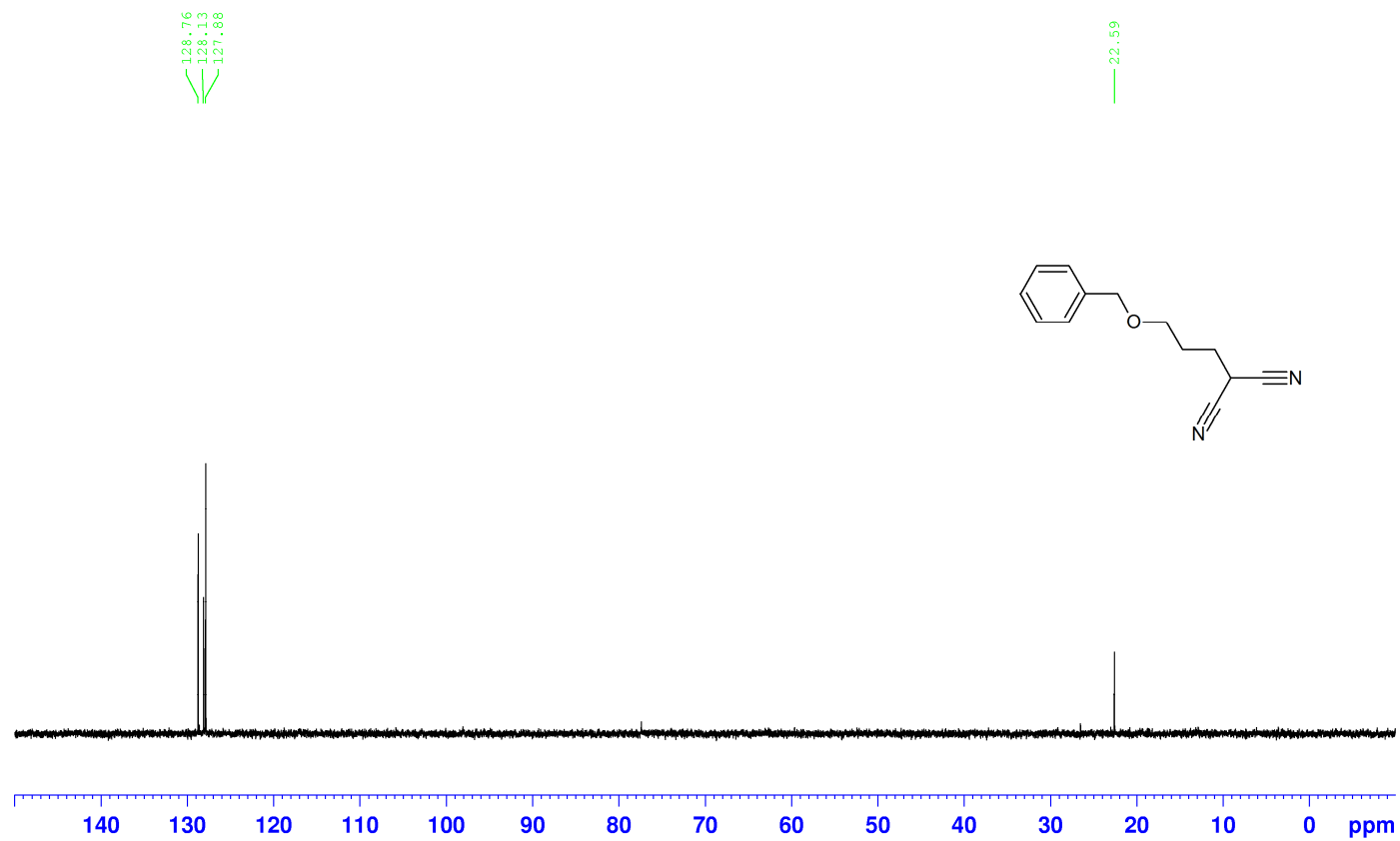
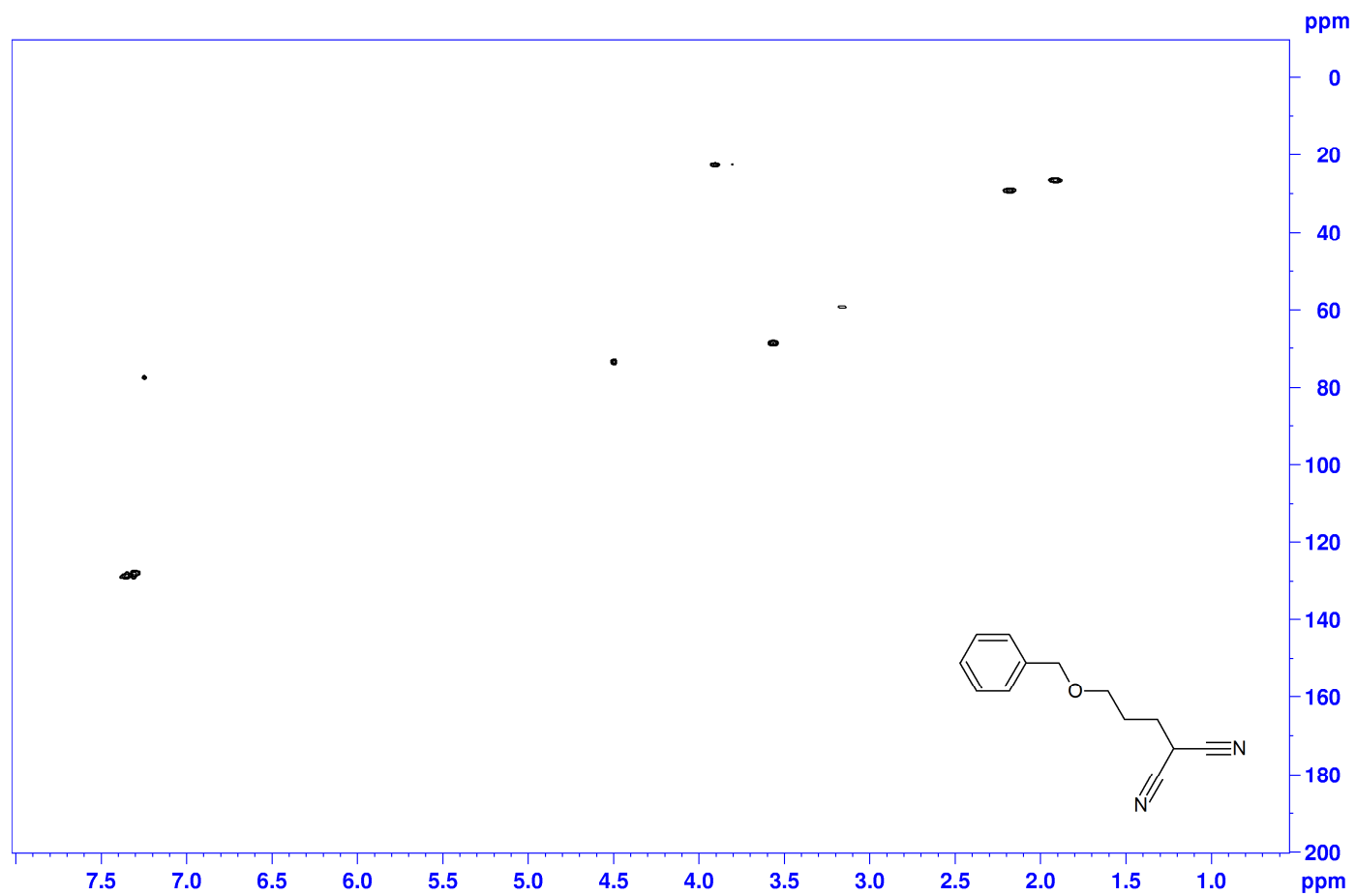


Fig. A58. DEPT 90 NMR spectrum of [3-(benzyloxy)propyl]propanedinitrile.

[3-(benzyloxy)propyl]propanedinitrile, HSQC, CDCl<sub>3</sub>



**Fig. A59.** HSQC NMR spectrum of [3-(benzyloxy)propyl]propanedinitrile.

[3-(benzyloxy)propyl]propanedinitrile, LRMS

13mn LRMS 24 (0.392) Cm (1:31)

TOF MS ES+  
4.18e4

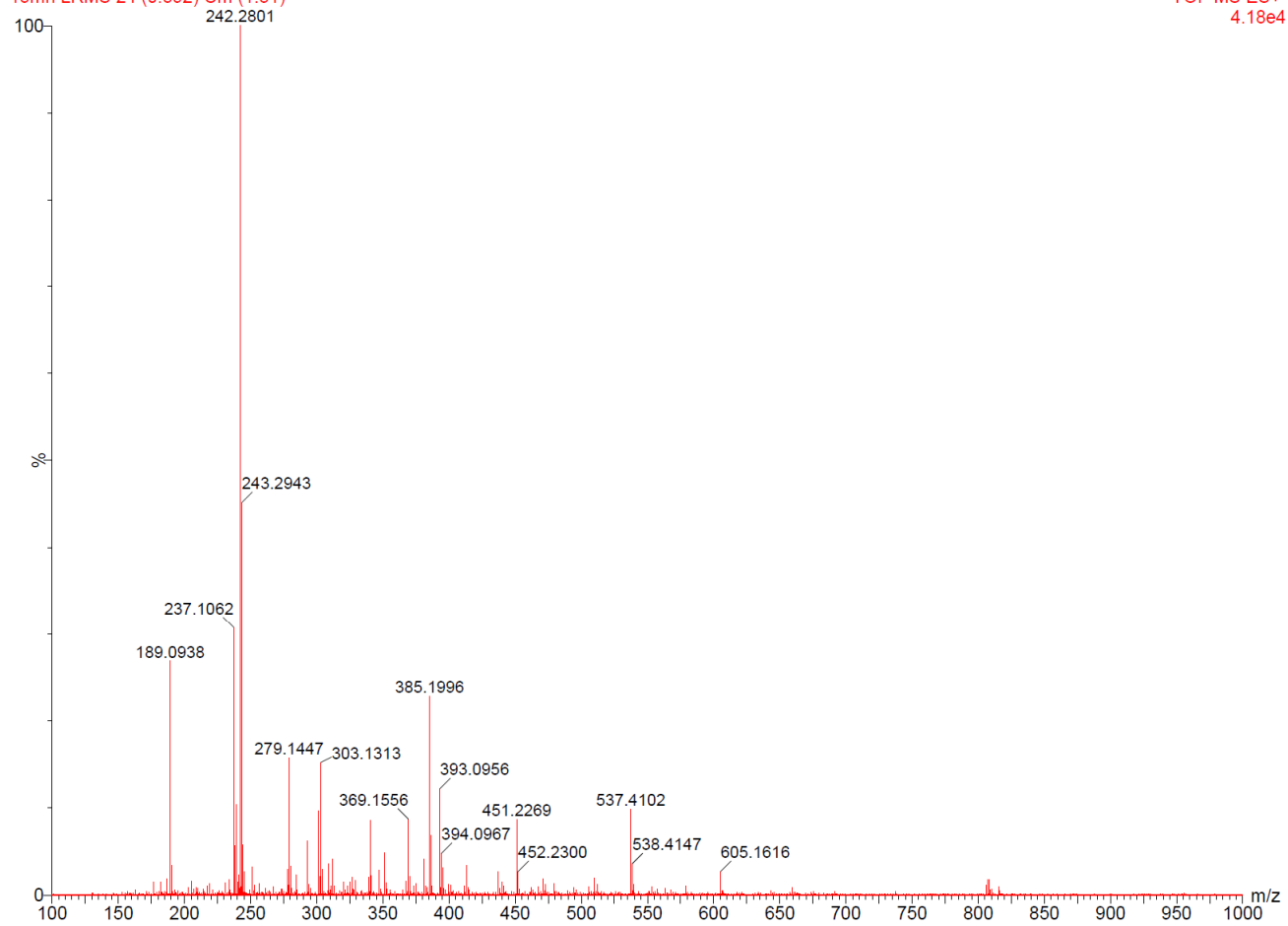


Fig. A60. Mass spectrum of [3-(benzyloxy)propyl]propanedinitrile without mass lock.

**Single Mass Analysis**

Tolerance = 5.0 PPM / DBE: min = -1.5, max = 50.0

Element prediction: Off

Number of isotope peaks used for i-FIT = 3

Monoisotopic Mass, Even Electron Ions

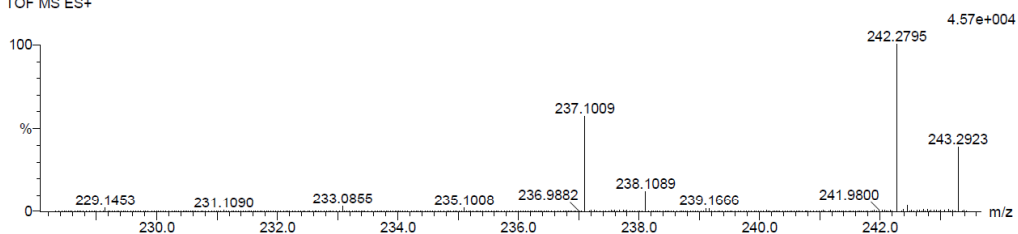
38 formula(e) evaluated with 1 results within limits (up to 50 best isotopic matches for each mass)

Elements Used:

C: 10-15 H: 10-15 N: 0-5 O: 0-5 Na: 0-1

13mn 5 (0.069) Cm (1:31)

TOF MS ES+



Minimum: -1.5  
 Maximum: 5.0 5.0 50.0

Mass	Calc. Mass	mDa	PPM	DBE	i-FIT	i-FIT (Norm)	Formula
237.1009	237.1004	0.5	2.1	7.5	500.1	0.0	C13 H14 N2 O Na

**Fig. A61.** Mass spectrum of [3-(benzyloxy)propyl]propanedinitrile with mass lock.

2-(2-hydroxyethyl)propane-1,3-diaminium dichloride, 1H, D2O

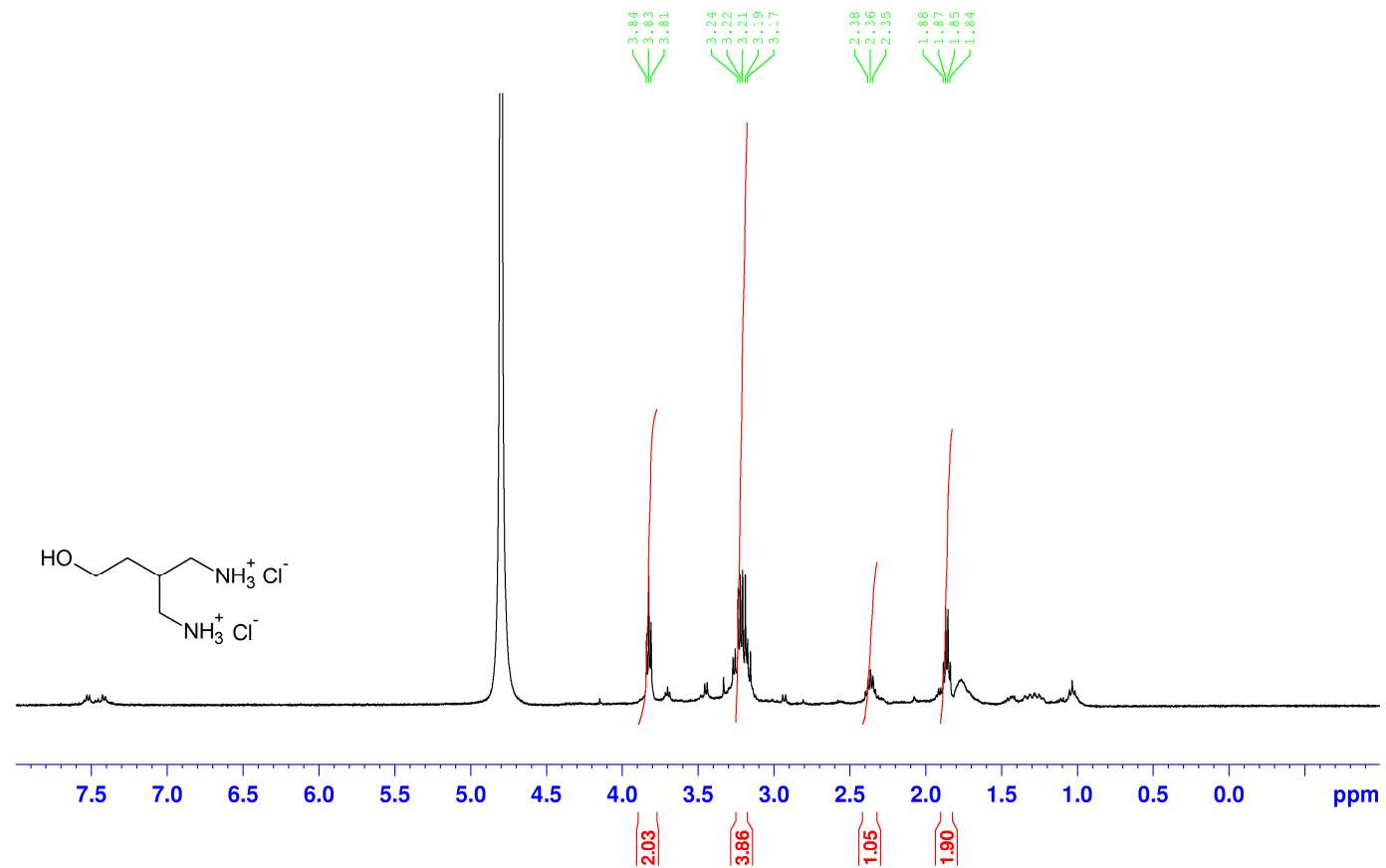
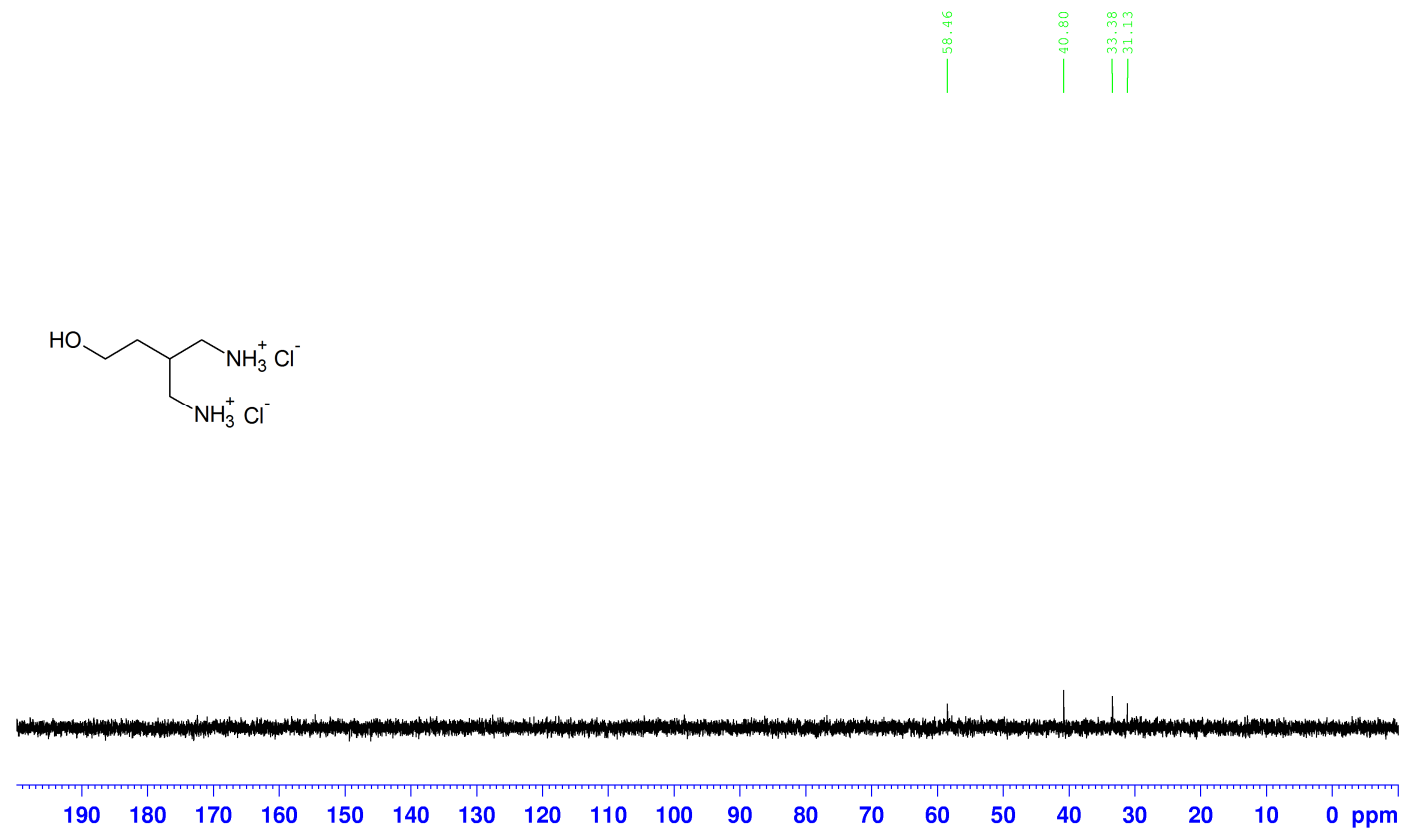


Fig. A62. <sup>1</sup>H NMR spectrum of 2-(2-hydroxyethyl)propane-1,3-diaminium dichloride.

2-(2-hydroxyethyl)propane-1,3-diaminium dichloride,  $^{13}\text{C}$ , D $_2\text{O}$



**Fig. A63.**  $^{13}\text{C}$  NMR spectrum of 2-(2-hydroxyethyl)propane-1,3-diaminium dichloride.

2-(2-hydroxyethyl)propane-1,3-diaminium dichloride, DEPT 135, D2O

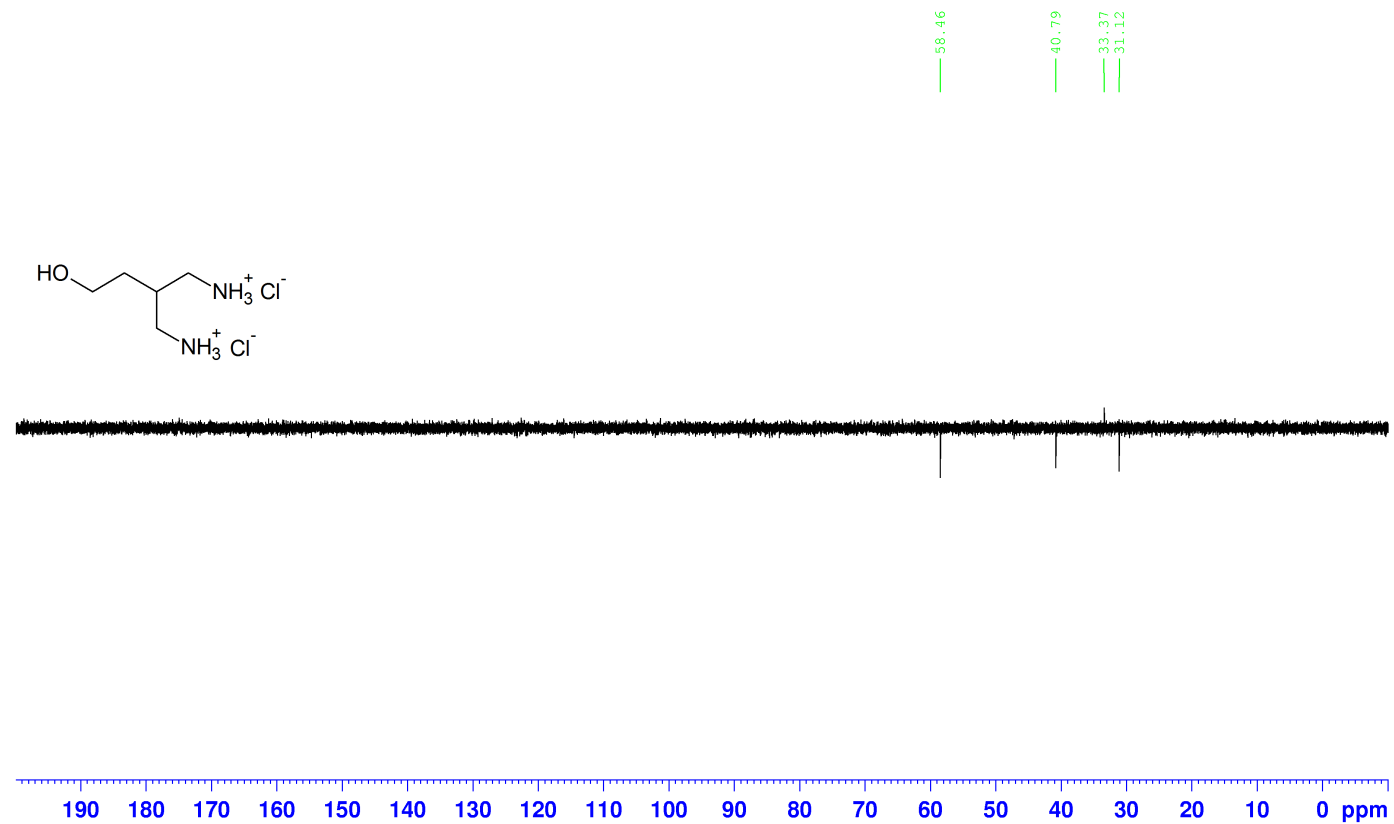


Fig. A64. DEPT 135 NMR spectrum of 2-(2-hydroxyethyl)propane-1,3-diaminium dichloride.

2-(2-hydroxyethyl)propane-1,3-diaminium dichloride, HSQC, D2O

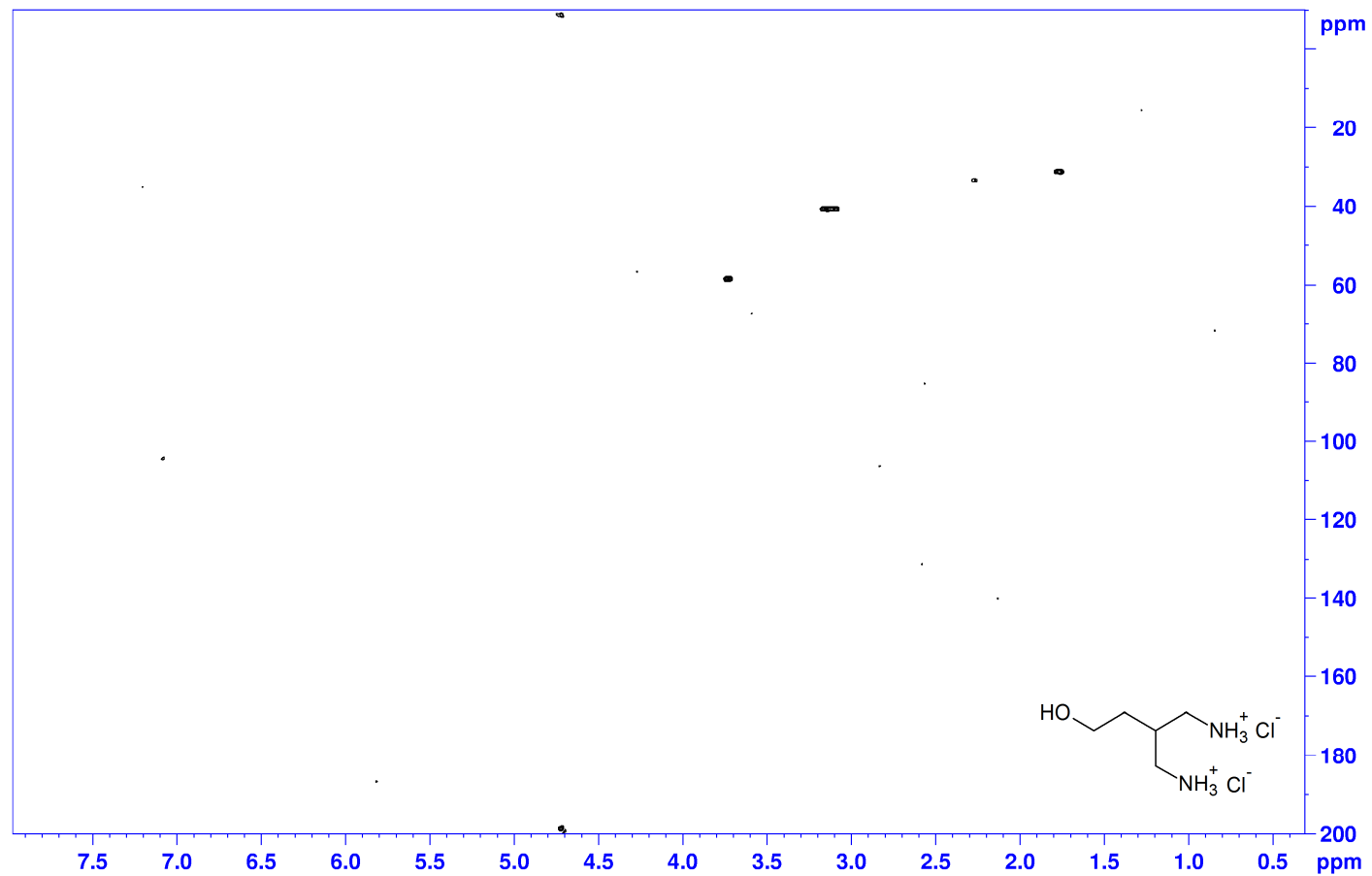
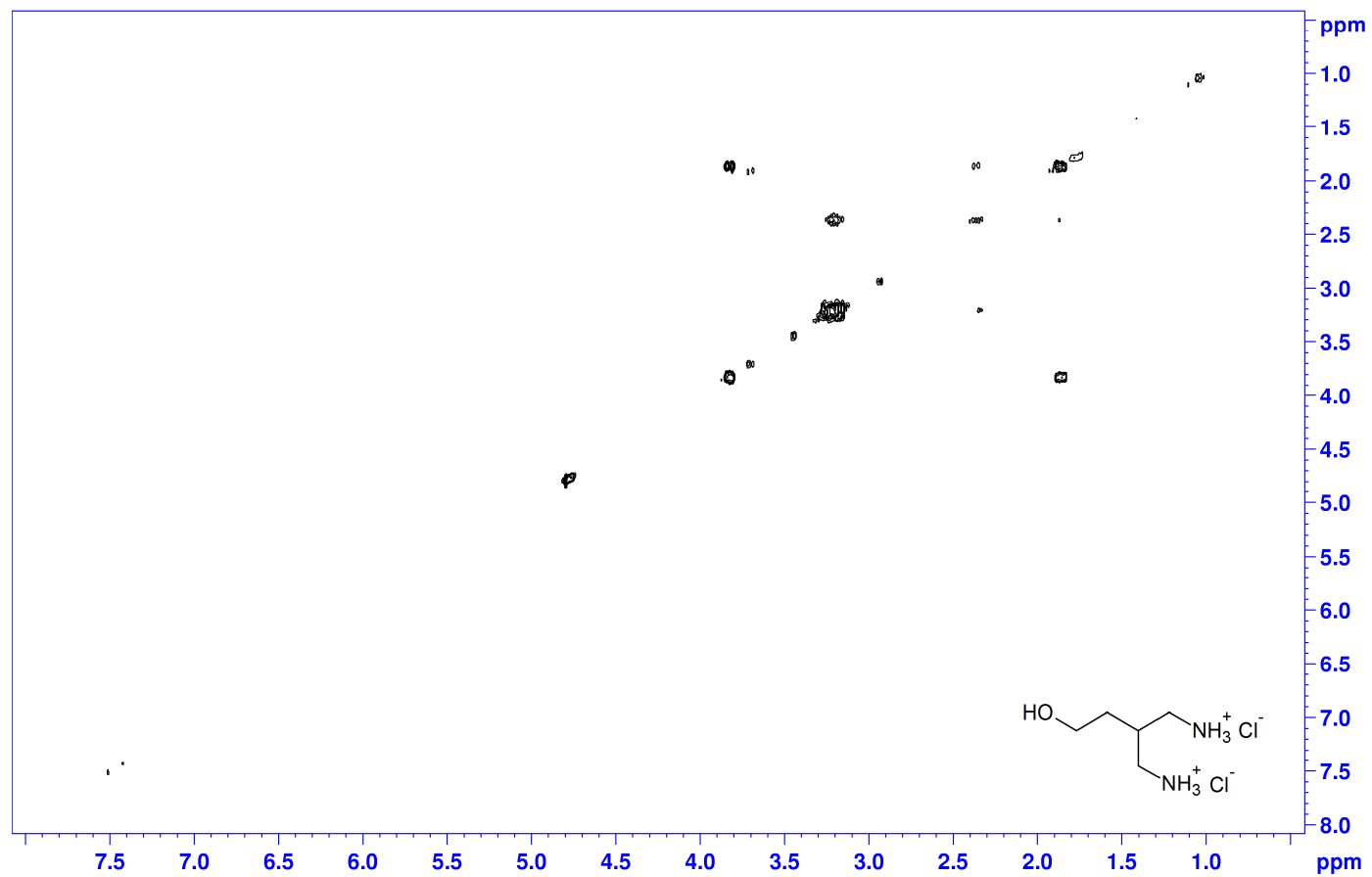


Fig. A65. HSQC NMR spectrum of 2-(2-hydroxyethyl)propane-1,3-diaminium dichloride.



2-(2-hydroxyethyl)propane-1,3-diaminium dichloride, COSY, D2O



**Fig. A66.** COSY NMR spectrum of 2-(2-hydroxyethyl)propane-1,3-diaminium dichloride.

*N,N'*-ethane-1,2-diylbis(2-cyanoacetamide), 1H, DMSO-d6

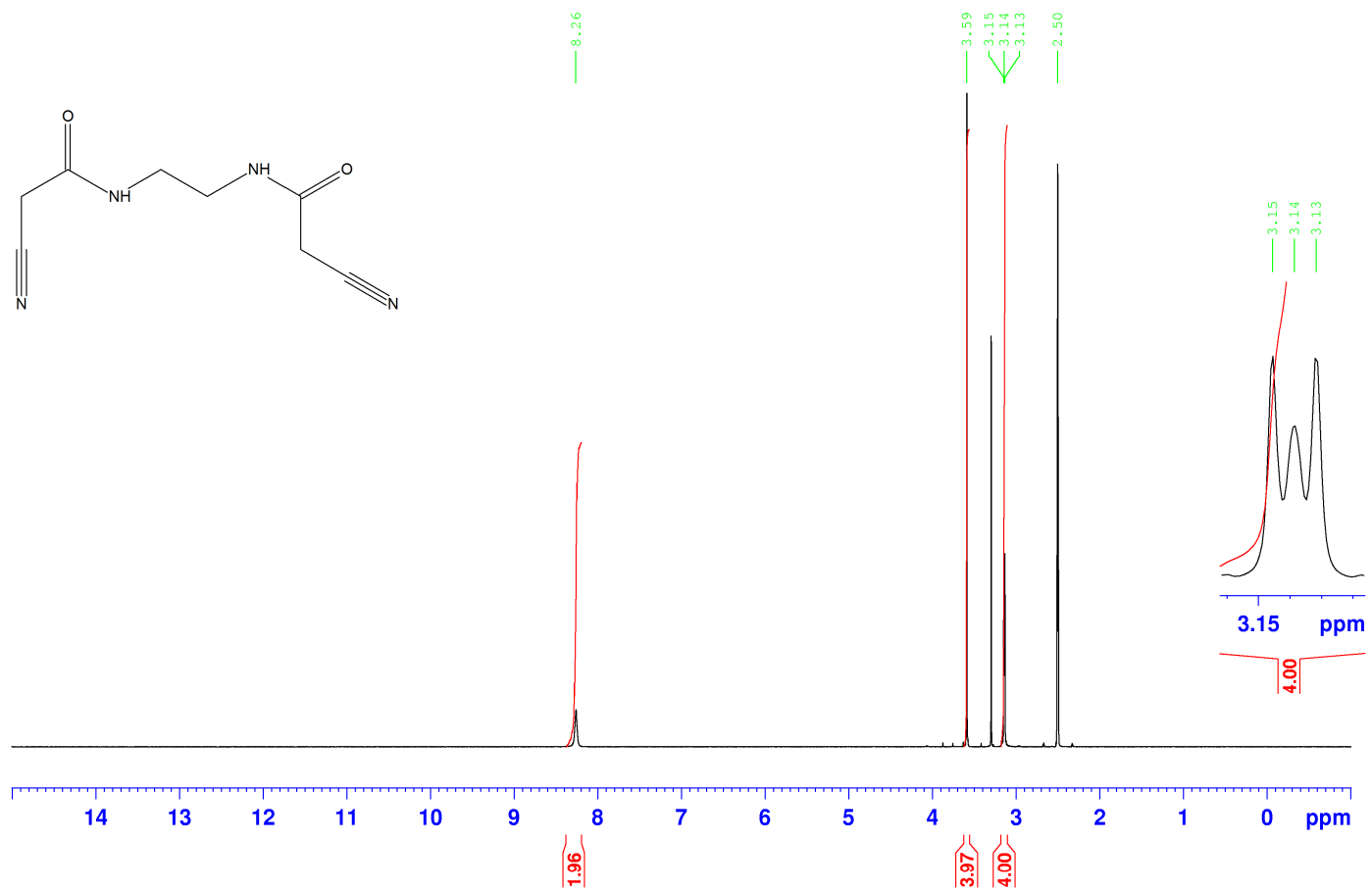


**Fig. B1.** <sup>1</sup>H NMR spectrum of *N,N'*-ethane-1,2-diylbis(2-cyanoacetamide).

*N,N'*-ethane-1,2-diylbis(2-cyanoacetamide),  $^{13}\text{C}$ ,  $\text{DMSO-d}_6$

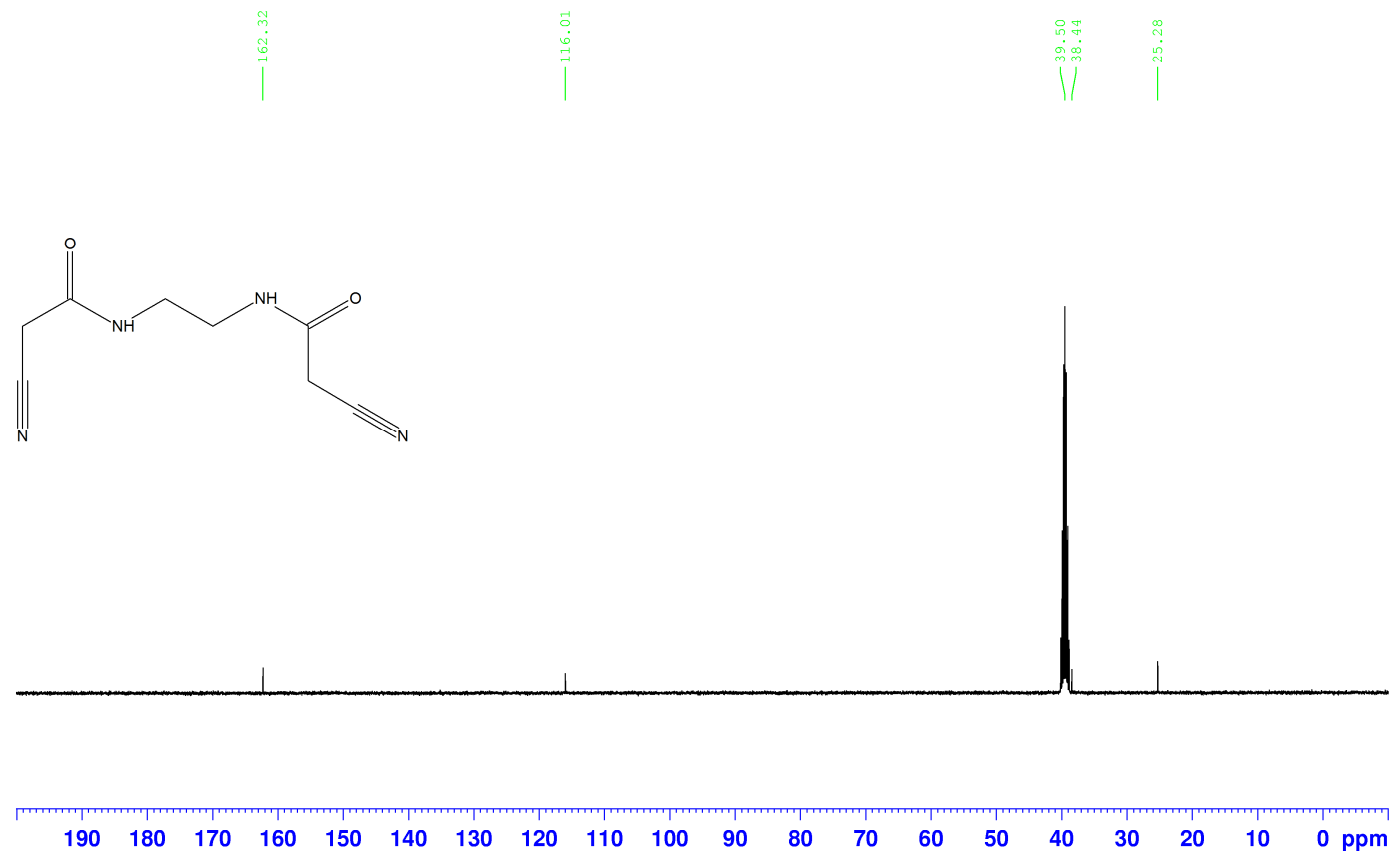


**Fig. B2.**  $^{13}\text{C}$  NMR spectrum of *N,N'*-ethane-1,2-diylbis(2-cyanoacetamide).

*N,N'*-ethane-1,2-diylbis(2-cyanoacetamide), DEPT 135, DMSO-d<sub>6</sub>

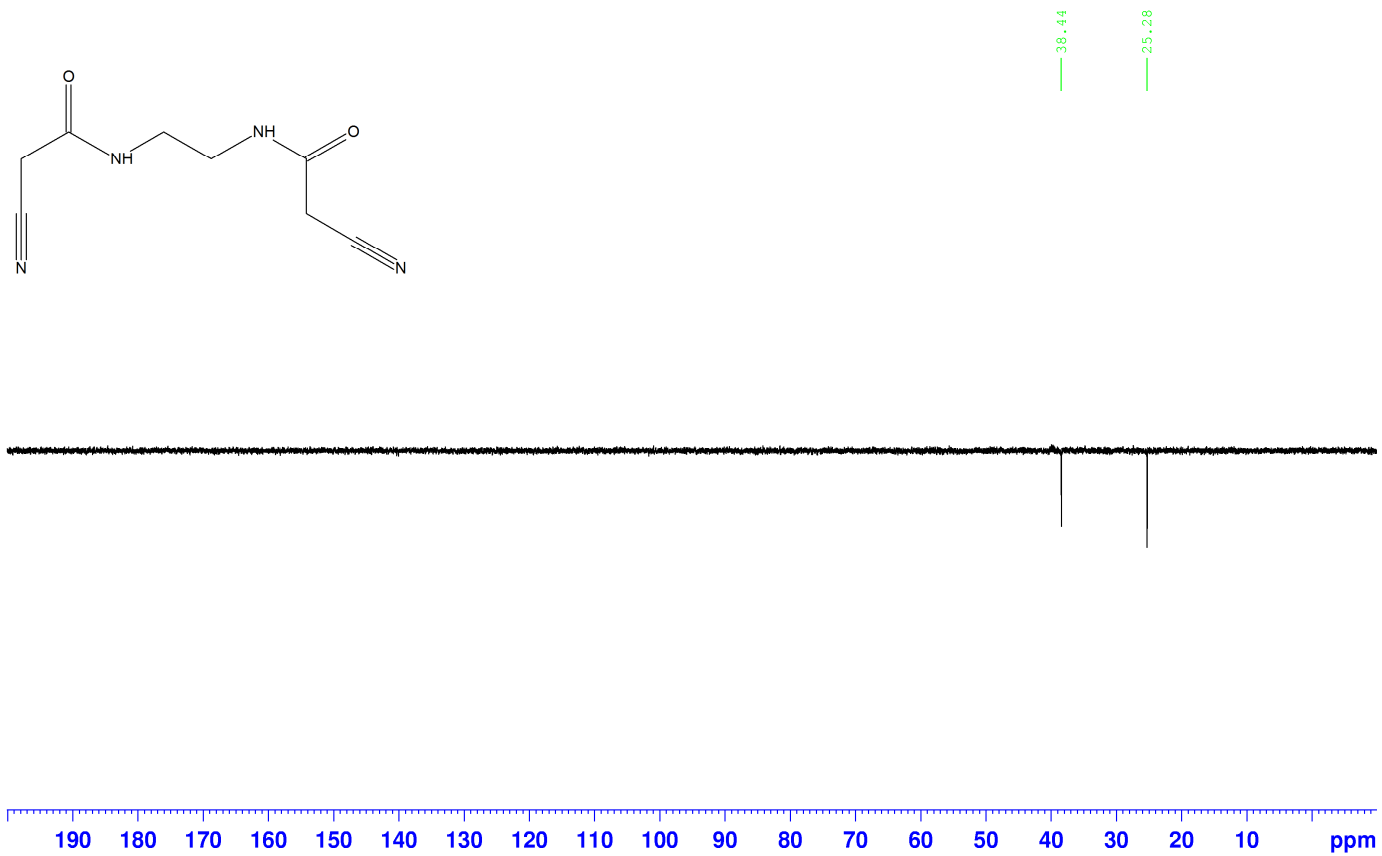


**Fig. B3.** DEPT 135 NMR spectrum of *N,N'*-ethane-1,2-diylbis(2-cyanoacetamide).

N,N'-ethane-1,2-diylbis(2-cyanoacetamide), CHN

**ATLANTIC MICROLAB, INC.**

Sample No. (464) SUBMITTER

Company / School Missouri State University

Address 901 South National Avenue

Dept. Chemistry, Temple Hall 456

6180 Atlantic Blvd., Suite M  
Norcross, GA 30071

www.atlanticmicrolab.com

PROFESSOR/SUPERVISOR: Prof. N. Gerasimchuk NAME Dr. Gerasimchuk DATE 10/27/12

PO# / CC#: 04172 PHONE (417) 836-5165

Element	Theory	Found	Single <input checked="" type="checkbox"/>	Duplicate <input type="checkbox"/>
C	49.4800	49.70	Elements Present: C, N, H, O	
H	5.1900	5.20	Analyze for: C, H, N	
N	28.8500	28.57	Hygroscopic: <input type="checkbox"/> Explosive: <input type="checkbox"/>	
			M.P. _____ B.P. _____	
			To be dried: Yes <input type="checkbox"/> No <input type="checkbox"/>	
			Temp. _____ Vac. _____ Time _____	
			RUSH SERVICE <input type="checkbox"/> Rush service laboratory analyses will be completed and results available by 5pm EST on the day the sample is received by 11 a.m.	
			Include Email Address: <u>Fax # 836-5165</u>	

Date Received OCT 31 P.M. Date Completed NOV 01 2012

Remarks:

Fig. B4. CHN chromatogram of N,N'-ethane-1,2-diylbis(2-cyanoacetamide).

*N,N'*-propane-1,3-diylbis(2-cyanoacetamide), 1H, DMSO-d<sub>6</sub>

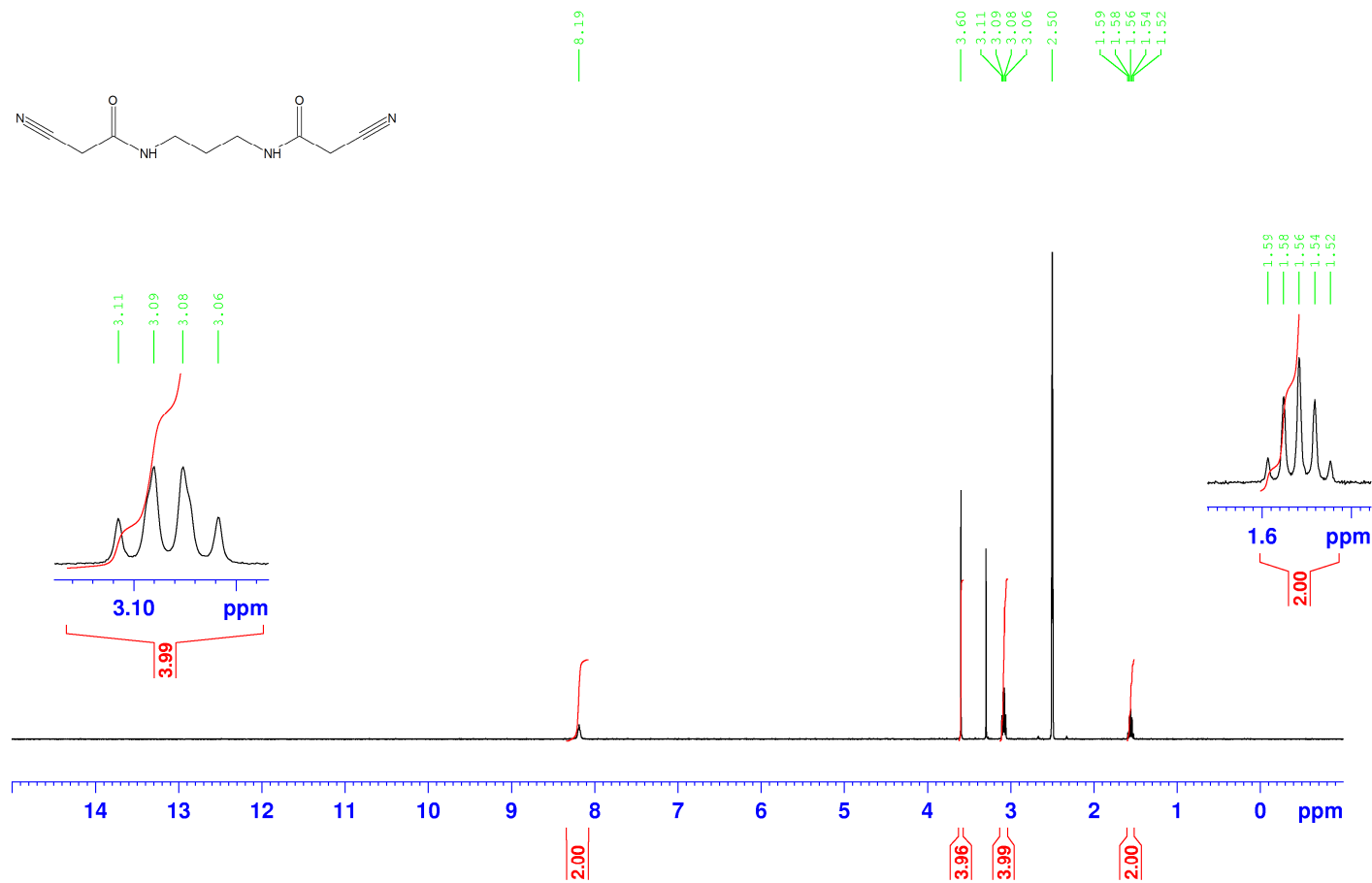


**Fig. B5.** <sup>1</sup>H NMR spectrum of *N,N'*-propane-1,3-diylbis(2-cyanoacetamide).

*N,N'*-propane-1,3-diylbis(2-cyanoacetamide),  $^{13}\text{C}$ ,  $\text{DMSO-d}_6$

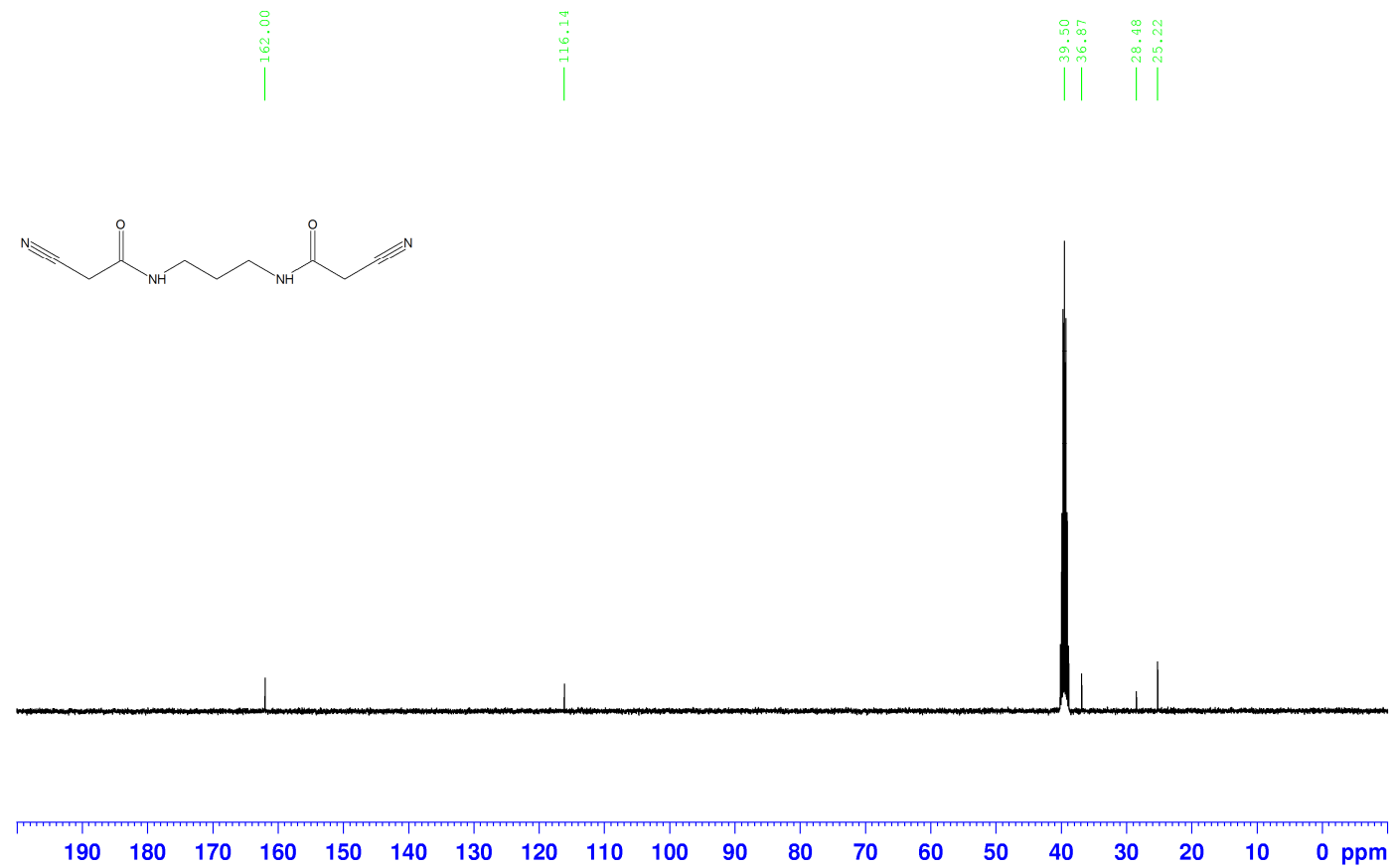


**Fig. B6.**  $^{13}\text{C}$  NMR spectrum of *N,N'*-propane-1,3-diylbis(2-cyanoacetamide).

*N,N'*-propane-1,3-diylbis(2-cyanoacetamide), DEPT 135, DMSO-D6

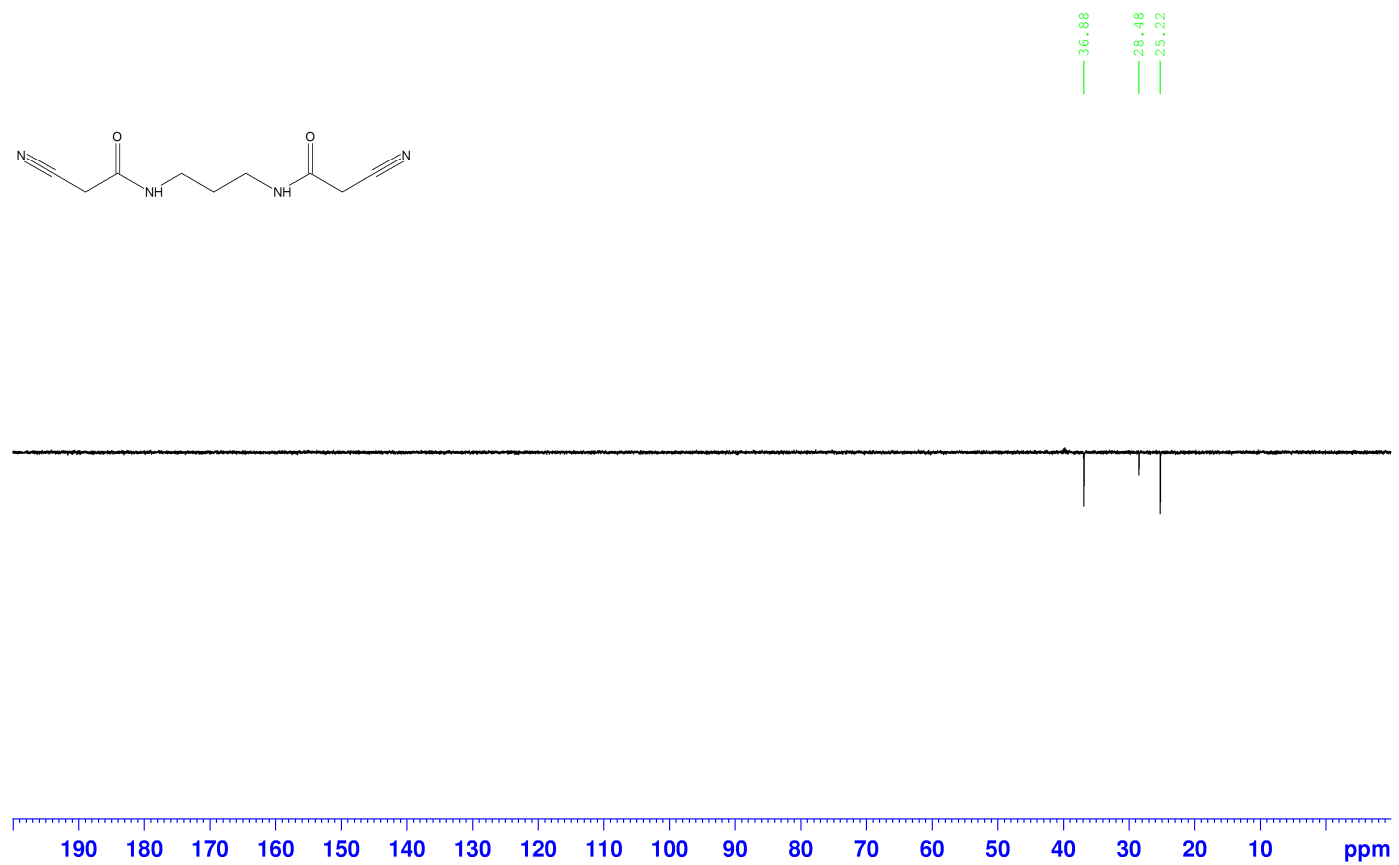


**Fig. B7.** DEPT 135 NMR spectrum of *N,N'*-propane-1,3-diylbis(2-cyanoacetamide).



*N,N'*-butane-1,4-diylbis(2-cyanoacetamide), 1H, DMSO-d6

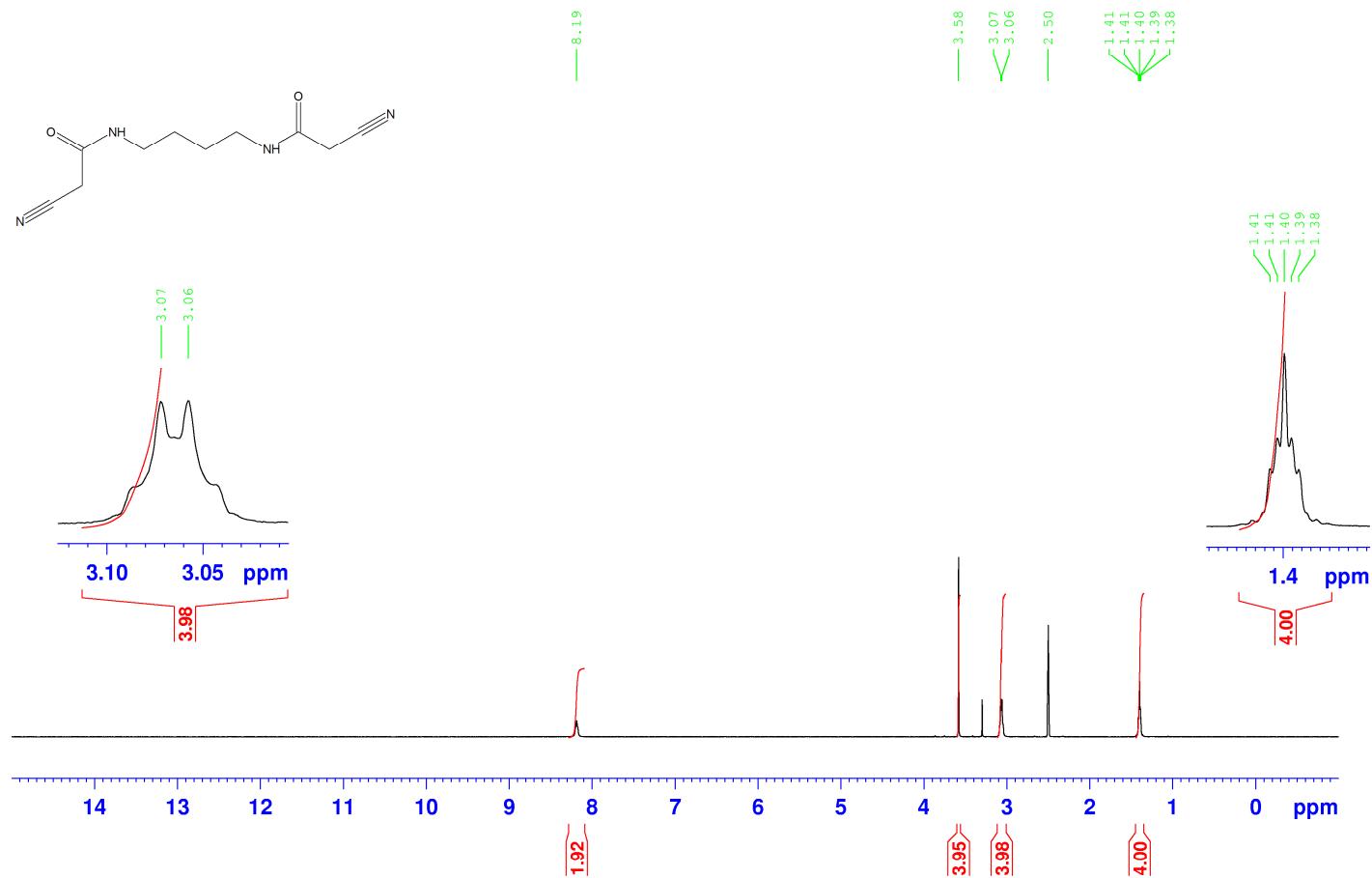


**Fig. B8.** <sup>1</sup>H NMR spectrum of *N,N'*-butane-1,4-diylbis(2-cyanoacetamide).

*N,N'*-butane-1,4-diylbis(2-cyanoacetamide),  $^{13}\text{C}$ ,  $\text{DMSO-d}_6$

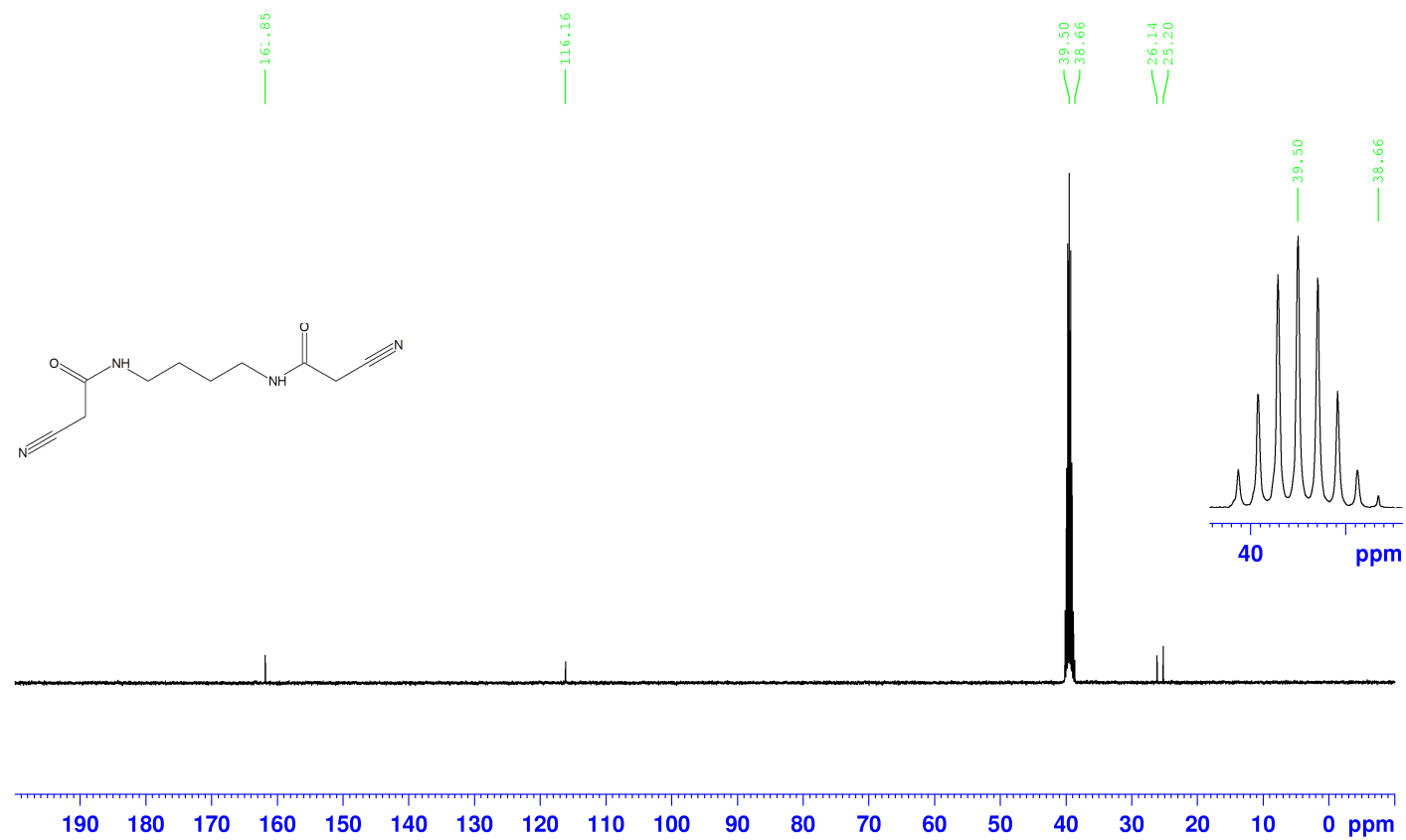


**Fig. B9.**  $^{13}\text{C}$  NMR spectrum of *N,N'*-butane-1,4-diylbis(2-cyanoacetamide).

*N,N'*-butane-1,4-diylbis(2-cyanoacetamide), DEPT 135, DMSO-D6

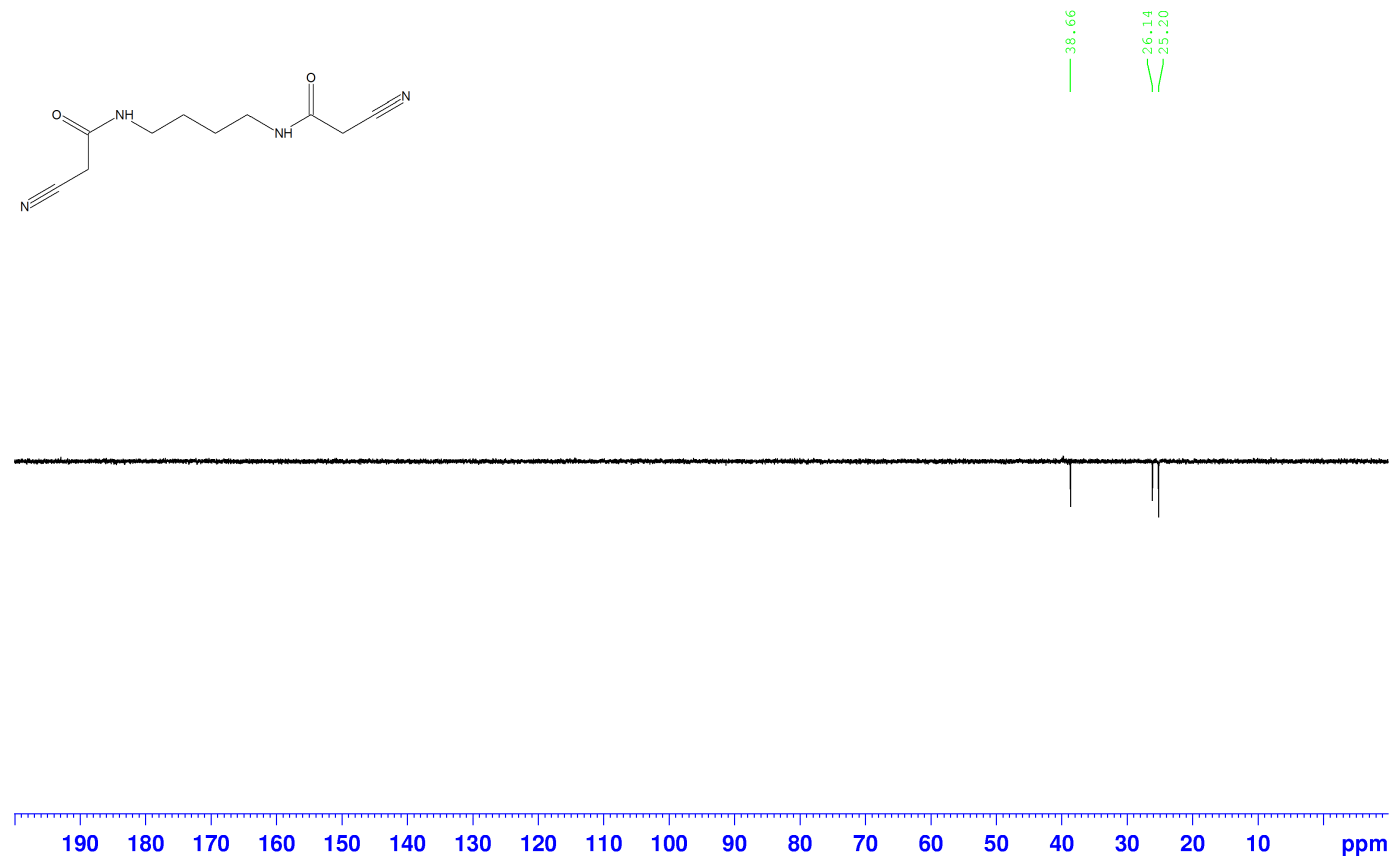
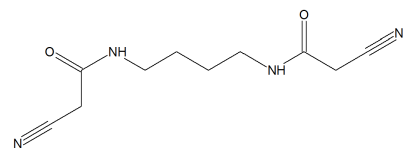


**Fig. B10.** DEPT 135 NMR spectrum of *N,N'*-butane-1,4-diylbis(2-cyanoacetamide).

*N,N'*-(2-hydroxypropane-1,3-diyl)bis(2-cyanoacetamide), 1H, DMSO-d<sub>6</sub>

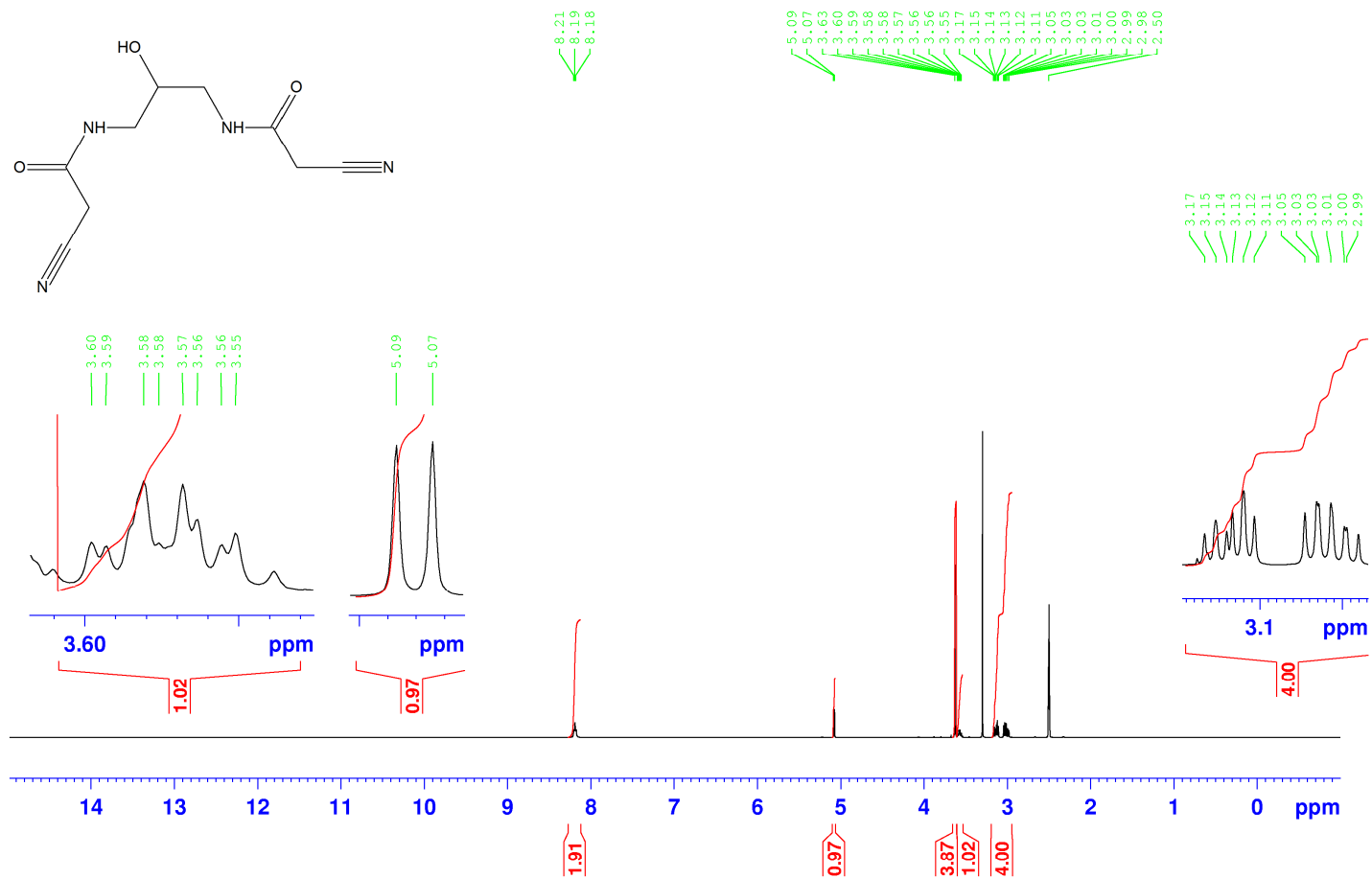


**Fig. B11.** <sup>1</sup>H NMR spectrum of *N,N'*-(2-hydroxypropane-1,3-diyl)bis(2-cyanoacetamide).

*N,N'*-(2-hydroxypropane-1,3-diyl)bis(2-cyanoacetamide), 13C, DMSO-d6

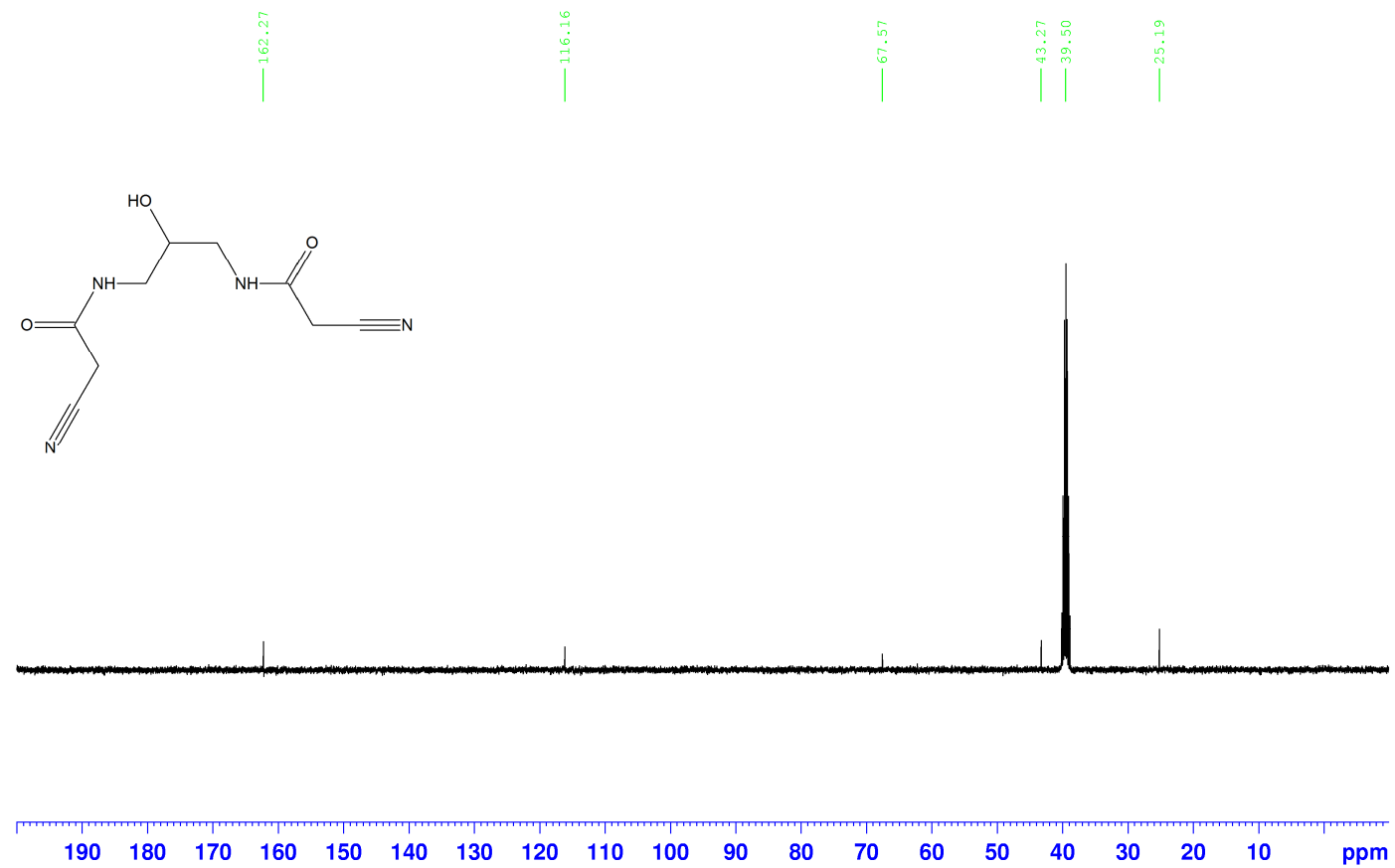


**Fig. B12.** <sup>13</sup>C NMR spectrum of *N,N'*-(2-hydroxypropane-1,3-diyl)bis(2-cyanoacetamide).

*N,N'*-(2-hydroxypropane-1,3-diyl)bis(2-cyanoacetamide), DEPT 135, DMSO-d<sub>6</sub>

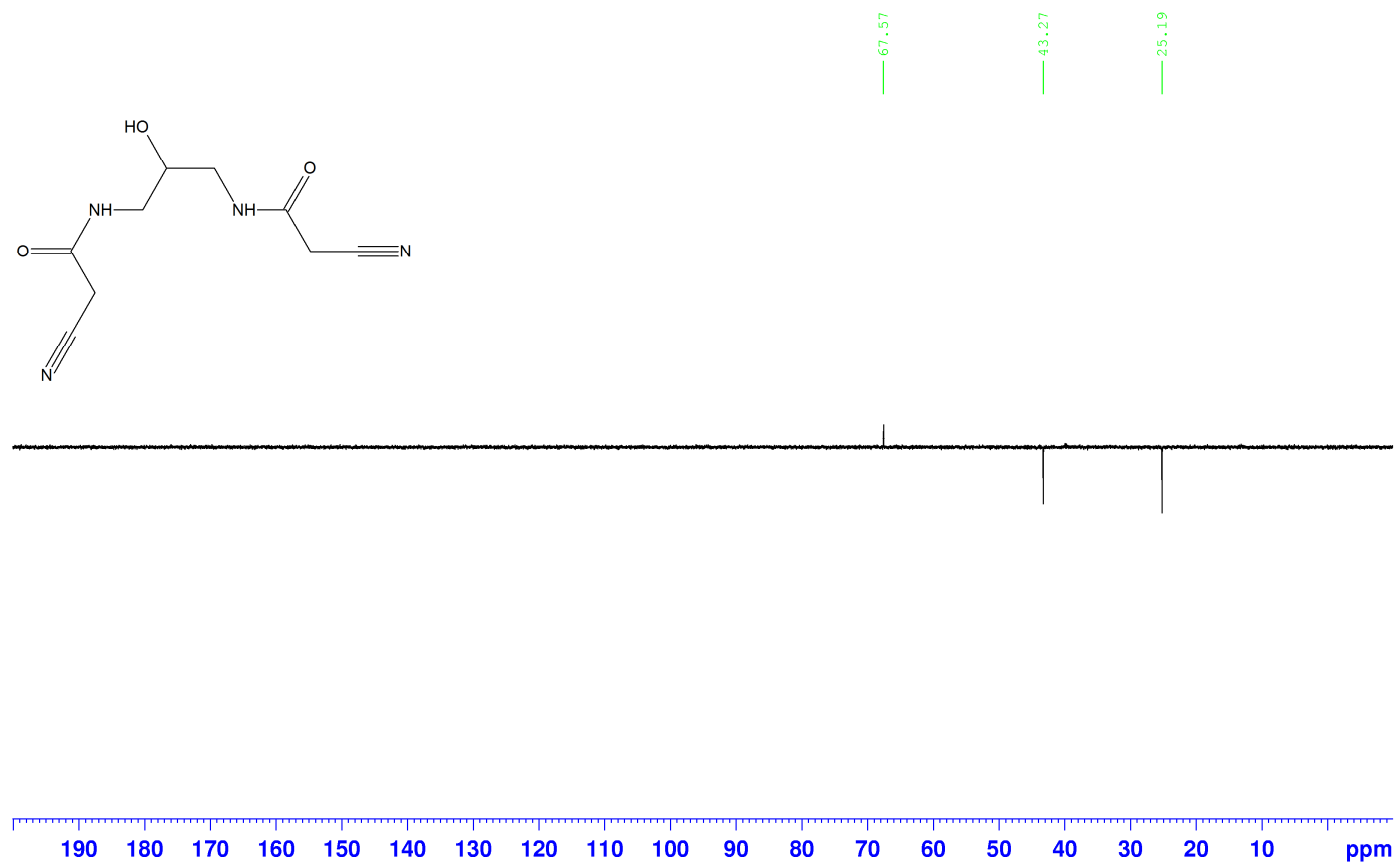


**Fig. B13.** DEPT 135 NMR spectrum of *N,N'*-(2-hydroxypropane-1,3-diyl)bis(2-cyanoacetamide).

**Single Mass Analysis**

Tolerance = 5.0 PPM / DBE: min = -1.5, max = 50.0

Element prediction: Off

Number of isotope peaks used for i-FIT = 3

Monoisotopic Mass, Even Electron Ions

48 formula(e) evaluated with 1 results within limits (up to 50 best isotopic matches for each mass)

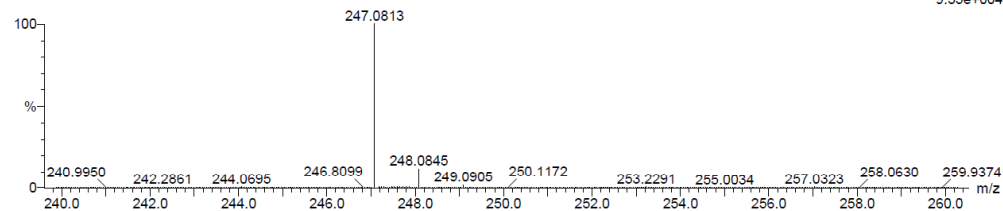
Elements Used:

C: 5-10 H: 10-15 N: 0-5 O: 0-5 Na: 0-1

eco-pnoh-p0-et-sl 22 (0.359) Cm (1:30)

TOF MS ES+

9.35e+004



Minimum:

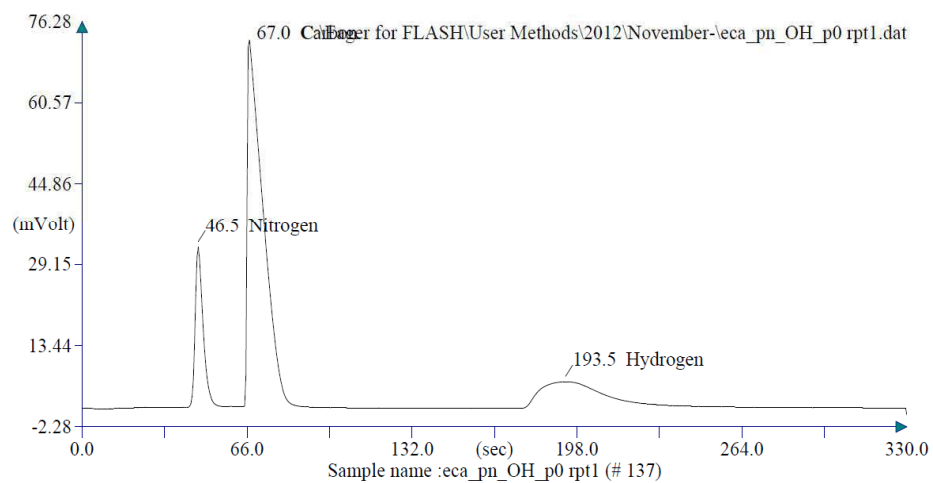
Maximum: 5.0 5.0 -1.5

Mass Calc. Mass mDa PPM DBE i-FIT i-FIT (Norm) Formula

247.0813 247.0807 0.6 2.4 5.5 601.6 0.0 C9 H12 N4 O3 Na

**Fig. B14.** Mass spectrum of *N,N'*-(2-hydroxypropane-1,3-diyl)bis(2-cyanoacetamide) without mass lock.

*N,N'*-(2-hydroxypropane-1,3-diyl)bis(2-cyanoacetamide), CHN



Retention Time (min)	Element Name	Element %
0.775	Nitrogen	25.207
1.117	Carbon	48.144
3.225	Hydrogen	5.007
		<u>78.358</u>

**Fig. B15.** CHN chromatogram of *N,N'*-(2-hydroxypropane-1,3-diyl)bis(2-cyanoacetamide)



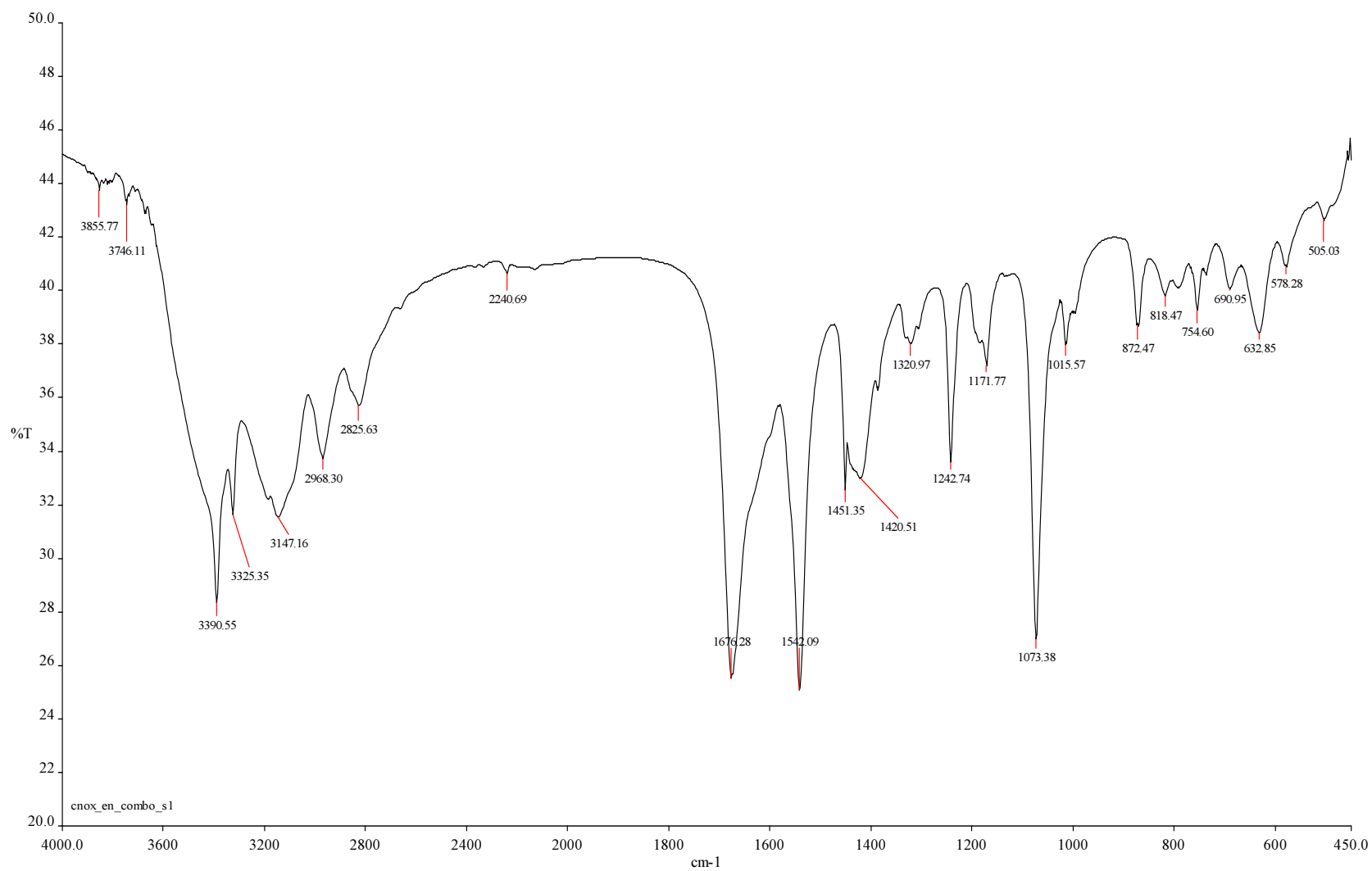


**Fig. B16.** IR spectrum of *N,N'*-ethane-1,2-diylbis[2-cyano-2-(hydroxyimino)ethanamide], KBr disk.

*N,N'*-ethane-1,2-diylbis[2-cyano-2-(hydroxyimino)ethanamide], 1H, DMSO-d6

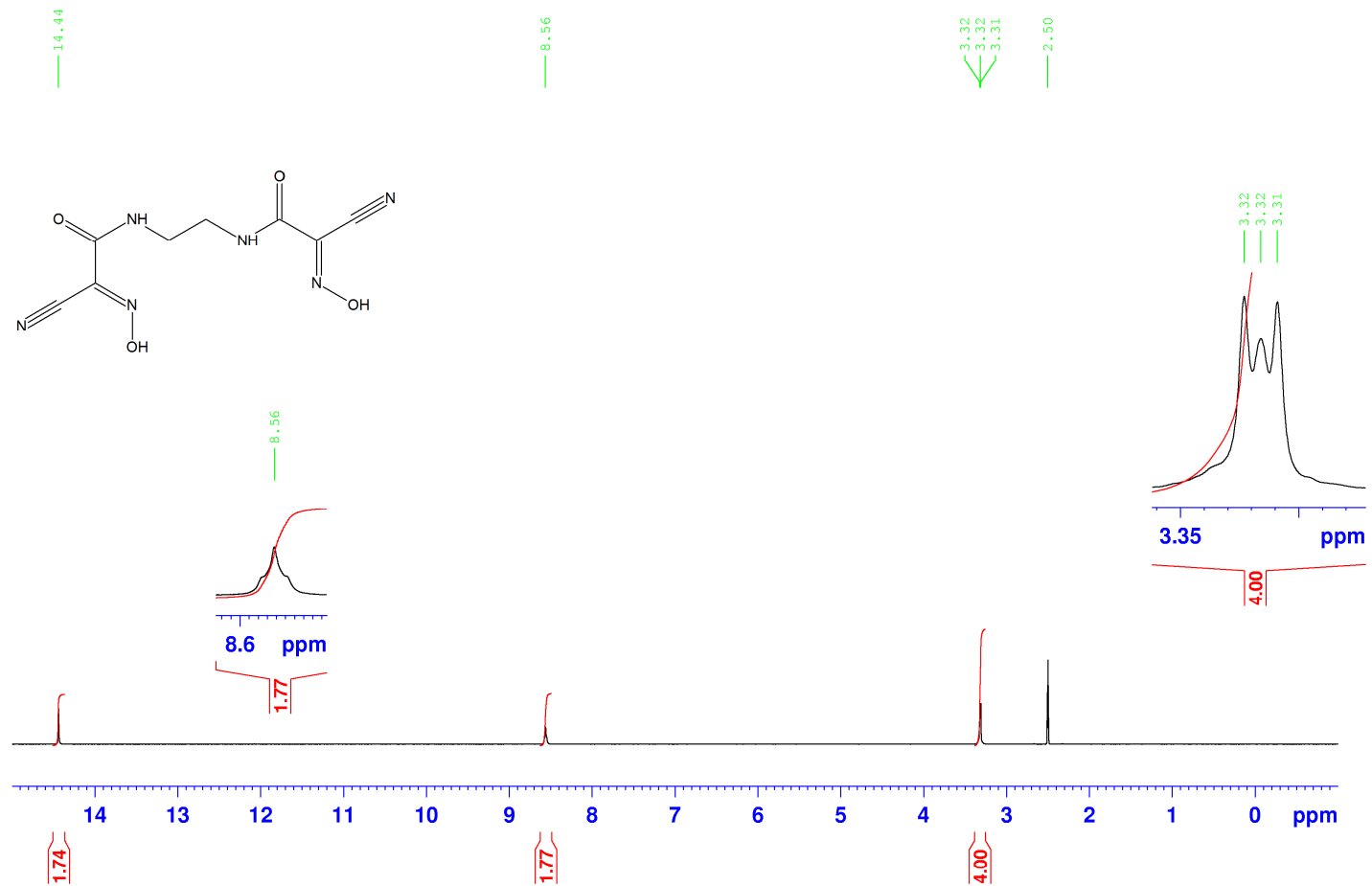


**Fig. B17.** <sup>1</sup>H NMR spectrum *N,N'*-ethane-1,2-diylbis[2-cyano-2-(hydroxyimino)ethanamide].

*N,N'*-ethane-1,2-diylbis[2-cyano-2-(hydroxyimino)ethanamide], <sup>13</sup>C, DMSO-d<sub>6</sub>

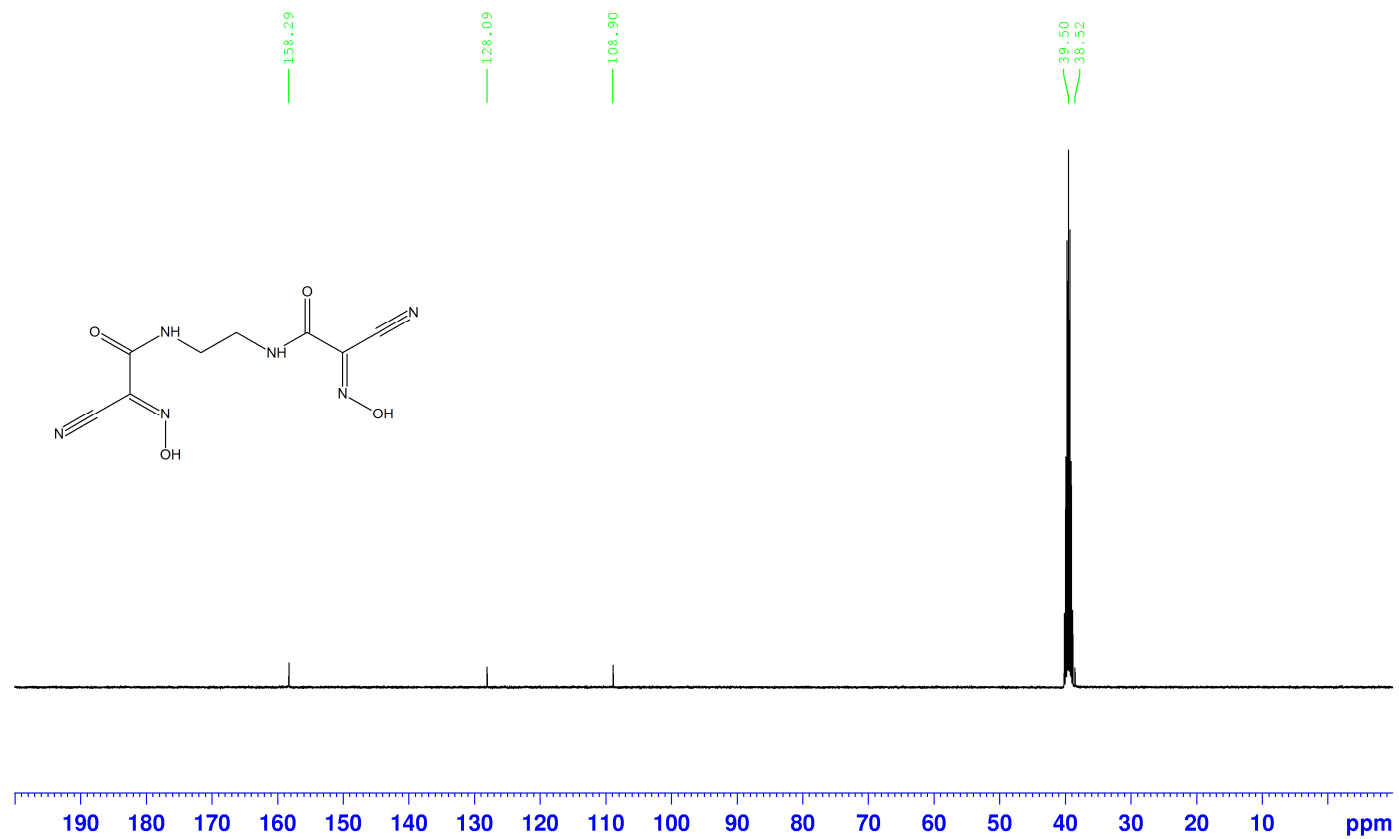


**Fig. B18.** <sup>13</sup>C NMR spectrum *N,N'*-ethane-1,2-diylbis[2-cyano-2-(hydroxyimino)ethanamide].

*N,N'*-ethane-1,2-diylbis[2-cyano-2-(hydroxyimino)ethanamide], DEPT 135, DMSO-d<sub>6</sub>

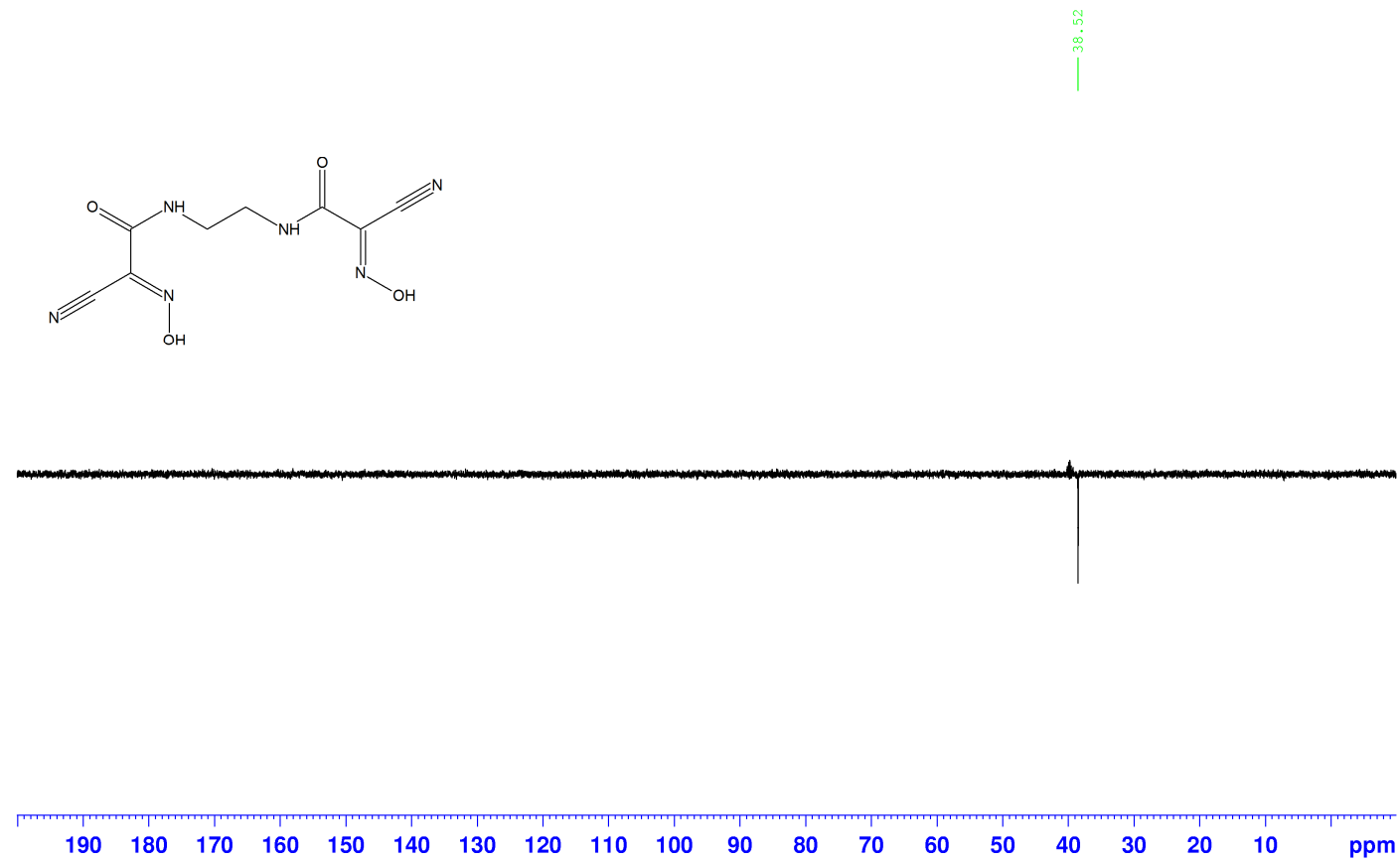


**Fig. B19.** DEPT 135 NMR spectrum *N,N'*-ethane-1,2-diylbis[2-cyano-2-(hydroxyimino)ethanamide].

*N,N'*-ethane-1,2-diylbis[2-cyano-2-(hydroxyimino)ethanamide], HSQC, DMSO-d<sub>6</sub>

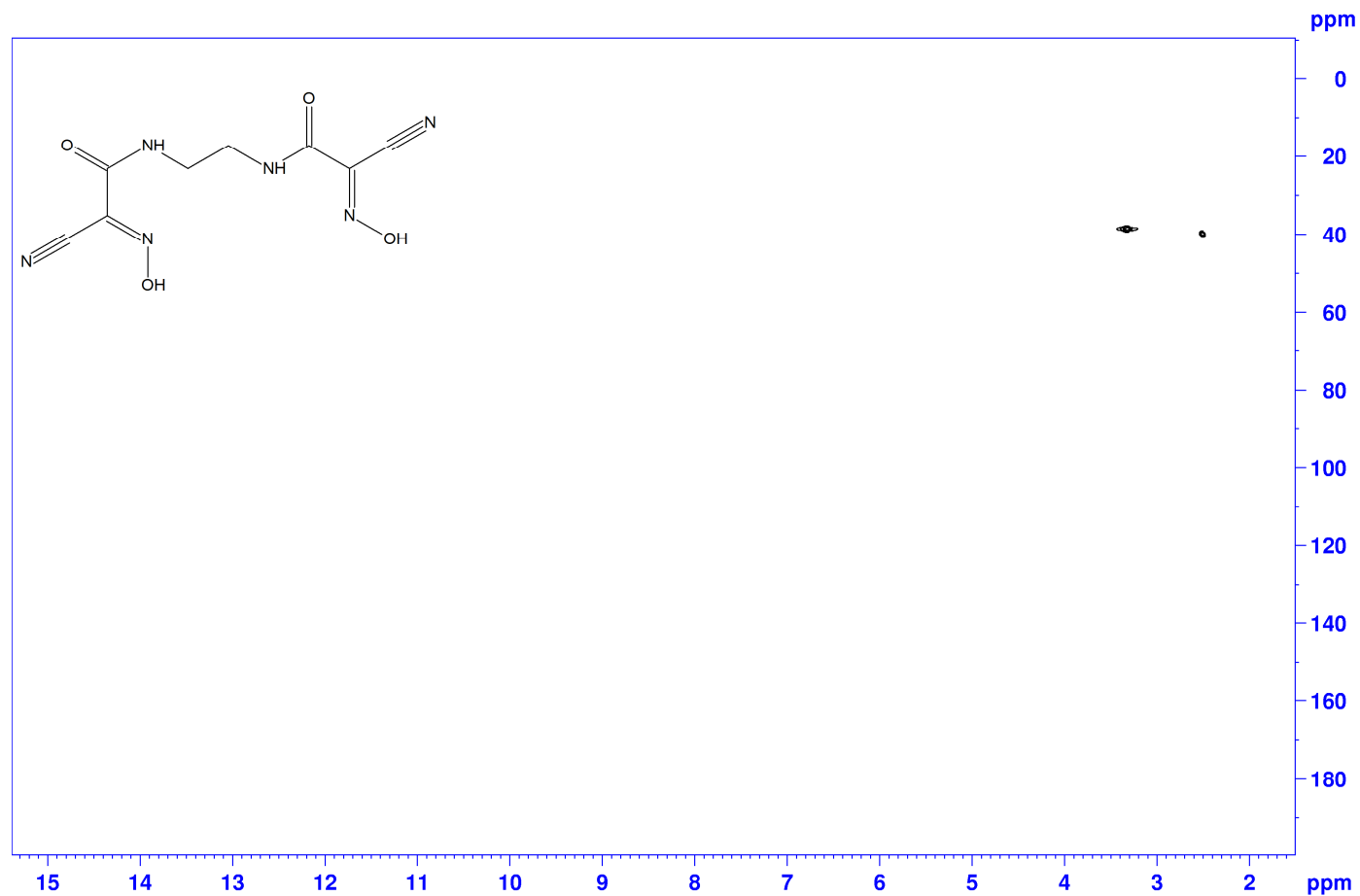


**Fig. B20.** HSQC NMR spectrum *N,N'*-ethane-1,2-diylbis[2-cyano-2-(hydroxyimino)ethanamide].

*N,N'*-ethane-1,2-diylbis[2-cyano-2-(hydroxyimino)ethanamide], HMBC, DMSO-d<sub>6</sub>

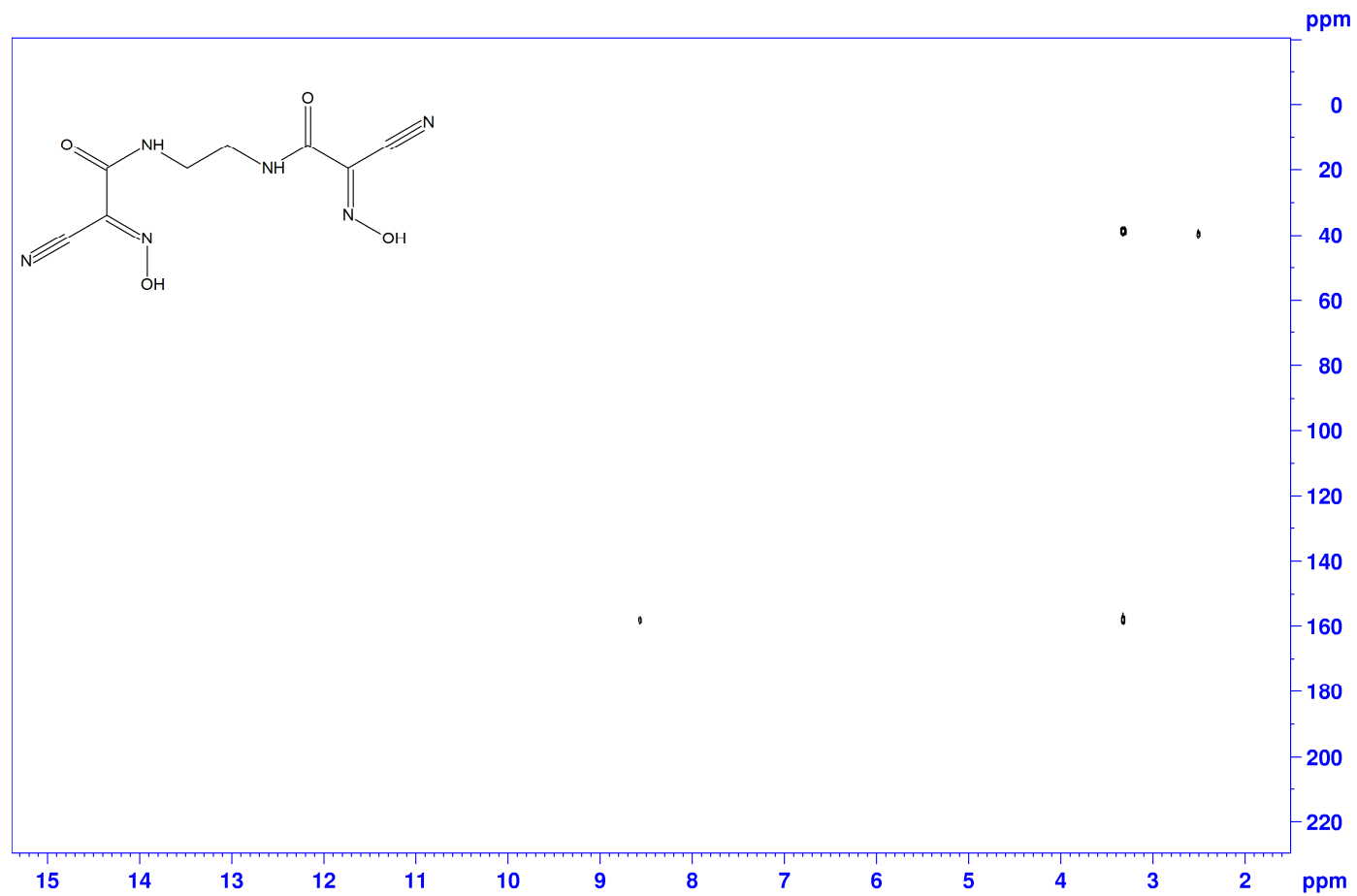


**Fig. B21.** HMBC NMR spectrum *N,N'*-ethane-1,2-diylbis[2-cyano-2-(hydroxyimino)ethanamide].

*N,N'*-ethane-1,2-diylbis[2-cyano-2-(hydroxyimino)ethanamide], COSY, DMSO-d6

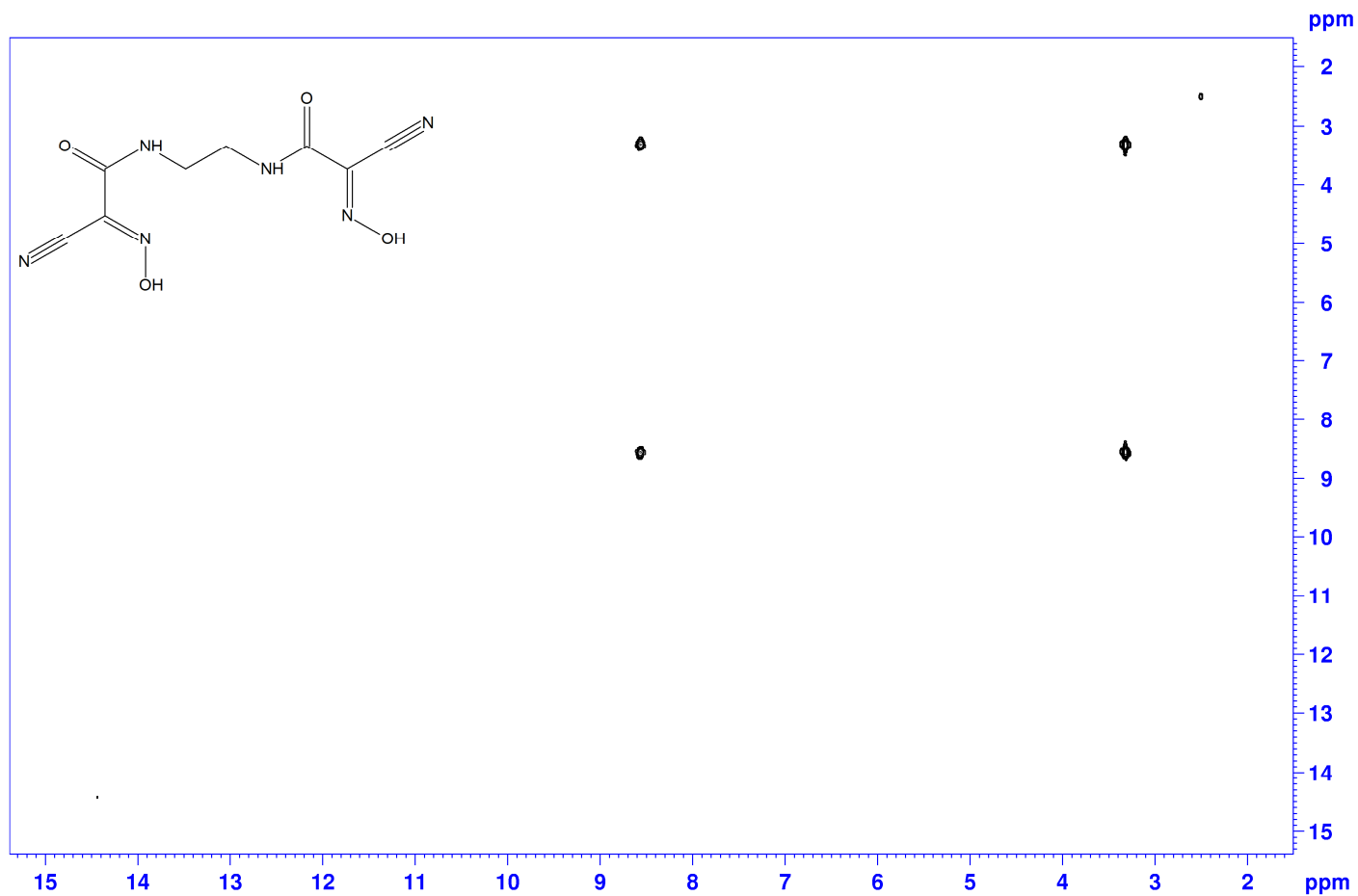


**Fig. B22.** COSY NMR spectrum of *N,N'*-ethane-1,2-diylbis[2-cyano-2-(hydroxyimino)ethanamide].

*N,N'*-ethane-1,2-diylbis[2-cyano-2-(hydroxyimino)ethanamide], LRMS

cnox\_jen\_combo\_sl LRMS 2 (0.017) Cm (1:30)

TOF MS ES-  
2.16e5

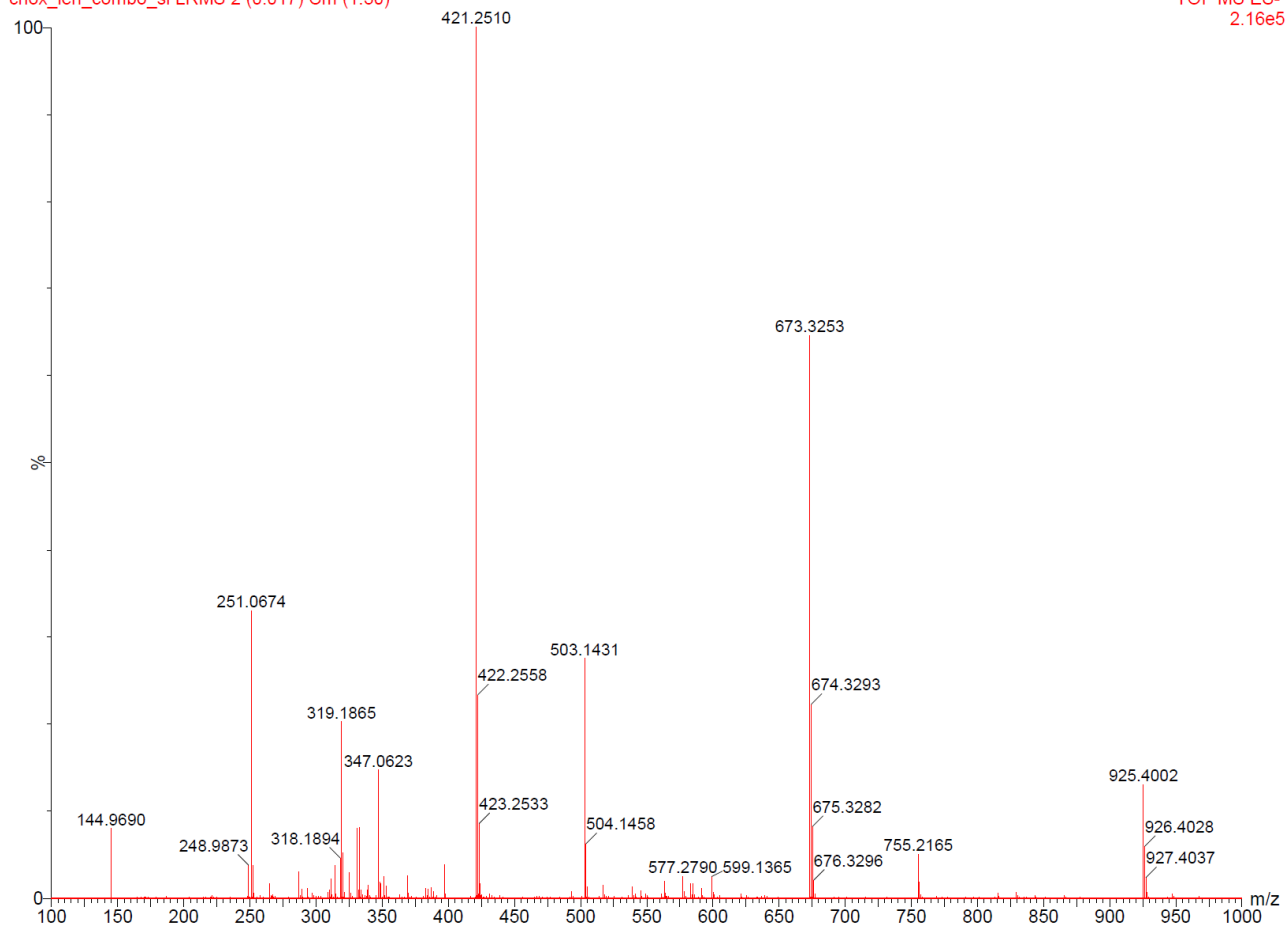


**Fig. B23.** Mass spectrum *N,N'*-ethane-1,2-diylbis[2-cyano-2-(hydroxyimino)ethanamide] without mass lock.



**Single Mass Analysis**

Tolerance = 3.0 PPM / DBE: min = -1.5, max = 100.0

Element prediction: Off

Number of isotope peaks used for i-FIT = 3

Monoisotopic Mass, Even Electron Ions

16 formula(e) evaluated with 1 results within limits (up to 50 best isotopic matches for each mass)

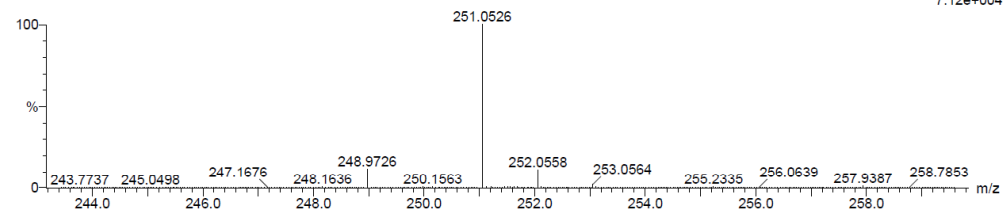
Elements Used:

C: 5-10 H: 5-10 N: 5-10 O: 0-5

cnox\_jen\_combo\_sl LRMS 2 (0.017) Cm (1:30)

TOF MS ES-

7.12e+004



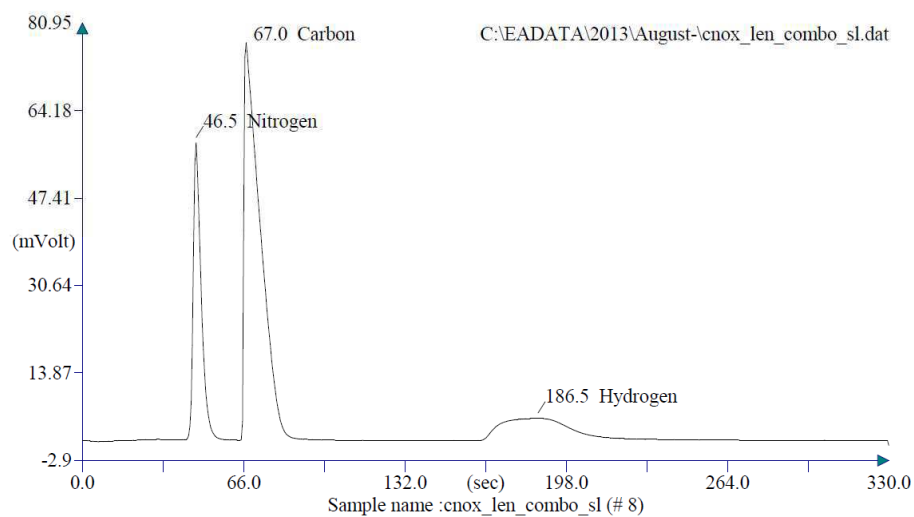
Minimum:

Maximum: 5.0 3.0 -1.5

Mass	Calc. Mass	mDa	PPM	DBE	i-FIT	i-FIT (Norm)	Formula
251.0526	251.0529	-0.3	-1.2	8.5	524.2	0.0	C8 H7 N6 O4

**Fig. B24.** Mass spectrum *N,N'*-ethane-1,2-diylbis[2-cyano-2-(hydroxyimino)ethanamide] with mass lock.

*N,N'*-ethane-1,2-diylbis[2-cyano-2-(hydroxyimino)ethanamide], CHN



Retention Time (min)	Element Name	Element %
0.775	Nitrogen	33.169
1.117	Carbon	37.782
3.108	Hydrogen	3.024
		<u>73.975</u>

**Fig. B25.** CHN chromatogram of *N,N'*-ethane-1,2-diylbis[2-cyano-2-(hydroxyimino)ethanamide].

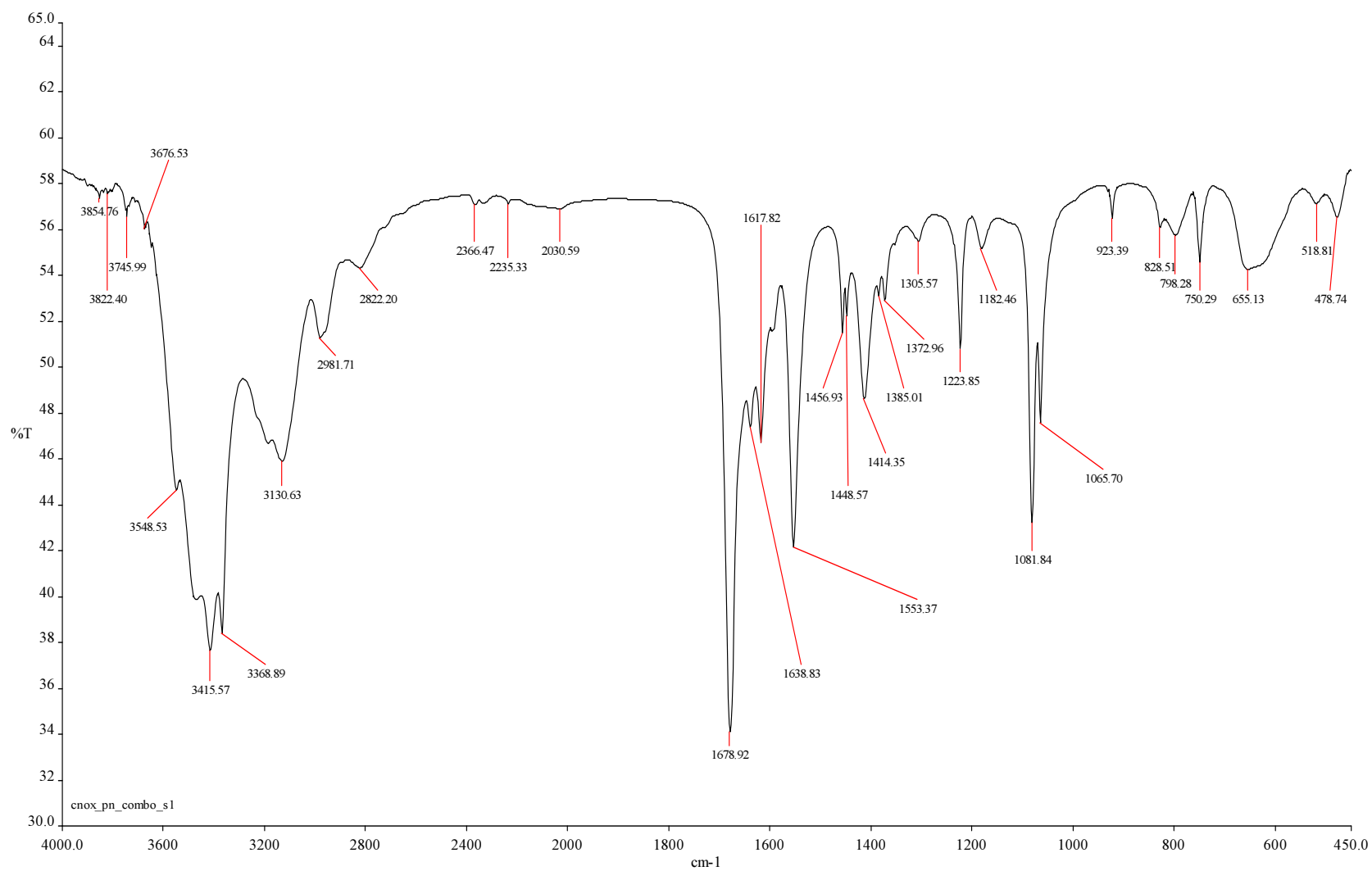


**Fig. B26.** IR spectrum of *N,N'*-propane-1,3-diybis[2-cyano-2-(hydroxyimino)ethanamide], KBr disk.

*N,N'*-propane-1,3-diylbis[2-cyano-2-(hydroxyimino)ethanamide], <sup>1</sup>H, DMSO-d<sub>6</sub>

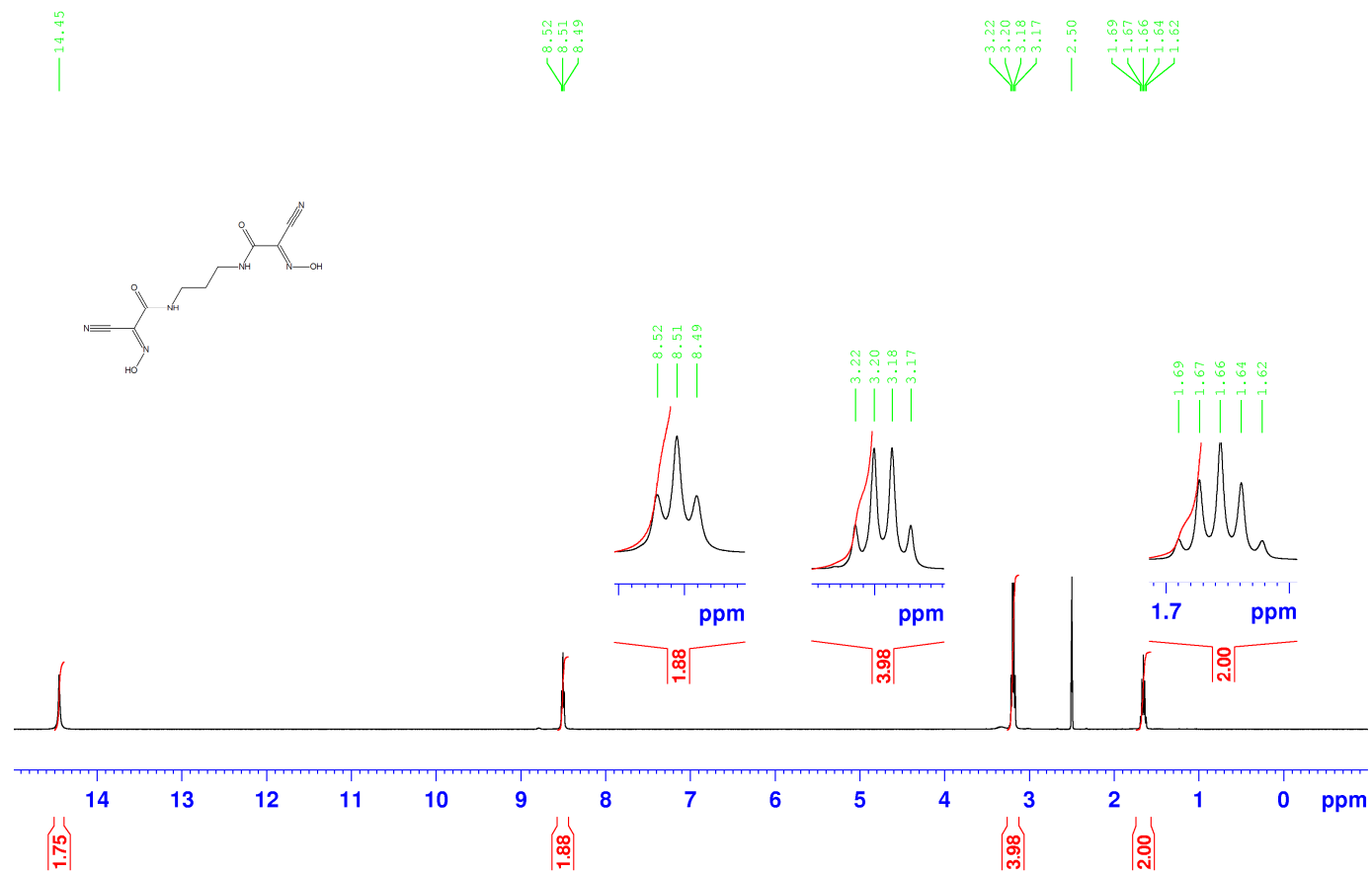


**Fig. B27.** <sup>1</sup>H NMR spectrum of *N,N'*-propane-1,3-diylbis[2-cyano-2-(hydroxyimino)ethanamide].

*N,N'*-propane-1,3-diylbis[2-cyano-2-(hydroxyimino)ethanamide],  $^{13}\text{C}$ ,  $\text{DMSO-d}_6$

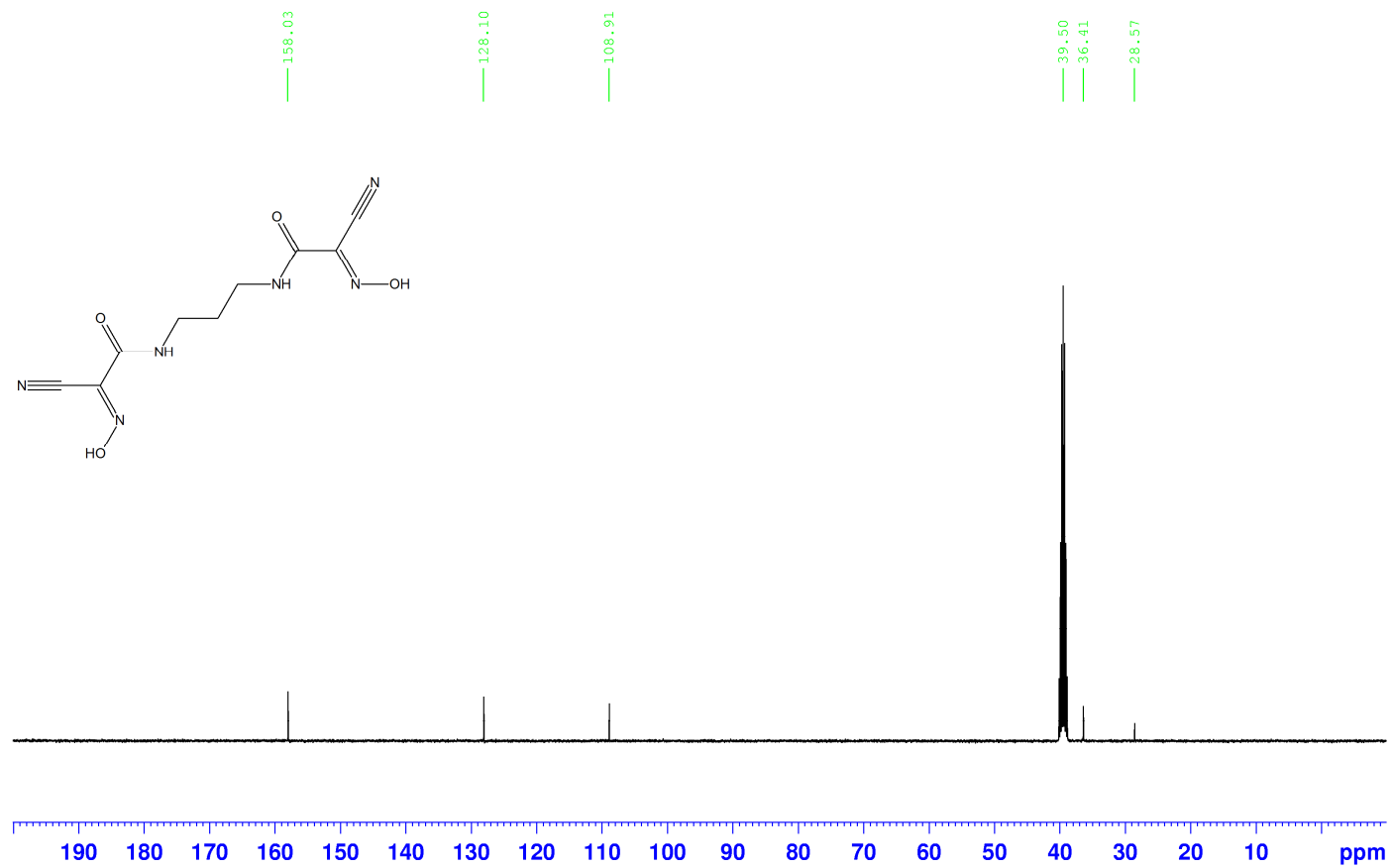


**Fig. B28.**  $^{13}\text{C}$  NMR spectrum of *N,N'*-propane-1,3-diylbis[2-cyano-2-(hydroxyimino)ethanamide].

*N,N'*-propane-1,3-diylbis[2-cyano-2-(hydroxyimino)ethanamide], DEPT 135, DMSO-d<sub>6</sub>

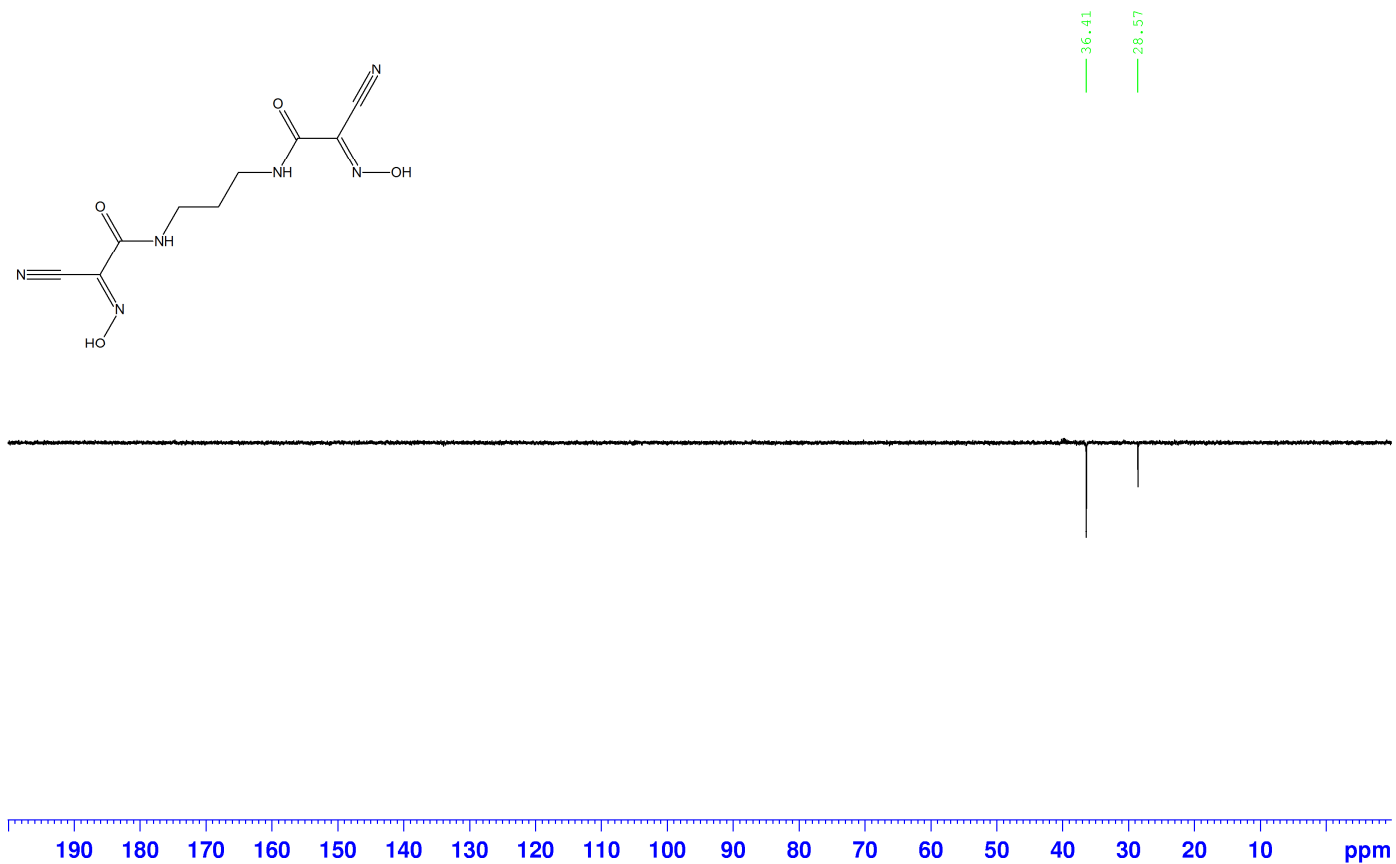


**Fig. B29.** DEPT 135 NMR spectrum of *N,N'*-propane-1,3-diylbis[2-cyano-2-(hydroxyimino)ethanamide].

*N,N'*-propane-1,3-diylbis[2-cyano-2-(hydroxyimino)ethanamide], HSQC, DMSO-d<sub>6</sub>

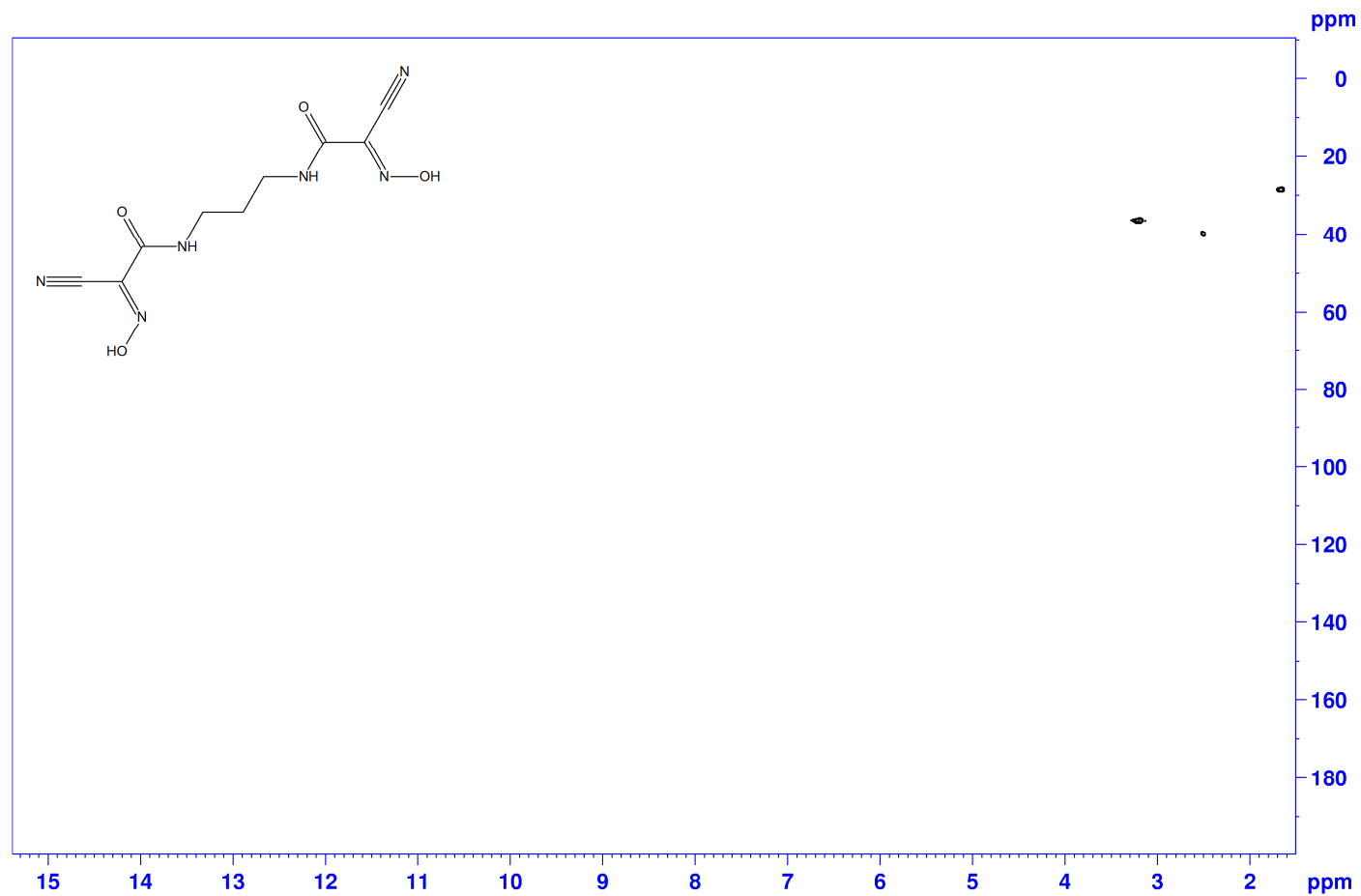


**Fig. B30.** HSQC NMR spectrum of *N,N'*-propane-1,3-diylbis[2-cyano-2-(hydroxyimino)ethanamide].

*N,N'*-propane-1,3-diylbis[2-cyano-2-(hydroxyimino)ethanamide], HMBC, DMSO-d<sub>6</sub>

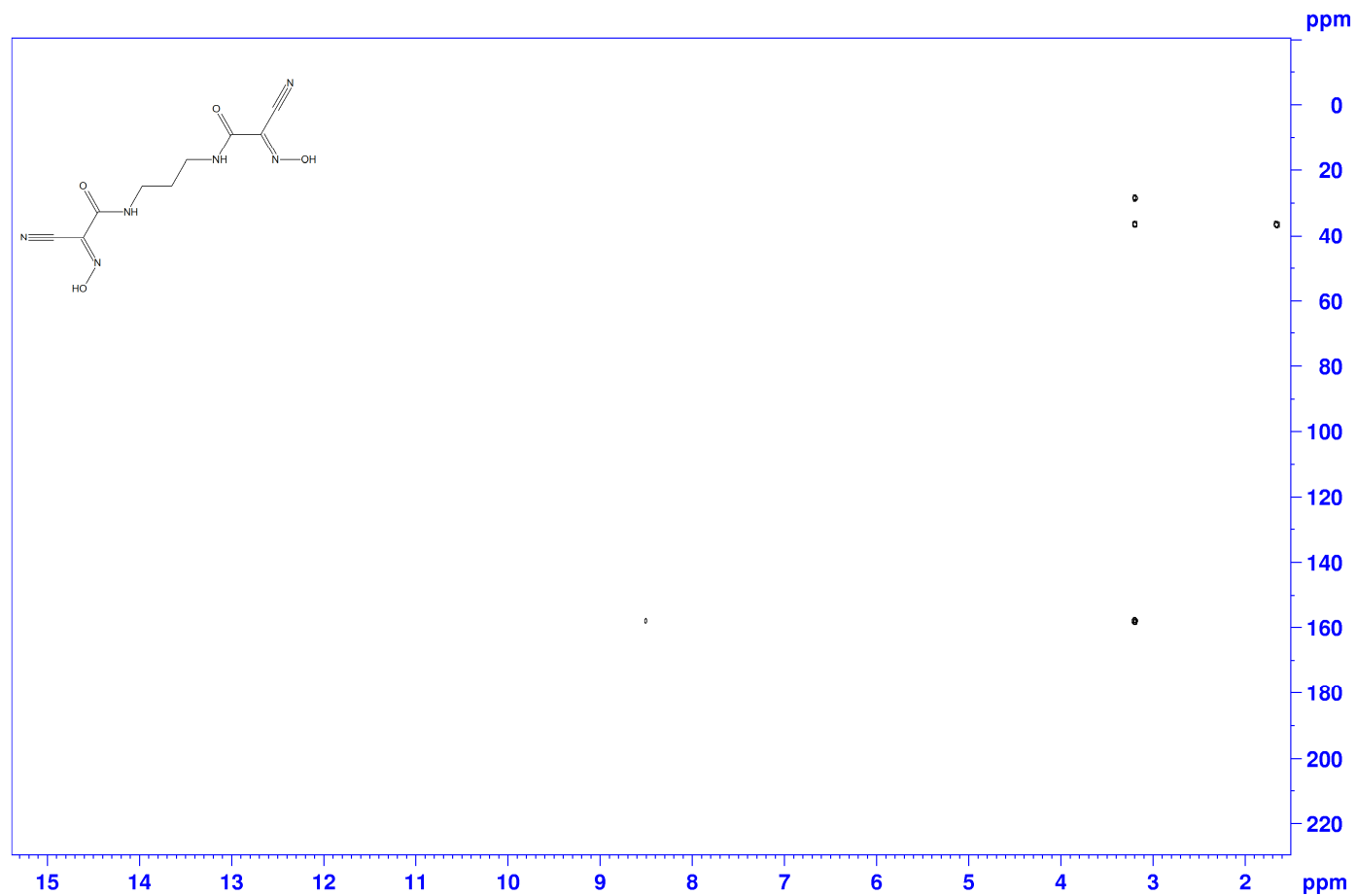


**Fig. B31.** HMBC NMR spectrum of *N,N'*-propane-1,3-diylbis[2-cyano-2-(hydroxyimino)ethanamide].



*N,N'*-propane-1,3-diylbis[2-cyano-2-(hydroxyimino)ethanamide], COSY, DMSO-d<sub>6</sub>

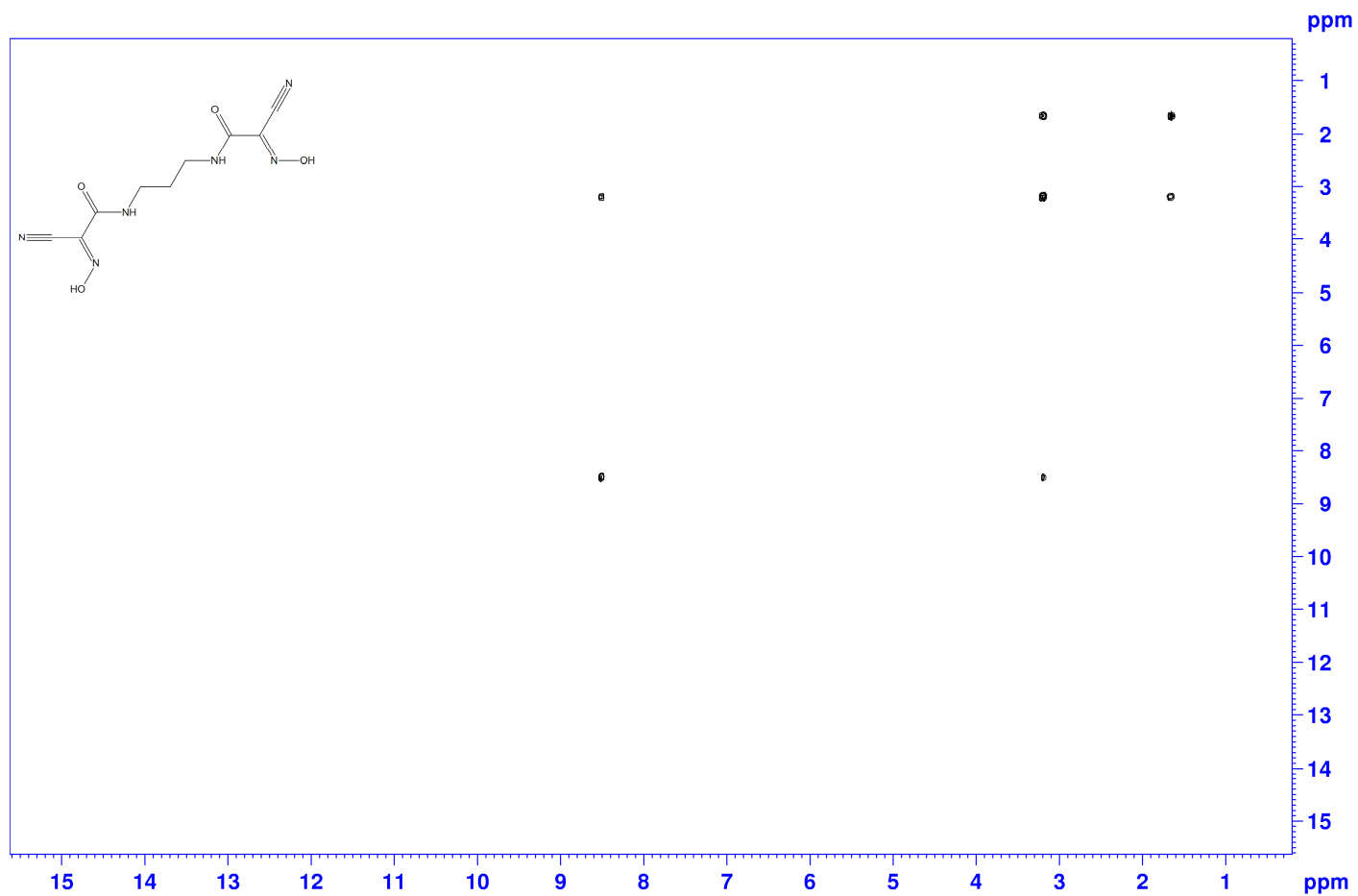


**Fig. B32.** COSY NMR spectrum of *N,N'*-propane-1,3-diylbis[2-cyano-2-(hydroxyimino)ethanamide].

*N,N'*-propane-1,3-diylbis[2-cyano-2-(hydroxyimino)ethanamide], LRMS

cnox-lpn-combo-sl LRMS 2 (0.017) Cm (1:31)

TOF MS ES-  
1.46e4

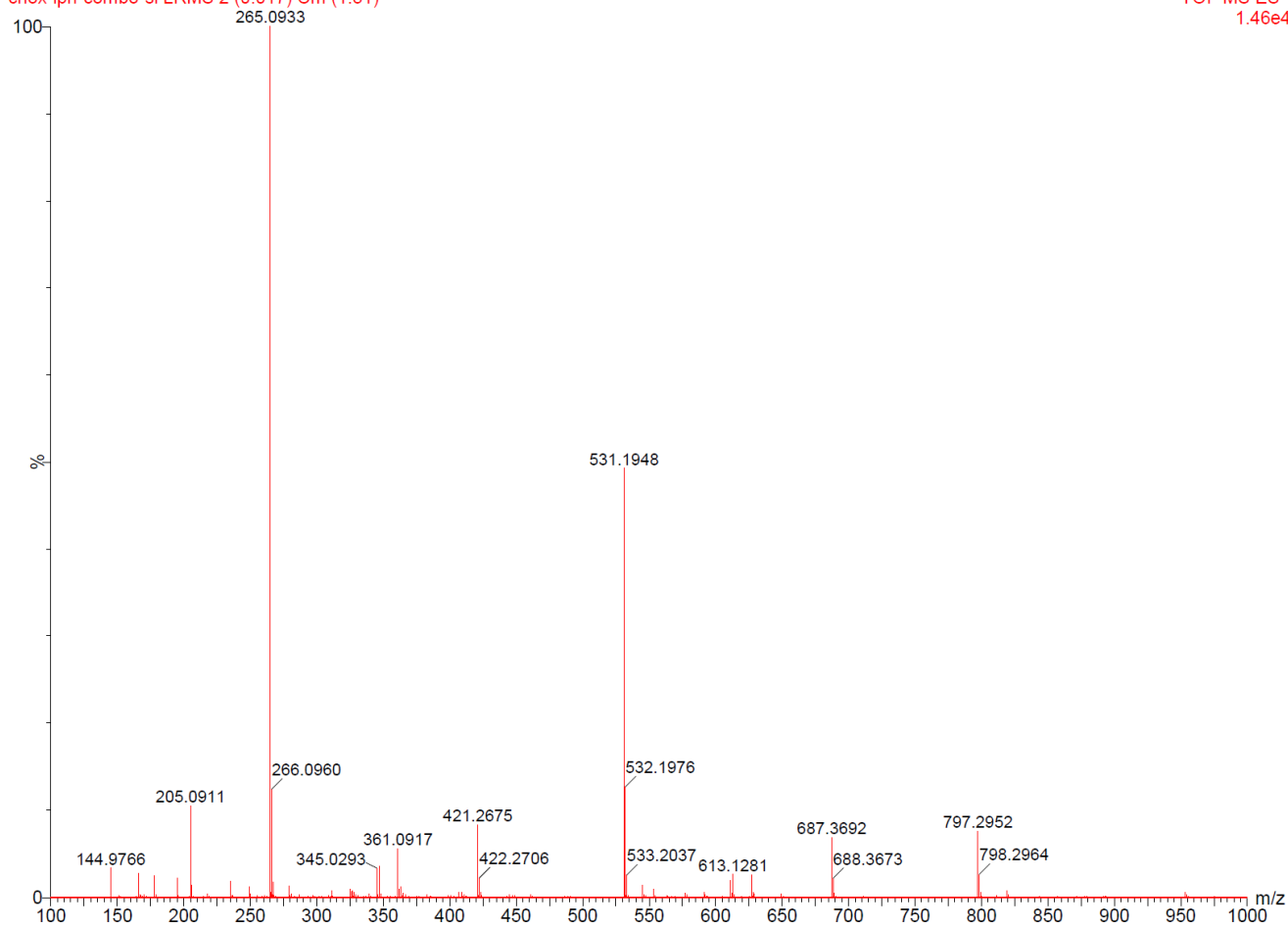


**Fig. B33.** Mass spectrum of *N,N'*-propane-1,3-diylbis[2-cyano-2-(hydroxyimino)ethanamide] without mass lock.

**Single Mass Analysis**

Tolerance = 3.0 PPM / DBE: min = -1.5, max = 100.0

Element prediction: Off

Number of isotope peaks used for i-FIT = 3

Monoisotopic Mass, Even Electron Ions

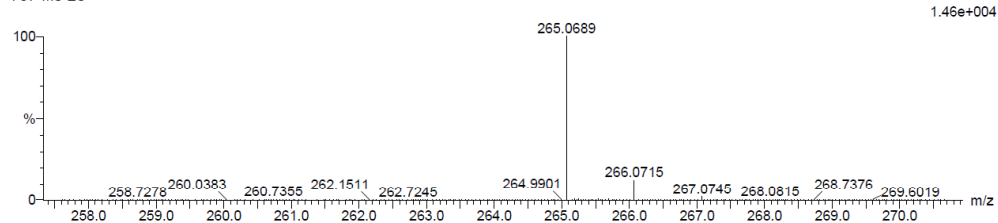
17 formula(e) evaluated with 1 results within limits (up to 50 best isotopic matches for each mass)

Elements Used:

C: 5-10 H: 5-10 N: 5-10 O: 0-5

cnox-1pn-combo-sl LRMS 2 (0.017) Cm (1:31)

TOF MS ES-



Mass	Calc. Mass	mDa	PPM	DBE	i-FIT	i-FIT (Norm)	Formula
265.0689	265.0685	0.4	1.5	8.5	316.0	0.0	C9 H9 N6 O4

**Fig. B34.** Mass spectrum of *N,N'*-propane-1,3-diylbis[2-cyano-2-(hydroxyimino)ethanamide] with mass lock.

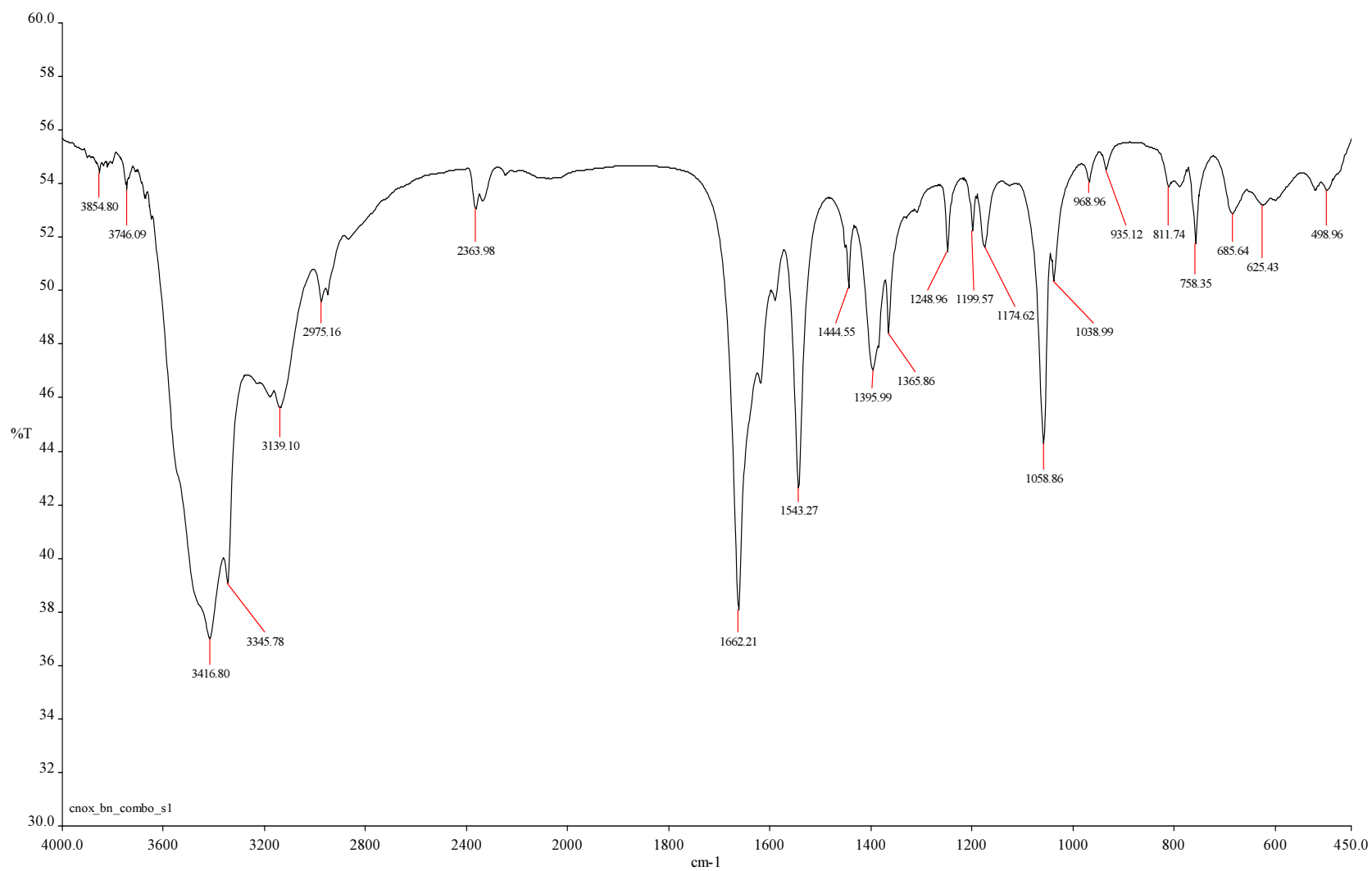


**Fig. B35.** IR spectrum of *N,N'*-butane-1,4-diylbis[2-cyano-2-(hydroxyimino)ethanamide] , KBr disk.

*N,N'*-butane-1,4-diylbis[2-cyano-2-(hydroxyimino)ethanamide], 1H, DMSO-d6

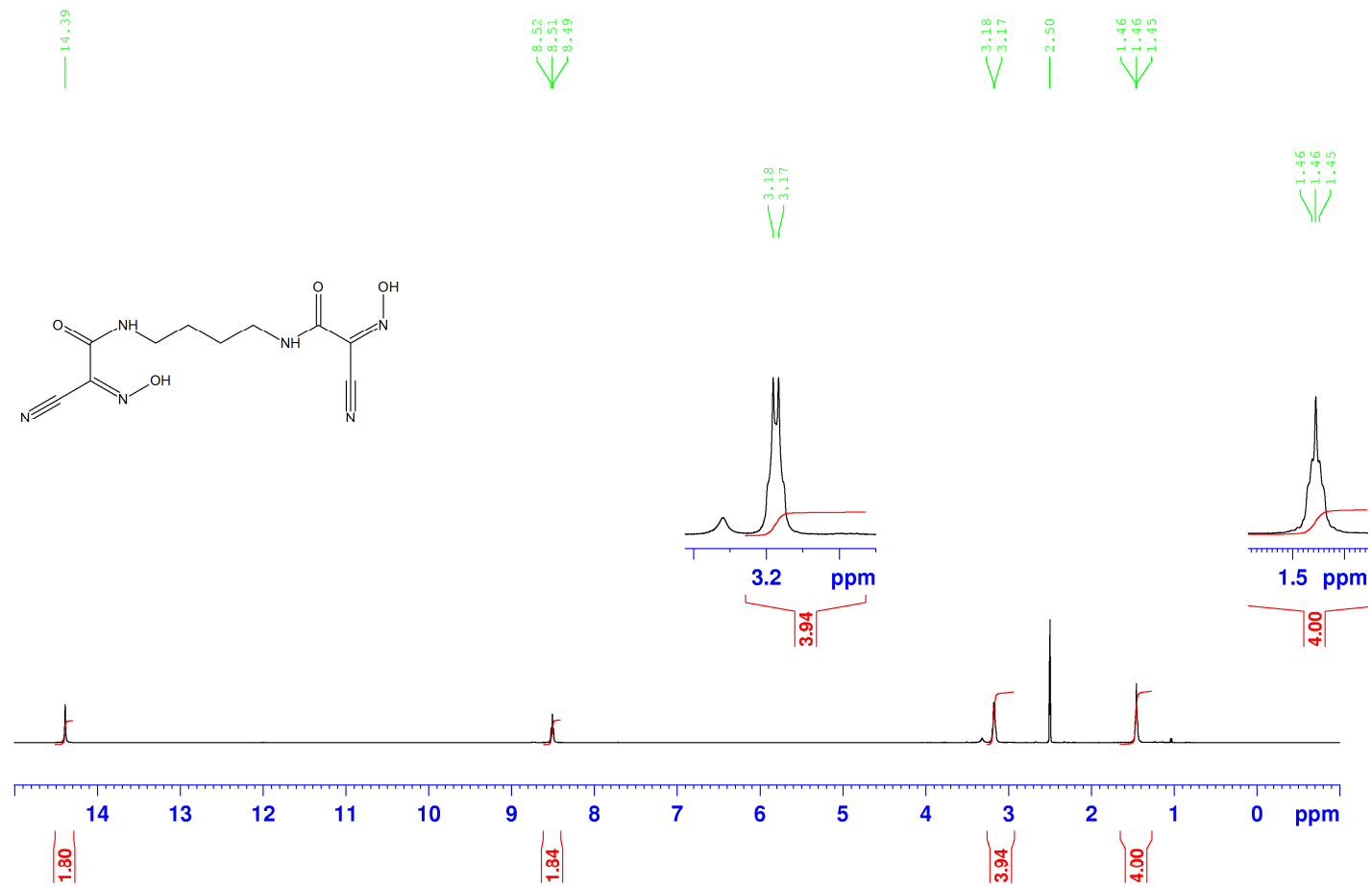


**Fig. B36.** <sup>1</sup>H NMR spectrum of *N,N'*-butane-1,4-diylbis[2-cyano-2-(hydroxyimino)ethanamide].

*N,N'*-butane-1,4-diylbis[2-cyano-2-(hydroxyimino)ethanamide],  $^{13}\text{C}$ , DMSO- $d_6$

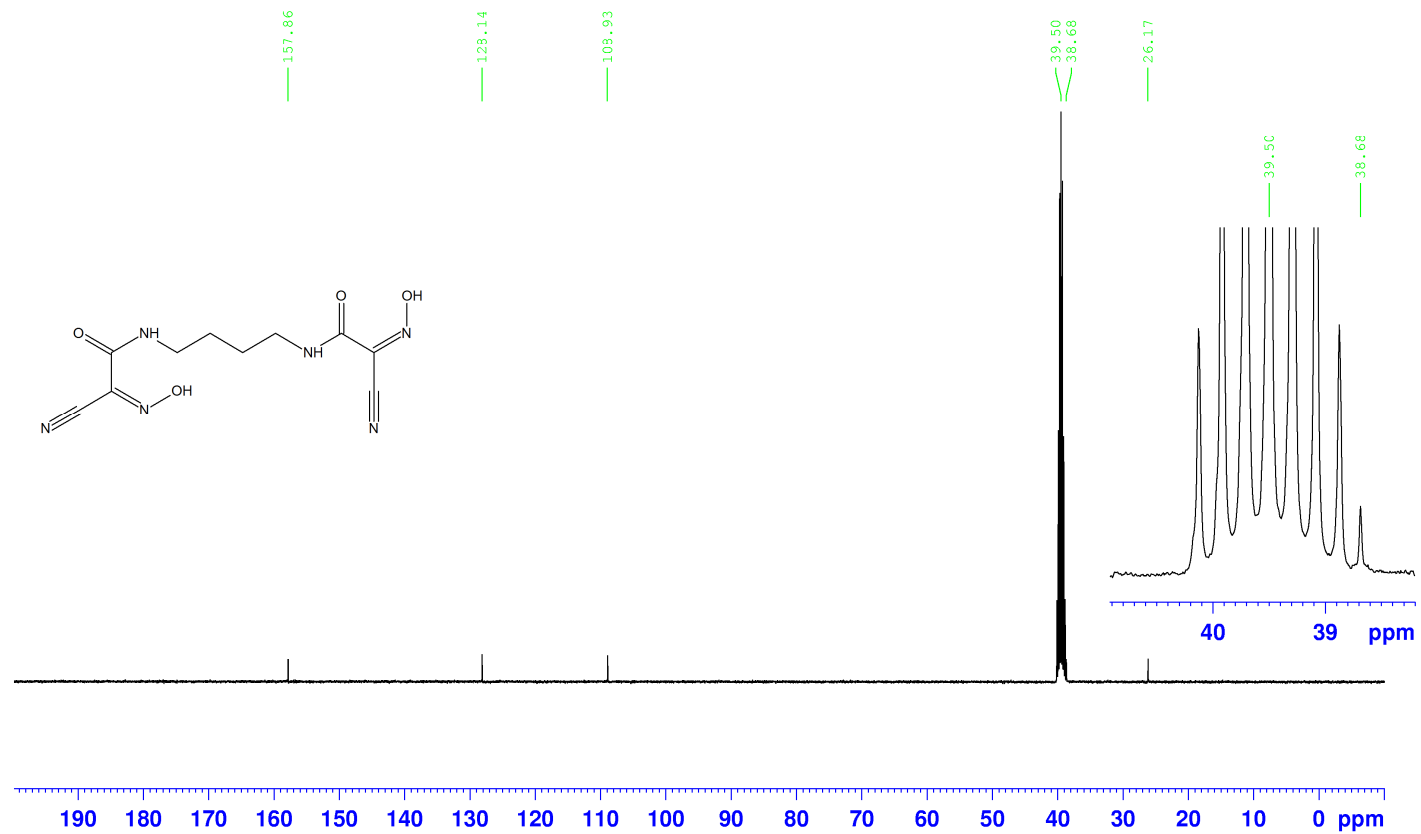


**Fig. B37.**  $^{13}\text{C}$  NMR spectrum of *N,N'*-butane-1,4-diylbis[2-cyano-2-(hydroxyimino)ethanamide].

*N,N'*-butane-1,4-diylbis[2-cyano-2-(hydroxyimino)ethanamide], <sup>13</sup>C, DMSO-d<sub>6</sub>

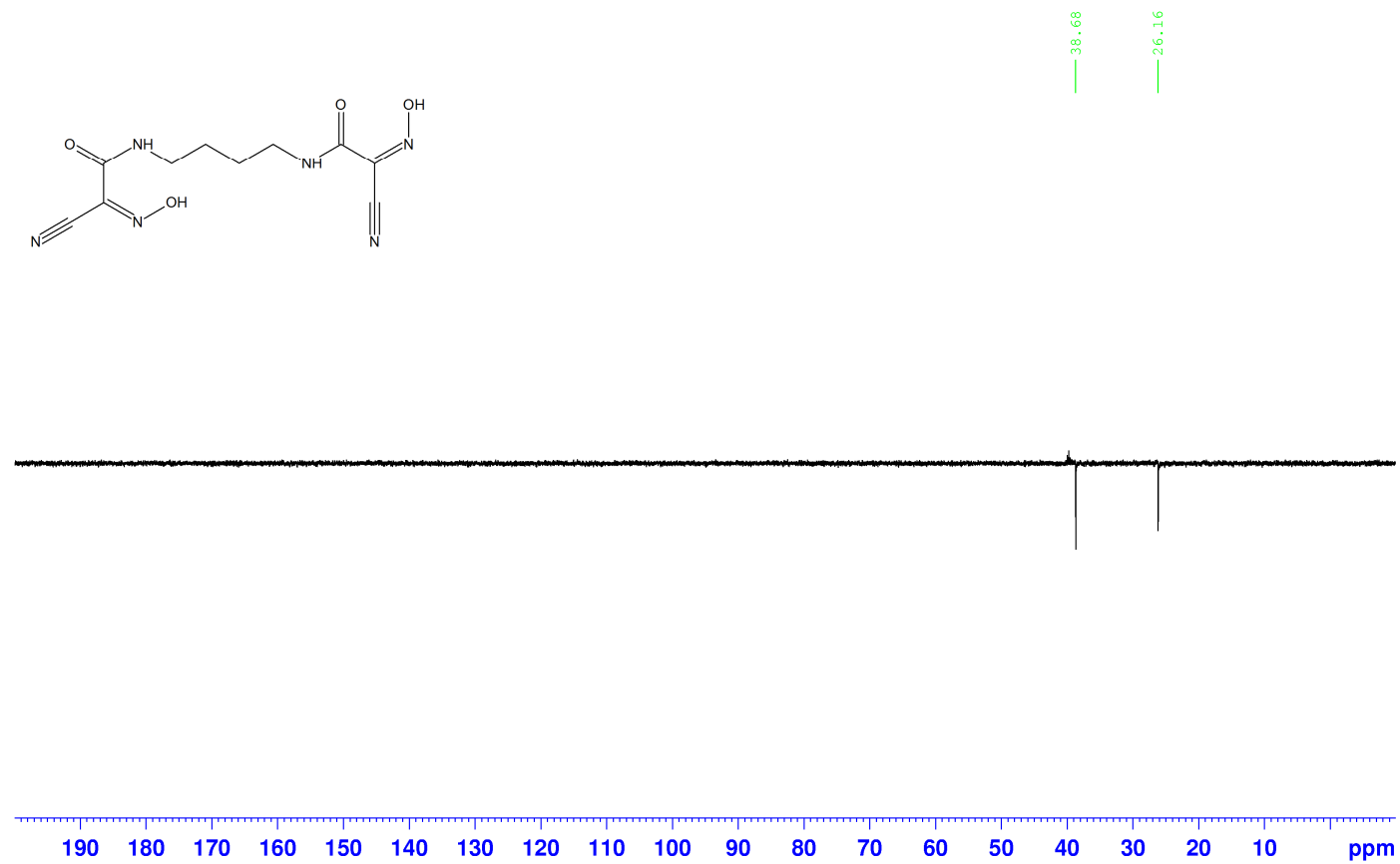
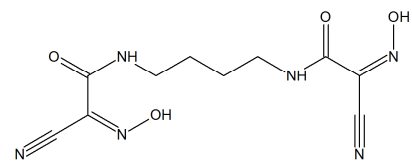


**Fig. B38.** DEPT 135 NMR spectrum of *N,N'*-butane-1,4-diylbis[2-cyano-2-(hydroxyimino)ethanamide].

*N,N'*-butane-1,4-diylbis[2-cyano-2-(hydroxyimino)ethanamide], HSQC, DMSO-d<sub>6</sub>

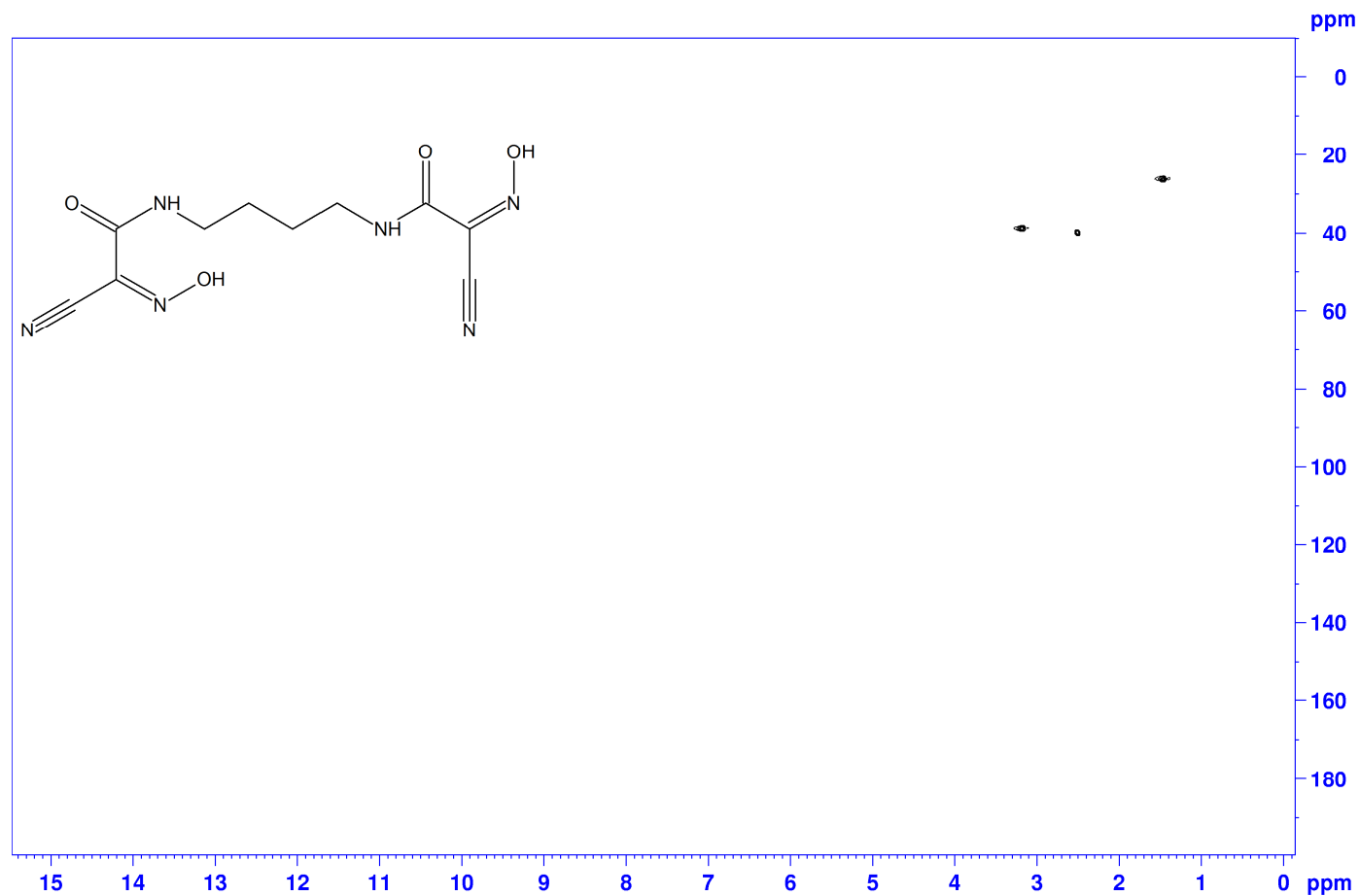


**Fig. B39.** HSQC NMR spectrum of *N,N'*-butane-1,4-diylbis[2-cyano-2-(hydroxyimino)ethanamide].



*N,N'*-butane-1,4-diylbis[2-cyano-2-(hydroxyimino)ethanamide], HMBC, DMSO-d<sub>6</sub>

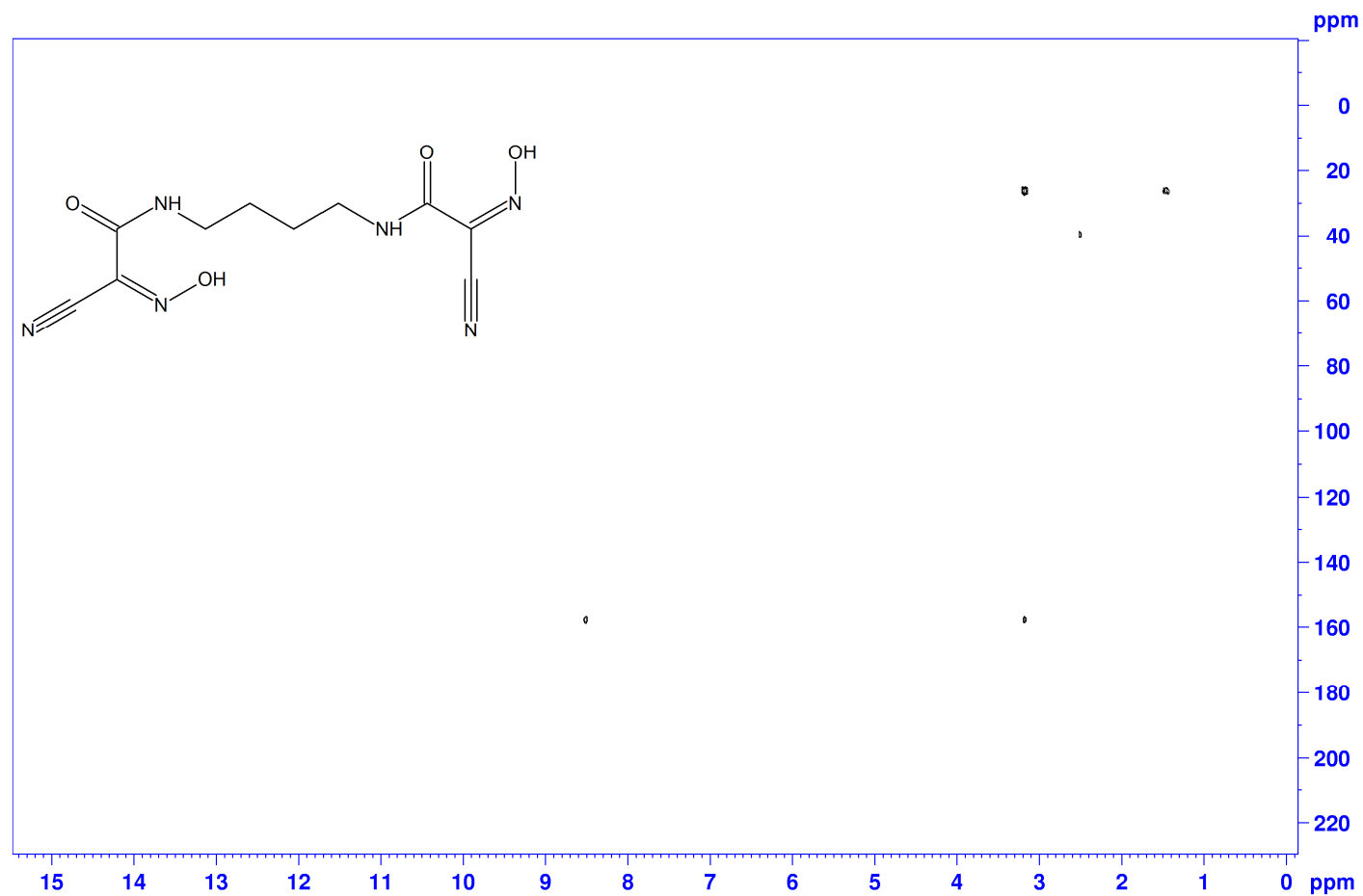


**Fig. B40.** HMBC NMR spectrum of *N,N'*-butane-1,4-diylbis[2-cyano-2-(hydroxyimino)ethanamide].

*N,N'*-butane-1,4-diylbis[2-cyano-2-(hydroxyimino)ethanamide], COSY, DMSO-d<sub>6</sub>

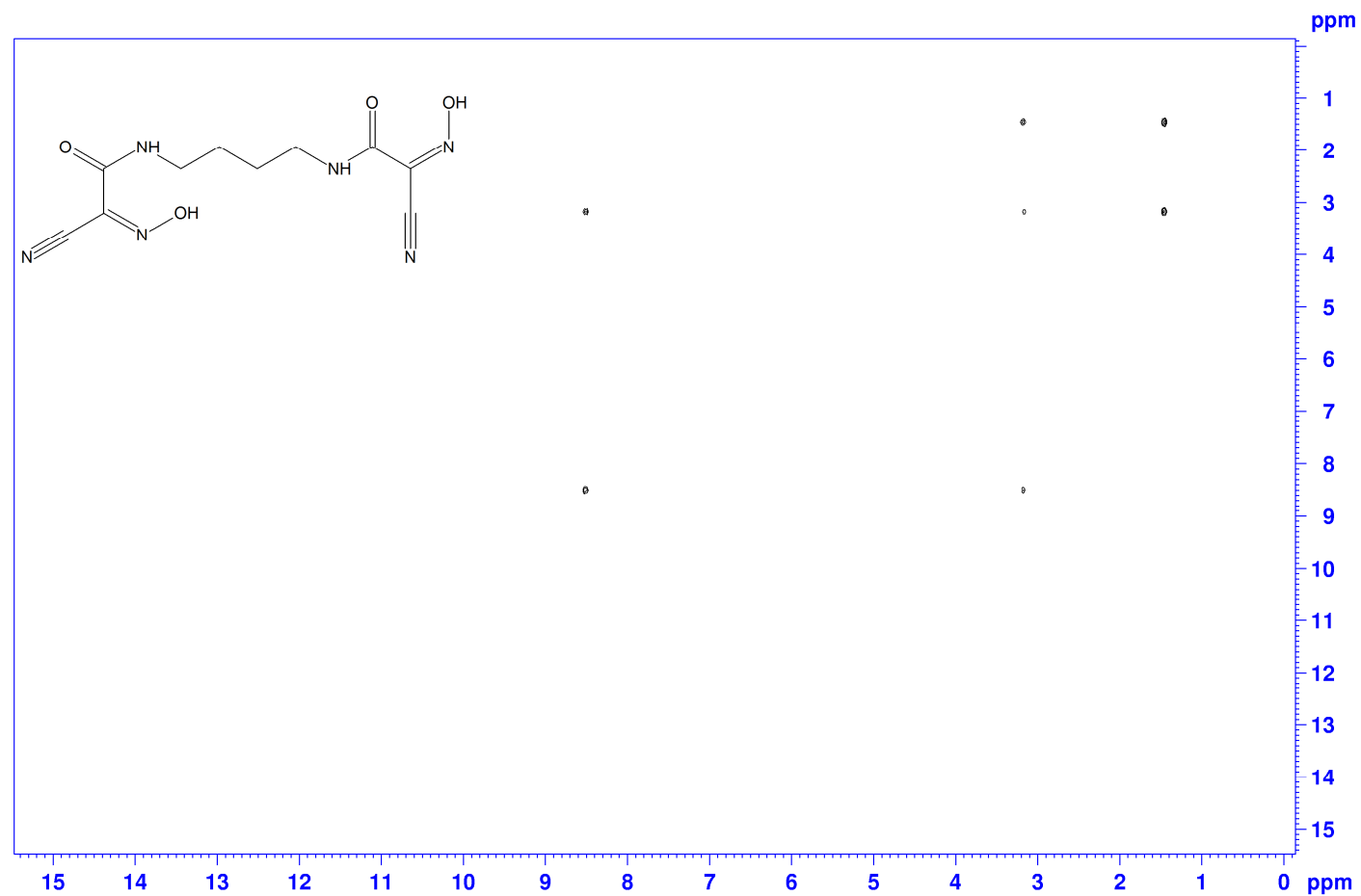


**Fig. B41.** COSY NMR spectrum of *N,N'*-butane-1,4-diylbis[2-cyano-2-(hydroxyimino)ethanamide].

*N,N'*-butane-1,4-diylbis[2-cyano-2-(hydroxyimino)ethanamide], LRMS

cnox-lbn-combo-sl LRMS 4 (0.052) Cm (1:31)

TOF MS ES-  
2.52e4

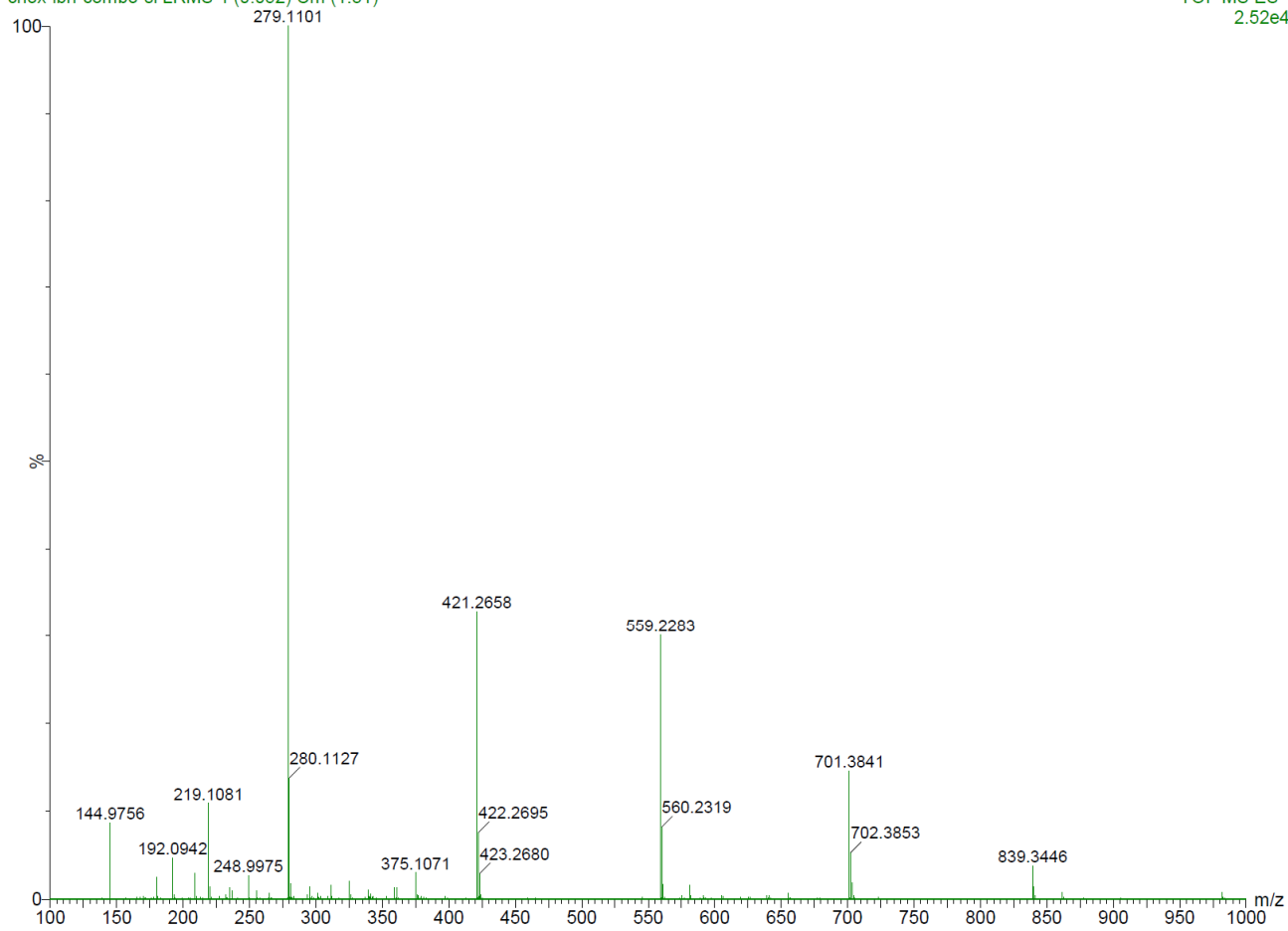


**Fig. B42.** Mass spectrum of *N,N'*-butane-1,4-diylbis[2-cyano-2-(hydroxyimino)ethanamide] without mass lock.

**Single Mass Analysis**

Tolerance = 5.0 PPM / DBE: min = -1.5, max = 100.0

Element prediction: Off

Number of isotope peaks used for i-FIT = 3

Monoisotopic Mass, Even Electron Ions

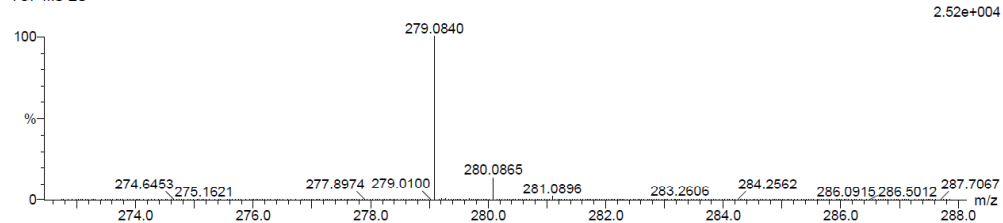
20 formula(e) evaluated with 1 results within limits (up to 50 best isotopic matches for each mass)

Elements Used:

C: 5-10 H: 10-15 N: 5-10 O: 0-5

cnx-lbn-combo-sl LRMS 4 (0.052) Cm (1:31)

TOF MS ES-



Minimum:

5.0 5.0 -1.5

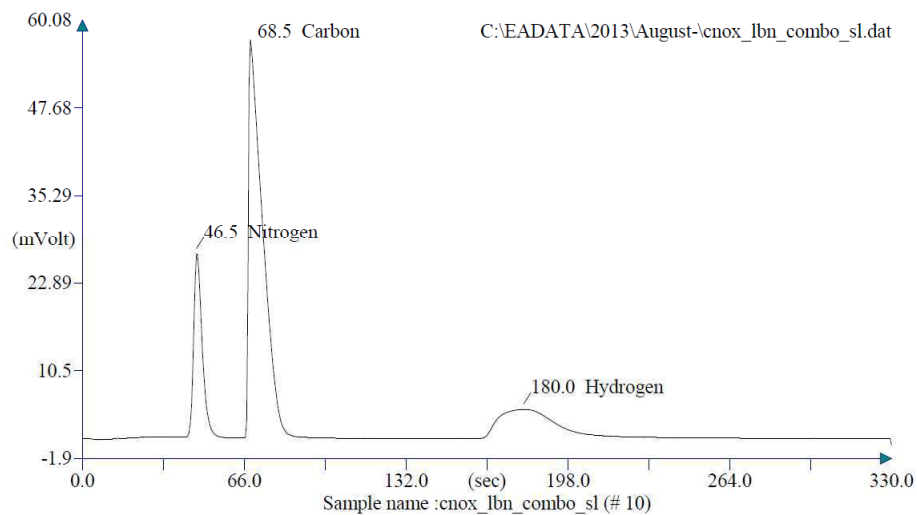
Maximum:

100.0 100.0

Mass	Calc. Mass	mDa	PPM	DBE	i-FIT	i-FIT (Norm)	Formula
279.0840	279.0842	-0.2	-0.7	8.5	371.7	0.0	C10 H11 N6 O4

**Fig. B43.** Mass spectrum of *N,N'*-butane-1,4-diylbis[2-cyano-2-(hydroxyimino)ethanamide] with mass lock.

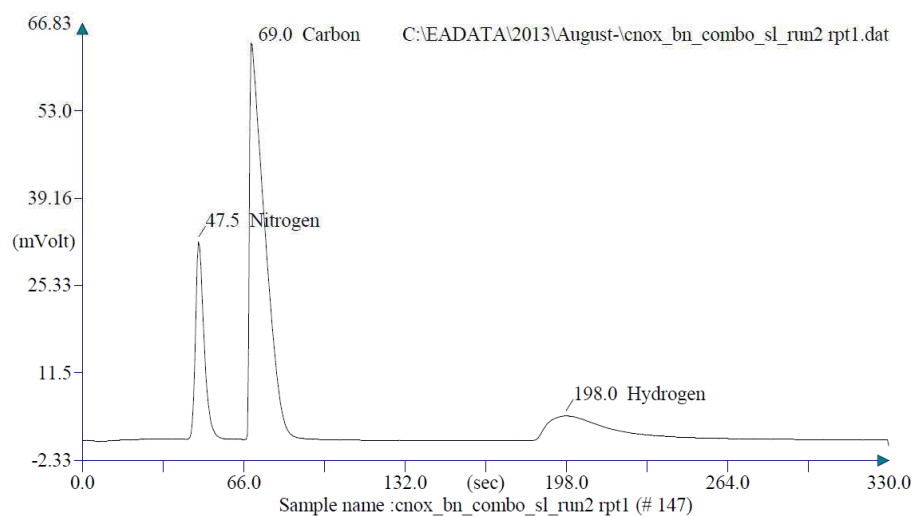
*N,N'*-butane-1,4-diylbis[2-cyano-2-(hydroxyimino)ethanamide], CHN



Retention Time (min)	Element Name	Element %
0.775	Nitrogen	28.923
1.142	Carbon	43.241
3.000	Hydrogen	4.256
		<hr/>
		76.420

**Fig. B44.** CHN chromatogram of *N,N'*-butane-1,4-diylbis[2-cyano-2-(hydroxyimino)ethanamide] 1.

*N,N'*-butane-1,4-diylbis[2-cyano-2-(hydroxyimino)ethanamide], CHN



Retention Time (min)	Element Name	Element %
0.792	Nitrogen	29.612
1.150	Carbon	43.993
3.300	Hydrogen	3.810
		<u>77.415</u>

**Fig. B45.** CHN chromatogram of *N,N'*-butane-1,4-diylbis[2-cyano-2-(hydroxyimino)ethanamide] 2.

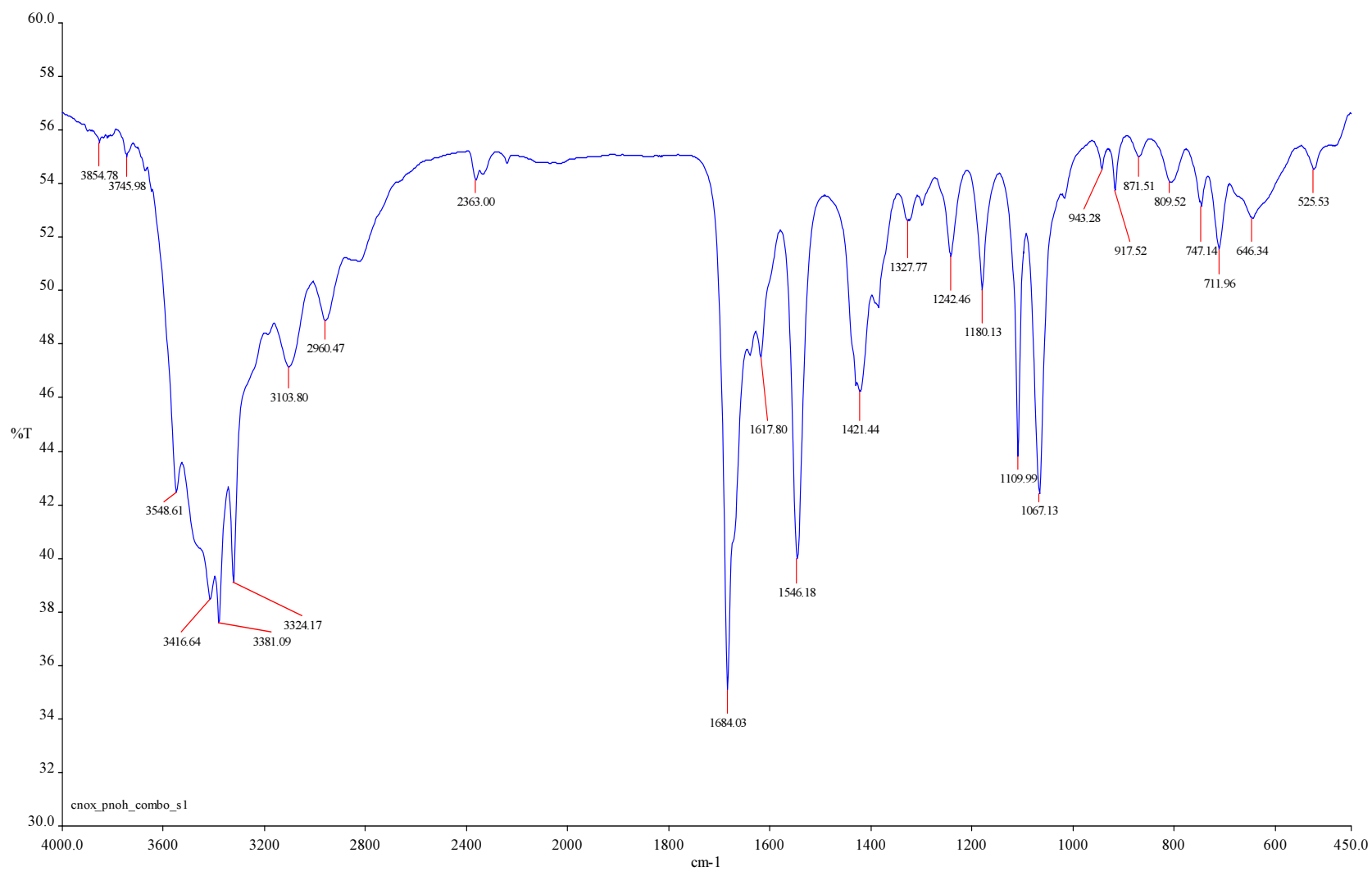


**Fig. B46.** IR spectrum of *N,N'*-butane-1,4-diylbis[2-cyano-2-(hydroxyimino)ethanamide] , KBr disk.

*N,N'*-(2-hydroxypropane-1,3-diyl)bis[2-cyano-2-(hydroxyimino)ethanamide], 1H, DMSO-d6

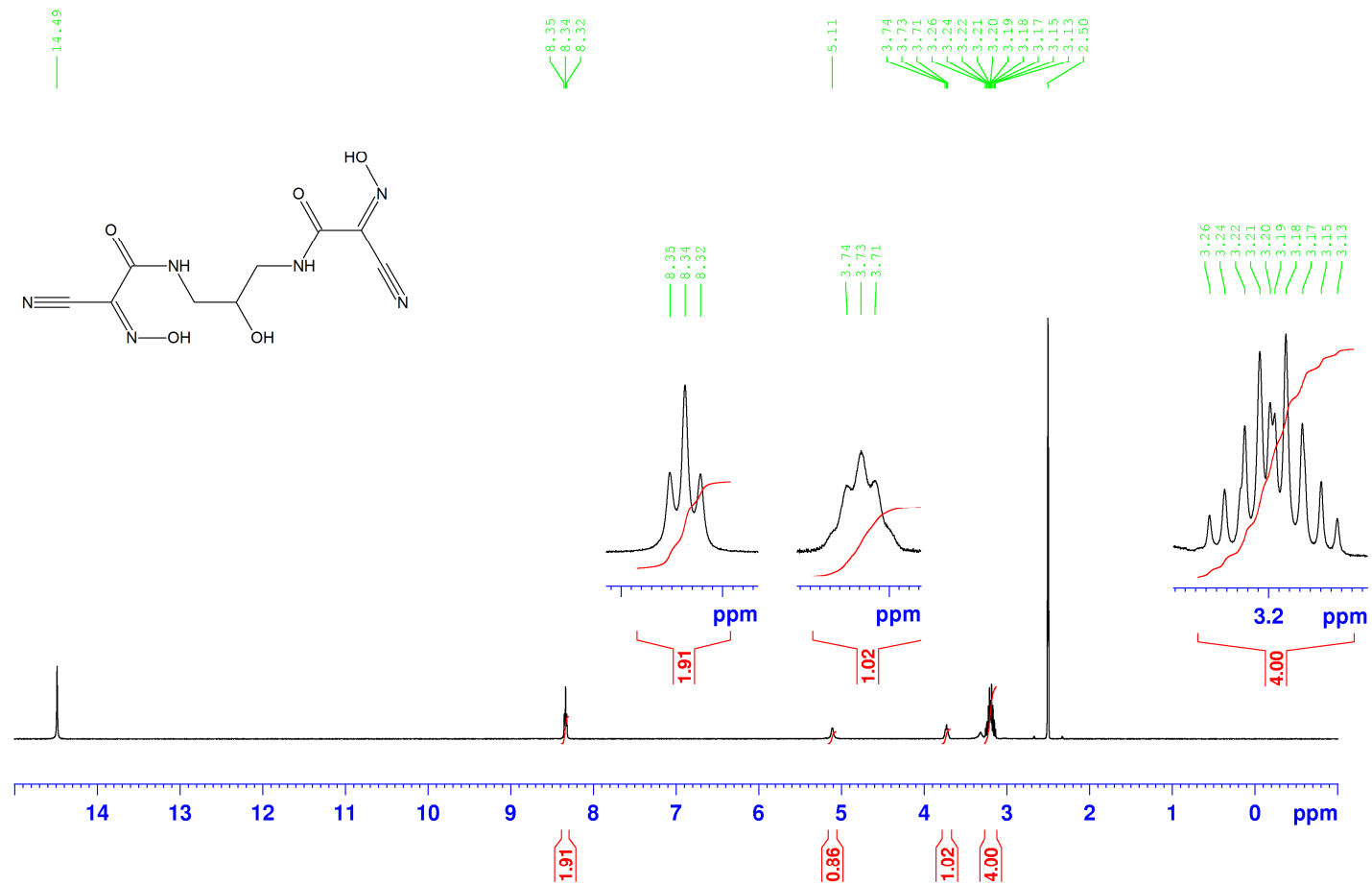


**Fig. B47.** <sup>1</sup>H NMR spectrum of *N,N'*-(2-hydroxypropane-1,3-diyl)bis[2-cyano-2-(hydroxyimino)ethanamide].



*N,N'*-(2-hydroxypropane-1,3-diyl)bis[2-cyano-2-(hydroxyimino)ethanamide], <sup>13</sup>C, DMSO-d<sub>6</sub>

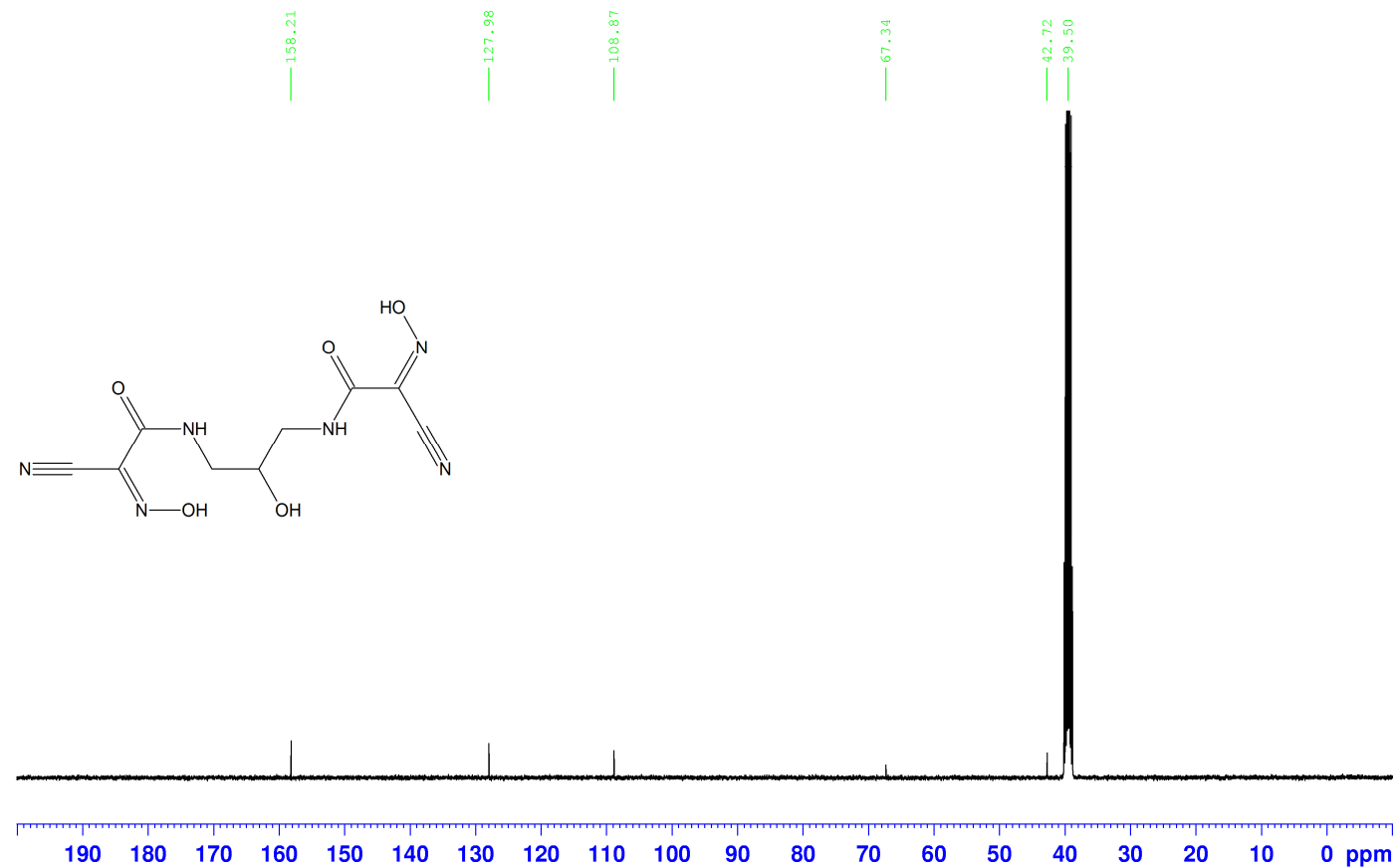


**Fig. B48.** <sup>13</sup>C NMR spectrum of *N,N'*-(2-hydroxypropane-1,3-diyl)bis[2-cyano-2-(hydroxyimino)ethanamide].

*N,N'*-(2-hydroxypropane-1,3-diyl)bis[2-cyano-2-(hydroxyimino)ethanamide], DEPT 135, DMSO-d<sub>6</sub>

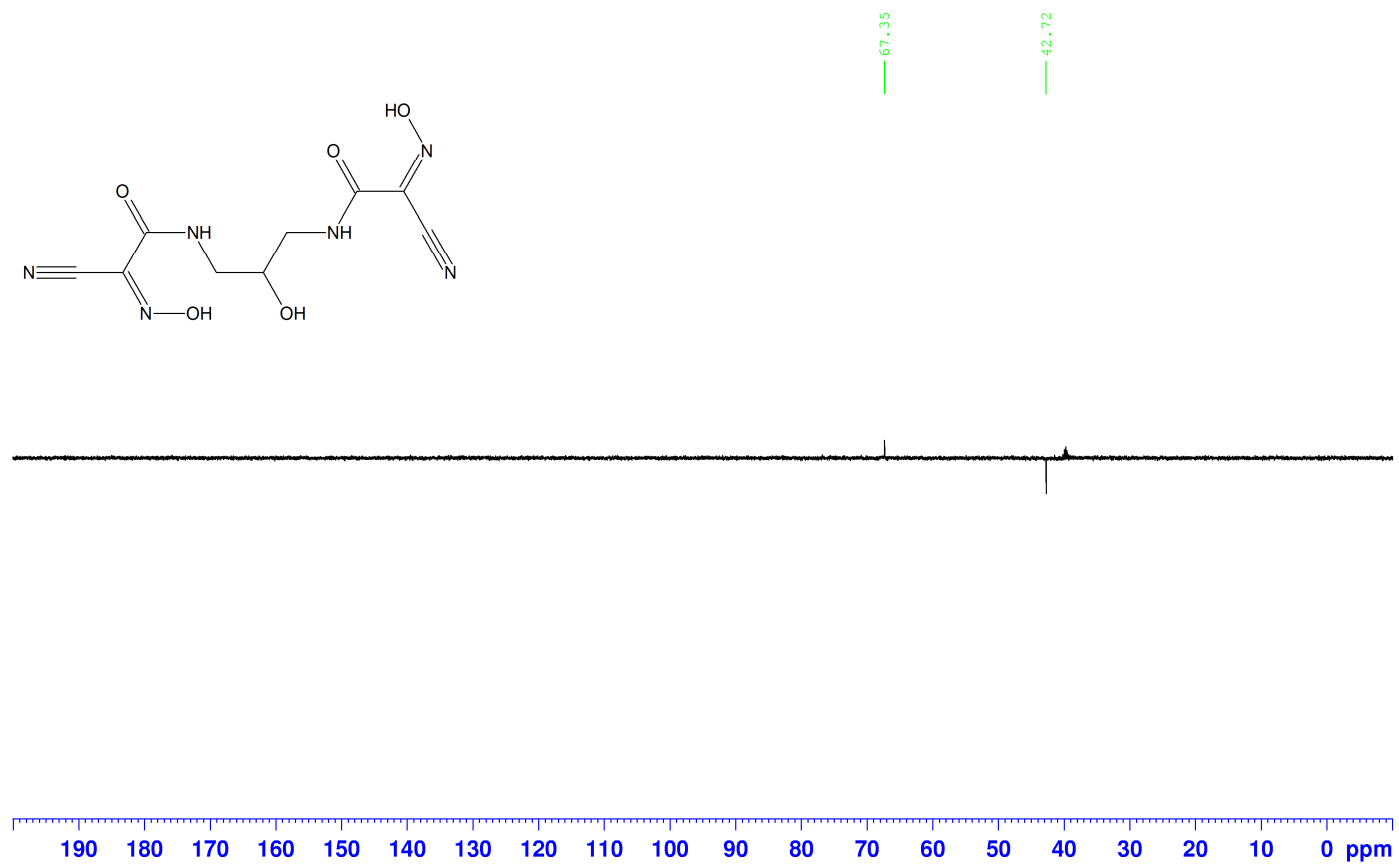


**Fig. B49.** DEPT 135 NMR spectrum of *N,N'*-(2-hydroxypropane-1,3-diyl)bis[2-cyano-2-(hydroxyimino)ethanamide].

*N,N'*-(2-hydroxypropane-1,3-diyl)bis[2-cyano-2-(hydroxyimino)ethanamide], HSQC, DMSO-d<sub>6</sub>

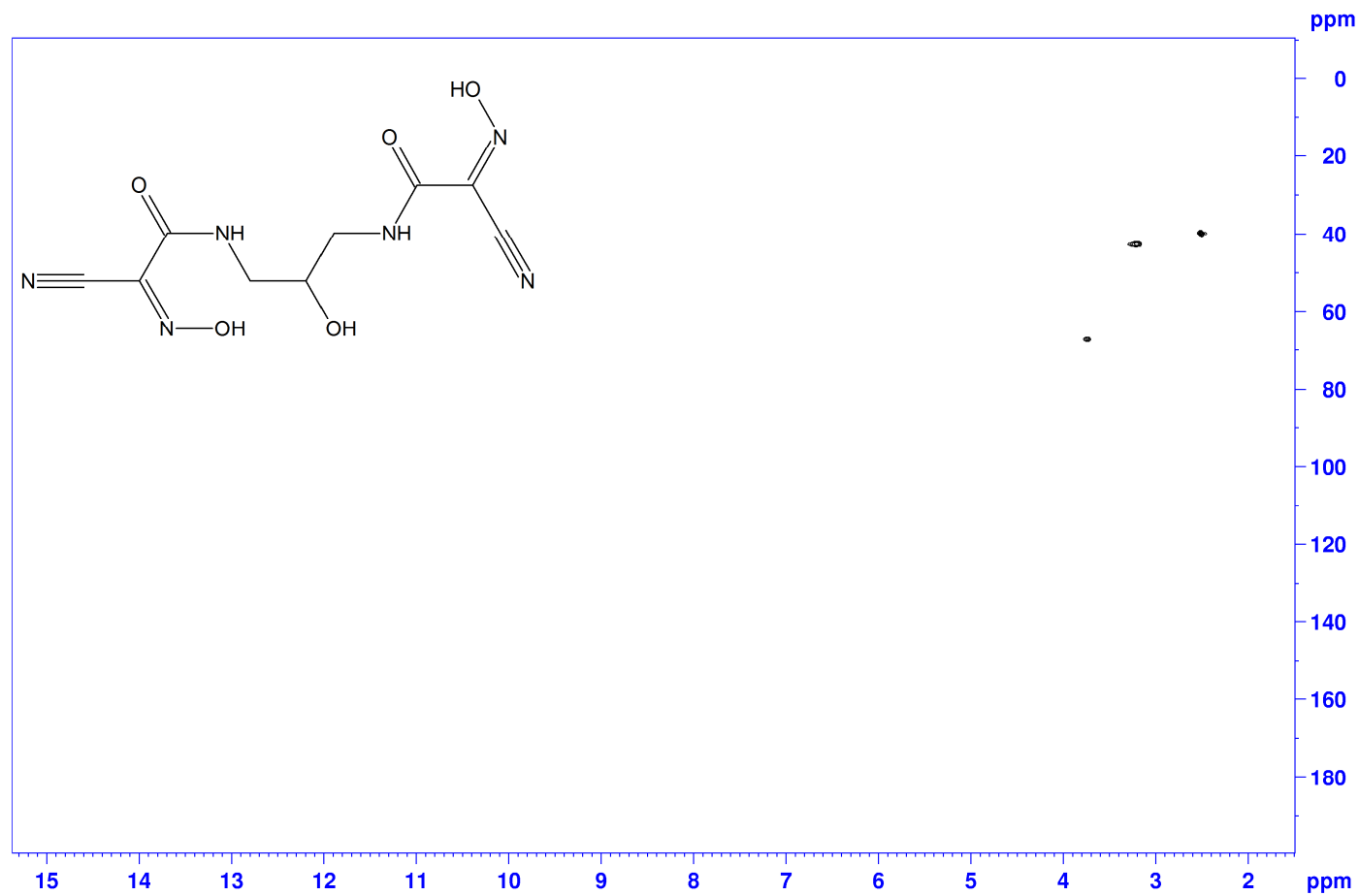


**Fig. B50.** HSQC NMR spectrum of *N,N'*-(2-hydroxypropane-1,3-diyl)bis[2-cyano-2-(hydroxyimino)ethanamide].

*N,N'*-(2-hydroxypropane-1,3-diyl)bis[2-cyano-2-(hydroxyimino)ethanamide], HMBC, DMSO-d<sub>6</sub>

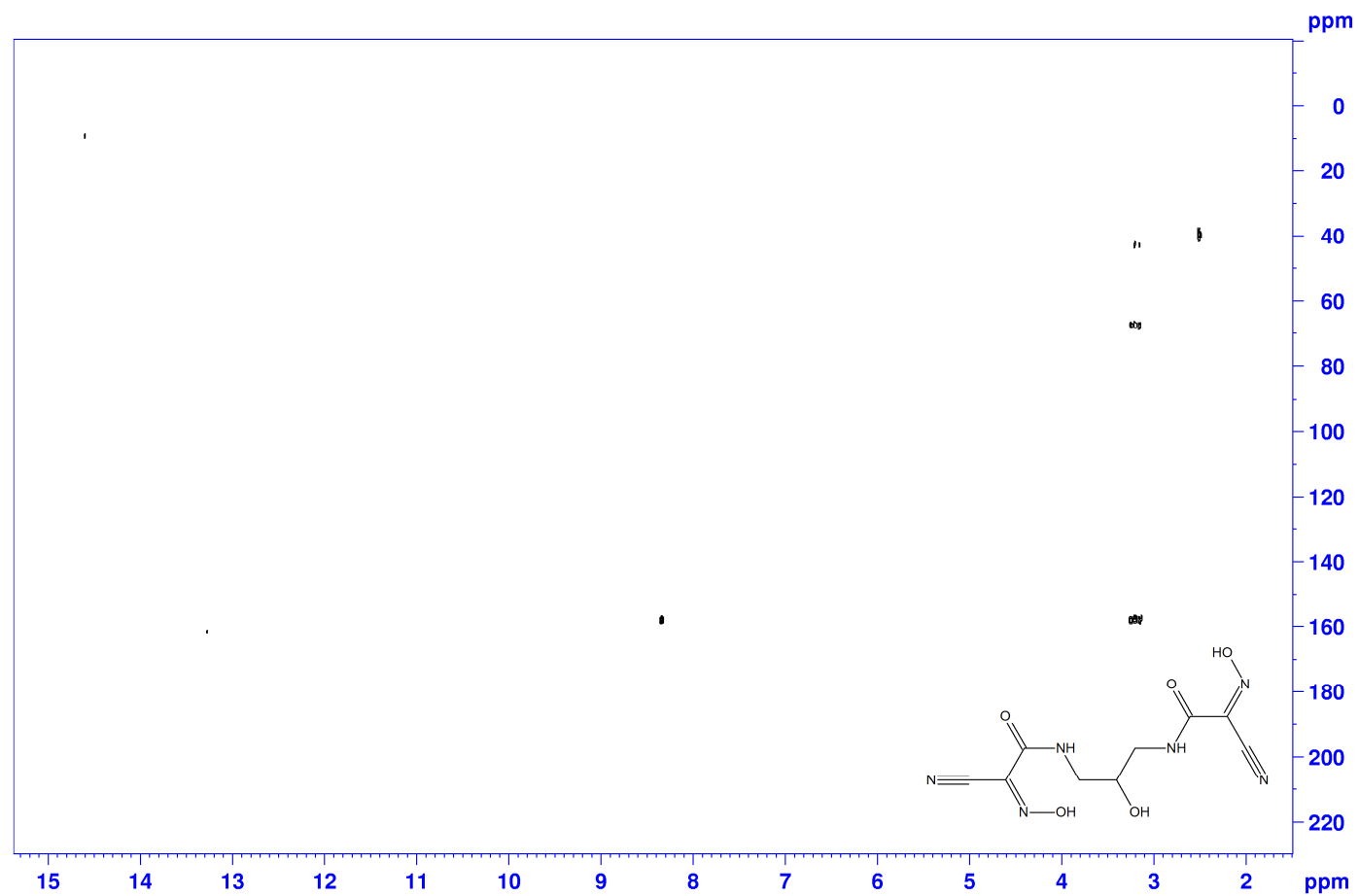


**Fig. B51.** HMBC NMR spectrum of *N,N'*-(2-hydroxypropane-1,3-diyl)bis[2-cyano-2-(hydroxyimino)ethanamide].

*N,N'*-(2-hydroxypropane-1,3-diyl)bis[2-cyano-2-(hydroxyimino)ethanamide], COSY, DMSO-d<sub>6</sub>

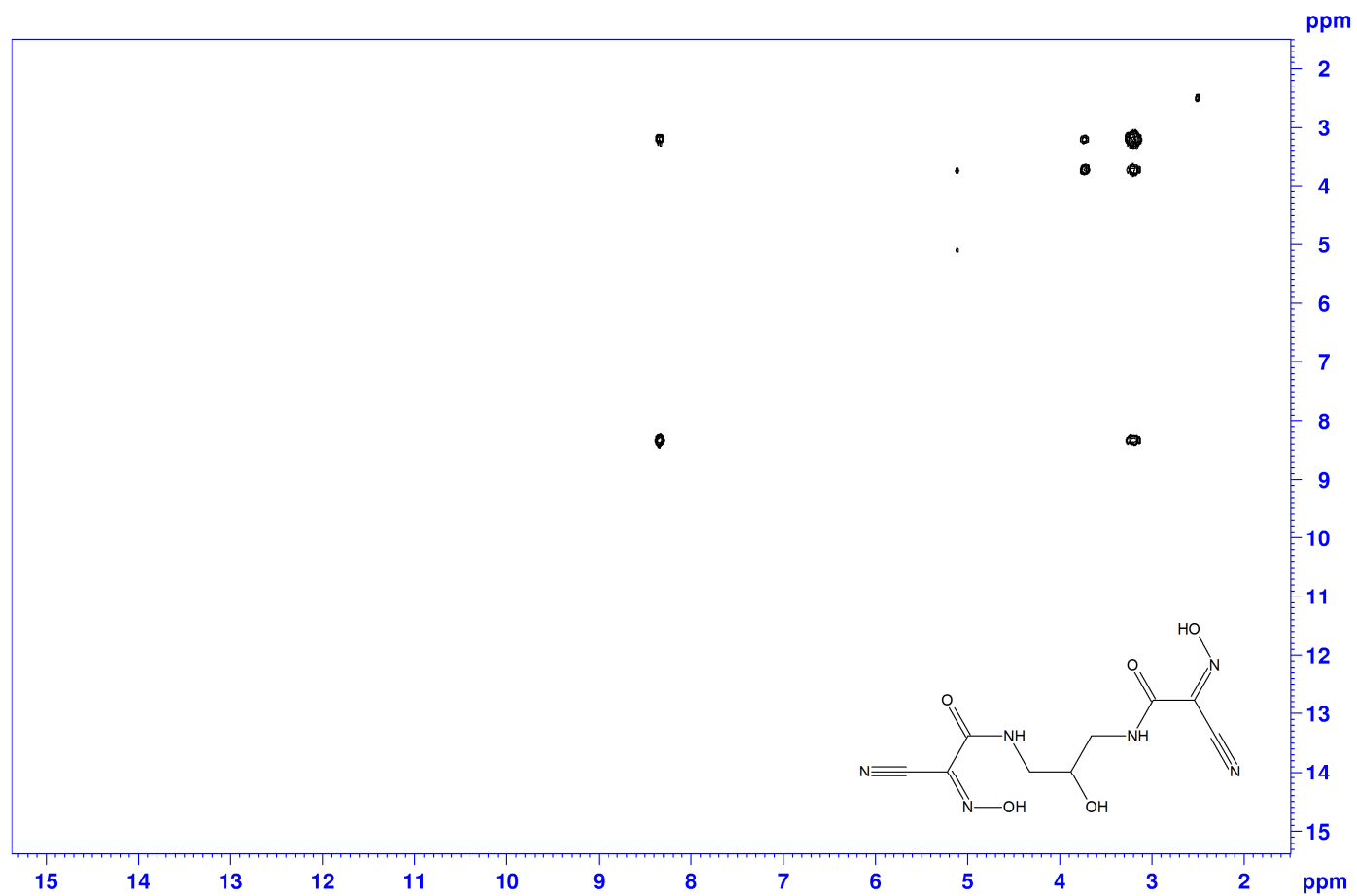


**Fig. B52.** COSY NMR spectrum of *N,N'*-(2-hydroxypropane-1,3-diyl)bis[2-cyano-2-(hydroxyimino)ethanamide].

*N,N'*-(2-hydroxypropane-1,3-diyl)bis[2-cyano-2-(hydroxyimino)ethanamide], LRMS

cnox\_lpnoh\_combo\_sl 14 (0.222) Cm (1:30)

TOF MS ES-  
3.71e4

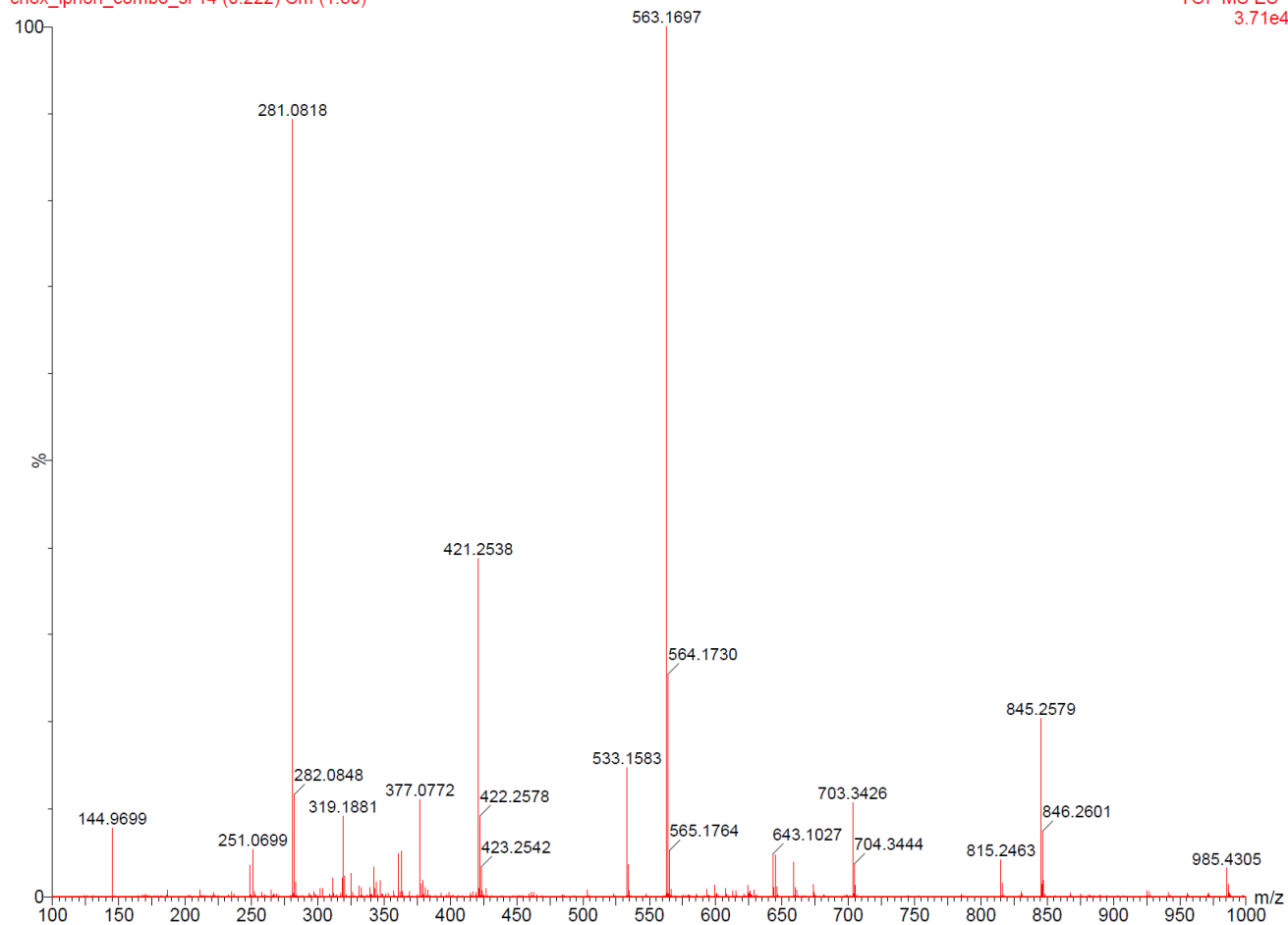


**Fig. B53.** Mass spectrum of *N,N'*-(2-hydroxypropane-1,3-diyl)bis[2-cyano-2-(hydroxyimino)ethanamide] without mass lock.

**Single Mass Analysis**

Tolerance = 3.0 PPM / DBE: min = -1.5, max = 100.0

Element prediction: Off

Number of isotope peaks used for i-FIT = 3

Monoisotopic Mass, Even Electron Ions

18 formula(e) evaluated with 1 results within limits (up to 50 best isotopic matches for each mass)

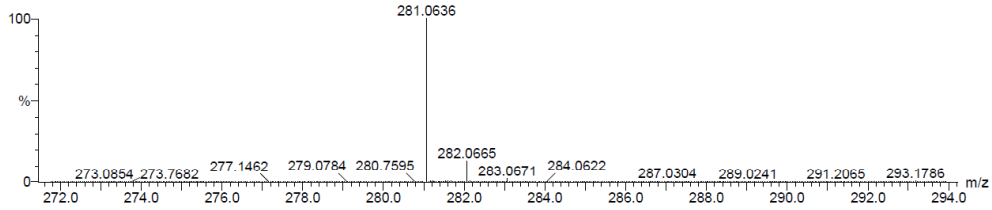
Elements Used:

C: 5-10 H: 5-10 N: 5-10 O: 0-5

cnox\_ipnoh\_combo\_sl 14 (0.222) Cm (1:30)

TOF MS ES-

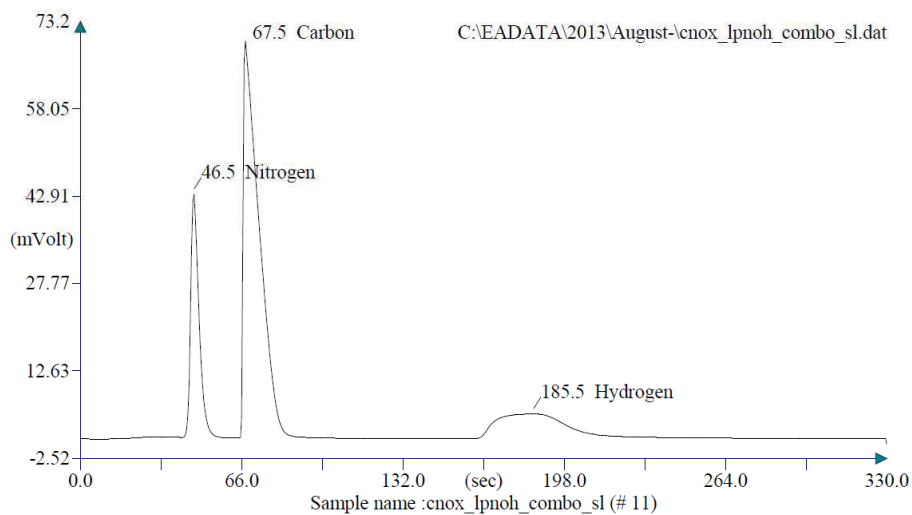
3.32e+004



Minimum:				-1.5				
Maximum:		5.0	3.0	100.0				
Mass	Calc. Mass	mDa	PPM	DBE	i-FIT	i-FIT (Norm)	Formula	
281.0636	281.0634	0.2	0.7	8.5	452.5	0.0	C9 H9 N6 O5	

**Fig. B54.** Mass spectrum of *N,N'*-(2-hydroxypropane-1,3-diyl)bis[2-cyano-2-(hydroxyimino)ethanamide] with mass lock.

*N,N'*-(2-hydroxypropane-1,3-diyl)bis[2-cyano-2-(hydroxyimino)ethanamide], CHN



Retention Time (min)	Element Name	Element %
0.775	Nitrogen	29.626
1.125	Carbon	38.147
3.092	Hydrogen	3.434
		71.206

**Fig. B55.** CHN chromatogram of *N,N'*-(2-hydroxypropane-1,3-diyl)bis[2-cyano-2-(hydroxyimino)ethanamide].



Ethyl-cyano(hydroxyimino)ethanoate, 1H, DMSO-d6

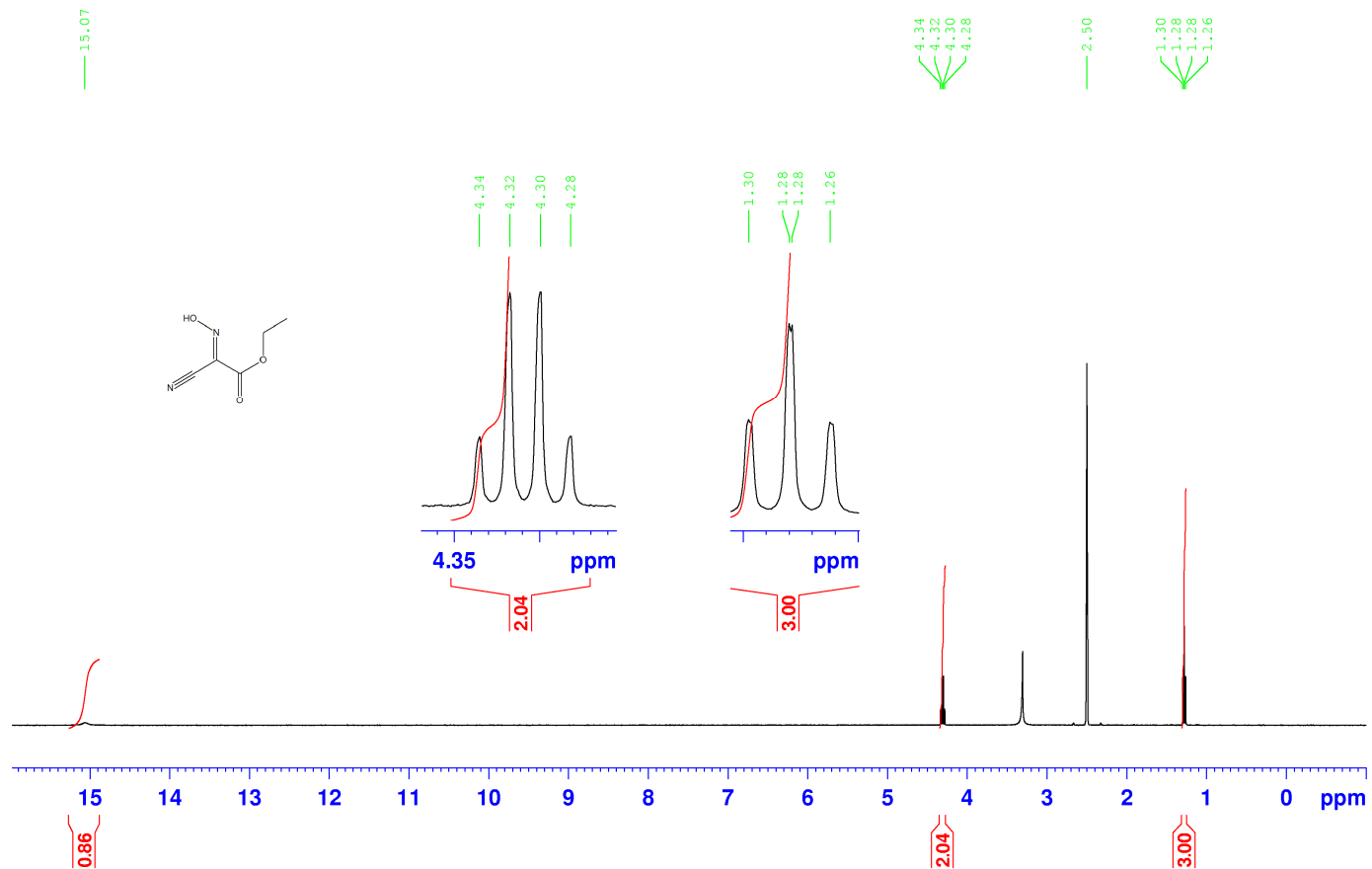
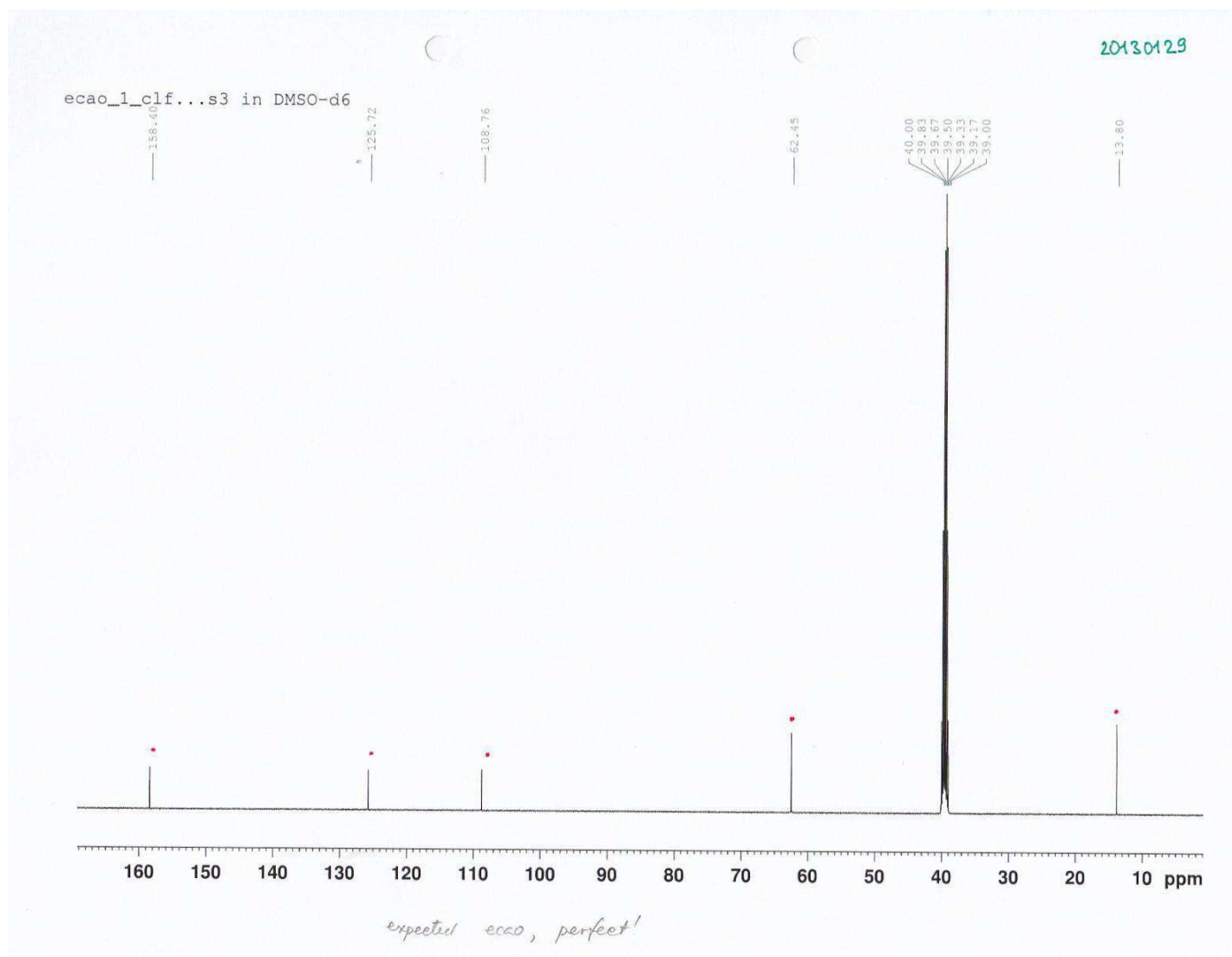


Fig. B56. <sup>1</sup>H NMR spectrum of ethyl-cyano(hydroxyimino)ethanoate.



**Fig. B57.**  $^{13}\text{C}$  NMR spectrum of ethyl-cyano(hydroxyimino)ethanoate

# checkCIF/PLATON (standard)

You have not supplied any structure factors. As a result the full set of tests cannot be run. THIS REPORT IS FOR GUIDANCE ONLY. IF USED AS PART OF A REVIEW PROCEDURE FOR PUBLICATION, IT SHOULD NOT REPLACE THE EXPERTISE OF AN EXPERIENCED CRYSTALLOGRAPHIC REFEREE.

No syntax errors found. [CIF dictionary](#)  
Please wait while processing ....  
[Interpreting this report](#)

## Datablock: in\_tj\_cnox\_en3

Bond precision: C-C = 0.0020 Å Wavelength=0.71073  
Cell: a=4.4555(5) b=8.7443(7) c=11.6123(10)  
alpha=90 beta=99.125(7) gamma=90  
Temperature: 100 K

	Calculated	Reported
Volume	446.69(7)	446.69(7)
Space group	P 21/c	P21/c
Hall group	-P 2ybc	?
Moiety formula	C8 H10 N4 O2	?
Sum formula	C8 H10 N4 O2	C4 H5 N2 O
Mr	194.20	97.10
Dx, g cm <sup>-3</sup>	1.444	1.444
Z	2	4
Mu (mm <sup>-1</sup> )	0.108	0.108
F000	204.0	204.0
F000'	204.08	
h, k, lmax	5, 10, 14	5, 10, 14
Nref	913	862
Tmin, Tmax	0.987, 0.989	0.974, 0.989
Tmin'	0.973	
Correction method= ?		
Data completeness= 0.944	Theta(max)= 26.270	
R(reflections)= 0.0408( 782)	wR2(reflections)= 0.1190( 862)	
S = 1.090	Npar= Npar = 64	

The following ALERTS were generated. Each ALERT has the format **test-name\_ALERT\_alert-type\_alert-level**. Click on the hyperlinks for more details of the test.

### Alert level B

[SHFSU01\\_ALERT\\_2\\_B](#) The absolute value of parameter shift to su ratio > 0.10  
Absolute value of the parameter shift to su ratio given 0.115  
Additional refinement cycles may be required.

[PLAT029\\_ALERT\\_3\\_B](#)  
\_diffn\_measured\_fraction\_theta\_full Low .....  
0.944 Note

PLAT080\_ALERT\_2\_B Maximum Shift/Error  
..... 0.12

---

## ● Alert level C

PLAT052\_ALERT\_1\_C Info on Absorption  
Correction Method Not Given . Please Do !  
PLAT250\_ALERT\_2\_C Large U3/U1 Ratio for  
Average U(i,j) Tensor .... 2.2 Note

---

## ● Alert level G

PLAT005\_ALERT\_5\_G No  
\_iucr\_refine\_instructions\_details in the CIF  
Please Do !  
PLAT007\_ALERT\_5\_G Number of Unrefined Donor-  
H Atoms ..... 1 Why ?  
PLAT045\_ALERT\_1\_G Calculated and Reported Z  
Differ by ..... 0.50 Ratio  
PLAT066\_ALERT\_1\_G Predicted and Reported  
Tmin&Tmax Range Identical ? Check  
PLAT093\_ALERT\_1\_G No su's on H-positions,  
refinement reported as . mixed  
PLAT104\_ALERT\_1\_G The Reported Crystal  
System is Inconsistent with P21/c Check  
PLAT710\_ALERT\_4\_G Delete 1-2-3 or 2-3-4 Linear  
Torsion Angle ... # 1 Do !  
N1 -C1 -C2 -C3 103.00 11.00 1.555  
1.555 1.555 1.555

---

0 **ALERT level A** = Most likely a serious  
problem - resolve or explain  
3 **ALERT level B** = A potentially serious  
problem, consider carefully  
2 **ALERT level C** = Check. Ensure it is not  
caused by an omission or oversight  
7 **ALERT level G** = General information/check it  
is not something unexpected

5 ALERT type 1 CIF construction/syntax error,  
inconsistent or missing data  
3 ALERT type 2 Indicator that the structure  
model may be wrong or deficient  
1 ALERT type 3 Indicator that the structure  
quality may be low  
1 ALERT type 4 Improvement, methodology,  
query or suggestion  
2 ALERT type 5 Informative message, check

---

---

It is advisable to attempt to resolve as many as possible of the alerts in all categories. Often the minor alerts point to easily fixed oversights, errors and omissions in your CIF or refinement strategy, so attention to these fine details can be worthwhile. In order to resolve some of the more serious problems it may be necessary to carry out additional measurements or structure refinements. However, the purpose of your study may justify the reported deviations and the more serious of these should normally be commented upon in the discussion or experimental section of a paper or in the "special\_details" fields of the CIF. checkCIF was carefully designed to identify outliers and unusual parameters, but every test has its limitations and alerts that are not important in a particular case may appear. Conversely, the absence of alerts does not guarantee there are no aspects of the results needing attention. It is up to the individual to critically assess their own results and, if necessary, seek expert advice.

## Publication of your CIF in IUCr journals

A basic structural check has been run on your CIF. These basic checks will be run on all CIFs submitted for publication in IUCr journals (*Acta Crystallographica*, *Journal of Applied Crystallography*, *Journal of Synchrotron Radiation*); however, if you intend to submit to *Acta Crystallographica Section C* or *E*, you should make sure that [full publication checks](#) are run

on the final version of your CIF prior to submission.

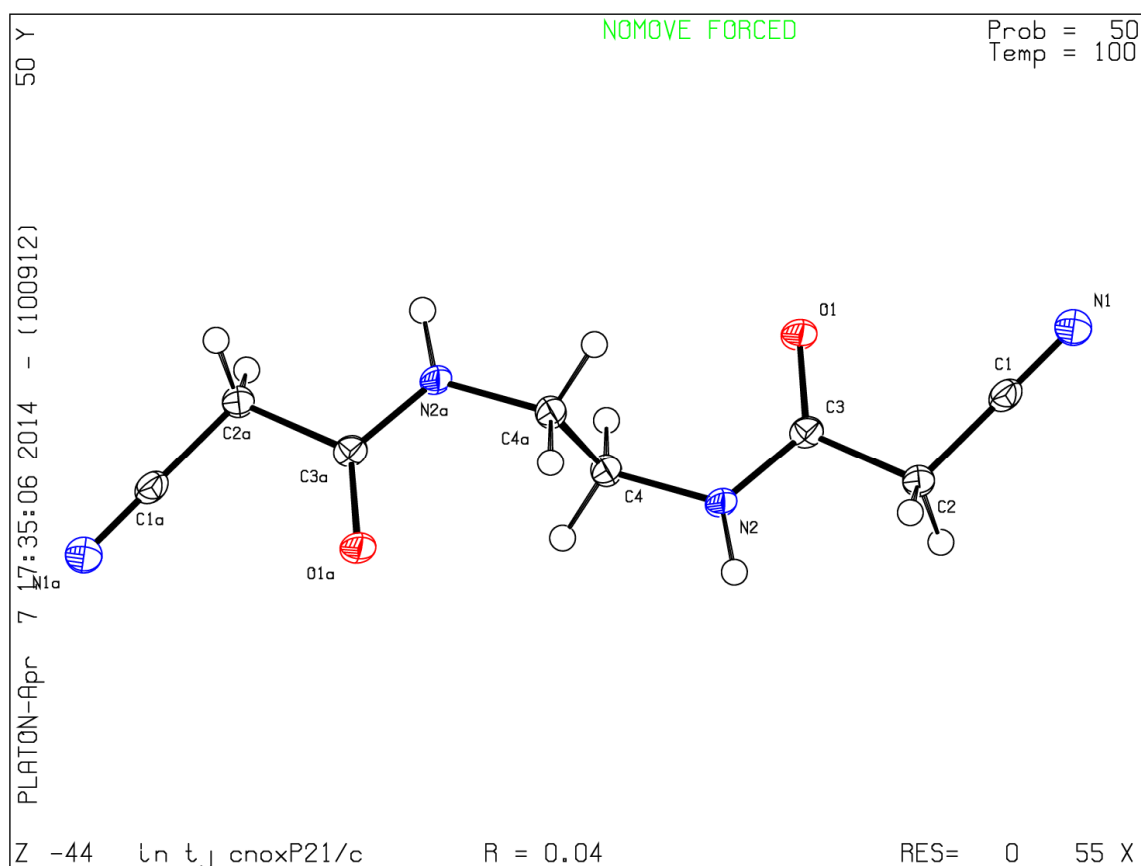
### Publication of your CIF in other journals

Please refer to the *Notes for Authors* of the relevant journal for any special instructions relating to CIF submission.

---

PLATON version of 05/02/2014; check.def file version of 05/02/2014

## Datablock in\_tj\_cnox\_en3 - ellipsoid plot



---

[Download CIF editor \(pubCIF\) from the IUCr](#)

[Download CIF editor \(enCIFer\) from the CCDC](#)

[Test a new CIF entry](#)

Fig. B58

Cifcheck for 4a

## checkCIF/PLATON (full publication check)

---

**Structure factors have been supplied for datablock(s) I**

THIS REPORT IS FOR GUIDANCE ONLY. IF USED AS PART OF A REVIEW PROCEDURE FOR PUBLICATION, IT SHOULD NOT REPLACE THE EXPERTISE OF AN EXPERIENCED CRYSTALLOGRAPHIC REFEREE.

No syntax errors found.

Please wait while processing ...

Structure factor report

CIF dictionary

Interpreting this report

### Datablock: I

### NG\_844\_H2L1\_En

---

Bond precision: C-C = 0.0033 A Wavelength=0.71073

Cell: a=8.170(2) b=6.6782(18) c=10.309(3)  
alpha=90 beta=99.320(4) gamma=90

Temperature: 120 K

	Calculated	Reported
Volume	555.0(3)	555.1(3)
Space group	P 21/n	P 21/n
Hall group	-P 2yn	-P 2yn
Moiety formula	C8 H8 N6 O4	C8 H8 N6 O2
Sum formula	C8 H8 N6 O4	C4 H4 N3 O2
Mr	252.20	126.10
Dx, g cm <sup>-3</sup>	1.509	1.509
Z	2	4
Mu (mm <sup>-1</sup> )	0.124	0.124
F000	260.0	260.0
F000'	260.13	
h, k, lmax	10, 8, 13	10, 8, 13
Nref	1275	1273
Tmin, Tmax	0.966, 0.989	0.727, 0.746
Tmin'	0.959	

Correction method= MULTI-SCAN

Data completeness= 0.998 Theta(max)= 27.485

R(reflections)= 0.0459( 897) wR2(reflections)= 0.1260( 1273)

S = 1.039 Npar= Npar = 97

---

The following ALERTS were generated. Each ALERT has the format

**test-name\_ALERT\_alert-type\_alert-level.**

Click on the hyperlinks for more details of the test.

---

#### ● Alert level C

PLAT975\_ALERT\_2\_C Check Calcd Residual Density 0.89A From N1 0.45 eA-3

---

#### ● Alert level G

FORMU01\_ALERT\_1\_G There is a discrepancy between the atom counts in the `_chemical_formula_sum` and `_chemical_formula_moiety`. This is usually due to the moiety formula being in the wrong format.

Atom count from `_chemical_formula_sum`: C4 H4 N3 O2

Atom count from `_chemical_formula_moiety`: C8 H8 N6 O2

PLAT042\_ALERT\_1\_G Calc. and Reported MoietyFormula Strings Differ Please Check

PLAT045\_ALERT\_1\_G Calculated and Reported Z Differ by ..... 0.50 Ratio  
PLAT720\_ALERT\_4\_G Number of Unusual/Non-Standard Labels ..... 2 Note  
PLAT912\_ALERT\_4\_G Missing # of FCF Reflections Above STh/L= 0.600 2 Note

- 0 **ALERT level A** = Most likely a serious problem - resolve or explain
- 0 **ALERT level B** = A potentially serious problem, consider carefully
- 1 **ALERT level C** = Check. Ensure it is not caused by an omission or oversight
- 5 **ALERT level G** = General information/check it is not something unexpected

3 ALERT type 1 CIF construction/syntax error, inconsistent or missing data

- 1 ALERT type 2 Indicator that the structure model may be wrong or deficient
- 0 ALERT type 3 Indicator that the structure quality may be low
- 2 ALERT type 4 Improvement, methodology, query or suggestion
- 0 ALERT type 5 Informative message, check

PLATON version of 05/02/2014; check.def file version of 05/02/2014

## Datablock I - ellipsoid plot

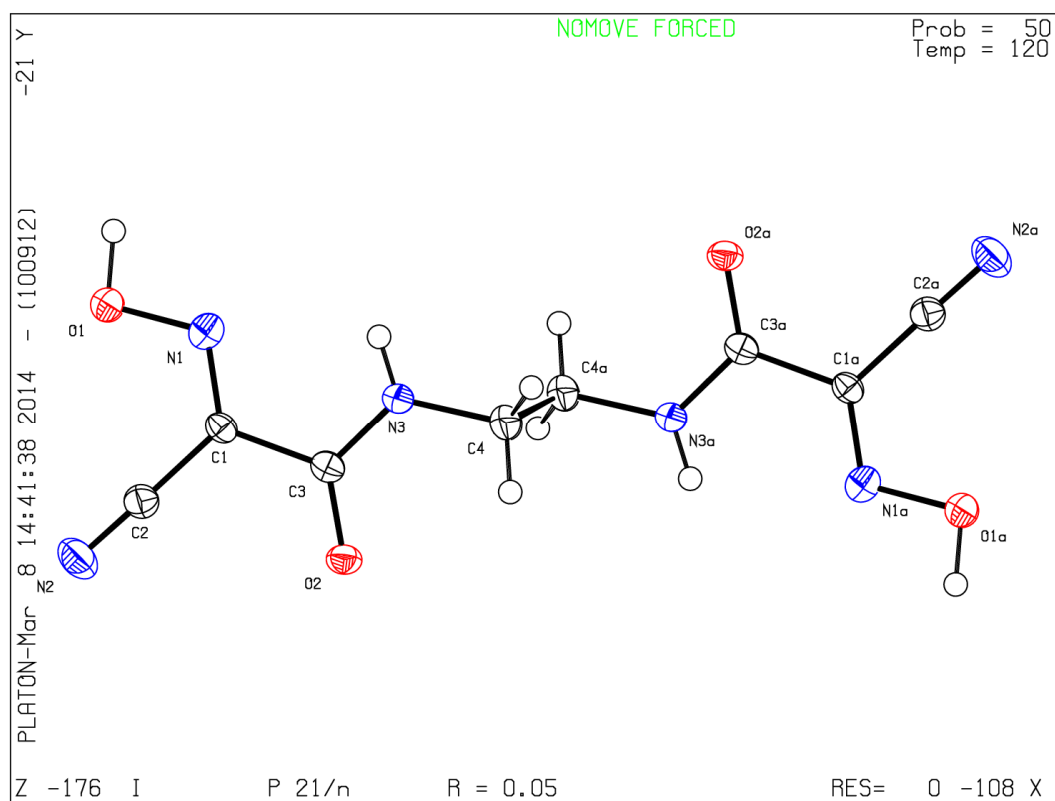


Fig. B59 Cifcheck for 5a